Development of New Classes of Palladium and Nickel Catalyzed Carbonylation Reactions

Jevgenijs Tjutrins

A thesis submitted to McGill University in partial fulfillment of the requirements of the degree of Doctor of Philosophy

Department of Chemistry

McGill University

Montreal, Quebec, Canada

H3A 0B8

June, 2017

Abstract

This thesis describes the development of new palladium and nickel catalyzed carbonylation reactions to efficiently and rapidly generate products with minimal waste. These reactions can be carried out using commercially and/or readily available starting materials, including imines, acid chlorides, aryl iodides, alkynes, alkenes and carbon monoxide.

In chapter 2, we describe a palladium catalyzed carbonylative synthesis of polysubstituted imidazoles. This transformation involves a tandem catalytic process, where a single palladium catalyst mediates both the carbonylation of aryl halides to form acid chlorides, as well as cyclocarbonylation of α-chloroamides, to generate 1,3-dipoles. Finally, a regioselective 1,3-dipolar cycloaddition with electron poor imines furnishes tetra-substituted imidazoles. Overall this provides a route to prepare imidazoles from five readily available building blocks: two electronically distinct imines, aryl halides and two molecules of CO.

In chapter 3, we describe a nickel catalyzed approach to synthesize of isoindolinones via the carbonylation of aryl iodides in the presence of imines. In this, the nickel catalyzed *in situ* generation of acid chlorides via aryl halide carbonylation allows the formation of α-chloroamides, which in turn undergo an intramolecular cyclization to form isoindolinones. This reaction offers an efficient alternative to traditional syntheses of isoindolinones, which often require the initial assembly of the appropriate aryl-tethered precursors for cyclization.

In chapter 4, we describe the development of a palladium catalyzed, electrophilic approach to the carbonylative C-H bond functionalization of a range of heterocycles. Mechanistic studies show that the Pd/P^{t}Bu$_3$ catalyst can mediate the *in situ* formation of highly electrophilic aroyl iodide intermediates, which react with heterocycles forming aryl-(hetero)aryl ketones. This provides a general methodology to construct ketones from aryl iodides and electron rich heterocycles without the need to prefunctionalize the heterocycle, install directing groups, or exploit high energy starting materials (e.g. acid chlorides).

Chapter 5 describes mechanistic studies on the palladium catalyzed multicomponent synthesis of 1,3-oxazolium-5-olates (Münchnones). Previous work in our laboratory has shown

that Münchnones can be generated via the palladium catalyzed multicomponent coupling of acid chlorides, imines and CO. In order to better understand this reaction, we synthesized and characterized key reactive intermediates, studied stoichiometric model reactions, and performed kinetic studies on catalytic reaction. These allowed the elucidation of the role of the catalyst structure, rate determining steps, as well as the importance of off cycle steps in this transformation.

In chapter 6, we show how the mechanistic insights laid out in the previous chapter can be applied to create a highly active catalytic system for synthesis of 1,3-oxazolium-5-olates. By employing a sterically encumbered pyrrole-based phosphine ligand, which can be more easily displaced by carbon monoxide for carbonylation, we have created a catalyst that is more than ten times more active that previous systems for this reaction. When coupled with alkyne cycloaddition, this offers a broadly generalizable route to form polysubstituted pyrroles from simple imines, acid chlorides and alkynes. This approach has been applied to the multicomponent synthesis of Atorvastatin (i.e., Lipitor).

Résumé

Cette thèse décrit le développement de nouvelles réactions de carbonylation catalysées au palladium et au nickel pour générer efficacement et rapidement des produits avec un minimum de pertes. Ces réactions peuvent être effectuées en utilisant des sources commerciales et/ou des composés de départ facilement disponibles, comme des imines, chlorures d'acide, iodures d'aryle, alcènes, alcynes, et le monoxyde de carbone.

Dans le chapitre 2, nous décrivons la synthèse carbonylative d'imidazoles polysubstitués catalysée au palladium. Cette transformation repose sur un procédé tandem où un seul catalyseur de palladium est impliqué autant dans la carbonylation des halogénures d'aryle que dans la cyclocarbonylation des α-chloroamides, pour générer des 1,3-dipôles. Finalement, une cycloaddition 1,3-dipolaire régiosélective avec des imines pauvres en électrons produit des imidazoles tétrasubstitués. Globalement, ceci procure une voie efficace pour préparer des imidazoles à partir de cinq composantes disponibles et faciles d'approche : deux imines électroniquement distinctes, halogénures d'aryle ainsi que deux molécules de monoxyde de carbone.

Dans le chapitre 3, nous décrivons une approche catalysée au nickel à l'égard de la synthèse d'isoindolines via la carbonylation d'iodures d'aryle en présence d'imines. La génération *in situ* catalysée au nickel de chlorure d'acide via la carbonylation d'halogénure d'aryle permet la génération de α-chloroamides, qui à son tour subit une cyclisation intramoléculaire pour former des isoindolinones. Cette réaction offre une alternative efficace aux synthèses traditionnelles d'isoindolinones, qui pour la plupart demandent l'assemblage initial des précurseurs appropriés pour la cyclisation contenant des aryles préalablement connectés.

Dans le chapitre 4, nous décrivons le développement d'une approche électrophile catalysée au palladium à l'égard de la fonctionnalisation C-H carbonylative d'une gamme d'hétérocycles. Des études mécanistiques montrent que le catalyseur Pd/P^tBu_3 peut générer *in situ* des iodures d'acyles hautement électrophiles qui réagissent avec des hétérocycles formant des cétones de type aryl-(hétéro)aryl. Ceci fournit une méthodologie générale pour construire des cétones à partir d'iodures d'aryle et d'hétérocycles riches en électrons sans le besoin de

préfonctionaliser ces derniers, d'installer des groupes directeurs ou d'exploiter des composés de départ hautement énergétiques (p. ex. chlorures d'acide).

Le chapitre 5 décrit les études mécanistiques sur la synthèse multicomposante de 1,3-oxazolium-5-olates (Münchnones) catalysée au palladium. Les travaux précédemment faits dans notre laboratoire ont montré que les Münchnones peuvent être générés via un couplage multicomposante de chlorure d'acide, d'imines et de monoxyde de carbone catalysé au palladium. Afin de mieux comprendre cette réaction, nous avons synthétisé et caractérisé les intermédiaires réactifs clés, étudié des réactions stœchiométriques et effectué des études cinétiques sur des réactions catalytiques. Ceux-ci ont permis d'élucider le rôle de la structure catalytique, les étapes cinétiquement déterminantes, ainsi que l'importance des étapes hors cycle dans cette transformation.

Dans le chapitre 6, nous montrons comment les connaissances décrites dans le chapitre précédent peuvent être appliquées pour créer un système catalytique extrêmement actif pour la synthèse de 1,3-oxazolium-5-olates. En utilisant un ligand phosphine encombré de type pyrrole, qui peut plus facilement être remplacé par le monoxyde de carbone pour la carbonylation, nous avons créé un catalyseur qui est dix fois plus actif que le système précédant pour cette réaction. En combinaison avec la cycloaddition d'alcynes, ceci offre une voie générale pour former des pyrroles polysubstituées à partir d'imines simples, de chlorures d'acide et d'alcynes. Cette approche a été appliquée à la synthèse multicomposante de l'Atorvastatin (i.e. Lipitor).

Acknowledgements

To my supervisor, Prof. Bruce Arndtsen: I would like to thank you for your guidance and for pushing me at the right times leading to great results.

I would like to thank the *doctors* of the Arndtsen Lab – Dr. Laure Kayser, Dr. Jeffrey Quesnel and Dr. Boran Xu, who have been next to me throughout the journey of graduate school and have given me tremendous support and mentoring.

I would like to thank Prof. Audrey Moores, Prof. Nicolas Moitessier, Prof. Youla Tsantrizos and Prof. Jim Gleason for being part of my review committees.

I would like to express my great acknowledgements to the NMR facility staff – Dr. Fred Morin and Robin Stein for teaching me all the tips and tricks as well as for taking tremendous time with my NMR endeavours. As well as all the support staff around the department: Rick Rossi, Weihua Wang, Jean-Philippe Guay, Dr. Nadim Saadeh, Dr. Alex Wahba, Chantal Marotte, Claude Perryman, Mario Perone, Stephanie Trempe, Jean-Marc Gauthier, Sandra Aerssen, Colleen McNamee, Jennifer Marleau, Linda Del Paggio, Karen Turner, Inna Perepichka, and Jacqueline Farrell.

I would like to thank my bestie Dr. Michelle Bezanson, who has made my time at McGill exciting and has supported me emotionally with lots of wine, movie nights and some tough love. Thanks to Monika Rak for all the hugs over the course of seven years, to Mary Bateman for being one of the nicest and most adorable people I know. Thanks to Nicklas Häggman, Graeme Cambridge, Thomas Knauber for great food and awesome parties. Very big thanks to Patrick Julien for being a great roommate for many years and tolerating me.

I would like to thank all the other members of the Arndtsen lab not mentioned above for being supportive and for all the brainstorming done together: Dr. David Leitch, Dr. Fabio Lorenzini, Dr. Han Zhi-Yong, Sara Aly, Evan Keyzer, Vicky Jackiewicz, Richard Garrison Kinney, Gerardo Martin-Torres, Huseyin Erguven, Elizabeth Hartigan, Giancarlo Feula, Maximilliano De La Higuera Macias, Pierre-Louis Lagueux-Tremblay, Yi Liu, Nina Liu, Oliver Williams, Anthony Lau and Alexander Fabrikant.

Lastly I would like to thank my family, in particular my parents, for their unconditional and everlasting support towards my studies.

Table of Contents

List of Schemes

List of Figures

List of Tables

List of Abbreviations

Ac	Acetyl
Ad	Adamantyl
Ar	Aryl
Atm	Atmosphere
BQ	1,4-Benzoquinone
Bu	Butyl
t-Bu	*tert*-butyl
BINOL	2,2-binapthol
n-BuLi	*n*-Butyllithium
bpy	2,2-Bipyridine
Cy	cyclohexyl
dba	Dibenzylideneacetone 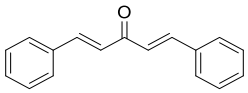
DBU	1,8-Diazabicyclo(5.4.0)undec-7-ene 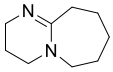
DCM	Dichloromethane
Dcpp	1,3-Bis(dicyclohexylphosphino)propane 
DMF	Dimethylformamide
DMSO	Dimethylsufoxide

DpePhos	Bis[(2-diphenylphosphino)phenyl]ether 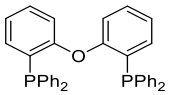
Dppb	1,4-Bis(diphenylphosphino)butane 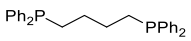
Dppe	1,2-Bis(diphenylphosphino)ethane 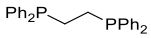
Dppf	1,1'-Bis(diphenylphosphino)ferrocene 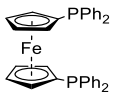
d^{i}ppp	1,3-Bis(diiisopropylphosphino)propane 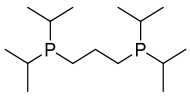
Dtbpx	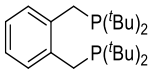
Et	Ethyl
EWG	Electron Withdrawing Group
FT-IR-ATR	Fourier Transform – Infrared spectroscopy - Attenuated Total Reflectance
JosiPhos	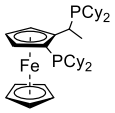
Hex	Hexyl
*i*Pr	Isopropyl
Leu	Leucene
LG	Leaving Group
Me	Methyl

Men	Menthyl
MHz	Megahertz
MS	Molecular Sieves
mg	Milligram
mmol	Millimole
mL	Milliliter
NMI	N-Methylimidazole 
NMP	N-Methyl-2-pyrrolidone
NMR	Nuclear Magnetic Resonance Spectroscopy
Piv	Pivalate
Ph	Phenyl
Phen	1,10-Phenanthroline
PG	Protecting Group
PMB	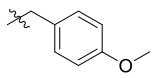
PMP	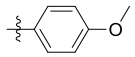
TEMPO	
TMEDA	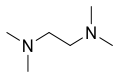
THF	Tetrahydrofuran
Tf	
TFA	Trifluoroacetate

TFAA	Trifluoroacetic acid
o-Tol	*ortho*-Tolyl
Ts	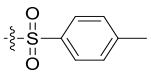
XantPhos	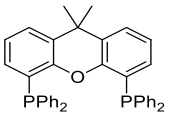

Contributions of Co-Authors

This thesis consists of six chapters. The first chapter is an introduction to the work described in this thesis, and chapter 7 will present conclusions and suggestions for future work. The main body includes four publications (Chapter 2, 3, 4, 5) and one paper to be submitted (Chapter 6). All the work was carried out as part of my degree of Doctor of Philosophy in chemistry under the supervision of Dr. Bruce Arndtsen. As such, he is the corresponding author on all manuscripts.

These papers are:

Chapter 2: "A Palladium-Catalyzed Synthesis of (Hetero)Aryl-Substituted Imidazoles from Aryl Halides, Imines and Carbon monoxide", Tjutrins, J.; Arndtsen, B. A.* *Chem. Sci.* **2017**, 8, 1002-1007.

Chapter 3: "A Nickel-Based, Tandem Catalytic Approach to Isoindolinones from Imines, Aryl Iodides, and CO", Tjutrins, J.; Shao, J. L.; Yempally, V.; Bengali, A. A.; Arndtsen, B. A.* *Organometallics* **2015**, *34*, 1802-1805.

Chapter 4: "An Electrophilic Approach to the Palladium-Catalyzed Carbonylative C-H Functionalization of Heterocycles", Tjutrins, J.; Arndtsen, B. A.* *J. Am. Chem. Soc.* **2015**, 137, 12050-12954.

Chapter 5: "Mechanism of the Palladium-Catalyzed Synthesis of Münchnones: The Role of Ligands in N-Acyl Iminium Salt Carbonylation", Tjutrins, J.; Dhawan, R.; Lu, Y.; Arndtsen, B. A.* *Chem. Eur. J.* **2016**, 22, 15945-15954.

All the experiments reported in this thesis were performed by myself with the following exceptions:

Chapter 3: Jia Lun Shao and Dr. Yempally performed some catalyst screening experiments and synthesized products **3.2c** and **3.2d**.

Chapter 5: Dr. Dhawan and Dr. Lu performed the mercury poisoning experiments, obtained X-ray crystal structures of compounds **5.2b** and **5.7b** as well as performed initial kinetic studies.

Chapter 1. Introduction: Palladium and Nickel Catalyzed Carbonylation Reactions

1.1. Perspective

The field of transition metal catalysis has undergone a dramatic expansion in the last 50 years. Areas as diverse as organic chemistry, pharmaceutical and agrochemical synthesis, polymer chemistry, fine chemical production, materials science, and many others all now exploit transition metal catalysis as a routine, and often integral, tool for molecular synthesis. A plethora of new catalytic reactions have been developed during this period, which can allow, for example, the efficient manipulation of functional groups, the formation of products with high selectivity, or coupling reactions to form new bonds. An important example of this area is the rapid evolution of palladium catalyzed cross-coupling reactions (Scheme 1.1a).[1] These transformations can provide a mild method to generate carbon-carbon and related carbon-heteroatom bonds from stable reagents, and are at the core of many current pharmaceutical syntheses. This field was highlighted in the 2010 Nobel Prize in chemistry awarded to R. Heck, E. Negishi and A. Suzuki.[2]

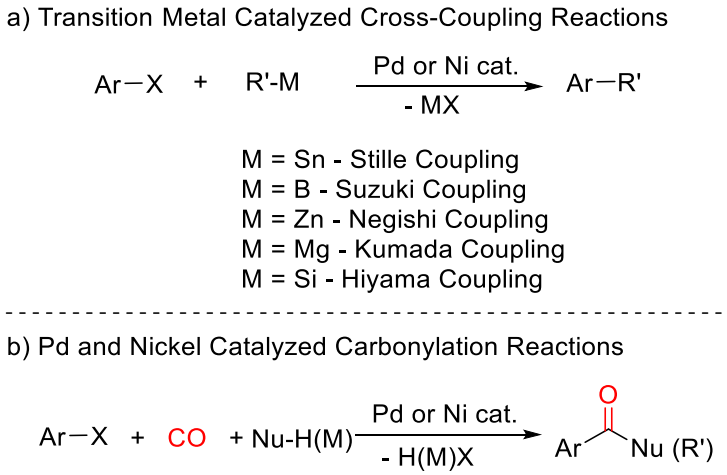

Scheme 1.1. Palladium and Nickel Catalyzed Cross-Coupling and Carbonylation Reactions.

A useful variant of cross-coupling reactions are palladium catalyzed carbonylative coupling reactions (Scheme 1.1b).[3] Unlike cross-coupling reactions, which typically generate inert aryl-aryl or aryl-alkyl bonds, carbonylative coupling reactions provide a route to incorporate a reactive carbonyl group into the final product. While classical approaches to prepare carbon-containing products typically involve coupling reactions with carboxylic acid derivatives using high energy stoichiometric reagents and additives (e.g. $SOCl_2$, PCl_3, carbodiimides (DCC), etc.), palladium catalyzed carbonylation reactions form these same products using simple carbon monoxide, which is one of the most readily available feedstocks in the chemical industry.[4]

Since the seminal work of Heck in the 1970s, a tremendous variety of palladium and nickel catalyzed carbonylative coupling reactions have been developed.[5] The products of these transformations are aldehydes, ketones or carboxylic acid derivatives, which are vital intermediates or products in the manufacture of pharmaceuticals, dyes, agrochemicals and other industrial products. Representative examples are shown in Figure 1.1.[6] Thus, the development of simple, cost-efficient and reliable carbonylation methodologies continues to be of great interest. This chapter will highlight the general types of these transformations, including examples of efforts towards creating new catalysts (Section 1.2), their application to more elaborate products (Section 1.3), and new uses in C-H bond functionalization (Section 1.4). This will provide the background for this thesis, which is focused upon development of new nickel and palladium catalyzed carbonylation reactions of utility in heterocycle synthesis, as well as new platforms for carbonylative C-H bond functionalization.

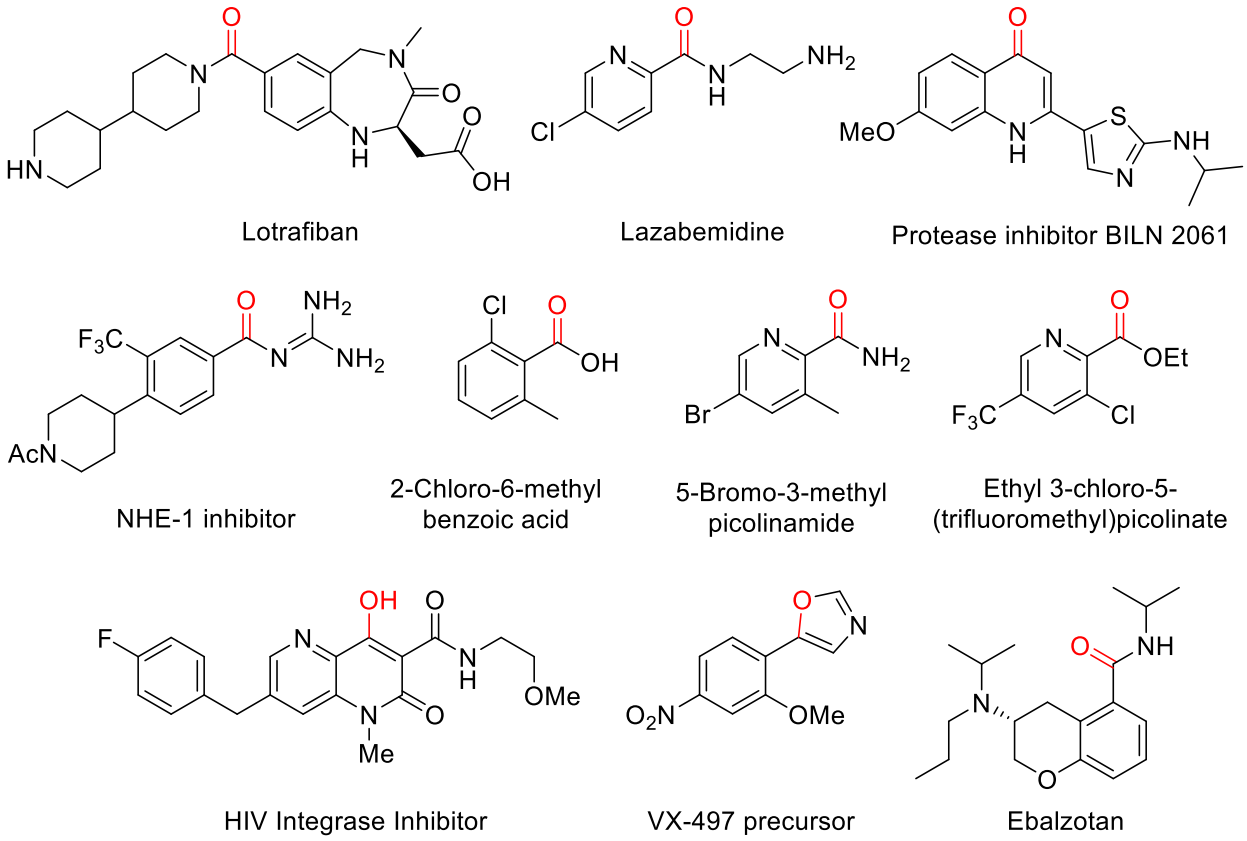

Figure 1.1. Representative Examples of Pharmaceuticals and Chemical Intermediates Produced via Aryl-Halide Carbonylation.

1.2. Palladium and Nickel Catalyzed Aryl-Halide Carbonylation Reactions

1.2.1. Overview of Mechanism

Palladium and nickel catalyzed carbonylation reactions cover a large number of closely related transformations in which carbon monoxide is coupled between an organic R-X electrophile and nucleophile. These most commonly involve the use of (hetero)aryl- or vinyl-halides as the electrophilic substrate, although alkyl and related sp^3 C-X bonds can also be employed. A number of studies have been conducted to elucidate the exact mechanism of carbonylation reactions.[7] The most commonly involved mechanism for these reactions is outlined in Scheme 1.2.

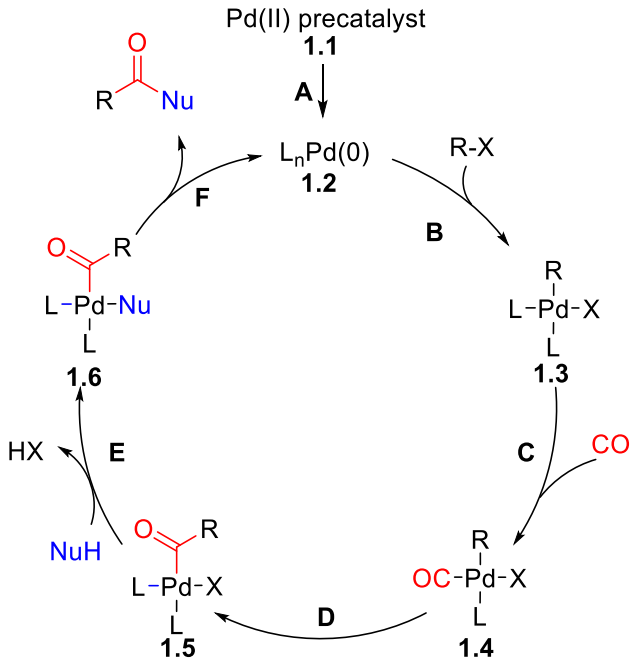

Scheme 1.2. Simplified Mechanism for Alkoxy- or Aminocarbonylation Reactions.

Carbonylation reactions typically require initiation steps (**A**) to activate the pre-catalyst (**1.1**). Many readily available (and oxygen stable) palladium precursors are Pd(II) salts, which must be converted to Pd(0) in order to enter the catalytic cycle. Catalyst reduction can be achieved *in situ* with added ligand (e.g. phosphines), amine base, or CO itself, each of which can be oxidized to convert Pd(II) to Pd(0). Once reduced, the ligated Pd(0) complex can then undergo oxidative addition of the aryl halide electrophile (**B**). This step, which is common in most cross coupling reactions, has been widely investigated, and is typically favored by electron rich phosphine ligands, as their donation into palladium lowers the activation barrier for the formal oxidation of palladium to form **1.3**.[7c,8] The oxidative addition propensity of aryl halides is strongly dependent upon the halide in the substrate, and typically follows the trend: Ar-I > Ar-Br > Ar-OTf > Ar-Cl.[3] This reflects to a large degree the strength of these bonds. For example, while the relatively weak carbon-iodide bond in aryl iodides can be activated by a range of palladium catalysts, highly sterically encumbered or bidentate ligands are often required for the aryl-chloride or -triflate carbonylations.[7a] In general, carbonylation reactions can suffer from lower rates of oxidative addition relative to cross-coupling reactions due to the presence of CO in

the reaction mixture. Carbon monoxide is a strong π-backbonding ligand, and its coordination can reduce electron density on palladium, thus slowing oxidative processes.

The next step in carbonylation is the migratory insertion of the CO into Pd-C bond. This requires the initial coordination of CO to palladium, and, for smaller phosphine ligands, is typically postulated to involve CO displacement of a coordinated phosphine (**C**). In the case of more sterically encumbered phosphines, which generate coordinatively unsaturated Pd(0), CO can coordinate to an empty Pd(II) coordination site, or may even be present on palladium during oxidative addition. The insertion of CO into the Pd-Ar bond is influenced by the strength of the Pd-CO and Pd-C bonds. Generally, electron withdrawing groups in the Ar group decrease the rate of carbonylation in comparison to electron donating groups, since it strengthens the Pd-C bond. On the other hand, electron rich ligands increase the backbonding to CO, thus for reactions where oxidative addition is not rate determining, aryl substituted phosphines often can yield faster reactions than the corresponding alkyl phosphines.[7c]

The last steps of the catalytic cycle are the reaction of **1.5** with the nucleophile and elimination of the product. Variation of the nucleophile can lead to a range of different products. For example, early studies of aryl halide carbonylation often employed alcohol or amine nucleophiles (alkoxy- and aminocarbonylation respectively). Initial observations by Heck suggested a direct nucleophilic attack on palladium aroyl ligand in **1.5** leads to the product. However extensive kinetic studies by Yamamoto and others have shown that the operating mechanism for most is the coordination of the deprotonated nucleophile to palladium generating **1.6** (Step **E**) followed by reductive elimination (Step **F**).[5,7b,9]

A number of other reagents can be employed as the nucleophile component in the reactions (Scheme 1.3.). For example, the use of terminal alkynes as coupling partners generates a range of alkynones. It is believed that alkyne π-coordination allows for an easy deprotonation of the terminal C-H bond, thus generating an Pd-acetylide which in turn can reductively eliminate the product. Hydrogen can also be employed as the coupling partner to form aldehydes. In a different mechanism, the use of alkenes in carbonylation reactions leads to the synthesis of chalcones, where an alkene insertion and β-hydride elimination are the product forming steps. Aryl and alkyl organometallic reagents can be similarly employed as the coupling partners to undergo a transmetallation step prior to reductive elimination to form ketone products. The use

of high CO pressure in aminocarbonylation reactions can lead to palladium coordinated CO to react with the amines forming palladium carbamoyl species, which upon reductive elimination form 1,2-ketoamides.

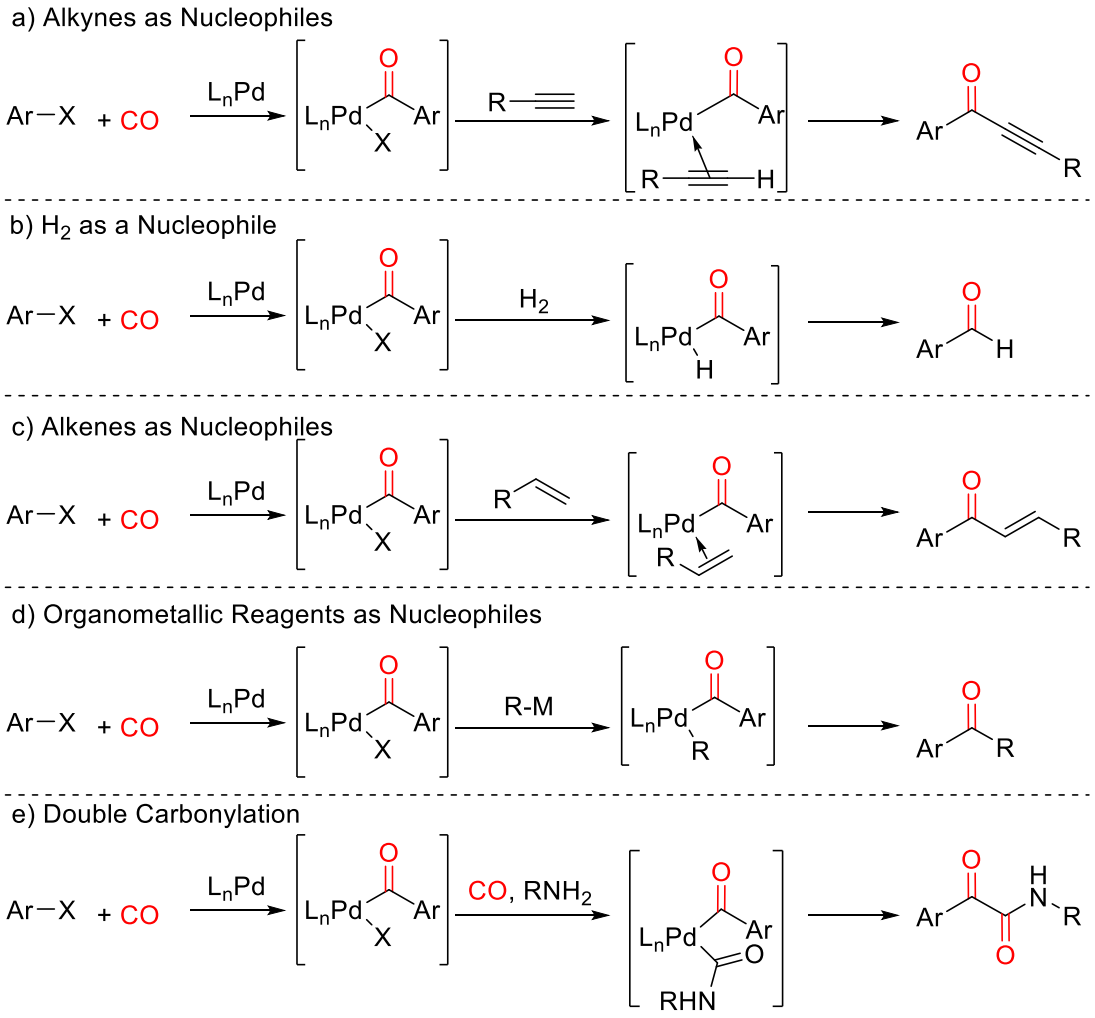

Scheme 1.3. Transition Metal Catalyzed Carbonylation Reactions with Nucleophiles.

1.2.2. Nickel Catalyzed Carbonylation Reactions

In 1888, Ludwig Mond reported the first nickel-carbonyl complex, $Ni(CO)_4$,[10] as the product of the reaction of impure nickel ores and carbon monoxide. The unusual properties of $Ni(CO)_4$ – it has a boiling point near ambient temperature – allowed for the facile purification of nickel metal, and thus initiated the development of organonickel chemistry. In the first part of

20th century, Walter Reppe at BASF developed several industrially important nickel catalyzed carbonylations of acetylene, ethene and benzylic alcohols, which are now more commonly referred to as Reppe carbonylations or Reppe chemistry (Scheme 1.4).[11]

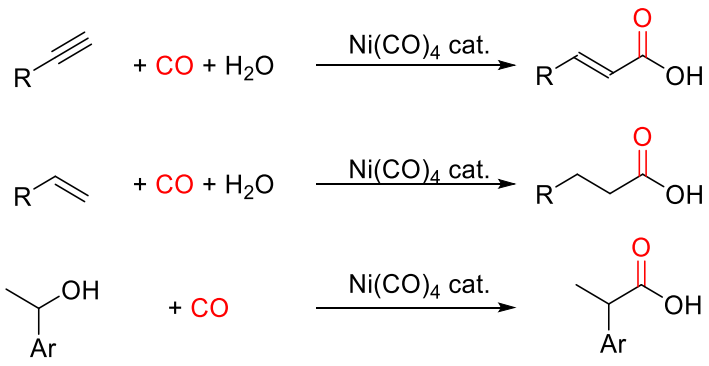

Scheme 1.4. Nickel Catalyzed Carbonylation of Alkynes, Alkenes and Alcohols.

It was not until 1954 when Yamamoto and Sato reported the first nickel catalyzed carbonylation of aryl halides. In this work, 1 mol% of nickel(II) iodide was found to catalyze the carbonylation of aryl-iodides and –chlorides into carboxylic acids at very high temperatures and pressures (250-300 °C, 250 atm CO).[12] The use of iodobenzene resulted in the quantitative formation of benzoic acid, whereas chlorobenzene led to diminished yields.

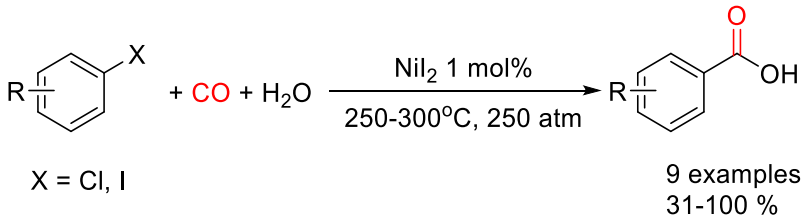

Scheme 1.5. Nickel Catalyzed Hydroxycarbonylation of Aryl Halides.

Several mechanistic studies on the $Ni(CO)_4$ catalyzed carbonylation of aryl halides were conducted by Mizoroki group between 1967 - 1971 (Scheme 1.6a).[13] The carbonylation of 1-bromonaphtalene or bromobenzene were used as the model system in this work. Kinetic studies show that rate of catalysis is dependent on concentration of aryl bromide, water and $Ni(CO)_4$ and

inversely related to CO pressure (Scheme 1.6b). This was rationalized by an initial, disfavored displacement of CO from $Ni(CO)_4$ to form $Ni(CO)_3$ for the rate determining oxidative addition of the aryl bromide. In this scenario, the oxidative addition of aryl halide to $Ni(CO)_3$ is in competition with recombination with CO to form $Ni(CO)_4$. As the regeneration of $Ni(CO)_4$ is rapid (especially at the high CO pressures used to drive this reaction), and $Ni(CO)_3$ is an electron deficient Ni(0) complex that disfavours oxidative addition, this can create a significant barrier to the formation of the aryl halide oxidative addition product. Interestingly the kinetics under lower pressure (below 150 atm) are much different: rate $\propto$ $[Ni(CO)_4][KOAc]$. This was explained by the slow regeneration of $Ni(CO)_4$ at the end of catalytic cycle from $Ni(CO)_2(H)Br$.

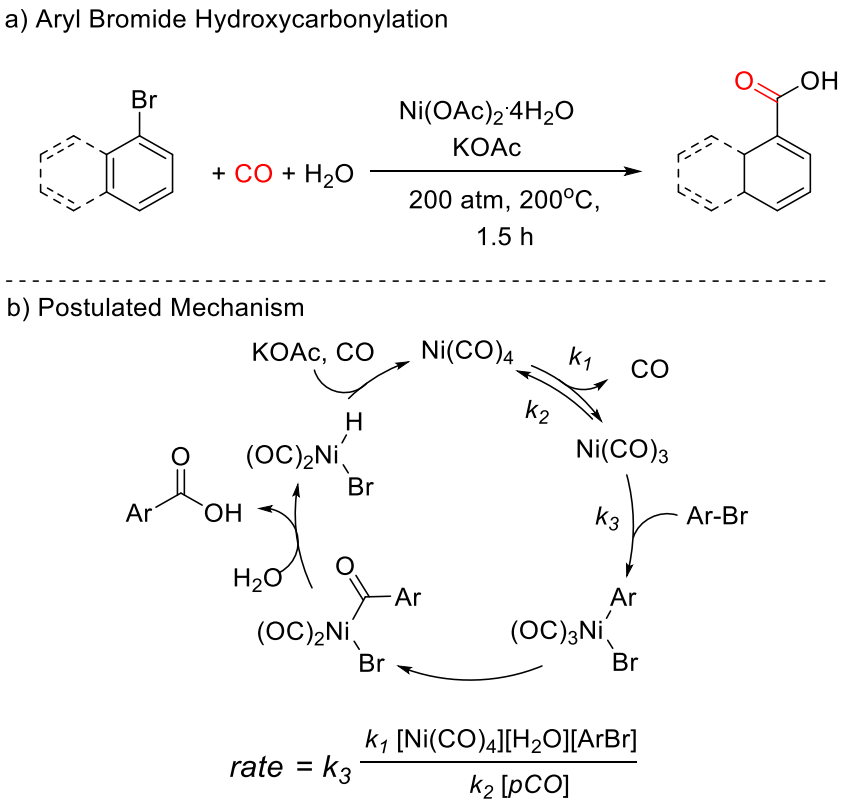

Scheme 1.6. Model System for Nickel Catalyzed Hydroxycarbonylation of Aryl Halides.

Cassar and Foa demonstrated that nickel catalyzed carbonylations can be performed at just 1 atmosphere of CO by using highly polar solvents and $Ca(OH)_2$ base.[14] Kinetic studies of

this reaction indicated that the reaction is autocatalytic, where the buildup of chloride and bromide ions throughout the course of the reaction allows the generation of the active nickel catalyst - $[Ni(CO)_3X]^-$ (X = Cl, Br). Polar solvents stabilize this ionic intermediate in the reaction mixture. Consistent with this postulate, if stoichiometric amounts of chloride salt are added to the reaction mixture, the reaction is no longer autocatalytic and instead displays simple first order kinetics in aryl halide concentration. Based on Hammett plots and kinetic studies, it was suggested that oxidative addition is the rate determining step in this system.

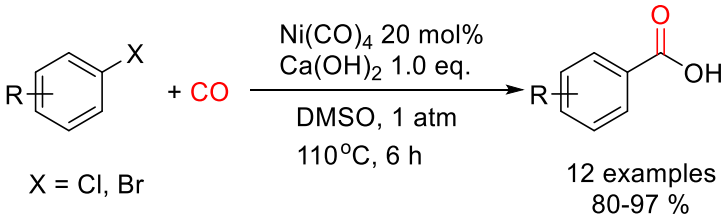

Scheme 1.7. Nickel Catalyzed Hydroxycarbonylation of Aryl Halides.

The Alper group developed a more mild aryl iodide carbonylation using a commercially available $Ni(CN)_2$ catalyst (90°C, 1 atm CO, Scheme 1.8).[15] The reaction was shown to afford carboxylic acids with a range of aryl iodides, and even 2-thiophenyliodide. It is believed that $[Ni(CO)_3CN]^-$ is generated *in situ* in this system, and upon CO dissociation forms a more electron rich nickel complex, $Ni(CO)_2CN^-$ (relative to $Ni(CO)_3$), for oxidative addition of the aryl iodide. Interestingly the presence of tetraalkylammonium bromide is critical for this transformation, and no carbonylation was observed in the absence of the organic salt. The authors suggest that the role of this phase-transfer catalyst could be the dissolution of $Ni(CN)_2$ in the toluene solvent, as well as providing a solvent cage for a radical pair that may be generated upon a single electron transfer mechanism from the aryl iodide.

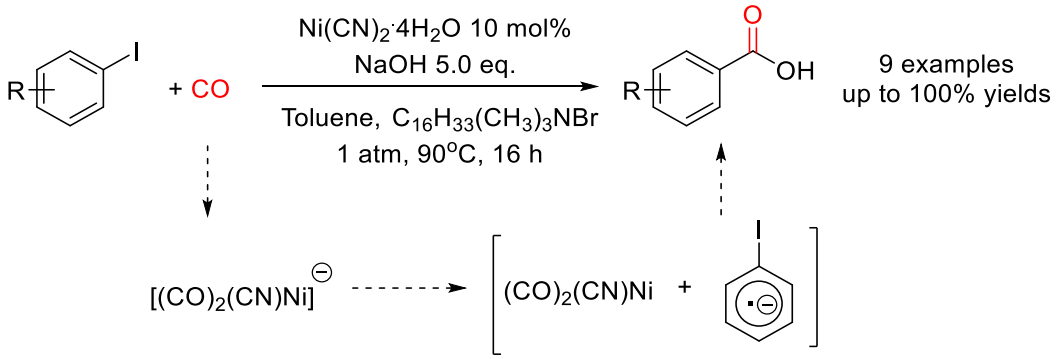

Scheme 1.8. Nickel Catalyzed Hydroxycarbonylation of Aryl Halides Using a Tetraalkylammonium Bromide.

Unlike studies with palladium catalysts (*vide infra*), strong donor ligands such as phosphines are not generally employed in nickel catalyzed carbonylation reactions. This is presumably the result of their formation of even more stable (phosphine)nickel-carbonyl complexes that cannot readily lose CO to enter the catalytic cycle, e.g., a disfavoured equilibrium of $(R_3P)Ni(CO)_3 \leftrightarrows (R_3P)Ni(CO)_2 + CO$. However, Giannoccaro and coworkers showed that $Ni(CO)_2(PPh_3)_2$ can catalyze the aminocarbonylation of aryl iodides.[16] A range of primary anilines as well as secondary aryl, alkyl-amines were viable reaction partners affording the amides in moderate to good yields. This reaction does require high temperatures and CO pressures.

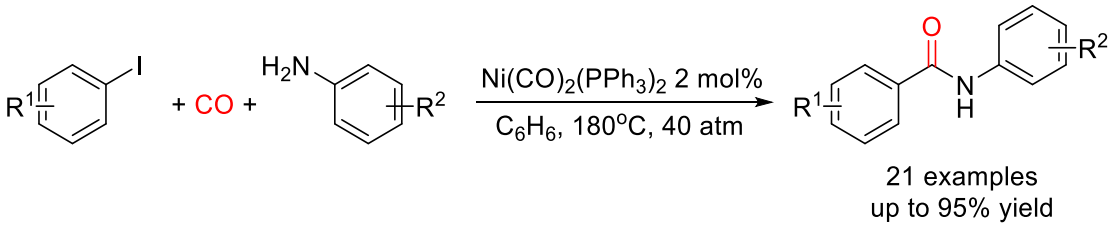

Scheme 1.9. Nickel Catalyzed Aminocarbonylation of Aryl Halides.

Nickel catalyzed carbonylations have also been applied to more elaborate products. For example, Prichard observed in 1956 an unusual carbonylation of aryl halides in the presence of

$Ni(CO)_4$ catalyst and Na_2CO_3 to form phthalic anhydrides (Scheme 1.10).[17] In this system, aryl halides are postulated to be initially converted to benzoic anhydrides, presumably via the initial generation of benzoic acid, which can act as the nucleophile in a second carbonylation. Interestingly, however, the benzoic anhydride is found to undergo a rearrangement under the reaction conditions to phthalic anhydrides and arenes. While the exact mechanism of the latter step remains unclear, control experiments suggest that $Ni(CO)_4$ and CO are required to convert benzoic anhydride to phthalic anhydride. This may represent an early example of chelation assisted arene C-H functionalization via the mechanism shown below.

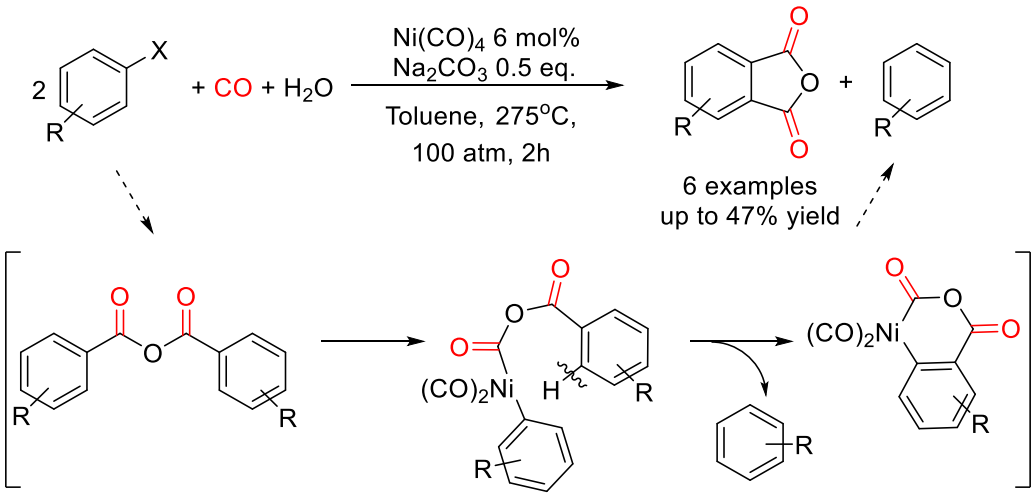

Scheme 1.10. Nickel Catalyzed Carbonylative Synthesis of Phthalic anhydrides.

1.2.3. Palladium Catalyzed Carbonylation Reactions

While nickel catalysts have been known for some time to mediate aryl halide carbonylations, the pressing condition required for the reaction, moderate scope, and toxicity of $Ni(CO)_4$, have limited their utility. A significant advance in the field was the report by Heck in 1974 using palladium complexes to catalyze aryl halide carbonylation.[5a] In this study, it was found that aryl-iodides and -bromides could undergo carbonylative coupling with *n*-butanol with 1.5 mol% of $Pd(OAc)_2$ or $PdBr_2(PPh_3)_2$ catalyst to form esters (Scheme 1.11a-b). Importantly, and unlike many nickel catalyzed carbonylations, this transformation proceeds at relatively mild temperatures (100 °C) and pressures (1-2 atm CO). Aryl halides bearing electron withdrawing

groups increased the reaction rates, while electron donating groups slowed the reaction, suggesting that oxidative addition was at least partially involved in the rate determining step.[7b] In addition to aryl iodides, a range of vinyl iodides and bromides were found to be similarly converted to the corresponding esters in goods yields. However, this reaction forms a mixture of cis and trans products. In a follow-up report, Heck described analogous aminocarbonylation reaction with aniline derivatives as the nucleophile (Scheme 1.11c-d).[5b]

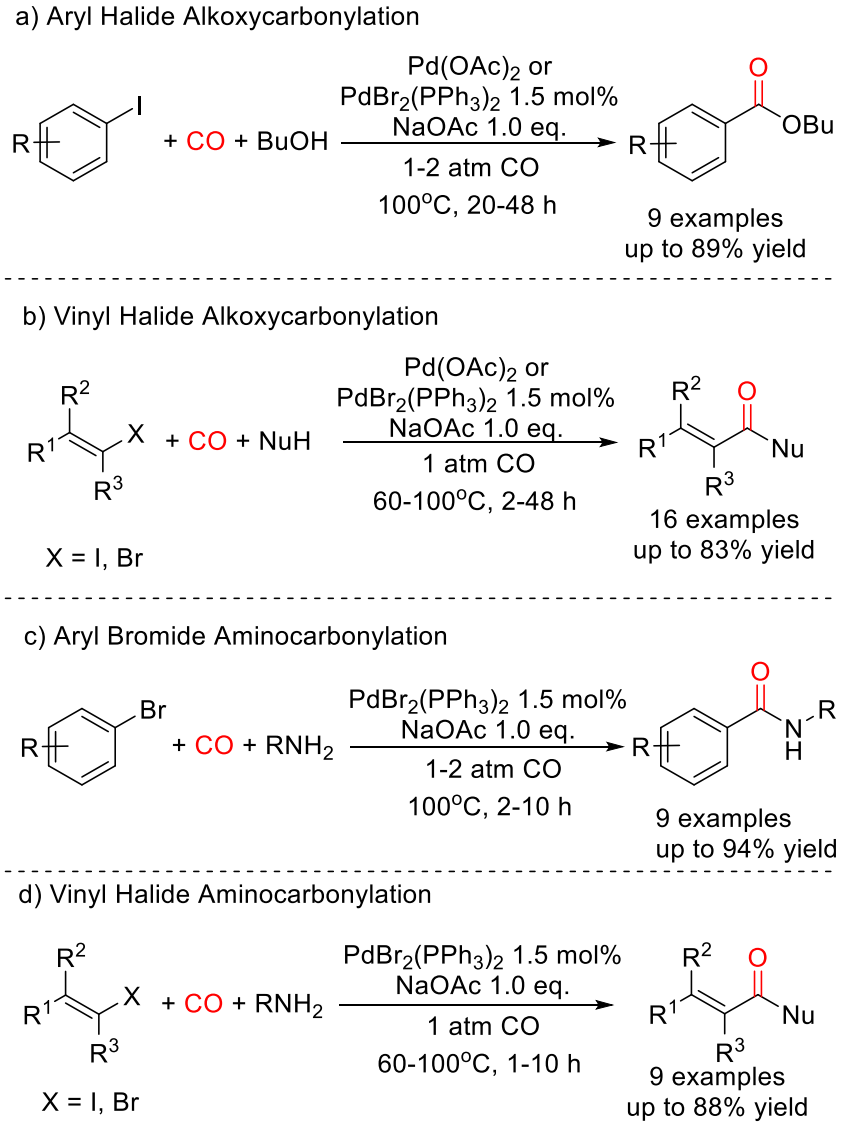

Scheme 1.11. Palladium Catalyzed Amino and Alkoxy-Carbonylation.

Since this pioneering work by Heck, there has been significant effort directed toward developing more active catalysts for carbonylations. Highlights of these are provided below.[18] For example, while the carbonylation of aryl iodides can be achieved by using simple, *in situ* reduced palladium salts without added ligands (e.g. $Pd(OAc)_2$), the activation of stronger bonds often requires the incorporation of donor ligands onto palladium. This latter presumably creates a more electron rich Pd(0) for oxidative addition. As first noted by Heck, the addition of 2 equivalents of PPh_3 to a $Pd(OAc)_2$ catalyst allows for the carbonylation of aryl bromides at synthetically useful rates and in good yields (Scheme 1.11c).

More recently, a range of ligands have been developed and explored to overcome the issues with substrate activation or catalyst degradation.[19] Representative examples from these studies are highlighted below (Scheme 1.12).[†]

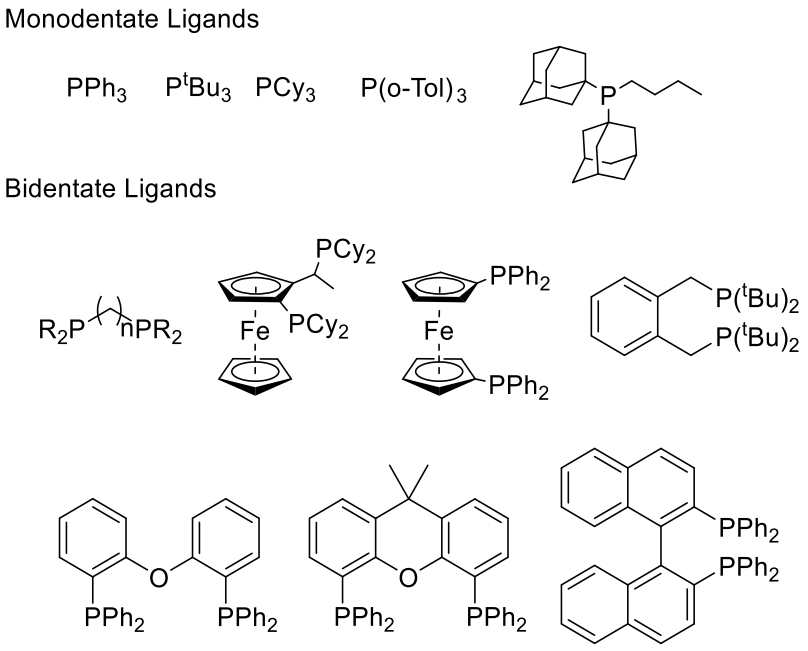

Scheme 1.12. Ligands in Palladium Catalyzed Carbonylation Reactions.

Notable progress with PPh_3 as a ligand was demonstrated by the Beller group. Rigorous optimization of reaction parameters, such as temperature, CO pressure, the catalyst precursor,

[†] For examples of phosphines not highlighted in this chapter see ref. 18.

and the Pd/ligand ratio allowed the authors to develop a catalytic system for alkoxycarbonylation of 4-bromoacetophenone with turnover numbers up to 7000 (Scheme 1.13a).[20] It was found that 80-fold excess of the ligand was necessary to prevent the palladium catalyst from forming colloids and retain its activity. Increasing the catalyst loading to 0.1 mol% allowed for near quantitative conversion to the corresponding butyl esters. Using a similar palladium catalyst, Chaudhari and co-workers described a highly efficient palladium catalyzed carbonylation-polycondensation protocol for the synthesis of polyamidoesters from *para*-diiodoarenes and amine-substituted phenols (Scheme 1.13b).[21]

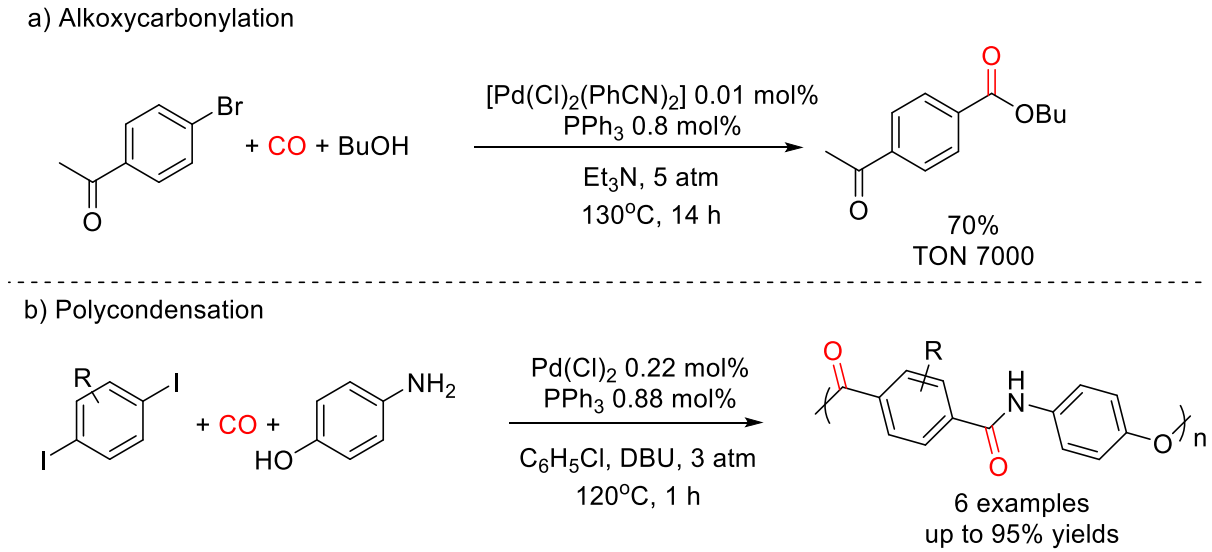

Scheme 1.13. Developments in Palladium Catalyst Activity using PPh_3 as a Ligand.

Beller and co-workers have also developed a range of palladium catalyzed carbonylation reactions based on a new phosphine ligand – di(1-adamantyl)-*n*-butyl-phosphine ($BuAd_2P$). This ligand is more electron donating and sterically encumbered than PPh_3, and presumably can generate a more electron rich Pd(0) catalyst. In addition, its the steric encumbrance may more easily generate an empty coordination site on palladium. These features would favour the formation of an electron rich, unsaturated Pd(0) for oxidative addition of the R-X substrate. The first example on the use of this ligand in palladium catalyzed carbonylations was in the synthesis of aromatic aldehydes. Using only 0.05-0.33 mol% of a palladium catalyst and synthesis gas, a range of aryl and heteroaryl bromides could be converted to the corresponding aldehydes in good

to excellent yields (Scheme 1.14a).[22] The stability of the ligand allows the reaction to be set up in air without any loss of catalyst activity. The Pd/$BuAd_2P$ catalyst system can also be used in alkoxycarbonylations with *n*-butanol to form esters with nearly quantitative yields (Scheme 1.14b),[23] as well as aminocarbonylations to generate amides. The latter studies demonstrate that not only are simple amines viable substrates, but also more challenging nucleophiles, such as secondary amines, pyrroles, or *tert*-butylamine. Primary amides, which are important intermediates in organic synthesis, as well as phenoxyesters, can also be accessed via a similar protocols, both affording the products in good yields (Scheme 1.14c-d).[24] In addition to its use in carbonylation reactions, $BuAd_2P$ has seen application in a range of cross-coupling reactions.[25]

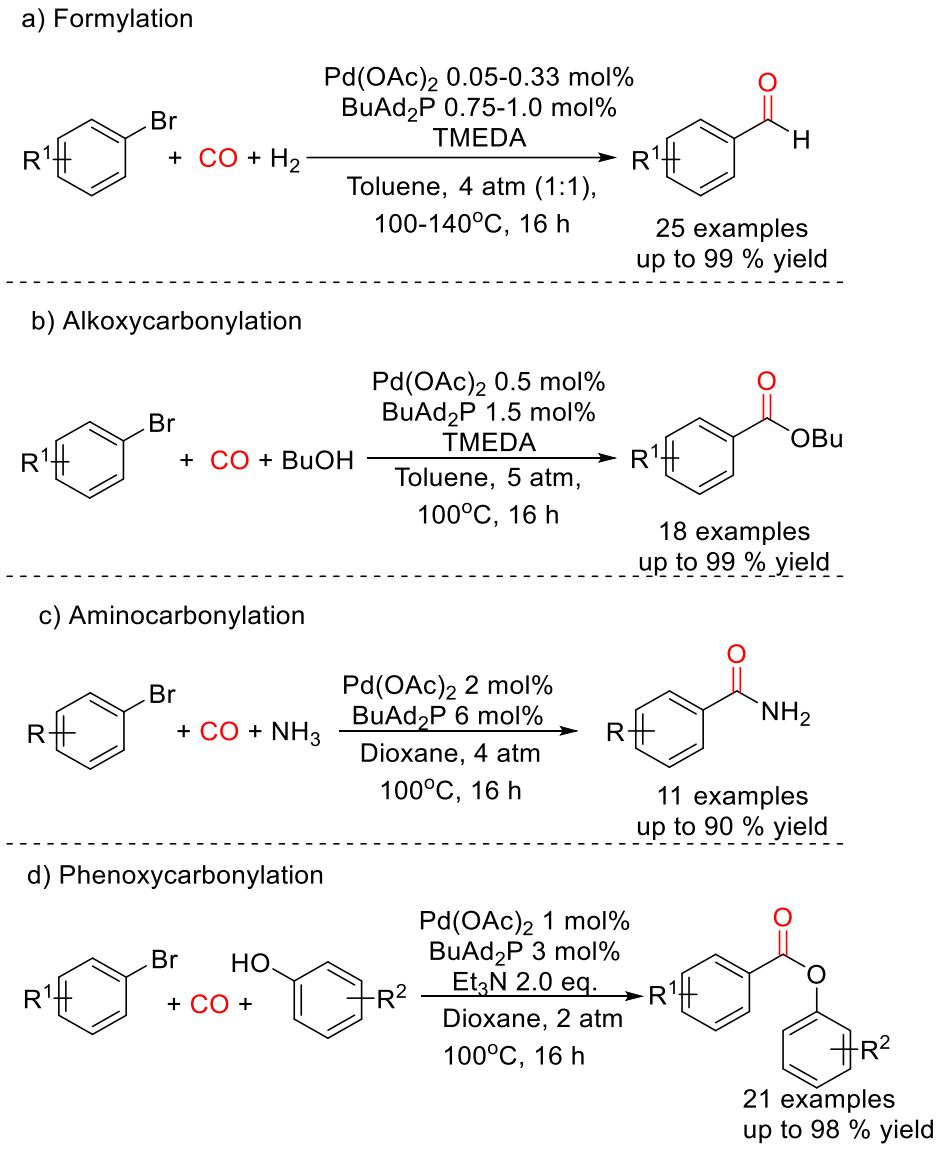

Scheme 1.14. Palladium Catalyzed Formylation and Alkoxycarbonylation of Aryl Bromides.

In a collaboration between the Stradiotto and Beller groups, it was shown that acetone and acetophenone derivatives can behave as carbon nucleophiles in carbonylations with aryl iodides to form a range of 1,3-diketones (Scheme 1.15a).[26] In this system, *in situ* deprotonation of the acidic α-C-H bond can form an enolate that can couple with the palladium-aroyl intermediate. To highlight the utility of this methodology, a one pot, two step procedure was

developed to synthesize pyrazoles, via the subsequent condensation of the carbonylated product with hydrazines (See section 1.3.2). In an another collaborative work between these groups, vinyl benzoates were synthesized via a carbonylative coupling between more sterically encumbered enolizable ketones and aryl halides (Scheme 1.15b).[27]

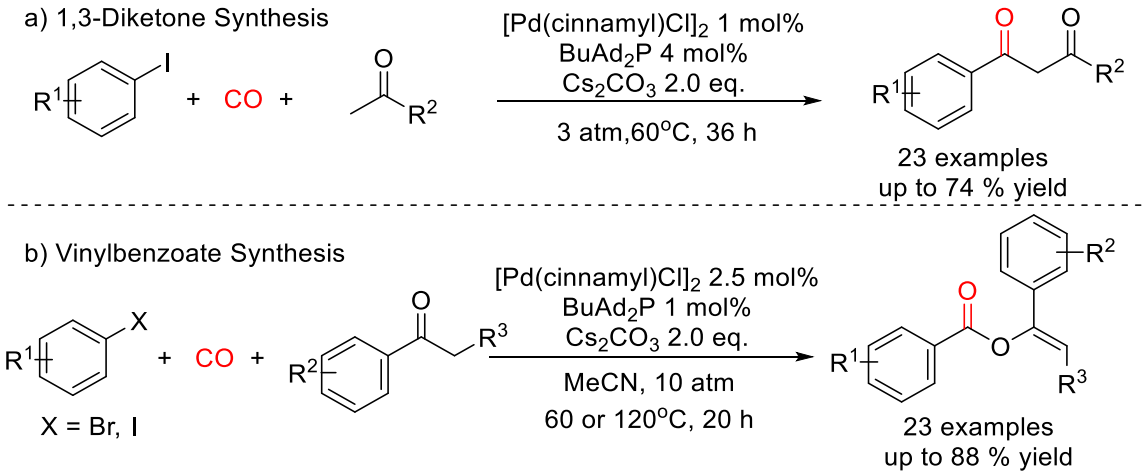

Scheme 1.15. $BuAd_2P$ Ligand in Palladium Catalyzed Carbonylation with Ketones.

Beller and coworkers further extended the use of $BuAd_2P$ ligand to the palladium catalyzed carbonylative synthesis of di(hetero)aryl ketones (Scheme 1.16a).[28-30] In these systems, it was found that CO pressure could influence product formation, and sufficiently high pressure is required to supress the competitive non-carbonylative Suzuki reaction. This protocol was extended to a one pot, two step double carbonylative synthesis of the non-steroid anti-inflammatory drugs Ketoprofen and Suprofen (Scheme 1.16b). In this latter synthesis, the authors found that increasing the CO pressure and adding H_2O/HCl after the carbonylative ketone synthesis led to a Reppe-type carbonylation of the alkene with the same catalyst to afford the desired pharmaceuticals in good yields.

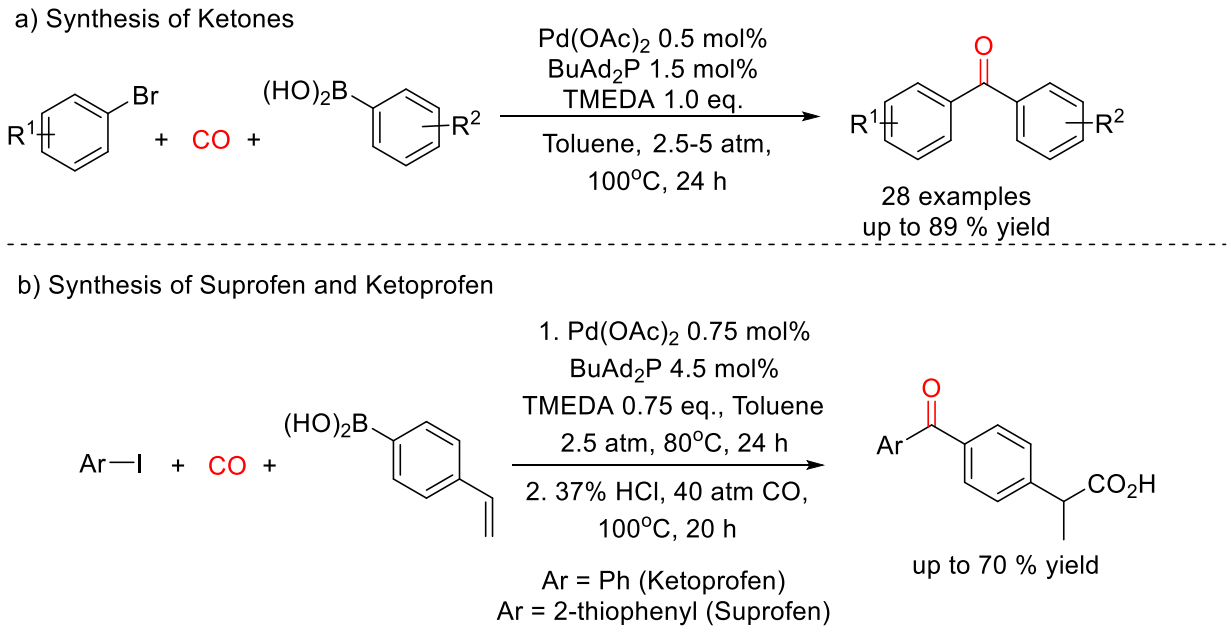

Scheme 1.16. $BuAd_2P$ Ligand in Palladium Catalyzed Carbonylative Suzuki Reactions.

The Skrydstrup lab has also been very active in developing palladium catalyzed carbonylative coupling reactions. These often exploit their dual chamber systems to generate CO from acid chlorides (Scheme 1.17a), where a palladium catalyzed decarbonylation of acid chlorides can be used to afford a controlled amount of CO gas for use in carbonylation reactions in a second chamber, and avoids the need for CO gas.[31] This system has been used in the $BuAd_2P/[Pd(cinnamyl)Cl]_2$ catalyzed carbonylative synthesis of ureas and α,β-unsaturated ketones (Scheme 1.17b-c).[32] The methodology was also used for the ^{13}C isotopic labeling of the carbonyl unit, since it utilizes a nearly equimolar amounts of CO.

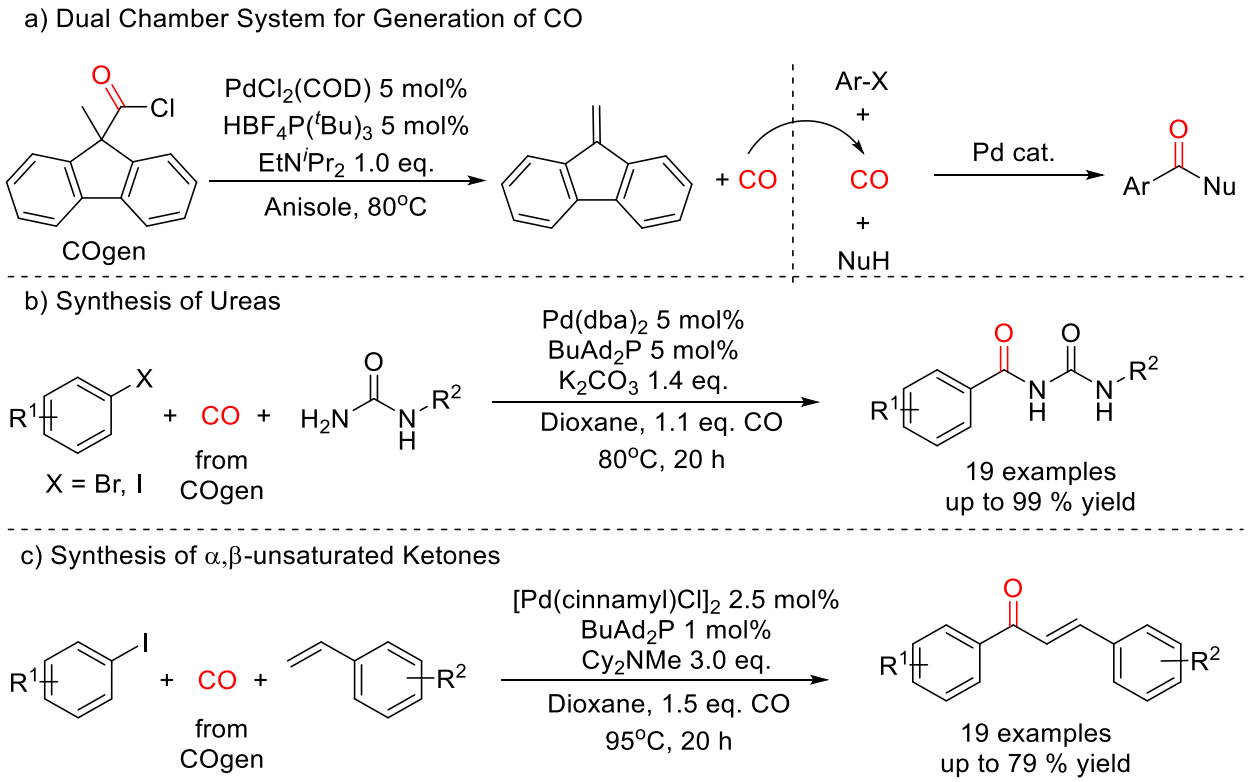

Scheme 1.17. Two Chamber System Generated CO in Palladium Catalyzed Carbonylations.

Aryl- and vinyl-triflates are attractive substrates in transition metal catalyzed reactions, since they can be readily accessed from ketones or phenols by treatment with triflic anhydride. The Cacchi and Ortar research groups developed the first aryl- and enol-triflate carbonylations using PPh_3 as the ligand (Scheme 1.18a-b).[33] While enol-triflate aminocarbonylation proceeded at room temperature and mild CO pressures, the alkoxycarbonylation of aryl triflates required prolonged heating to afford the corresponding esters. Soon after, reports by Dolle and co-workers showed that the use of bidentate ligands (e.g. dppp) led to a *ca.* 500-fold rate enhancement in the palladium catalyzed alkoxycarbonylation of aryl triflates compared to catalysis with PPh_3 (Scheme 1.18c).[34] Similarly, Gerlach and co-workers reported the synthesis of tetralone carboxylic acid esters using a $Pd(OAc)_2$/dppp catalytic system under mild conditions (2-5 h, 70°C).[35]

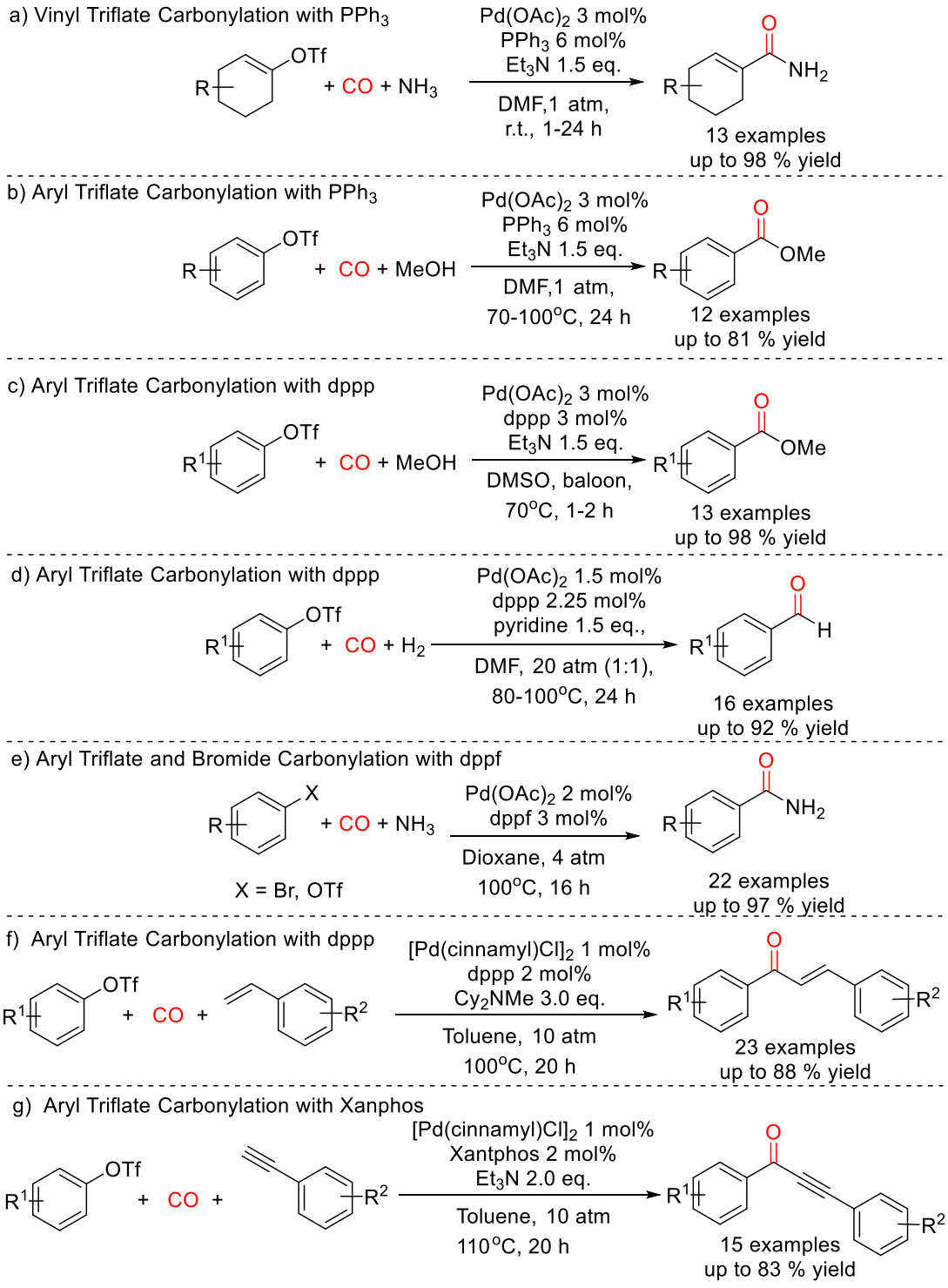

Scheme 1.18. Bidentate Ligands in Palladium Catalyzed Carbonylations of Aryl Triflates.

The utility of these chelate ligands is presumably related to their ability to tightly associate two phosphines to palladium, which could inhibit multiple CO associations to Pd(0) and generate a more electron rich palladium center for the oxidative addition step.

Beller and co-workers reported that a similar chelating phosphine ligand can allow the mild formylation of aromatic triflates using synthesis gas (Scheme 1.18d),[36] while the dppf ligand can be used in the aminocarbonylation of aryl triflates to form amides (Scheme 1.18e).[37] In the latter study, it was shown that dppf created a much more active catalyst than the $BuAd_2P$ ligand, and led to catalyst turnover numbers up to 1100. Alkenes have also been used as coupling partners in a carbonylative Heck reaction of aryl triflates (Scheme 1.18f).[38] While many substrates proceed in good yields, reactions with bulky aryl triflates lead to the competitive direct Heck coupling without CO insertion. Alternatively, the carbonylative coupling of aryl triflates and terminal alkynes can be used to form alkynones (Scheme 1.18g).[39]

A breakthrough in aryl chloride carbonylation came with the use of the chelating, bulky d^ippp ligand by the Milstein group (Scheme 1.19).[40] The ability of these systems to activate the robust Ar-Cl bond was attributed to the high donor ability of the electron rich phosphine, as well as the inhibition of CO coordination due to the steric bulk of the ligand, both of which would favour oxidative addition to Pd(0). A range of alcohols, water, as well as secondary amines were employed as coupling partners in this transformation. In a follow up report, the group extended the use of d^ippp/$Pd(OAc)_2$ towards the synthesis of aromatic aldehydes, using sodium formate as the reducing agent.[41] This catalytic system was also applied in the synthesis of polyamides from aromatic dichlorides and diamines.[42]

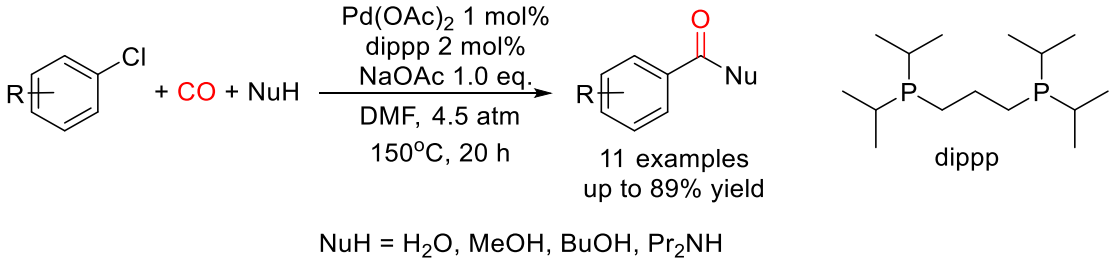

Scheme 1.19. Aryl-Chloride Amino and Alkoxy Carbonylation.

In 2001, Beller and coworkers reported the carbonylation of activated and unactivated aryl chlorides at simply atmospheric pressure of CO using the large mondodentate ligand Josiphos (Scheme 1.20a).[43] A range O- and N- nucleophiles could serve as coupling partners, and afforded the corresponding carbonylated products in good yields. Unfortunately, an excess of ligand relative to palladium was necessary to inhibit palladium colloid formation. Turnover numbers up to 1600 were observed for the coupling of chlorobenzene and *n*-butanol.

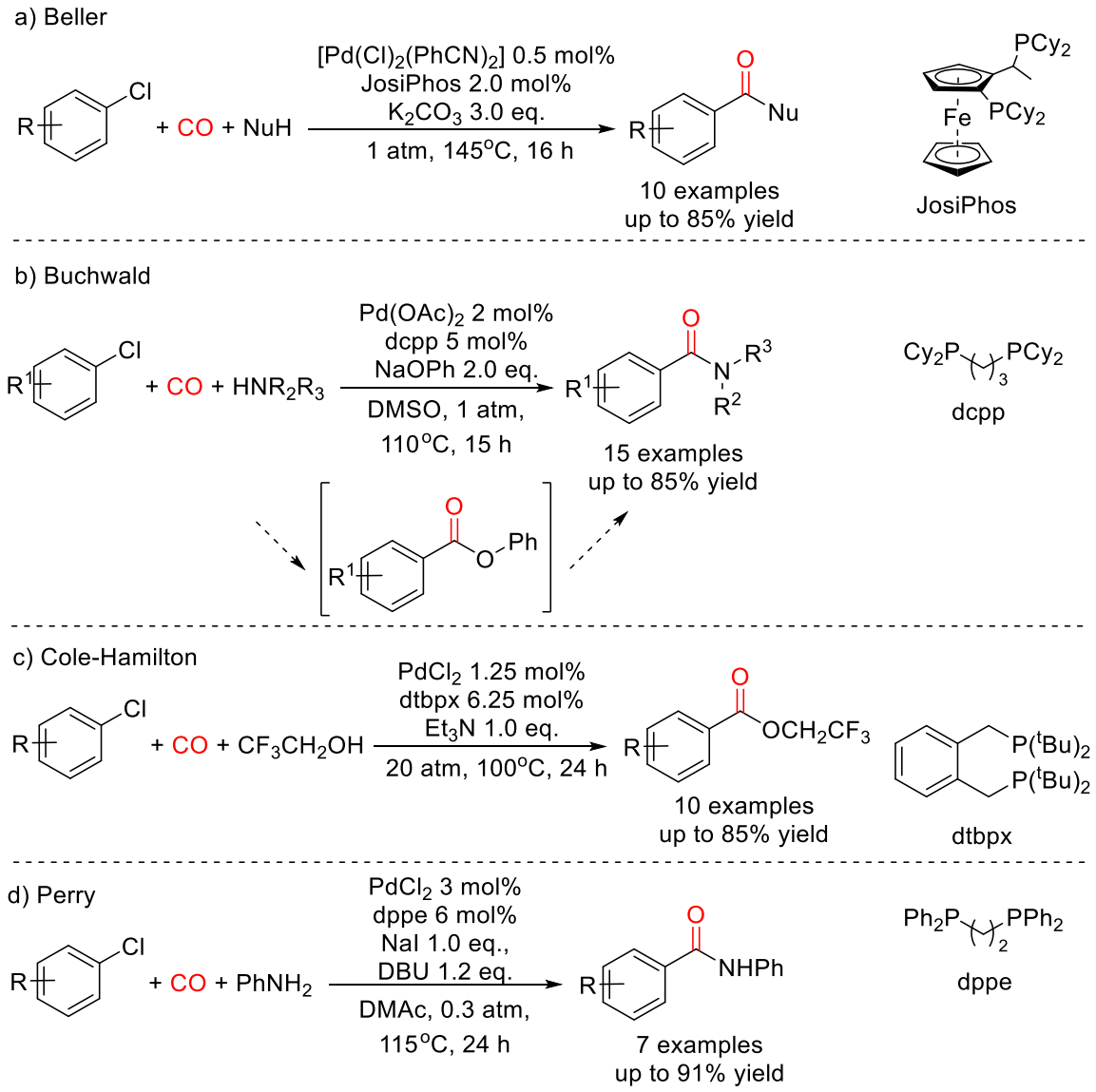

Scheme 1.20. Aryl-Chloride Carbonylation with Alcohols and Amines.

In 2007, Buchwald and coworkers developed a general approach to the aminocarbonylation of aryl chlorides using the chelating dppp ligand (Scheme 1.20b).[44] Primary, α-branched primary, cyclic secondary, and aryl amines afforded the amides in good yields. The relatively mild reaction conditions were found to be the result of the sodium phenoxide used in the reaction, which led to the rapid generation of the corresponding phenoxy ester. This provided an alternative to the more common requirement of nucleophile association to palladium for reductive elimination, and can undergo subsequent coupling with a range of amines to form the observed amide products.

Recently, Cole-Hamilton and co-workers have used the 1,2-bis(di-*tert*-butylphoshanyl)-*ortho*-xylene (dtbpx) ligand for the carbonylation of aryl chlorides under similar conditions (Scheme 1.20c).[45] In related work, Perry and coworkers developed a sodium iodide promoted aminocarbonylation of activated aryl chlorides under low CO pressures (Scheme 1.20d).[46] The authors suggest that an anionic palladium(0) complex of the form $[L_nPd(0)I]^-$ is formed in the catalytic system, and that these reactive species enhance the oxidative addition rate with aryl chlorides.

Chloropyridines, while of high industrial interest, have been shown to be one of the most challenging substrates in carbonylation chemistry, presumably due to the ligating nature of pyridine. Early examples of the carbonylation of these substrates relied on extremely high pressures and temperatures.[47] In 2001, Beller and co-workers developed butoxycarbonylation of 2- and 3-chloropyridines using similar dppf and dppb ligands. By varying the Pd/P ratio, turnover numbers up to 13000 were obtained for carbonylation of heterocyclic aryl chlorides (Scheme 1.21a).[48] In a related report Albaneze-Walker has shown that $(BINAP)PdCl_2$ could mediate the carbonylation of chloropyridines at low pressures and temperatures.[49] These bidentate ligand systems have been exploited in a range of subsequent studies with chloropyridines, including the development of compound libraries,[50] selective carbonylation (Scheme 1.21c),[6a] and the industrial synthesis of Lazabemide hydrochloride, a monoamine oxidase B inhibitor, by Hoffmann-La Roche (Scheme 1.21b).[6b]

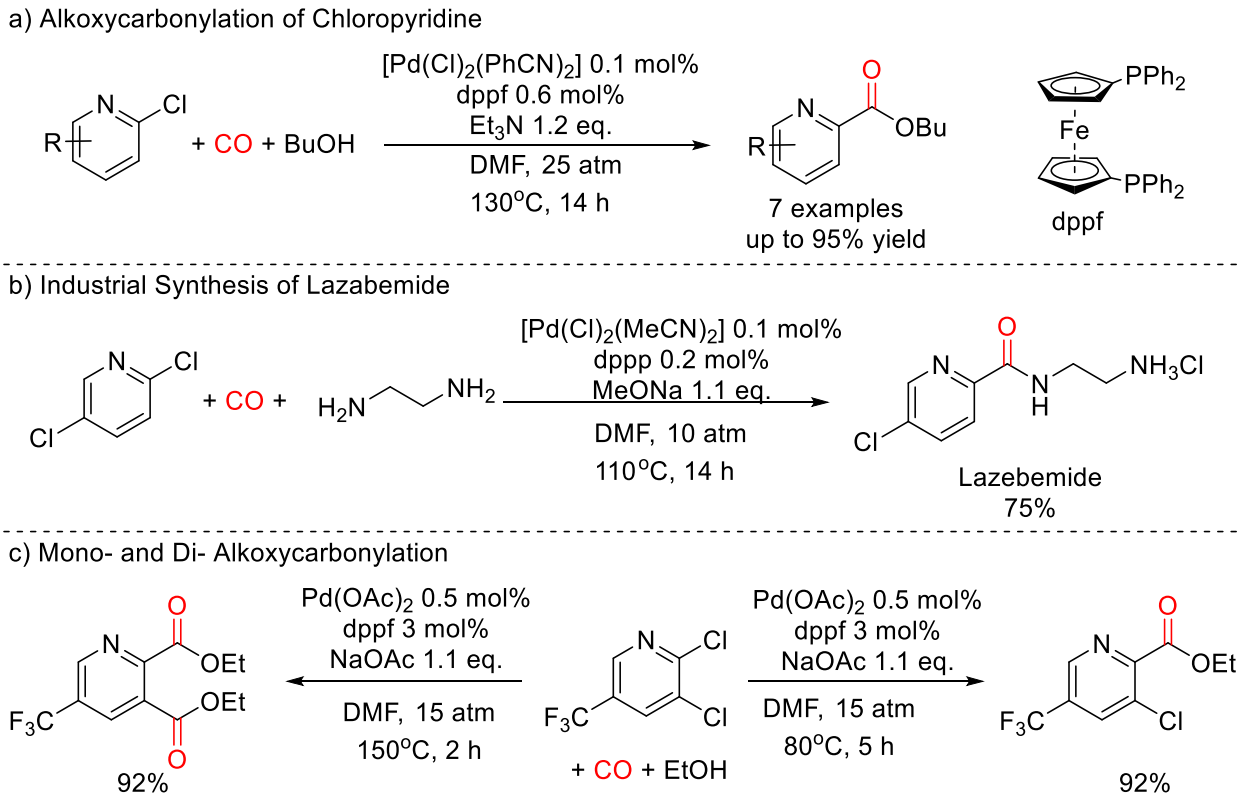

Scheme 1.21. Palladium Catalyzed Carbonylation of Pyridil-Chloride.

Vinyl chlorides are also viable substrates in carbonylation reactions. For example, Roulland and co-workers have developed a fully chemo- and stereoselective carbonylation of 1,1-dichloro-1-alkenes and various alcohols (Scheme 1.22).[51] In these systems, the large bite angle of DpePhos was found to be instrumental for the chemoselectivity between two chlorides, and the sterically less hindered C-Cl bond undergoes selective carbonylation.

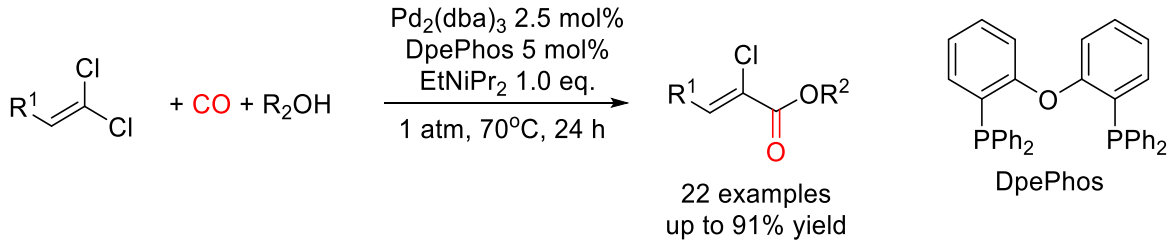

Scheme 1.22. Palladium Catalyzed Carbonylation of 1,1-dichloroalkenes.

1.3. Palladium Catalyzed Multicomponent Carbonylation Reactions

In addition to simple carbonylation reactions, palladium catalyzed carbonylations have also been instrumental in the design of multicomponent reactions. Multicomponent coupling reactions (MCRs) couple three or more reagents together at once, and can therefore offer useful alternatives to more classical multistep syntheses. The spontaneous assembly of several substrates in MCRs usually requires some element of control, such that these compounds not only react, but do so selectively, within the complex mixture. For traditional non-catalytic MCRs, this reactivity and selectivity are often incorporated into each component.[52] While effective, these substrates can themselves require an initial synthesis, and detract from the overall efficiency of MCRs. In contrast, transition metal catalyzed MCRs can employ the reactivity of the catalyst to activate simple, often unreactive substrates towards reactions.[53] In addition, the metal catalyst, rather than substrates themselves, can be used to control selectivity, via the order of steps that occur on the metal center. This can provide an attractive synthetic method to convert several simple and readily available building blocks directly into products in efficient, one pot transformations.

Most palladium catalyzed carbonylation reactions are formally MCRs involving three components. However, since CO is a non-diversifiable unit, discussions of carbonylative MCRs usually involve reactions of four components, or where three or more bonds are assembled during the transformation.[54] This section will highlight palladium catalyzed carbonylative MCRs of this form, and in particular those that access heterocycles from substrates that are both readily available and easily tuned, as these can provide methods to readily assemble molecular complexity.

1.3.1. Multicomponent Cyclocarbonylations with ortho-Substituted Aryl Halides

A broad range of palladium catalyzed multicomponent cyclocarbonylation reactions have been developed to generate fused heterocyclic products. These typically involve the carbonylative coupling of aryl halides bearing a nucleophile in the *ortho* position with an unsaturated A=B substrate (Scheme 1.23). This approach can offer routes to a number of heterocycles such as flavones, chromones, quinolones and others.

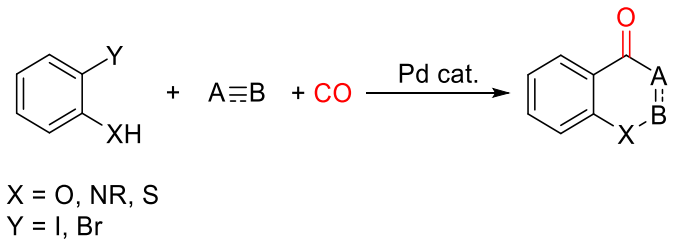

Scheme 1.23. Palladium Catalyzed Cyclocarbonylation of Aryl Halides Bearing *ortho*-Nucleophiles.

An early approach to this chemistry was demonstrated by Kalinin and coworkers. In this, the palladium catalyzed reaction of *ortho*-iodophenols and terminal alkynes under carbonylative conditions led to the generation of flavones and chromones (Scheme 1.24a).[55] This reaction is believed to proceed via an initial carbonylative Sonogoshira reaction, followed by a spontaneous, intramolecular Michael addition of the phenol oxygen onto the alkyne. The reaction proceeds at low catalyst loadings and has been shown to tolerate aryl, heteroaryl and aliphatic terminal alkynes. In a later report Alper demonstrated that this reaction could proceed without phosphine ligands and at low pressures of CO (1 atm) in a phosphonium salt ionic liquid (Scheme 1.24b).[56] This platform can also be applied to nitrogen-heterocycle synthesis via the use *ortho*-halogenated anilines, as shown by Kalinin and Torii (Scheme 1.24c).[57] An interesting four-component variant of this reaction was described by Wu to access thiochromones (Scheme 1.24d).[58] The one pot reaction employed a wax reagent capsule containing Na_2S which prevented the catalyst poisoning during the catalytic generation of the alkynone intermediate. Subsequent release of Na_2S and raising the reaction temperature triggered the cyclization.

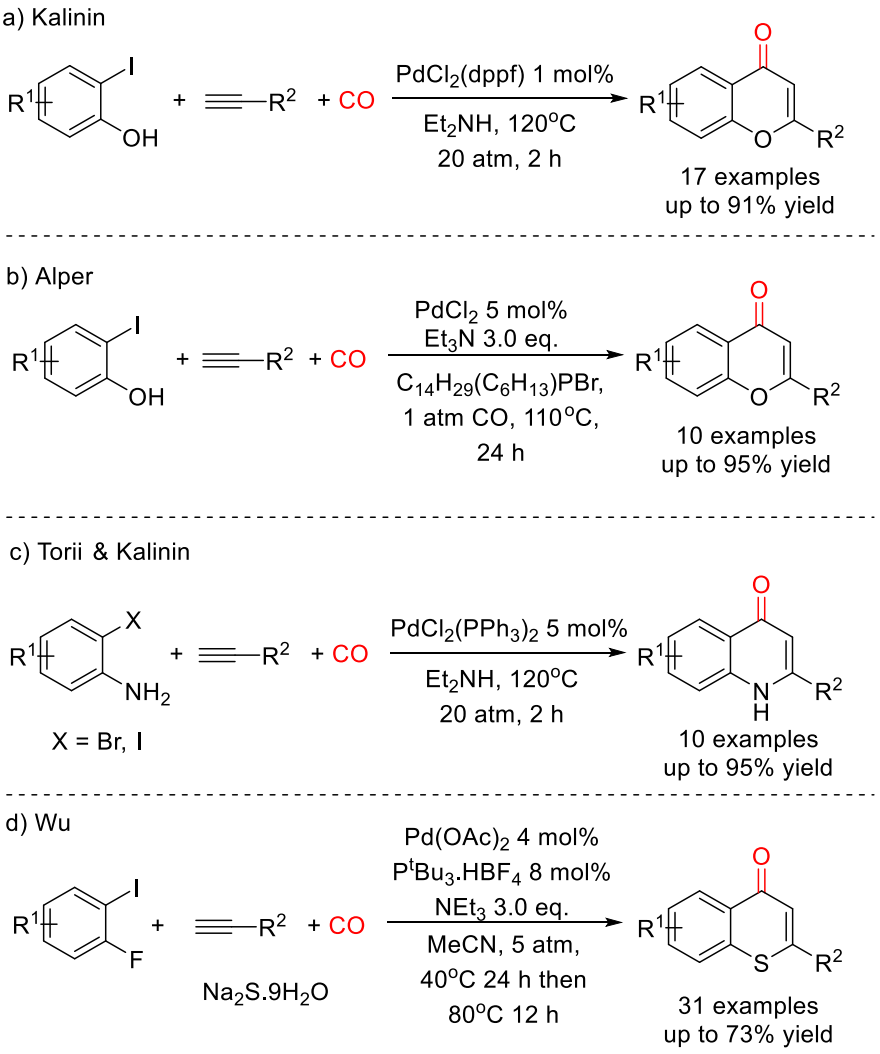

Scheme 1.24. Palladium Catalyzed Multicomponent Cyclocarbonylations with Terminal Alkynes.

A diverse variety of other A=B unsaturated reagents can be used in this approach. Examples of these include electrophilic substrates such as carbodiimides, isocyanates or acid chlorides (Scheme 1.25).[59] Unlike the carbonylative Sonogashira reactions above, these are believed to involve an initial reaction of the phenol or aniline with the electrophile, followed by palladium catalyzed intramolecular carbonylative ester or amide formation. Cacchi, Marinelli and Beller have each reported that the acid chloride in the latter reaction can be replaced with aryl halides and CO (Scheme 1.26).[60] These reactions are believed to proceed via an initial

aminocarbonylation of the bromobenzene and aniline, followed by cyclocarbonylation. Notably, the selectivity in these systems are driven by the electronics of the aryl halides, where the more electron rich aniline derivatives react presumably more slowly with the palladium catalyst, and therefore can only cyclize with the *in situ* generated amide. Alper extended this approach further to the synthesis of quinazolinones (Scheme 1.27),[61] via the palladium catalyzed cyclocarbonylation of *ortho*-iodoanilines, imidoyl chlorides and CO.

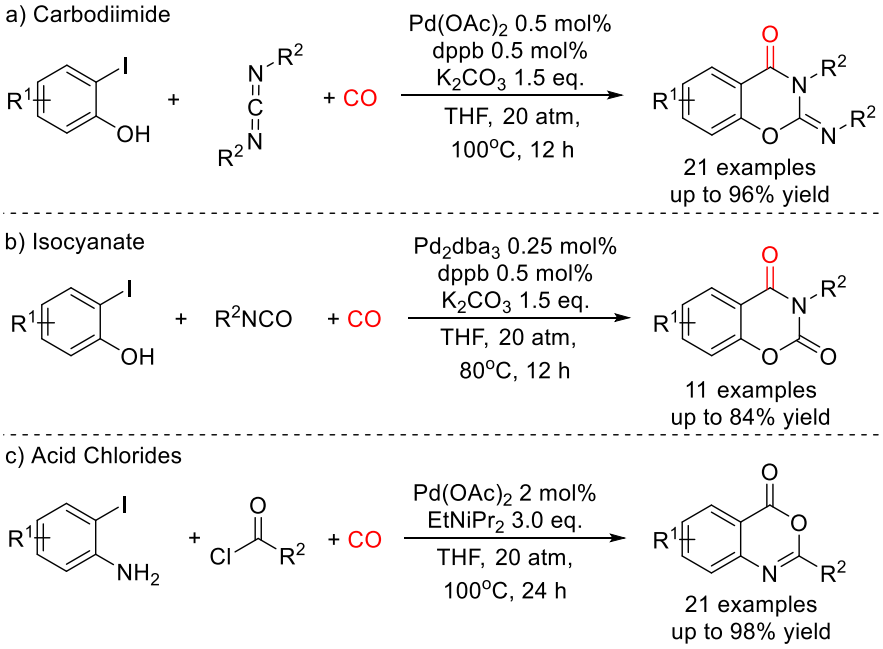

Scheme 1.25. Palladium Catalyzed Cyclocarbonylations with Carbodiimides, Isocyanates and Acid Chlorides.

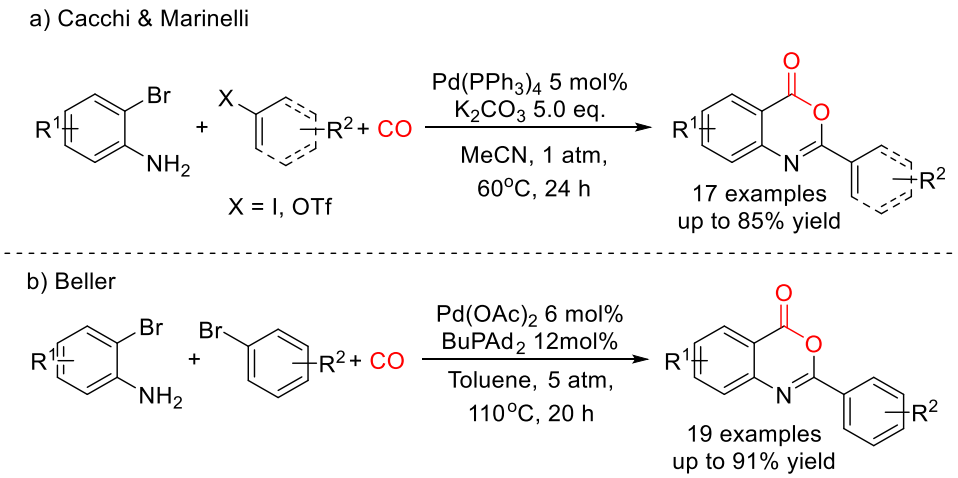

Scheme 1.26. Palladium Catalyzed Cyclocarbonylative Synthesis of Benzoxazinones.

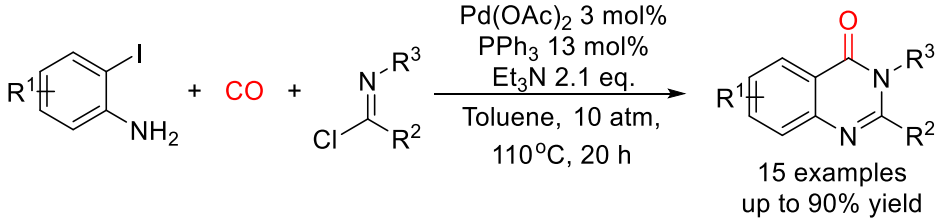

Scheme 1.27. Palladium Catalyzed Cyclocarbonylative Synthesis of Quinazolinones.

Allenes and internal alkynes can also be employed in these carbonylative cyclizations (Scheme 1.28).[62] Such transformations are believed to proceed via the carbonylation of the aryl halide, followed by allene or alkyne insertion and subsequent Pd-mediated C-N bond formation. In contrast to the studies with terminal alkynes, internal alkynes provide access to coumarins and quinolinones.[63]

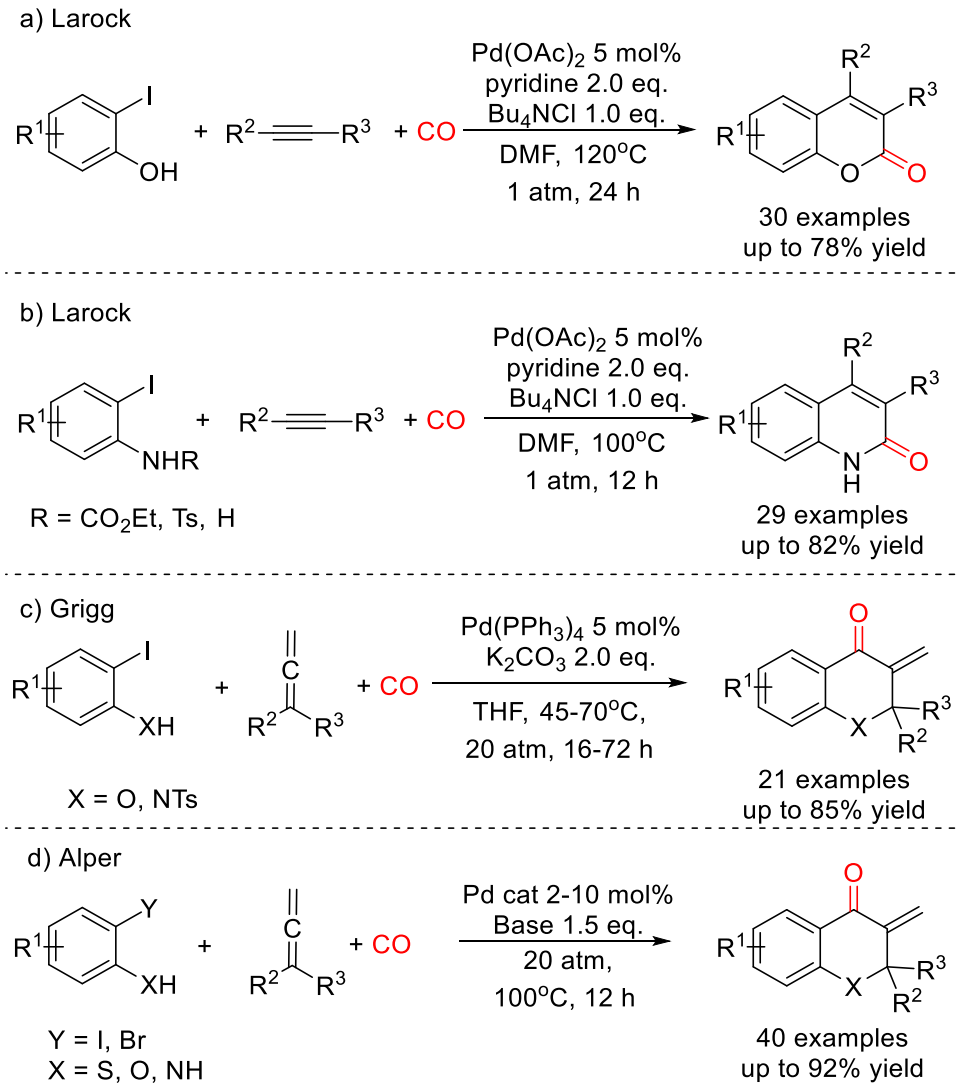

Scheme 1.28. Palladium Catalyzed Cyclocarbonylation with Allenes and Internal Alkynes.

In an alternative approach, Alper has shown that the alkynylation and carbonylative amidation of *ortho*-bromoiodoarenes can occur selectively in a single reaction, where the Sonogashira coupling proceeds more rapidly (and therefore on the C-I bond) than aminocarbonylation. Spontaneous cyclization can allow the build up of 3-methylene isoindolinones from *ortho*-bromoiodobenzene, terminal alkynes, amines and CO (Scheme 1.29a).[64] Grigg and co-workers have reported a four-component approach to isoindolinone derivatives through a sequential Petasis reaction/palladium catalyzed aminocarbonylation

(Scheme 1.29b).[65] The reaction had to be carried out in two steps to minimize the undesired Suzuki reaction between aryl iodide and boronic acid.

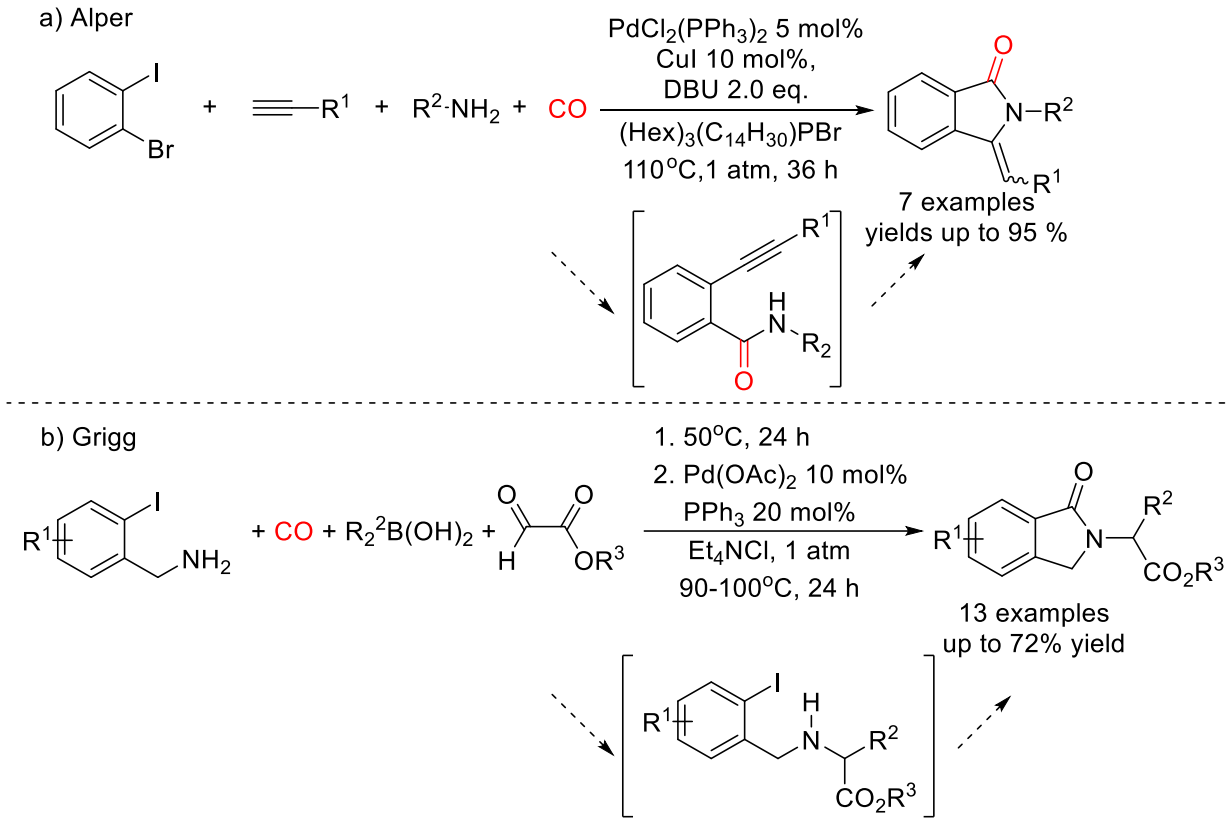

Scheme 1.29. Palladium Catalyzed Multicomponent Synthesis of Isoindolinones.

The Beller and Wu research groups have developed a palladium catalyzed four component carbonylative methodology for the synthesis of quinazolinones (Scheme 1.30).[66] This reaction is believed to proceed via an initial reaction of aniline and orthoformate to afford a formamide intermediate, while the aryl bromide undergoes a palladium catalyzed aminocarbonylation with a primary amine. This product undergoes a spontaneous intramolecular condensation to form the final product.

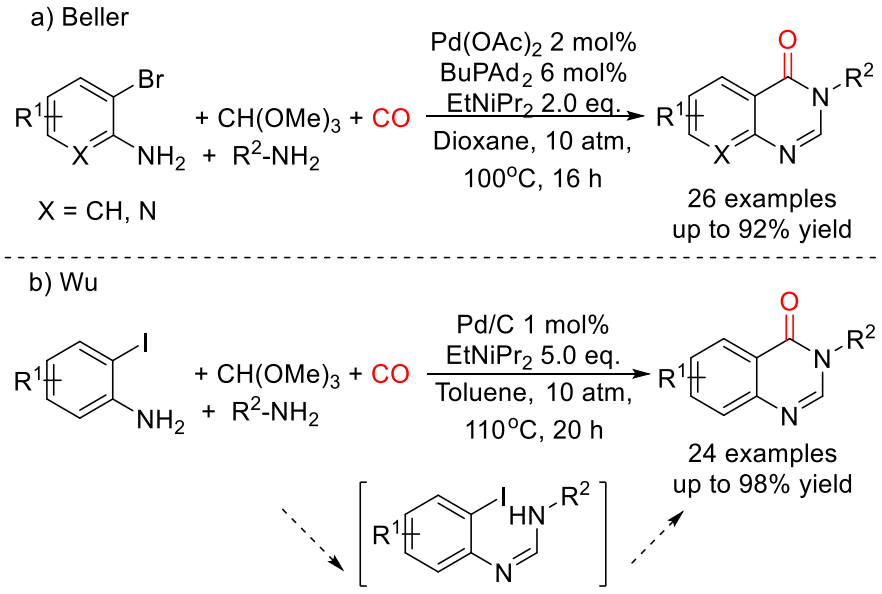

Scheme 1.30. Palladium Catalyzed Four Component Synthesis of Quinazolinones.

A number of other variants of these transformations have also been reported.[67] These include a number of double carbonylation reactions, which can allow the build-up of complex scaffolds involving generation of five or more bonds (Scheme 1.31).

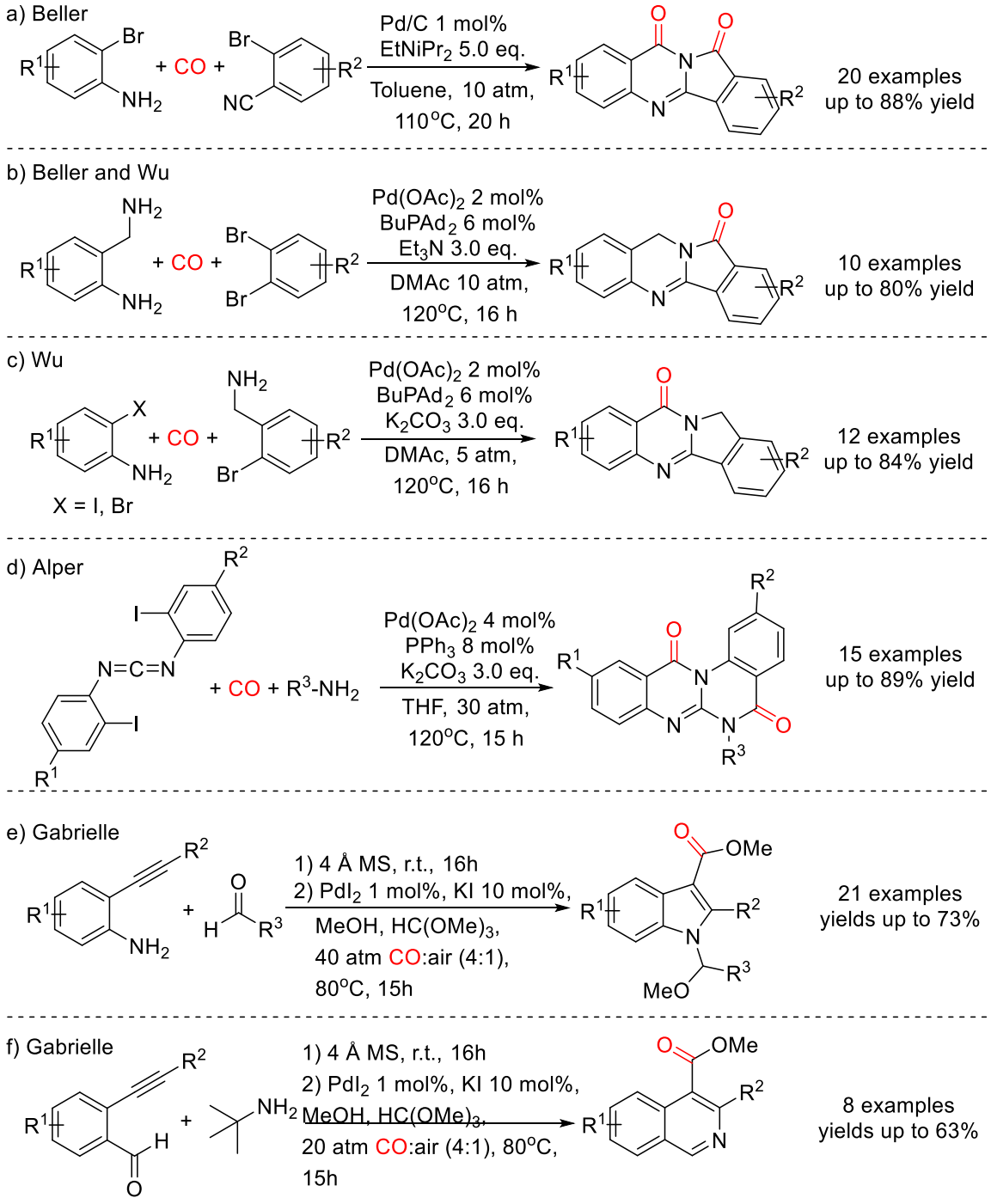

Scheme 1.31. Palladium Catalyzed Multicomponent Aminocarbonylation and Double Carbonylation Reactions.

As an alternative to unsaturated substrates, the Alper group has shown that strained rings such as aziridines can be used in the generation of 7-membered heterocycles (Scheme 1.32).[68] Seven membered ring products can also be formed with *ortho*-bromo-substituted Baylis Hillman acetates, primary amines and CO under palladium catalysis.[69]

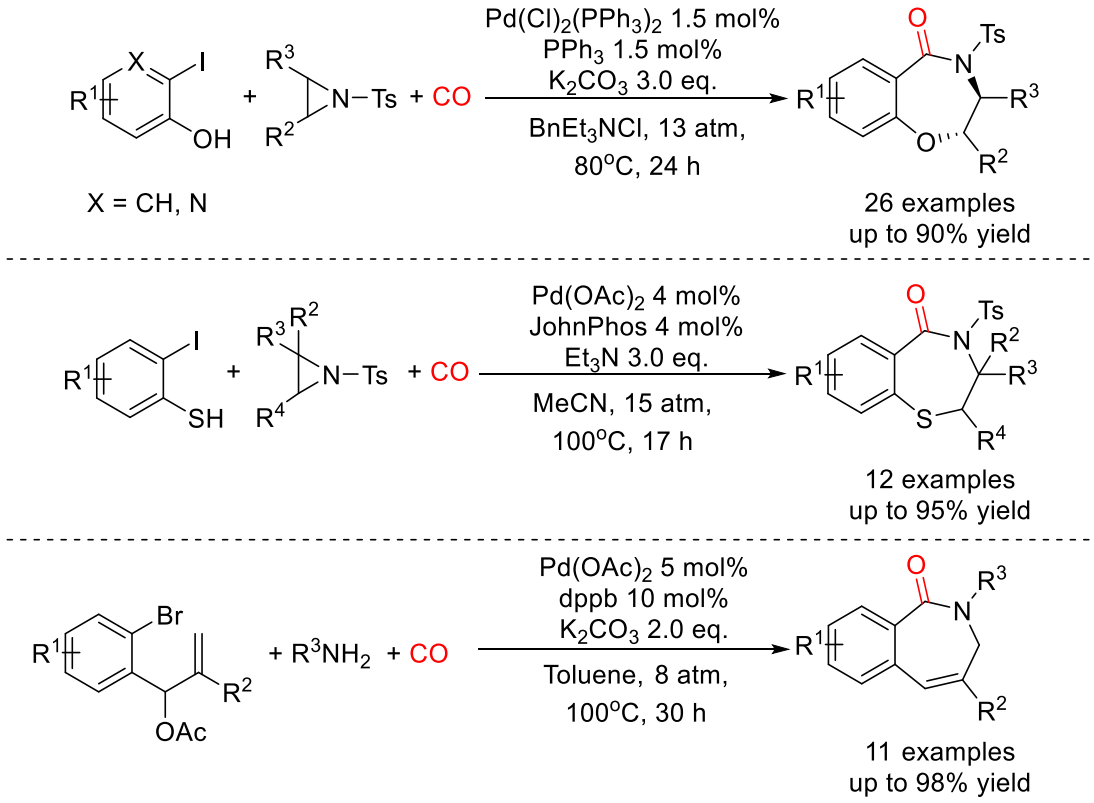

Scheme 1.32. Palladium Catalyzed Synthesis 7-Membered Heterocycles.

1.3.2. Cyclization of Carbonylation Products

Palladium catalyzed carbonylation reactions can also be used as a route to build up carbonyl-containing products that can undergo subsequent cyclization to generate a wide range of heterocycles. Perhaps the most heavily exploited variant of this chemistry involves the *in situ* generation of yones via palladium-catalyzed carbonylative Sonogashira reactions (Scheme 1.33).

By using the diverse reactivity of this intermediate, this approach has provided modular syntheses of a range of five- and six-membered heterocycles.

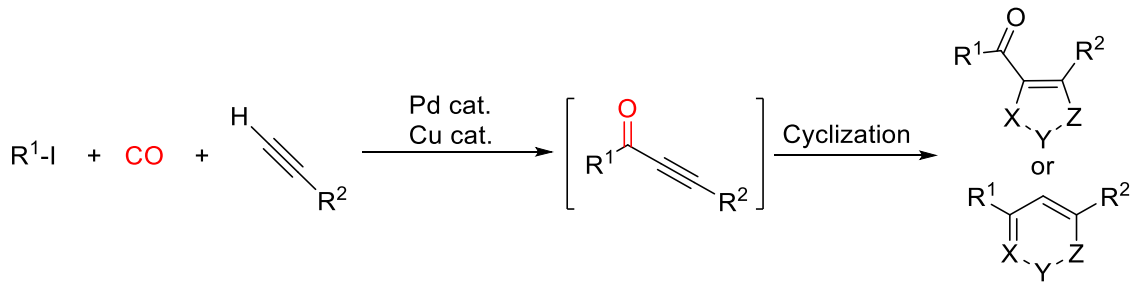

Scheme 1.33. Palladium Catalyzed Synthesis of Heterocycles via Carbonylative Sonogoshira reaction/Cyclization.

An early example of this approach was reported by Mori in the four component, palladium catalyzed coupling of terminal alkynes, CO, aryl iodide and hydrazines (or oximes) to form pyrazole and oxazole derivatives (Scheme 1.34a).[70] This reaction proceeds at room temperature, under 1 atm of CO, and can even be performed in water. Beller demonstrated that this approach could be extended to aryl-bromide substrates by use of the $BuPAd_2$ ligand system (Scheme 1.34b).[26] Stonehouse and Iranpoor groups have utilized $Cr(CO)_6$ and $Mo(CO)_6$ as the CO source for the multicomponent synthesis of these products.[71] Alternatively the Li research group has shown that Pd nanoparticles supported on porous N-doped carbon ($Pd@CN^T$) could be used as well for the synthesis of pyrazoles in a one step fashion, affording the products in good to excellent yields.[72]

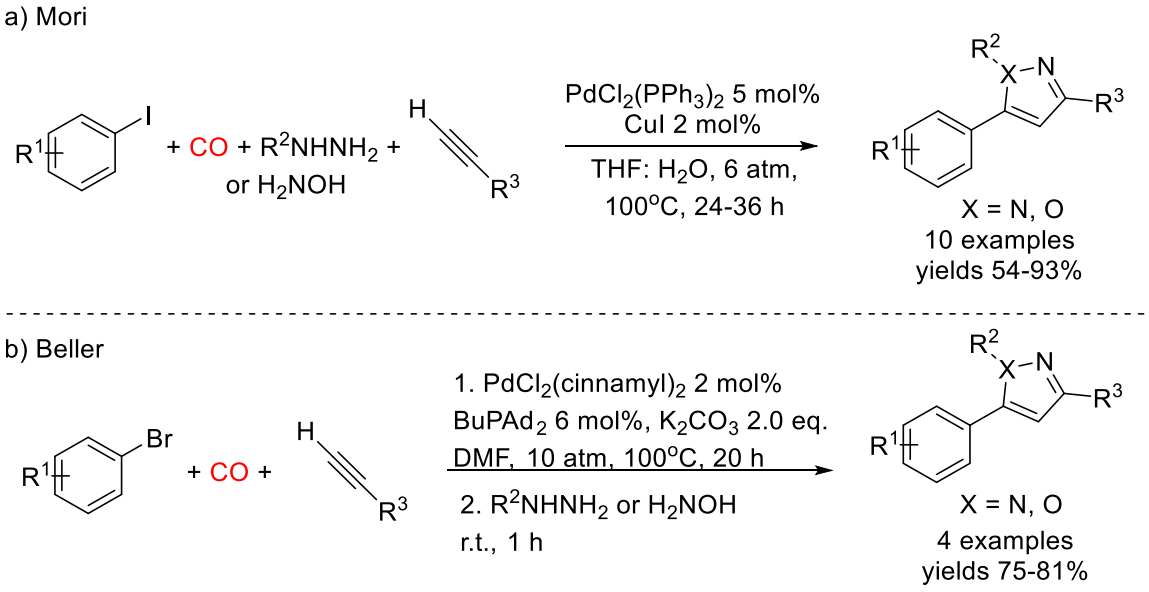

Scheme 1.34. Palladium Catalyzed Multicomponent Synthesis of Oxazoles and Pyrazoles.

The Müller lab has exploited the reactivity of alkynones to design a diverse array of palladium catalyzed MCRs.[73] Typically these alkynones intermediates are accessed via a palladium catalyzed Sonogoshira-type reaction between acid chlorides and terminal alkynes and undergo cycloaddition or cyclization reactions with a number of dinucleophiles or 1,3-dipolarophiles. However, they have also exploited carbonylations in some of these reactions. For example, they have found that 6-membered pyrimidines can be formed via the carbonylative coupling of aryl iodides, terminal alkynes and CO with amidinium salts (Scheme 1.35).[73d]

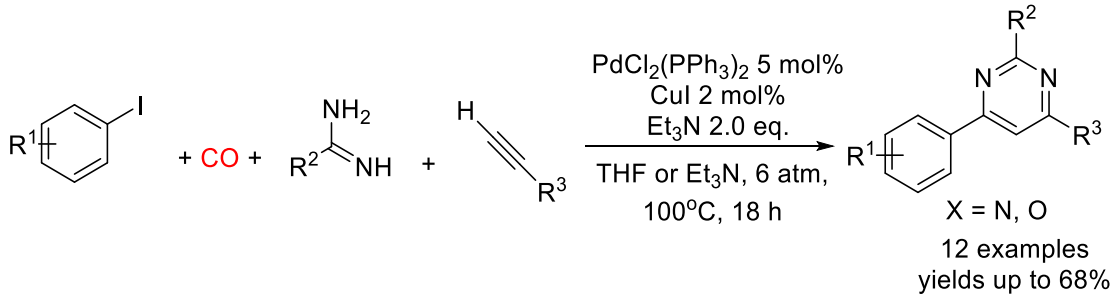

Scheme 1.35. Palladium Catalyzed Carbonylative Four Component Synthesis Pyrimidines.

Ynone reactions have also been applied to generate fused ring products. As shown by Torii and Rossi, this can allow the build-up of quinolones from 2-aminophenacetylenes, aryl iodides, amines and CO (Scheme 1.36).[74] While there are multiple potential palladium catalyzed transformations possible with these reagents (e.g. a direct Sonogoshira coupling, aminocarbonylation, or dimerization of alkyne), balancing of the reaction conditions and catalyst allowed the *in situ* generation of ynones for a subsequent amine initiated cyclization to form the product.

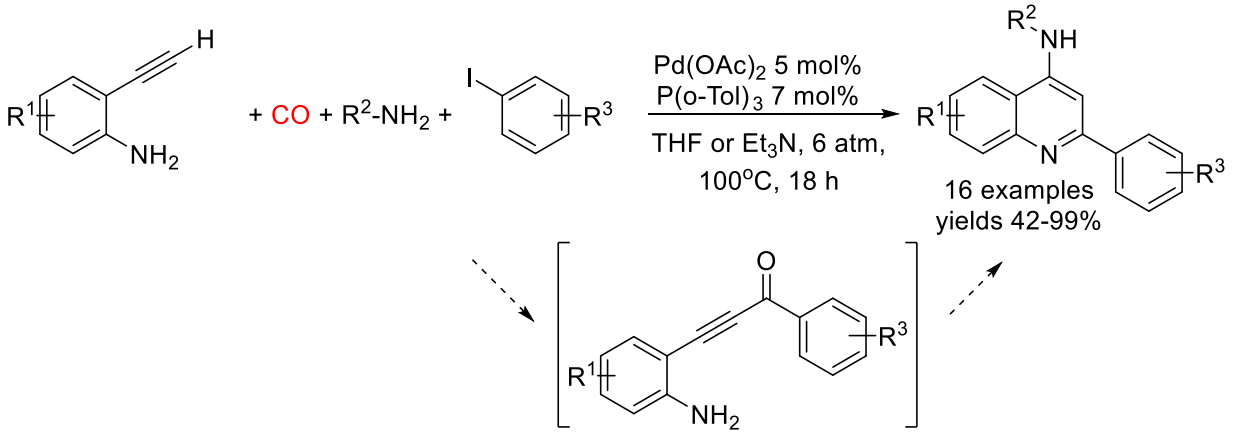

Scheme 1.36. Palladium Catalyzed Cyclocarbonylation Towards the Synthesis of Quinolines.

As an alternative to the use of ynone intermediates, Staben has reported that the four component reaction of aryl iodides, amidines, carbon monoxide, and hydrazines can provide an efficient approach to prepare triazoles (Scheme 1.37).[75] In this, $Pd(OAc)_2$/Xantphos was found to mediate the carbonylative coupling of aryl halides and amidinium salts forming an enamide intermediate. These can then undergo an *in situ* cyclization with hydrazines to allow the formation substituted triazoles. This protocol was applied for the synthesis of deferasirox – a metal chelator used in the treatment of chronic iron overload.

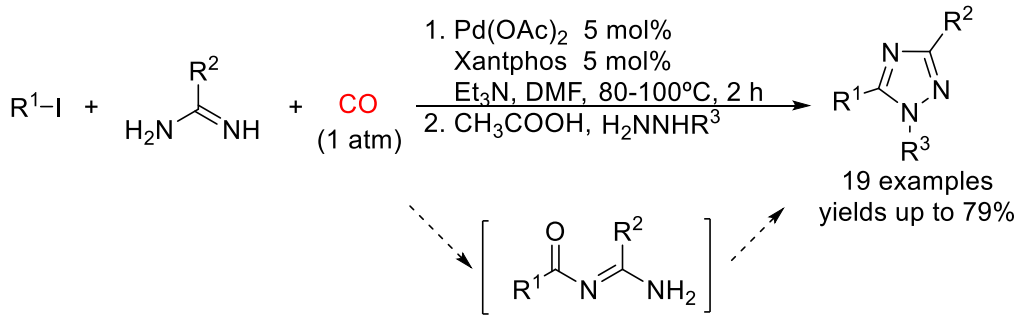

Scheme 1.37. Palladium Catalyzed Carbonylative Four Component Synthesis Triazoles.

1.3.3. Palladium Catalyzed Carbonylative Synthesis of 1,3-Dipoles

Our research group has reported an alternative approach to exploit carbonylations in MCRs, where CO is used to generate 1,3-dipoles (1,3-oxazolium-5-oxides, or Münchnones) for cycloaddition reactions. This transformation is believed to proceed via the initial reaction of an imine with an acid chloride generating an α-chloroamide, which can undergo rapid oxidative addition to Pd(0) generating a palladacycle (Scheme 1.38).[76] Subsequent CO insertion and reductive elimination (along with HCl loss) generates the 1,3-dipole. The ligand coordinated to the palladium catalyst has been found to be critical to this coupling, with strongly coordinating phosphines inhibiting the reaction, presumably by blocking CO association to intermediate. Instead, this reaction proceeds rapidly in the presence of bulky phosphines, such a P(*o*-Tol)$_3$. Since imines and acid chlorides can be easily tuned, a range of 1,3-dipoles can be readily prepared by this approach.

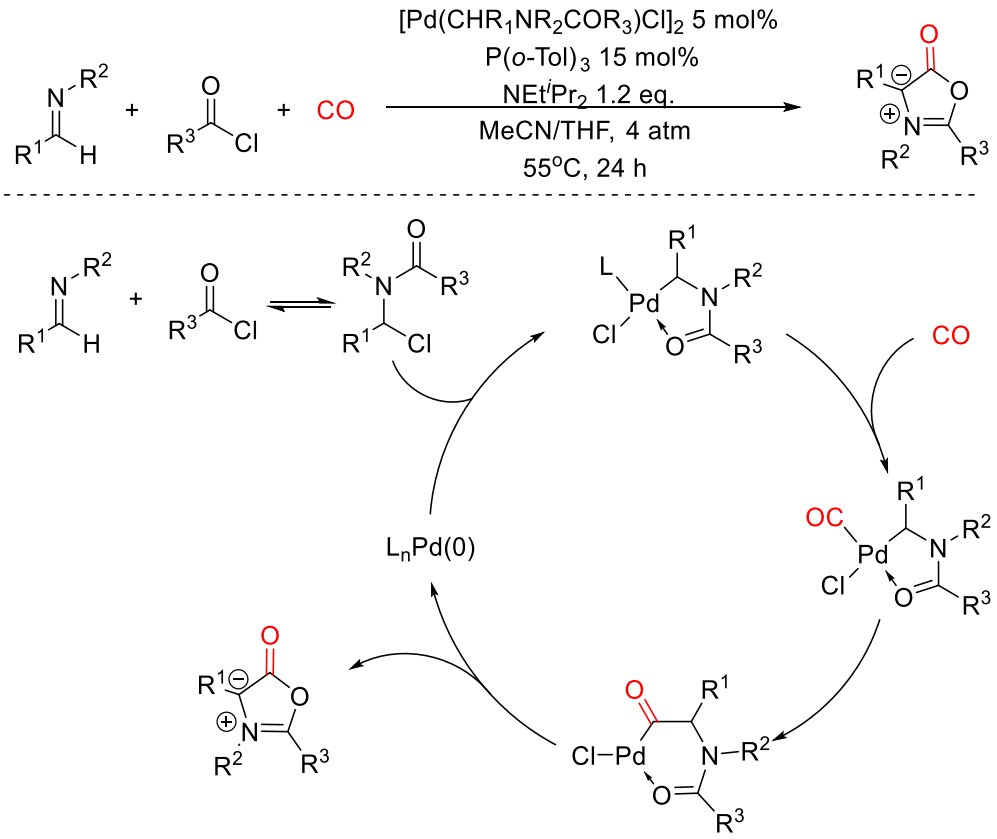

Scheme 1.38. Palladium Catalyzed Multicomponent Synthesis of Münchnones.

Coupling the generation of Münchnones with their 1,3-dipolar cycloaddition can allow the modular synthesis of a range of products. In these reactions, CO serves overall as a reducing agent to form a 1,3-dipole unit from imine and acid chloride, and eliminates CO_2 upon cycloaddition (Scheme 1.39a). For example, the palladium catalyzed generation of Münchnones in concert with alkyne cycloaddition allows the overall synthesis of polysubstituted pyrroles (Scheme 1.39b).[77] Various non-acidic functionalities on the acid chloride and imine, as well as a range of electron deficient alkynes are tolerated by this approach. Alternatively, the cycloaddition of N-tosyl substituted imine forms polysubstituted imidazoles (Scheme 1.39c).[78] In this system, cycloaddition is observed exclusively with the N-tosyl imine, despite the presence of two imines in the reaction mixture. The latter is believed to result from the favoured generation of acyl iminium salts with the N-alkyl or N-aryl substituted imines, while cycloaddition is most rapid with electron deficient imines. This can provide a route to a range of fully substituted

imidazoles with high selectivity. Alternatively, the cycloaddition of protonated imine, generated *in situ* by the liberated acid in the reaction, can form imidazolium carboxylate salts (Scheme 1.39d).[79] Initial reports of this reaction involved the same imine in both positions. However, more recent studies have shown that the addition of a second imine under acid conditions to the *in situ* generated Münchnone can allow the generation of imidazolium heterocycles with independent control of five substituents.[80]

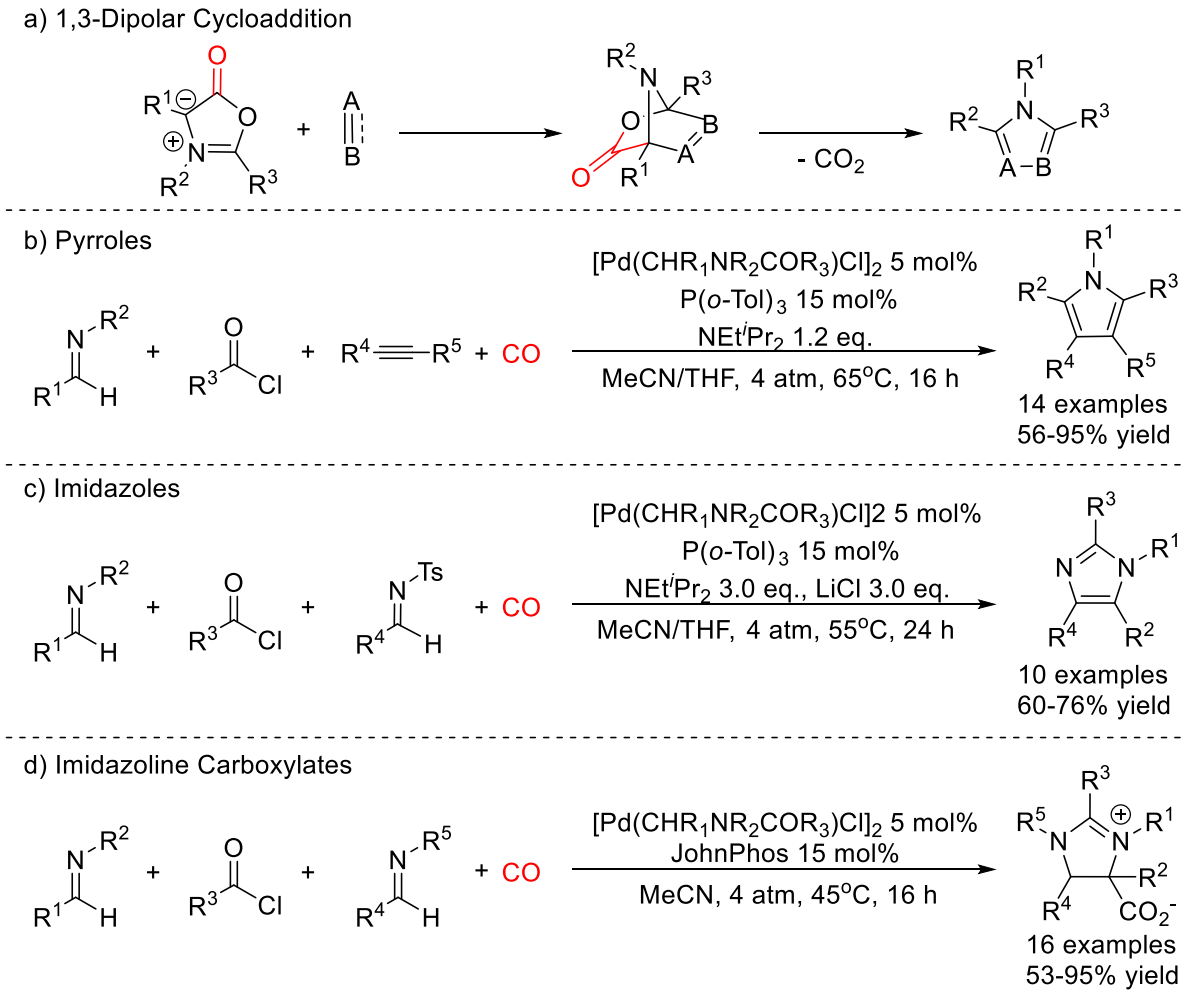

Scheme 1.39. 1,3-Dipoles in the Synthesis of Heterocycles.

Münchnones are known to exist in equilibrium with their acyclic ketene tautomer. Thus, while Münchnones undergo rapid 1,3-dipolar cycloaddition to protonated imines, removal of acid from reaction with amine base results in a slower [2+2] trapping of the ketene with the imine to generate 3-amido-substituted β-lactams (Scheme 1.40).[81] The catalyst in this case involves weakly coordinated oxazoline ligands. While most of the products employ identical imines in both positions, the initial generation of Münchnones followed by the addition of a second imine can allow the assembly of diversely substituted products.

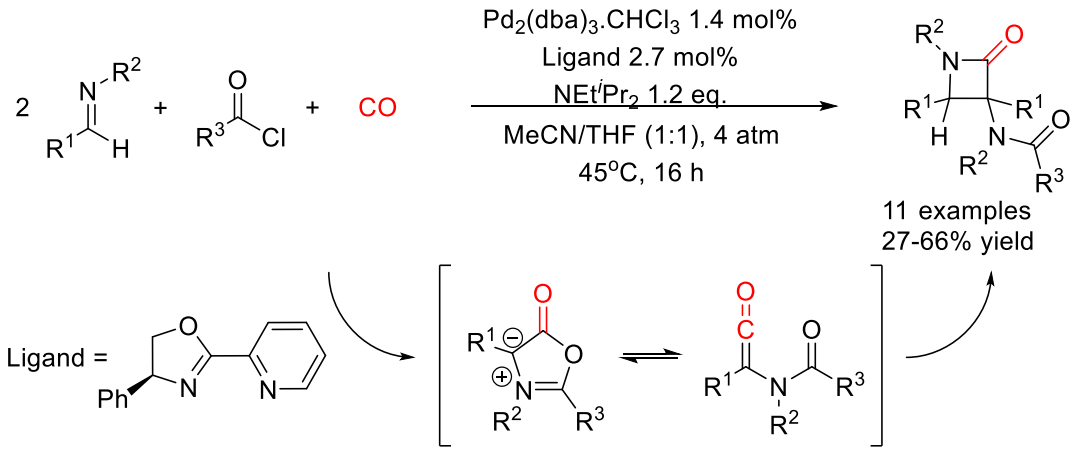

Scheme 1.40. Palladium Catalyzed Carbonylative Synthesis of β-Lactams.

More recently, our lab has demonstrated that the carbonylation of aryl iodides in the presence of a chloride salt can allow the construction of acid chlorides.[82] This transformation relies on the use of a bulky tri-*tert*-butyl phosphine ligand, which in conjunction with CO favors the reductive elimination of acid chlorides. This can be used to replace acid chlorides in the above chemistry to form Münchnones with aryl iodides, in a reaction that involves two consecutive (and concurrent) carbonylations using a single $Pd(P^tBu_3)_2$ catalyst. Combining the generation of these 1,3-dipoles with imine cycloaddition can be used to generate a modular synthesis of imidazolinium carboxylates from two imines, aryl iodides and two molecules of CO in a five component coupling reaction (Scheme 1.41a).[83] Polysubstituted pyrroles can be generated by a similar protocol (Scheme 1.41b-c).[84]

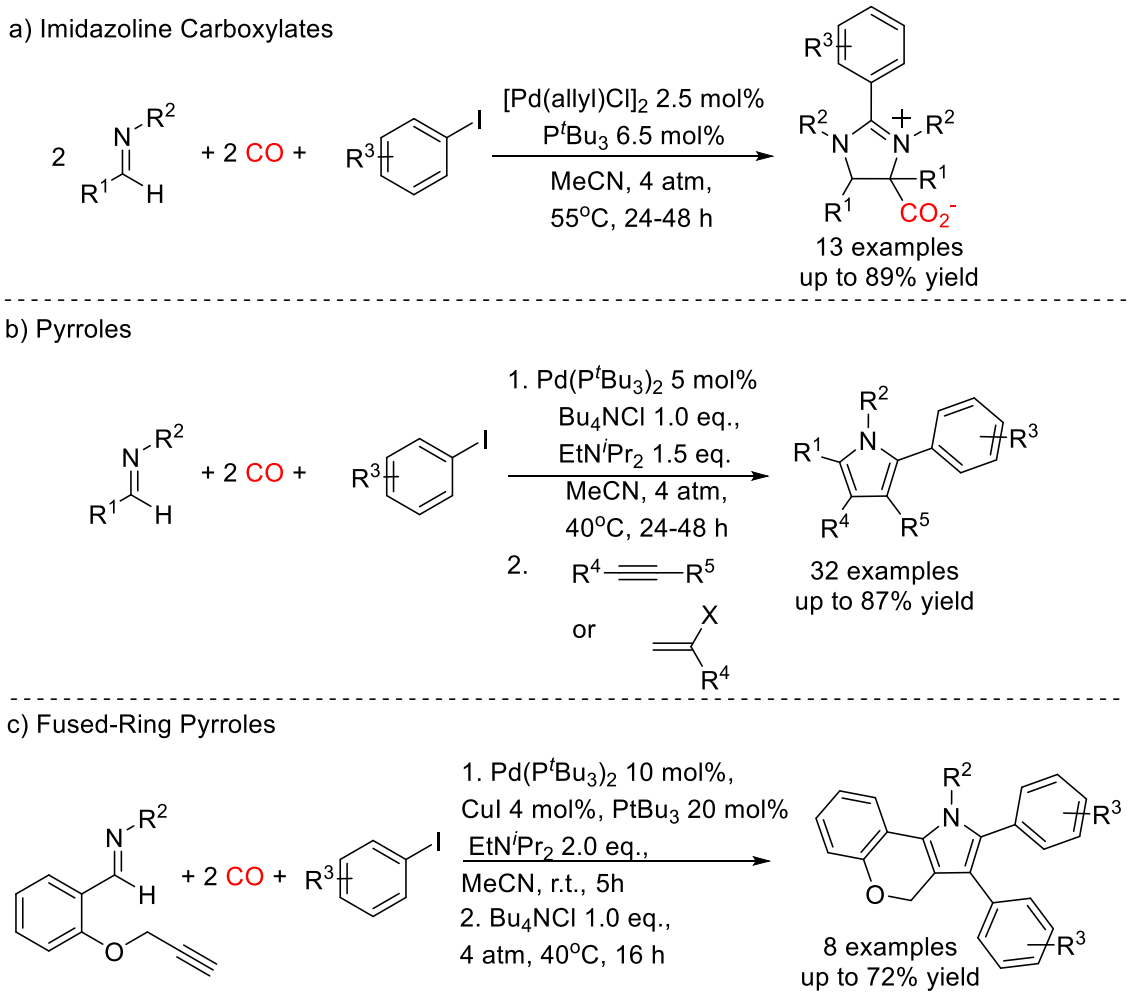

Scheme 1.41. Palladium Catalyzed Carbonylative Synthesis of Heterocycles from Aryl Halides.

1.4. Palladium Catalyzed Carbonylative C-H Bond Functionalization

Palladium catalyzed carbonylation reactions have also seen growing application in the field of C-H bond functionalization.[85] The use of metal catalysts to mediate the functionalization of traditionally unreactive arene and alkane C-H bonds (C-H bond functionalization) has garnered significant research attention in the last decade, since it provides with an efficient route to create new C-C and C-heteroatom bonds from available and unfunctionalized reagents.[86] In the case of palladium catalysis, these often involve the use of palladium-carboxylate derivatives (e.g. $Pd(OAc)_2$), where it is thought that association of the substrate to palladium allows a low

barrier concerted metalation-deprotonation (CMD) with the acetate ligand to form a palladium-carbon bond for subsequent chemistry (Scheme 1.42).[87]

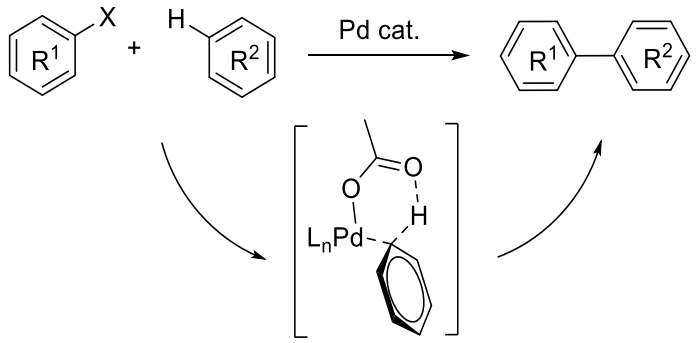

Scheme 1.42. Concerted Metalation-Deprotonation Mediated C-H Activation.

While palladium catalyzed C-H bond functionalization has been extensively employed in (hetero)ary-aryl and –alkyl bond forming chemistry, carbonylative variants of these reaction have been slower to develop. This may arise from several factors, including:

a) Pd(II) complexes can be readily reduced to Pd(0) under carbonylative conditions, thus inhibiting certain modes for palladium catalyzed C-H bond cleavage (i.e. the CMD mechanism).

b) The strong affinity of CO to palladium can potentially inhibit the coordination of the substrate.

c) CO is itself reactive, and can interact with the base (e.g. acetate) often employed in these reactions.

Despite these limits, the catalytic carbonylation of arenes and heterocycles was one of the earliest examples of palladium catalyzed C-H bond functionalization. Fujiwara and coworkers reported in 1980 that stoichiometric amounts of $Pd(OAc)_2$ can allow the conversion of arenes to carboxylic acids in the presence of CO when the arene substrate was used as solvent (Scheme 1.43a).[88] In 1982, the catalytic version of this transformation was reported using tert-butyl

peroxide as an oxidant (Scheme 1.43b).[89] The transformation is believed to proceed via an initial acetate assisted concerted metalation deprotonation mechanism forming the Pd-aryl bond, followed by CO coordination, insertion, and reductive elimination of an anhydride (which is subsequently hydrolysed to form the product). The palladium(0) generated in this last step is re-oxidized by *tert*-butyl peroxide to continue catalysis.

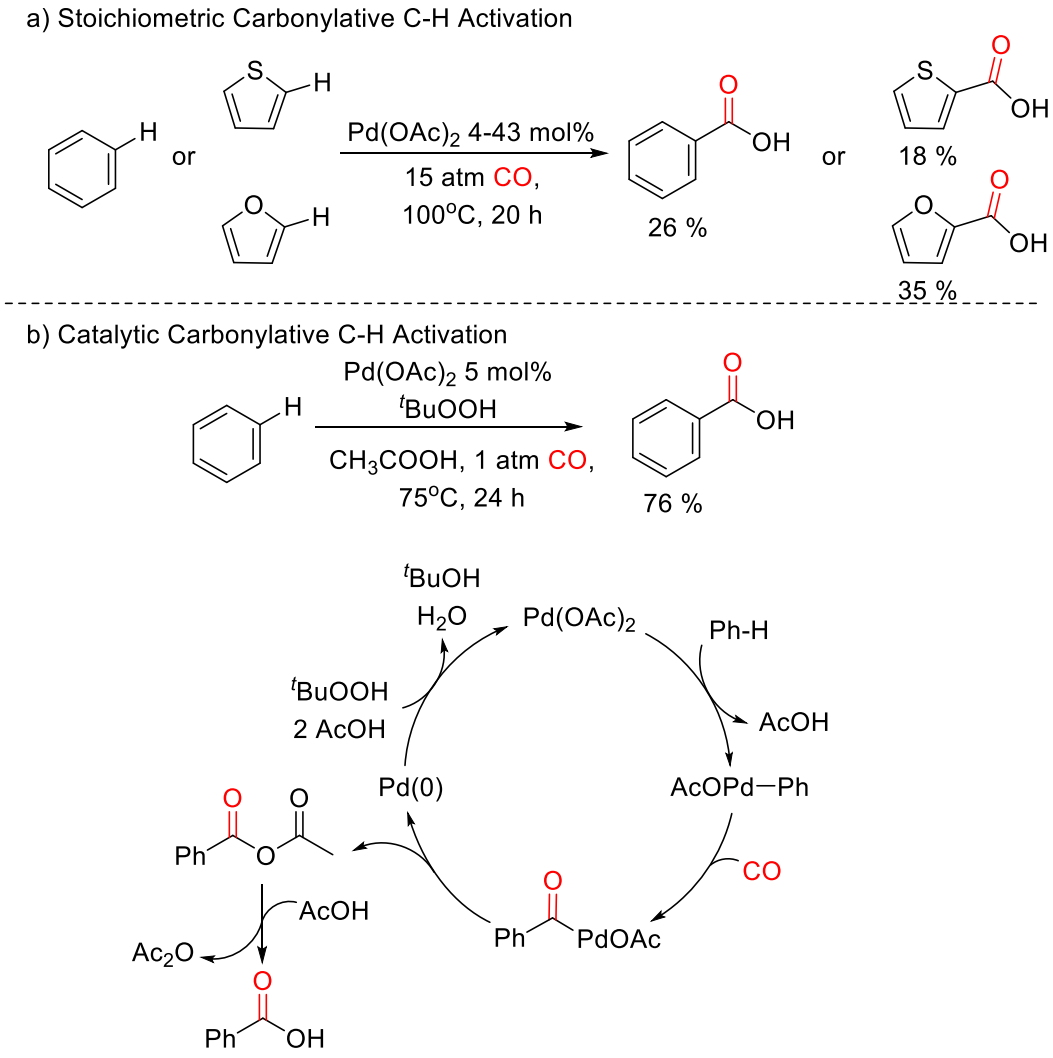

Scheme 1.43. Carbonylative C-H Activation of Simple Arenes and Heteroarenes.

Subsequent studies have shown that various oxidants can be employed in this reaction. For example, concurrent with the report of Fujiwara, Itahara showed that $Na_2S_2O_8$ could be used as the oxidant in the carbonylative C-H activation of indoles, thiophenes and dimethyluracil (Scheme 1.44a).[90] Moreover, this transformation could proceed at simply 1 atm CO. Reports by Dixneuf and Ugo have shown that copper and mercury salts can be used as co-catalysts and oxidants for the carbonylation of 5-membered heterocycles (Scheme 1.44b).[91] More recently, the group of Ishii has shown several examples of carbonylative C-H functionalization using oxygen as the terminal oxidant, where molybdovanadophosphates are used as co-catalysts that facilitate the reoxidation of Pd(0) (Scheme 1.44c).[92] In all of these examples, the (hetero)arene is employed in high concentration to help drive the reaction.

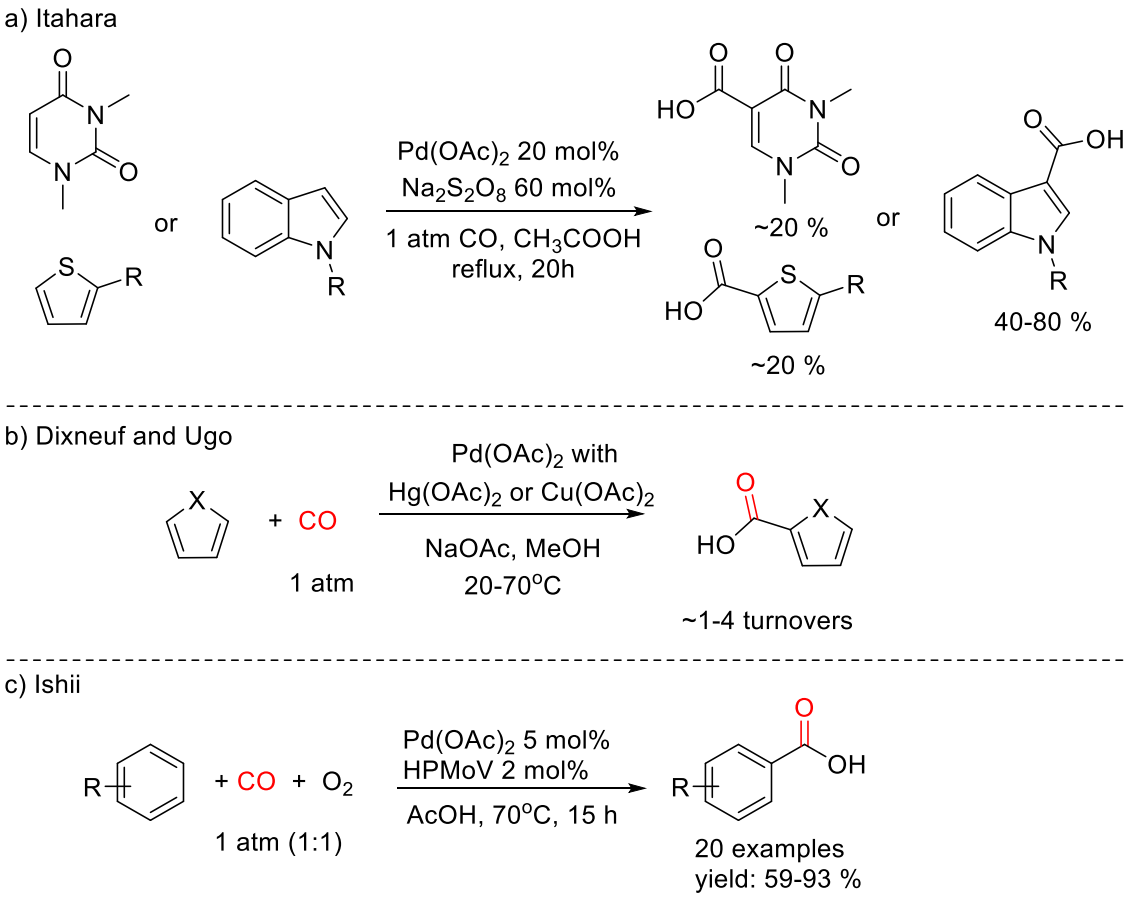

Scheme 1.44. Terminal Oxidants in Carbonylative C-H Activation of Simple Arenes and Heteroarenes.

Palladium acetate catalyzed C-H functionalization has also been used for the alkoxy- and amino-carbonylation. In 2011, Lei and coworkers developed a regioselective aerobic oxidative alkoxycarbonylation of indoles (Scheme 1.45a).[93] This reaction proceeds using an atmosphere of CO and air mixture, and affords 3-indole carboxylic esters in yields up to 86%. If unprotected indoles are employed in this transformation, N-carbamates are obtained as the only carbonylation product. This reaction is thought to proceed through an electrophilic carbopalladation at the C-3 position of the indole (Scheme 1.45b). A copper co-catalyst in this reaction serves as an oxidant for palladium, and is regenerated by oxidation with air. Alternatively, Li and coworkers reported the carbonylation of indoles using a $Pd(OAc)_2$ and stoichiometric I_2, where I_2 reacts with indoles to generate 3-iodoindoles for a more traditional aryl halide carbonylation, described in section 1.2 (Scheme 1.45c).[94]

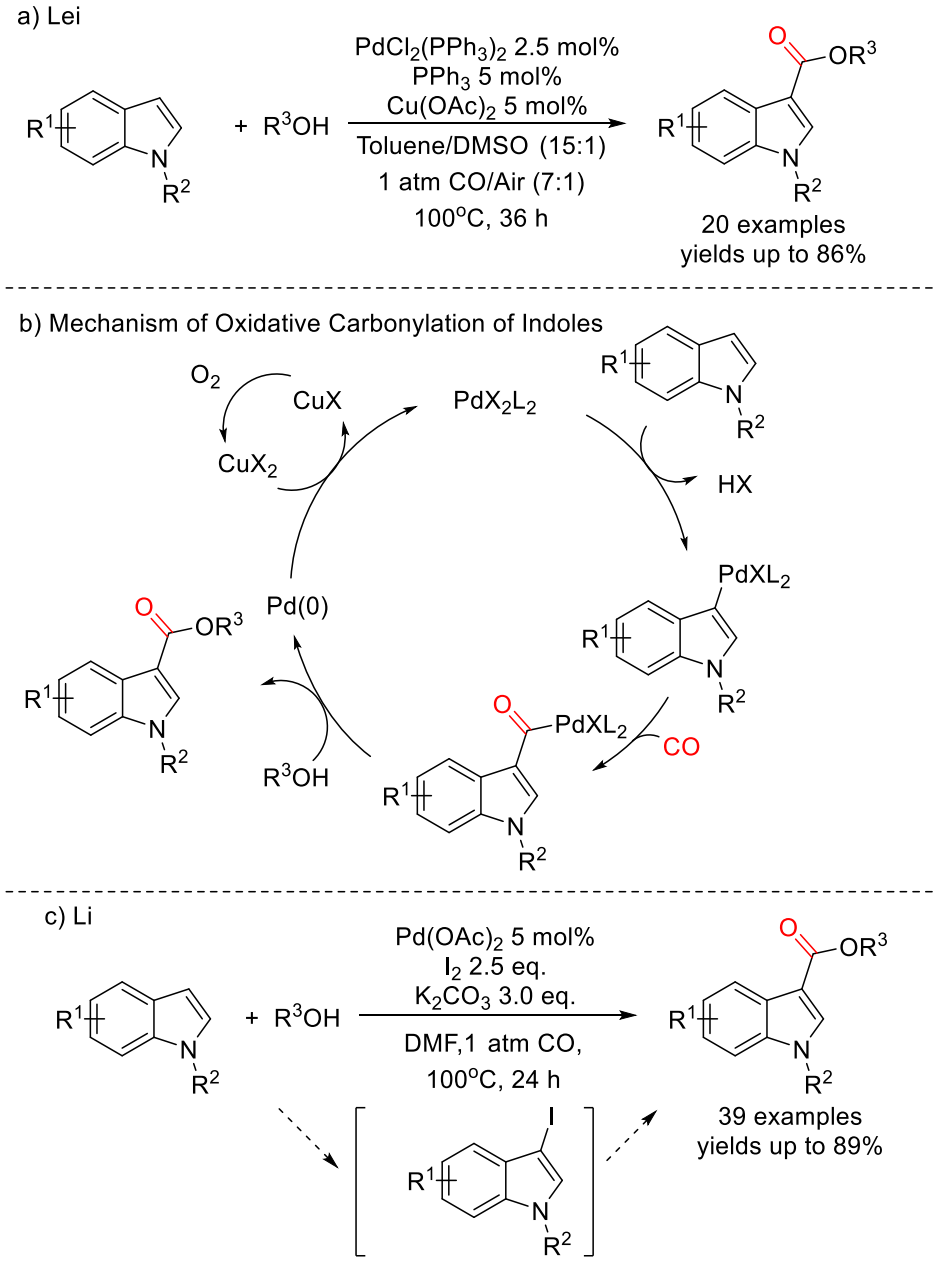

Scheme 1.45. Direct Alkoxycarbonylation of Indoles.

1.4.1. Chelation Assisted Carbonylative C-H Functionalization

A limitation of $Pd(O_2CR)_2$ catalyzed carbonylative C-H functionalization relative to non-carbonylative chemistry is the reactivity of the *in situ* generated Pd-(CO)R complex with the acetate base. Thus, these systems are often limited to the generation of anhydrides or anhydride

derived products. A method to avoid this limitation is via chelation assistance. This general field has been the subject of several reviews.[95] Chelation assistance provides a powerful method to accelerate C-H functionalization and control selectivity, where coordination of palladium to a directing group allows a rapid, intramolecular reaction of the C-H bond (Scheme 1.46). In catalytic carbonylative chemistry, this directing group is often also incorporated into the carbonyl-containing functionality.

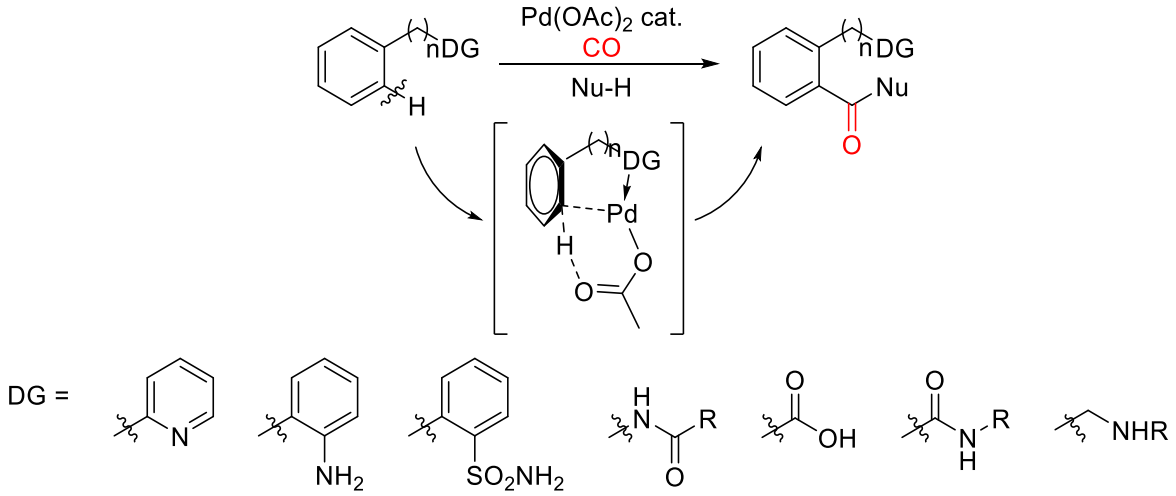

Scheme 1.46. Chelation assisted C-H functionalization reactions.

One of the earliest examples of this chemistry was developed by the Orito group and involved amine-directed intramolecular carbonylative C-H bond functionalization (Scheme 1.47a).[96] This transformation proceeds at mild pressure of CO, and generates five- and six-membered benzolactams with high selectivity. By modifying the oxidant, Gaunt and co-workers have extended this methodology to proceed at ambient temperature (Scheme 1.47b).[97] In this case, benzoquinone serves to rapidly reoxidize Pd(0) to Pd(II) in the presence of O_2. This latter reaction is tolerant of various functionalities on the tether, including stereogenic centers. Albert and Granell reported an analogous catalyst system which can allow the use of primary amines as directing groups, including quaternary aromatic α-amino esters (Scheme 1.47c).[98]

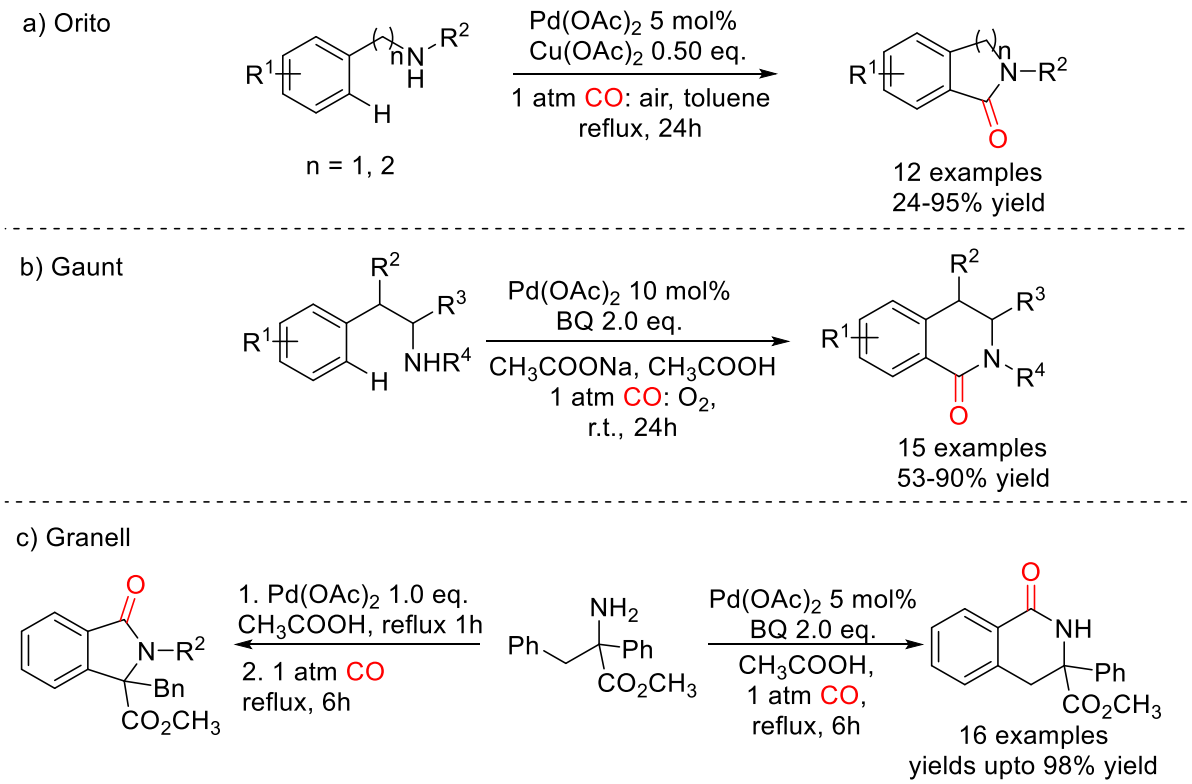

Scheme 1.47. Amine Directed Carbonylative C-H Activation Towards the Synthesis of Benzolactams.

Biaryls have been similarly exploited in amine directed C-H functionalization and lactam synthesis. Chuang and co-workers have shown a mild carbonylative synthesis of phenanthridinone derivatives from N-sulfonyl-2-aminobiaryls using a balloon of CO and silver acetate as the oxidant (Scheme 1.48a).[99] In 2013, the independent groups of Zhu and Zhang were able to extend this approach to unsubstituted aniline derivatives (Scheme 1.48b-c).[100] In both cases, an acidic additive (TFA) or solvent (trifluoroethanol) was necessary to prevent side carbonylation reactions involving the generation of ureas. This approach was also applied to several *ortho*-heteroarene substituted anilines.

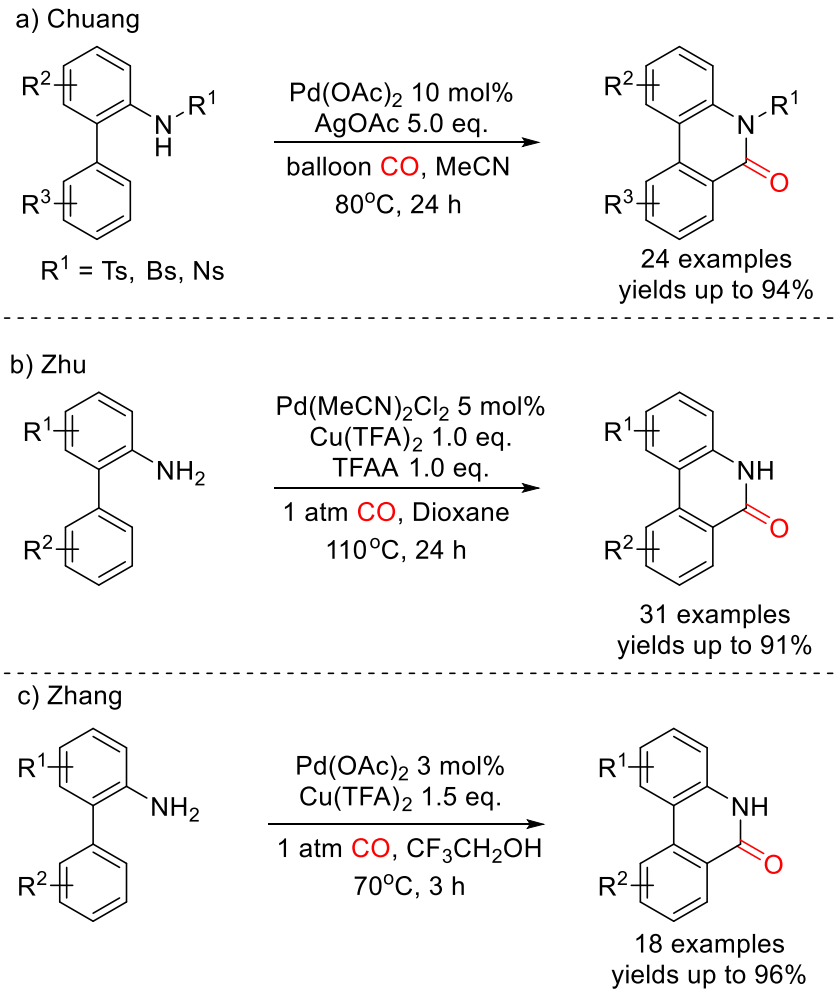

Scheme 1.48. Amine Directed Carbonylative C-H Activation Towards the Synthesis of Phenanthridinone.

The amine functionality in simple anilines can also be used to direct C-H functionalization. This approach was shown by the Guan research group in 2012 to lead to the double carbonylative formation of isatoic anhydrides (Scheme 1.49a).[101] The mechanism for this carbonylation proposed by the authors involves an initial electrophilic palladation of the C-H bond followed by an insertion of the first molecule of CO and reductive elimination forming a carboxylic acid. Subsequent reaction of this carboxylic acid with $Pd(OAc)_2$ then generates the Pd-O bound intermediate shown in scheme 1.49a. This intermediate undergoes a CO insertion followed by reductive elimination to form the final isatoic anhydride.

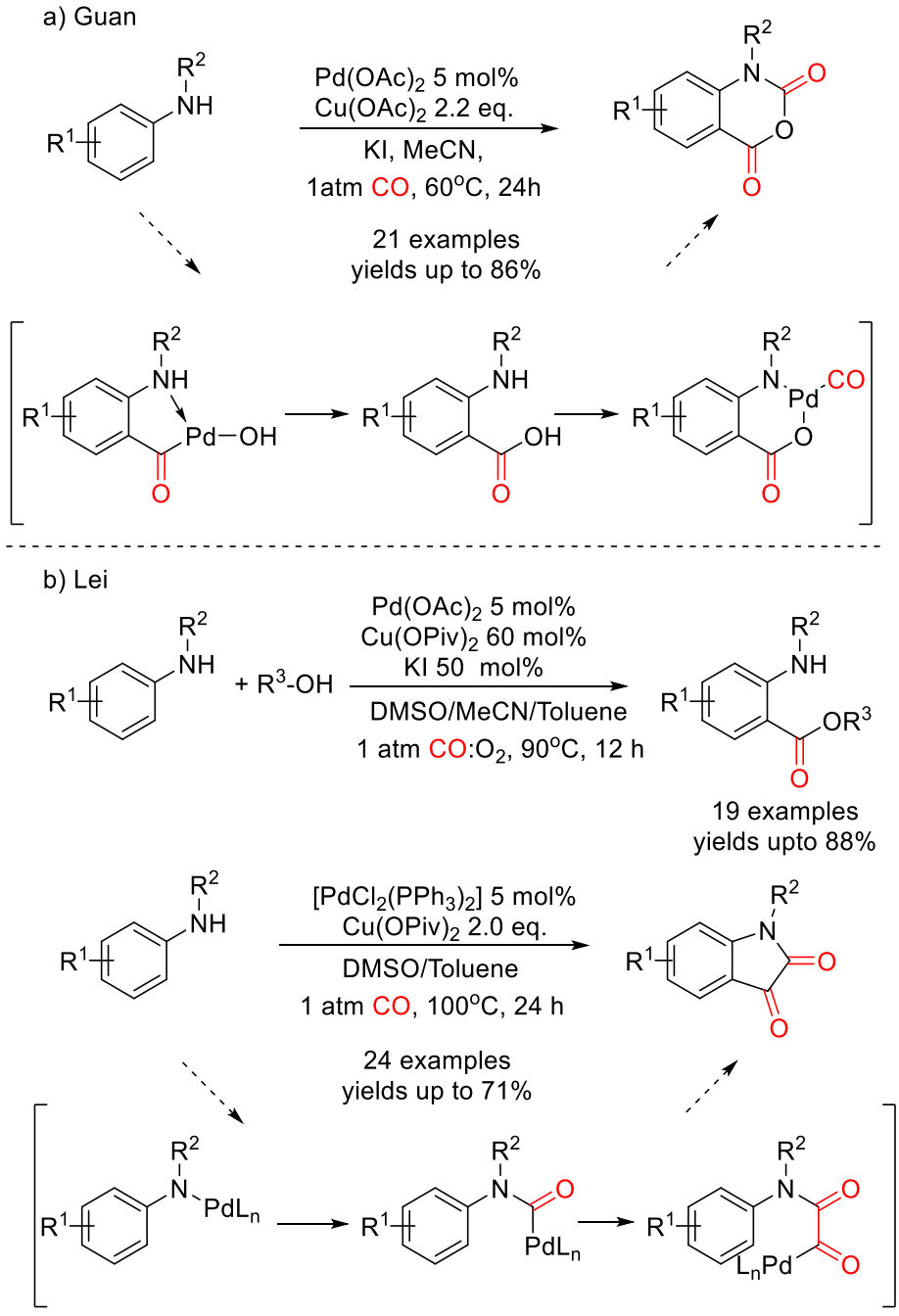

Scheme 1.49. Secondary Amine Directed Carbonylative C-H Activation.

Alternatively, Lei has shown that external nucleophiles can be employed in this reaction to form esters (Scheme 1.49b),[102] while removing the nucleophile leads to the double carbonylative formation of isatin derivatives.[103] In this latter case authors attribute the generation

of isatin derivatives to the initial N-H bond activation followed by double CO insertion. Concerted metalation deprotonation generates a six membered cyclic carbamoyl intermediate, which upon reductive elimination gives the isatin product.

Chelation assistance can also be applied to the carbonylation of C_{sp^3}-H bonds. Yu has shown that amide directing groups can allow the palladium catalyzed carbonylative synthesis of a range of succinimide derivatives. This catalytic system relies on TEMPO and AgOAc as the oxidant (Scheme 1.50).[104] While the role of TEMPO is still to be elucidated, the authors speculate that it may reoxidize Pd(0) to Pd(II) more efficiently than just AgOAc. This transformation requires higher temperatures than non-carbonylative variants, which was attributed to the inhibition of C-H bond interaction with palladium due to CO association. Notably, other directing groups that were previously utilized in their laboratory for the activation of C_{sp^3}-H bonds (e.g. carboxylates, pyridines or hydroximic acids) were unreactive under these carbonylative conditions.

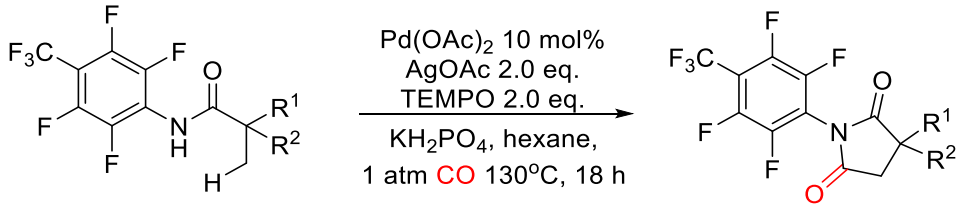

Scheme 1.50. Amide Directed Intermolecular Carbonylative C-H Activation of sp^3 bonds.

In 2016, Gaunt demonstrated that amines can also direct aliphatic C-H bond carbonylations to form β-lactams (Scheme 1.51).[105] This reaction is postulated to proceed via an usual mechanism, where CO insertion into the palladium-acetate bond forms a palladium-anhydride intermediate, which reacts with the amine. Subsequent C-H functionalization forms a 5-membered ring palladacycle that then eliminates the β-lactam product. This reaction is general with a range of secondary amines, and can be applied to the synthesis of several pharmaceutical products.

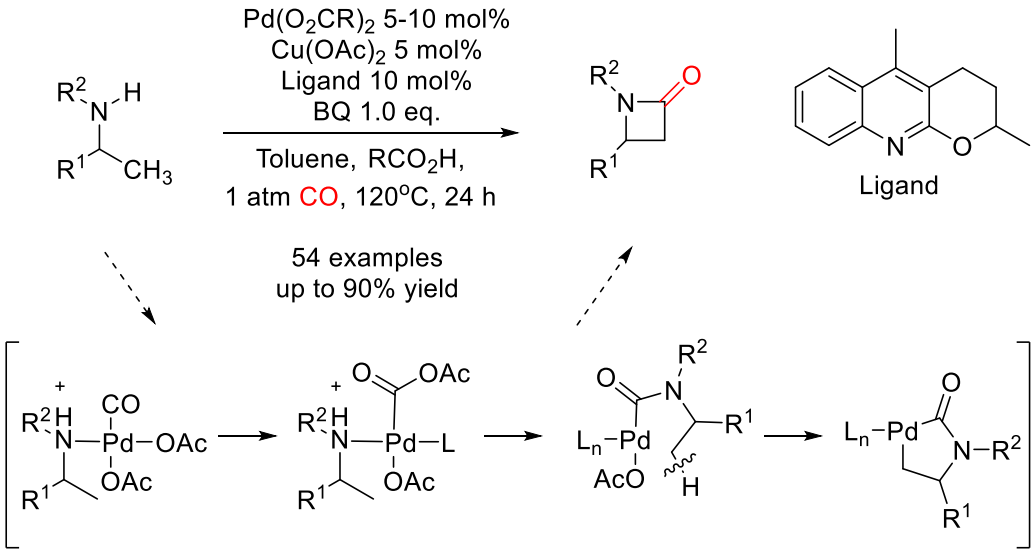

Scheme 1.51. Palladium Catalyzed Carbonylative Synthesis of β-lactams.

Oxygen directing groups have been employed in a similar fashion to amines in C-H bond carbonylations. As with amines, these can serve as directing groups and nucleophiles to afford lactones, or simply directing groups in concert with other nucleophiles to form various carboxylic acid derivatives. Representative examples of these are summarized in Schemes 1.52-1.53, and include the work of Yu towards the synthesis of carboxylic acids and lactones from various aromatic reagents (Scheme 1.52a-d),[106] the use of biaryls by Shi and Chuang in constructing polycyclic lactones (Scheme 1.52e-f),[107] and Booker-Milburn for ureas and other derivatives (Scheme 1.53). [108]

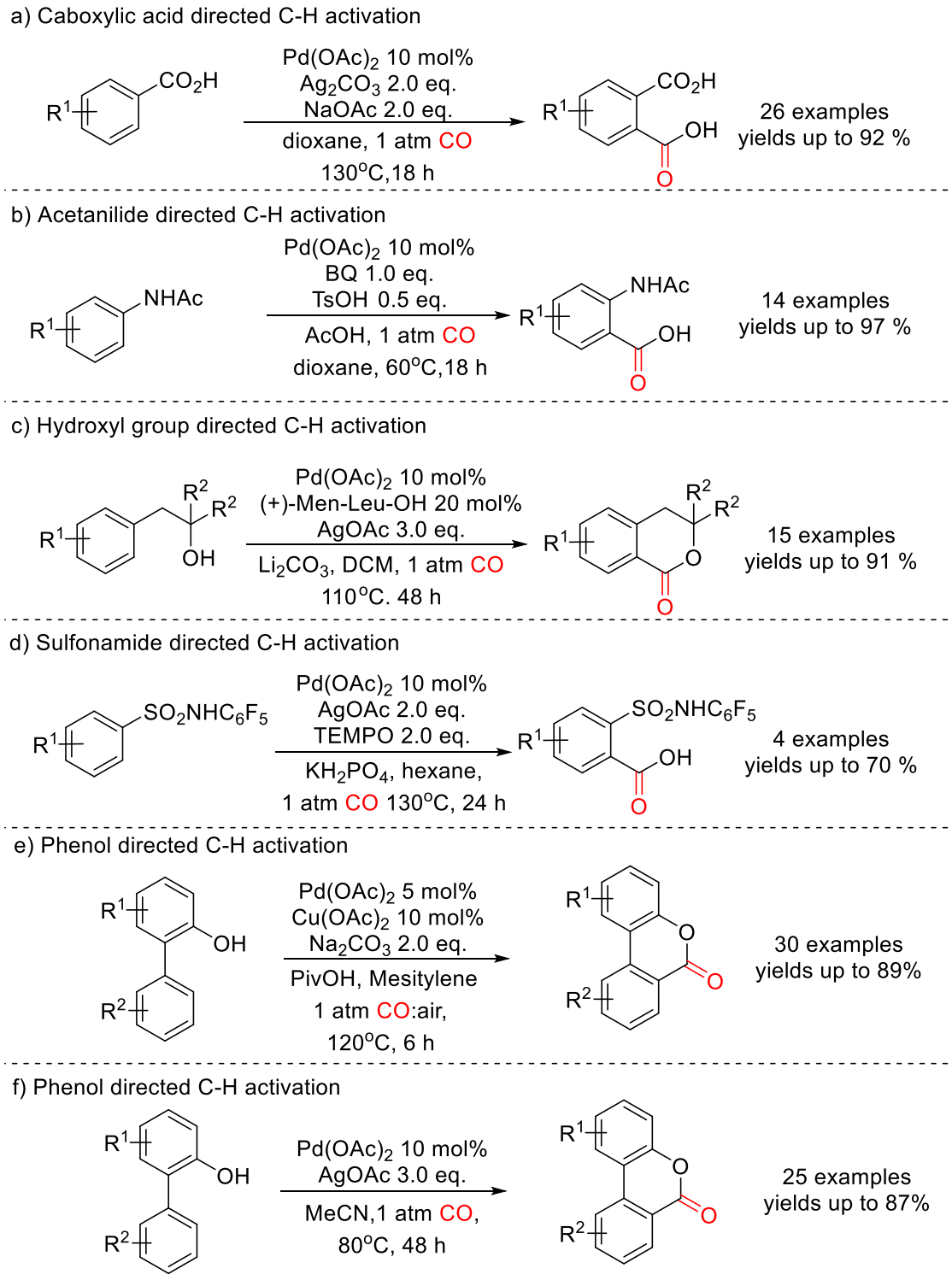

Scheme 1.52. Oxygen Directed Carbonylative C-H Activations.

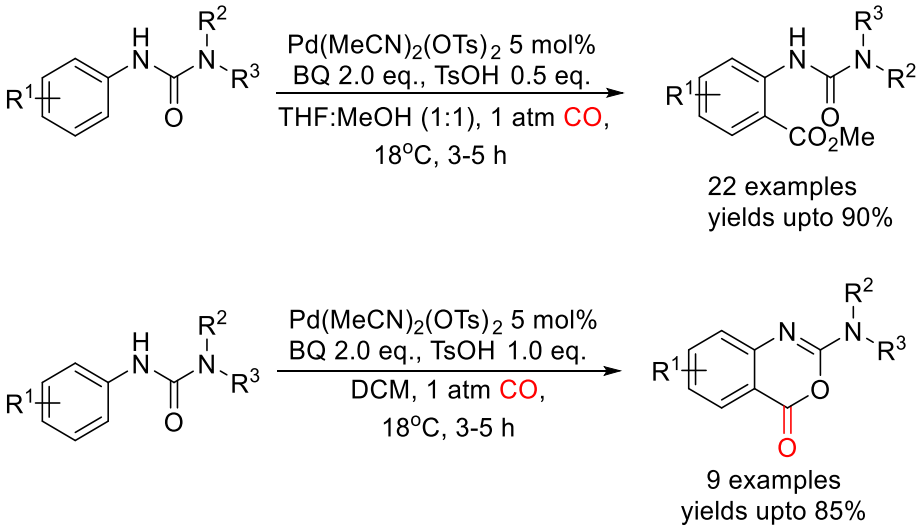

Scheme 1.53. Urea Directed Carbonylative C-H Activations.

1.4.2. Carbonylative C-H Activation in the Synthesis of Ketones

Unlike many examples in non-carbonylative C-H bond functionalization, palladium catalyzed carbonylative C-C bond formation has to date seen limited success, despite the potential utility of these ketone products. This can be attributed, at least in part, to the reactivity of the carboxylate base commonly used in these systems, which can react with the Pd(CO)R complex more rapidly than the steps required to form a Pd-C bond for reductive elimination. As a result, most Pd-catalyzed carbonylative C-H functionalizations have led to carboxylic acid derivatives.

One approach to avoid this limitation is via intramolecular reactions. Larock pioneered this methodology in intramolecular cyclocarbonylation of 2-halobiphenyls to form fluorenones (Scheme 1.54).[109] This system employs the commercially available $Pd(PCy_3)_2$ catalyst and stoichiometric NaO_2C^tBu, and presumably involves C-H functionalization of the tethered arene followed by CO insertion and reductive elimination. A follow-up paper showed that this approach could be extended to a wide range of heterocycles, including thiophenes, indoles, benzofurans, and furans.[110]

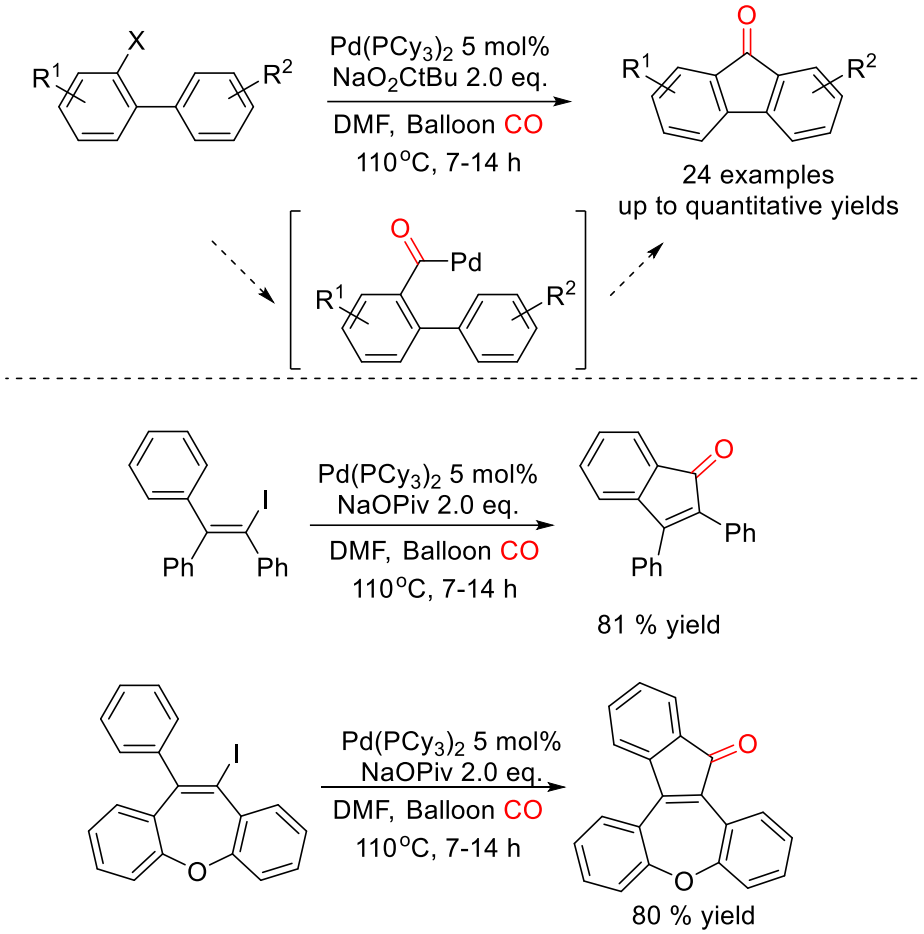

Scheme 1.54. Intramolecular Carbonylative C-H Activation of 2-Halobiphenyls Towards the Synthesis of Fluorenones.

Lei and co-workers demonstrated that aryl halides are not required in this reaction, and instead simple diaryl ethers can undergo a double C-H functionalization / carbonylation to form xantones (Scheme 1.55).[111] The reaction utilized a simple $Pd(OAc)_2$ catalyst with $K_2S_2O_8$ as the oxidant and under 1 atm of CO, and afforded 20 different xantones in moderate to good yields. Kinetic studies using IR spectroscopy showed that the rate-determining step was intramolecular C-H activation of the second aromatic ring.

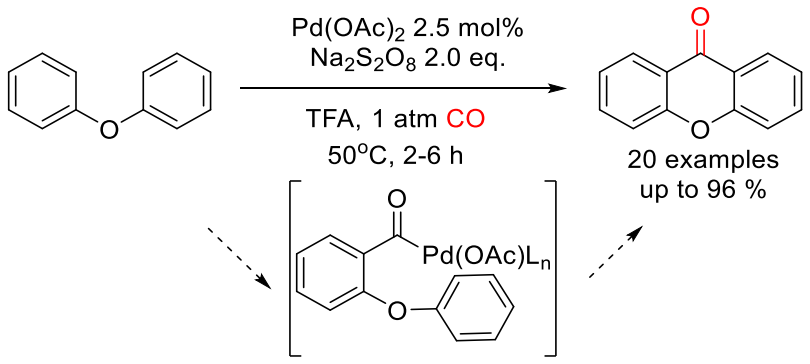

Scheme 1.55. Double Carbonylative C-H Activation of Diarylethers Towards the Synthesis of Xantones.

An alternative approach to generate ketones via carbonylative C-H functionalization that has seen some success is to employ highly activated substrates. This was described by Beller in the first carbonylative intermolecular C-H functionalization of heteroarenes to form diaryl(heteroaryl)ketones (Scheme 1.56).[112] While this at first glance appears to involve a palladium catalyzed heterocycle functionalization, this system employs a stoichiometric CuI salt, who's role is to first react with the acidic C-H bond of the heterocycle in the presence of base to form a metallated heterocycle. This then undergoes a more traditional palladium catalyzed carbonylative coupling reaction. The high CO pressure in the reaction (40 atm) was necessary to prevent the formation of the direct non-carbonylative coupled product. A range of heterocycles, including benzoxazoles, benzimidazoles, benzothiazoles, and oxazoles, were found to give the corresponding ketones in good yields.

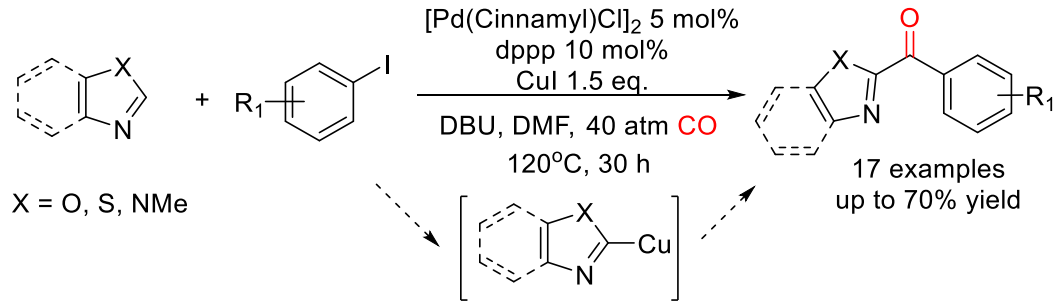

Scheme 1.56. Intermolecular Carbonylative C-H Activation Towards the Synthesis of diaryl(heteroaryl)ketones.

Recently, Skrydstrup reported the first palladium-based intermolecular C-H bond carbonylation to form ketones. This transformation employs highly activated/acidic perfluorinated arenes, who's CMD by the palladium catalyst can complete with acetate reductive elimination within the palladium-acyl intermediate to form the corresponding ketone products (Scheme 1.57).[113] This reaction proceeds efficiently under moderate reaction temperatures, but requires the use of highly fluorinated arenes in order to accelerate the C-H bond activation and minimize the formation of carboxylic acids.

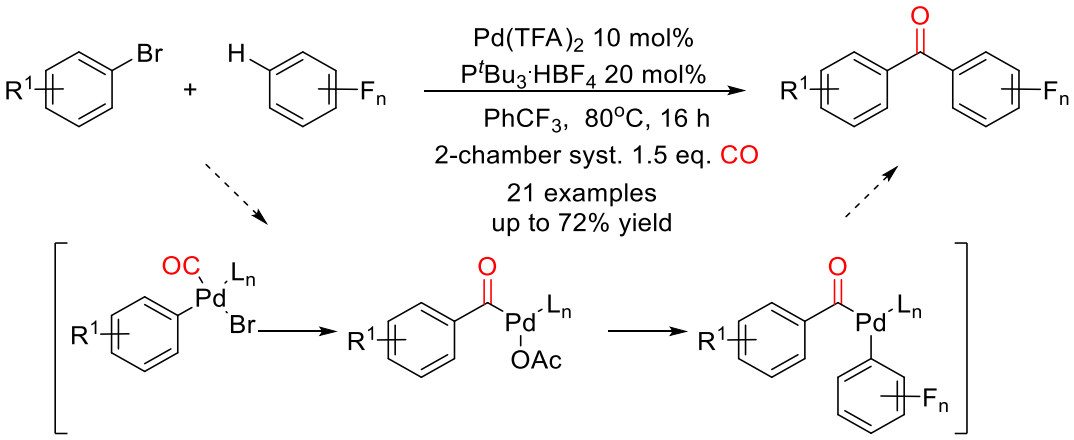

Scheme 1.57. Carbonylative C-H Activation of Fluorinated Arenes Towards the Synthesis of Diarylketones.

1.5. Overview of the Thesis

The studies outlined above show that a diverse range of transition metal catalyzed carbonylation reactions have been developed in the last four decades. Tremendous effort has been directed towards rational catalyst design, activation of challenging substrates, and the development of multicomponent protocols. Furthermore, these reactions provide with a method to combine a widely available feedstock, CO, together with other reagents (alcohols, amines, alkenes, alkynes, aldehydes, etc.) to generate products of added value that have great relevance in pharmaceutical, synthetic, agrochemical and polymer chemistry.

The research described in this thesis is directed towards developing new variants of these carbonylation reactions, and in particular those that use readily available building blocks and employ simple protocols. These transformations rely on the generation and trapping of the highly electrophilic organic intermediates, which has allowed for the development of several new variants of these reactions.

In chapter 2, we describe a tandem catalytic and multicomponent approach to the synthesis of imidazoles from readily available imines, aryl halides and CO. This reaction uses a simple Pd/P^tBu_3 catalyst that is able to mediate both aryl halide carbonylation as well as α-chloroamide carbonylation yielding a 1,3-dipole (a Münchnone). When performed in conjunction with 1,3-dipolar cycloaddition, this allows the efficient one pot synthesis of aryl-substituted imidazoles.

Chapter 3 describes a new nickel-catalyzed synthesis of isoindolinones via the carbonylation of aryl iodides in the presence of imines. The use of simple $Ni(COD)_2$ catalyst in the presence of 1 atm of CO allows for the mild carbonylation of aryl halides to generate *in situ* acid chlorides. These rapidly react with an imine to form an α-chloroamide, which undergoes a catalytic cyclization to yield the isoindolinone products.

Chapter 4 describes our efforts in the field of palladium catalyzed carbonylative C-H functionalization, and the functionalization of electron rich heterocycles into ketones. This transformation relies on formation of highly electrophilic intermediates, aroyl iodides, via the Pd/P^tBu_3 catalyzed carbonylation of aryl iodides. The decoupling of palladium catalyst from C-H

functionalization step allows the design of an efficient and simple protocol for the generation of a broad range of aryl-(hetero)aryl ketones from aryl iodides, CO and heterocycles.

As laid out in section 1.3.3, our laboratory has done extensive work in the palladium catalyzed carbonylative synthesis of mesoionic Münchnone intermediates. Chapter 5 describes our work towards understanding the mechanism of this catalytic system. It includes the synthesis of key catalytic intermediates, performing model reactions, as well as kinetic studies that support the role of these compounds in catalysis. Overall, this allowed the elucidation of the mechanism of this transformation, including the role of palladium nanoparticles and ligands in facilitating catalysis.

In chapter 6, we show how this mechanistic data can be used to create a highly active catalyst for the carbonylative synthesis of Münchnones, and, from these, pyrroles. This includes its application to a novel one step, palladium catalyzed synthesis of Atorvastatin (i.e., Lipitor) from simple imines, acid chlorides and alkynes.

1.6. References

(1) (a) Amatore, C.; Jutand, A. *Acc. Chem. Res.* **2000**, *33*, 314-321; (b) Alberico, D.; Scott, M. E.; Lautens, M. *Chem. Rev.* **2007**, *107*, 174-238; (c) Martin, R.; Buchwald, S. L. *Acc. Chem. Res.* **2008**, *41*, 1461-1473; (d) Chartoire, A.; Nolan, S. P. In *New Trends in Cross-Coupling: Theory and Applications*; The Royal Society of Chemistry: 2015, p 139-227.

(2) (a) Johansson Seechurn, C. C. C.; Kitching, M. O.; Colacot, T. J.; Snieckus, V. *Angew. Chem. Int. Ed.* **2012**, *51*, 5062-5085.

(3) For reviews on palladium catalyzed carbonylations, see: (a) Brennführer, A.; Neumann, H.; Beller, M. *Angew. Chem. Int. Ed.* **2009**, *48*, 4114-4133; (b) Gadge, S. T.; Bhanage, B. M. *RSC Advances* **2014**, *4*, 10367-10389; (c) Skoda-Földes, R. In *Ionic Liquids (ILs) in Organometallic Catalysis*; Dupont, J., Kollár, L., Eds.; Springer: Berlin, Heidelberg, 2015, p 145-161; (d) Wu, X.-F.; Fang, X.; Wu, L.; Jackstell, R.; Neumann, H.; Beller, M. *Acc. Chem. Res.* **2014**, *47*, 1041-1053; (d) Beller, M.; Wu, X.-F. *Transition Metal Catalyzed Carbonylation Reactions*; Springer: Berlin Heidelberg, 2013; (e) Sumino, S.; Fusano, A.; Fukuyama, T.; Ryu, I.

Acc. Chem. Res. **2014**, *47*, 1563-1574; (f) Wu, X.-F.; Neumann, H.; Beller, M. *Chem. Soc. Rev.* **2011**, *40*, 4986-5009.

(4) Bierhals, J. In *Ullmann's Encyclopedia of Industrial Chemistry*; Wiley-VCH Verlag GmbH & Co. KGaA: 2000.

(5) (a) Schoenberg, A.; Bartoletti, I.; Heck, R. F. *J. Org. Chem.* **1974**, *39*, 3318-3326; (b) Schoenberg, A.; Heck, R. F. *J. Org. Chem.* **1974**, *39*, 3327-3331.

(6) Industrial processes (a) Crettaz, R.; Waser, J.; Bessard, Y. *Org. Process Res. Dev.* **2001**, *5*, 572-574; (b) M. Scalone, P. Vogt, (Hoffmann–La Roche, Switzerland), EP 0385210, 1990, A2; (c) Andrews, I. P.; Atkins, R. J.; Breen, G. F.; Carey, J. S.; Forth, M. A.; Morgan, D. O.; Shamji, A.; Share, A. C.; Smith, S. A. C.; Walsgrove, T. C.; Wells, A. S. *Org. Process Res. Dev.* **2003**, *7*, 655-662; (d) Karpf, M. In *Pharmaceutical Process Chemistry*; Wiley-VCH Verlag GmbH & Co. KGaA: 2010, p 1-37; (e) Yee, N. K.; Farina, V.; Houpis, I. N.; Haddad, N.; Frutos, R. P.; Gallou, F.; Wang, X.-j.; Wei, X.; Simpson, R. D.; Feng, X.; Fuchs, V.; Xu, Y.; Tan, J.; Zhang, L.; Xu, J.; Smith-Keenan, L. L.; Vitous, J.; Ridges, M. D.; Spinelli, E. M.; Johnson, M.; Donsbach, K.; Nicola, T.; Brenner, M.; Winter, E.; Kreye, P.; Samstag, W. *J. Org. Chem.* **2006**, *71*, 7133-7145; (f) Daniewski, A. R.; Liu, W.; Püntener, K.; Scalone, M. *Org. Process Res. Dev.* **2002**, *6*, 220-224; (g) Herr, R. J.; Fairfax, D. J.; Meckler, H.; Wilson, J. D. *Org. Process Res. Dev.* **2002**, *6*, 677-681.

(7) (a) Barnard, C. F. J. *Organometallics* **2008**, *27*, 5402-5422; (b) Garrou, P. E.; Heck, R. F. *J. Am. Chem. Soc.* **1976**, *98*, 4115-4127; (c) Portnoy, M.; Milstein, D. *Organometallics* **1993**, *12*, 1655-1664; (d) Portnoy, M.; Milstein, D. *Organometallics* **1993**, *12*, 1655-1664; (e) Parshall, G. W. *J. Am. Chem. Soc.* **1974**, *96*, 2360-2366.; (e) Torborg, C.; Beller, M. *Adv. Synth. Catal.* **2009**, *351*, 3027-3043; (f) Kubota, Y.; Hanaoka, T.-a.; Takeuchi, K.; Sugi, Y. *J. Mol. Catal. A: Chem.* **1996**, *111*, L187-L192; (g) Satoh, T.; Ikeda, M.; Miura, M.; Nomura, M. *J. Mol. Catal. A: Chem.* **1996**, *111*, 25-31; (h) Moser, W. R.; Wang, A. W.; Kildahl, N. K. *J. Am. Chem. Soc.* **1988**, *110*, 2816-2820.

(8) (a) Hamann, B. C.; Hartwig, J. F. *J. Am. Chem. Soc.* **1998**, *120*, 7369-7370; (b) Qadir, M.; Möchel, T.; Hii, K. K. *Tetrahedron* **2000**, *56*, 7975-7979.

(9) (a) Ozawa, F.; Kawasaki, N.; Okamoto, H.; Yamamoto, T.; Yamamoto, A. *Organometallics* **1987**, *6*, 1640-1651; (b) Yamamoto, A.; Ozawa, F.; Osakada, K.; Huang, L.; Son, T. I.; Kawasaski, N.; Doh, M. K. *Pure Appl. Chem.* **1991**, *63*, 687-696.

(10) Keim, W. Angew. Chem. Int. Ed. 1990, 29, 235-244.

(11) Lascelles, K.; Morgan, L. G.; Nicholls, D.; Beyersmann, D. In *Ullmann's Encyclopedia of Industrial Chemistry*; Wiley-VCH Verlag GmbH & Co. KGaA: 2000.

(12) Yamamoto, K.; Sato, K. *Bull. Chem. Soc. Jpn.* **1954**, *27*, 389-392.

(13) a) Mizoroki, T.; Nakayama, M. *Bull. Chem. Soc. Jpn.* **1967**, *40*, 2203-2203; (b) Nakayama, M.; Mizoroki, T. *Bull. Chem. Soc. Jpn.* **1969**, *42*, 1124-1129; (c) Nakayama, M.; Mizoroki, T. *Bull. Chem. Soc. Jpn.* **1970**, *43*, 569-572; (d) Nakayama, M.; Mizoroki, T. *Bull. Chem. Soc. Jpn.* **1971**, *44*, 508-513.

(14) (a) Cassar, L.; Foà, M. *J. Organomet. Chem.* **1973**, *51*, 381-393; (b) Cassar, L.; Foà, M. *Inorg. Nucl. Chem. Lett.* **1970**, *6*, 291-294.

(15) Amer, I.; Alper, H. *J. Org. Chem.* **1988**, *53*, 5147-5148.

(16) Giannoccaro, P.; Pannacciulli, E. *J. Organomet. Chem.* **1987**, *319*, 119-127.

(17) Prichard, W. W. J. Am. Chem. Soc. 1956, 78, 6137-6139.

(18) (a) Fang, W.; Zhu, H.; Deng, Q.; Liu, S.; Liu, X.; Shen, Y.; Tu, T. *Synthesis* **2014**, *46*, 1689-1708; (b) Brennfuehrer, A.; Neumann, H.; Beller, M. *Angew. Chem. Int. Ed.* **2009**, *48*, 4114-4133; (c) Wu, X.-F.; Fang, X.; Wu, L.; Jackstell, R.; Neumann, H.; Beller, M. *Acc. Chem. Res.* **2014**, *47*, 1041-1053; (d) Skoda-Foldes, R.; Kollar, L. *Current Organic Chemistry* **2002**, *6*, 1097-1119; (e) Gadge, S. T.; Bhanage, B. M. *RSC Advances* **2014**, *4*, 10367-10389; (f) Wu, X.-F.; Neumann, H.; Beller, M. *Chem. Rev.* **2013**, *113*, 1-35; (g) Barnard, C. F. J. *Organometallics* **2008**, *27*, 5402-5422; (h) Beller, M.; Wu, X.-F. *Transition Metal Catalyzed Carbonylation Reactions*; Springer: Berlin Heidelberg, 2013; (i) Wu, L.; Fang, X.; Liu, Q.; Jackstell, R.; Beller, M.; Wu, X.-F. *ACS Catal.* **2014**, *4*, 2977-2989; (j) Wu, X.-F. *RSC Advances* **2016**, *6*, 83831-83837.

(19) Fang, W.; Zhu, H.; Deng, Q.; Liu, S.; Liu, X.; Shen, Y.; Tu, T. *Synthesis* **2014**, *46*, 1689-1708.

(20) Mägerlein, W.; Beller, M.; Indolese, A. F. *J. Mol. Catal. A: Chem.* **2000**, *156*, 213-221.

(21) Kulkarni, S. M.; Kelkar, A. A.; Chaudhari, R. V. *Chem. Commun.* **2001**, 1276-1277.

(22) Klaus, S.; Neumann, H.; Zapf, A.; Strübing, D.; Hübner, S.; Almena, J.; Riermeier, T.; Groß, P.; Sarich, M.; Krahnert, W.-R.; Rossen, K.; Beller, M. *Angew. Chem. Int. Ed.* **2006**, *45*, 154-158.

(23) Neumann, H.; Brennführer, A.; Groß, P.; Riermeier, T.; Almena, J.; Beller, M. *Adv. Synth. Catal.* **2006**, *348*, 1255-1261.

(24) (a) Wu, X.-F.; Neumann, H.; Beller, M. *Chem. Eur. J.* **2010**, *16*, 9750-9753; (b) Wu, X.-F.; Neumann, H.; Beller, M. *ChemCatChem* **2010**, *2*, 509-513.

(25) (a) Ehrentraut, A.; Zapf, A.; Beller, M. *Synlett* **2000**, *2000*, 1589-1592; (b) Zapf, A.; Ehrentraut, A.; Beller, M. *Angew. Chem. Int. Ed.* **2000**, *39*, 4153-4155; (c) Köllhofer, A.; Pullmann, T.; Plenio, H. *Angew. Chem. Int. Ed.* **2003**, *42*, 1056-1058.

(26) Wu, X. F.; Neumann, H.; Beller, M. *Chem. Eur. J.* **2010**, *16*, 12104-12107.

(27) Schranck, J.; Tlili, A.; Neumann, H.; Alsabeh, P. G.; Stradiotto, M.; Beller, M. *Chem. Eur. J.* **2012**, *18*, 15592-15597.

(28) Neumann, H.; Brennführer, A.; Beller, M. *Chem. Eur. J.* **2008**, *14*, 3645-3652;

(29) Neumann, H.; Brennführer, A.; Beller, M. *Adv. Synth. Catal.* **2008**, *350*, 2437-2442.

(30) Sharif, M.; Pews-Davtyan, A.; Lukas, J.; Schranck, J.; Langer, P.; Rolfs, A.; Beller, M. *Eur. J. Org. Chem.* **2014**, *2014*, 222-230.

(31) For reviews on CO surrogate use in carbonylation reactions, see: (a) Friis, S. D.; Lindhardt, A. T.; Skrydstrup, T. *Acc. Chem. Res.* **2016** *49*, 594-605; (b) Morimoto, T.; Kakiuchi, K. *Angew. Chem. Int. Ed.* **2004**, *43*, 5580-5588; (c) Wu, L.; Liu, Q.; Jackstell, R.; Beller, M. *Angew. Chem. Int. Ed.* **2014**, *53*, 6310-6320; (d) Gautam, P.; Bhanage, B. M. *Catal. Sci. Technol.* **2015**, *5*, 4663-4702.

(32) (a) Bjerglund, K.; Lindhardt, A. T.; Skrydstrup, T. *J. Org. Chem.* **2012**, *77*, 3793-3799; (b) Hermange, P.; Gøgsig, T. M.; Lindhardt, A. T.; Taaning, R. H.; Skrydstrup, T. *Org. Lett.* **2011**, *13*, 2444-2447.

(33) (a) Cacchi, S.; Morera, E.; Ortar, G. *Tetrahedron Lett.* **1984**, *25*, 2271-2274; (b) Cacchi, S.; Morera, E.; Ortar, G. *Tetrahedron Lett.* **1985**, *26*, 1109-1112; (c) Cacchi, S.; Ciattini, P. G.; Morera, E.; Ortar, G. *Tetrahedron Lett.* **1986**, *27*, 3931-3934; (d) Cacchi, S.; Lupi, A. *Tetrahedron Lett.* **1992**, *33*, 3939-3942.

(34) Dolle, R. E.; Schmidt, S. J.; Kruse, L. I. *J. Chem. Soc., Chem. Commun.* **1987**, 904-905.

(35) Gerlach, U.; Wollmann, T. *Tetrahedron Lett.* **1992**, *33*, 5499-5502.

(36) (a) Baillargeon, V. P.; Stille, J. K. *J. Am. Chem. Soc.* **1986**, *108*, 452-461; (b) Brennführer, A.; Neumann, H.; Beller, M. *Synlett* **2007**, *2007*, 2537-2540.

(37) Wu, X.-F.; Neumann, H.; Beller, M. *Chem. Asian J.* **2010**, *5*, 2168-2172.

(38) Wu, X.-F.; Neumann, H.; Beller, M. *Angew. Chem. Int. Ed.* **2010**, *49*, 5284-5288.

(39) Wu, X.-F.; Sundararaju, B.; Neumann, H.; Dixneuf, P. H.; Beller, M. *Chem. Eur. J.* **2011**, *17*, 106-110.

(40) (a) Ben-David, Y.; Portnoy, M.; Milstein, D. *J. Am. Chem. Soc.* **1989**, *111*, 8742-8744; (b) Portnoy, M.; Milstein, D. *Organometallics* **1993**, *12*, 1655-1664.

(41) Ben-David, Y.; Portnoy, M.; Milstein, D. *J. Chem. Soc., Chem. Commun.* **1989**, 1816-1817.

(42) Kim, J. S.; Sen, A. *J. Mol. Catal. A: Chem.* **1999**, *143*, 197-201.

(43) (a) Mägerlein, W.; Indolese, A. F.; Beller, M. *Angew. Chem. Int. Ed.* **2001**, *40*, 2856-2859; (b) Mägerlein, W.; Indolese, A. F.; Beller, M. *J. Organomet. Chem.* **2002**, *641*, 30-40.

(44) Martinelli, J. R.; Clark, T. P.; Watson, D. A.; Munday, R. H.; Buchwald, S. L. *Angew. Chem. Int. Ed.* **2007**, *46*, 8460-8463.

(45) Jimenez-Rodriguez, C.; Eastham, G. R.; Cole-Hamilton, D. J. *Dalt. Trans.* **2005**, 1826-1830.

(46) Perry, R. J.; Wilson, B. D. *J. Org. Chem.* **1996**, *61*, 7482-7485.

(47) Bessard, Y.; Roduit, J. P. *Tetrahedron* **1999**, *55*, 393-404.

(48) Beller, M.; Mägerlein, W.; Indolese, A. F.; Fischer, C. *Synthesis* **2001**, *2001*, 1098-1109.

(49) Albaneze-Walker, J.; Bazaral, C.; Leavey, T.; Dormer, P. G.; Murry, J. A. *Org. Lett.* **2004**, *6*, 2097-2100.

(50) Blaser, H.-U.; Diggelmann, M.; Meier, H.; Naud, F.; Scheppach, E.; Schnyder, A.; Studer, M. *J. Org. Chem.* **2003**, *68*, 3725-3728.

(51) Arthuis, M.; Lecup, A.; Roulland, E. *Chem. Commun.* **2010**, *46*, 7810-7812.

(52) For reviews on non-catalytic MCRs, see (a) Dömling, A.; Ugi, I. *Angew. Chem. Int. Ed.* **2000**, *39*, 3168-3210; (b) Ramón, D. J.; Yus, M. *Angew. Chem. Int. Ed.* **2005**, *44*, 1602-1634; (c) Ruijter, E.; Scheffelaar, R.; Orru, R. V. A. *Angew. Chem. Int. Ed.* **2011**, *50*, 6234-6246; (d) Dömling, A. *Chem. Rev.* **2006**, *106*, 17-89; (e) Toure, B. B.; Hall, D. G. *Chem. Rev.* **2009**, *109*, 4439-4486; (f) Estevez, V.; Villacampa, M.; Menendez, J. C. *Chem. Soc. Rev.* **2010**, *39*, 4402-4421; (g) Levi, L.; Muller, T. J. J. *Chem. Soc. Rev.* **2016**, *45*, 2825-2846; (h) Sunderhaus, J. D.; Martin, S. F. *Chem. Eur. J.* **2009**, *15*, 1300-1308; (i) Balme, G.; Bossharth, E.; Monteiro, N. *Eur. J. Org. Chem.* **2003**, 4101-4111.

(53) For reviews on transition metal catalyzed MCRs, see: (a) (b) Balme, G. *Angew. Chem. Int. Ed.* **2004**, *43*, 6238-6241; (c) Beller, M.; Eckert, M. *Angew. Chem. Int. Ed.* **2000**, *39*, 1010-1027; (d) Gibson, S. E.; Mainolfi, N. *Angew. Chem. Int. Ed.* **2005**, *44*, 3022-3037; (e) Gibson, S. E.; Stevenazzi, A. *Angew. Chem. Int. Ed.* **2003**, *42*, 1800-1810; (f) Mihovilovic, M. D.; Stanetty, P. *Angew. Chem. Int. Ed.* **2007**, *46*, 3612-3615; (g) Balme, G.; Bouyssi, D.; Mont, N. In *Multicomponent Reactions*; Zhu, J., Bienaymé, H., Eds.; Wiley-VCH: Weinheim, 2005, p 224-276; (h) Ros, A.; Matas, I. In *Multicomponent Reactions*; John Wiley & Sons, Inc: 2015, p 72-126; (i) Lorenzini, F.; Tjutrins, J.; Quesnel, J. S.; Arndtsen, B. A. In *Multicomponent Reactions in Organic Synthesis*; Wiley-VCH Verlag GmbH & Co. KGaA: 2014, p 207-230; (j) Arndtsen, B. A.; Tjutrins, J. In *Science of Synthesis, Multicomponent Reactions*; Georg Thieme Verlag: 2014; Vol. 2, p 475-533.

(54) Shen, C.; Wu, X.-F. *Chem. Eur. J.* **2017**, *23*, 2973-2987.

(55) Kalinin, V. N.; Shostakovsky, M. V.; Ponomaryov, A. B. *Tetrahedron Lett.* **1990**, *31*, 4073-4076.

(56) Yang, Q.; Alper, H. *J. Org. Chem.* **2010**, *75*, 948-950.

(57) (a) Torii, S.; Okumoto, H.; Xu, L. H. *Tetrahedron Lett.* **1991**, *32*, 237-240; (b) Kalinin, V. N.; Shostakovsky, M. V.; Ponomaryov, A. B. *Tetrahedron Lett.* **1992**, *33*, 373-376; (c) Torii, S.; Okumoto, H.; Xu, L. H.; Sadakane, M.; Shostakovsky, M. V.; Ponomaryov, A. B.; Kalinin, V. N. *Tetrahedron* **1993**, *49*, 6773-6784.

(58) Shen, C.; Spannenberg, A.; Wu, X.-F. *Angew. Chem. Int. Ed.* **2016**, *55*, 5067-5070.

(59) (a) Larksarp, C.; Alper, H. *Org. Lett.* **1999**, *1*, 1619-1622; (b) Salvadori, J.; Balducci, E.; Zaza, S.; Petricci, E.; Taddei, M. *J. Org. Chem.* **2010**, *75*, 1841-1847; (c) Zheng, Z.; Alper, H. *Org. Lett.* **2009**, *11*, 3278-3281.

(60) Cacchi, S.; Fabrizi, G.; Marinelli, F. *Synlett* **1996**, *1996*, 997-998; (b) Wu, X.-F.; Schranck, J.; Neumann, H.; Beller, M. *Chem. Eur. J.* **2011**, *17*, 12246-12249.

(61) Zheng, Z.; Alper, H. *Org. Lett.* **2008**, *10*, 829-832.

(62) Okuro, K.; Alper, H. *J. Org. Chem.* **1997**, *62*, 1566-1567; (b) Xiao, W.-J.; Alper, H. *J. Org. Chem.* **1999**, *64*, 9646-9652; (c) Ye, F.; Alper, H. *J. Org. Chem.* **2007**, *72*, 3218-3222; (d) Grigg, R.; Liu, A.; Shaw, D.; Suganthan, S.; Woodall, D. E.; Yoganathan, G. *Tetrahedron Lett.* **2000**, *41*, 7125-7128.

(63) (a) Kadnikov, D. V.; Larock, R. C. *Org. Lett.* **2000**, *2*, 3643-3646; (b) Kadnikov, D. V.; Larock, R. C. *J. Organomet. Chem.* **2003**, *687*, 425-435; (c) Kadnikov, D. V.; Larock, R. C. *J. Org. Chem.* **2003**, *68*, 9423-9432; (d) Kadnikov, D. V.; Larock, R. C. *J. Org. Chem.* **2004**, *69*, 6772-6780; (e) Cao, H.; Xiao, W.-J. *Can. J. Chem.* **2005**, *83*, 826-831.

(64) Cao, H.; McNamee, L.; Alper, H. *Org. Lett.* **2008**, *10*, 5281-5284.

(65) Grigg, R.; Sridharan, V.; Thayaparan, A. *Tetrahedron Lett.* **2003**, *44*, 9017-9019.

(66) (a) He, L.; Li, H.; Neumann, H.; Beller, M.; Wu, X.-F. *Angew. Chem.* **2014**, *126*, 1444-1448; (b) Natte, K.; Neumann, H.; Wu, X.-F. *Catal. Sci. Technol.* **2015**, *5*, 4474-4480.

(67) (a) Li, H.; Li, W.; Spannenberg, A.; Baumann, W.; Neumann, H.; Beller, M.; Wu, X.-F. *Chem. Eur. J.* **2014**, *20*, 8541-8544; (b) Chen, J.; Neumann, H.; Beller, M.; Wu, X.-F. *Org. Biomol. Chem.* **2014**, *12*, 5835-5838; (c) Wu, X.-F.; He, L.; Neumann, H.; Beller, M. *Chem. Eur. J.* **2013**, *19*, 12635-12638; (d) Shen, C.; Man, N. Y. T.; Stewart, S.; Wu, X.-F. *Org. Biomol. Chem.* **2015**, *13*, 4422-4425; (e) Gabriele, B.; Plastina, P.; Salerno, G.; Mancuso, R.; Costa, M. *Org. Lett.* **2007**, *9*, 3319-3322; (f) Gabriele, B.; Veltri, L.; Salerno, G.; Mancuso, R.; Costa, M. *Adv. Synth. Catal.* **2010**, *352*, 3355-3363; (g) Gabriele, B.; Veltri, L.; Maltese, V.; Spina, R.; Mancuso, R.; Salerno, G. *Eur. J. Org. Chem.* **2011**, *2011*, 5626-5635.

(68) (a) Zeng, F.; Alper, H. *Org. Lett.* **2010**, *12*, 5567-5569; (b) Chouhan, G.; Alper, H. *Org. Lett.* **2009**, *12*, 192-195.

(69) Cao, H.; Vieira, T. O.; Alper, H. *Org. Lett.* **2010**, *13*, 11-13.

(70) Mohamed Ahmed, M. S.; Kobayashi, K.; Mori, A. *Org. Lett.* **2005**, *7*, 4487-4489.

(71) (a) Stonehouse, J. P.; Chekmarev, D. S.; Ivanova, N. V.; Lang, S.; Pairaudeau, G.; Smith, N.; Stocks, M. J.; Sviridov, S. I.; Utkina, L. M. *Synlett* **2008**, *2008*, 100-104; (b) Iranpoor, N.; Firouzabadi, H.; Etemadi-Davan, E. *Tetrahedron Lett.* **2016**, *57*, 837-840.

(72) Li, Z.; Liu, J.; Huang, Z.; Yang, Y.; Xia, C.; Li, F. *ACS Catal.* **2013**, *3*, 839-845.

(73) (a) Deni; Nordmann, J.; Dziambor, J.; Mayer, B.; Frank, W.; Muller, T. J. J. *RSC Advances* **2015**, *5*, 33838-33854; (b) Moni, L.; Denißen, M.; Valentini, G.; Müller, T. J. J.; Riva, R. *Chem. Eur. J.* **2015**, *21*, 753-762; (c) Merkul, E.; Boersch, C.; Frank, W.; Müller, T. J. J. *Org. Lett.* **2009**, *11*, 2269-2272; (d) Karpov, A. S.; Merkul, E.; Rominger, F.; Müller, T. J. J. *Angew. Chem. Int. Ed.* **2005**, *44*, 6951-6956.

(74) (a) Torii, S.; Xu, L. H.; Sadakane, M.; Okumoto, H. *Synlett* **1992**, *1992*, 513-514; (b) Abbiati, G.; Arcadi, A.; Canevari, V.; Capezzuto, L.; Rossi, E. *J. Org. Chem.* **2005**, *70*, 6454-6460.

(75) Staben, S. T.; Blaquiere, N. *Angew. Chem. Int. Ed.* **2010**, *49*, 325-328.

(76) (a) Dhawan, R.; Dghaym, R. D.; Arndtsen, B. A. *J. Am. Chem. Soc.* **2003**, *125*, 1474-1475; (b) Arndtsen, B. A. *Chem. Eur. J.* **2009**, *15*, 302-313.

(77) Dhawan, R.; Arndtsen, B. A. *J. Am. Chem. Soc.* **2004**, *126*, 468-469.

(78) Siamaki, A. R.; Arndtsen, B. A. *J. Am. Chem. Soc.* **2006**, *128*, 6050-6051.

(79) Dghaym, R. D.; Dhawan, R.; Arndtsen, B. A. *Angew. Chem. Int. Ed.* **2001**, *40*, 3228-3230.

(80) (a) Worrall, K.; Xu, B.; Bontemps, S.; Arndtsen, B. A. *J. Org. Chem.* **2011**, *76*, 170-180; (b) Xu, B.; Worrall, K.; Arndtsen, B. A. *Molecules* **2012**, *17*, 13759-13768.

(81) Dhawan, R.; Dghaym, R. D.; St. Cyr, D. J.; Arndtsen, B. A. *Org. Lett.* **2006**, *8*, 3927-3930.

(82) Quesnel, J. S.; Arndtsen, B. A. *J. Am. Chem. Soc.* **2013**, *135*, 16841-16844.

(83) Bontemps, S.; Quesnel, J. S.; Worrall, K.; Arndtsen, B. A. *Angew. Chem. Int. Ed.* **2011**, *50*, 8948-8951.

(84) (a) Torres, G. M.; De La Higuera Macias, M.; Quesnel, J. S.; Williams, O. P.; Yempally, V.; Bengali, A. A.; Arndtsen, B. A. *J. Org. Chem.* **2016**; (b) Torres, G. M.; Quesnel, J. S.; Bijou, D.; Arndtsen, B. A. *J. Am. Chem. Soc.* **2016**, *138*, 7315-7324; (c) Firoozi, N.; Torres, G. M.; Arndtsen, B. A. *J. Org. Chem.* **2016**, *81*, 11145-11152.

(85) (a) Gadge, S. T.; Gautam, P.; Bhanage, B. M. *The Chemical Record* **2016**, *16*, 835-856; (b) Wu, X.-F.; Barnard, C. F. J. In *New Trends in Cross-Coupling: Theory and Applications*; The Royal Society of Chemistry: 2015, p 479-520; (c) Beller, M.; Wu, X.-F. In *Transition Metal Catalyzed Carbonylation Reactions*; Springer: Berlin Heidelberg, 2013, p 113-132; (d) Chen, J.; Wu, X.-F. In *Transition Metal-Catalyzed Heterocycle Synthesis via C-H Activation*; Wiley-VCH Verlag GmbH & Co. KGaA: 2016, p 467-504; (e) Lang, R.; Xia, C.; Li, F. *New Journal of Chemistry* **2014**, *38*, 2732-2738.

(86) (a) Shi, Z.; Yu, J.-Q. In *C-H activation*; Springer: Berlin, 2010; (b) Hartwig, J. F. *Acc. Chem. Res.* **2012**, *45*, 864-873; (c) Jia, C.; Kitamura, T.; Fujiwara, Y. *Acc. Chem. Res.* **2001**, *34*, 633-639; (d) Neufeldt, S. R.; Sanford, M. S. *Acc. Chem. Res.* **2012**, *45*, 936-946; (e) Yamaguchi,

J.; Yamaguchi, A. D.; Itami, K. *Angew. Chem. Int. Ed.* **2012**, *51*, 8960-9009; (f) Alberico, D.; Scott, M. E.; Lautens, M. *Chem. Rev.* **2007**, *107*, 174-238; (g) Lyons, T. W.; Sanford, M. S. *Chem. Rev.* **2010**, *110*, 1147-1169; (h) Davies, H. M. L.; Du Bois, J.; Yu, J.-Q. *Chem. Soc. Rev.* **2011**, *40*, 1855-1856; (i) Wencel-Delord, J.; Droge, T.; Liu, F.; Glorius, F. *Chem. Soc. Rev.* **2011**, *40*, 4740-4761.

(87) (a) Lapointe, D.; Fagnou, K. *Chemistry Letters* **2010**, *39*, 1118-1126; (b) Liégault, B.; Lapointe, D.; Caron, L.; Vlassova, A.; Fagnou, K. *J. Org. Chem.* **2009**, *74*, 1826-1834; (c) Liégault, B.; Petrov, I.; Gorelsky, S. I.; Fagnou, K. *J. Org. Chem.* **2010**, *75*, 1047-1060.

(88) Fujiwara, Y.; Kawauchi, T.; Taniguchi, H. *J. Chem. Soc., Chem. Commun.* **1980**, 220-221.

(89) (a) Fujiwara, Y.; Kawata, I.; Kawauchi, T.; Taniguchi, H. *J. Chem. Soc., Chem. Commun.* **1982**, 132-133; (b) Fujiwara, Y.; Kawata, I.; Sugimoto, H.; Taniguchi, H. *J. Organomet. Chem.* **1983**, *256*, C35-C36; (c) Jintoku, T.; Fujiwara, Y.; Kawata, I.; Kawauchi, T.; Taniguchi, H. *J. Organomet. Chem.* **1990**, *385*, 297-306.

(90) (a) Itahara, T. *Chemistry Letters* **1982**, *11*, 1151-1152; (b) Itahara, T. *Chemistry Letters* **1983**, *12*, 127-128.

(91) (a) Jaouhari, R.; Dixneuf, P. H.; Lécolier, S. *Tetrahedron Lett.* **1986**, *27*, 6315-6318; (b) Ugo, R.; Chiesa, A.; Nardi, P.; Psaro, R. *J. Mol. Catal.* **1990**, *59*, 23-31.

(92) (a) Ohashi, S.; Sakaguchi, S.; Ishii, Y. *Chem. Commun.* **2005**, 486-488; (b) Yamada, S.; Sakaguchi, S.; Ishii, Y. *J. Mol. Catal. A* **2007**, *262*, 48-51; (c) Yamada, S.; Ohashi, S.-i.; Obora, Y.; Sakaguchi, S.; Ishii, Y. *J. Mol. Catal. A* **2008**, *282*, 22-27.

(93) Zhang, H.; Liu, D.; Chen, C.; Liu, C.; Lei, A. *Chem. Eur. J.* **2011**, *17*, 9581-9585.

(94) (a) Lang, R.; Shi, L.; Li, D.; Xia, C.; Li, F. *Org. Lett.* **2012**, *14*, 4130-4133; (b) Xing, Q.; Shi, L.; Lang, R.; Xia, C.; Li, F. *Chem. Commun.* **2012**, *48*, 11023-11025.

(95) For reviews on Chelation assisted C-H activation, see: (a) Colby, D. A.; Bergman, R. G.; Ellman, J. A. *Chem. Rev.* **2010**, *110*, 624-655; (b) Ackermann, L. *Chem. Rev.* **2011**, *111*, 1315-1345; (c) Arockiam, P. B.; Bruneau, C.; Dixneuf, P. H. *Chem. Rev.* **2012**, *112*, 5879-5918; (d) Engle, K. M.; Mei, T.-S.; Wasa, M.; Yu, J.-Q. *Acc. Chem. Res.* **2012**, *45*, 788-802.

(96) (a) Orito, K.; Horibata, A.; Nakamura, T.; Ushito, H.; Nagasaki, H.; Yuguchi, M.; Yamashita, S.; Tokuda, M. *J. Am. Chem. Soc.* **2004**, *126*, 14342-14343; (b) Orito, K.; Miyazawa,

M.; Nakamura, T.; Horibata, A.; Ushito, H.; Nagasaki, H.; Yuguchi, M.; Yamashita, S.; Yamazaki, T.; Tokuda, M. *J. Org. Chem.* **2006**, *71*, 5951-5958.

(97) Haffemayer, B.; Gulias, M.; Gaunt, M. J. *Chem. Sci.* **2011**, *2*, 312-315.

(98) (a) Lopez, B.; Rodriguez, A.; Santos, D.; Albert, J.; Ariza, X.; Garcia, J.; Granell, J. *Chem. Commun.* **2011**, *47*, 1054-1056; (b) Albert, J.; Ariza, X.; Calvet, T.; Font-Bardia, M.; Garcia, J.; Granell, J.; Lamela, A.; López, B.; Martinez, M.; Ortega, L.; Rodriguez, A.; Santos, D. *Organometallics* **2013**, *32*, 649-659.

(99) Rajeshkumar, V.; Lee, T.-H.; Chuang, S.-C. *Org. Lett.* **2013**, *15*, 1468-1471.

(100) (a) Liang, D.; Hu, Z.; Peng, J.; Huang, J.; Zhu, Q. *Chem. Commun.* **2013**, *49*, 173-175; (b) Liang, Z.; Zhang, J.; Liu, Z.; Wang, K.; Zhang, Y. *Tetrahedron* **2013**, *69*, 6519-6526.

(101) Guan, Z.-H.; Chen, M.; Ren, Z.-H. *J. Am. Chem. Soc.* **2012**, *134*, 17490-17493.

(102) Li, W.; Duan, Z.; Jiang, R.; Lei, A. *Org. Lett.* **2015**, *17*, 1397-1400.

(103) Li, W.; Duan, Z.; Zhang, X.; Zhang, H.; Wang, M.; Jiang, R.; Zeng, H.; Liu, C.; Lei, A. *Angew. Chem. Int. Ed.* **2015**, *54*, 1893-1896.

(104) Yoo, E. J.; Wasa, M.; Yu, J.-Q. *J. Am. Chem. Soc.* **2010**, *132*, 17378-17380.

(105) Willcox, D.; Chappell, B. G. N.; Hogg, K. F.; Calleja, J.; Smalley, A. P.; Gaunt, M. J. *Science* **2016**, *354*, 851-857.

(106) (a) Giri, R.; Yu, J.-Q. *J. Am. Chem. Soc.* **2008**, *130*, 14082-14083; (b) Giri, R.; Yu, J.-Q. *J. Am. Chem. Soc.* **2008**, *130*, 14082-14083; (c) Lu, Y.; Leow, D.; Wang, X.; Engle, K. M.; Yu, J.-Q. *Chem. Sci.* **2011**, *2*, 967-971; (d) Dai, H.-X.; Stepan, A. F.; Plummer, M. S.; Zhang, Y.-H.; Yu, J.-Q. *J. Am. Chem. Soc.* **2011**, *133*, 7222-7228.

(107) (a) Luo, S.; Luo, F.-X.; Zhang, X.-S.; Shi, Z.-J. *Angew. Chem. Int. Ed.* **2013**, *52*, 10598-10601; (b) Lee, T.-H.; Jayakumar, J.; Cheng, C.-H.; Chuang, S.-C. *Chem. Commun.* **2013**, *49*, 11797-11799.

(108) (a) Wrigglesworth, J. W.; Cox, B.; Lloyd-Jones, G. C.; Booker-Milburn, K. I. *Org. Lett.* **2011**, *13*, 5326-5329; (b) Houlden, C. E.; Hutchby, M.; Bailey, C. D.; Ford, J. G.; Tyler, S. N. G.; Gagné, M. R.; Lloyd-Jones, G. C.; Booker-Milburn, K. I. *Angew. Chem. Int. Ed.* **2009**, *48*, 1830-1833.

(109) Campo, M. A.; Larock, R. C. *Org. Lett.* **2000**, *2*, 3675-3677.

(110) Campo, M. A.; Larock, R. C. *J. Org. Chem.* **2002**, *67*, 5616-5620.

(111) Zhang, H.; Shi, R.; Gan, P.; Liu, C.; Ding, A.; Wang, Q.; Lei, A. *Angew. Chem. Int. Ed.* **2012**, *51*, 5204-5207.

(112) Wu, X.-F.; Anbarasan, P.; Neumann, H.; Beller, M. *Angew. Chem. Int. Ed.* **2010**, *49*, 7316-7319.

(113) Lian, Z.; Friis, S. D.; Skrydstrup, T. *Chem. Commun.* **2015**, *51*, 1870-1873.

Chapter 2. A Palladium-Catalyzed Synthesis of (Hetero)Aryl-Substituted Imidazoles from Aryl Halides, Imines and Carbon Monoxide

2.1. Preface

As described in chapter 1 (Section 1.3.3), the Arndtsen research group has previously reported a palladium catalyzed synthesis of Münchnones from aryl iodides, carbon monoxide and imines. This transformation was applied to the multicomponent synthesis of pyrroles and β-lactams. In this chapter, we describe the extension of this approach to prepare imidazoles in a single palladium catalyzed operation from aryl iodides, two imines and two equivalents of CO. Mechanistic studies show that the reaction involves an initial catalytic carbonylative coupling of aryl halides with imines to form a 1,3-dipole, which undergo a spontaneous 1,3-dipolar cycloaddition with an electron deficient N-tosyl imine. Overall, this offers an alternative to more classical cross coupling or C-H bond functionalization reactions to construct the (hetero)aryl-imidazole motif, where variation of the building blocks can allow the synthesis of broad families of imidazoles with independent control of all substituents. This work has been published *Chemical Science* (**2016**, 8, 1002-1007).

2.2. Introduction

The aryl-(hetero)aryl motif is among the most common structural motifs found in pharmaceutical design.[1] An important example of these are aryl- and heteroaryl-substituted imidazoles, which are key units in a diverse range of anti-inflammatory[2] and other pharmaceutically relevant agents,[3] as well as electronic materials,[4] polymers,[5] metal coordinating ligands,[6] and other areas of application.[7] Traditional approaches to assemble aryl-substituted imidazoles involve the cyclization of pre-synthesized diamines with electrophiles.[8] While effective, these require the initial multistep synthesis of the substituted precursors, and can suffer from poor regioselectivity. In this regard, the rapid rise in the use of cross-coupling reactions with heterocycles has had a tremendous impact. These commonly exploit the reaction of halogenated imidazoles with organometallic reagents (scheme 2.1a).[9] More recently, efforts by a number of research groups have demonstrated that cross-coupling can be replaced with even more efficient metal catalyzed C-H bond functionalization (scheme 2.1b).[10] The latter obviate

the need to pre-activate the imidazole unit and the use metallated coupling partners, and instead can employ the broad range of commercially available (hetero)aryl halides.

Despite the many attractive features of coupling reactions, there remain drawbacks to their use in assembling substituted imidazoles. Perhaps most importantly, intrinsic to this chemistry is the need for the pre-formed, substituted imidazole for use in bond formation. These must be prepared, often by classical cyclization chemistry, and can make the systematic tuning of the imidazole core an involved process. Other routes to imidazoles have been developed,[11] including our own Pd-catalyzed synthesis with *N*-acyl iminium salts,[11b] but these also often involve reactive and/or synthetic reagents.

a) Metal-Catalyzed Cross-Coupling Reactions

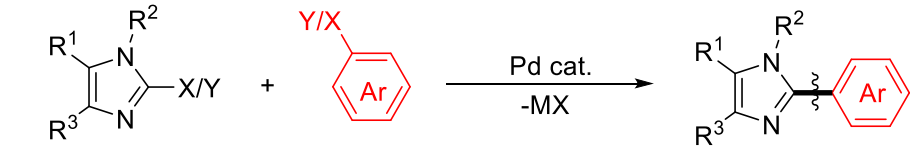

(X = Br, I; Y = $SnBu_3$, $B(OH)_2$, ZnI)

b) Metal-Catalyzed C-H Coupling Reactions

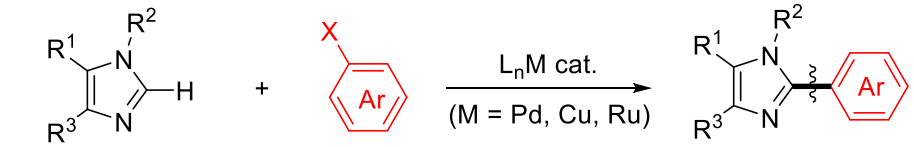

c) This work: Tandem Catalytic Imidazole Synthesis

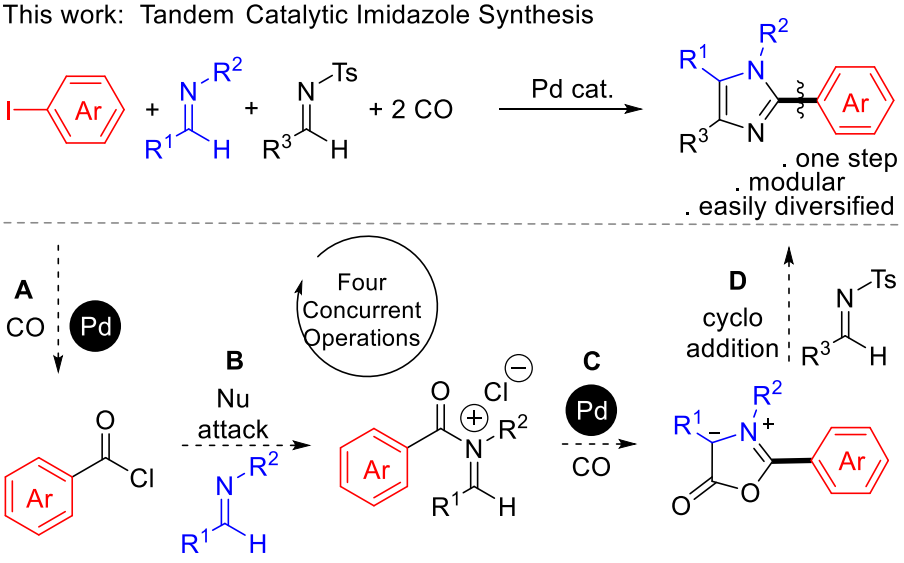

Scheme 2.1. Transition Metal-Catalyzed Approaches to Aryl-Substituted Imidazoles.

In principle, a more flexible method to generate these products would be to assemble the aryl-imidazole bond at the same time as the heterocycle. A potential approach to such a synthesis is to exploit tandem catalysis. Tandem catalytic reactions have seen growing interest due to their ability to generate multiple bonds through a series of spontaneous catalytic operations.[12] We questioned if these features might be applied to design a synthesis of imidazoles from aryl halides, via the reaction illustrated in Figure 2.1c.

We have recently shown that aryl halides can undergo palladium catalyzed carbonylation into reactive acid chlorides.[13] Performing this reaction in the presence of an imine can initiate a second carbonylation and the overall generation of 1,3-dipolar Münchnones.[14] An interesting facet of the latter reaction is its ability to generate a reactive, 1,3-dipole intermediate from an aryl halide, which has the ability to undergo cycloaddition.[15] The overall sequence in Figure 2.1c would offer what is to our knowledge a rare example of a tandem catalytic reaction involving five separate reagents.[16] While each of these steps has precedent, the complete transformation requires the performance of two separate palladium catalyzed carbonylation reactions (**A** and **C**), together with nucleophilic attack (**B**) and cycloaddition (**D**) with perfect selectivity. Similarly, the catalyst, multiple reagents, reactive intermediates, coordinating product and two separate imines must all be compatible and react in sequence in a single reaction mixture.

We describe below our efforts towards this goal. This has led to a novel route to assemble imidazoles from combinations of substrates that are available, easily diversified and stable (aryl halides, two imines and CO). The catalytic reaction proceeds with high chemoselectivity, and opens an alternative to coupling reactions to prepare aryl-imidazoles from aryl halides, where variation of the substrates can allow the formation of broad families of products.

2.3. Results and Discussion

Our initial studies involved the $Pd(P^tBu_3)_2$ catalyzed coupling of aryl iodide with the two imines shown in Table 2.1, based upon our previous observations of the activity of these catalysts in aryl iodide carbonylation. This led to minimal product after several days at elevated temperatures (entry 1). Modulation of the reaction conditions did not favor the reaction, nor did

changing the palladium coordinating ligand (entries 2-5, see Table 2.5 for full catalyst development). We have previously noted that the presence of chloride can dramatically accelerate carbonylations with aryl iodides by allowing the *in situ* build-up of acid chlorides.[13] Similarly, the addition of Bu_4NCl, or the even more straightforward use of $[Pd(allyl)Cl]_2$ as the catalyst and chloride sources allowed the formation of imidazole **2.1a** in moderate yield (entries 6,7). No subsequent optimization improved this yield.

Closer examination of the reaction mixture shows that the *N*-benzyl imine is fully consumed, suggesting that the initial catalytic carbonylation cycle may be effective, but subsequent steps are inhibited. We suspected that this may arise from the formation of the sulfinate byproduct of cycloaddition. Control experiments show that the addition of stoichiometric sodium sulfinate completely blocks catalysis.[17] Attempts to improve the reaction yield by varying this leaving group did not increase the yield of imidazole (entries 8-10), nor did the addition of potential sulfinate trapping agents.[18] However, the simple change of making the *N*-tosyl imine the limiting reagent dramatically improved catalysis (entry 11). From a synthetic perspective this proved useful, as *N*-tosyl imines are the most valuable building blocks in the reaction. Under these conditions, imidazole **2.1a** is formed in high yield and with the exclusive incorporation of two separate imines (*vide infra*).

In considering the substrates employed in this reaction, we next questioned if even more broadly available and inexpensive aryl bromides might also be employed in the catalytic sequence. A challenge in the use of aryl bromides is the required use of pressing conditions required to activate the Ar-Br bond, which must be compatible with the sensitive iminium salt or Münchnone intermediates generated in this reaction. However, after probing various reaction conditions (see Table 2.6 for details), we have found that the rapid trapping of the intermediates to imidazoles (*vide infra*) can allow this tandem catalytic sequence to be performed with aryl bromides, and affords imidazole with similar efficiency (entry 13).

Table 2.1. Catalyst Development for the Generation of Aryl-Imidazoles[a]

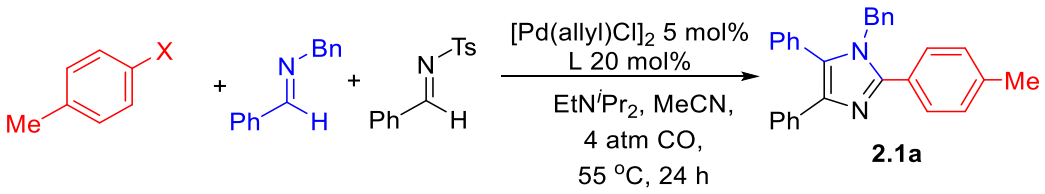

entry	L	**2.1a** (%)[b]	entry	L	**2.1a** (%)[b]
X = I					
1	$Pd(P^tBu_3)_2$	4	6[b]	$Pd(P^tBu_3)_2$	43
2	P(*o*-tolyl)$_3$	5	7	P^tBu_3	42
3	DPPE	-	8[c]	P^tBu_3	-
4		7	9[d]	P^tBu_3	30
			10[e]	P^tBu_3	12
5		7	11[f]	P^tBu_3	77 (75)[g]
X = Br					
12[b,f]	$Pd(P^tBu_3)_2$	-	13[b,f,h]	P^tBu_3	73 (65)[i]

[a]*p*-iodotoluene (109 mg, 0.50 mmol), PhC=NBn (20 mg, 0.10 mmol), PhC=NTs (31 mg, 0.12 mmol), $[Pd(allyl)Cl]_2$ (0.005 mmol), L (0.02 mmol), EtN^iPr_2 (0.3 mmol), 0.7 mL CD_3CN, 4 atm CO. b 10% $Pd(P^iBu_3)_2$, 0.1 mmol Bu_4NCl. [c]PhC=NMs. [d]PhC=$NSO_2C_6H_4Cl$. [e]PhC=NNs. [f]*p*-halotoluene (0.3 mmol), PhC=NBn (39 mg, 0.2 mmol). [g]isolated; [h]95 °C, 25 atm CO, 20 % P^tBu_3. [i]4 atm CO.

A feature of this catalytic synthesis is its ability to generate substituted imidazoles from combinations of building blocks that can be easily diversified. This can allow for the modular assembly of a diverse range of these products (Table 2.2 and Table 2.3).

Table 2.2. Diversity of the Imine Reaction Partner

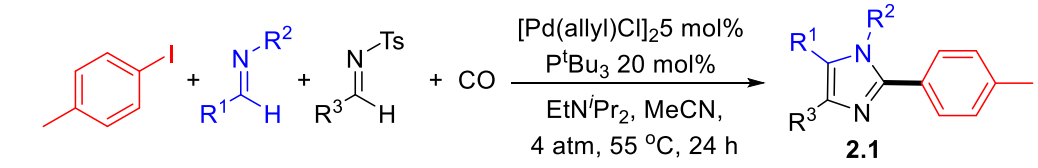

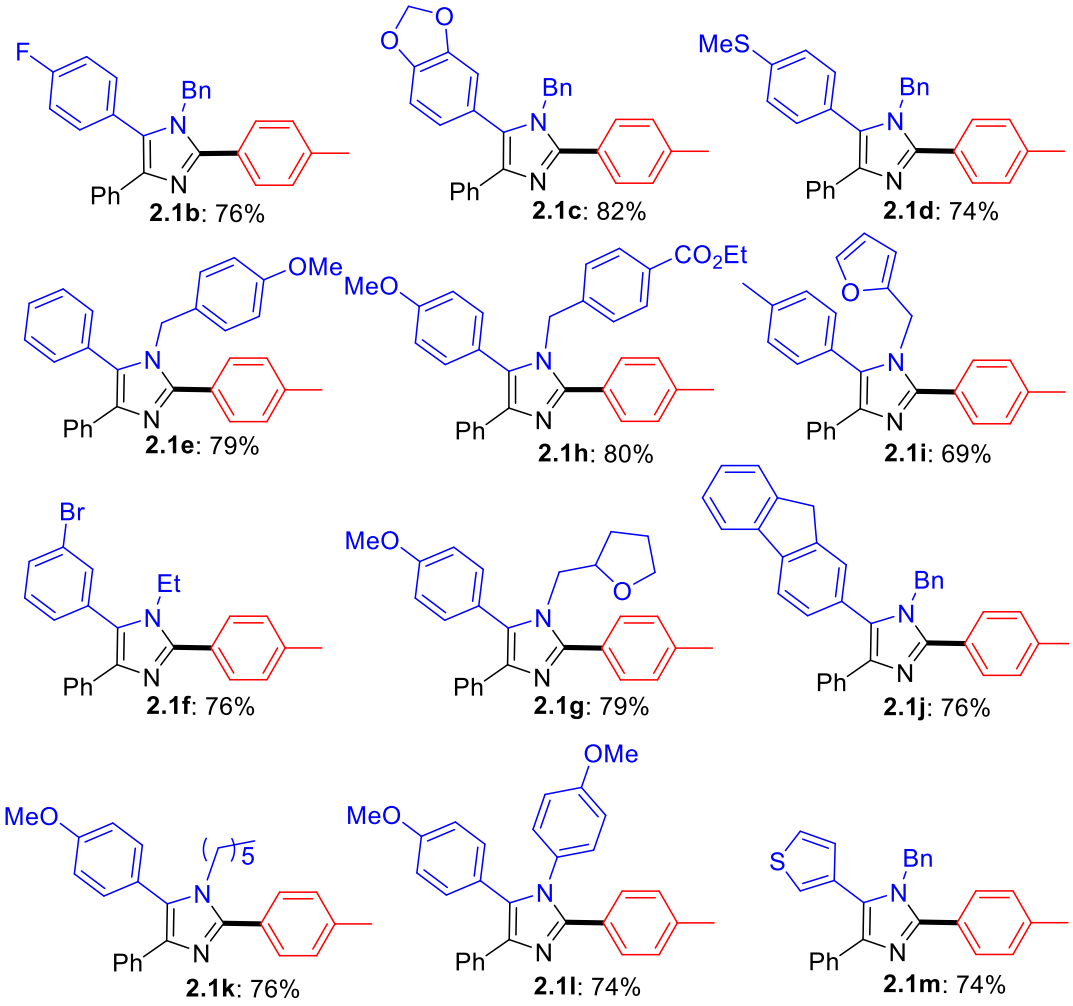

[a]aryl iodide (327 mg, 1.50 mmol), imine (1.0 mmol), N-Ts imine (0.50 mmol), $[Pd(allyl)Cl]_2$ (9 mg, 0.025 mmol), $PtBu_3$ (20 mg, 0.10 mmol), EtN^iPr_2 (194 mg, 1.50 mmol), MeCN (2.0 mL), 4 atm CO, 55 °C, 24h. [b]N-Ts imine added after Münchnone formation.

Table 2.3. Diversity of the N-Ts Imine Reaction Partner

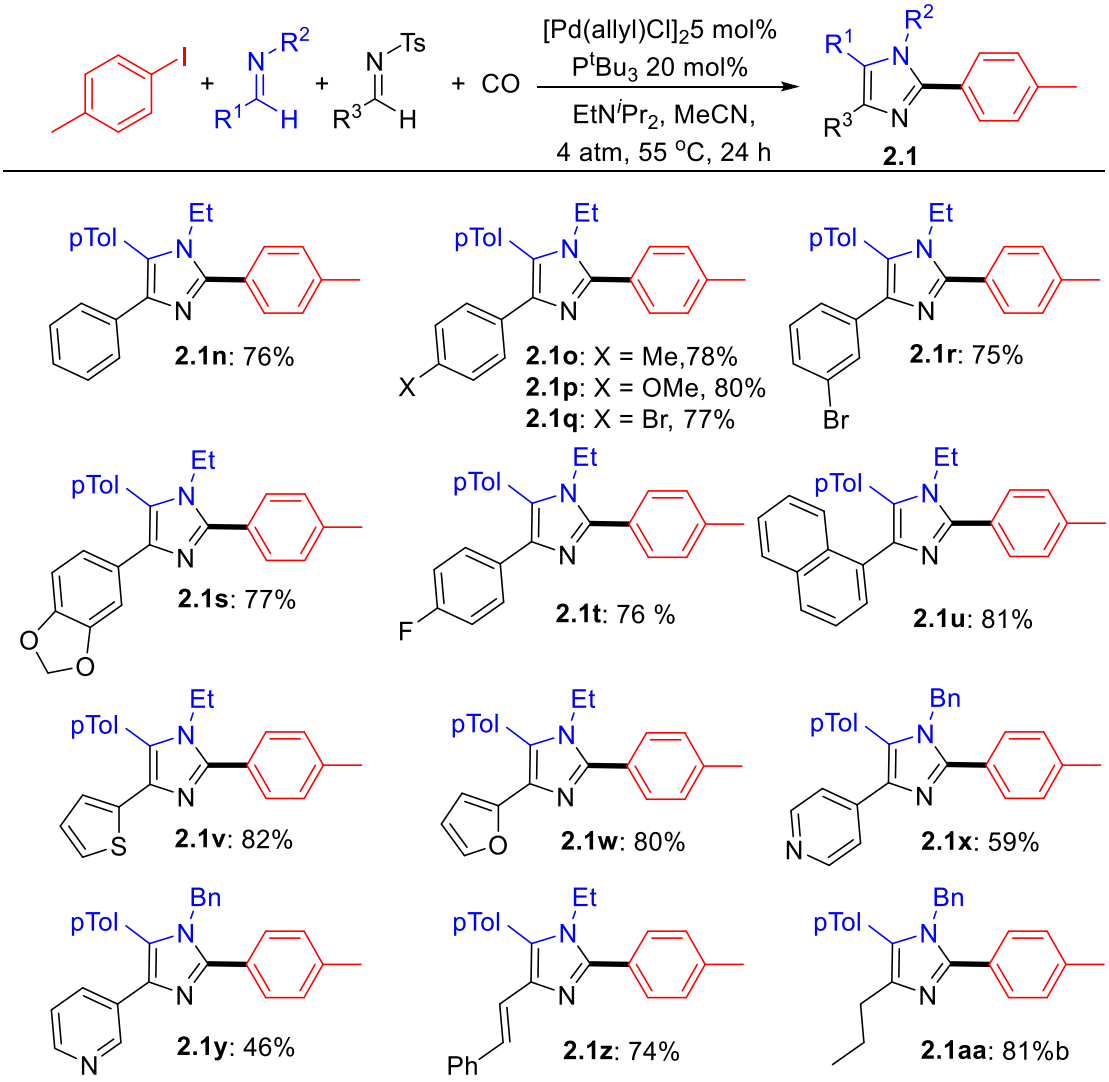

[a]aryl iodide (327 mg, 1.50 mmol), imine (1.0 mmol), N-Ts imine (0.50 mmol), $[Pd(allyl)Cl]_2$ (9 mg, 0.025 mmol), $PtBu_3$ (20 mg, 0.10 mmol), EtN^iPr_2 (194 mg, 1.50 mmol), MeCN (2.0 mL), 4 atm CO, 55 °C, 24h. [b]N-Ts imine added after Münchnone formation.

For example, a number of simple imines can be incorporated into the reaction, including those with phenyl substituents on the imine carbon, electron deficient aromatics (**2.1b**,**f**) those with donor substituents (**2.1c**,**d**,**h**,**k**) as well as heterocyclic imines (**2.1m**). Each of these form imidazoles in good yields. Similarly, those with various *N*-alkyl, -benzyl and -aryl substituents are viable partners, as are those with heteroaromatic units. The *N*-tosyl substituted imine can be even more widely diversified as a tool to modulate the 4-imidazole position. Examples of these latter can involve electron rich or electron deficient aromatics (**2.1n-t**) or naphthyl substituents

(**2.1u**). α,β-Unsataturated *N*-tosyl imines are also viable substrates, as are those with heteroaromatic (thiophene, furan, pyridine) units (**2.1w-z**). The reaction also tolerates the use of enolizable, *C*-alkyl substituted *N*-tosyl imines (**2.1aa**). Since the latter imine is thermally unstable, it was added to the reaction mixture after the catalytic formation of Münchnone.

Table 2.4. Scope of Aryl Halide Reaction Partner

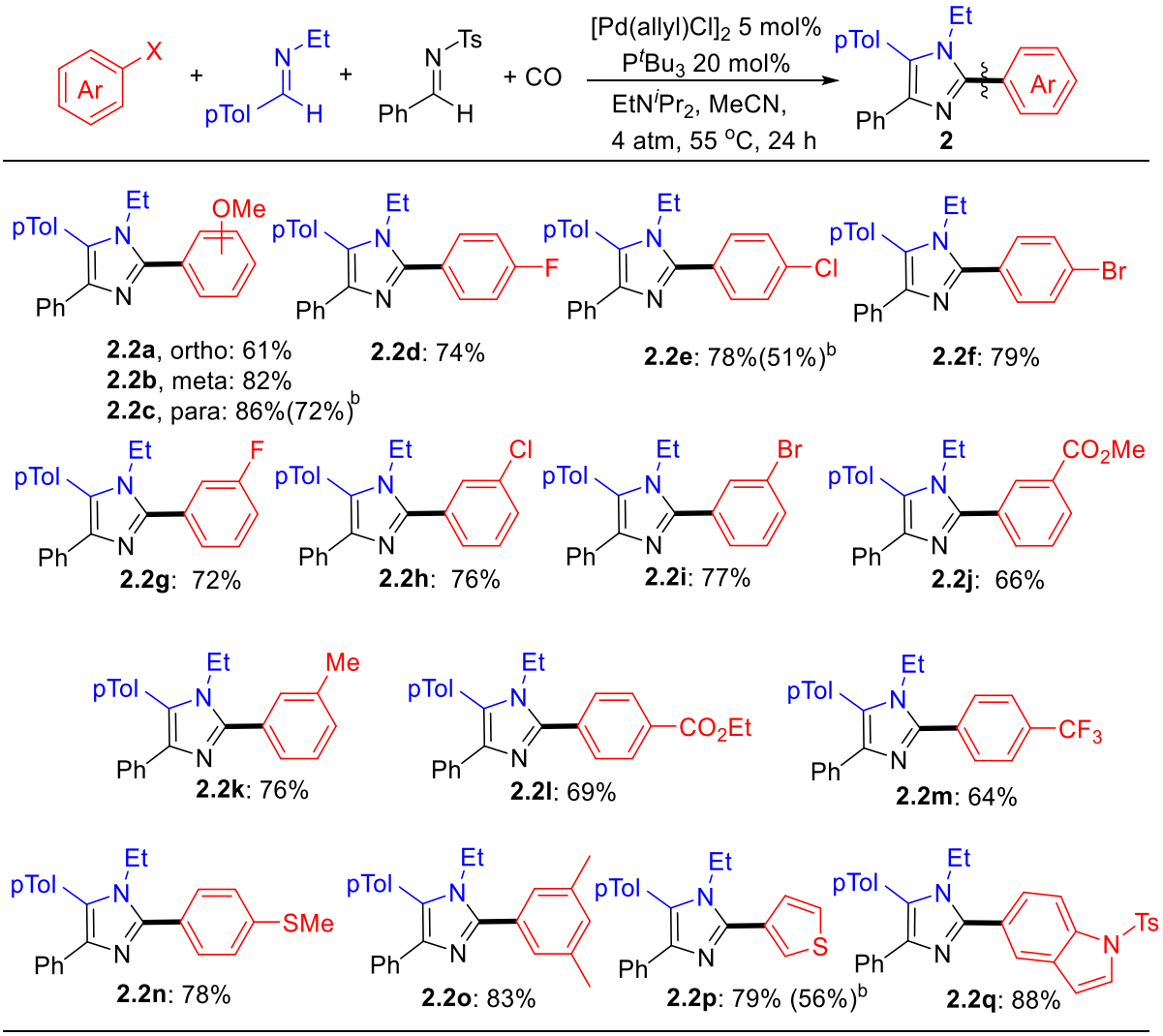

[a]Reaction conditions of Table 2.2. [b]Reaction performed with aryl bromide.

As shown in Table 2.4, the aryl iodide coupling partner can also be modulated in this transformation. As representative examples, various para-, meta-, and even sterically encumbered ortho-substituents can be incorporated onto the aryl-iodide or -bromide (**2.2a-n**), as can those with palladium reactive functionalities (**2.2d-i**). Electron rich aryl halides generally

lead to slightly higher yields (**2.2c,n,o**), but electron withdrawing substituents are also viable reagents. However, aryl halides with *ortho*-substituents other than a MeO- group are not viable reaction partners (e.g. 2-bromoiodobenzene, 2-chloroiodobenzene), potentially due to the slow oxidative addition of the N-acyl iminium salt to Pd(0). Similarly, *p*-CN and *p*-CHO substituted aryl iodides generate a mixture of products, including what is preliminarily characterized as the same isoindolinones as reported in chapter 3 (*vide infra*). This chemistry can be extended to the use of heteroaryl iodides, such as those with thiophene and indole units (**2.2p,q**). When combined with the diversity of imine(s) that can be employed, this transformation provides what is to our knowledge a novel method to prepare imidazoles from aryl halides, where every substituent can be varied at the same time as the imidazole-(hetero)aryl bond is generated.

We have performed preliminary studies to probe the mechanism of this catalytic reaction. Monitoring the reaction by ^{1}H and ^{31}P NMR analysis shows the build-up of palladium-aroyl complex **2.3** (Scheme 2.2) as the catalyst resting state, suggesting the elimination of acid chloride (step **A**) is rate determining in catalysis.[19] This data is consistent with the results in Table 2.1, where the sterically encumbered P^{t}Bu$_3$ ligand and a chloride source are both required for efficient catalysis, as they can favor acid chloride reductive elimination.[13] Once acid chloride is formed, it presumably reacts rapidly with the imine to form an *N*-acyl iminium salt. *In situ* ^{1}H NMR analysis shows no evidence for iminium salt **2.4**, and likely reflects its more rapid oxidative addition to palladium than aryl iodide for subsequent cyclocarbonylation to Münchnone (step **C**). The final cycloaddition of *N*-tosyl imine leads to the liberation of sulfinate. ^{1}H NMR analysis shows that this sulfinate is rapidly trapped with iminium salt to form PhCON(Bn)CH(*p*-Tol)Ts (**2.5**), and does not therefore block either of the two palladium catalyzed carbonylation cycles. The high imine selectivity in this system presumably arises from their different electronic characteristics, wherein the poorly nucleophilic *N*-tosyl imine cannot react with acid chloride to form iminium salt. Conversely, once Münchnone is generated, it undergoes selective 1,3-dipolar cycloaddition with the more electron deficient imine and aromatization.

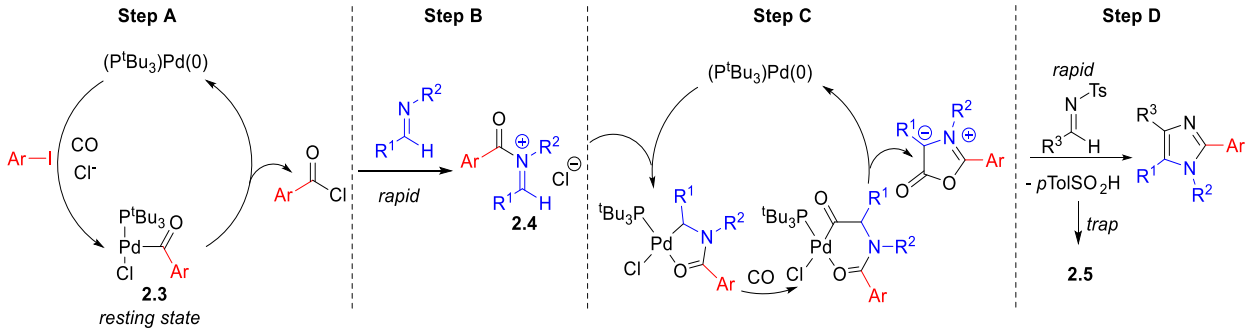

Scheme 2.2. Catalytic Cascade to Generate (Hetero)Aryl-Substituted Imidazoles.

Finally, as an illustration of the potential utility of this transformation, we have probed its use in more targeted synthesis. Imidazole **2.6** (Scheme 2.3) has attracted attention as a potent Tie2 kinase inhibitor.[20] While **2.6** is typically prepared via cyclization of preformed polysubstituted ketones, this palladium catalyzed platform can allow access to the imidazole core of **2.6** directly from combinations of two imines, CO and aryl iodide. The modularity of this catalytic reaction should in principle allow facile access to variants of this product, by systematic tuning of either the imine or aryl halide building blocks.

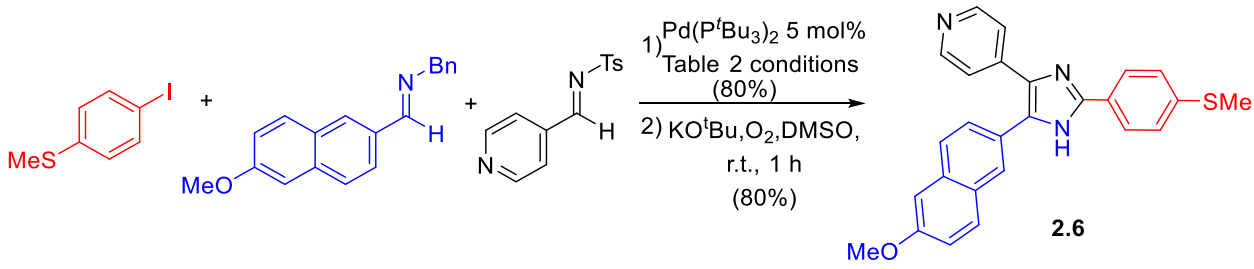

Scheme 2.3. Aryl Iodide Carbonylative Synthesis of Imidazole 2.6.

2.4. Conclusions

In conclusion, we have described a new palladium-based tandem catalytic transformation that can allow the generation of polysubstituted imidazoles from combinations of imines, aryl halides and carbon monoxide. This provides an alternative route to prepare the (hetero)aryl-

substituted imidazoles, where the imidazole unit is generated at the same time as the aryl-heteroaryl bond. The reaction proceeds with high selectivity, and allows the build-up of these products in one operation, from available substrates, and with independent control of all substituents.

2.5. Supporting Information

2.5.1. General Considerations

All reactions were carried out under an inert atmosphere in a glovebox or using standard Schlenk techniques, unless otherwise indicated. Research grade carbon monoxide (99.99%) was used as received. All solvents were dried using a solvent purification system and stored in glovebox over activated 4 Å molecular sieves. Deuterated solvents were dried over CaH_2, vacuum transferred and stored over 4 Å molecular sieves. N-alkyl, N-aryl imines, and N-tosyl imines were prepared according to literature procedures.[21-24] All other reagents were purchased from commercial suppliers and used as received. All ^1H and ^{13}C NMR spectra were acquired on 400 and 500 MHz spectrometers. High resolution mass spectra were obtained using a quadrupole-time of flight and an Orbitrap detector by direct infusion in positive ESI mode.

2.5.2. Synthetic Procedures

Typical Procedure for Catalyst Screening (Table 2.1.)

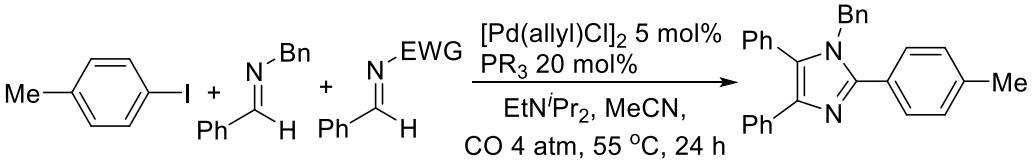

In a glovebox, 4-iodotoluene (109 mg, 0.50 mmol), PhC=NBn (20 mg, 0.10 mmol), PhC=NTs (31 mg, 0.12 mmol), EtN^iPr_2 (40 mg, 0.3 mmol), $[Pd(allyl)Cl]_2$ (2 mg, 0.005 mmol), P^tBu_3 (4 mg, 0.02 mmol), and benzyl benzoate internal standard were dissolved in CD_3CN (0.7 mL) and added to a J-Young NMR tube. The tube was removed from the glovebox, frozen in liquid

nitrogen, the headspace evacuated, and 4 atm carbon monoxide was condensed into the NMR tube. (Procedure: The CO manifold shown in Figure 2.1 has a volume of 67 mL. This was evacuated, filled with 760 torr CO, then closed to the CO tank, and the valve to the liquid nitrogen frozen NMR tube was opened until CO pressure in the manifold dropped by 120 torr (0.45 mmol) due to condensation of CO into the NMR tube. As the headspace of the NMR tube is 2.5 mL, this corresponds to 4 atm CO). The reaction was then heated at 55 ^{o}C and monitored by ^{1}H NMR spectroscopy. The yield of **2.1a** (43%) was determined by ^{1}H NMR analysis relative to the internal standard. Also, monitoring the reaction during the course of catalysis by ^{1}H and ^{31}P NMR shows the generation of the palladium complex (^{t}Bu$_3$P)Pd(CO*p*-Tol)Cl (^{31}P NMR: 73.1 ppm) as the major observable phosphine-containing intermediate, and the formation of (N-benzylbenzamido)(phenyl)methyl 4-methylbenzenesulfinate **2.5** in 48% yield at the end of catalysis. The results of screening of other ligands, reagents and additives to the reaction are shown in Table 2.5 below.

Figure 2.1. Experimental Setup for Condensation of CO in to a J-Young Tube.

Table 2.5. Catalyst Development for Generation of Aryl-Imidazoles from Aryl Iodides

Entry	PR_3	EWG	Yield, %	Entry	PR_3	EWG	Additive	Yield, %
1	$Pd(P^tBu_3)_2$	Ts	4	10	$Pd(P^tBu_3)_2$	Ts	Bu_4NCl	43
2	PPh_3	Ts	0	11	P^tBu_3	Ts		42
3	PCy_3	Ts	0	12	P^tBu_3	$SO_2C_6H_4Cl$		30
4	$P(o\text{-Tol})_3$	Ts	5	13	P^tBu_3	NS		12
5	DPPE	Ts	0	14	P^tBu_3	Ms		0
6		Ts	7	15	P^tBu_3	Ts		0
7	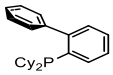	Ts	7	16	P^tBu_3	Ts	*n*-propyl-Br	0
8	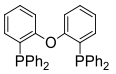	Ts	0	17	P^tBu_3	Ts	TMSCl	32
9		Ts	8	18	P^tBu_3	Ts		77 (75)

Typical Procedure for Catalyst Screening with Aryl Bromides (Table 2.1.)

In a glovebox, 4-bromotoluene (68 mg, 0.40 mmol), PhC=NBn (40 mg, 0.20 mmol), PhC=NTs (26 mg, 0.12 mmol), EtN^iPr_2 (40 mg, 0.3 mmol), $Pd(P^tBu_3)_2$ (5 mg, 0.01 mmol), Bu_4NCl (28 mg, 0.1 mmol), P^tBu_3 (4 mg, 0.02 mmol), and benzyl benzoate internal standard were dissolved in MeCN (1 mL) in a vial with a loosely capped screw cap and added to a high-pressure reactor. The reactor was removed from the glovebox, and was pressurized with 25 atm carbon monoxide. The reaction was heated at 95 °C for 24 h. The reaction was then cooled to room temperature, carbon monoxide was removed and all volatiles were evaporated in vacuo. The yield of **2.1a** (73%) was determined by ^1H NMR analysis relative to the internal standard. The results of screening other conditions and additives is provided in Table 2.6.

Table 2.6. Catalyst Development for Generation of Aryl-Imidazoles from Aryl Bromides

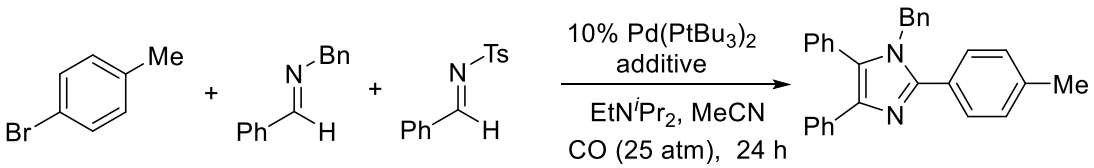

Entry	Temp., °C	Additive	Yield, %
1[a]	85	-	31%
2	75	1.0 eq. Bu_4NCl	35%
3	85	1.0 eq. Bu_4NCl	36%
4	95	1.0 eq. Bu_4NCl	39%
5	95	0.1 eq. Bu_4NCl	31%
6	95	0.1 eq. Bu_4NCl 20 mol% P^tBu_3	40%
7[b]	95	1.0 eq. Bu_4NCl, 20 mol% P^tBu_3	72%
8[c]	95	1.0 eq. Bu_4NCl, 20 mol% P^tBu_3	65%
9	95	1.0 eq. Bu_4NCl, 20 mol% P^tBu_3	73%

[a] $[Pd(allyl)Cl]_2/P^tBu_3$ used as catalyst. [b] 10 eq. of *p*-bromotoluene. [c] CO pressure 4 atm.

Typical Synthesis of Imidazoles (Tables 2.2. and 2.3.)

In a glovebox, 4-iodotoluene (327 mg, 1.50 mmol), PhC=NBn (98 mg, 1.00 mmol), Ph=NTs (130 mg, 0.50 mmol), NEt^iPr_2 (194 mg, 1.50 mmol), $[Pd(allyl)Cl]_2$ (9 mg, 0.025 mmol), P^tBu_3 (20 mg, 0.10 mmol) were combined in acetonitrile (2 mL) and added to a 50 mL Teflon sealed, thick walled glass reaction vessel. The vessel was closed, removed from the glovebox, and pressurized to 4 atm CO. (Procedure: The 50 mL glass reaction vessel was connected to a CO gas cylinder via a rubber hose that was also connected to a vacuum manifold (see Figure 2.2). The hose was evacuated and backfilled with carbon monoxide 3 times. Afterwards, the reaction vessel was opened to the line, and pressurized to 4 atm (4 bar) of carbon monoxide according to the outlet pressure gauge on the regulator for the gas cylinder.) The reaction was heated at 55 °C for 24 h. After the reaction was cooled to room temperature, all volatiles were removed in vacuo. The crude product was purified by column chromatography (silica gel, gradient hexane / ethyl

acetate 4% to 20% with 1 % Et_3N additive) affording pure imidazole **2.1a** as a pale yellow solid in 75% yield (151 mg).

For the synthesis of **1aa**, the reaction was performed as above without the initial addition of the *N*-tosyl imine. After the reaction was complete, the CO was removed, the pressure vessel was brought back into glovebox and freshly synthesized (propyl)HC=NTs (225 mg, 1.00 mmol) in 1 mL acetonitrile was added to the reaction mixture. This imine was prepared as previously reported.[23] (Procedure: a solution 4-methyl-N-(1-tosylbutyl)benzenesulfonamide (762 mg, 2.0 mmol) in EtOAc (25 mL) was treated with aqueous NaOH (1M, 25 mL) for 45 seconds. The organic solution was collected, and the solvent removed in vacuo to afford the imine (propyl)HC=NTs as a colorless oil. This was brought into the glovebox and weighed for use.) The reaction heated at 55 °C for 5 h, then cooled to room temperature, and all volatiles were removed in vacuo. The crude product was purified by column chromatography (silica gel, gradient hexane / ethyl acetate 4% to 20% with 1 % Et_3N additive) affording imidazole **2.1aa** as a colorless oil in 81% yield (155 mg).

Figure 2.2. Experimental Setup for Carbonylation Reactions (1-4 atm).

Procedure for the Synthesis of Imidazoles from Aryl Bromides

In a glovebox, 4-bromotoluene (342 mg, 2.0 mmol), Ph=NBn (195 mg, 1.0 mmol), PhC=NTs (130 mg, 0.5 mmol), EtN^iPr_2 (193 mg, 1.5 mmol), $[Pd(P^tBu_3)_2$ (12 mg, 0.025 mmol), P^tBu_3 (10 mg, 0.1 mmol), and benzyl benzoate internal standard were combined in MeCN (5.0 mL) and added to a 50 mL Anton-Paar high-pressure reactor. The reactor was removed from the glovebox and pressurized to 25 atm CO. (Procedure: The high-pressure reactor was connected to a multiwell Anton-Paar system through a steel hose (see Figure 2.3). The tubing of the Anton-Paar system was evacuated and backfilled with CO 3 times. Afterwards, the high-pressure reactor was opened to the multiwell system and was pressurized with 25 atm carbon monoxide according to the digital pressure sensor reader.) The reactor was closed, and the reaction was heated at 95 °C

for 24 h in an oil bath. The reaction was then cooled to room temperature, carbon monoxide was removed and all volatiles were evaporated in vacuo. The crude product was purified by column chromatography (silica gel, gradient hexane / ethyl acetate 4% to 20% with 1 % Et_3N additive) affording pure imidazole **2.1a** as a pale yellow solid in 70% yield (140.0 mg).

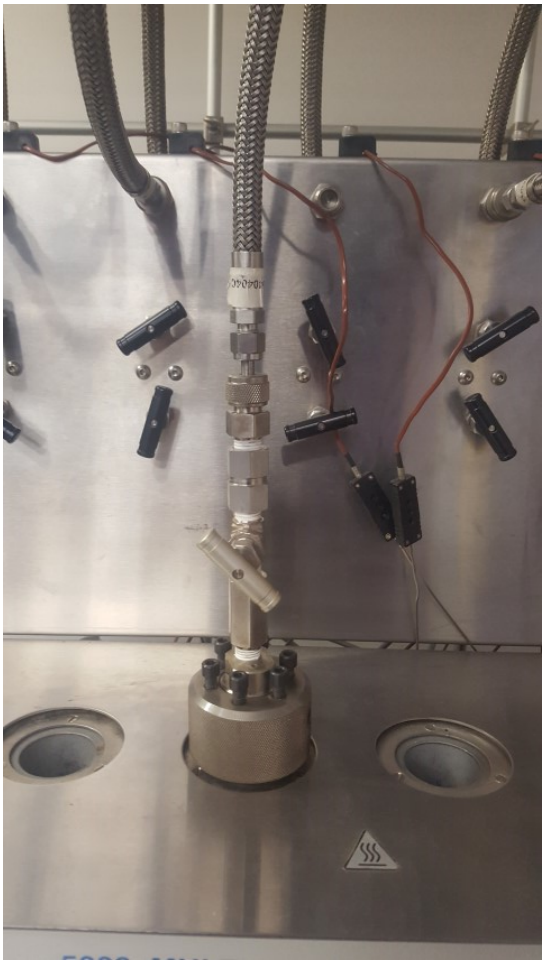

Figure 2.3. Experimental Setup for High Pressure Carbonylation Reactions (5-100 atm).

Procedure for the Synthesis of 4-(5-(6-methoxynaphthalen-2-yl)-2-(4-(methylthio)phenyl)-1H-imidazol-4-yl)pyridine **2.6**.

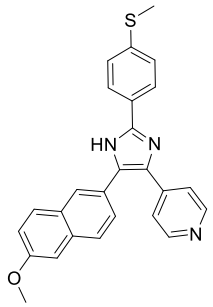

In a glovebox, 4-iodothioanisole (1000 mg, 4.0 mmol), N-benzyl-1-(6-methoxynaphthalen-2-yl)methanimine (275 mg, 1.00 mmol), NEt^iPr_2 (194 mg, 1.50 mmol), $Pd(P^tBu_3)_2$ (12 mg, 0.05 mmol), and Bu_4NCl (278 mg, 1.0 mmol) were combined in acetonitrile (15 mL) and added to a 50 mL sealable pressure vessel. The vessel was closed, removed from the glovebox, and pressurized with 4 atm of carbon monoxide. The reaction was heated at 40°C for 24 h. After the reaction was cooled to room temperature, the CO was removed on a Schlenk line, and the pressure vessel was brought into a glovebox. 4-Methyl-N-(pyridin-4-ylmethylene)benzenesulfonamide (260 mg, 1.00 mmol) was added to the crude mixture and stirred for 4 h at 40°C. Afterwards all the volatiles were removed in vacuo, and the crude mixture was purified by column chromatography (silica gel, gradient hexane / ethyl acetate 4% to 85% with 1 % Et_3N additive) affording the imidazole as a pale yellow solid in 80% yield (413 mg).

Based on literature procedure,[25] this product, [4-(1-benzyl-5-(6-methoxynaphthalen-2-yl)-2-(4-(methylthio)phenyl)-1H-imidazol-4-yl)pyridine], (102 mg, 0.2 mmol), DMSO (156 mg, 2.0 mmol) and potassium tert-butoxide (1.4 mL, 1 mol/L in THF) were combined in a flame-dried flask. The reaction was stirred and oxygen was bubbled through the solution for 1h. Upon completion, the reaction mixture was quenched with aqueous sodium carbonate solution. The THF was removed in vacuo, and the product was extracted three times with EtOAc. The organics were combined, dried and concentrated in vacuo. The crude mixture was purified by column chromatography (silica gel, gradient hexane / ethyl acetate 30% to 85%) affording the imidazole. An ethyl acetate solution of the product was washed with a saturated solution of Na_2CO_3, and then dried in vacuo to yield **6** as a pale brown solid in 80% yield (67 mg).

Reaction of N-Acyliminium Salt with Sodium *p*-Toluenesulfinate

Ph(H)C=NBn (20 mg, 0.10 mmol), benzoyl chloride (21 mg, 0.15 mmol), and benzyl benzoate internal standard were dissolved in 0.7 mL of CD_3CN and stirred at room temperature for 10 min. To this solution was added sodium *p*-toluenesulfinate (27 mg, 0.15 mmol), and the obtained mixture was heated at 55 ºC and reaction was monitored by *in situ* ^{1}H NMR. ^{1}H NMR shows generation of (N-benzylbenzamido)(phenyl)methyl 4-methylbenzenesulfinate in 52% yield after 18 h,[11c] and N-benzylbenzamide in 6% yield compared to internal standard.

2.5.3. Spectroscopic Data

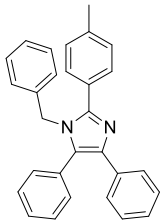

1-Benzyl-4,5-diphenyl-2-(p-tolyl)-1H-imidazole 2.1a. Pale yellow solid, 151 mg, 75% yield. ^{1}H NMR (500 MHz, $CDCl_3$) δ 7.62 (d, *J* = 7.2 Hz, 2H), 7.59 (d, *J* = 8.1 Hz, 2H), 7.34 (m, 3H), 7.27 – 7.21 (m, 9H), 7.17 (t, *J* = 7.3 Hz, 1H), 6.88 – 6.82 (m, 2H), 5.13 (s, 2H), 2.40 (s, 3H). ^{13}C NMR (126 MHz, $CDCl_3$) δ 148.2, 138.8, 138.0, 137.7, 134.6, 131.15, 131.10, 129.9, 129.3, 129.0, 128.8*, 128.6, 128.08, 128.05, 127.3, 126.8, 126.3, 126.0, 48.3, 21.4. HRMS. Calculated for $C_{29}H_{25}N_2$ ($M+H^+$): 401.2012, found: 401.1994.

*Selective HSQC NMR experiment indicates that signal at δ 128.8 ppm corresponds to two carbons.

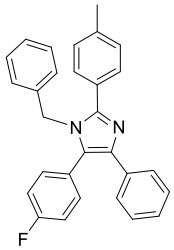

1-Benzyl-5-(4-fluorophenyl)-4-phenyl-2-(p-tolyl)-1H-imidazole 2.1b. White solid, 159 mg, 76% yield. ^{1}H NMR (500 MHz, $CDCl_3$) δ 7.59 (d, *J* = 8.2 Hz, 4H), 7.27 – 7.21 (m, 7H), 7.20 – 7.16 (m, 3H), 7.02 (t, *J* = 8.7 Hz, 2H), 6.84 (dd, *J* = 7.3, 1.9 Hz, 2H), 5.11 (s, 2H), 2.40 (s, 3H). ^{13}C NMR (126 MHz, $CDCl_3$) δ 162.84 (d, *J* = 248.8 Hz), 148.4, 139.0, 138.3, 137.5, 134.4, 133.0 (d, *J* = 8.3 Hz), 129.3, 129.1 (d, *J* = 59.9 Hz), 128.9, 128.7, 128.1, 127.9, 127.5, 127.13 (d, *J* = 3.4 Hz), 126.8, 126.5, 126.0, 115.9 (d, *J* = 21.5 Hz), 48.3, 21.4. HRMS. Calculated for $C_{29}H_{24}N_2F$ ($M+H^+$): 419.1918, found: 419.1918.

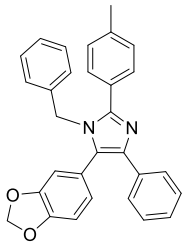

5-(Benzo[d][1,3]dioxol-5-yl)-1-benzyl-4-phenyl-2-(p-tolyl)-1H-imidazole 2.1c. Pale yellow solid, 182 mg, 82% yield. ^{1}H NMR (500 MHz, $CDCl_3$) δ 7.66 (d, *J* = 7.5 Hz, 2H), 7.57 (d, *J* = 7.8 Hz, 2H), 7.22 (m, 8H), 6.87 (d, *J* = 6.6 Hz, 2H), 6.78 (d, *J* = 7.9 Hz, 1H), 6.71 (d, *J* = 7.8 Hz, 1H), 6.67 (s, 1H), 5.99 (s, 2H), 5.13 (s, 2H), 2.39 (s, 3H). ^{13}C NMR (126 MHz, $CDCl_3$) δ 148.0, 147.9, 147.9, 138.8, 138.0, 137.7, 134.5, 129.4, 129.3, 128.9, 128.6, 128.1, 128.0, 127.4, 126.7, 126.3, 126.0, 125.1, 124.4, 111.3, 108.7, 101.3, 48.2, 21.4. HRMS. Calculated for $C_{30}H_{25}N_2O_2$ ($M+H^+$): 445.1911, found: 445.1913.

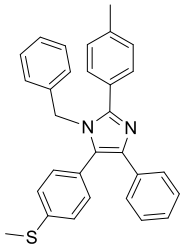

1-Benzyl-5-(4-(methylthio)phenyl)-4-phenyl-2-(p-tolyl)-1H-imidazole 2.1d. Colorless oil 165 mg, 74% yield. ^{1}H NMR (500 MHz, $CDCl_3$) δ 7.63 (d, *J* = 7.2 Hz, 2H), 7.58 (d, *J* = 8.0 Hz, 2H), 7.27 – 7.21 (m, 7H), 7.20 – 7.17 (m, 3H), 7.12 (d, *J* = 8.4 Hz, 2H), 6.84 (d, *J* = 7.8 Hz, 2H), 5.13 (s, 2H), 2.51 (s, 3H), 2.39 (s, 3H). ^{13}C NMR (126 MHz, $CDCl_3$) δ 148.0, 139.7, 137.3, 131.9, 131.3, 129.4, 129.1, 128.7, 128.2, 128.2, 127.7, 127.5, 127.2, 127.1, 127.0, 126.7, 126.2, 126.0, 124.0, 48.4, 21.4, 15.2. HRMS. Calculated for $C_{30}H_{27}N_2S$ ($M+H^+$): 447.1889, found: 447.1893.

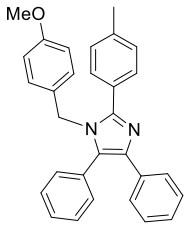

1-(4-Methoxybenzyl)-4,5-diphenyl-2-(p-tolyl)-1H-imidazole 2.1e. Pale yellow solid, 170 mg, 79% yield. ^{1}H NMR (400 MHz, $CDCl_3$) δ 7.61 (t, *J* = 7.7 Hz, 4H), 7.40 – 7.32 (m, 3H), 7.30 – 7.21 (m, 6H), 7.17 (d, *J* = 7.3 Hz, 1H), 6.80 – 6.69 (m, 4H), 5.07 (s, 2H), 3.77 (s, 3H), 2.41 (s, 3H). ^{13}C NMR (126 MHz, $CDCl_3$) δ 158.8, 148.1, 138.8, 137.9, 134.5, 131.2, 131.1, 129.9, 129.7, 129.3, 129.0, 128.8, 128.6, 128.1, 127.3, 126.8, 126.3, 113.9, 113.7, 55.2, 47.8, 21.4. HRMS. Calculated for $C_{30}H_{27}N_2O$ ($M+H^+$): 431.2118, found: 431.2125.

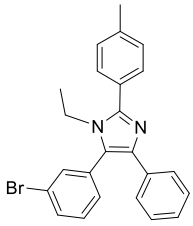

5-(3-Bromophenyl)-1-ethyl-4-phenyl-2-(p-tolyl)-1H-imidazole 2.1f. Pale yellow solid, 159 mg, 76% yield. ^{1}H NMR (500 MHz, $CDCl_3$) δ 7.89 – 7.57 (m, 3H), 7.54 (d, *J* = 7.2 Hz, 1H), 7.45 – 7.36 (m, 2H), 7.33 (d, *J* = 8.1 Hz, 2H),

7.25 (dd, *J* = 8.1, 6.8 Hz, 3H), 7.18 (t, *J* = 7.3 Hz, 1H), 7.05 (t, *J* = 7.9 Hz, 1H), 4.00 – 3.93 (m, 2H), 2.45 (s, 3H), 1.05 (t, *J* = 7.2 Hz, 3H). ^{13}C NMR (126 MHz, Chloroform-*d*) δ 148.1, 139.2, 136.7, 133.7, 133.6, 133.3, 132.1, 131.9, 130.7, 130.6, 129.9, 129.8, 129.7, 129.6, 129.4, 129.4, 129.4, 129.1, 129.0, 128.2, 128.1, 128.0, 127.5, 126.9, 126.6, 125.1, 123.0, 122.9, 122.5, 39.8, 21.4, 16.3. Calculated for $C_{24}H_{22}N_2Br$ ($M+H^+$): 417.0961, found: 417.0963.

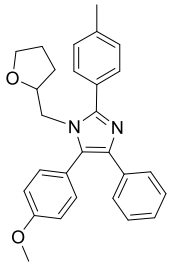

5-(4-Methoxyphenyl)-4-phenyl-1-((tetrahydrofuran-2-yl)methyl)-2-(p-tolyl)-1H-imidazole 2.1g. White solid, 168 mg, 79% yield. ^{1}H NMR (500 MHz, $CDCl_3$). δ 7.64 (d, *J* = 8.1 Hz, 2H), 7.57 (d, *J* = 7.0 Hz, 2H), 7.37 (d, *J* = 8.7 Hz, 2H), 7.32 – 7.26 (m, 2H), 7.21 (dd, *J* = 8.4, 6.9 Hz, 2H), 7.13 (t, *J* = 7.2 Hz, 1H), 7.02 (d, *J* = 8.7 Hz, 2H), 4.02 (dd, *J* = 14.3, 7.5 Hz, 2H), 3.89 (s, 3H), 3.74 (dd, *J* = 7.4, 5.7 Hz, 1H), 3.60 – 3.35 (m, 2H), 2.43 (s, 3H), 1.80 – 1.47 (m, 2H), 1.26 – 1.14 (m, 2H). ^{13}C NMR (126 MHz, $CDCl_3$) δ 159.7, 148.1, 138.5, 137.6, 134.9, 132.5, 129.4, 129.3, 129.2, 128.9, 127.9, 126.9, 126.0, 123.6, 114.5, 77.1, 67.7, 55.3, 48.5, 29.0, 25.1, 21.4. HRMS. Calculated for $C_{28}H_{29}N_2O_2$ ($M+H^+$): 425.2224, found: 425.2229.

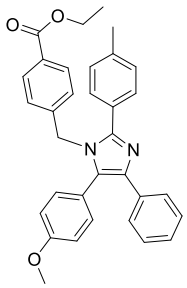

Ethyl 4-((5-(4-methoxyphenyl)-4-phenyl-2-(p-tolyl)-1H-imidazol-1-yl)methyl) benzoate 2.1h. Pale yellow solid, 201 mg, 80% yield. ^{1}H NMR (500 MHz, $CDCl_3$). δ 7.93 (d, *J* = 8.2 Hz, 2H), 7.63 (d, *J* = 7.3 Hz, 2H), 7.53 (d, *J* = 8.1 Hz, 2H), 7.26 – 7.19 (m, 5H), 7.14 (d, *J* = 8.7 Hz, 2H), 6.93 (d, *J* = 8.2 Hz, 2H), 6.86 (d, *J* = 8.7 Hz, 2H), 5.14 (s, 2H), 4.38 (q, *J* = 7.2 Hz, 2H), 3.82 (s, 3H), 2.38 (s, 3H), 1.40 (t, *J* = 7.1 Hz, 3H). ^{13}C NMR (126 MHz, $CDCl_3$) δ 166.2, 159.9, 148.0, 142.8, 138.9, 138.0, 134.5, 132.3, 129.9, 129.7, 129.6, 129.3, 128.8, 128.1, 127.9, 126.7, 126.3, 125.9, 122.9, 114.4, 61.0, 55.2, 48.0, 21.3, 14.3. HRMS. Calculated for $C_{33}H_{31}N_2O_3$ ($M+H^+$): 503.2329, found: 503.2342.

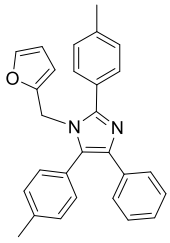

1-(furan-2-ylmethyl)-4-phenyl-2,5-di-p-tolyl-1H-imidazole 2.1i. Yellow solid, 140 mg, 69% yield. ^{1}H NMR (500 MHz, $CDCl_3$). δ 7.64 (d, *J* = 8.1 Hz, 2H), 7.59

(d, J = 7.2 Hz, 2H), 7.33 – 7.27 (m, 3H), 7.26 – 7.19 (m, 6H), 7.15 (t, J = 7.3 Hz, 1H), 6.22 (dd, J = 3.2, 1.8 Hz, 1H), 5.71 (d, J = 2.9 Hz, 1H), 5.01 (s, 2H), 2.44 (s, 3H), 2.43 (s, 3H).^{13}C NMR (126 MHz, $CDCl_3$) δ 150.1, 147.9, 142.1, 138.6, 137.4, 131.0, 129.7, 129.6, 129.3, 129.2, 128.0, 127.9, 126.8, 126.3, 110.4, 108.0, 42.1, 21.4, 21.4. HRMS. Calculated for $C_{28}H_{25}N_2O$ ($M+H^+$): 405.1963, found: 405.1973.

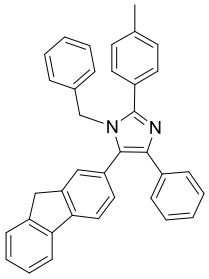

1-benzyl-5-(9H-fluoren-2-yl)-4-phenyl-2-(p-tolyl)-1H-imidazole 2.1j. Pale yellow solid, 185 mg, 76% yield. ^{1}H NMR (500 MHz, $CDCl_3$). δ 7.83 (d, J = 7.5 Hz, 1H), 7.77 (d, J = 7.8 Hz, 1H), 7.69 (d, J = 7.3 Hz, 2H), 7.64 (d, J = 8.1 Hz, 2H), 7.58 (d, J = 7.5 Hz, 1H), 7.43 (t, J = 7.3 Hz, 1H), 7.39 – 7.33 (m, 2H), 7.30 – 7.20 (m, 8H), 7.17 (t, J = 7.2 Hz, 1H), 6.87 (dd, J = 6.5, 2.7 Hz, 2H), 5.17 (s, 2H), 3.83 (s, 2H), 2.42 (s, 3H). ^{13}C NMR (126 MHz, $CDCl_3$) δ 148.2, 143.6, 143.5, 142.0, 141.1, 138.8, 137.9, 137.8, 134.7, 130.3, 129.8, 129.4, 129.3, 129.0, 128.6, 128.1, 127.8, 127.3, 127.2, 127.0, 126.8, 126.3, 126.1, 125.2, 120.2, 48.4, 36.9, 21.4. HRMS. Calculated for $C_{36}H_{29}N_2$ ($M+H^+$): 489.2325, found: 489.2329.

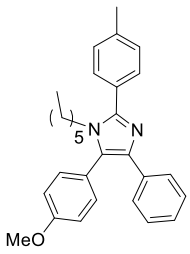

1-Hexyl-5-(4-methoxyphenyl)-4-phenyl-2-(p-tolyl)-1H-imidazole 2.1k. White solid, 161 mg, 76% yield. ^{1}H NMR (500 MHz, $CDCl_3$) δ 7.60 (m, 4H), 7.35 (d, J = 8.7 Hz, 2H), 7.31 (d, J = 7.9 Hz, 2H), 7.22 (t, J = 7.6 Hz, 2H), 7.14 (t, J = 7.3 Hz, 1H), 7.03 (d, J = 8.7 Hz, 2H), 3.90 (s, 3H), 3.89 – 3.85 (m, 2H), 2.44 (s, 3H), 1.43 – 1.34 (m, 2H), 1.10 (m, 2H), 0.99 (m, 4H), 0.78 (t, J = 7.3 Hz, 3H). ^{13}C NMR (126 MHz, $CDCl_3$) δ 159.8, 147.5, 138.7, 137.4, 134.7, 132.3, 129.9, 129.3, 129.3, 129.1, 128.6, 128.0, 126.8, 126.1, 123.6, 114.5, 55.3, 44.6, 30.8, 30.3, 25.9, 22.2, 21.4, 13.9. HRMS. Calculated for $C_{29}H_{33}N_2O$ ($M+H^+$): 425.2587, found: 425.2591.

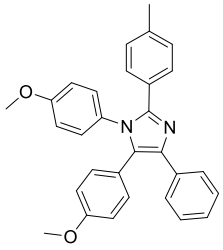

1,5-bis(4-methoxyphenyl)-4-phenyl-2-(p-tolyl)-1H-imidazole 2.1l. Yellow solid, 165 mg, 74% yield. ^{1}H NMR (500 MHz, $CDCl_3$) δ 7.65 (d, J = 7.4 Hz, 2H), 7.37 (d, J = 8.1 Hz, 2H), 7.28 (dd, J = 10.6, 4.4 Hz, 2H), 7.20 (t, J = 7.3

Hz, 1H), 7.08 (d, *J* = 8.6 Hz, 4H), 6.99 (d, *J* = 8.8 Hz, 2H), 6.79 (d, *J* = 7.7 Hz, 4H), 3.80 (s, 3H), 3.80 (s, 3H), 2.33 (s, 3H).^{13}C NMR (126 MHz, $CDCl_3$) δ 159.2, 159.0, 147.0, 137.9, 137.7, 134.8, 132.4, 130.8, 130.2, 129.5, 128.8, 128.7, 128.1, 127.9, 127.3, 126.3, 123.1, 114.2, 113.8, 55.4, 55.1, 21.3. HRMS. Calculated for $C_{30}H_{27}N_2O_2$ ($M+H^+$): 447.2067, found: 447.2067.

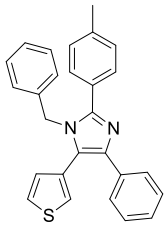

1-benzyl-4-phenyl-5-(thiophen-3-yl)-2-(p-tolyl)-1H-imidazole 2.1m. White solid, 150 mg, 74% yield. ^{1}H NMR (500 MHz, $CDCl_3$) δ 7.64 (d, *J* = 8.1 Hz, 2H), 7.56 (d, *J* = 8.1 Hz, 2H), 7.33 – 7.25 (m, 6H), 7.21 (dd, *J* = 10.4, 7.6 Hz, 3H), 7.11 (dd, *J* = 2.9, 1.2 Hz, 1H), 6.94 (d, *J* = 6.7 Hz, 2H), 6.88 (dd, *J* = 5.0, 1.2 Hz, 1H), 5.14 (s, 2H), 2.39 (s, 3H).^{13}C NMR (126 MHz, $CDCl_3$) δ 148.4, 138.9, 138.0, 134.6, 130.8, 129.5, 129.3, 128.8, 128.8, 128.1, 128.0, 127.4, 126.7, 126.4, 126.3, 126.0, 125.8, 124.6, 48.4, 21.4. HRMS. Calculated for $C_{27}H_{23}N_2S$ ($M+H^+$): 407.1576, found: 407.1595.

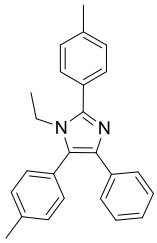

1-Ethyl-4-phenyl-2,5-di-p-tolyl-1H-imidazole 2.1n. white solid, 134 mg, 76% yield. ^{1}H NMR (500 MHz, $CDCl_3$) δ 7.62 (d, *J* = 8.1 Hz, 2H), 7.58 (d, *J* = 7.2 Hz, 2H), 7.39 – 7.29 (m, 8H), 7.22 (t, *J* = 7.6 Hz, 2H), 7.14 (t, *J* = 7.3 Hz, 1H), 3.95 (q, *J* = 7.2 Hz, 2H), 2.47 (s, 3H), 2.45 (s, 3H), 1.04 (t, *J* = 7.2 Hz, 3H).^{13}C NMR (126 MHz, $CDCl_3$) δ 147.3, 138.7, 138.5, 137.5, 134.8, 130.9, 129.8, 129.29, 129.28, 129.0, 128.63, 128.59, 128.0, 126.7, 126.0, 39.5, 21.4, 21.4, 16.3. HRMS. Calculated for $C_{25}H_{25}N_2$ ($M+H^+$): 353.2012, found: 353.2018.

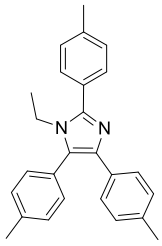

1-Ethyl-2,4,5-tri-p-tolyl-1H-imidazole 2.1o. Pale yellow solid, 143 mg, 78% yield. ^{1}H NMR (500 MHz, $CDCl_3$) δ 7.62 (d, *J* = 8.1 Hz, 2H), 7.47 (d, *J* = 8.2 Hz, 2H), 7.32 (dt, *J* = 8.0, 6.4 Hz, 6H), 7.04 (d, *J* = 8.0 Hz, 2H), 3.94 (q, *J* = 7.2 Hz, 2H), 2.47 (s, 3H), 2.45 (s, 3H), 2.30 (s, 3H), 1.04 (t, *J* = 7.2 Hz, 3H). ^{13}C NMR (126 MHz, $CDCl_3$) δ 147.2, 138.6, 138.4, 137.6, 135.6, 132.0, 131.0, 129.7, 129.3,

129.1, 128.8, 128.72, 128.71, 128.68, 126.7, 39.5, 21.44, 21.39, 21.1, 16.3. HRMS. Calculated for $C_{26}H_{27}N_2$ ($M+H^+$): 367.2169, found: 367.2162.

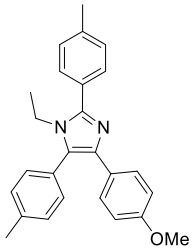

1-Ethyl-4-(4-methoxyphenyl)-2,5-di-p-tolyl-1H-imidazole 2.1p. Pale yellow solid, 153 mg, 80% yield. ^{1}H NMR (500 MHz, $CDCl_3$) δ 7.62 (d, *J* = 8.1 Hz, 2H), 7.51 (d, *J* = 8.9 Hz, 2H), 7.32 (m, 6H), 6.78 (d, *J* = 8.9 Hz, 2H), 3.94 (q, *J* = 7.1 Hz, 2H), 3.77 (s, 3H), 2.46 (s, 3H), 2.44 (s, 3H), 1.03 (t, *J* = 7.2 Hz, 3H). ^{13}C NMR (126 MHz, $CDCl_3$) δ 158.1, 147.1, 138.6, 138.3, 137.4, 131.0, 129.8, 129.3, 129.0, 128.8, 128.7, 128.3, 127.9, 127.7, 113.5, 55.1, 39.5, 21.43, 21.38, 16.3. HRMS. Calculated for $C_{26}H_{27}N_2O$ ($M+H^+$): 383.2118, found: 383.2120.

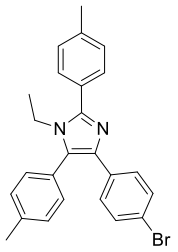

4-(4-bromophenyl)-1-ethyl-2,5-di-p-tolyl-1H-imidazole 2.1q. Pale yellow solid, 166 mg, 77% yield. ^{1}H NMR (500 MHz, $CDCl_3$) δ 7.60 (d, *J* = 8.1 Hz, 2H), 7.44 (d, *J* = 8.7 Hz, 2H), 7.35 – 7.29 (m, 8H), 3.93 (q, *J* = 7.2 Hz, 2H), 2.47 (s, 3H), 2.45 (s, 3H), 1.03 (t, *J* = 7.2 Hz, 3H). ^{13}C NMR (126 MHz, $CDCl_3$) δ 147.5, 138.8, 138.8, 136.5, 133.9, 131.1, 130.8, 129.9, 129.6, 129.3, 129.0, 128.4, 128.3, 128.2, 119.9, 39.6, 21.44, 21.39, 16.3. HRMS. Calculated for $C_{25}H_{24}N_2Br$ ($M+H^+$): 431.1117, found: 431.1132.

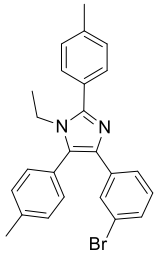

4-(3-Bromophenyl)-1-ethyl-2,5-di-p-tolyl-1H-imidazole 2.1r. Pale yellow solid, 162 mg, 75% yield. ^{1}H NMR (500 MHz, $CDCl_3$) δ 7.88 (t, *J* = 1.8 Hz, 1H), 7.60 (d, *J* = 8.1 Hz, 2H), 7.35 – 7.30 (m, 7H), 7.25 (ddd, *J* = 7.9, 2.0, 1.0 Hz, 1H), 7.02 (t, *J* = 7.9 Hz, 1H), 3.93 (q, *J* = 7.2 Hz, 2H), 2.48 (s, 3H), 2.45 (s, 3H), 1.03 (t, *J* = 7.2 Hz, 3H). ^{13}C NMR (126 MHz, $CDCl_3$) δ 147.5, 138.9, 138.8, 137.0, 136.1, 130.8, 130.0, 129.9, 129.6, 129.4, 129.3, 129.0, 128.9, 128.3, 128.1, 125.0, 122.4, 39.6, 21.5, 21.4, 16.3. HRMS. Calculated for $C_{25}H_{24}N_2Br$ ($M+H^+$): 431.1117, found: 431.1107.

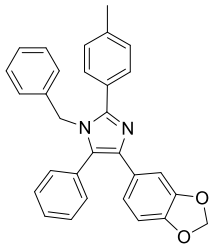

4-(Benzo[d][1,3]dioxol-5-yl)-1-benzyl-5-phenyl-2-(p-tolyl)-1H-imidazole 2.1s. Pale yellow solid, 171 mg, 77% yield. ^{1}H NMR (500 MHz, $CDCl_3$) δ 7.55 (d, *J* = 8.1 Hz, 2H), 7.38 – 7.30 (m, 3H), 7.21 (td, *J* = 5.3, 2.2 Hz, 8H), 7.11 (dd, *J* = 8.1, 1.7 Hz, 1H), 7.08 (d, *J* = 1.5 Hz, 1H), 6.82 (dd, *J* = 7.2, 2.2 Hz, 2H), 6.69 (d, *J* = 8.1 Hz, 1H), 5.90 (s, 2H), 5.10 (s, 2H), 2.39 (s, 3H). ^{13}C NMR (126 MHz, $CDCl_3$) δ δ 147.9, 147.3, 146.1, 138.8, 137.7, 131.1, 129.3, 129.1, 128.9, 128.8, 128.6, 128.5, 127.3, 126.0, 120.5, 108.1, 107.6, 100.7, 48.3, 21.3 HRMS. Calculated for $C_{30}H_{25}N_2O_2$ ($M+H^+$): 445.1911, found: 445.1921.

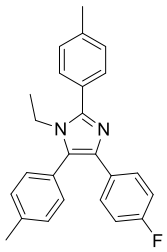

1-Ethyl-4-(4-fluorophenyl)-2,5-di-p-tolyl-1H-imidazole 2.1t. Pale yellow solid, 141 mg, 76% yield. ^{1}H NMR (500 MHz, $CDCl_3$) δ 7.61 (d, *J* = 8.1 Hz, 2H), 7.53 (dd, *J* = 9.0, 5.5 Hz, 2H), 7.36 – 7.30 (m, 6H), 6.90 (t, *J* = 8.9 Hz, 2H), 3.94 (q, *J* = 7.2 Hz, 2H), 2.47 (s, 3H), 2.45 (s, 3H), 1.03 (t, *J* = 7.2 Hz, 3H). ^{13}C NMR (126 MHz, $CDCl_3$) δ 161.51 (d, *J* = 244.6 Hz), 147.3, 138.8, 138.6, 136.7, 131.0 (d, *J* = 3.0 Hz), 130.9, 129.9, 129.3, 129.2, 129.0, 128.5, 128.4, 128.3 (d, *J* = 7.8 Hz), 114.8 (d, *J* = 21.2 Hz), 39.6, 21.43, 21.38, 16.3. HRMS. Calculated for $C_{25}H_{24}N_2F$ ($M+H^+$): 371.1918, found: 371.1923.

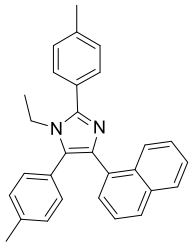

1-Ethyl-4-(naphthalen-1-yl)-2,5-di-p-tolyl-1H-imidazole 2.1u. Pale yellow solid, 163 mg, 81% yield. ^{1}H NMR (500 MHz, $CDCl_3$) δ 8.17 (s, 1H), 7.74 (dd, *J* = 8.5, 6.4 Hz, 2H), 7.69 – 7.64 (m, 3H), 7.60 (m, 1H), 7.43 – 7.31 (m, 8H), 3.98 (q, *J* = 7.1 Hz, 2H), 2.49 (s, 3H), 2.47 (s, 3H), 1.06 (t, *J* = 7.2 Hz, 3H). ^{13}C NMR (126 MHz, $CDCl_3$) δ 147.5, 138.8, 138.6, 137.5, 133.6, 132.3, 132.2, 133.0, 129.8, 129.8, 129.3, 129.1, 129.0, 128.6, 128.2, 127.5, 127.3, 125.6, 125.4, 125.1, 125.1, 39.6, 21.5, 21.4, 16.3. HRMS. Calculated for $C_{29}H_{27}N_2$ ($M+H^+$): 403.2169, found: 403.2177.

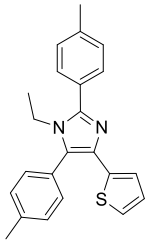

1-Ethyl-4-(thiophen-2-yl)-2,5-di-p-tolyl-1H-imidazole 2.1v. White solid, 147 mg, 82% yield. ^{1}H NMR (500 MHz, $CDCl_3$) δ 7.60 (d, *J* = 8.0 Hz, 2H), 7.37 (q, *J* = 8.0

Hz, 4H), 7.31 (d, *J* = 7.9 Hz, 2H), 7.07 (d, *J* = 5.0 Hz, 1H), 6.95 (d, *J* = 2.7 Hz, 1H), 6.88 (dd, *J* = 4.9, 3.7 Hz, 1H), 3.91 (q, *J* = 7.1 Hz, 2H), 2.49 (s, 3H), 2.44 (s, 3H), 1.05 (t, *J* = 7.2 Hz, 3H). ^{113}C NMR (126 MHz, $CDCl_3$) δ 147.2, 139.0, 138.8, 138.5, 133.5, 131.1, 129.8, 129.3, 129.1, 128.3, 128.3, 127.7, 127.0, 122.9, 122.3, 39.7, 21.5, 21.4, 16.3. HRMS. Calculated for $C_{23}H_{23}N_2S$ ($M+H^+$): 359.1576, found: 359.1581.

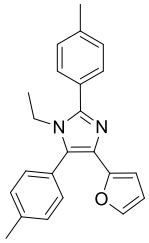

1-Ethyl-4-(furan-2-yl)-2,5-di-p-tolyl-1H-imidazole 2.1w. Pale yellow solid, 137 mg, 80% yield. ^{1}H NMR (500 MHz, $CDCl_3$) δ 7.57 (d, *J* = 8.1 Hz, 2H), 7.38 – 7.19 (m, 7H), 6.27 (dd, *J* = 3.3, 1.8 Hz, 1H), 6.09 (dd, *J* = 3.3, 0.7 Hz, 1H), 3.92 (q, *J* = 7.2 Hz, 2H), 2.44 (s, 3H), 2.41 (s, 3H), 0.99 (t, *J* = 7.2 Hz, 3H). ^{13}C NMR (126 MHz, $CDCl_3$). HRMS. Calculated for $C_{23}H_{23}N_2O$ ($M+H^+$): 343.1805, found: 343.1814.

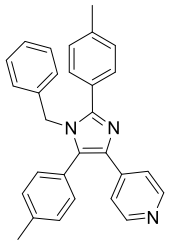

4-(1-benzyl-2,5-di-p-tolyl-1H-imidazol-4-yl)pyridine 2.1x. Pale yellow solid, 122 mg, 59% yield. ^{1}H NMR (500 MHz, $CDCl_3$δ 8.41 (d, *J* = 6.3 Hz, 2H), 7.53 (d, *J* = 8.1 Hz, 2H), 7.47 (d, *J* = 6.3 Hz, 2H), 7.24 – 7.21 (m, 5H), 7.18 (d, *J* = 7.9 Hz, 2H), 7.10 (d, *J* = 8.1 Hz, 2H), 6.84 – 6.78 (m, 2H), 5.09 (s, 2H), 2.40 (s, 3H), 2.38 (s, 3H). ^{13}C NMR (126 MHz, $CDCl_3$) δ 149.6, 148.7, 142.2, 139.2, 139.2, 137.3, 135.1, 132.6, 130.6, 129.8, 129.4, 128.9, 128.6, 127.6, 127.4, 127.1, 126.0, 120.6, 48.2, 21.4, 21.4. HRMS. Calculated for $C_{29}H_{26}N_3$ ($M+H^+$): 416.2121, found: 416.2131.

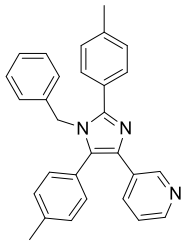

3-(1-benzyl-2,5-di-p-tolyl-1H-imidazol-4-yl)pyridine 2.1y. Pale yellow solid, 96 mg, 46% yield. ^{1}H NMR (500 MHz, $CDCl_3$) δ 8.71 (d, *J* = 1.5 Hz, 1H), 8.38 (dd, *J* = 4.7, 1.7 Hz, 1H), 7.98 (d, *J* = 8.1 Hz, 1H), 7.54 (d, *J* = 8.1 Hz, 2H), 7.22 (d, *J* = 7.3 Hz, 5H), 7.19 – 7.07 (m, 5H), 6.87 – 6.83 (m, 2H), 5.12 (s, 2H), 2.39 (s, 3H), 2.38 (s, 3H).^{13}C NMR (126 MHz, $CDCl_3$) δ 148.6, 148.0, 147.2, 139.0, 138.9, 137.5, 135.1, 133.7, 131.0, 130.7, 130.7, 129.8, 129.3, 128.9, 128.6, 127.8, 127.4, 127.2, 126.0, 123.1, 48.2, 21.4. HRMS. Calculated for $C_{29}H_{26}N_3$ ($M+H^+$): 416.2121, found: 416.2123.

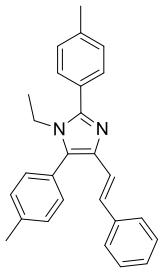

(E)-1-Ethyl-4-styryl-2,5-di-p-tolyl-1H-imidazole 2.1z. Pale yellow solid, 141 mg, 74% yield. ^{1}H NMR (500 MHz, $CDCl_3$) δ 7.60 (d, *J* = 8.1 Hz, 2H), 7.46 (m, 3H), 7.36 (m, 4H), 7.34 – 7.25 (m, 4H), 7.18 (t, *J* = 7.3 Hz, 1H), 6.92 (d, *J* = 16.0 Hz, 1H), 4.01 (q, *J* = 7.1 Hz, 2H), 2.49 (s, 3H), 2.45 (s, 3H), 0.99 (t, *J* = 7.2 Hz, 3H). ^{13}C NMR (126 MHz, $CDCl_3$) δ 148.4, 138.9, 138.3, 138.3, 136.9, 131.7, 130.4, 129.6, 129.3, 129.1, 128.4, 127.2, 126.84, 126.82, 126.7, 126.2, 119.6, 39.8, 21.41, 21.40, 16.1. HRMS. Calculated for $C_{27}H_{27}N_2$ ($M+H^+$): 379.2169, found: 379.2180.

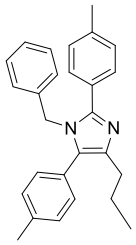

1-benzyl-4-propyl-2,5-di-p-tolyl-1H-imidazole 2.1aa. Colorless oil, 155 mg, 81% yield. ^{1}H NMR (500 MHz, $CDCl_3$) δ 7.49 (d, *J* = 8.1 Hz, 2H), 7.24 – 7.16 (m, 5H), 7.14 (d, *J* = 7.9 Hz, 2H), 7.10 (d, *J* = 8.2 Hz, 2H), 6.79 (d, *J* = 6.3 Hz, 2H), 5.12 (s, 2H), 2.57 (dd, *J* = 8.4, 7.0 Hz, 2H), 2.36 (s, 6H), 1.74 (h, *J* = 7.4 Hz, 2H), 0.93 (t, *J* = 7.4 Hz, 3H). ^{13}C NMR (126 MHz, $CDCl_3$) δ 147.4, 140.0, 138.3, 138.2, 137.6, 130.5, 129.9, 129.13, 129.08, 128.8, 128.5, 128.4, 127.7, 127.1, 125.9, 48.3, 29.6, 23.6, 21.3, 21.3, 14.1 Calculated for $C_{27}H_{29}N_2$ ($M+H^+$): 381.2325, found: 381.2333.

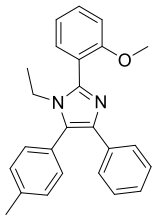

1-Ethyl-2-(2-methoxyphenyl)-4-phenyl-5-(p-tolyl)-1H-imidazole 2.2a. White solid, 112 mg, 61% yield. ^{1}H NMR (500 MHz, $CDCl_3$) δ 7.58 (d, *J* = 7.5 Hz, 2H), 7.49 – 7.41 (m, 1H), 7.36 (d, *J* = 7.9 Hz, 2H), 7.32 – 7.25 (m, 3H), 7.20 (t, *J* = 7.6 Hz, 2H), 7.11 (dt, *J* = 11.1, 7.4 Hz, 2H), 7.02 (d, *J* = 8.3 Hz, 1H), 3.86 (s, 3H), 3.77 (q, *J* = 7.2 Hz, 2H), 2.47 (s, 3H), 0.93 (t, *J* = 7.2 Hz, 3H). ^{13}C NMR (126 MHz, $CDCl_3$) δ 157.6, 144.6, 138.3, 137.4, 134.8, 132.7, 130.9, 130.8, 129.7, 128.8, 128.7, 127.9, 126.7, 125.9, 120.9, 120.7, 111.0, 55.6, 39.5, 21.4, 15.9. HRMS. Calculated for $C_{25}H_{25}N_2O$ ($M+H^+$): 369.1961, found: 369.1966.

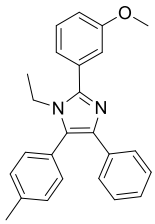

1-Ethyl-2-(3-methoxyphenyl)-4-phenyl-5-(p-tolyl)-1H-imidazole 2.2b. Pale yellow solid, 151 mg, 82% yield. ^{1}H NMR (500 MHz, $CDCl_3$) δ 7.58 (d, *J* = 7.2

Hz, 2H), 7.41 (t, *J* = 7.9 Hz, 1H), 7.35 – 7.27 (m, 6H), 7.22 (t, *J* = 7.5 Hz, 2H), 7.14 (t, *J* = 7.3 Hz, 1H), 7.02 (dd, *J* = 8.2, 2.5 Hz, 1H), 3.96 (q, *J* = 7.2 Hz, 2H), 3.90 (s, 3H), 2.47 (s, 3H), 1.05 (t, *J* = 7.2 Hz, 3H). ^{13}C NMR (126 MHz, $CDCl_3$) δ 159.7, 147.0, 138.6, 137.6, 134.3, 132.8, 130.0, 129.1, 129.6, 129.5, 128.5, 128.0, 126.7, 126.1, 121.4, 114.9, 114.5, 55.4, 39.6, 21.5, 16.3. HRMS. Calculated for $C_{25}H_{25}N_2O$ ($M+H^+$): 369.1961, found: 369.1961.

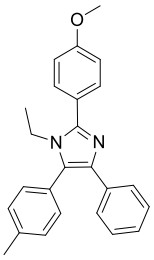

1-Ethyl-2-(4-methoxyphenyl)-4-phenyl-5-(p-tolyl)-1H-imidazole 2.2c. Pale brown solid, 158 mg, 86% yield. ^{1}H NMR (500 MHz, $CDCl_3$) δ 7.66 (d, *J* = 8.8 Hz, 2H), 7.57 (d, *J* = 7.1 Hz, 2H), 7.36 – 7.29 (m, 4H), 7.22 (t, *J* = 7.5 Hz, 2H), 7.17 – 7.11 (m, 1H), 7.03 (d, *J* = 8.8 Hz, 2H), 3.93 (q, *J* = 7.2 Hz, 2H), 3.88 (s, 3H), 2.47 (s, 3H), 1.04 (t, *J* = 7.2 Hz, 3H). ^{13}C NMR (126 MHz, $CDCl_3$) δ 160.0, 147.1, 138.5, 137.4, 134.8, 130.9, 130.5, 129.8, 129.2, 128.6, 128.0, 126.7, 126.0, 124.0, 114.0, 55.4, 39.5, 21.4, 16.3. HRMS. Calculated for $C_{25}H_{25}N_2O$ ($M+H^+$): 369.1961, found: 369.1962.

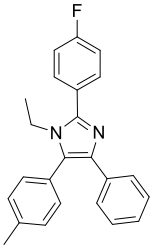

1-Ethyl-2-(4-fluorophenyl)-4-phenyl-5-(p-tolyl)-1H-imidazole 2.2d. Pale yellow solid, 132 mg, 74% yield. ^{1}H NMR (500 MHz, $CDCl_3$) δ 7.72 (dd, *J* = 8.8, 5.4 Hz, 2H), 7.57 (d, *J* = 7.2 Hz, 2H), 7.35 – 7.30 (m, 4H), 7.21 (dt, *J* = 10.7, 8.1 Hz, 4H), 7.15 (t, *J* = 7.3 Hz, 1H), 3.92 (q, *J* = 7.2 Hz, 2H), 2.47 (s, 3H), 1.04 (t, *J* = 7.2 Hz, 3H). ^{13}C NMR (126 MHz, $CDCl_3$) δ 163.1 (d, *J* = 248.7 Hz), 146.2, 138.6, 137.7, 134.7, 131.0 (d, *J* = 8.4 Hz), 130.9, 129.9, 129.5, 128.4, 128.0, 127.7 (d, *J* = 3.3 Hz), 126.7, 126.2, 115.7 (d, *J* = 21.7 Hz), 39.6, 21.5, 16.3. HRMS. Calculated for $C_{24}H_{22}N_2F$ ($M+H^+$): 357.1762, found: 357.1767.

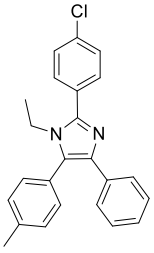

2-(4-Chlorophenyl)-1-ethyl-4-phenyl-5-(p-tolyl)-1H-imidazole 2.2e. White solid, 145 mg, 78% yield. ^{1}H NMR (500 MHz, $CDCl_3$) δ 7.69 (d, *J* = 8.5 Hz, 2H), 7.55 (d, *J* = 7.3 Hz, 2H), 7.49 (d, *J* = 8.5 Hz, 2H), 7.35 – 7.31 (m, 4H), 7.22 (t, *J* = 7.5 Hz, 2H), 7.15 (t, *J* = 7.3 Hz, 1H), 3.94 (q, *J* = 7.2 Hz, 2H), 2.48 (s, 3H), 1.05 (t, *J* = 7.2 Hz, 3H). ^{13}C NMR (126 MHz, $CDCl_3$) δ 145.9, 138.7, 137.8, 134.9, 134.5,

130.9, 130.4, 129.9, 129.9, 129.8, 128.9, 128.2, 128.1, 126.7, 126.3, 39.6, 21.5, 16.3. HRMS. Calculated for $C_{24}H_{22}N_2Cl$ ($M+H^+$): 373.1466, found: 373.1469.

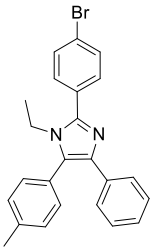

2-(4-Bromophenyl)-1-ethyl-4-phenyl-5-(p-tolyl)-1H-imidazole 2.2f. Pale yellow solid, 164 mg, 79% yield. ^{1}H NMR (500 MHz, $CDCl_3$) δ 7.63 (q, *J* = 8.7 Hz, 4H), 7.54 (d, *J* = 7.2 Hz, 2H), 7.32 (s, 4H), 7.22 (t, *J* = 7.5 Hz, 2H), 7.15 (t, *J* = 7.3 Hz, 1H), 3.94 (q, *J* = 7.2 Hz, 2H), 2.47 (s, 3H), 1.05 (t, *J* = 7.2 Hz, 3H). ^{13}C NMR (126 MHz, $CDCl_3$) δ 145.9, 138.7, 137.9, 134.5, 131.8, 130.9, 130.6, 130.4, 129.8, 128.2, 128.1, 126.7, 126.2, 123.1, 39.6, 21.4, 16.3. HRMS. Calculated for $C_{24}H_{22}N_2Br$ ($M+H^+$): 417.0961, found: 417.0972.

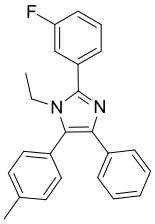

1-Ethyl-2-(3-fluorophenyl)-4-phenyl-5-(p-tolyl)-1H-imidazole 2.2g. White solid, 128 mg, 72% yield. ^{1}H NMR (500 MHz, $CDCl_3$) δ 7.57 – 7.50 (m, 3H), 7.47 (dd, *J* = 7.9, 2.0 Hz, 2H), 7.32 (s, 4H), 7.23 (d, *J* = 7.3 Hz, 2H), 7.16 (d, *J* = 7.4 Hz, 2H), 3.97 (d, *J* = 7.2 Hz, 2H), 2.48 (s, 3H), 1.06 (t, *J* = 7.2 Hz, 3H). ^{13}C NMR (126 MHz, $CDCl_3$) δ 162.8 (d, *J* = 246.6 Hz), 145.7 (d, *J* = 2.6 Hz), 138.7, 137.9, 134.5, 133.5 (d, *J* = 8.2 Hz), 130.9, 130.2 (d, *J* = 8.4 Hz), 129.8, 128.2, 128.0, 126.7, 126.2, 124.70, 124.67, 116.2 (d, *J* = 22.7 Hz), 115.7 (d, *J* = 21.1 Hz), 39.6, 21.4, 16.3. HRMS. Calculated for $C_{24}H_{22}N_2F$ ($M+H^+$): 357.1762, found: 357.1769.

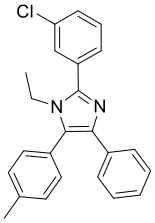

2-(3-Chlorophenyl)-1-ethyl-4-phenyl-5-(p-tolyl)-1H-imidazole 2.2h. White solid, 142 mg, 76% yield. ^{1}H NMR (500 MHz, $CDCl_3$) δ 7.76 (d, *J* = 1.0 Hz, 1H), 7.64 – 7.61 (m, 1H), 7.55 (d, *J* = 7.2 Hz, 2H), 7.46 – 7.44 (m, 2H), 7.32 (s, 4H), 7.23 (t, *J* = 7.5 Hz, 2H), 7.16 (t, *J* = 7.3 Hz, 1H), 3.96 (q, *J* = 7.2 Hz, 2H), 2.48 (s, 3H), 1.06 (t, *J* = 7.2 Hz, 3H). ^{13}C NMR (126 MHz, $CDCl_3$) δ 145.6, 138.8, 137.8, 134.6, 134.2, 133.0, 130.9, 130.9, 129.9, 129.8, 129.3, 129.0, 128.8, 128.1, 127.1, 126.7, 126.3, 39.7, 21.4, 16.3. Calculated for $C_{24}H_{22}N_2Cl$ ($M+H^+$): 373.1466, found: 373.1468.

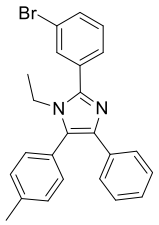

2-(3-Bromophenyl)-1-ethyl-4-phenyl-5-(p-tolyl)-1H-imidazole 2.2i. White solid, 161 mg, 77% yield. ^{1}H NMR (500 MHz, $CDCl_3$) δ 7.93 (t, *J* = 1.7 Hz, 1H), 7.66 (d, *J* = 7.7 Hz, 1H), 7.60 (d, *J* = 7.1 Hz, 1H), 7.55 (d, *J* = 7.2 Hz, 2H), 7.38 (t, *J* = 7.9 Hz, 1H), 7.32 (s, 4H), 7.22 (t, *J* = 7.5 Hz, 2H), 7.16 (t, *J* = 7.3 Hz, 1H), 3.96 (q, *J* = 7.2 Hz, 2H), 2.48 (s, 3H), 1.06 (t, *J* = 7.2 Hz, 3H). ^{13}C NMR (126 MHz, $CDCl_3$) δ 145.5, 138.8, 137.9, 134.3, 133.3, 132.2, 131.9, 130.9, 130.1, 129.9, 129.87, 128.09, 128.07, 127.5, 126.7, 126.3, 122.7, 39.7, 21.5, 16.3. HRMS. Calculated for $C_{24}H_{22}N_2Br$ ($M+H^+$): 417.0961, found: 417.0969.

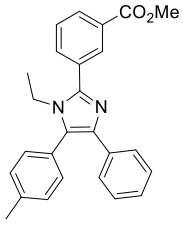

Methyl 3-(1-ethyl-4-phenyl-5-(p-tolyl)-1H-imidazol-2-yl)benzoate 2.2j. Pale yellow solid, 131 mg, 66% yield. ^{1}H NMR (500 MHz, $CDCl_3$) δ 8.41 (s, 1H), 8.15 (d, *J* = 7.9 Hz, 1H), 7.99 (d, *J* = 7.7 Hz, 1H), 7.61 (t, *J* = 7.8 Hz, 1H), 7.57 (d, *J* = 7.2 Hz, 2H), 7.35 – 7.31 (m, 4H), 7.23 (t, *J* = 7.5 Hz, 2H), 7.16 (t, *J* = 7.3 Hz, 1H), 4.00 – 3.95 (m, 5H), 2.47 (s, 3H), 1.06 (t, *J* = 7.2 Hz, 3H). ^{13}C NMR (126 MHz, $CDCl_3$) δ 166.6, 145.9, 138.8, 137.6, 134.1, 133.7, 131.4, 130.9, 130.6, 130.0, 129.9, 129.86, 128.9, 128.1, 128.0, 126.8, 126.4, 52.3, 39.8, 21.5, 16.2. HRMS. Calculated for $C_{26}H_{25}N_2O_2$ ($M+H^+$): 397.1911, found: 397.1920.

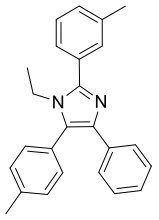

1-Ethyl-4-phenyl-2-(m-tolyl)-5-(p-tolyl)-1H-imidazole 2.2k. Pale yellow solid, 134 mg, 76% yield. ^{1}H NMR (500 MHz, $CDCl_3$) δ 7.61 – 7.55 (m, 3H), 7.49 (d, *J* = 7.6 Hz, 1H), 7.39 (t, *J* = 7.6 Hz, 1H), 7.33 (q, *J* = 8.1 Hz, 4H), 7.28 (d, *J* = 5.6 Hz, 1H), 7.22 (t, *J* = 7.6 Hz, 2H), 7.15 (t, *J* = 7.3 Hz, 1H), 3.96 (q, *J* = 7.1 Hz, 2H), 2.47 (s, 3H), 2.46 (s, 3H), 1.04 (t, *J* = 7.2 Hz, 3H). ^{13}C NMR (126 MHz, $CDCl_3$) δ 147.4, 138.5, 138.4, 137.6, 134.8, 131.4, 130.9, 130.1, 129.8, 129.6, 129.4, 128.6, 128.4, 128.0, 126.7, 126.1, 126.0, 39.6, 21.5, 21.4, 16.3. HRMS. Calculated for $C_{25}H_{25}N_2$ ($M+H^+$): 353.2012, found: 353.2018.

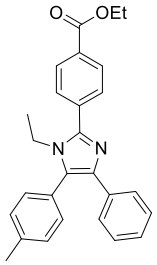

Ethyl 4-(1-ethyl-4-phenyl-5-(p-tolyl)-1H-imidazol-2-yl)benzoate 2.2l. White solid, 142 mg, 69% yield. ^{1}H NMR (500 MHz, $CDCl_3$) δ 8.19 (d, *J* = 8.5 Hz, 2H), 7.84 (d, *J* = 8.4 Hz, 2H), 7.55 (d, *J* = 7.2 Hz, 2H), 7.33 (s, 4H), 7.23 (t, *J* = 7.5 Hz, 2H), 7.16 (t, *J* = 7.3 Hz, 1H), 4.44 (q, *J* = 7.2 Hz, 2H), 3.99 (q, *J* = 7.2 Hz, 2H), 2.48 (s, 3H), 1.45 (t, *J* = 7.2 Hz, 3H), 1.06 (t, *J* = 7.2 Hz, 3H). ^{13}C NMR (126 MHz, $CDCl_3$) δ 166.3, 146.0, 138.7, 138.2, 135.7, 134.5, 130.8, 130.4, 130.3, 129.8, 129.8, 128.8, 128.1, 128.1, 126.7, 126.3, 61.2, 39.7, 21.4, 16.3, 14.4. HRMS. Calculated for $C_{27}H_{27}N_2O_2$ ($M+H^+$): 411.2067, found: 411.2067.

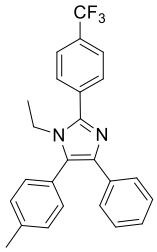

1-Ethyl-4-phenyl-5-(p-tolyl)-2-(4-(trifluoromethyl)phenyl)-1H-imidazole 2.2m. White solid, 130 mg, 64% yield. ^{1}H NMR (500 MHz, $CDCl_3$) δ 7.90 (d, *J* = 8.1 Hz, 2H), 7.78 (d, *J* = 8.2 Hz, 2H), 7.56 (d, *J* = 7.1 Hz, 2H), 7.33 (m, 4H), 7.23 (t, *J* = 7.4 Hz, 2H), 7.17 (t, *J* = 7.3 Hz, 1H), 3.99 (q, *J* = 7.2 Hz, 2H), 2.48 (s, 3H), 1.07 (t, *J* = 7.2 Hz, 3H). ^{13}C{^{19}F} NMR (126 MHz, $CDCl_3$) δ 145.3, 139.0, 137.8, 134.4, 133.9, 130.8, 130.2, 129.9, 129.4, 128.1, 126.8, 126.5, 125.6, 125.1, 122.9, 39.8, 21.4, 16.3. ^{19}F NMR (470 MHz, $CDCl_3$) δ -62.7. HRMS. Calculated for $C_{25}H_{22}N_2F_3$ ($M+H^+$): 407.1730, found: 407.1727.

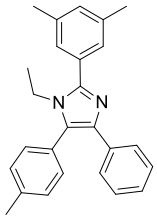

2-(3,5-Dimethylphenyl)-1-ethyl-4-phenyl-5-(p-tolyl)-1H-imidazole 2.2o. Yellow solid, 152 mg, 83% yield. ^{1}H NMR (500 MHz, $CDCl_3$) δ 7.56 (d, *J* = 7.2 Hz, 2H), 7.36 – 7.29 (m, 6H), 7.21 (t, *J* = 7.5 Hz, 2H), 7.14 (t, *J* = 7.3 Hz, 1H), 7.10 (s, 1H), 3.95 (q, *J* = 7.2 Hz, 2H), 2.47 (s, 3H), 2.41 (s, 6H), 1.04 (t, *J* = 7.2 Hz, 3H). ^{13}C NMR (126 MHz, $CDCl_3$) δ 147.6, 138.4, 138.1, 137.5, 134.8, 131.3, 130.9, 130.5, 129.8, 129.2, 128.6, 128.0, 127.0, 126.8, 126.0, 39.6, 21.43, 21.37, 16.3. HRMS. Calculated for $C_{26}H_{27}N_2$ ($M+H^+$): 367.2169, found: 367.2174.

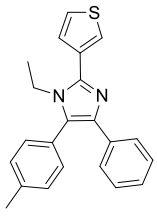

1-Ethyl-4-phenyl-2-(thiophen-3-yl)-5-(p-tolyl)-1H-imidazole 2.2p. Pale red solid, 136 mg, 79% yield. ^{1}H NMR (500 MHz, $CDCl_3$) δ 7.67 (dd, *J* = 2.9, 1.2 Hz,

1H), 7.57 – 7.53 (m, 3H), 7.45 (dd, *J* = 5.0, 3.0 Hz, 1H), 7.31 (m, 4H), 7.22 (t, *J* = 7.5 Hz, 2H), 7.16 – 7.12 (m, 1H), 3.98 (q, *J* = 7.2 Hz, 2H), 2.47 (s, 3H), 1.14 (t, *J* = 7.2 Hz, 3H). ^{13}C NMR (126 MHz, $CDCl_3$) δ 142.69, 138.59, 137.51, 134.69, 132.07, 130.95, 129.79, 129.33, 128.73, 128.35, 128.20, 128.00, 126.66, 126.57, 126.11, 125.85, 124.30, 39.42, 21.44, 16.29. HRMS. Calculated for $C_{22}H_{21}N_2S$ ($M+H^+$): 345.1420, found: 345.1427.

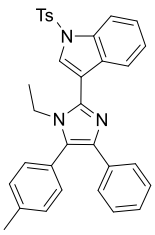

3-(1-Ethyl-4-phenyl-5-(p-tolyl)-1H-imidazol-2-yl)-1-tosyl-1H-indole 2.2q. White solid, 234 mg, 88% yield. ^{1}H NMR (500 MHz, $CDCl_3$) δ 8.13 (d, *J* = 8.6 Hz, 1H), 7.87 (d, *J* = 1.2 Hz, 1H), 7.79 (d, *J* = 8.4 Hz, 2H), 7.67 (dd, *J* = 8.6, 1.6 Hz, 1H), 7.64 (d, *J* = 3.7 Hz, 1H), 7.57 (d, *J* = 7.2 Hz, 2H), 7.33 (q, *J* = 8.1 Hz, 4H), 7.24 (d, *J* = 8.1 Hz, 2H), 7.21 (t, *J* = 7.5 Hz, 2H), 7.13 (t, *J* = 7.3 Hz, 1H), 6.74 (dd, *J* = 3.6, 0.4 Hz, 1H), 3.95 (q, *J* = 7.1 Hz, 2H), 2.47 (s, 3H), 2.36 (s, 3H), 1.01 (t, *J* = 7.2 Hz, 3H). ^{13}C NMR (126 MHz, $CDCl_3$) δ 147.2, 145.2, 138.6, 137.6, 135.1, 135.0, 134.8, 131.0, 130.9, 130.0, 129.8, 129.4, 128.5, 128.0, 127.3, 126.9, 126.8, 126.7, 126.1, 125.8, 122.3, 113.8, 109.4, 39.6, 21.6, 21.5, 16.3. HRMS. Calculated for $C_{33}H_{30}N_3OS$ ($M+H^+$): 532.2053, found: 532.2065.

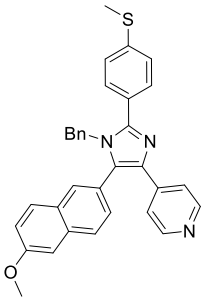

4-(1-benzyl-5-(6-methoxynaphthalen-2-yl)-2-(4-(methylthio) phenyl)-1H-imidazol-4-yl)pyridine. Pale yellow solid in 80% yield (413 mg). ^{1}H NMR (500 MHz, $CDCl_3$) δ 8.38 (d, *J* = 6.3 Hz, 2H), 7.74 (d, *J* = 8.4 Hz, 1H), 7.64 – 7.58 (m, 4H), 7.46 (d, *J* = 6.4 Hz, 2H), 7.30 (d, *J* = 8.5 Hz, 2H), 7.26 – 7.22 (m, 4H), 7.19 (d, *J* = 8.7 Hz, 2H), 6.83 (dd, *J* = 6.5, 3.0 Hz, 2H), 5.14 (s, 2H), 3.97 (s, 3H), 2.52 (s, 3H). ^{13}C NMR (126 MHz, $CDCl_3$) δ 158.6, 149.7, 148.3, 141.9, 140.3, 137.3, 135.6, 134.6, 132.8, 130.2, 129.7, 129.2, 128.7, 128.7, 128.4, 127.7, 127.6, 127.0, 126.2, 126.0, 125.0, 120.6, 119.6, 105.6, 55.4, 48.4, 15.4. HRMS. Calculated for $C_{33}H_{28}N_3OS$ ($M+H^+$): 514.1948, found: 514.1964.

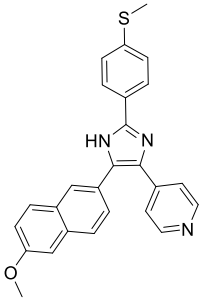

Procedure for the Synthesis of 4-(5-(6-methoxynaphthalen-2-yl)-2-(4-(methylthio)phenyl)-1H-imidazol-4-yl)pyridine 2.6.

Pale brown solid, 80% yield (67 mg). ^{1}H NMR (500 MHz, DMSO-d_6) δ 13.02 (s, 1H), 8.45 (d, J = 5.8 Hz, 2H), 8.08 (d, J = 8.7 Hz, 3H), 7.88 (t, J = 8.9 Hz, 2H), 7.56 (dd, J = 8.5, 1.6 Hz, 1H), 7.52 (d, J = 6.3 Hz, 2H), 7.38 (d, J = 8.7 Hz, 3H), 7.22 (dd, J = 8.9, 2.4 Hz, 1H), 3.91 (s, 3H), 2.54 (s, 3H). ^{13}C NMR (126 MHz, DMSO-d_6) δ 158.2, 150.1, 139.2, 134.3, 132.1, 131.9, 130.0, 129.1, 128.85, 127.79, 127.78, 127.56, 127.53, 127.26, 127.25, 126.29, 126.25, 121.3, 119.6, 106.5, 55.7, 14.9. HRMS. Calculated for $C_{26}H_{22}N_3OS$ ($M+H^+$): 424.1478, found: 424.1483.

2.6. References

(1) (a) Shen, H. C. In *Applications of Transition Metal Catalysis in Drug Discovery and Development*; Matthew L. Crawley, Trost, B. M., Eds.; John Wiley & Sons, Inc.: Hoboken, **2012**, p 25-95; (b) Carey, J. S.; Laffan, D.; Thomson, C.; Williams, M. T. *Org. Biomol. Chem.* **2006***, 4*, 2337-2347; (c) Horton, D. A.; Bourne, G. T.; Smythe, M. L. *Chem. Rev.* **2003**, *103*, 893-930; (d) Yamaguchi, J.; Yamaguchi, A. D.; Itami, K. Itami *Angew. Chem. Int. Ed.* **2012**, *51*, 8960-9009; (e) Roughley, S. D.; Jordan, A. M. *J. Med. Chem.* **2011**, *54*, 3451-3479; (f) Baumann, M.; Baxendale, I. R.; Ley, S. V.; Nikbin, N. *Beilstein J. Org. Chem.* **2011**, *7*, 442-495.

(2) For review: (a) Bellina, F.; Cauteruccio, S.; Rossi, R. *Tetrahedron* **2007**, *63*, 4571-4624. For examples: (b) Lee, J. C.; Laydon, J. T.; McDonnell, P. C.; Gallagher, T. F.; Kumar, S.; Green, D.; McNulty, D.; Blumenthal, M. J.; Keys, J. R.; Land vatter, S. W.; Strickler, J. E.; McLaughlin, M. M.; Siemens, I. R.; Fisher, S. M.; Livi, G. P.; White, J. R.; Adams, J. L.; Young, P. R. *Nature* **1994**, *372*, 739-746; (c) Ting-Ting, K.; Cheng-Mei, Z.; Zhao-Peng, L. *Curr. Med. Chem.* **2013**, *20*, 1997-2016; (d) Sisko, J. *J. Org. Chem.* **1998**, *63*, 4529-4531; (e) Newton, R.; Holden, N. S. *Drug Discov. Today: Dis. Mech.* **2006**, *3*, 53–61.

(3) For example: (a) Atwell, G. J.; Fan, J.-Y.; Tan, K.; Denny, W. A. *J. Med. Chem.* **1998**, *41*, 4744-4754; (b) Wang, L.; Woods, K. W.; Li, Q.; Barr, K. J.; McCroskey, R. W.; Hannick, S. M.; Gherke, L.; Credo, R. B.; Hui, Y.-H.; Marsh, K.; Warner, R.; Lee, J. Y.; Zielinski-Mozng, N.; Frost, D.; Rosenberg, S. H.; Sham, H. L.*J. Med. Chem.* **2002**, *45*, 1697-1711; (c) Williams,

D. R.; Ko, S.-K.; Park, S.; Lee, M.-R.; Shin, I. *Angew. Chem. Int. Ed.* **2008**, *47*, 7466-7469; (d) Williams, D. R.; Lee, M.-R.; Song, Y.-A.; Ko, S.-K.; Kim, G.-H.; Shin, I. *J. Am. Chem. Soc.* **2007**, *129*, 9258-9259; (e) Sakagami, H.; Kobayashi, M.; Ishihara, M.; Kikuchi, H.; Nakamura, Y.; Kawase, M.; Motohashi, N. In *Bioactive Heterocycles VI: Flavonoids and Anthocyanins in Plants, and Latest Bioactive Heterocycles I*; Motohashi, N., Ed.; Springer Berlin Heidelberg: Berlin, Heidelberg, **2008**, p 173-199; (f) Bonezzi, K.; Taraboletti, G.; Borsotti, P.; Bellina, F.; Rossi, R.; Giavazzi, R. *J. Med. Chem.* **2009**, *52*, 7906-7910; (g) Leschke, C.; Elz, S.; Garbarg, M.; Schunack, W. *J. Med. Chem.* **1995**, *38*, 1287-1294; (h) Zhang, L.; Peng, X.-M.; Damu, G. L. V.; Geng, R.-X.; Zhou, C.-H. *Med. Res. Rev.* **2014**, *34*, 340-437.

(4) (a) Kulkarni, A. P.; Tonzola, C. J.; Babel, A.; Jenekhe, S. A. *Chem. Mater.* **2004**, *16*, 4556-4573; (b) Wang, Z.; Lu, P.; Chen, S.; Gao, Z.; Shen, F.; Zhang, W.; Xu, Y.; Kwok, H. S.; Ma, Y. *J. Mater. Chem.* **2011**, *21*, 5451-5456; (c) Zhu, M.; Yang, C. *Chem. Soc. Rev.* **2013**, *42*, 4963-4976; (d) Kumar, D.; Justin Thomas, K. R.; Lee, C.-P.; Ho, K.-C. *J. Org. Chem.* **2014**, *79*, 3159-3172; (e) Li, W.; Lin, W.; Wang, J.; Guan, X. *Org. Lett.* **2013**, *15*, 1768-1771; (f) Levi, L.; Muller, T. J. J. *Chem. Soc. Rev.* **2016**, *45*, 2825-2846.

(5) Reviews: (a) Anderson, E. B.; Long, T. E. *Polymer* **2010**, *51*, 2447-2454; (b) Kulhanek, J.; Bures, F. *Beilstein J. Org. Chem.* **2012**, *8*, 25-49.

(6) Contreras, R.; Flores-Parra, A.; Mijangos, E.; Téllez, F.; López-Sandoval, H.; Barba-Behrens, N. *Coord. Chem. Rev.* **2009**, *253*, 1979-1999.

(7) (a) Hopkinson, M. N.; Richter, C.; Schedler, M.; Glorius, F. *Nature* **2014**, *510*, 485-496; (b) Herrmann, W. A. *Angew. Chem. Int. Ed.* **2002**, *41*, 1290-1309; (c) Levin, E.; Ivry, E.; Diesendruck, C. E.; Lemcoff, N. G. *Chem. Rev.* **2015**, *115*, 4607-4692.

(8) For reviews: (a) Grimmett, M. R. In *Imidazole and Benzimidazole Synthesis*; Grimmett, M. R., Ed.; Academic Press: San Diego, **1997**, p 151-165; (b) Yet, L. In *Progress in Heterocyclic Chemistry*; Gordon, W. G., John, A. J., Eds.; Elsevier: **2012**; Vol. 24, p 243-279.

(9) For reviews: (a) Schnürch, M.; Flasik, R.; Khan, A. F.; Spina, M.; Mihovilovic, M. D.; Stanetty, P. *Eur. J. Org. Chem.* **2006**, *2006*, 3283-3307; (b) Bellina, F.; Rossi, R. *Adv. Synth. Catal.* **2010**, *352*, 1223-1276; (c) Caron, S.; Ghosh, A.; Gut Ruggeri, S.; Ide, N. D.; Nelson, J. D.; Ragan, J. A. In *Practical Synthetic Organic Chemistry*; Caron, S., Ed.; John Wiley & Sons, Inc.: Hoboken, **2011**, p 279-340; (d) Schröter, S.; Stock, C.; Bach, T. *Tetrahedron* **2005**, *61*, 2245-2267.

(10) Rh-catalyzed: (a) Lewis, J. C.; Bergman, R. G.; Ellman, J. A. *Acc. Chem. Res.* **2008**, *41*, 1013-1025; (b) Lewis, J. C.; Wu, J. Y.; Bergman, R. G.; Ellman, J. A. *Angew. Chem. Int. Ed.* **2006**, *45*, 1589-1591; (c) J Lewis, J. C.; Berman, A. M.; Bergman, R. G.; Ellman, J. A. *J. Am. Chem. Soc.* **2008**, *130*, 2493-2500; Pd/Ni catalyzed: (d) Joo, J. M.; Touré, B. B.; Sames, D. *J. Org. Chem.* **2010**, *75*, 4911-4920; (e) Zhao, D.; Wang, W.; Lian, S.; Yang, F.; Lan, J.; You, J. *Chem. Eur. J.* **2009**, *15*, 1337-1340; (f) Campeau, L.-C.; Stuart, D. R.; Leclerc, J.-P.; Bertrand-Laperle, M.; Villemure, E.; Sun, H.-Y.; Lasserre, S.; Guimond, N.; Lecavallier, M.; Fagnou, K. *J. Am. Chem. Soc.* **2009**, *131*, 3291-3306; (g) Canivet, J.; Yamaguchi, J.; Ban, I.; Itami, K. *Org. Lett.* **2009**, *11*, 1733-1736; (h) Hachiya, H.; Hirano, K.; Satoh, T.; Miura, M. *Angew. Chem. Int. Ed.* **2010**, *49*, 2202-2205; (i) Muto, K.; Hatakeyama, T.; Yamaguchi, J.; Itami, K. *Chem. Sci.* **2015**, *6*, 6792-6798; (j) Shibahara, F.; Yamaguchi, E.; Murai, T. *J. Org. Chem.* **2011**, *76*, 2680-2693.; Cu-catalyzed: (k) Daugulis, O.; Do, H.-Q.; Shabashov, D. *Acc. Chem. Res.* **2009**, *42*, 1074-1086; (l) Do, H.-Q.; Khan, R. M. K.; Daugulis, O. *J. Am. Chem. Soc.* **2008**, *130*, 15185-15192; (m) Do, H.-Q.; Daugulis, O. *J. Am. Chem. Soc.* **2007**, *129*, 12404-12405; (n) Zhao, D.; Wang, W.; Yang, F.; Lan, J.; Yang, L.; Gao, G.; You, J. *Angew. Chem. Int. Ed.* **2009**, *48*, 3296-3300.

(11) Review: (a) Kamijo, S.; Yamamoto, Y. *Chem. Asian J.* **2007**, *2*, 568-578; Recent examples: (b) Siamaki, A. R.; Arndtsen, B. A. *J. Am. Chem. Soc.* **2006**, *128*, 6050-6051; (c Chen, C.-Y.; Hu, W.-P.; Yan, P.-C.; Senadi, G. C.; Wang, J.-J. *Org. Lett.* **2013**, *15*, 6116-6119; (d) Pérez-Caaveiro, C.; Pérez Sestelo, J.; Martínez, M. M.; Sarandeses, L. A. *J. Org. Chem.* **2014,** *79*, 9586-9593; (e) Li, S.; Li, Z.; Yuan, Y.; Peng, D.; Li, Y.; Zhang, L.; Wu, Y. *Org. Lett.* **2012**, *14*, 1130-1133; (f) Hu, B.; Wang, Z.; Ai, N.; Zheng, J.; Liu, X.-H.; Shan, S.; Wang, Z. *Org. Lett.* **2011**, *13*, 6362-6365; (g) Shen, H.; Xie, Z.*J. Am. Chem. Soc.* **2010**, *132*, 11473-11480. For routes to symmetrical products: (h) Huang, H.; Ji, X.; Wu, W.; Jiang, H. *Adv. Synth. Cat.* **2013**, *355*, 170-180; (i) Garcia, J. J.; Zerecero-Silva, P.; Reyes-Rios, G.; Crestani, M. G.; Arevalo, A.; Barrios-Francisco, R. *Chem. Comm.* **2011**, *47*, 10121-10123.

(12) (a) Lohr, T. L.; Marks, T. J. *Nat Chem* **2015**, *7*, 477-482; (b) Fogg, D. E.; dos Santos, E. N. *Coord. Chem. Rev.* **2004**, *248*, 2365-2379; (c) Wasilke, J.-C.; Obrey, S. J.; Baker, R. T.; Bazan, G. C. *Chem. Rev.* **2005**, *105*, 1001-1020; (d) Mata, J. A.; Hahn, F. E.; Peris, E. *Chem. Sci.* **2014**, *5*, 1723-1732.

(13) (a) Quesnel, J. S.; Arndtsen, B. A. *J. Am. Chem. Soc.* **2013**, *135*, 16841-16844; (b) Quesnel, J. S.; Kayser, L. V.; Fabrikant, A.; Arndtsen, B. A. *Chem. Eur. J.* **2015**, *21*, 9550-9555.

(14) These dipoles can be trapped in a subsequent step to from pyrroles: Torres, G. M.; Quesnel, J. S.; Bijou, D.; Arndtsen, B. A. *J. Am. Chem. Soc.* **2016**, *138*, 7315-7324.

(15) For reviews on Münchnone reactivity: (a) Gribble, G. W. In *Oxazoles: Synthesis, Reactions, and Spectroscopy, Part A*; Palmer, D. C., Ed.; John Wiley & Sons, Inc.: Hoboken, **2003**, p 473-576; (b) Gribble, G. W. In *Synthetic Applications of 1,3-Dipolar Cycloaddition Chemistry Toward Heterocycles and Natural Products*; Padwa, A., Pearson, W. H., Eds.; John Wiley & Sons, Inc.: New York, **2003**, p 681-753. For *N*-tosyl imine cycloaddition to Münchnones: (c) Dalla Croce, P.; Ferraccioli, R.; La Rosa, C. *Tetrahedron* **1999**, *55*, 201-210.

(16) For a related approach to triazoles, see: (a) Staben, S. T.; Blaquiere, N. *Angew. Chem. Int. Ed.* **2010**, *49*, 325-328; (b) Ackermann, L.; Potukuchi, H. K.; Landsberg, D.; Vicente, R. *Org. Lett.* **2008**, *10*, 3081-3084.

(17) Performing the catalytic reaction in the presence of *p*-TolSO_2Na (17 mg, 0.1 mmol) leads to no product after 24h.

(18) The addition of TMSCl or *n*-propylbromide (0.1 mmol) to the catalytic reaction was probed, and did not improve the product yield.

(19) Palladium aroyl complex **2.3** can be synthesized and isolated based on literature procedure.[13] Using **2.3** as the Palladium source and the conditions described in table 2.1, entry 11, the reaction affords the imidazole product in 72% yield.

(20) (a) Semones, M.; Feng, Y.; Johnson, N.; Adams, J. L.; Winkler, J.; Hansbury, M. *Bioorg. Med. Chem. Lett.* **2007**, *17*, 4756-4760; (b) Johnson, N. W.; Semones, M.; Adams, J. L.; Hansbury, M.; Winkler, J. *Bioorg. Med. Chem. Lett.* **2007**, *17*, 5514-5517. For a synthetic approach by sequential C-H bond functionalization, see ref. 10j.

(21) Layer W. R. *Chem. Rev.* **1963**, 63, 489-510.

(22) Vishwakarma, L. C.; Stringer, O. D.; Davis F. A. *Org. Synth.*, **1988**, 66, 203.

(23) Chemla, F.; Hebbe, V.; Normant, J.-F. *Synthesis*, **2000**, *1*, 75-77.

(24) Boultwood, T.; Bull, J. A. *Org. Lett.* **2014**, *16*, 2740-2743.

(25) Haddach, A.A.; Kelleman, A.; Deaton-Rewolinski, M.V. *Tetrahedron Lett*. **2002**, *43*, 399-402.

Chapter 3. A Nickel-Based, Tandem Catalytic Approach to Isoindolinones from Imines, Aryl Iodides and CO

3.1. Preface

In our studies on the synthesis of imidazoles in chapter 2, we showed how the palladium catalyzed carbonylation of aryl iodides in the presence of imines can allow the *in situ* generation of *N*-acyl iminium salts, which undergoes a second spontaneous cyclocarbonylation to form Münchnones. One of the limitations of this transformation is its reliance on palladium as the catalyst, which is an expensive and relative scarce metal. In an attempt to address this issue, we explore in this chapter the replacement of palladium with a first row nickel catalyst. Similar to the observations with palladium catalysts, it was found that $Ni(COD)_2$ in concert with chloride salts can catalyze the carbonylation of aryl iodides in the presence of imines to form *N*-acyl iminium chloride salts. However, in contrast to the palladium system, these *N*-acyl iminium salts undergo a spontaneous nickel catalyzed cyclization affording isoindolinone products. A range of aryl iodides and imines have been found to be viable substrates in this reaction, providing a modular route to generate substituted isoindolinones with high atom economy. This work was performed in collaboration with Jia Lun Shao (undergraduate student) and Dr. Veeranna Yempally (visiting postdoctoral fellow), who synthesized products **3.2c** and **3.2d**. This work was published in *Organometallics* (**2015**, *34*, 1802-1805).

3.2. Introduction

Transition metal catalyzed carbonylation reactions have seen growing use in synthetic chemistry.[1] In addition to simple esters, amides, ketones and related carboxylic acid derivatives, there has been significant recent application of carbonylations to the assembly of more elaborate carbocyclic and heterocyclic products. Examples of these can range from carbonylative cyclizations,[2] ring expansions,[3] Pauson-Khand type reactions,[4] and others.[5] One important class of heterocyclic products towards which carbonylations have been applied are isoindolinones. These heterocycles represent the core unit in a variety of natural products and other

pharmaceutically relevant compounds, including antitumor, anesthetic, anti-inflammatory agents, antidiabetic and others.[6] A number of approaches have been reported for the carbonylative synthesis of isoindolinones with *ortho*-functionalized aryl halides, including those with *ortho*-imino and *ortho*-vinyl substituted arenes (Scheme 3.1a).[7] However, similar to other approaches to isoindolinones, these often require the initial assembly of the appropriate aryl-tethered precursors for cyclization.

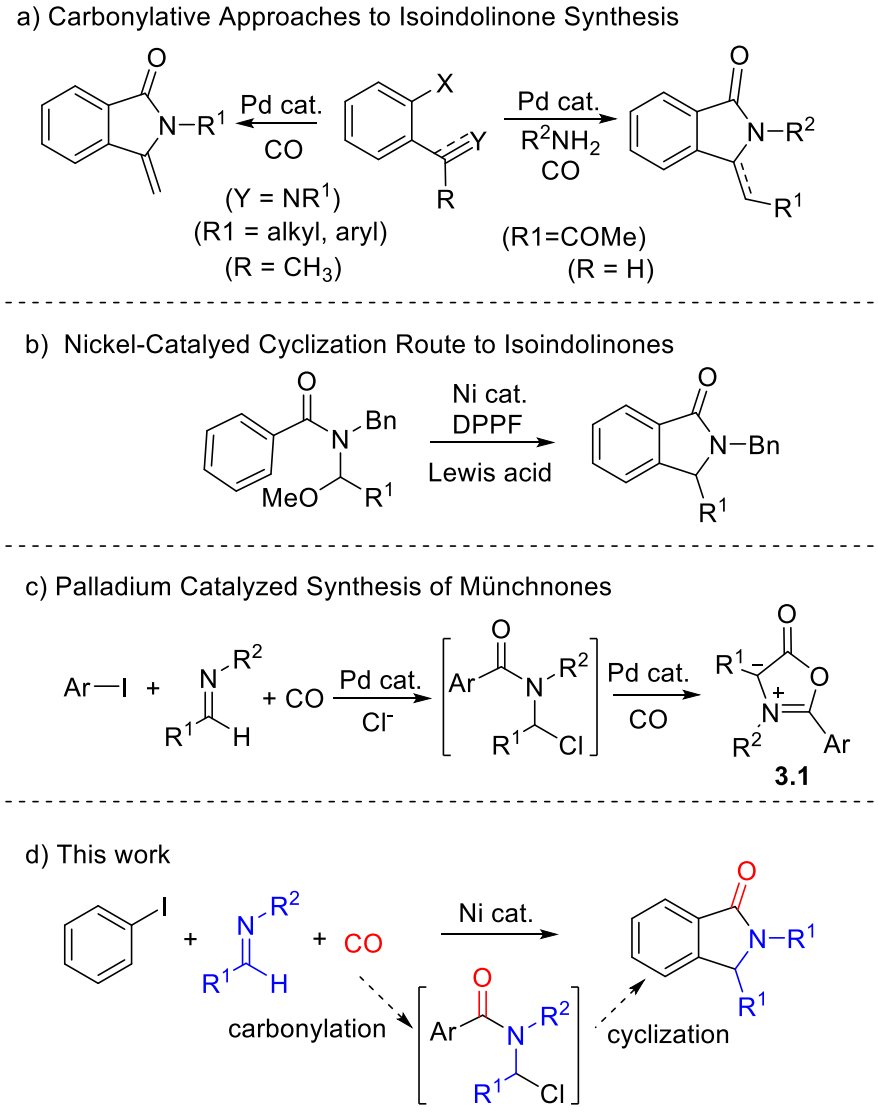

Scheme 3.1. Catalytic Synthesis to Isoindolinones

In considering the structure of isoindolinones, we postulated that a more modular approach to these products might be via the carbonylative coupling of aryl halides and imines. Watson and co-workers demonstrated that nickel catalysts can mediate the cyclization of synthetic *N*-benzoylaminals to isoindolinones (Scheme 3.1b).[8] An alternative would be to generate the *N*-acyl iminium salt intermediates via carbonylation. We have recently reported that palladium catalysts can be employed to generate acid chlorides from aryl iodides, which are reactive with even weak nucleophiles such as imines.[9] However, these palladium systems are potent carbonylation catalysts, and mediate a second, spontaneous carbonylation of the *N*-acyl iminium salt to form mesoionic 1,3-oxazolium-5-oxides **3.1** (i.e. Münchnones, Scheme 3.1c).[10] Relative to palladium, nickel catalysts often show diminished reactivity in carbonylations.[11] This suggests that nickel catalysts may be better suited to mediate a tandem carbonylation/C-H functionalization reaction (Scheme 1d), rather than the double carbonylative formation of **3.1**. We describe herein the successful realization of this goal, and the efficient, tandem catalytic approach to isoindolinones.

3.3. Results and Discussion

Our initial studies of this transformation examined the carbonylative coupling of 4-iodotoluene and imine (Table 3.1). The use of nickel(0)biscyclooctadiene [$Ni(COD)_2$] catalyst led to only trace amounts of isoindolinone **3.2a**, and instead generated amide **3.3a** in low yield (**Safety note:** *$Ni(CO)_4$ is a potential product generated in nickel-based carbonylations, and is extremely toxic and volatile. See Section 3.5.1. for details on safe practices on handling $Ni(CO)_4$*). The addition of various ligands to this reaction also did not afford significant amounts of **3.2a**. We have previously noted in our studies of palladium catalyzed carbonylation that chloride sources can facilitate coupling with weakly nucleophilic substrates by allowing the *in situ* generation of acid chlorides.[9a] As was hoped, the addition of tetrabutylammonium chloride to the catalytic reaction with simple $Ni(COD)_2$ catalyst resulted in the high yield formation of isoindolinone **3.2a** as the major reaction product. Most added ligands retard the formation of **3.2a**, with only the bulky and weak donor P(*o*-tolyl)$_3$ leading to yields approaching that of simple $Ni(COD)_2$. These suggest that the active catalyst for this system is an unligated nickel(0).[12]

Decreasing the reaction pressure to 1 atm doesn't appear to influence the product yield (entry 16).

Table 3.1. Catalyst Design for Carbonylative Isoindolinone Synthesis[a]

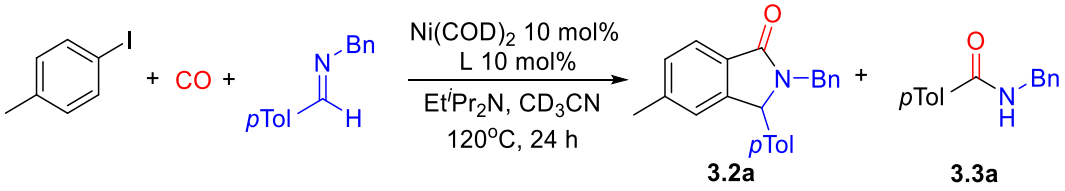

3.2a **3.3a**

Entry	L	Additive	**3.2a** (%)	**3.3a** (%)
1	-	-	2	28
2	PPh_3	-	-	-
3	P^tBu_3	-	-	-
4	P(*o*-tolyl)$_3$	-	3	-
5	-	Bu_4NCl	79	17
6	-	CsCl	5	16
7	-	Ph_4PCl	69	28
8	PCy_3	Bu_4NCl	0	0
9	DPPE	Bu_4NCl	0	0
10	DPPF	Bu_4NCl	0	5
11	PPh_3	Bu_4NCl	7	3
12	P^tBu_3	Bu_4NCl	10	5
13	P(*o*-tolyl)$_3$	Bu_4NCl	60	13
14		Bu_4NCl	11	4
15	XantPhos	Bu_4NCl	48	23
16[b]	-	Bu_4NCl	79 (78)[c]	17

[a] *p*-Tol-I (44 mg, 0.20 mmol), imine (21 mg, 0.10 mmol), Et $^iPr_2N$ (16 mg, 0.12 mmol), additive (0.10 mmol), $Ni(COD)_2$ (3 mg, 0.01 mmol), 4 atm CO, CD_3CN (0.7 mL), 120°C for 24 h, NMR yield; [b] 1 atm CO; [c] isolated.

With the optimized reaction conditions in hand, we explored the substrate diversity of the aryl halide reaction partner (Table 3.2). Both electron-rich (**3.2e**) and electron-deficient (**3.2b, 3.2c, 3.2f-2h**) aryl iodides can participate in this reaction, and lead to products in good yields. In addition to simple *para*-substituted aryl iodides, symmetrically di-substituted aryl iodides are viable substrates in this chemistry (**3.2i**). On the other hand, *ortho*-substituted aryl iodides such

as 2-iodotoluene or 2-iodoanisole failed to produce any of the corresponding isoindolinones products under these conditions. Simple *meta*-substituted aryl iodides lead to a mixture of isomeric products (**3.2j**).

The compatibility of this reaction with imines was also examined (Table 3.3). A number of *N*-alkyl (**3.2k**, **3.2l**) and -benzyl (**3.2n, 3.2o**) substituted imines can undergo carbonylative cyclization to form isoindolinones. However, *N*-aryl substituted imines yield only starting material under these conditions, presumably due to their decreased nucleophilicity for *N*-acyl iminium salt formation *(vide infra*). The imine carbon can tolerate a range of aromatic units,

Table 3.2. Aryl Iodide Diversity in Isoindolinone Synthesis[a]

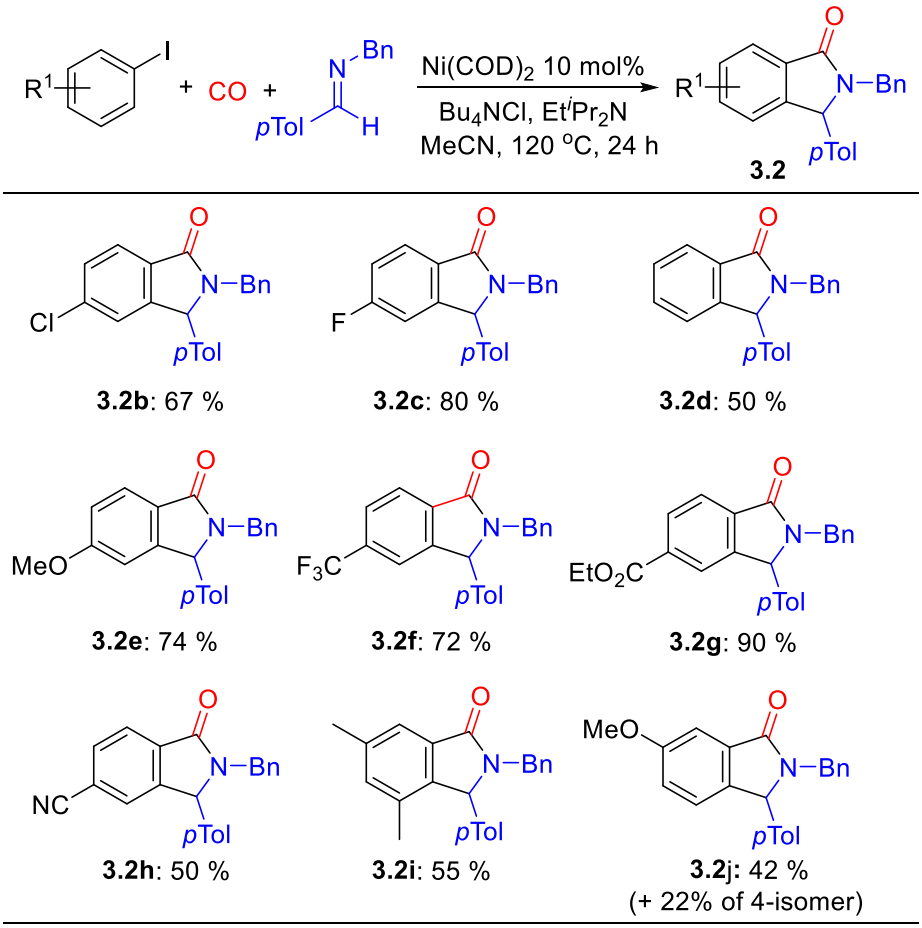

[a] Ar-I (1.00 mmol), imine (105 mg, 0.50 mmol), Et^{i}Pr$_2$N (77 mg, 0.60 mmol), Bu$_4$NCl (134 mg, 0.50 mmol), and Ni(COD)$_2$ (14 mg, 0.05 mmol), 1 atm CO, MeCN (2 mL) at 120°C for 24 h; Isolated yields.

Table 3.3. Imine Diversity in Isoindolinone Synthesis[a]

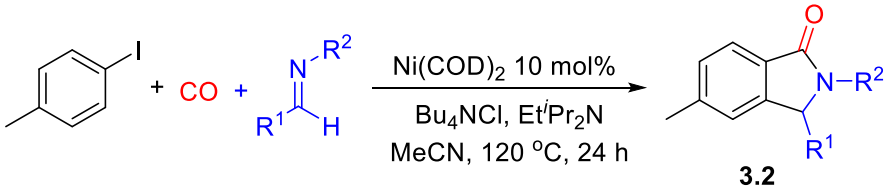

3.2

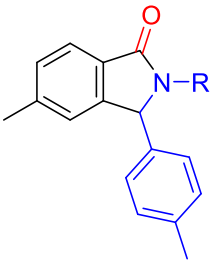

3.2k: R=Et, 70 %
3.2l: R=^{i}Pr, 55%

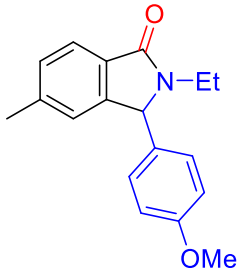

3.2m: 65 %

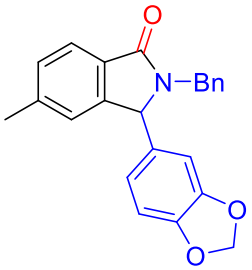

3.2n: 65 %

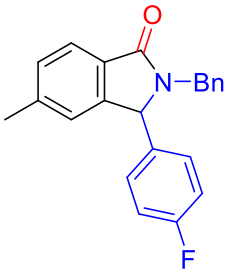

3.2o: 80 % (77 %)[b]

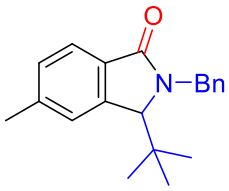

3.2p: 74 %

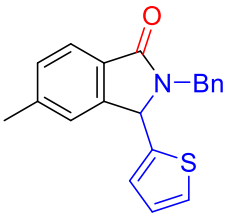

3.2q: 56 %

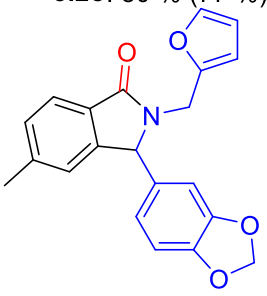

3.2r: 68 %

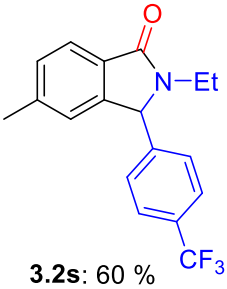

3.2s: 60 %

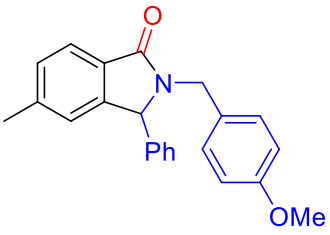

3.2t: 50 %

[a] *p*-Tol-I (218 mg, 1.00 mmol), imine (0.50 mmol), Et^{i}Pr$_2$N (77 mg, 0.60 mmol) , Bu$_4$NCl (134 mg, 1.0 mmol) and Ni(COD)$_2$ (14 mg, 0.05 mmol), 1 atm CO, MeCN (2 mL) at 120°C for 24 h; Isolated yields. [b] Reaction performed on 4 mmol scale.

including those with electron withdrawing (**3.2o**) and electron donating (**3.2m, 3.2n**) arenes, or heteroaryl units (**3.2q**). As shown with isoindolinone **3.2p**, ^{t}Bu-substituted imines can also be employed in this chemistry. This reaction can be applied to a gram scale synthesis of isoindolinones (e.g. **3.2o**).

While the mechanism of this transformation is still under investigation, based on preliminary studies we postulate a dual role of the nickel catalyst in this reaction (Scheme 3.2a). The required use of chloride in catalysis (Table 1) is similar to that observed with palladium systems that lead to acid chloride synthesis.[9] Thus, although it is possible that an *in situ* generated nickel-aroyl complex (**II**) can react directly with imine, the critical role of chloride in this chemistry is more consistent with the nickel catalyzed formation of acid chloride. As shown in Scheme 2b, acid chloride can rapidly react with an imine forming an *N*-acyl iminium chloride. Unlike traditional Pictet–Spengler reactions, **3.4a** does not undergo cyclization, even upon heating at 120 ^{o}C, and instead slowly decomposes to yield amide **3.3a**. However, the addition of $Ni(COD)_2$ to **3.4a** leads to the formation of isoindolinone in similar yield to that noted in catalysis (Scheme 3.2b). As noted by Watson, the nickel catalyst could play several roles in this cyclization, including that of a Lewis acid (e.g. **III**) or more directly in facilitating C-H bond functionalization.[8] While we at present cannot distinguish between these mechanisms, the conversion of *N*-acyl iminium chloride to the more electrophilic iodide or triflate salt also leads to cyclization, consistent with a Lewis acidic role of the nickel catalyst.

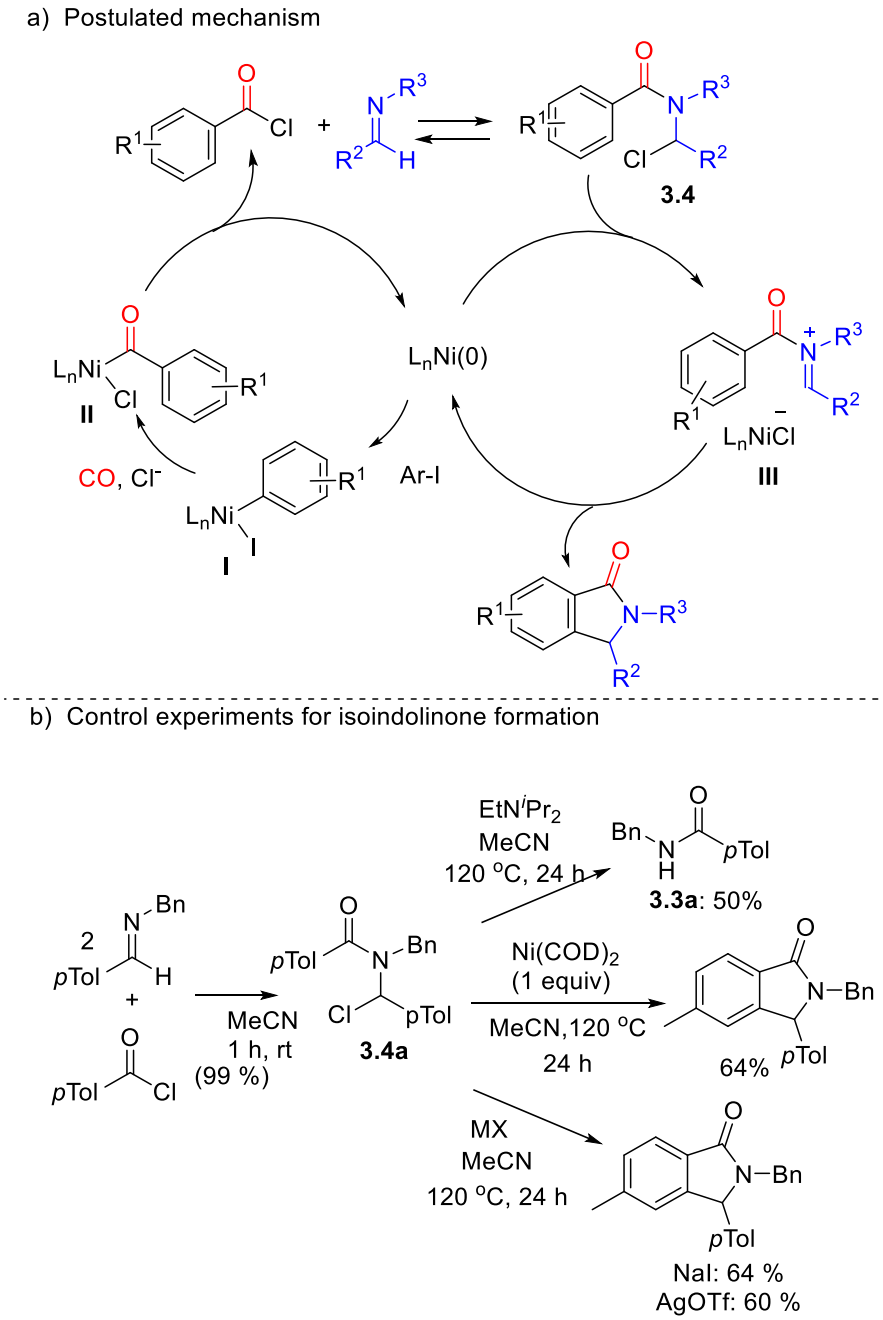

Scheme 3.2. Mechanism of Isoindolinone Synthesis

3.4. Conclusions

In conclusion, we have developed a nickel catalyzed process for the synthesis of highly substituted isoindolinones from aryl iodides, imines and carbon monoxide. This reaction is believed to proceed via the *in situ* generation of an *N*-acyl iminium chloride which further can

undergo a nickel mediated annulation. Overall, this provides a modular synthesis of isoindolinones from available substrates, and is directly amenable to structural diversification.

3.5. Supplementary information

3.5.1. General Considerations

All reactions were carried out under an inert atmosphere in a glovebox or using standard Schlenk techniques, unless otherwise indicated. Research grade carbon monoxide (99.99%) was used as received. All solvents were dried with using a solvent purification system and stored in glovebox over activated 4 Å molecular sieves. Deuterated solvents were dried over CaH_2, vacuum transferred and stored over 4 Å molecular sieves. Tetrabutylammonium chloride was dried in the glovebox by dissolving in dichloromethane, allowing it to stand overnight over activated 4 Å molecule sieves, then filtering and removing the solvent *in vacuo*. N-alkyl and -aryl imines were prepared according to literature procedures.[13] All other reagents were purchased from commercial suppliers and used as received. All ^{1}H and ^{13}C NMR spectra were acquired on 400 and 500 MHz spectrometers

Safety note: ***$Ni(CO)_4$ is a potential product generated in nickel-based carbonylations, and is extremely toxic and volatile.*** Precautions must be taken to avoid all contact with the reaction prior to quenching. All manipulations of the catalysis solutions after CO introduction were therefore rigorously performed in sealed vessels with no contact to air or person. In order to quench any possible traces of $Ni(CO)_4$, all volatiles from reaction mixtures were removed *in vacuo* on a Schlenk line and collected into a solvent trap charged with excess PPh_3, followed by the addition of water, as noted by Nolan.[14]

3.5.2. Synthetic Procedures

<u>Typical Procedure for the Ligand Screening (Table 3.1)</u>

In a glovebox, 4-iodotoluene (44 mg, 0.20 mmol), *p*-Tol(H)C=NBn (21 mg, 0.10 mmol), N,N-diisopropylethylamine (16 mg, 0.12 mmol), tetrabutylammonium chloride (28 mg, 0.10 mmol), $Ni(COD)_2$ (3 mg, 0.010 mmol) and benzyl benzoate internal standard were combined in CD_3CN (0.7 mL) and added to a J-Young NMR tube. The tube was removed from the glovebox, frozen

in liquid nitrogen, the headspace evacuated, and 4 atm carbon monoxide was condensed into the NMR tube. The reaction was heated at 120 °C and monitored by NMR spectroscopy. Yield of **3.2a** and **3.3a** was determined by ^{1}H NMR analysis relative to the internal standard. Procedures noted above were used to remove any potential traces of $Ni(CO)_4$.

Typical Procedure for the Catalytic Synthesis of Isoindolinones

In a glovebox, 4-iodotoluene (218 mg, 1.00 mmol), *p*-Tol(H)C=NBn (105 mg, 0.50 mmol), N,N-diisopropylethylamine (77 mg, 0.60 mmol), tetrabutylammonium chloride (134 mg, 0.50 mmol), $Ni(COD)_2$ (14 mg, 0.05 mmol) were combined in acetonitrile (2 mL) and added to a 50 mL sealable pressure vessel. The vessel was closed, removed from the glovebox, and pressurized with 1 atm carbon monoxide. The reaction was heated at 120°C for 24 h. Note: $Ni(CO)_4$ is a potential product generated in nickel-based carbonylations, and is extremely toxic and volatile. Therefore, all manipulations of the catalysis solutions after CO introduction were rigorously performed in an isolated, sealed vessel, with no contact to air or person prior to quenching of the potential $Ni(CO)_4$. After the reaction was cooled to room temperature, all volatiles were removed *in vacuo* on a Schlenk line and collected into a liquid N_2 cooled solvent trap charged with excess PPh_3 (to which water was subsequently added), in order to quench any possible traces of $Ni(CO)_4$. The crude product was purified by column chromatography (Silica gel, gradient hexane / ethyl acetate 4% to 20 %) affording isoindolinone **3.2a** as a pale white solid in 78 % yield (129 mg).

Generation of **3.4a** (Scheme 3.2b) In a glovebox, *p*-Tol(H)C=NBn (42 mg, 0.20 mmol), *p*-toluoyl chloride (16 mg, 0.10 mmol) and benzyl benzoate (internal standard) were combined in CD_3CN (0.7 mL) and stirred for 1 h. ^{1}H NMR analysis shows the formation of **3.4a** in quantitative yield (99%). **3.4a** is generated in a dynamic equilibrium with the acid chloride and imine, and an excess of imine was employed to favor its formation. In light of this equilibrium, **3.4a** was characterized *in situ*, in analogy to other iminium salts.[15] ^{1}H NMR (400 MHz, CD_3CN) δ 7.54 (d, J = 8.1 Hz, 2H), 7.44 (d, J = 8.2 Hz, 2H), 7.39 – 7.32 (m, 3H), 7.19 (m, 5H), 7.11 – 7.06 (m, 2H), 4.57 (s, 2H), 2.41 (s, 3H), 2.33 (s, 3H).

Generation of Thermal Reaction of **3.4a** (Scheme 3.2b)

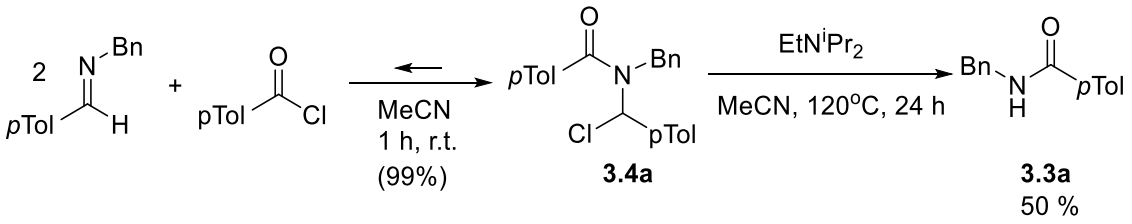

In a glovebox, *p*-Tol(H)C=NBn (42 mg, 0.20 mmol), *p*-toluoyl chloride (16 mg, 0.10 mmol) and benzyl benzoate (internal standard) were combined in CD_3CN (0.7 mL) and stirred for 1 h. The formation of **3.4a** (99%) was confirmed by ^{1}H NMR analysis. N,N-diisopropylethylamine (13 mg, 0.10 mmol) was added, and the reaction mixture transferred to a J-Young tube. The reaction mixture was heated to 120°C. ^{1}H NMR analysis after 24 h showed generation of amide **3.3a** in 50% yield relative to the internal standard.[16]

Reaction of **3.4a** with $Ni(COD)_2$ (Scheme 3.2b)

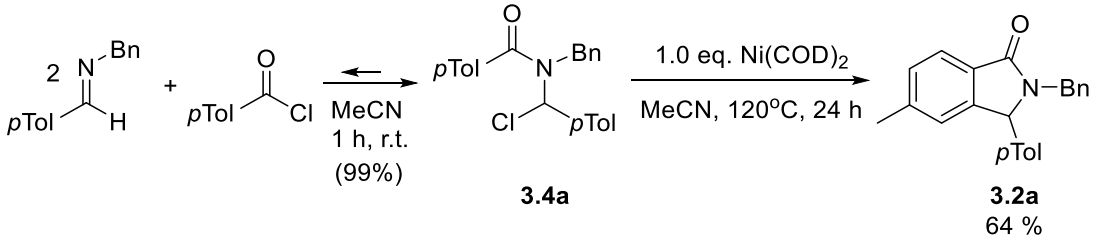

In a glovebox, *p*-Tol(H)C=NBn (42 mg, 0.20 mmol), *p*-toluoyl chloride (16 mg, 0.10 mmol) and benzyl benzoate (internal standard) were combined in CD_3CN (0.7 mL) and stirred for 1 h. As above, the quantitative formation of **3.4a** was confirmed by ^{1}H NMR analysis. $Ni(COD)_2$ (27 mg, 0.10 mmol) was added, and the reaction mixture transferred to a J-Young tube. The reaction mixture was heated to 120°C. ^{1}H NMR analysis after 24 h showed generation of **3.2a** in 64% yield relative to the internal standard.

Reaction of **3.4a** with AgOTf (Scheme 3.2b)

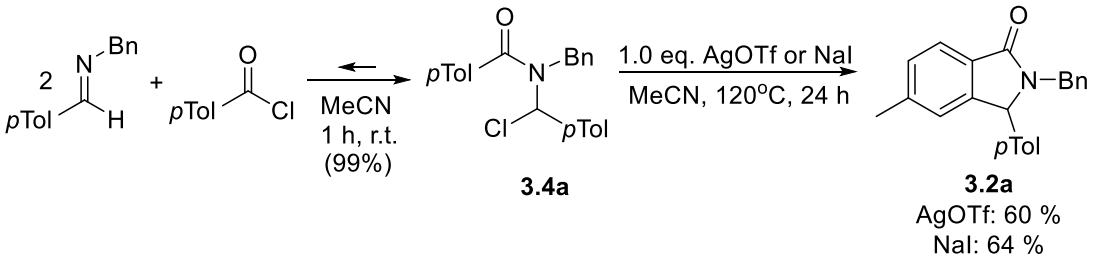

In a glovebox, *p*-Tol(H)C=NBn (42 mg, 0.20 mmol), *p*-toluoyl chloride (16 mg, 0.10 mmol) and benzyl benzoate (internal standard) were combined in CD_3CN (0.7 mL) and stirred for 1 h. As above, the formation of **3.4a** was confirmed by ^1H NMR analysis. Silver trifluoromethanesulfonate (26 mg, 0.10 mmol) was added, and the reaction mixture was transferred to a J-Young tube. The reaction mixture was heated to 120°C. ^1H NMR analysis after 24 h showed generation of **3.2a** in 60% relative to the internal standard.

3.5.3. Spectroscopic Data on Isoiondolinones 3.2

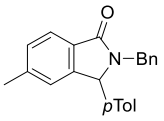

2-Benzyl-5-methyl-3-(p-tolyl)isoindolin-1-one (3.2a). Pale white solid, 127 mg, 78 % yield. ^{1}H NMR (500 MHz, $CDCl_3$) δ 7.84 (d, *J* = 7.8 Hz, 1H), 7.35 – 7.25 (m, 4H), 7.20 (dd, *J* = 7.1, 4.0 Hz, 4H), 6.99 (d, *J* = 8.0 Hz, 2H), 6.93 (s, 1H), 5.40 (d, *J* = 14.9 Hz, 1H), 5.18 (s, 1H), 3.73 (d, *J* = 14.9 Hz, 1H), 2.39 (s, 3H), 2.36 (s, 3H). ^{13}C NMR (126 MHz, $CDCl_3$) δ 168.6, 146.9, 142.5, 138.5, 137.3, 133.9, 129.8, 129.3, 128.9, 128.7, 128.4, 127.7, 127.5, 123.6, 123.5, 63.2, 43.7, 21.83 21.2. FT-IR-ATR (cm^{-1}): 1674.4 (C=O). HRMS. Calculated for $C_{23}H_{22}NO$ (M+H): 328.1696; found: 328.1692.

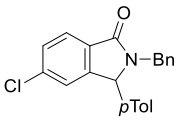

2-Benzyl-5-chloro-3-(p-tolyl)isoindolin-1-one (3.2b). White solid, 116 mg, 67 % yield. ^{1}H NMR (500 MHz, $CDCl_3$) δ 7.88 (d, *J* = 8.1 Hz, 1H), 7.45 (dd, *J* = 8.1, 1.5 Hz, 1H), 7.30 (dd, *J* = 11.3, 7.7 Hz, 3H), 7.20 (t, *J* = 7.6 Hz, 4H), 7.11 (s, 1H), 6.97 (d, *J* = 7.9 Hz, 2H), 5.39 (d, *J* = 14.9 Hz, 1H), 5.20 (s, 1H), 3.73 (d, *J* = 14.9 Hz, 1H), 2.40 (s, 3H). ^{13}C NMR (126 MHz, $CDCl_3$) δ 167.4, 148.1, 138.9, 138.2, 136.9, 132.8, 130.0, 129.9, 128.9, 128.8, 128.7, 128.5, 127.7, 124.9, 123.6, 62.9, 43.8, 21.2. FT-IR-ATR (cm^{-1}): 1677.6 (C=O). HRMS. Calculated for $C_{22}H_{18}ClNNaO$ (M+Na): 370.0969; found: 370.0970.

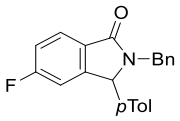

2-Benzyl-5-fluoro-3-(p-tolyl)isoindolin-1-one (3.2c). White solid, 116 mg, 80 % yield. ^{1}H NMR (500 MHz, $CDCl_3$) δ 7.94 (dd, *J* = 8.4, 5.0 Hz, 1H), 7.40 – 7.26 (m, 3H), 7.25 – 7.11 (m, 5H), 6.98 (d, *J* = 7.9 Hz, 2H), 6.81 (dd, *J* = 8.0, 1.8 Hz, 1H), 5.39 (d, *J* = 14.9 Hz, 1H), 5.20 (s, 1H), 3.74 (d, *J* = 14.9 Hz, 1H), 2.39 (s, 3H). ^{13}C NMR (126 MHz, $CDCl_3$) δ 167.5, 165.3 (d, J = 251.8 Hz), 149.0 (d, J = 9.6 Hz), 138.9, 137.0, 133.0, 130.0, 128.7, 128.8, 127.7, 127.6, 127.5 (d, J = 2.0 Hz), 125.7 (d, J = 9.7 Hz), 116.1 (d, J = 23.5 Hz), 110.5 (d, J = 24.1 Hz), 63.0 (d, J = 2.6 Hz), 43.9, 21.2. FT-IR-ATR (cm^{-1}): 1680.4 (C=O). HRMS. Calculated for $C_{22}H_{19}NOF$ (M+H): 332.1445; found: 332.1440.

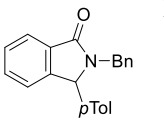

2-Benzyl-3-(p-tolyl)isoindolin-1-one (3.2d). Pale white solid, 78 mg, 50 % yield. ^{1}H NMR (500 MHz, $CDCl_3$) δ 7.96 (d, *J* = 6.4 Hz, 1H), 7.49 – 7.44 (m, 2H), 7.30

(dt, *J* = 6.8, 4.4 Hz, 3H), 7.20 (dd, *J* = 12.5, 7.4 Hz, 4H), 7.15 – 7.12 (m, 1H), 6.98 (d, *J* = 7.9 Hz, 2H), 5.42 (d, *J* = 14.9 Hz, 1H), 5.23 (s, 1H), 3.74 (d, *J* = 14.9 Hz, 1H), 2.39 (s, 3H). ^{13}C NMR (126 MHz, $CDCl_3$) δ 168.5, 146.6, 138.6, 137.2, 133.7, 131.8, 131.4, 129.8, 128.7, 128.5, 128.2, 127.7, 127.5, 123.7, 123.1, 63.32, 43.7, 21.2. FT-IR-ATR (cm^{-1}): 1685.0 (C=O). HRMS. Calculated for $C_{22}H_{19}NONa$ (M+Na): 336.1359; found: 336.1364.

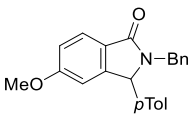

2-Benzyl-5-methoxy-3-(p-tolyl)isoindolin-1-one (3.2e). Pale yellow solid, 127 mg, 74 % yield. ^{1}H NMR (500 MHz, $CDCl_3$) δ 7.86 (d, *J* = 8.4 Hz, 1H), 7.30 (dt, *J* = 12.9, 6.5 Hz, 3H), 7.23 – 7.14 (m, 4H), 6.99 (t, *J* = 6.0 Hz, 3H), 6.59 (s, 1H), 5.38 (d, *J* = 14.9 Hz, 1H), 5.17 (s, 1H), 3.77 (s, 3H), 3.69 (t, *J* = 14.2 Hz, 1H), 2.39 (s, 3H). ^{13}C NMR (126 MHz, $CDCl_3$) δ 168.3, 163.0, 148.8, 138.5, 137.4, 133.8, 129.8, 128.7, 128.4, 127.8, 127.4, 125.0, 124.1, 115.0, 107.9, 63.1, 55.6, 43.7, 21.2. FT-IR-ATR (cm^{-1}): 1675.8 (C=O). HRMS. Calculated for $C_{23}H_{22}NO_2$ (M+H): 344.1645; found: 344.1641.

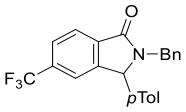

2-Benzyl-3-(p-tolyl)-5-(trifluoromethyl)isoindolin-1-one (3.2f). Pale yellow solid, 139 mg, 72 % yield. ^{1}H NMR (500 MHz, $CDCl_3$) δ 8.07 (d, *J* = 7.9 Hz, 1H), 7.76 (d, *J* = 7.9 Hz, 1H), 7.39 (s, 1H), 7.36 – 7.26 (m, 3H), 7.21 (t, *J* = 8.0 Hz, 4H), 6.98 (d, *J* = 7.9 Hz, 2H), 5.42 (d, *J* = 14.8 Hz, 1H), 5.28 (s, 1H), 3.76 (d, *J* = 14.8 Hz, 1H), 2.40 (s, 3H). ^{13}C NMR (126 MHz, $CDCl_3$) δ 167.0, 146.8, 139.1, 136.7, 134.7, 133.8 (q, J = 32.5 Hz), 132.4, 130.1, 128.8, 128.5, 127.8, 127.7, 125.61 (q, J = 3.6 Hz), 124.3, 123.7 (q, J = 273.0 Hz), 120.5 (q, J = 3.8 Hz), 63.4, 43.9, 21.2. FT-IR-ATR (cm^{-1}): 1699.0 (C=O). HRMS. Calculated for $C_{23}H_{18}F_3NNaO$ (M+Na): 404.1233; found: 404.1240.

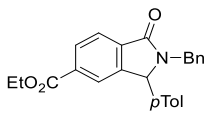

Ethyl 2-benzyl-1-oxo-3-(p-tolyl)isoindoline-5-carboxylate (3.2g). White solid, 171 mg, 90 % yield. ^{1}H NMR (500 MHz, $CDCl_3$) δ 8.17 (d, *J* = 8.0 Hz, 1H), 8.01 (d, *J* = 7.9 Hz, 1H), 7.80 (s, 1H), 7.37 – 7.26 (m, 3H), 7.23 – 7.16 (m, 4H), 6.98 (d, *J* = 8.0 Hz, 2H), 5.41 (d, *J* = 14.8 Hz, 1H), 5.28 (s, 1H), 4.50 – 4.22 (m, 2H), 3.76 (d, *J* = 14.8 Hz, 1H), 2.39 (s, 3H), 1.36 (t, *J* = 7.1 Hz, 3H). ^{13}C NMR (126 MHz, $CDCl_3$) δ 167.5, 165.8, 146.4, 138.84, 136.8, 135.2, 133.7, 132.8, 130.0, 129.7, 128.8, 128.5, 127.8, 127.7,

124.5, 123.7, 63.4, 61.4, 43.9, 21.2, 14.3. FT-IR-ATR (cm^{-1}): 1715.2 (CO_2Et), 1694.4 (C=O). HRMS. Calculated for $C_{25}H_{24}NO_3$ (M+H): 386.1751; found: 386.1740.

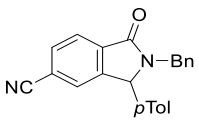

2-Benzyl-1-oxo-3-(p-tolyl)isoindoline-5-carbonitrile (3.2h). Pale yellow solid, 85 mg, 50 % yield. ^{1}H NMR (500 MHz, $CDCl_3$) δ 8.05 (d, *J* = 7.9 Hz, 1H), 7.77 (d, *J* = 7.9 Hz, 1H), 7.42 (s, 1H), 7.37 – 7.29 (m, 3H), 7.25 – 7.15 (m, 4H), 6.96 (d, *J* = 8.0 Hz, 2H), 5.41 (d, *J* = 14.8 Hz, 1H), 5.27 (s, 1H), 3.77 (d, *J* = 14.8 Hz, 1H), 2.41 (s, 3H). ^{13}C NMR (126 MHz, $CDCl_3$) δ 166.5, 146.9, 139.4, 136.4, 135.3, 132.3, 132.0, 130.2, 128.9, 128.5, 127.9, 127.6, 127.2, 124.6, 118.1, 115.3, 63.16, 44.0, 21.23. FT-IR-ATR (cm^{-1}): 2229.0 (CN), 1682.1 (C=O). HRMS. Calculated for $C_{23}H_{19}N_2O$ (M+H): 339.1492; found: 339.1502.

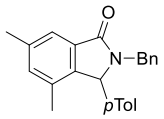

2-Benzyl-4,6-dimethyl-3-(p-tolyl)isoindolin-1-one (3.2i). Pale white solid, 94 mg, 55 % yield. ^{1}H NMR (500 MHz, $CDCl_3$) δ 7.64 (s, 1H), 7.36 – 7.26 (m, 3H), 7.22 (d, *J* = 6.9 Hz, 2H), 7.15 (d, *J* = 7.9 Hz, 2H), 7.08 (s, 1H), 6.93 (d, *J* = 7.3 Hz, 2H), 5.36 (d, *J* = 15.0 Hz, 1H), 5.13 (s, 1H), 3.61 (d, *J* = 15.0 Hz, 1H), 2.44 (s, 3H), 2.38 (s, 3H), 1.89 (s, 3H). ^{13}C NMR (126 MHz, $CDCl_3$) δ 168.6, 141.7, 138.6, 138.4, 137.5, 134.3, 133.0, 133.0, 132.1, 129.6, 128.7, 128.4, 127.4, 121.5, 62.8, 43.40, 21.4, 21.2, 17.8. FT-IR-ATR (cm^{-1}): 1684.8 (C=O). HRMS. Calculated for $C_{24}H_{24}NO$ (M+H): 342.1852; found: 342.1846.

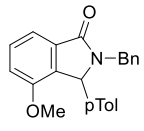

2j: 42%

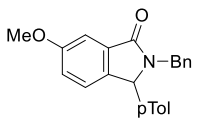

2j': 22%

2-Benzyl-4-methoxy-3-(p-tolyl)isoindolin-1-one (3.2j) and 2-benzyl-6-methoxy-3-p-tolylisoindolin-1 one (3.2j'). Isolated as a mixture of both isomers, and characterized by comparison to previous reports.[5] Colorless oil, 109 mg, 64 % yield. ^{1}H NMR (500 MHz, $CDCl_3$) δ 7.56 (d, *J* = 7.1 Hz, 1H, major isomer), 7.44 (t, *J* = 7.8 Hz, 1H, both isomers), 7.34 – 7.23 (m, 4H, both isomers), 7.21 – 7.13 (m, 4H, both isomers), 7.02 – 6.93 (m, 2H, both isomers), 6.92 (d, *J* = 8.0 Hz, 1H, major isomer), 5.39 (d, *J* = 15.1 Hz, 1H, minor isomer), 5.36 (d, *J* = 14.9 Hz, 1H, major isomer), 5.25 (s, 1H, major isomer), 5.17 (s, 1H, minor isomer), 3.88 (s, 3H, minor isomer), 3.72 (d, *J* = 14.9 Hz, 1H, minor isomer), 3.65 (d, *J* = 14.9

Hz, 1H, major isomer), 3.62 (s, 3H, major isomer), 2.36 (s, 3H, both isomers). ^{13}C NMR (126 MHz, $CDCl_3$) δ 168.5, 168.3, 160.1, 154.7, 138.9, 138.5, 137.9, 137.3, 137.2, 133.93, 133.91, 133.4, 133.0, 132.8, 130.1, 129.8, 129.3, 128.68, 128.65, 128.5, 128.4, 127.9, 127.7, 127.5, 127.4, 124.0, 120.1, 115.8, 113.7, 106.4, 62.9, 61.6, 55.7, 55.5, 43.8, 43.5, 21.3, 21.2.

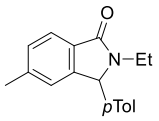

2-Ethyl-5-methyl-3-(p-tolyl)isoindolin-1-one (3.2k). Pale yellow solid, 92 mg, 70 % yield. ^{1}H NMR (500 MHz, $CDCl_3$) δ 7.77 (d, *J* = 7.8 Hz, 1H), 7.24 (d, *J* = 7.7 Hz, 1H), 7.17 (d, *J* = 7.8 Hz, 2H), 7.05 (d, *J* = 8.0 Hz, 2H), 6.97 (s, 1H), 5.40 (s, 1H), 3.96 (dq, *J* = 14.5, 7.3 Hz, 1H), 2.96 (dq, *J* = 14.2, 7.1 Hz, 1H), 2.35 (d, *J* = 2.4 Hz, 6H), 1.13 (t, *J* = 7.2 Hz, 3H). ^{13}C NMR (126 MHz, $CDCl_3$) δ 168.4, 146.8, 142.2, 138.4, 134.3, 129.7, 129.3, 129.2, 127.5, 123.5, 123.2, 63.7, 34.9, 21.8, 21.2, 13.5. FT-IR-ATR (cm^{-1}): 1667.9 (C=O). HRMS. Calculated for $C_{18}H_{20}NO$ (M+H): 266.1539; found: 266.1543.

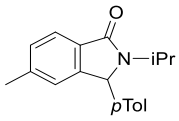

2-Isopropyl-5-methyl-3-(p-tolyl)isoindolin-1-one (3.2l). Pale yellow solid, 77 mg, 55 % yield. ^{1}H NMR (500 MHz, $CDCl_3$) δ 7.75 (d, *J* = 7.7 Hz, 1H), 7.24 (d, *J* = 7.7 Hz, 1H), 7.15 (d, *J* = 7.8 Hz, 2H), 7.09 (d, *J* = 7.8 Hz, 2H), 6.88 (s, 1H), 5.42 (s, 1H), 4.32 (hept, *J* = 6.9 Hz, 1H), 2.36 (s, 3H), 2.34 (s, 3H), 1.35 (d, *J* = 6.9 Hz, 3H), 1.04 (d, *J* = 6.9 Hz, 3H) ^{13}C NMR (126 MHz, $CDCl_3$) δ 168.9, 147.4, 142.2, 138.2, 136.0, 129.5, 129.5, 129.1, 127.7, 123.3, 123.0, 63.5, 45.1, 21.8, 21.3, 21.2, 20.6. FT-IR-ATR (cm^{-1}): 1667.2 (C=O). HRMS. Calculated for $C_{19}H_{22}NO$ (M+H): 280.1696; found: 280.1697.

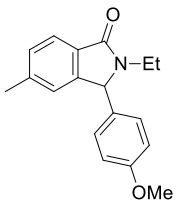

2-Ethyl-3-(4-methoxyphenyl)-5-methylisoindolin-1-one (3.2m). Pale yellow oil, 91 mg, 65 % yield. ^{1}H NMR (500 MHz, $CDCl_3$) δ 7.77 (d, *J* = 7.7 Hz, 1H), 7.26 (d, *J* = 7.7 Hz, 1H), 7.08 (d, *J* = 8.6 Hz, 2H), 6.97 (s, 1H), 6.89 (d, *J* = 8.7 Hz, 2H), 5.39 (s, 1H), 3.94 (d, *J* = 14.1, 7.2 Hz, 1H), 3.82 (s, 3H), 2.96 (dd, *J* = 14.1, 7.1 Hz, 1H), 2.37 (s, 3H), 1.13 (t, *J* = 7.2 Hz, 3H). ^{13}C NMR (126 MHz, $CDCl_3$) δ 168.3, 159.8, 146.9, 142.2, 129.3, 129.2, 129.2, 128.8, 123.5, 123.1, 114.4, 63.4, 55.3, 34.8, 21.8, 13.6. FT-IR-ATR (cm^{-1}): 1677.7 (C=O). HRMS. Calculated for $C_{18}H_{19}NO_2Na$ (M+Na): 304.1308; found: 304.1322.

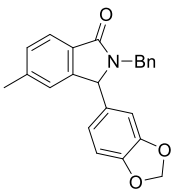

3-(Benzo[d][1,3]dioxol-4-yl)-2-benzyl-5-methylisoindolin-1-one (3.2n). Yellow solid, 116 mg, 65 % yield. ^{1}H NMR (500 MHz, $CDCl_3$) δ 7.83 (d, *J* = 7.8 Hz, 1H), 7.33 – 7.24 (m, 4H), 7.21 (d, *J* = 6.8 Hz, 2H), 6.94 (s, 1H), 6.81 (d, *J* = 7.9 Hz, 1H), 6.67 (dd, *J* = 7.9, 1.5 Hz, 1H), 6.42 (d, *J* = 1.5 Hz, 1H), 5.96 (dd, *J* = 8.8, 1.3 Hz, 2H), 5.37 (d, *J* = 14.9 Hz, 1H), 5.13 (s, 1H), 3.78 (d, *J* = 14.9 Hz, 1H), 2.36 (s, 3H). ^{13}C NMR (126 MHz, $CDCl_3$) δ 168.5, 148.5, 148.0, 146.8, 142.6, 137.3, 130.6, 129.4, 129.2, 128.8, 128.7, 128.4, 127.5, 127.1, 123.6, 123.5, 121.9, 108.5, 107.3, 101.4, 63.2, 43.7, 21.9. FT-IR-ATR (cm^{-1}): 1680.5 (C=O). HRMS. Calculated for $C_{23}H_{20}NO_3$ (M+H): 358.1438; found: 358.14388.

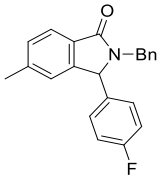

2-Benzyl-3-(4-fluorophenyl)-5-methylisoindolin-1-one (3.2o). White solid, 132 mg, 80 % yield. ^{1}H NMR (500 MHz, $CDCl_3$) δ 7.84 (d, *J* = 7.8 Hz, 1H), 7.34 – 7.26 (m, 5H), 7.20 – 7.14 (m, 2H), 7.09 – 7.03 (m, 4H), 6.90 (s, 1H), 5.39 (d, *J* = 14.9 Hz, 1H), 5.19 (s, 1H), 3.73 (d, *J* = 14.9 Hz, 1H), 2.37 (s, 3H). ^{13}C NMR (126 MHz, $CDCl_3$) δ 168.5, 162.8 (d, J = 247.6 Hz), 146.6, 142.7, 137.1, 132.8 (d, J = 3.2 Hz), 129.6 (d, J = 8.3 Hz), 129.5 (s), 128.8 (s), 128.6 (d, J = 43.3 Hz), 127.6 (s), 123.6 (s), 123.6, 116.2, 116.0, 62.7, 43.8, 21.8. FT-IR-ATR (cm^{-1}): 1680.9 (C=O). HRMS. Calculated for $C_{22}H_{19}NOF$ (M+H): 332.1445; found: 332.1444.

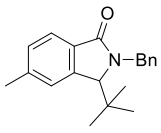

2-Benzyl-3-(tert-butyl)-5-methylisoindolin-1-one (3.2p). Colorless oil, 108 mg, 74 % yield. ^{1}H NMR (500 MHz, $CDCl_3$) δ 7.80 (d, *J* = 7.7 Hz, 1H), 7.32 – 7.21 (m, 5H), 7.13 (d, *J* = 7.2 Hz, 2H), 5.63 (d, *J* = 15.6 Hz, 1H), 4.42 (d, *J* = 15.6 Hz, 1H), 4.10 (s, 1H), 2.45 (s, 3H), 1.01 (s, 9H). ^{13}C NMR (126 MHz, $CDCl_3$) δ 170.9, 145.7, 141.2, 137.4, 130.8, 130.4, 129.0, 128.8, 128.8, 128.8, 128.7, 128.4, 128.3, 128.2, 127.72, 127.70, 127.3, 125.0, 123.6, 68.0, 47.6, 36.6, 27.7, 26.4, 22.1. FT-IR-ATR (cm^{-1}): 1685.9 (C=O). HRMS. Calculated for $C_{20}H_{24}NO$ (M+H): 294.1852; found: 294.1856.

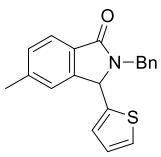

2-Benzyl-5-methyl-3-(thiophen-2-yl)isoindolin-1-one (3.2q). Colorless oil, 90 mg, 56 % yield. ^{1}H NMR (500 MHz, $CDCl_3$) δ 7.83 (d, *J* = 7.8 Hz, 1H), 7.36 – 7.28 (m, 5H), 7.28 – 7.21 (m, 2H), 7.07 – 7.00 (m, 3H), 5.54 (s, 1H), 5.40 (d, *J* = 15.0 Hz, 1H), 3.89 (d, *J* = 15.0 Hz, 1H), 2.40 (s, 3H). ^{13}C NMR (126 MHz, $CDCl_3$) δ 168.0, 146.0, 142.7, 140.5, 137.2, 129.7, 128.7, 128.6, 128.4, 127.6, 127.5, 126.9, 126.6, 123.6, 123.6, 58.6, 43.7, 21.9. FT-IR-ATR (cm^{-1}): 1686.6 (C=O). HRMS. Calculated for $C_{20}H_{18}NOS$ (M+H): 320.1104; found: 320.1095.

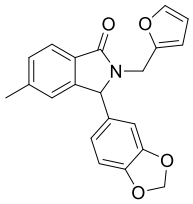

3-(Benzo[d][1,3]dioxol-4-yl)-2-(furan-2-ylmethyl)-5-methylisoindolin-1-one (3.2r). Colorless oil, 117 mg, 68 % yield. ^{1}H NMR (500 MHz, $CDCl_3$) δ 7.79 (d, *J* = 7.8 Hz, 1H), 7.34 (d, *J* = 1.0 Hz, 1H), 7.30 – 7.23 (m, 1H), 6.96 (s, 1H), 6.82 (d, *J* = 7.9 Hz, 1H), 6.75 (dd, *J* = 7.9, 1.4 Hz, 1H), 6.46 (d, *J* = 1.2 Hz, 1H), 6.33 – 6.27 (m, 1H), 6.19 (d, *J* = 3.1 Hz, 1H), 5.96 (dd, *J* = 7.9, 1.1 Hz, 2H), 5.28 (s, 1H), 5.22 (d, *J* = 15.6 Hz, 1H), 3.90 (d, *J* = 15.6 Hz, 1H), 2.37 (s, 3H). ^{13}C NMR (126 MHz, $CDCl_3$) δ 168.2, 150.0, 148.4, 148.0, 146.7, 142.6, 142.4, 130.6, 129.4, 128.7, 123.6, 123.5, 121.9, 110.3, 108.5, 108.4, 107.4, 101.3, 63.7, 36.5, 21.9. FT-IR-ATR (cm^{-1}): 1685.8 (C=O). HRMS. Calculated for $C_{21}H_{18}NO_4$ (M+H): 348.1230; found: 348.1228.

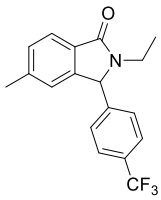

2-Ethyl-5-methyl-3-(4-(trifluoromethyl)phenyl)isoindolin-1-one (3.2s). Pale yellow solid, 96 mg, 60 % yield. ^{1}H NMR (500 MHz, $CDCl_3$) δ 7.79 (d, *J* = 7.8 Hz, 1H), 7.64 (d, *J* = 8.1 Hz, 2H), 7.31 (d, *J* = 8.0 Hz, 2H), 7.30 – 7.26 (m, 1H), 6.95 (s, 1H), 5.50 (s, 1H), 4.00 (dd, *J* = 14.2, 7.2 Hz, 1H), 2.95 (dd, *J* = 14.1, 7.1 Hz, 1H), 2.37 (s, 3H), 1.15 (t, *J* = 7.2 Hz, 3H). ^{13}C NMR (126 MHz, $CDCl_3$) δ 168.4, 145.8, 142.6, 141.8, 130.9 (q, J = 32.6 Hz), 129.7, 129.10, 127.9, 126.1 (q, J = 3.7 Hz), 123.9 (q, J = 272.2 Hz), 123.5, 123.4, 63.3, 35.1, 21.8, 13.5. FT-IR-ATR (cm^{-1}): 1672.5 (C=O). HRMS. HRMS. Calculated for $C_{18}H_{17}F_3NO$ (M+H): 320.1257; found: 320.1269.

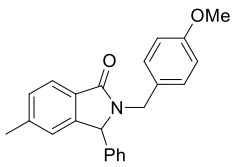

2-(4-Methoxybenzyl)-5-methyl-3-phenylisoindolin-1-one (3.2t). Pale yellow oil, 100 mg, 53 % yield. ^{1}H NMR (500 MHz, $CDCl_3$) δ 7.83 (d, *J* = 7.8 Hz, 1H), 7.42 – 7.33 (m, 3H), 7.27 (d, *J* = 8.6 Hz, 1H), 7.17 – 7.07 (m, 4H), 6.92 (s, 1H), 6.87 – 6.79 (m, 2H), 5.35 (d, *J* = 14.8 Hz, 1H), 5.20 (s, 1H), 3.80 (s, 3H), 3.68 (d, *J* = 14.8 Hz, 1H), 2.35 (s, 3H). ^{13}C NMR (126 MHz, $CDCl_3$) δ 168.5, 159.0, 146.8, 142.47, 137.1, 129.8, 129.3, 129.3, 129.1, 128.9, 128.6, 127.8, 123.6, 123.5, 114.0, 63.3 55.3, 43.2, 21.8. FT-IR-ATR (cm^{-1}): 1680.0 (C=O). HRMS. HRMS. Calculated for $C_{23}H_{22}NO_2$ (M+H): 344.1645; found: 344.1649.

3.6. References

(1) (a) Gadge, S. T.; Bhanage, B. M. *RSC Advances* **2014**, *4*, 10367-10389; (b) Beller, M.; Wu, X.-F. *Transition Metal Catalyzed Carbonylation Reactions*; Springer: Berlin Heidelberg, **2013**, pp 1-11; (c) Rossi, E. In *Modern Carbonylation Methods*; Kollár, L., Ed.; Wiley-VCH: Weinheim, 2008.

(2) (a) Wu, X.-F.; Neumann, H.; Beller, M. *Chem. Rev.* **2013**, *113*, 1-35; (b) Zeni, G.; Larock, R. C. *Chem. Rev.* **2006**, *106*, 4644-4680.

(3) (a) Khumtaveeporn, K.; Alper, H. *Acc. Chem. Res.* **1995**, *28*, 414-422; (b) Lu, S.-M.; Alper, H. *J. Org. Chem.* **2004**, *69*, 3558-3561; (c) Rowley, J. M.; Lobkovsky, E. B.; Coates, G. W. *J. Am. Chem. Soc.* **2007**, *129*, 4948-4960. (d) Xu, H.; Jia, L. *Org. Lett.* **2003**, *5*, 1575-1577.

(4) (a) Kitagaki, S.; Inagaki, F.; Mukai, C. *Chem. Soc. Rev.* **2014**, *43*, 2956-2978; (b) Gibson, S. E.; Mainolfi, N. *Angew. Chem. Int. Ed.* **2005**, *44*, 3022-3037.

(5) (a) Mohamed Ahmed, M. S.; Kobayashi, K.; Mori, A. *Org. Lett.* **2005**, *7*, 4487-4489; (b) Stonehouse, J. P.; Chekmarev, D. S.; Ivanova, N. V.; Lang, S.; Pairaudeau, G.; Smith, N.; Stocks, M. J.; Sviridov, S. I.; Utkina, L. M. *Synlett* **2008**, *2008*, 100-104; (c) Staben, S. T.; Blaquiere, N., *Angew. Chem. Int. Ed.* **2010**, *49*, 325-328. (d) Worrall, K.; Xu, B.; Bontemps, S.; Arndtsen, B. A. *J. Org. Chem.* **2011**, *76*, 170-180; (e) Dhawan, R.; Dghaym, R. D.; St. Cyr, D. J.; Arndtsen, B. A. *Org. Lett*. **2006**, *8*, 3927-3930.

(6) For examples: (a) Riedinger, C.; Endicott, J. A.; Kemp, S. J.; Smyth, L. A.; Watson, A.; Valeur, E.; Golding, B. T.; Griffin, R. J.; Hardcastle, I. R.; Noble, M. E.; McDonnell, J. M. *J. Am. Chem. Soc.* **2008**, *130*, 16038-16044; (b) Guillaumel, J.; Léonce, S.; Pierré, A.; Renard, P.;

Pfeiffer, B.; Arimondo, P. B.; Monneret, C. *Eur. J. Med. Chem.* **2006**, *41*, 379-386; (c) Zhang, L.; Chen, X.; Liu, J.; Zhu, Q.; Leng, Y.; Luo, X.; Jiang, H.; Liu, H. *Eur. J. Med. Chem.* **2012**, *58*, 624-639; (d) Hardcastle, I. R.; Valeur, E.; Watson, A.; Blackburn, T. J.; Clegg, W.; Golding, B. T.; Griffin, R. J.; Haggerty, K.; Harrington, R. W.; Kemp, S.; Payne, S. L.; Revill, C. H.; Liu, J.; Ahmed, S. U.; Bennaceur, K.; Drummond, C.; Hutton, C.; Lu, X.; Newell, D. R.; Xu, Q.; Lunec, J.; Endicott, J. A.; Gruber, J.; McDonnell, J. M.; Noble, M. E. M.; Riedinger, C. *J. Med. Chem*. **2011**, *54*, 1233-1243; (e) Luzzio, F. A.; Mayorov, A. V.; Ng, S. S. W.; Kruger, E. A.; Figg, W. D. *J. Med. Chem*. **2003**, *46*, 3793-3799.

(7) (a) Cao, H.; McNamee, L.; Alper, H. *Org. Lett.* **2008**, *10*, 5281-5284; (b) Cho, C. S.; Shim, H. S.; Choi, H.-J.; Kim, T.-J.; Shim, S. C. *Synth. Commun.* **2002**, *32*, 1821-1827; (c) Ju, J.; Qi, C.; Zheng, L.; Hua, R. *Tetrahedron Lett.* **2013**, *54*, 5159-5161; (d) Uozumi, Y.; Kawasaki, N.; Mori, E.; Mori, M.; Shibasaki, M. *J. Am. Chem. Soc.* **1989**, *111*, 3725-3727; (e) Gai, X.; Grigg, R.; Khamnaen, T.; Rajviroongit, S.; Sridharan, V.; Zhang, L.; Collard, S.; Keep, A. *Tetrahedron Lett.* **2003**, *44*, 7441-7443.

(8) Shacklady-McAtee, D. M.; Dasgupta, S.; Watson, M. P. *Org. Lett.* **2011**, *13*, 3490-3493.

(9) (a) Quesnel, J. S.; Arndtsen, B. A. *J. Am. Chem. Soc.* **2013**, *135*, 16841-16844; (b) Bontemps, S.; Quesnel, J. S.; Worrall, K.; Arndtsen, B. A. *Angew. Chem. Int. Ed.* **2011**, *50*, 8948-8951; (c) Dhawan, R.; Arndtsen, B. A. *J. Am. Chem. Soc.* **2004**, *126*, 468-469.

(10) (a) Dhawan, R.; Dghaym, R. D.; Arndtsen, B. A. *J. Am. Chem. Soc.* **2003**, *125*, 1474-1475; (b) Arndtsen, B. A. *Chem. Eur. J.* **2009**, *15*, 302-313.

(11) (a) Tamaru, Y. Carbonylation and Decarbonylation. In *Modern Organonickel Chemistry*; Wiley-VCH Verlag GmbH & Co. KGaA: **2005**, pp 224-239; (b) Cubiak; C. P. Nickel, Palladium, and Platinum. In: Comprehensive Organometallic Chemistry II; Wilkinson, G., Abel, E. W., Stone, G. A., Eds.; Elsevier: Oxford, **1995**, pp 1-27.

(12) Caution: $Ni(CO)_4$ is a potential product generated in nickel-based carbonylations, and is extremely toxic and volatile. Precautions must be taken to avoid all contact with the reaction prior to quenching. All manipulations of the catalysis solutions after CO introduction were therefore rigorously performed in sealed vessels and an isolated atmosphere with no contact to air or person. To remove $Ni(CO)_4$, all volatiles from reaction were immediately transferred *in vacuo* on a Schlenk line into a liquid N_2 cooled solvent trap charged with excess PPh_3, then

exposed to water, as noted in: Dorta, R.; Stevens, E. D.; Scott, N. M.; Costabile, C.; Cavallo, L.; Hoff, C. D.; Nolan, S. P. *J. Am. Chem. Soc.* **2005**, *127*, 2485-2495.

(13) Layer W. R. *Chem. Rev.* **1963**, *63*, 489-510.

(14) Dorta, R.; Stevens, E. D.; Scott, N. M.; Costabile, C.; Cavallo, L.; Hoff, C. D.; Nolan, S. P. *J. Am. Chem. Soc.* **2005**, *127*, 2485-2495.

(15) Ratts, K. W.; Chupp, J. P. *J. Org. Chem.* **1974**, *39*, 3745-3747.

(16) Morimoto, H.; Fujiwara, R.; Shimizu, Y.; Morisaki, K.; Ohshima, T. *Org. Lett.* **2014**, *16*, 2018-2021.

Chapter 4. An Electrophilic Approach to the Palladium-Catalyzed Carbonylative C-H Functionalization of Heterocycles

4.1. Preface

Chapters 2 and 3 demonstrate that the palladium or nickel catalyzed carbonylation of aryl iodides in the presence of chloride salts can allow the *in situ* generation of acid chlorides. This has allowed the use of weak nucleophiles such as imines in carbonylative coupling reactions to generate iminium salts. We next became interested in the potential use of this chemistry to perform carbonylative coupling reactions with even less potent nucleophiles. In this chapter, we demonstrate how the *in situ* generation of highly electrophilic acylating agents via the carbonylation of aryl iodides can offer a new approach to the intermolecular C-H bond functionalization of nitrogen-containing heterocycles. This transformation is mediated by P^tBu_3-coordinated palladium catalyst, and allows the conversion of a diverse range of heterocycles, including pyrroles, indoles, imidazoles, benzoxazoles and furans, into ketones, and without the typical need to exploit pre-metallated heterocycles in carbonylative coupling chemistry. This work has been published in the *Journal of American Chemical Society* (**2015**, *137*, 12050-12054).

4.2. Introduction

The palladium catalyzed C-H functionalization of arenes and heteroarenes has emerged as one of the most important new approaches in synthetic chemistry.[1] Extensive research efforts have been directed towards the discovery of new approaches to these transformations, with examples including such powerful platforms as chelation-assisted functionalization,[2] concerted metalation deprotonation (CMD),[3] radical reactions,[4] and others.[5] In contrast, the design of methods to incorporate reactive functionalities such as CO into C-H bond functionalization has to date presented a challenge. Unlike reactions that generate robust and relatively inert aryl-(hetero)aryl, -alkyl, or -heteroatom bonds, palladium catalyzed carbonylations provide an efficient route to synthesize a number of the most easily manipulated functional groups in

synthetic chemistry, such as carboxylic acid derivatives or ketones.[6] Unfortunately, carbon monoxide is also a π-acidic and reactive ligand with the potential to interfere with many modes of Pd-based bond activation. In this regard, Fujiwara and others have demonstrated the palladium catalyzed oxidative carbonylation of arenes and heteroarenes to carboxylic acids and esters.[7,8] More recently, examples of the application of this chemistry to coupling with aryl halides have emerged involving either intramolecular or chelation assisted carbonylations by Larock, Beller, Yu, Lei and others (Scheme 4.1a),[9] or the use of activated substrates, such as perfluoroarenes, reported by Skrydstrup (Scheme 4.1b) [10] or alternatively via *in situ* halogenation of heterocycles followed by their carbonylation.[11] However, a general carbonylative coupling of heterocycles and aryl halides is to our knowledge not known. These products are instead often prepared via palladium catalyzed cross coupling reactions,[12] or via Friedel-Crafts acylations with acid chlorides and strong Lewis acids;[13] both of which require the synthesis of high energy substrates and/or create significant waste.

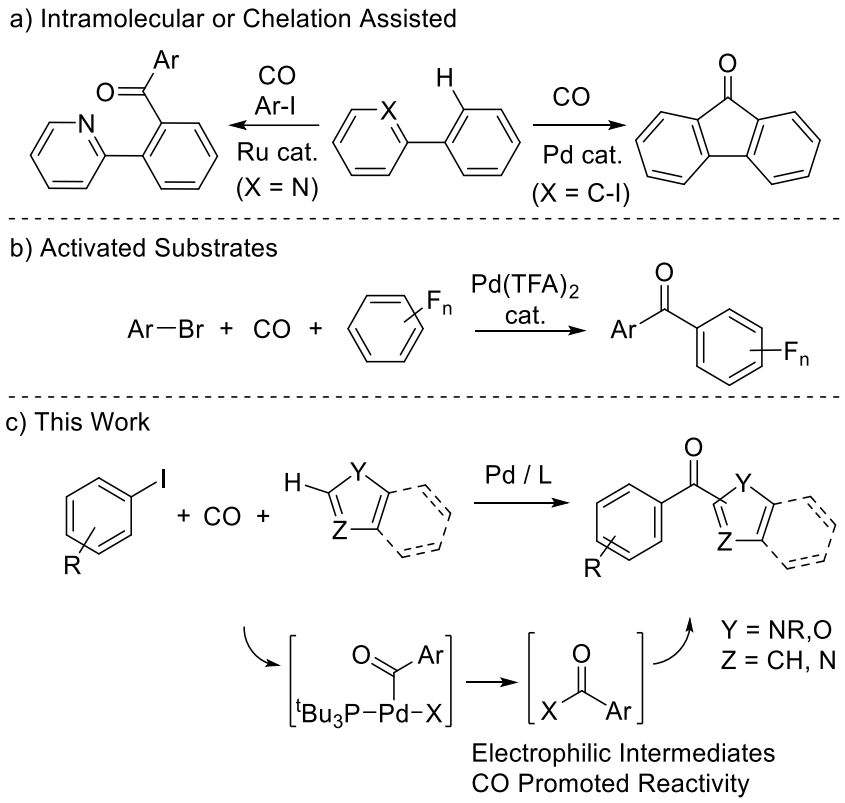

Scheme 4.1. An Electrophilic Approach to Pd-Catalyzed Carbonylative C-H Bond Functionalization.

In considering these issues, we postulated that the features unique to carbonylation may offer an alternative approach to C-H functionalization. We have recently reported that the highly sterically encumbered ligands such as P^{t}Bu$_3$ can induce the reductive elimination and Pd-catalyzed generation of acid chlorides from aryl halides and CO.[14] In contrast to the moderate reactivity of the palladium-acyl intermediates formed in traditional carbonylations, acid chlorides are highly electrophilic, and have allowed the application of carbonylation to a range of new classes of weak nucleophiles. The formation of acid chlorides is driven by the unusual energetics of carbon monoxide, whose reduction is sufficiently exothermic as to allow the formation of a weak aroyl-chloride bond. These results led us to question if carbonylations might be used to create even more high energy products than acid chlorides, including those sufficiently electrophilic to react directly aromatic systems (Scheme 4.1c). We describe here the

results of these studies. These have led to the design of what is to our knowledge the first broadly applicable approach to perform carbonylative C-H functionalization of heterocycles, without directing groups, and via a mechanism that is promoted, rather than inhibited, by carbon monoxide.

4.3. Results and Discussion

Our initial studies involved the carbonylation of 4-iodoanisole in the presence of the electron rich *N*-benzyl pyrrole employing the conditions we have reported for the catalytic, *in situ* formation of acid chlorides (Pd/P^{t}Bu$_3$, Bu$_4$NCl). As shown in Table 1, this leads to the generation of the carbonylative arene/pyrrole coupling product **4.1a** in 44% yield (entry 1). This reaction proceeds in highest yields with P^{t}Bu$_3$ (entries 2 – 5), presumably due to its ability to facilitate acid chloride reductive elimination. The formation of **4.1a** is slow under these conditions, and generates a mixture of 2- and 3-substituted isomers (3.2:1 ratio). These features mirror the reactivity of aromatic acid chlorides with pyrroles.[15]

While effective, the observed yields in this reaction are moderate, and product scope expected to be limited to substrates reactive towards acid chlorides. In probing methods to increase reactivity, we questioned if acid chloride formation is indeed necessary for carbonylative coupling. A simple experiment in this regard was to omit the addition of chloride to the reaction of aryl iodide, pyrrole and CO. Rather than inhibiting catalysis, this led to a dramatic *increase* in aroylation and **4.1a** yield (entries 6 and 7). Examination of ligand effects reveals that the large cone angle P^{t}Bu$_3$ ligand creates the most reactive catalyst for this transformation, and smaller ligands show diminished activity (entries 8-15). Bidentate ligands, which have become common in many Pd-catalyzed carbonylation reactions, almost fully shut down catalysis (entries 16-20). Increasing the reaction temperature to 115 ^{o}C with the most active ligand, P^{t}Bu$_3$, allowed us to decrease the catalyst loading to 5 mol% and obtain the near quantitative formation of ketone **4.1a** as a mixture of 2- and 3-substituted isomers (3.2:1 ratio) (entry 21).

Table 4.1. Catalyst for Carbonylative Functionalization[a]

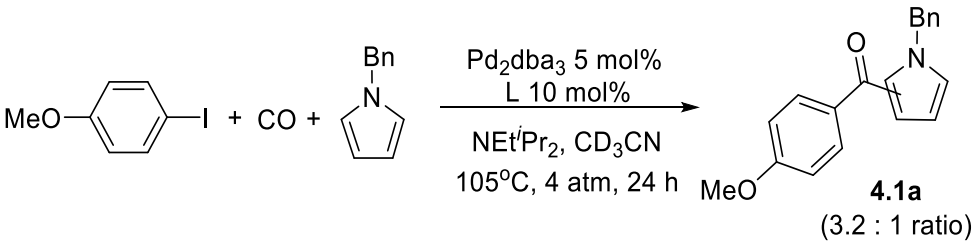

entry	L	additive	% **4.1a**[c]	entry	L	% **4.1a**[c]
1	P^{t}Bu$_3$	Bu$_4$NCl	44	12	-	45
2	PPh$_3$	Bu$_4$NCl	0	13	PCy$_3$	15
3	P(*o*-tolyl)$_3$	Bu$_4$NCl	27	14		9
4	PCy$_3$	Bu$_4$NCl	0			
5		Bu$_4$NCl	24	15		21
6	P^{t}Bu$_3$	-	84	16	DPPE	0
7	Pd(P^{t}Bu$_3$)$_2$	-	79	17	DPPP	0
8	PPh$_3$		60	18	DPPF	0
9	P(*o*-tolyl)$_3$	-	62	19	DCPE	0
10		-	64	20	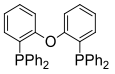	11
11		-	72	21	Pd(P^{t}Bu$_3$)$_2$[b]	97 (73)[d]

[a]$CH_3OC_6H_4I$ (47 mg, 0.20 mmol), pyrrole (16 mg, 0.10 mmol), Pd (0.010 mmol), L (0.010 mmol), NEt^{i}Pr$_2$ (15 mg, 0.12 mmol) 4 atm CO, 0.7 mL CD3CN ; [b]115 °C, 0.005 mmol Pd; [c]NMR yield of 2- and 3- isomers; [d]isolated yield of 2-aroyl pyrrole.

The optimized catalyst system can mediate carbonylative C-H functionalization with a range of aryl iodides and pyrroles (Table 4.2). Electron-acceptor and electron-donor substituents are tolerated in all positions of the aryl iodide, and lead to substituted pyrroles in good yield. This

includes a number of palladium-reactive functionalities (**4.1c-d, 4.1f-g, 4.1i-j**), and *ortho*-functionalized substrates (**4.1h-1j, 4.1m, 4.1p, 4.1s**).

Table 4.2. Pd-Catalyzed Functionalization of Pyrroles[a]

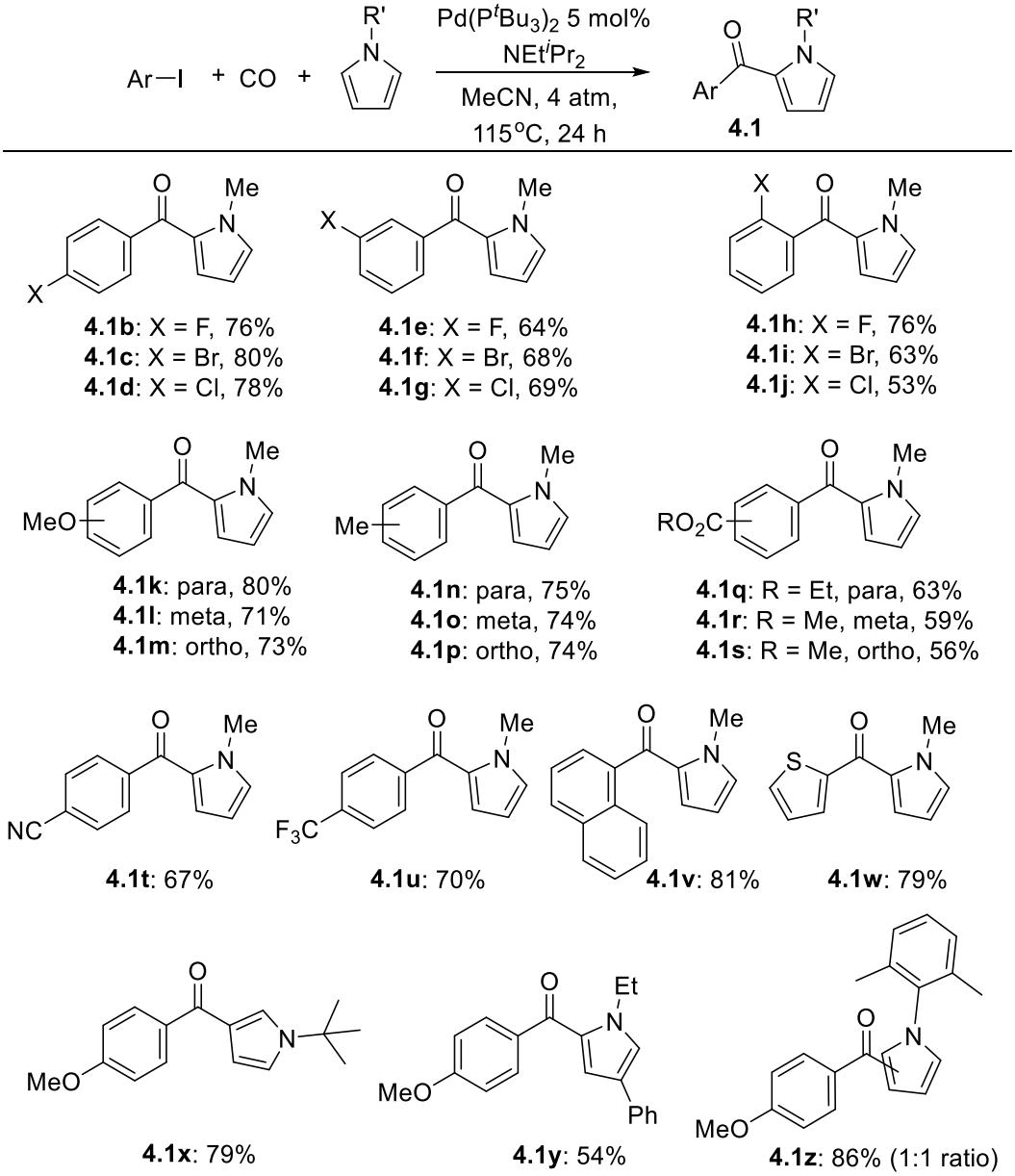

[a]ArI (1.0 mmol), pyrrole (0.50 mmol), NEt^{i}Pr$_2$ (77 mg, 0.60 mmol) 4 atm CO and Pd(P^{t}Bu$_3$)$_2$ (13 mg, 0.025 mmol) in MeCN (2 mL) at 115 °C for 24 h; Isolated yield of isomer shown.

Sterically encumbered arenes are also viable in this transformation (**4.1v**), and the chemistry can be extended to the use of thiophenyl iodides (**4.1w**). With *N*-methylpyrrole, the 2-derivatized

isomer is obtained in all cases as the isolated product.[16] In the case of more sterically encumbered N-2,6-dimethylpyrrole, both regio-isomers were observed in moderate yields (**4.1z**). However, increasing the steric bulk on the pyrrole to a *tert*-butyl group allows for the generation of 3-subsitututed pyrroles (**4.1x**). Substituents can also be incorporated onto the pyrrole backbone (**4.1y**).

The ability to carbonylatively functionalize pyrroles with aryl iodides opens a number of mechanistic questions. As no chloride salts are present in these transformations, acid chloride is not a viable intermediate. Nevertheless, the reactivity and product selectivity observed are consistent with an electrophilic pathway. In light of our previously observed acid chloride synthesis, one possibility is that without chloride, aroyl iodide (ArCO-I) itself can undergo reductive elimination (Scheme 4.2a, path A). Although the latter is analogous to acid chloride formation, it is notable that aroyl iodides are much more reactive and electrophilic products, and have not been previously observed in Pd-catalyzed carbonylation chemistry. As such, we also consider the potential that the palladium-aroyl intermediates of carbonylation (**4.2**) could directly react with pyrroles, such as via a Friedel-Crafts reaction with the aroyl ligand (path B), or the electrophilic palladation of pyrrole (path C), in analogy to known non-carbonylative reactions.[17]

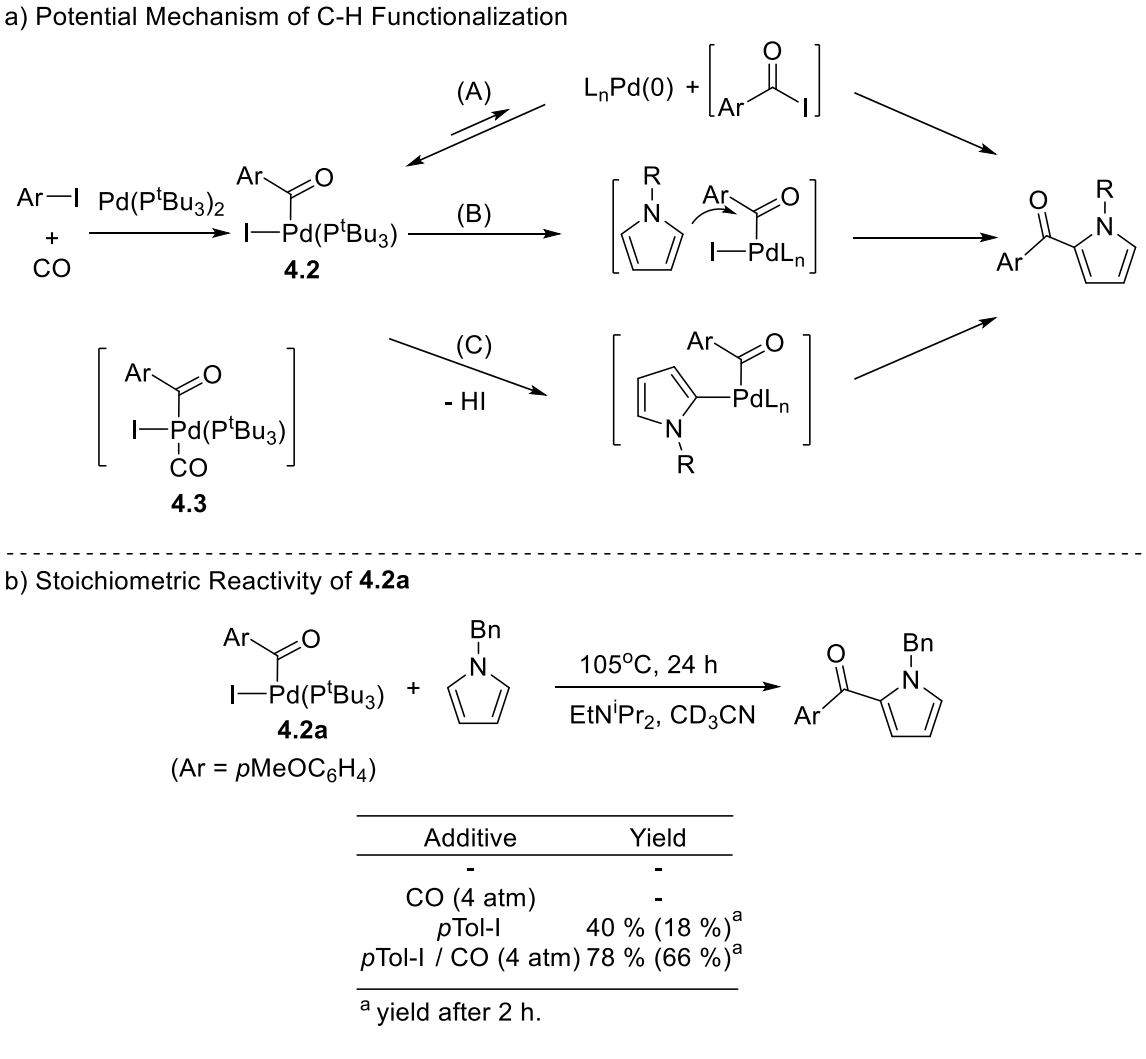

Additive	Yield
-	-
CO (4 atm)	-
*p*Tol-I	40 % (18 %)[a]
*p*Tol-I / CO (4 atm)	78 % (66 %)[a]

[a] yield after 2 h.

Scheme 4.2. Mechanistic Studies on the Carbonylative Functionalization of Pyrroles.

Preliminary studies shed some light on the pathway followed in this reaction. Monitoring the catalytic reaction by *in situ* by ^{1}H and ^{31}P NMR spectrometry reveals the formation of the three-coordinate palladium-aroyl complex **4.2a** (Scheme 4.2a) as the major palladium containing intermediate and presumed catalyst resting state. Complex **4.2a** can be independently generated from $Pd(P^{t}Bu_3)_2$, aryl iodide and CO,[18] and its reactivity examined. Interestingly, **4.2a** does not itself react with the pyrrole at elevated temperatures with or without CO present (Scheme 4.2b). These data suggests that the palladium-aroyl complex, even with CO coordinated, is not sufficiently electrophilic to directly react with pyrrole, either at the aroyl ligand or palladium.

However, the addition of the other reagent present in catalysis, iodotoluene, to the stoichiometric reaction of **4.2a** initiates a reaction with pyrrole to form the functionalized pyrrole product. In considering the mechanistic postulates, while it is possible that aryl iodide reacts directly with **4.2a** to form a Pd(IV) intermediate, an alternative role would be to trap any Pd(0) generated upon reversible reductive elimination in the rate determining step (path A). Unlike even acid chlorides, the ArCO-I bond is very weak and reactive, making its formation an equilibrium process that would heavily favor palladium-aroyl complex **4.2**. In the presence of excess aryl iodide, palladium can be converted to palladium-aryl complex and allow the subsequent reaction of aroyl iodide with pyrrole. Consistent with this mechanism, the introduction of CO significantly accelerates the stoichiometric reaction (Scheme 4.2b).[19] The latter has been noted to facilitate reductive elimination by creating a sterically encumbered, electron poor palladium intermediate **4.3**.[14] Kinetic studies show that the reaction between **4.2a** and the pyrrole in the presence of CO and iodotoluene follow 1st order kinetics in pyrrole concentration, however this observation doesn't discount any of the three mechanistic pathways.

Table 4.3. Pd-Catalyzed Carbonylative Functionalization of Heterocycles[a]

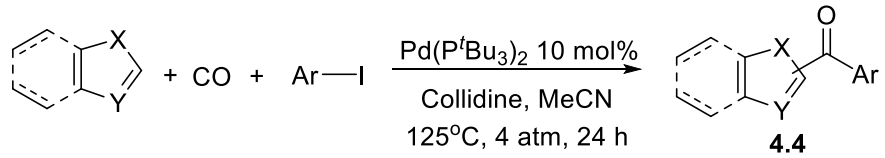

4.4

a) Indoles

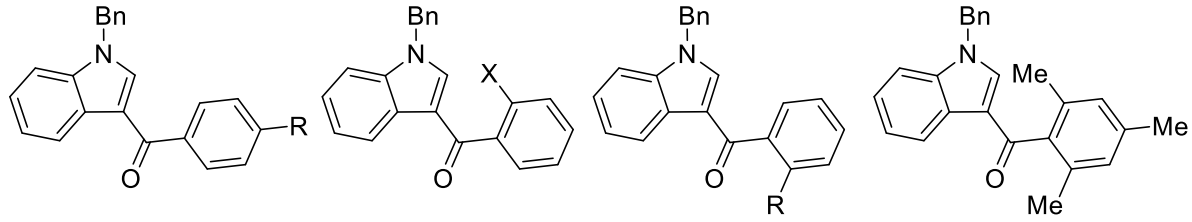

4.4a: R = OMe, 83%
4.4b: R = CO_2Et, 91%

4.4c: X = F, 77%
4.4d: X = Cl, 72%
4.4e: X = Br, 68%

4.4f: R = OMe, 74%
4.4g: R = Me, 74%

4.4h: 76%

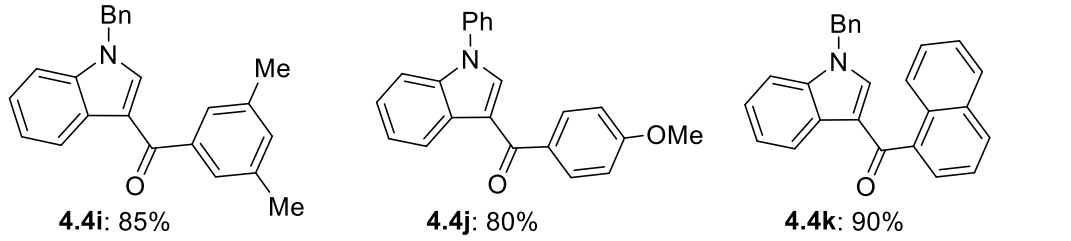

4.4i: 85%

4.4j: 80%

4.4k: 90%

b) Benzimidazoles and Benzoxazoles

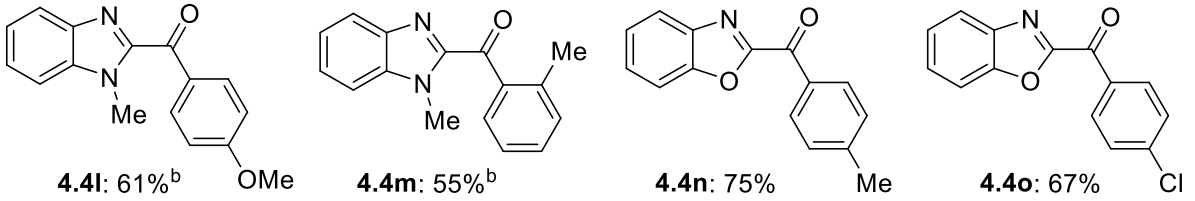

4.4l: 61%[b]

4.4m: 55%[b]

4.4n: 75%

4.4o: 67%

c) Imidazoles and Furan

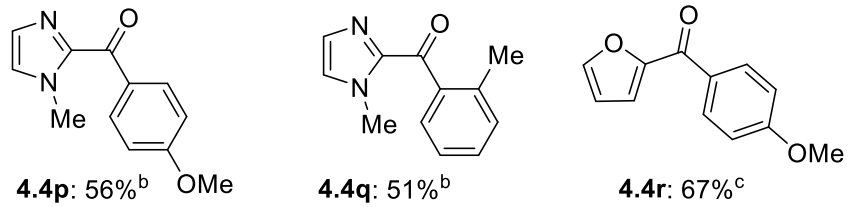

4.4p: 56%[b]

4.4q: 51%[b]

4.4r: 67%[c]

[a]ArI (1.0 mmol), heterocycle (0.5 mmol), collidine (73 mg, 0.6 mmol), Pd(P^{t}Bu$_3$)$_2$ (25 mg, 0.05 mmol), 2 mL MeCN, 125 °C, 24 h; [b] 20 atm CO; [c] 150 °C, 48 h.

As far as we are aware, the catalytic formation of potent electrophilic products for carbonylative C-H bond functionalization has not been previously described. This high

reactivity provides the ability to functionalize a variety of less reactive heterocycles. As examples, indoles can be converted into ketones in good to excellent yields with this catalyst system (**4.4a**-**k**, Table 4.3).

Collidine is required as a base in these reactions to avoid the aroylation of the amine base by these reactive intermediates.[20] In all cases, the 3-substituted indole derivative is generated. The reaction proceeds with electron rich (**4.4a**, **4.4f**, **4.4j**), electron poor (**4.4b-e**), or sterically encumbered (**4.4f-h**) aryl iodides. Less reactive heterocycles can also be functionalized, such as those containing two heteroatoms. Benzimidazoles undergo clean carbonylative coupling with aryl iodides to form ketones (**4.4l,m**). Similar reactivity is observed with benzoxazoles (**4.4n,o**), and with the monocyclic *N*-methyl imidazole (**4.4p,q**). It is also possible to move beyond nitrogen heterocycles, with simple furan undergoing carbonylative functionalization in good yield (**4.4r**).

As an illustration of the potential utility of this chemistry, we noted that the carbonylative C-H functionalization is mechanistically orthogonal to many of the more established Pd-based methods for heterocycle derivatization. The latter can be exploited for the selective, sequential functionalization of heterocycles. As examples, the carbonylative functionalization of indole with *ortho*-bromoiodobenzene followed by direct arylation can allow the selective generation of polycyclic **4.5** (Scheme 4.3a). As both of these steps are palladium catalyzed, this reaction can be extended to a one pot, sequential C-H functionalization reaction, where the same palladium catalyzed is employed in both steps via the stepwise addition of ligands ($Pd(P^tBu_3)_2$ and PPh_3/K_2CO_3) for each functionalization. We see no evidence for cross-over in functionalization in this chemistry (e.g. non-carbonylative coupling), presumably due to the distinct mechanisms for the two processes. The same transformation is available with pyrroles (**4.6**), and allows the selective functionalization of two C-H bonds via differing methods in one pot. Alternatively, this chemistry can be applied in synthesis, such as the preparation of Tolmetin (**4.7**, Scheme 4.3b), a potent nonsteroidal anti-inflammatory agent, in two steps using available 4-iodotoluene and CO.[21]

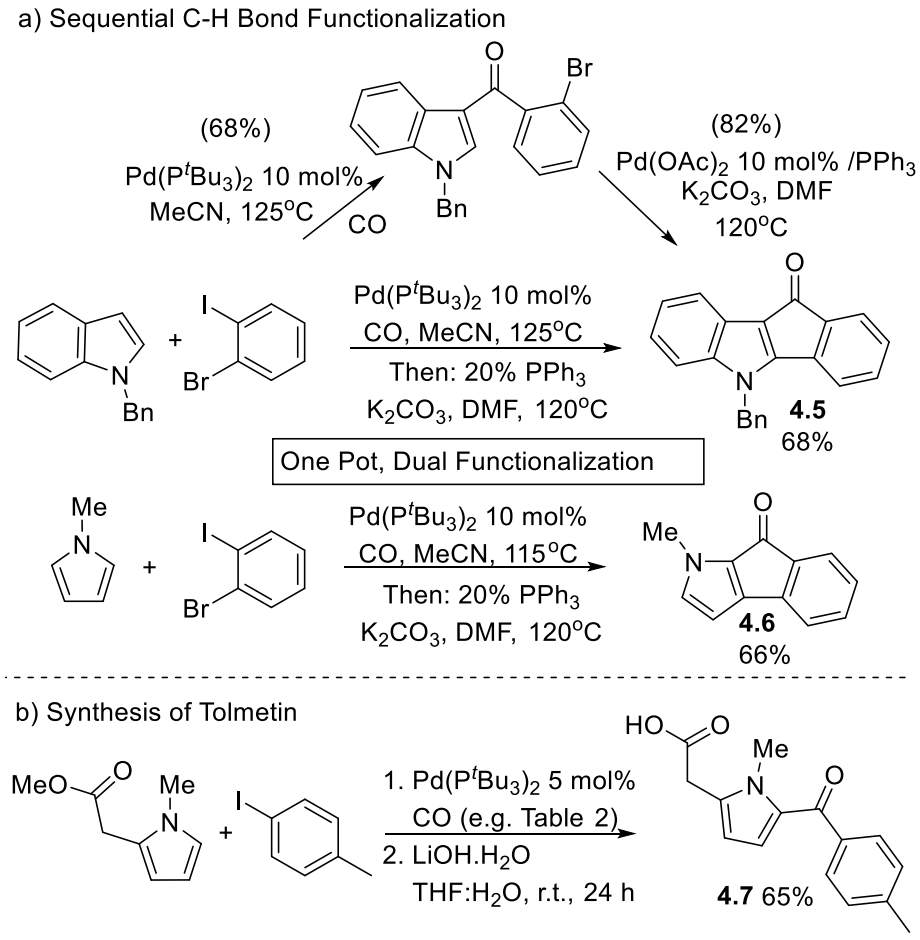

Scheme 4.3. Application of Palladium Catalyzed Carbonylative Heterocycle Functionalization

4.4. Conclusions

In conclusion, we have reported a new approach to palladium catalyzed carbonylative C-H functionalization. This provides an efficient method to synthesize functionalized heterocycles with high atom economy, using stable reagents (aryl iodides and CO), and without the need to prefunctionalize the heterocycle, install directing groups, or exploit high energy building blocks. Considering the high electrophilicity of the intermediates in this chemistry, and the CO promoted, rather than diminished, reactivity, this suggests the potential application of carbonylation in a range of new products classes. Studies directed towards the latter are underway.

4.5. Supplementary information

4.5.1. General Considerations

All reactions were carried out under an inert atmosphere in a glovebox or using standard Schlenk techniques, unless otherwise indicated. Research grade carbon monoxide (99.99%) was used as received. All solvents were dried with using a solvent purification system and stored in glovebox over activated 4 Å molecular sieves. Deuterated solvents were dried over CaH_2, vacuum transferred and stored over 4 Å molecular sieves. Tetrabutylammonium chloride was dried in the glovebox by dissolving in dichloromethane, allowing it to stand overnight over activated 4 Å molecule sieves, then filtering and removing the solvent *in vacuo*. $Pd_2dba_3{\cdot}CHCl_3$ was prepared according to literature procedures and stored at -35 °C in the glovebox to avoid decomposition.[22] N-substituted pyrroles, and N-substituted indoles were prepared according to literature procedures.[23-26] All other reagents were purchased from commercial suppliers and used as received. All ^1H and ^{13}C NMR spectra were acquired on 400 and 500 MHz spectrometers. High resolution mass spectra were obtained using a quadrupole-time of flight and an orbitrap detector by direct infusion in positive ESI mode.

4.5.2. Synthetic Procedures

General Procedure for Phosphine Ligand Screening (Table 4.1)

In a glovebox, 4-iodoanisole (47 mg, 0.20 mmol), N-benzylpyrrole (16 mg, 0.10 mmol), NEt^iPr_2 (15 mg, 0.12 mmol), Pd catalyst (0.010 mmol), ligand (0.020 mmol), additive (0.10 mmol) and benzyl benzoate internal standard were dissolved in CD_3CN (0.7 mL) and added to a J-Young NMR tube. The tube was removed from the glovebox, frozen in liquid nitrogen, the headspace evacuated, and 4 atm carbon monoxide was condensed into the NMR tube. The reaction was heated at 105 °C and monitored by ^1H NMR spectroscopy. Yield of 2- and 3-substituted **4.1a** was determined by ^1H NMR analysis relative to the internal standard.

Typical Procedure for the Catalytic Synthesis of Diarylketones **1** (Table 4.2)

In a glovebox, 4-iodoanisole (236 mg, 1.00 mmol), N-benzylpyrrole (79 mg, 0.50 mmol), NEt^iPr_2 (77 mg, 0.60 mmol), $Pd(P^tBu_3)_2$ (13 mg, 0.025 mmol) were combined in acetonitrile (2 mL) and added to a 50 mL sealable pressure vessel. The vessel was closed, removed from the glovebox, and pressurized with 4 atm of carbon monoxide. The reaction was heated at 115 °C for 24 h. After the reaction was cooled to room temperature, all volatiles were removed *in vacuo*. The crude product was purified by column chromatography (Silica gel, gradient hexane / ethyl acetate 4% to 20%) affording pure diarylketone **4.1a** as a pale white solid in 73% yield (106 mg).

Typical Procedure for the Catalytic Synthesis of Diarylketones **4.4** (Table 4.3)

4-Iodoanisole (234 mg, 1.00 mmol), N-benzylindole (104 mg, 0.50 mmol), 2,4,6-collidine (73 mg, 0.60 mmol), $Pd(P^tBu_3)_2$ (25 mg, 0.05 mmol) were combined in acetonitrile (2 mL) and added to a 50 mL sealable pressure vessel. The vessel was closed, removed from the glovebox, and pressurized with 4 atm of carbon monoxide. The reaction was heated at 125 °C for 24 h. After the reaction was cooled to room temperature, all volatiles were removed *in vacuo*. The crude product was purified by column chromatography (Silica gel, gradient hexane / ethyl acetate 4% to 30%) affording pure diarylketone **4.4a** as a white solid in 83% yield (141 mg).

Synthesis of Palladium-Acyl Complex [4-$MeOC_6H_4$(CO)Pd(P^tBu_3)I] **4.2a**

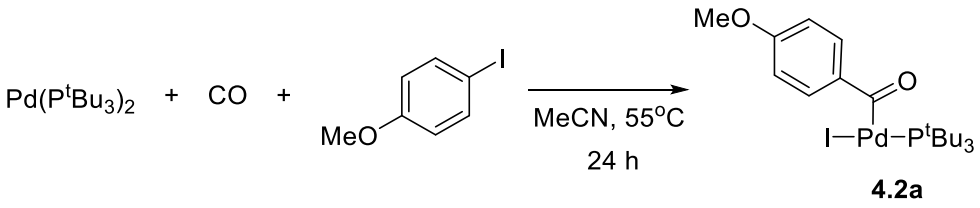

4.2a

Based on a literature procedure,[18] $Pd(P^tBu_3)_2$ (51 mg, 0.10 mmol) and 4-iodoanisole (70 mg, 0.30 mmol) were combined in acetonitrile (4 mL) in a 50 mL sealable pressure vessel in a glovebox. The vessel was closed, removed from the glovebox, and pressurized with 4 atm of carbon monoxide upon which the reaction mixture turned bright yellow. The reaction mixture was heated and stirred at 55 °C for 24 h. The solvent was removed *in vacuo* and the resulting residue

was washed and triturated with pentane (3 x 8 mL) affording **4.2a** as yellow-orange powder in 86 % yield (46 mg). ^{1}H NMR (400 MHz, $CDCl_3$) δ 8.21 (d, J = 8.9 Hz, 2H), 6.89 (d, J = 8.9 Hz, 2H), 3.88 (s, 3H), 1.45 (d, J = 12.8 Hz, 27H). ^{13}C NMR (126 MHz, $CDCl_3$) δ 194.0 (d, J = 5.3 Hz), 163.4, 133.7, 127.6 (d, J = 14.3 Hz), 113.4, 55.6, 39.9 (d, J = 7.3 Hz), 32.2 (d, J = 4.2 Hz). ^{31}P NMR (162 MHz, $CDCl_3$) δ 71.1.

Reaction of Acid Chloride with *N*-benzylpyrrole

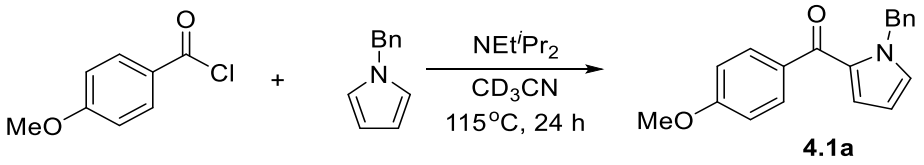

In a glovebox, 4-methoxybenzoyl chloride (34 mg, 0.2 mmol), N-benzylpyrrole (16 mg, 0.10 mmol), NEt^{i}Pr$_2$ (16 mg, 0.12 mmol), and benzyl benzoate internal standard were dissolved in CD_3CN (0.7 mL) and added to a J-Young NMR tube. The tube was removed from the glovebox, and the reaction was heated at 115 °C and monitored by ^{1}H NMR spectroscopy. After 24 h ^{1}H NMR analysis showed generation of 43% yield of 2- and 3-substituted **4.1a** (3.2:1 ratio) relative to the internal standard.

Reaction of **4.2a** with *N*-benzylpyrrole (Scheme 4.2b, entry 1)

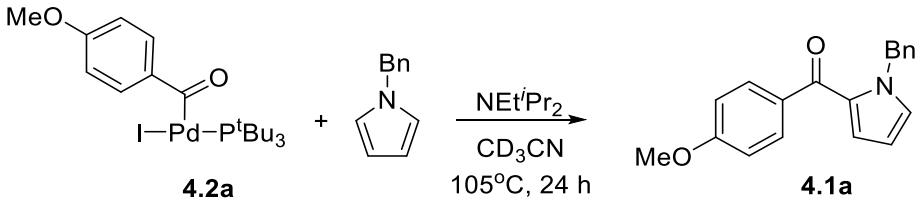

In a glovebox, [4-$CH_3OC_6H_4$(CO)Pd(P^{t}Bu$_3$)I] **4.2a** (13 mg, 0.025 mmol), N-benzylpyrrole (12 mg, 0.075 mmol), N,N-diisopropylethylamine (5 mg, 0.0375 mmol) and benzyl benzoate internal standard were dissolved in CD_3CN (0.7 mL) and added to a J-Young NMR tube. The tube was removed from the glovebox, and the reaction was heated at 105 °C for 24 h. ^{1}H NMR analysis relative to the internal standard after 24 h showed no evidence for **4.1a** formation.

Reaction of **2a** with *N*-benzylpyrrole and CO (Scheme 4.2b, entry 2)

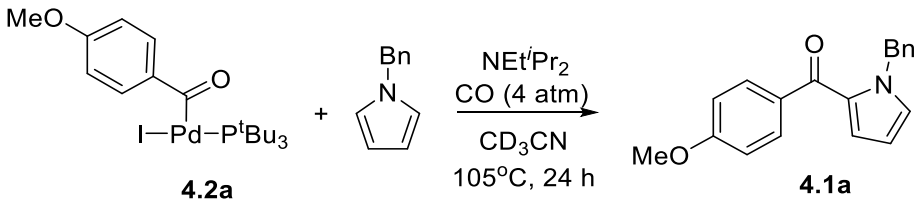

In a glovebox, [4-$CH_3OC_6H_4$(CO)Pd(P^{t}Bu$_3$)I] **4.2a** (13 mg, 0.025 mmol), N-benzylpyrrole (12 mg, 0.075 mmol), N,N-diisopropylethylamine (5 mg, 0.0375 mmol) and benzyl benzoate internal standard were dissolved in CD_3CN (0.7 mL) and added to a J-Young NMR tube. The tube was removed from the glovebox, frozen in liquid nitrogen, the headspace evacuated, and 4 atm carbon monoxide was condensed into the NMR tube. The reaction was heated at 105 °C for 24 h. ^{1}H NMR analysis relative to the internal standard after 24 h showed no evidence for **4.1a** formation.

Reaction of **4.2a** with *N*-benzylpyrrole and 4-iodotoluene (Scheme 4.2b, entry 3)

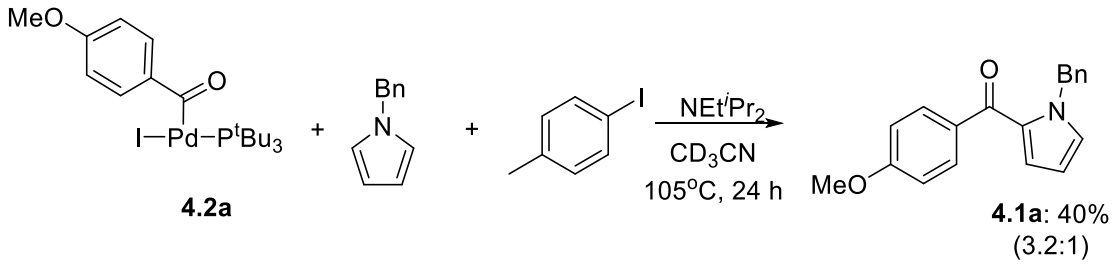

In a glovebox, [4-$CH_3OC_6H_4$(CO)Pd(P^{t}Bu$_3$)I] **4.2a** (13 mg, 0.025 mmol), N-benzylpyrrole (12 mg, 0.075 mmol), 4-iodotoluene (27 mg, 0.125 mmol), N,N-diisopropylethylamine (5 mg, 0.0375 mmol) and benzyl benzoate internal standard were dissolved in CD_3CN (0.7 mL) and added to a J-Young NMR tube. The tube was removed from the glovebox and was heated at 105 °C for 24 h. ^{1}H NMR analysis relative to the internal standard after 24 h showed generation of **4.1a** in 40% yield.

Reaction of **4.2a** with *N*-benzylpyrrole, 4-iodotoluene and CO (Scheme 4.2b, entry 4)

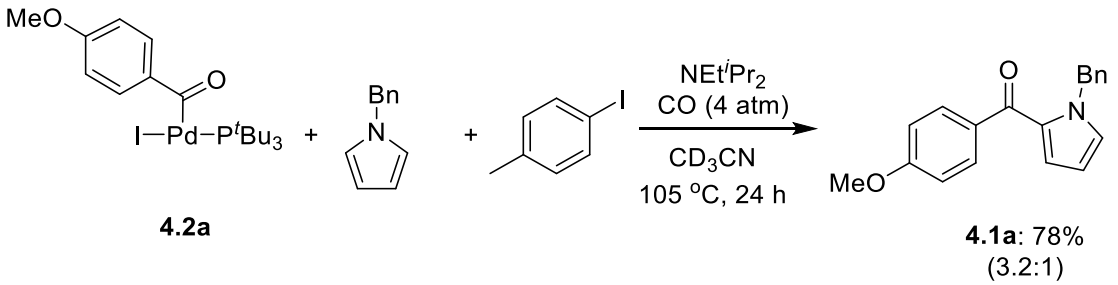

In a glovebox, [4-$CH_3OC_6H_4$(CO)Pd(P^{t}Bu$_3$)I] **4.2a** (13 mg, 0.025 mmol), N-benzylpyrrole (12 mg, 0.075 mmol), 4-iodotoluene (27 mg, 0.125 mmol), N,N-diisopropylethylamine (5 mg, 0.0375 mmol) and benzyl benzoate internal standard were dissolved in CD_3CN (0.7 mL) and added to a J-Young NMR tube. The tube was removed from the glovebox, frozen in liquid nitrogen, the headspace evacuated, and 4 atm carbon monoxide was condensed into the NMR tube. The reaction was heated at 105 °C for 24 h. ^{1}H NMR analysis relative to the internal standard after 24 h showed generation of **4.1a** in 78% yield.

Synthesis of **4.5** (Scheme 4.3a)

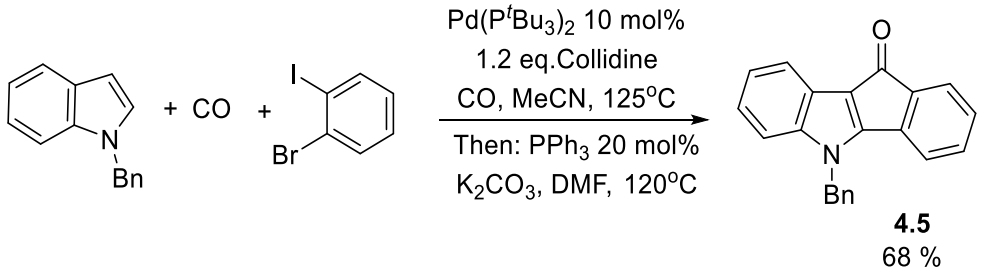

In a glovebox, 2-bromoiodobenzene (283 mg, 1.00 mmol), N-benzylindole (104 mg, 0.50 mmol), 2,4,6-collidine (73 mg, 0.60 mmol), Pd(P^{t}Bu$_3$)$_2$ (25 mg, 0.05 mmol) were combined in acetonitrile (2 mL) and added to a 50 mL sealable pressure vessel. The vessel was closed, removed from the glovebox, and pressurized with 4 atm of carbon monoxide. The reaction was heated at 115 °C for 24 h. After the reaction was cooled to room temperature it was brought into the glovebox, and all volatiles were removed *in vacuo*. Triphenylphosphine (26 mg, 0.10 mmol),

potassium carbonate (207 mg, 1.50 mmol) and DMF (4 mL) were added to the crude mixture. The pressure vessel was sealed again, and heated to 120 ºC for 24h. The reaction was cooled to room temperature, water (50 mL) was added to crude and the mixture was extracted with EtOAc (3 x 50 mL). The organic layer was washed with brine (3 x 100 mL), dried over $MgSO_4$ and evaporated. The crude product was purified by column chromatography (Silica gel, gradient hexane / ethyl acetate 4% to 20%) affording 1-methylindeno[2,1-b]pyrrol-8(1H)-one **4.5** as a bright red solid in 68% yield (105 mg).

Synthesis of **4.6** (Scheme 4.3a)

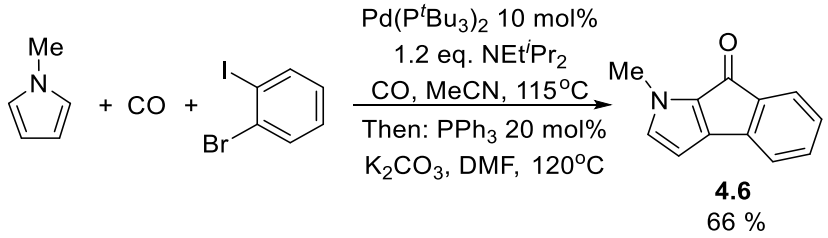

In a glovebox, 2-bromoiodobenzene (283 mg, 1.00 mmol), N-methylpyrrole (41 mg, 0.50 mmol), NEt^iPr_2 (77 mg, 0.60 mmol), $Pd(P^tBu_3)_2$ (25 mg, 0.05 mmol) were combined in acetonitrile (2 mL) and added to a 50 mL sealable pressure vessel. The vessel was closed, removed from the glovebox, and pressurized with 4 atm of carbon monoxide. The reaction was heated at 115 °C for 24 h. After the reaction was cooled to room temperature it was brought into the glovebox, and all volatiles were removed *in vacuo*. Triphenylphosphine (26 mg, 0.10 mmol), potassium carbonate (207 mg, 1.50 mmol) and DMF (4 mL) were added to the crude mixture. The pressure vessel was sealed again, and heated to 120 ºC for 24h. The reaction was cooled to room temperature, water (50 mL) was added to crude and the mixture was extracted with EtOAc (3 x 50 mL). The organic layer was washed with brine (3 x 100 mL), dried over $MgSO_4$ and evaporated. The crude product was purified by column chromatography (Silica gel, gradient hexane / ethyl acetate 4% to 20%) affording pure 1-methylindeno[2,1-b]pyrrol-8(1H)-one **4.6** as a bright red solid in 66% yield (60 mg).

Synthesis of Tolmetin **4.7** (Scheme 4.3b)

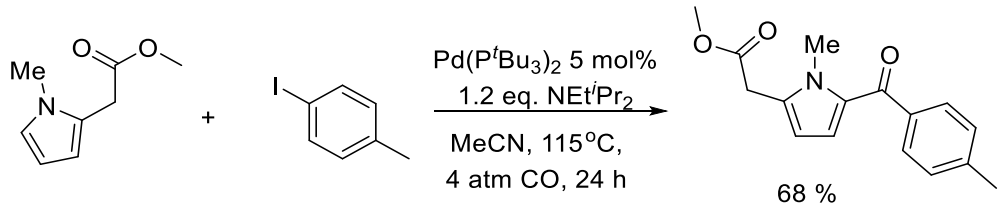

In a glovebox, 4-iodotoluene (218 mg, 1.00 mmol), methyl 2-(1-methyl-1H-pyrrol-2-yl)acetate[27] (77 mg, 0.50 mmol), NEt^{i}Pr$_2$ (77.4 mg, 0.60 mmol), Pd(P^{t}Bu$_3$)$_2$ (13 mg, 0.025 mmol) were combined in acetonitrile (2 mL) and added to a 50 mL sealable pressure vessel. The vessel was closed, removed from the glovebox, and pressurized with 4 atm of carbon monoxide. The reaction was heated at 115 °C for 24 h. After the reaction was cooled to room temperature, all volatiles were removed *in vacuo*. The crude product was purified by column chromatography (Silica gel, gradient hexane / ethyl acetate 4% to 20%) affording pure methyl 2-(1-methyl-5-(4-methylbenzoyl)-1H-pyrrol-2-yl)acetate **4.7a** as a pale yellow oil in 68% yield (92 mg).

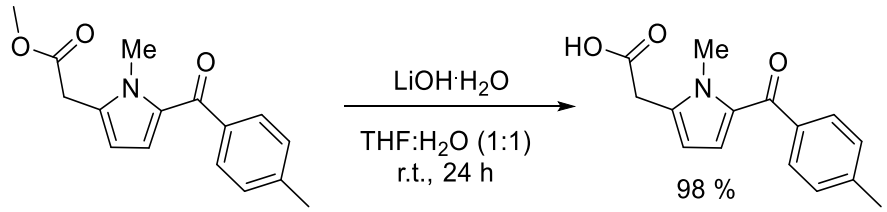

Methyl 2-(1-methyl-5-(4-methylbenzoyl)-1H-pyrrol-2-yl)acetate (90 mg, 0.33 mmol) was dissolved in THF:water mixture (1:1, 4 mL), to which LiOH·H$_2$O (28 mg, 0.66 mmol) was added. Reaction mixture was stirred overnight at room temperature. THF was evaporated and the pH of the aqueous layer was adjusted to 2 with (1M) to precipitate the product. The solid was vacuum filtered, washed with cold distilled water and dried, affording 2-(1-methyl-5-(4-methylbenzoyl)-1H-pyrrol-2-yl)acetic acid **4.7** as a pale white solid in 98% yield (83 mg).

4.5.3. Kinetic Studies

Typical Procedure for Kinetic Studies

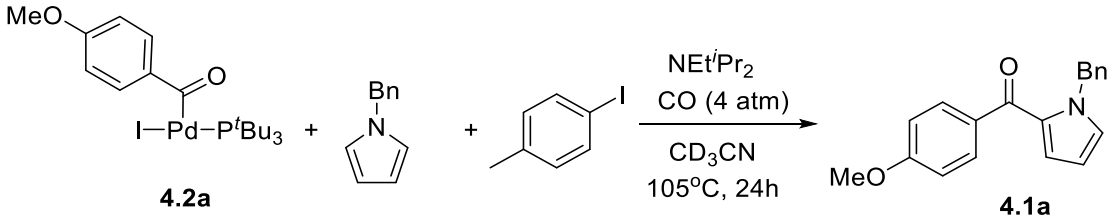

In a glovebox, [4-$CH_3OC_6H_4$(CO)Pd(P^tBu_3)I] **4.2a** (13 mg, 0.025 mmol), N-benzylpyrrole (16 mg, 0.10 mmol), 4-iodotoluene (27 mg, 0.125 mmol), N,N-diisopropylethylamine (5 mg, 0.0375 mmol) and benzyl benzoate internal standard were dissolved in CD_3CN (0.7 mL) and added to a J-Young NMR tube. The tube was removed from the glovebox, frozen in liquid nitrogen, the headspace evacuated, and 4 atm carbon monoxide was condensed into the NMR tube. The reaction was heated at 105 °C and the generation of **4.1a** and consumption of **4.2a** was determined by ^1H NMR analysis relative to the internal standard after 20, 40, 60, 80, 100, 120 and 140 min.

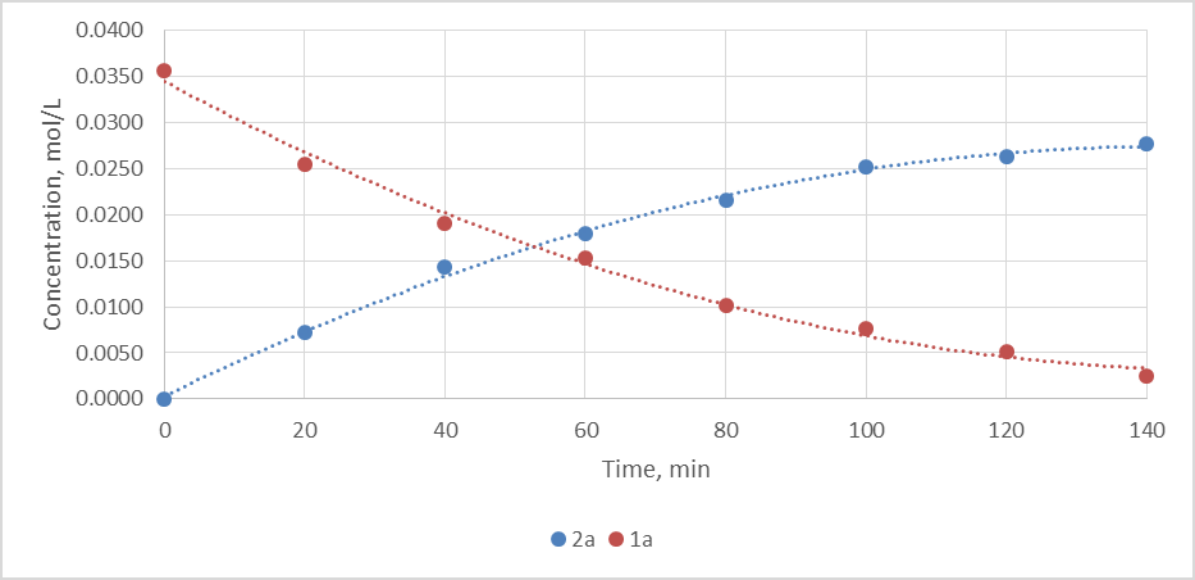

Figure 4.1. Kinetic plot for the generation of 4.1a and consumption 4.2a at initial concentration of pyrrole 0.189 mol/L.

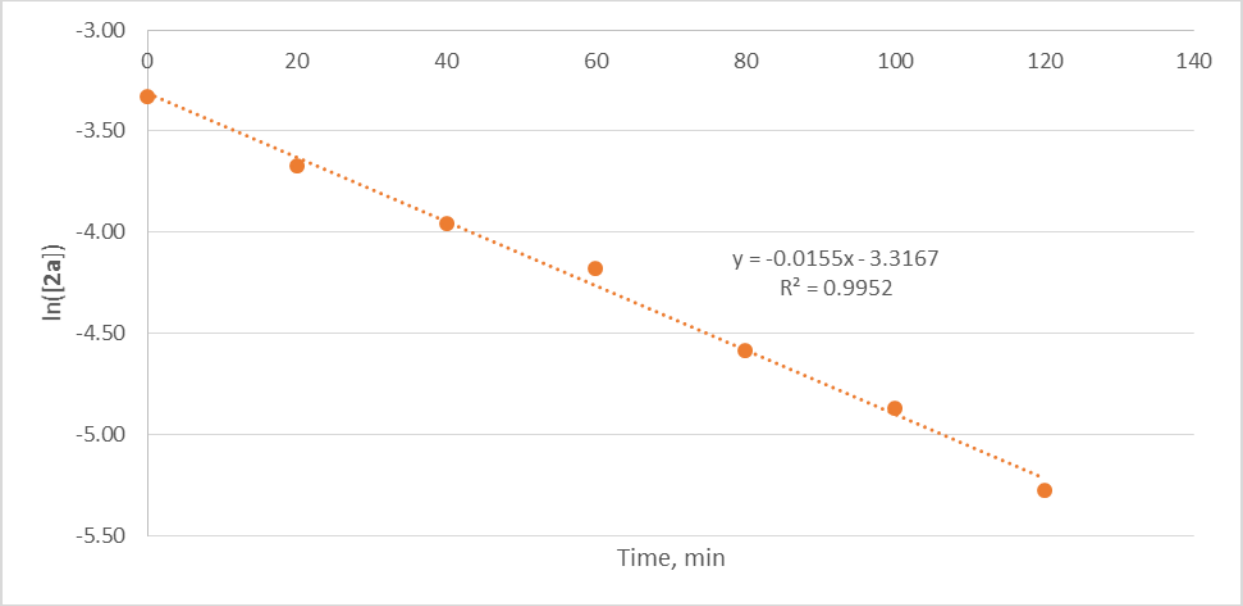

Figure 4.2. Sample kinetic plot for the consumption of 4.2a at initial concentration of pyrrole 0.189 mol/L

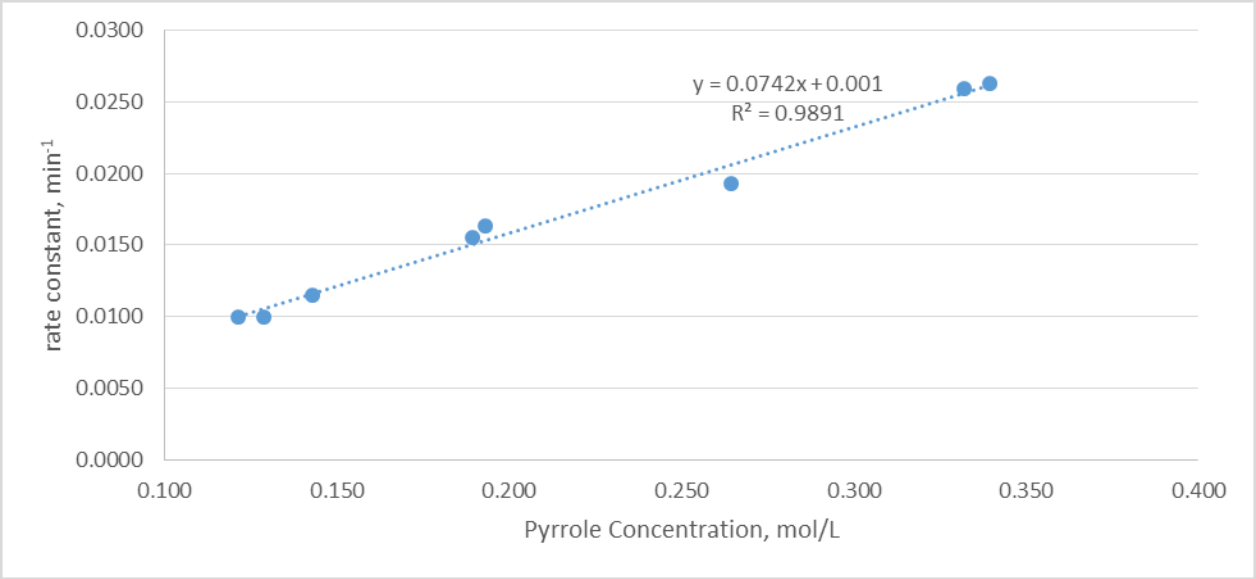

Figure 4.3. Relationship between pyrrole concentration and the observed rate constant of the reaction between N-benzylpyrrole and 4.2a.

Table 4.4. Relationship between pyrrole concentration and the observed rate constant of the reaction between N-benzylpyrrole and **4.2a**.

Pyrrole Concentration, mol/L	k_{obs}, min^{-1}
0.121	0.0100
0.129	0.0101
0.143	0.0115
0.189	0.0155
0.193	0.0163
0.264	0.0193
0.332	0.0259
0.339	0.0263

4.5.4. Spectroscopic Data on 4.1

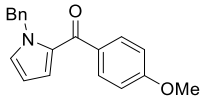

(1-Benzyl-1H-pyrrol-2-yl)(4-methoxyphenyl)methanone 4.1a. Pale yellow solid, 106 mg, 73% yield. ^{1}H NMR (400 MHz, $CDCl_3$) δ 7.81 (d, *J* = 8.8 Hz, 2H), 7.33 – 7.21 (m, 3H), 7.17 (d, *J* = 7.3 Hz, 2H), 6.99 (s, 1H), 6.93 (d, *J* = 8.7 Hz, 2H), 6.80 – 6.72 (m, 1H), 6.21 (dd, *J* = 3.5, 2.9 Hz, 1H), 5.65 (s, 2H), 3.87 (s, 3H). ^{13}C NMR (126 MHz, $CDCl_3$) δ 189.5, 162.3, 136.6, 132.5, 132.3, 131.2, 128.9, 128.2, 127.7, 127.2, 124.8, 122.4, 113.7, 113.4, 111.4, 55.4, 53.9. HRMS. Calculated for $C_{19}H_{17}NNaO_2$ ($M+Na^+$): 314.1151, found: 314.1150. FT-IR-ATR (cm^{-1}): 1619.7 (C=O).

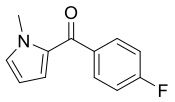

(4-Fluorophenyl)(1-methyl-1H-pyrrol-2-yl)methanone 4.1b. Yellow solid, 77 mg, 76% yield. ^{1}H NMR (500 MHz, $CDCl_3$) δ 7.83 (dd, *J* = 8.6, 5.5 Hz, 2H), 7.13 (t, *J* = 8.6 Hz, 2H), 6.93 (s, 1H), 6.71 (dd, *J* = 4.0, 1.5 Hz, 1H), 6.16 (dd, *J* = 3.9, 2.5 Hz, 1H), 4.02 (s, 3H). ^{13}C NMR (126 MHz, $CDCl_3$) δ 184.7, 164.8 (d, *J* = 252.0 Hz), 136.1 (d, *J* = 3.1 Hz), 131.6, 131.5, 130.3, 122.6, 115.1 (d, *J* = 21.7 Hz), 108.2, 37.3. HRMS. Calculated for $C_{12}H_{10}FNNaO$ ($M+Na^+$): 226.0639, found: 226.0645. FT-IR-ATR (cm^{-1}): 1624.0 (C=O).

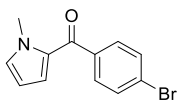

(4-Bromophenyl)(1-methyl-1H-pyrrol-2-yl)methanone 4.1c.[29] Dark yellow solid, 105 mg, 80% yield. ^{1}H NMR (500 MHz, $CDCl_3$) δ 7.72 – 7.66 (m, 2H), 7.64 – 7.58 (m, 2H), 6.98 – 6.92 (m, 1H), 6.73 (dd, *J* = 4.1, 1.7 Hz, 1H), 6.19 (dd, *J* = 4.1, 2.5 Hz, 1H), 4.05 (s, 3H). ^{13}C NMR (126 MHz, $CDCl_3$) δ 185.0, 138.8, 133.0, 131.4, 130.9, 130.3, 126.3, 123.0, 108.5, 37.5. HRMS. Calculated for $C_{12}H_{10}BrNNaO$ ($M+Na^+$): 285.9838, found: 285.9835. FT-IR-ATR (cm^{-1}): 1624.2 (C=O).

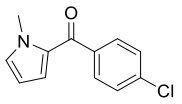

(4-Chlorophenyl)(1-methyl-1H-pyrrol-2-yl)methanone 4.1d.[30] Yellow solid, 86 mg, 78% yield. ^{1}H NMR (500 MHz, $CDCl_3$) δ 7.77 (d, *J* = 8.5 Hz, 2H), 7.45 (d, *J* = 8.5 Hz, 2H), 6.96 (s, 1H), 6.73 (dd, *J* = 4.1, 1.6 Hz, 1H), 6.19 (dd, *J* = 4.1, 2.5 Hz, 1H), 4.05 (s, 3H). ^{13}C NMR (126 MHz, $CDCl_3$) δ 184.8, 138.2, 137.6, 131.8, 130.6, 130.2, 128.3, 122.8, 108.3, 37.4. HRMS. Calculated for $C_{12}H_{10}ClNNaO$ ($M+Na^+$): 242.0343, found: 242.0353. FT-IR-ATR (cm^{-1}): 1623.1 (C=O).

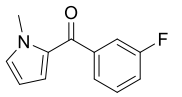

(3-Fluorophenyl)(1-methyl-1H-pyrrol-2-yl)methanone 4.1e. Dark yellow oil, 65 mg, 64% yield. ^{1}H NMR (500 MHz, $CDCl_3$) δ 7.80 (dd, *J* = 8.3, 1.3 Hz, 1H), 7.56 – 7.50 (m, 1H), 7.45 (t, *J* = 7.5 Hz, 2H), 6.92 (t, *J* = 2.0 Hz, 1H), 6.74 (dd, *J* = 4.1, 1.7 Hz, 1H), 6.16 (dd, *J* = 4.1, 2.5 Hz, 1H), 4.05 (s, 3H). ^{13}C NMR (126 MHz, $CDCl_3$) δ 184.5 (d, *J* = 2.1 Hz), 162.3 (d, *J* = 247.3 Hz), 142.0 (d, *J* = 6.4 Hz), 132.0, 130.1, 129.7 (d, *J* = 7.8 Hz), 124.9 (d, *J* = 3.0 Hz), 123.1, 118.3 (d, *J* = 21.4 Hz), 116.0 (d, *J* = 22.5 Hz), 108.4, 37.4. HRMS. Calculated for $C_{12}H_{11}ONF$ ($M+H^+$): 204.08192, found: 204.08177. FT-IR-ATR (cm^{-1}): 1622.4 (C=O).

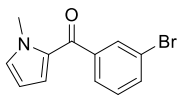

(3-Bromophenyl)(1-methyl-1H-pyrrol-2-yl)methanone 4.1f. Yellow oil, 89 mg, 68% yield. ^{1}H NMR (500 MHz, $CDCl_3$) δ 7.92 (t, *J* = 1.8 Hz, 1H), 7.73 – 7.69 (m, 1H), 7.65 (ddd, *J* = 8.0, 2.0, 1.1 Hz, 1H), 7.32 (t, *J* = 7.8 Hz, 1H), 6.94 (t, *J* = 2.1 Hz, 1H), 6.72 (dd, *J* = 4.1, 1.7 Hz, 1H), 6.17 (dd, *J* = 4.1, 2.5 Hz, 1H), 4.03 (s, 3H). ^{13}C NMR (126 MHz, $CDCl_3$) δ 184.3, 141.8, 134.3, 132.0, 130.05, 130.00, 129.6, 127.6, 123.2, 122.2, 108.4,

37.4. HRMS. Calculated for $C_{12}H_{10}BrNNaO$ ($M+Na^+$): 285.9838, found: 285.9839. FT-IR-ATR (cm^{-1}): 1620.9 (C=O).

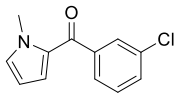

(3-Chlorophenyl)(1-methyl-1H-pyrrol-2-yl)methanone 4.1g. Dark yellow oil, 76 mg, 69% yield. ^1H NMR (500 MHz, $CDCl_3$) δ 7.77 (t, *J* = 1.8 Hz, 1H), 7.69 – 7.62 (m, 1H), 7.50 (ddd, *J* = 8.0, 2.1, 1.1 Hz, 1H), 7.38 (t, *J* = 7.8 Hz, 1H), 6.94 (t, *J* = 1.9 Hz, 1H), 6.73 (dd, *J* = 4.1, 1.7 Hz, 1H), 6.17 (dd, *J* = 4.1, 2.5 Hz, 1H), 4.03 (s, 3H). ^{13}C NMR (126 MHz, $CDCl_3$) δ 184.6, 141.7, 134.3, 132.1, 131.4, 130.2, 129.5, 129.3, 127.3, 123.3, 108.6, 37.6. HRMS. Calculated for $C_{12}H_{10}ClNNaO$ ($M+Na^+$): 242.0343, found: 242.0350. FT-IR-ATR (cm^{-1}): 1621.5 (C=O).

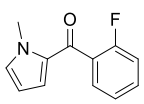

(2-Fluorophenyl)(1-methyl-1H-pyrrol-2-yl)methanone 4.1h. Dark yellow oil, 77 mg, 76% yield. ^1H NMR (500 MHz, $CDCl_3$) δ 7.50 (td, *J* = 7.3, 1.7 Hz, 1H), 7.44 (dd, *J* = 6.2, 1.9 Hz, 1H), 7.20 (td, *J* = 7.5, 0.8 Hz, 1H), 7.14 (t, *J* = 9.1 Hz, 1H), 6.92 (s, 1H), 6.65 – 6.59 (m, 1H), 6.13 (dd, *J* = 4.1, 2.4 Hz, 1H), 4.07 (s, 3H). ^{13}C NMR (126 MHz, $CDCl_3$) δ 182.4, 159.8 (d, *J* = 250.8 Hz), 132.4, 131.9 (d, *J* = 8.2 Hz), 131.1, 130.2 (d, *J* = 3.2 Hz), 128.8 (d, *J* = 15.6 Hz), 123.9 (d, *J* = 3.6 Hz), 123.8 (d, *J* = 2.0 Hz), 116.3 (d, *J* = 21.9 Hz), 108.7, 37.7. HRMS. Calculated for $C_{12}H_{11}ONF$ ($M+H^+$): 204.08192, found: 204.08198. FT-IR-ATR (cm^{-1}): 1620.6 (C=O).

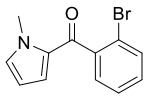

(2-Bromophenyl)(1-methyl-1H-pyrrol-2-yl)methanone 4.1i.[31] Dark yellow oil, 63 mg, 63% yield. ^1H NMR (500 MHz, $CDCl_3$) δ 7.64 – 7.58 (m, 1H), 7.40 – 7.33 (m, 2H), 7.31 – 7.27 (m, 1H), 6.94 (s, 1H), 6.45 (dd, *J* = 4.1, 1.6 Hz, 1H), 6.11 (dd, *J* = 4.1, 2.4 Hz, 1H), 4.09 (s, 3H). ^{13}C NMR (101 MHz, $CDCl_3$) δ 185.2, 141.8, 133.2, 132.7, 130.7, 130.4, 129.0, 126.9, 124.2, 119.9, 108.8, 37.7. HRMS. Calculated for $C_{12}H_{10}BrNNaO$ ($M+Na^+$): 285.9838, found: 285.9835. FT-IR-ATR (cm^{-1}): 1629.2 (C=O).

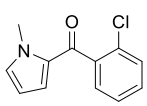

(2-Chlorophenyl)(1-methyl-1H-pyrrol-2-yl)methanone 4.1j. Yellow oil, 58 mg, 53% yield. ^{1}H NMR (500 MHz, $CDCl_3$) δ 7.45 – 7.34 (m, 3H), 7.30 (td, *J* = 7.4, 1.2 Hz, 1H), 6.93 (t, *J* = 1.9 Hz, 1H), 6.47 (dd, *J* = 4.1, 1.7 Hz, 1H), 6.11 (dd, *J* = 4.1, 2.4 Hz, 1H), 4.09 (s, 3H). ^{13}C NMR (126 MHz, $CDCl_3$) δ 184.4, 139.8, 132.6, 131.4, 130.7, 130.5, 130.1, 129.1, 126.3, 124.1, 108.8, 37.7. HRMS. Calculated for $C_{12}H_{10}ClNNaO$ ($M+Na^+$): 242.0343, found: 242.0348. FT-IR-ATR (cm^{-1}): 1624.7 (C=O).

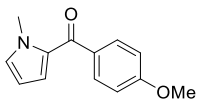

(4-Methoxyphenyl)(1-methyl-1H-pyrrol-2-yl)methanone 4.1k.[29] Yellow oil, 86 mg, 80% yield. ^{1}H NMR (400 MHz, $CDCl_3$) δ 7.83 (d, *J* = 8.8 Hz, 2H), 6.95 (d, *J* = 8.8 Hz, 2H), 6.90 – 6.87 (m, 1H), 6.72 (dd, *J* = 4.0, 1.6 Hz, 1H), 6.15 (dd, *J* = 4.0, 2.5 Hz, 1H), 4.01 (s, 3H), 3.87 (s, 3H). ^{13}C NMR (126 MHz, $CDCl_3$) δ 185.1, 162.4, 132.4, 131.4, 130.9, 130.6, 121.9, 113.3, 107.8, 55.4, 37.2. HRMS. Calculated for $C_{13}H_{13}NNaO_2$ ($M+Na^+$): 238.0838, found: 238.0846. FT-IR-ATR (cm^{-1}): 1619.5 (C=O).

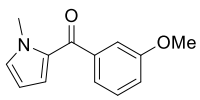

(3-Methoxyphenyl)(1-methyl-1H-pyrrol-2-yl)methanone 4.1l. Yellow oil, 76 mg, 71% yield. ^{1}H NMR (500 MHz, $CDCl_3$) δ 7.38 (m, 3H), 7.07 (dd, J = 8.0, 1.5 Hz, 1H), 6.92 (s, 1H), 6.77 (dd, *J* = 4.0, 1.6 Hz, 1H), 6.15 (dd, *J* = 4.0, 2.5 Hz, 1H), 4.03 (s, 3H), 3.85 (s, 3H). ^{13}C NMR (126 MHz, $CDCl_3$) δ 186.0, 159.4, 141.3, 131.7, 130.6, 129.1, 123.0, 121.9, 117.9, 113.8, 108.2, 55.5, 37.5. HRMS. Calculated for $C_{13}H_{13}NNaO_2$ ($M+Na^+$): 238.0838, found: 238.0841. FT-IR-ATR (cm^{-1}): 1622.5 (C=O).

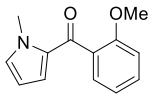

(2-Methoxyphenyl)(1-methyl-1H-pyrrol-2-yl)methanone 4.1m. Pale white solid, 79 mg, 73% yield. ^{1}H NMR (500 MHz, $CDCl_3$) δ 7.39 (ddd, *J* = 8.4, 7.5, 1.7 Hz, 1H), 7.33 (dd, *J* = 7.6, 1.8 Hz, 1H), 7.00 – 6.93 (m, 2H), 6.87 (t, *J* = 2.0 Hz, 1H), 6.51 (dd, *J* = 4.1, 1.7 Hz, 1H), 6.08 (dd, *J* = 4.1, 2.4 Hz, 1H), 4.07 (s, 3H), 3.80 (s, 3H). ^{13}C NMR (126 MHz, $CDCl_3$) δ 185.7, 157.0, 131.8, 131.5, 130.9, 130.3, 129.2, 123.5, 119.9, 111.4, 108.2, 55.8, 37.7. HRMS. Calculated for $C_{13}H_{13}NNaO_2$ ($M+Na^+$): 238.0838, found: 238.0841. FT-IR-ATR (cm^{-1}): 1618.9 (C=O).

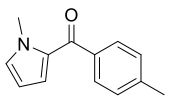

(4-Methylphenyl)(1-methyl-1H-pyrrol-2-yl)methanone 4.1n.[31] White solid, 75 mg, 75% yield. ^{1}H NMR (500 MHz, $CDCl_3$) δ 7.79 – 7.72 (m, 2H), 7.28 (d, *J* = 7.7 Hz, 2H), 6.93 (t, *J* = 2.0 Hz, 1H), 6.76 (dd, *J* = 4.0, 1.7 Hz, 1H), 6.18 (dd, *J* = 4.0, 2.5 Hz, 1H), 4.05 (s, 3H), 2.45 (s, 3H). ^{13}C NMR (126 MHz, $CDCl_3$) δ 186.0, 141.9, 137.2, 131.2, 130.7, 129.4, 128.7, 122.4, 108.0, 37.3, 21.6. HRMS. Calculated for $C_{13}H_{13}NNaO$ ($M+Na^+$): 222.0889, found: 222.0894. FT-IR-ATR (cm^{-1}): 1622.4 (C=O).

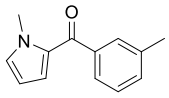

(3-Methylphenyl)(1-methyl-1H-pyrrol-2-yl)methanone 4.1o.[29] Yellow oil, 74 mg, 74% yield. ^{1}H NMR (500 MHz, $CDCl_3$) δ 7.64 – 7.57 (m, 2H), 7.38 – 7.30 (m, 2H), 6.94 – 6.88 (m, 1H), 6.74 (dd, *J* = 4.0, 1.7 Hz, 1H), 6.15 (dd, *J* = 4.0, 2.5 Hz, 1H), 4.03 (s, 3H), 2.42 (s, 3H). ^{13}C NMR (126 MHz, $CDCl_3$) δ 186.5, 140.0, 137.9, 132.2, 131.5, 130.7, 129.8, 128.0, 126.5, 122.9, 108.1, 37.5, 21.5. HRMS. Calculated for $C_{13}H_{13}NNaO$ ($M+Na^+$): 222.0889, found: 222.0894. FT-IR-ATR (cm^{-1}): 1621.6 (C=O).

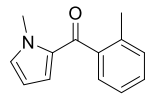

(2-Methylphenyl)(1-methyl-1H-pyrrol-2-yl)methanone 4.1p.[29] Yellow oil, 74 mg, 74% yield. ^{1}H NMR (500 MHz, $CDCl_3$) δ 7.37 (dd, *J* = 7.5, 1.4 Hz, 1H), 7.32 (dd, *J* = 7.5, 1.4 Hz, 1H), 7.26 – 7.18 (m, 2H), 6.93 – 6.88 (m, 1H), 6.48 (dd, *J* = 4.1, 1.7 Hz, 1H), 6.10 (dd, *J* = 4.1, 2.4 Hz, 1H), 4.08 (s, 3H), 2.37 (s, 3H). ^{13}C NMR (126 MHz, $CDCl_3$) δ 188.3, 140.2, 136.2, 132.0, 131.5, 130.8, 129.6, 128.2, 124.9, 123.7, 108.3, 37.7, 19.7. HRMS. Calculated for $C_{13}H_{13}NNaO$ ($M+Na^+$): 222.0889, found: 222.0891. FT-IR-ATR (cm^{-1}): 1622.7 (C=O).

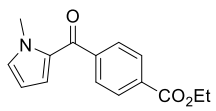

Ethyl 4-(1-methyl-1H-pyrrole-2-carbonyl)benzoate 4.1q.[32] Pale white solid, 81 mg, 63% yield. ^{1}H NMR (500 MHz, $CDCl_3$) δ 8.12 (d, *J* = 8.5 Hz, 2H), 7.91 – 7.74 (m, 2H), 6.95 (s, 1H), 6.70 (dd, *J* = 4.1, 1.7 Hz, 1H), 6.17 (dd, *J* = 4.1, 2.5 Hz, 1H), 4.41 (q, *J* = 7.1 Hz, 2H), 4.05 (s, 3H), 1.42 (t, *J* = 7.1 Hz, 3H). ^{13}C NMR (126 MHz, $CDCl_3$) δ 185.4, 166.2, 143.8, 132.8, 132.2, 130.4, 129.4, 129.0, 123.5, 108.6,

61.4, 37.6, 14.5. HRMS. Calculated for $C_{15}H_{15}NNaO_3$ ($M+Na^+$): 280.0944, found: 280.0955. FT-IR-ATR (cm^{-1}): 1709.8 (CO_2Et), 1623.9 (C=O).

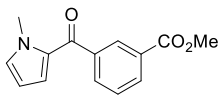

Methyl 3-(1-methyl-1H-pyrrole-2-carbonyl)benzoate 4.1r. Yellow solid, 72 mg, 59% yield. ^1H NMR (500 MHz, $CDCl_3$) δ 8.45 (t, *J* = 1.6 Hz, 1H), 8.22 – 8.19 (m, 1H), 7.98 (dd, *J* = 5.3, 3.8 Hz, 1H), 7.54 (t, *J* = 7.7 Hz, 1H), 6.97 – 6.92 (m, 1H), 6.71 (dd, *J* = 4.1, 1.6 Hz, 1H), 6.17 (dd, *J* = 4.1, 2.5 Hz, 1H), 4.05 (s, 3H), 3.94 (s, 3H). ^{13}C NMR (126 MHz, $CDCl_3$) δ 185.2, 166.7, 140.4, 133.4, 132.4, 132.1, 130.33, 130.33, 130.2, 128.5, 123.3, 108.6, 52.5, 37.6. HRMS. Calculated for $C_{14}H_{13}NNaO_3$ ($M+Na^+$): 266.0788, found: 266.0775. FT-IR-ATR (cm^{-1}): 1717.5 (CO_2Me), 1622.1 (C=O).

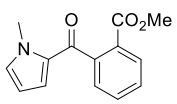

(2-Methylphenyl)(1-methyl-1H-pyrrol-2-yl)methanone 4.1s. Pale white solid, 68 mg, 56% yield. ^1H NMR (500 MHz, $CDCl_3$) δ 7.99 (dd, *J* = 7.8, 1.0 Hz, 1H), 7.60 (td, *J* = 7.5, 1.3 Hz, 1H), 7.53 (td, *J* = 7.6, 1.4 Hz, 1H), 7.49 (dd, *J* = 7.5, 1.1 Hz, 1H), 6.90 (t, *J* = 1.9 Hz, 1H), 6.33 (dd, *J* = 4.1, 1.7 Hz, 1H), 6.08 (dd, *J* = 4.1, 2.5 Hz, 1H), 4.12 (s, 3H), 3.75 (s, 3H). ^{13}C NMR (126 MHz, $CDCl_3$) δ 186.8, 167.0, 142.5, 131.9, 131.6, 131.3, 130.1, 129.5, 129.4, 128.3, 122.2, 108.4, 52.4, 37.5. HRMS. Calculated for $C_{14}H_{13}NNaO_3$ ($M+Na^+$): 266.0788, found: 266.0790. FT-IR-ATR (cm^{-1}): 1717.9 (CO_2Me), 1623.9 (C=O).

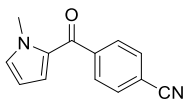

4-(1-methyl-1H-pyrrole-2-carbonyl)benzonitrile 4.1t. Yellow solid, 70 mg, 67% yield. ^1H NMR (500 MHz, $CDCl_3$) δ 7.85 (d, *J* = 8.6 Hz, 2H), 7.75 (d, *J* = 8.6 Hz, 2H), 7.00 – 6.94 (m, 1H), 6.67 (dd, *J* = 4.1, 1.7 Hz, 1H), 6.18 (dd, *J* = 4.1, 2.5 Hz, 1H), 4.04 (s, 3H). ^{13}C NMR (126 MHz, $CDCl_3$) δ 184.2, 143.8, 132.8, 132.1, 129.9, 129.6, 123.7, 118.4, 114.8, 108.9, 37.7. HRMS. Calculated for $C_{13}H_{10}N_2NaO$ ($M+Na^+$): 233.0685, found: 233.0691. FT-IR-ATR (cm^{-1}): 2226.9 (CN), 1621.1 (C=O).

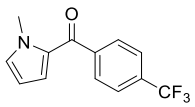

(1-methyl-1H-pyrrol-2-yl)(4-(trifluoromethyl)phenyl)methanone 4.1u. Pale yellow solid, 89 mg, 70% yield. ^1H NMR (500 MHz, $CDCl_3$) δ 7.88 (d, *J* = 8.0

Hz, 2H), 7.71 (d, *J* = 8.1 Hz, 2H), 7.05 – 6.89 (m, 1H), 6.70 (dd, *J* = 4.1, 1.7 Hz, 1H), 6.18 (dd, *J* = 4.1, 2.5 Hz, 1H), 4.05 (s, 3H). ^{13}C NMR (126 MHz, $CDCl_3$) δ 184.8, 143.2 (d, *J* = 1.2 Hz), 132.9 (d, *J* = 32.6 Hz), 132.4, 130.2, 129.4, 125.2 (q, *J* = 3.8 Hz), 125.0, 123.6, 108.7, 37.6. HRMS. Calculated for $C_{13}H_{10}F_3NNaO$ ($M+Na^+$): 276.0607, found: 276.0607. FT-IR-ATR (cm^{-1}): 1621.3 (C=O).

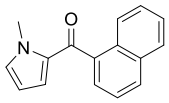

(1-methyl-1H-pyrrol-2-yl)(naphthalen-1-yl)methanone 4.1v. Yellow oil, 95 mg, 81% yield. ^{1}H NMR (500 MHz, $CDCl_3$) δ 8.16 (dd, *J* = 7.8, 2.0 Hz, 1H), 7.95 (d, *J* = 8.3 Hz, 1H), 7.92 – 7.87 (m, 1H), 7.65 (dd, *J* = 7.0, 1.2 Hz, 1H), 7.54 – 7.46 (m, 3H), 6.95 (t, *J* = 2.0 Hz, 1H), 6.53 (dd, *J* = 4.1, 1.7 Hz, 1H), 6.10 (dd, *J* = 4.1, 2.4 Hz, 1H), 4.17 (s, 3H). ^{13}C NMR (126 MHz, $CDCl_3$) δ 187.4, 138.0, 133.8, 132.2, 132.0, 131.0, 130.4, 128.3, 126.9, 126.7, 126.3, 125.8, 124.4, 124.0, 108.4, 37.8. HRMS. Calculated for $C_{16}H_{13}NNaO$ ($M+Na^+$): 258.0889, found: 258.0883. FT-IR-ATR (cm^{-1}): 1613.7 (C=O).

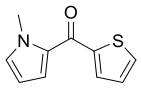

(1-methyl-1H-pyrrol-2-yl)(thiophen-2-yl)methanone 4.1w. Colorless oil, 76 mg, 79% yield. ^{1}H NMR (400 MHz, $CDCl_3$) δ 7.76 (dd, *J* = 3.7, 1.1 Hz, 1H), 7.61 (dd, *J* = 5.0, 1.0 Hz, 1H), 7.14 (dd, *J* = 4.9, 3.8 Hz, 1H), 7.04 (dd, *J* = 4.1, 1.6 Hz, 1H), 6.95 – 6.89 (m, 1H), 6.19 (dd, *J* = 4.0, 2.5 Hz, 1H), 3.99 (s, 3H). ^{13}C NMR (126 MHz, $CDCl_3$) δ 177.4, 144.9, 132.4, 132.1, 131.5, 130.4, 127.7, 121.1, 108.4, 37.3. HRMS. Calculated for $C_{10}H_9NNaOS$ ($M+Na^+$): 214.0297, found: 214.0290. FT-IR-ATR (cm^{-1}): 1601.9 (C=O).

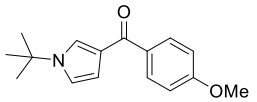

(1-(tert-butyl)-1H-pyrrol-3-yl)(4-methoxyphenyl)methanone 4.1x. Yellow solid, 102 mg, 79% yield. ^{1}H NMR (500 MHz, $CDCl_3$) δ 7.86 (d, *J* = 8.8 Hz, 2H), 7.46 – 7.40 (m, 1H), 6.94 (d, *J* = 8.8 Hz, 2H), 6.84 (dd, *J* = 2.9, 2.5 Hz, 1H), 6.63 (dd, *J* = 3.0, 1.8 Hz, 1H), 3.85 (s, 3H), 1.54 (s, 9H). ^{13}C NMR (126 MHz, $CDCl_3$) δ 189.7, 162.3, 132.8, 131.2, 124.6, 123.9, 119.1, 113.4, 110.8, 55.9, 55.4, 30.6. HRMS. Calculated for $C_{16}H_{19}NNaO_2$ ($M+Na^+$): 280.1308, found: 280.1318. FT-IR-ATR (cm^{-1}): 1623.9 (C=O).

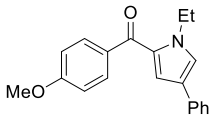

(1-ethyl-4-phenyl-1H-pyrrol-2-yl)(4-methoxyphenyl)methanone 4.1y. Yellow solid, 82 mg, 54% yield. ^{1}H NMR (500 MHz, $CDCl_3$) δ 7.90 (d, *J* = 8.7 Hz, 2H), 7.51 (d, *J* = 7.3 Hz, 2H), 7.37 (t, *J* = 7.7 Hz, 2H), 7.31 (d, *J* = 1.7 Hz, 1H), 7.23 (t, *J* = 7.4 Hz, 1H), 7.00 (dd, *J* = 5.2, 3.3 Hz, 3H), 4.49 (q, *J* = 7.2 Hz, 2H), 3.92 (s, 3H), 1.52 (t, *J* = 7.2 Hz, 3H). ^{13}C NMR (126 MHz, $CDCl_3$) δ 185.1, 162.5, 134.4, 132.6, 131.5, 130.6, 128.8, 126.2, 126.0, 125.1, 124.1, 119.1, 113.4, 55.5, 44.5, 17.1. HRMS. Calculated for $C_{20}H_{19}NNaO_2$ ($M+Na^+$): 328.1308, found: 328.1307. FT-IR-ATR (cm^{-1}): 1621.8 (C=O).

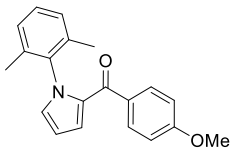

(1-(2,6-dimethylphenyl)-1H-pyrrol-2-yl)(4-methoxyphenyl)methanone 4.1z. White solid, 66 mg, 43% yield. ^{1}H NMR (500 MHz, $CDCl_3$) δ 7.86 (d, *J* = 8.9 Hz, 2H), 7.20 (dd, *J* = 8.0, 7.1 Hz, 1H), 7.11 (d, *J* = 7.6 Hz, 2H), 6.93 (d, *J* = 8.9 Hz, 2H), 6.89 (dd, *J* = 3.9, 1.6 Hz, 1H), 6.85 (dd, *J* = 2.5, 1.6 Hz, 1H), 6.40 (dd, *J* = 3.9, 2.6 Hz, 1H), 3.87 (s, 3H), 2.01 (s, 6H). ^{13}C NMR (126 MHz, $CDCl_3$) δ 183.7, 162.7, 139.7, 135.7, 131.81, 131.81, 131.4, 129.2, 128.1, 128.0, 120.6, 113.5, 109.4, 55.6, 17.8. HRMS. Calculated for $C_{20}H_{19}NNaO_2$ ($M+Na^+$): 328.1308, found: 328.1311. FT-IR-ATR (cm^{-1}): 1625.4 (C=O).

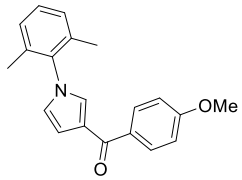

(1-(2,6-dimethylphenyl)-1H-pyrrol-3-yl)(4-methoxyphenyl)methanone 4.1z'. White solid, 66 mg, 43% yield. ^{1}H NMR (500 MHz, $CDCl_3$) δ 7.91 (d, *J* = 8.9 Hz, 2H), 7.25 (dd, *J* = 12.7, 4.7 Hz, 1H), 7.19 (t, *J* = 1.8 Hz, 1H), 7.15 (d, *J* = 7.6 Hz, 2H), 6.95 (d, *J* = 8.9 Hz, 2H), 6.87 (dd, *J* = 2.9, 1.7 Hz, 1H), 6.65 (dd, *J* = 2.8, 2.1 Hz, 1H), 3.86 (s, 3H), 2.08 (s, 6H). ^{13}C NMR (126 MHz, $CDCl_3$) δ 189.6, 162.4, 138.8, 135.7, 132.6, 131.21, 128.7, 128.3, 128.5, 125.2, 123.1, 113.42, 111.2, 55.4 17.4. HRMS. Calculated for $C_{20}H_{19}NNaO_2$ ($M+Na^+$): 328.1308, found: 328.1311. FT-IR-ATR (cm^{-1}): 1627.8 (C=O).

4.5.5. Spectroscopic Data on 4.4

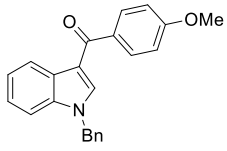

(1-Benzyl-1H-indol-3-yl)(4-methoxyphenyl)methanone 4.4a.[33] White solid, 141 mg, 83% yield. ^{1}H NMR (500 MHz, $CDCl_3$) δ 8.41 (dd, *J* = 8.6, 1.3 Hz, 1H), 7.87 (d, *J* = 8.8 Hz, 2H), 7.66 (s, 1H), 7.38 – 7.30 (m, 6H), 7.20 – 7.14 (m, 2H), 7.00 (d, *J* = 8.8 Hz, 2H), 5.40 (s, 2H), 3.91 (s, 3H). ^{13}C NMR (126 MHz, $CDCl_3$) δ 189.9, 162.4, 137.2, 136.5, 136.1, 133.5, 131.1, 129.2, 128.3, 127.7, 127.0, 123.8, 122.9, 122.7, 116.4, 113.7, 110.3, 55.6, 50.9. Calculated for $C_{23}H_{19}NNaO_2$ ($M+Na^+$): 364.1308, found: 364.1303. FT-IR-ATR (cm^{-1}): 1612.4 (C=O).

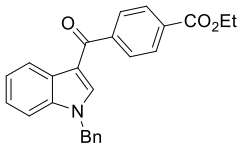

Ethyl 4-(1-benzyl-1H-indole-3-carbonyl)benzoate 4.4b. Pale yellow solid, 168 mg, 91% yield. ^{1}H NMR (500 MHz, $CDCl_3$) δ 8.46 (d, J = 8.3 Hz, 1H), 8.17 (d, *J* = 8.3 Hz, 2H), 7.88 (d, *J* = 8.3 Hz, 2H), 7.61 (s, 1H), 7.42 – 7.30 (m, 6H), 7.17 (d, *J* = 7.9 Hz, 2H), 5.39 (s, 2H), 4.45 (q, *J* = 7.1 Hz, 2H), 1.45 (t, *J* = 7.1 Hz, 3H). ^{13}C NMR (126 MHz, $CDCl_3$) δ 190.0, 166.1, 144.5, 137.3, 137.2, 135.6, 132.6, 129.6, 129.1, 128.5, 128.3, 127.3, 126.9, 124.0, 123.1, 122.8, 116.0, 110.3, 61.3, 50.9, 14.3. Calculated for $C_{25}H_{21}NO_3Na$ ($M+Na^+$): 406.1414, found: 406.1424. FT-IR-ATR (cm^{-1}): 1704.4 (CO_2Et), 1613.7 (C=O).

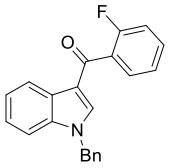

(1-Benzyl-1H-indol-3-yl)(2-fluorophenyl)methanone 4.4c. Pale yellow solid, 127 mg, 77% yield. ^{1}H NMR (500 MHz, $CDCl_3$) δ 8.46 (d, *J* = 7.8 Hz, 1H), 7.61 (t, *J* = 7.2 Hz, 1H), 7.57 (d, *J* = 1.4 Hz, 1H), 7.49 (dd, *J* = 14.0, 6.7 Hz, 1H), 7.39 – 7.30 (m, 6H), 7.29 – 7.23 (m, 1H), 7.19 (t, *J* = 9.1 Hz, 1H), 7.15 (d, *J* = 6.9 Hz, 2H), 5.36 (s, 2H). ^{13}C NMR (126 MHz, $CDCl_3$) δ 186.7, 159.4 (d, *J* = 250.2 Hz), 138.0 (d, *J* = 3.1 Hz), 137.18, 135.6, 131.8 (d, *J* = 8.1 Hz), 130.1 (d, *J* = 3.3 Hz), 129.4 (d, *J* = 16.1 Hz), 129.0, 128.2, 126.9, 126.7, 124.1 (d, *J* = 3.6 Hz), 123.9, 123.1, 122.7, 117.2, 116.2 (d, *J* = 22.0 Hz), 110.4, 50.9. Calculated for $C_{22}H_{16}NOFNa$ ($M+Na^+$): 352.1108, found: 352.1105. FT-IR-ATR (cm^{-1}): 1619.2 (C=O).

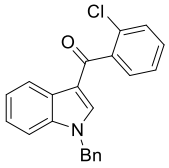

(1-Benzyl-1H-indol-3-yl)(2-chlorophenyl)methanone 4.4d. Pale yellow solid, 124 mg, 72% yield. ^{1}H NMR (500 MHz, $CDCl_3$) δ 8.39 (d, *J* = 7.8 Hz, 1H), 7.49

(dd, *J* = 7.0, 1.3 Hz, 2H), 7.46 – 7.39 (m, 2H), 7.39 – 7.29 (m, 7H), 7.14 (d, *J* = 6.6 Hz, 2H), 5.35 (s, 2H). ^{13}C NMR (126 MHz, $CDCl_3$) δ 189.0, 140.5, 138.2, 137.3, 135.6, 131.0, 130.4, 130.1, 129.0, 128.8, 128.2, 126.7, 126.7, 126.5, 124.0, 123.2, 122.7, 116.9, 110.4, 51.0. Calculated for $C_{22}H_{16}NOClNa$ ($M+Na^+$): 368.0813, found: 368.0813. FT-IR-ATR (cm^{-1}): 1620.0 (C=O).

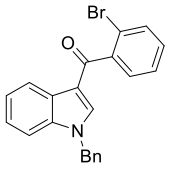

(1-Benzyl-1H-indol-3-yl)(2-bromophenyl)methanone 4.4e.[34] Pale yellow solid, 133 mg, 68% yield. ^{1}H NMR (500 MHz, $CDCl_3$) δ 8.39 (d, *J* = 7.6 Hz, 1H), 7.67 (d, *J* = 8.0 Hz, 1H), 7.48 – 7.39 (m, 3H), 7.38 – 7.27 (m, 7H), 7.14 (d, *J* = 6.6 Hz, 2H), 5.33 (s, 2H). ^{13}C NMR (126 MHz, $CDCl_3$) δ 189.7, 142.5, 138.3, 137.3, 135.6, 133.2, 130.5, 129.03, 129.03, 128.8, 128.2, 127.1, 126.7, 123.9, 123.2, 122.7, 119.6, 116.5, 110.4, 51.0. Calculated for $C_{22}H_{16}NOBrNa$ ($M+Na^+$): 412.0307, found: 412.0321. FT-IR-ATR (cm^{-1}): 1619.6 (C=O).

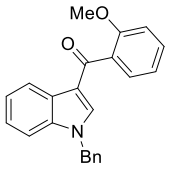

(1-Benzyl-1H-indol-3-yl)(2-methoxyphenyl)methanone 4f. Pale yellow solid, 126 mg, 74% yield. ^{1}H NMR (500 MHz, $CDCl_3$) δ 8.45 (d, J = 7.8 Hz, 1H), 7.50 (s, 1H), 7.45 (m, 2H), 7.38 – 7.26 (m, 6H), 7.13 (d, J = 6.4 Hz, 2H), 7.08 – 6.99 (m, 2H), 5.30 (s, 2H), 3.78 (s, 3H). ^{13}C NMR (126 MHz, $CDCl_3$) δ 190.2, 156.8, 138.1, 137.2, 135.9, 131.1, 130.9, 129.1, 128.97, 128.97, 128.1, 126.9, 126.8, 123.6, 122.8, 120.3, 117.6, 111.6, 110.3, 55.7, 50.8. Calculated for $C_{23}H_{19}NO_2Na$ ($M+Na^+$): 364.1308, found: 364.1325. FT-IR-ATR (cm^{-1}): 1618.2 (C=O).

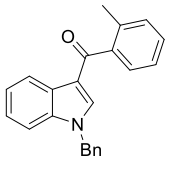

(1-Benzyl-1H-indol-3-yl)(o-tolyl)methanone 4.4g. Pale yellow solid, 120 mg, 74% yield. ^{1}H NMR (500 MHz, $CDCl_3$) δ 8.44 (d, *J* = 7.7 Hz, 1H), 7.46 (m, 2H), 7.42 – 7.25 (m, 9H), 7.15 (d, *J* = 6.6 Hz, 2H), 5.33 (s, 2H), 2.45 (s, 3H). ^{13}C NMR (126 MHz, $CDCl_3$) δ 193.0, 141.0, 138.0, 137.3, 136.0, 135.8, 130. 9, 129.4, 129.0, 128.2, 127.7, 127.0, 126.8, 125.2, 123.8, 123.0, 122.8, 117.6, 110.4, 50.9, 19.7. Calculated for $C_{23}H_{19}NONa$ ($M+Na^+$): 348.1359, found: 348.1367. FT-IR-ATR (cm^{-1}): 1620.0 (C=O).

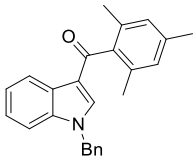

(1-Benzyl-1H-indol-3-yl)(mesityl)methanone 4.4h. Pale yellow solid, 134 mg, 76% yield. ^{1}H NMR (500 MHz, $CDCl_3$) δ 8.64 (s, 1H), 7.31 (m, 8H), 7.11 (s, 2H), 6.92 (s, 2H), 5.32 (s, 2H), 2.36 (s, 3H), 2.23 (s, 6H). ^{13}C NMR (126 MHz, $CDCl_3$) δ 194.7, 139.0, 137.9, 137.4, 135.8, 134.1, 129.0, 128.3, 128.1, 126.6, 126.4, 123.7, 122.9, 118.1, 110.4, 50.8, 21.2, 19.4. Calculated for $C_{25}H_{24}NONa$ ($M+Na^+$): 376.1672, found: 376.1684. FT-IR-ATR (cm^{-1}): 1623.9 (C=O).

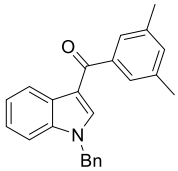

(1-Benzyl-1H-indol-3-yl)(3,5-dimethylphenyl)methanone 4.4i. Pale yellow solid, 144 mg, 85% yield. ^{1}H NMR (500 MHz, $CDCl_3$) δ 8.50 (d, J = 7.7 Hz, 1H), 7.64 (s, 1H), 7.46 (s, 2H), 7.39 – 7.30 (m, 6H), 7.21 (s, 1H), 7.18 (d, *J* = 6.5 Hz, 2H), 5.37 (s, 2H), 2.42 (s, 6H). ^{13}C NMR (126 MHz, $CDCl_3$) δ 191.3, 141.0, 137.9, 137.2, 137.1, 135.9, 132.8, 129.0, 128.2, 127.5, 127.0, 126.6, 123.7, 122.9, 122.8, 116.2, 110.2, 50.8, 21.4. Calculated for $C_{24}H_{21}NONa$ ($M+Na^+$): 362.1515, found: 362.1527. FT-IR-ATR (cm^{-1}): 1621.5 (C=O).

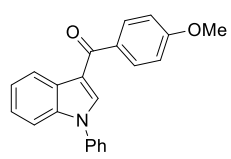

(4-methoxyphenyl)(1-phenyl-1H-indol-3-yl)methanone 4.4j. Pale white solid, 131 mg, 80% yield. ^{1}H NMR (500 MHz, $CDCl_3$) δ 8.48 (d, *J* = 7.6 Hz, 1H), 7.94 (d, *J* = 8.7 Hz, 2H), 7.82 (s, 1H), 7.57 (dt, *J* = 8.3, 7.6 Hz, 5H), 7.49 (d, *J* = 7.1 Hz, 1H), 7.45 – 7.33 (m, 2H), 7.02 (d, *J* = 8.7 Hz, 2H), 3.91 (s, 3H). ^{13}C NMR (126 MHz, $CDCl_3$) δ 190.0, 162.5, 138.6, 137.1, 135.9, 133.3, 131.1, 130.0, 128.0, 127.8, 125.0, 124.2, 123.1, 122.9, 117.5, 113.7, 110.9, 55.6. Calculated for $C_{22}H_{17}NNaO_2$ ($M+Na^+$): 350.1151, found: 350.1161. FT-IR-ATR (cm^{-1}): 1617.7 (C=O).

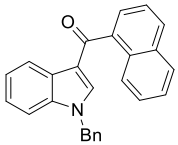

(1-Benzyl-1H-indol-3-yl)(naphthalen-1-yl)methanone 4.4k. Pale yellow solid, 163 mg, 90% yield. ^{1}H NMR (500 MHz, $CDCl_3$) δ 8.52 (d, J = 7.9 Hz, 1H), 8.24 (d, *J* = 8.3 Hz, 1H), 7.99 (d, *J* = 8.3 Hz, 1H), 7.93 (d, *J* = 7.6 Hz, 1H), 7.70 (dd, *J* = 7.0, 1.1 Hz, 1H), 7.57 – 7.48 (m, 3H), 7.46 (s, 1H), 7.38 (d, *J* = 8.0 Hz, 1H), 7.32 (m, 5H), 7.18

– 7.02 (m, 2H), 5.31 (s, 2H). ^{13}C NMR (126 MHz, $CDCl_3$) δ 192.1, 138.9, 138.2, 137.3, 135.6, 133.8, 130.8, 130.1, 129.0, 128.2, 128.2, 127.1, 126.8, 126.7, 126.3, 126.0, 124.5, 123.9, 123.0, 122.9, 118.1, 110.4, 50.9. Calculated for $C_{26}H_{19}NONa$ ($M+Na^+$): 384.1359, found: 384.1375. FT-IR-ATR (cm^{-1}): 1608.3 (C=O).

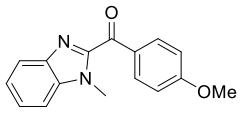

(4-methoxyphenyl)(1-methyl-1H-benzo[d]imidazol-2-yl)methanone 4.4l.[35] Pale white solid, 81 mg, 61% yield. ^{1}H NMR (500 MHz, $CDCl_3$) δ 8.42 (d, *J* = 9.0 Hz, 2H), 7.94 (d, *J* = 8.1 Hz, 1H), 7.48 (m, 2H), 7.42 – 7.37 (m, 1H), 7.03 (d, *J* = 9.0 Hz, 2H), 4.14 (s, 3H), 3.92 (s, 3H). ^{13}C NMR (126 MHz, $CDCl_3$) δ 184.8, 164.2, 147.2, 141.9, 136.5, 133.8, 129.8, 125.5, 123.6, 121.9, 113.8, 110.5, 55.7, 32.2. Calculated for $C_{16}H_{14}N_2NaO_2$ ($M+Na^+$): 289.0947, found: 289.0951. FT-IR-ATR (cm^{-1}): 1634.9 (C=O).

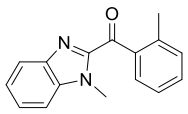

(1-Methyl-1H-benzo[d]imidazol-2-yl)(o-tolyl)methanone 4.4m. Pale yellow solid, 69 mg, 55% yield. ^{1}H NMR (500 MHz, $CDCl_3$) δ 7.92 (d, *J* = 8.2 Hz, 1H), 7.80 (d, *J* = 7.8 Hz, 1H), 7.55 – 7.43 (m, 3H), 7.40 – 7.36 (m, 1H), 7.33 (t, *J* = 7.9 Hz, 2H), 4.22 (s, 3H), 2.52 (s, 3H). ^{13}C NMR (126 MHz, $CDCl_3$) δ 190.0, 147.3, 141.9, 138.7, 137.2, 136.7, 131.7, 131.5, 131.4, 125.8, 125.3, 123.6, 122.3, 110.4, 32.3, 20.6. Calculated for $C_{16}H_{15}N_2O$ ($M+H^+$): 251.1179, found: 251.1178. FT-IR-ATR (cm^{-1}): 1650.2 (C=O).

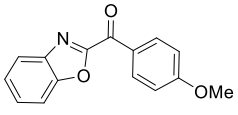

benzo[d]oxazol-2-yl(4-methoxyphenyl)methanone 4.4n. [35] Pale white solid, 95 mg, 75% yield. ^{1}H NMR (400 MHz, $CDCl_3$) δ 8.61 (d, *J* = 9.1 Hz, 2H), 7.94 (d, *J* = 7.7 Hz, 1H), 7.71 (d, *J* = 8.2 Hz, 1H), 7.54 (td, *J* = 7.8, 1.1 Hz, 1H), 7.46 (td, *J* = 7.8, 1.1 Hz, 1H), 7.04 (d, *J* = 9.0 Hz, 2H), 3.92 (s, 3H). ^{13}C NMR (101 MHz, $CDCl_3$) δ 178.9, 164.8, 157.6, 150.5, 140.9, 133.8, 128.2, 128.1, 125.7, 122.3, 114.1, 112.0, 55.8. Calculated for $C_{15}H_{11}NNaO_3$ ($M+Na^+$): 276.0631, found: 276.0636. FT-IR-ATR (cm^{-1}): 1646.4 (C=O).

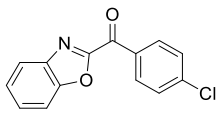

Benzo[d]oxazol-2-yl(4-chlorophenyl)methanone 4.4o. Pale yellow solid, 86 mg, 67% yield. ^{1}H NMR (500 MHz, $CDCl_3$) δ 8.55 (d, *J* = 8.7 Hz, 2H), 7.93 (d, *J* = 8.0 Hz, 1H), 7.70 (d, *J* = 8.2 Hz, 1H), 7.58 – 7.51 (m, 3H), 7.49 – 7.44 (m, 1H).^{13}C NMR (126 MHz, $CDCl_3$) δ 179.0, 156.8, 150.4, 141.0, 140.7, 133.7, 132.4, 129.0, 128.6, 125.8, 122.4, 111.9. Calculated for $C_{14}H_9NO_2Cl$ ($M+H^+$): 258.0322, found: 258.0312. FT-IR-ATR (cm^{-1}): 1657.1 (C=O).

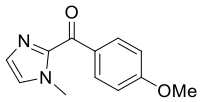

(4-methoxyphenyl)(1-methyl-1H-imidazol-2-yl)methanone 4.4p. Pale white solid, 61 mg, 56% yield. ^{1}H NMR (500 MHz, $CDCl_3$) δ 8.34 (d, *J* = 8.9 Hz, 2H), 7.21 (s, 1H), 7.08 (s, 1H), 6.96 (d, *J* = 8.9 Hz, 2H), 4.05 (s, 3H), 3.87 (s, 3H). ^{13}C NMR (126 MHz, $CDCl_3$) δ 182.8, 163.5, 143.5, 133.4, 130.2, 129.0, 126.5, 113.6, 55.6, 36.5. Calculated for $C_{12}H_{12}N_2NaO_2$ ($M+Na^+$): 239.0791, found: 239.0795. FT-IR-ATR (cm^{-1}): 1617.9 (C=O).

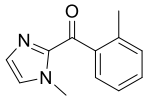

(1-Methyl-1H-imidazol-2-yl)(o-tolyl)methanone 4.4q. Pale yellow solid, 51 mg, 51% yield. ^{1}H NMR (500 MHz, $CDCl_3$) δ 7.64 (d, *J* = 7.3 Hz, 1H), 7.39 (t, *J* = 7.0 Hz, 1H), 7.28 (dd, *J* = 7.2, 4.1 Hz, 2H), 7.21 (s, 1H), 7.11 (s, 1H), 4.13 (s, 3H), 2.43 (s, 3H). ^{13}C NMR (126 MHz, $CDCl_3$) δ 188.0, 143.7, 137.9, 137.3, 131.1, 130.7, 129.9, 129.8, 127.0, 125.1, 36.3, 20.2. Calculated for $C_{12}H_{13}N_2O$ (M^+H^+): 201.1022, found: 201.1021. FT-IR-ATR (cm^{-1}): 1641.9 (C=O).

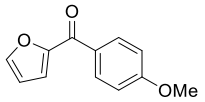

Furan-2-yl(4-methoxyphenyl)methanone 4.4r.[36] Pale yellow oil, 67 mg, 67% yield. ^{1}H NMR (500 MHz, $CDCl_3$) δ 8.10 – 7.96 (m, 2H), 7.69 (d, *J* = 0.9 Hz, 1H), 7.24 (d, *J* = 3.5 Hz, 1H), 6.99 (d, *J* = 8.9 Hz, 2H), 6.59 (dd, *J* = 3.5, 1.7 Hz, 1H), 3.89 (s, 3H). ^{13}C NMR (126 MHz, $CDCl_3$) δ 181.11, 163.30, 152.65, 146.52, 131.72, 129.84, 119.62, 113.71, 112.06, 55.48. Calculated for $C_{12}H_{11}O_3$ ($M+H^+$): 203.0708, found: 203.0700. FT-IR-ATR (cm^{-1}): 1630.1 (C=O).

4.5.6. Spectroscopic Data on 4.5

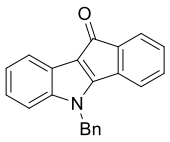

5-Benzylindeno[1,2-b]indol-10(5H)-one 4.5.[34] Bright red solid, 105 mg, 68% yield. ^{1}H NMR (500 MHz, $CDCl_3$) δ 7.84 (d, *J* = 7.8 Hz, 1H), 7.46 – 7.43 (m, 1H), 7.39 – 7.27 (m, 3H), 7.26 – 7.20 (m, 3H), 7.19 – 7.10 (m, 4H), 7.03 – 6.94 (m, 1H), 5.45 (s, 2H). ^{13}C NMR (126 MHz, $CDCl_3$) δ 185.1, 158.7, 142.7, 141.1, 135.5, 134.7, 132.0, 129.6, 129.2, 128.2, 126.3, 123.6, 123.3, 123.2, 123.0, 120.8, 118.5, 115.5, 111.1, 48.7. Calculated for $C_{22}H_{15}NaNO$ ($M+Na^+$): 332.1046, found: 332.1041. FT-IR-ATR (cm^{-1}): 1680.8 (C=O).

4.5.7. Spectroscopic Data on 4.6

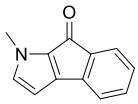

1-Methylindeno[2,1-b]pyrrol-8(1H)-one 4.6. Bright red solid, 60 mg, 66% yield. ^{1}H NMR (500 MHz, $CDCl_3$) δ 7.29 (d, *J* = 7.5 Hz, 1H), 7.21 – 7.15 (m, 1H), 7.00 (d, *J* = 7.1 Hz, 1H), 6.95 (d, *J* = 7.2 Hz, 1H), 6.65 (d, *J* = 2.2 Hz, 1H), 6.03 (d, *J* = 2.3 Hz, 1H), 3.73 (s, 3H). ^{13}C NMR (126 MHz, $CDCl_3$) δ 181.4, 142.8, 139.1, 138.4, 133.3, 132.9, 132.5, 126.7, 123.1, 118.9, 103.3, 34.5. Calculated for $C_{12}H_9NNaO$ ($M+Na^+$): 206.0576, found: 206.0577. FT-IR-ATR (cm^{-1}): 1679.0 (C=O).

4.5.8. Spectroscopic Data on 4.7

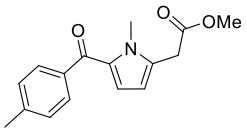

Methyl 2-(1-methyl-5-(4-methylbenzoyl)-1H-pyrrol-2-yl)acetate.[27] Pale yellow oil, 92 mg, yield: 68%. ^{1}H NMR (500 MHz, $CDCl_3$) δ 7.73 (d, *J* = 8.1 Hz, 2H), 7.27 (d, *J* = 8.0 Hz, 2H), 6.70 (d, *J* = 4.0 Hz, 1H), 6.13 (d, *J* = 4.0 Hz, 1H), 3.97 (s, 3H), 3.77 (s, 3H), 3.75 (s, 2H), 2.44 (s, 3H). ^{13}C NMR (126 MHz, $CDCl_3$) δ 185.9, 169.8, 141.9, 137.3, 134.3, 131.5, 129.4, 128.7, 122.2, 109.4, 52.5, 33.2, 32.8, 21.5. Calculated for $C_{16}H_{17}NNaO_3$ ($M+Na^+$): 294.1101 found: 294.1101.

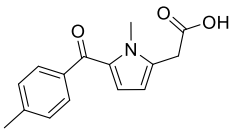

2-(1-Methyl-5-(4-methylbenzoyl)-1H-pyrrol-2-yl)acetic acid.[27] Pale white solid, 83 mg, yield: 98%. ^{1}H NMR (500 MHz, $CDCl_3$) δ 7.74 (d, J = 8.1 Hz, 2H), 7.34 – 7.16 (m, 2H), 6.71 (d, J = 4.0 Hz, 1H), 6.16 (d, J = 4.0 Hz, 1H), 3.98 (s, 3H), 3.80 (s, 2H), 2.45 (s, 3H). ^{13}C NMR (126 MHz, $CDCl_3$) δ 186.3, 174.8, 142.2, 137.3, 134.0, 131.7, 129.6, 128.9, 122.6, 109.9, 33.4, 32.7, 21.7. Calculated for $C_{15}H_{15}NNaO_3$ ($M+Na^+$): 280.0944 found: 280.0942. FT-IR-ATR (cm^{-1}): 1692.2 (COOH), 1624.52 (C=O).

4.6. References

(1) (a) Yu, J. Q.; Shi, Z. *C-H Activation*; Springer: Berlin, 2010; (b) Wencel-Delord, J.; Droge, T.; Liu, F.; Glorius, F. *Chem. Soc. Rev.* **2011**, *40*, 4740-4761; (c) Yamagucki, J.; Yamaguchi, A. D.; Itami, K. *Angew. Chem. Int. Ed.* **2012***, 51*, 8690-9009; (d) Davies, H. M. L.; Du Bois, J.; Yu, J.-Q. *Chem Soc. Rev.* **2011**, *40*, 1855-1856; (e) McMurray, L.; O'Hara, F.; Gaunt, M. J. *Chem. Soc. Rev.* **2011**, *40*, 1885-1898; (f) Godula, K.; Sames, D. *Science* **2006**, *312*, 67-72.

(2) (a) Lyons, T. W.; Sanford, M. S. *Chem. Rev.* **2010**, *110*, 1147-1169; (b) Colby, D. A.; Bergman, R. G.; Ellman, J. A. *Chem. Rev.* **2010**, *110*, 624-655; (c) Engle, K. M.; Mei, T.-S.; Wasa, M.; Yu, J.-Q. *Acc. Chem. Res.* **2012**, *45*, 788-802; (d) Daugulis, O.; Roane, J.; Tran, L. D. *Acc. Chem. Res.* **2015**, *48*, 1053-1064; (e) Arockiam, P. B.; Bruneau, C.; Dixneuf, P. H. *Chem. Rev.* **2012**, *112*, 5879-5918.

(3) (a) Lapointe, D.; Fagnou, K. *Chem. Lett.* **2010**, *39*, 1118-1126; (b) Ackermann, L. *Acc. Chem. Res.* **2014**, *47*, 281-295; (c) Ackermann, L. *Chem. Rev.* **2011**, *111*, 1315-1345; (d) Gorelsky, S. I. *Cord. Chem. Rev.* **2013**, *257*, 153-164.

(4) (a) White, M. C. *Science* **2012**, *335*, 807-809; (b) Roizen, J. L.; Harvey, M. E.; Du Bois, J. *Acc. Chem. Res.* **2012**, *45*, 911-922; (c) Tang, S.; Liu, K.; Liu, C.; Lei, A. *Chem. Soc. Rev*. **2015**, *44*, 1070-1082; (d) Song, R.-J.; Liu, Y.; Xie, Y.-X.; Li, J.-H. *Synthesis* **2015**, *47*, 1195-1209; (e) Shi, Z.; Zhang, C.; Tang, C.; Jiao, N. *Chem. Soc. Rev.* **2012**, *41*, 3381-3430.

(5) (a) Haibach, M. C.; Kundu, S.; Brookhart, M.; Goldman, A. S. *Acc. Chem. Res.* **2012**, *45*, 947-958; (b) Pérez, P. J. *Alkane C-H Activation by Single-Site Metal Catalysis*; Springer: Netherlands, 2012; (c) Kuhl, N.; Hopkinson, M. N.; Wencel-Delord, J.; Glorius, F. *Angew. Chem. Int. Ed.* **2012**, *51*, 10236-10254; (d) Davies, H. M. L.; Morton, D. *Chem. Soc. Rev.* **2011**, *40*, 1857-1869; (e) Girard, S. A.; Knauber, T.; Li, C.-J. *Angew. Chem. Int. Ed.* **2014**, *53*, 74-100; (f) Yeung, C. S.; Dong, V. M. *Chem. Rev.* **2011**, *111*, 1215-1292; (g) Sigman, M. S.; Werner, E. W. *Acc. Chem. Res.* **2012**, *45*, 874-884.

(6) For recent reviews on palladium catalyzed carbonylations: (a) Sumino, S.; Fusano, A.; Fukuyama, T.; Ryu, I. *Acc. Chem. Res.* **2014**, *47*, 1563-1574; (b) Wu, X.-F.; Neumann, H.; Beller, M. *Chem. Rev.* **2013**, *113*, 1-35; (c) Fang, W.; Zhu, H.; Deng, Q.; Liu, S.; Liu, X.; Shen,

Y.; Tu, T. *Synthesis* **2014**, *46*, 1689-1708; (d) Brennführer, A.; Neumann, H.; Beller, M. *Angew. Chem. Int. Ed.* **2009**, *48*, 4114-4133; (e) Barnard, C. F. J. *Organometallics* **2008**, *27*, 5402-5422.

(7) (a) Fujiwara, Y.; Kawauchi, T.; Taniguchi, H. *J. Chem. Soc., Chem. Comm.* **1980**, 220-221; (b) Fujiwara, Y.; Tabaki, K.; Taniguchi, Y. *Synlett* **1996**, *1996*, 591-599; (c) Jia, C.; Kitamura, T.; Fujiwara, Y. *Acc. Chem. Res.* **2001**, *34*, 633-639; (d) Itahara, T. *Chem. Lett.***1983**, *12*, 127-128; (e) Jaouhari, R., Dixneuf, P.H., Lécolier, S. *Tetrahedron Lett.* **1986**, *27*, 6315-6318; (f) Shibahara, F.; Kinoshita, S.; Nozaki, K. *Org. Lett.* **2004**, *6*, 2437-2439.

(8) For non-palladium catalyzed approaches to arene carbonylation, see: (a) Kunin, A. J.; Eisenberg, R. *J. Am. Chem. Soc.* **1986**, *108*, 535-536; (b) Kunin, A. J.; Eisenberg, R. *Organometallics* **1988**, *7*, 2124-2129; (c) Rosini, G. P.; Boese, W. T.; Goldman, A. S. *J. Am. Chem. Soc.* **1994**, *116*, 9498-9505; (d) Sakakura, T.; Sodeyama, T.; Sasaki, K.; Wada, K.; Tanaka, M. *J. Am. Chem. Soc.* **1990**, *112*, 7221-7229; (e) Guang Lan, Z.; Xuan Zhen, J. *Catal. Lett.* **2003**, *87*, 225-227; (f) Werner, H.; Höhn, A.; Dziallas, M. *Angew. Chem.* **1986**, *98*, 1112-1114.

(9) (a) Campo, M.A.; Larock, R.C. *Org. Lett.* **2000**, *2*, 3675-3677; (b) Tlili, A.; Schranck, J.; Pospech, J.; Neumann, H.; Beller, M. *Angew. Chem. Int. Ed.* **2013**, *52*, 6293-6297; (c) Giri, R.; Yu, J.-Q. *J. Am. Chem. Soc.* **2008**, *130*, 14082-14083; (d) Giri, R.; Lam, J.K.; Yu, J.-Q. *J. Am. Chem. Soc.* **2010**, *132*, 686-693; (e) Orito, K.; Horibata, A.; Nakamura, T.; Ushito, H.; Nagasaki, H.; Yuguchi, M.; Yamashita, S.; Tokuda, M. *J. Am. Chem. Soc.* **2004** *126*, 14342-14343; (f) Zhang, H.; Shi, R.; Gan, P.; Liu, C.; Ding, A.; Wang, Q.; Lei, A. *Angew. Chem. Int. Ed.* **2012,** *51*, 5204-5207; (g) Zhang, H.; Liu, D.; Chen, C.; Liu, C.; Lei, A. *Chem. Eur. J.* **2011**, *17*, 9581-9585.

(10) (a) Lian, Z.; Friis S. D.; Skrydstrup T. *Chem. Commun*., **2015**, *51*, 1870-1873; (b) For carbonylative coupling with *in situ* generated organocuprates with stoichiometric copper: Wu, X.-F.; Anbarasan, P.; Neumann, H.; Beller, M. *Angew. Chem. Int. Ed.* **2010**, *49*, 7316-7319.

(11) (a) Li, D.; Shan, S.; Shi, L.; Lang, R.; Xia, C.; Li, F. *Chinese J. Catal.* **2013**, *34*, 185-192; (b) Lang, R.; Shi, L.; Li, D.; Xia, C.; Li, F. *Org. Lett.* **2012**, *14*, 4130-4133; (c) Xing, Q.; Shi, L.; Lang, R.; Xia, C.; Li, F. *Chem. Commun.* **2012**, *48*, 11023-11025; (d) Zhao, M.-N.; Ran, L.; Chen, M.; Ren, Z.-H.; Wang, Y.-Y.; Guan, Z.-H. *ACS Catal.* **2015**, *5*, 1210-1213.

(12) (a) Beletskaya, I. P.; Cheprakov, A. V. In *Comprehensive Organometallic Chemistry III*; Crabtree, R.H; Mings, D. M. P., Eds.; Elsevier: Oxford, **2007**, 411-433; (b) Beller, M.; Wu, X. F.

Transition Metal Catalyzed Carbonylation Reactions: Carbonylative Activation of C-X Bonds; Springer: Berlin, Heidelberg, **2013**.

(13) (a) Olah, G. A. *Friedel-Crafts and Related Reactions*; Interscience Publishers: New York, **1963**; b) Olah, G. A. *Friedel-Crafts Chemistry*; John Wiley-Interscience: New York, **1973**.

(14) (a) Quesnel, J. S.; Arndtsen, B. A. *J. Am. Chem. Soc.* **2013**, *135*, 16841-16844; (b) Quesnel, J. S.; Kayser, L. V.; Fabrikant, A.; Arndtsen, B. A. *Chem. Eur. J.* **2015**, *21*, 9550-9555.

(15) The reaction of *N*-benzyl pyrrole (16 mg, 0.1 mmol) and *p*-anisoyl chloride (21 mg, 0.12 mmol) with NEt^iPr_2 (16 mg, 0.12 mmol) in CD_3CN (0.7 mL) at 115 ºC for 24 h leads to the 2- and 3-substituted pyrrole in 43% yield (in an identical 3.2:1 ratio). The catalytic reaction shows the generation of a mixture of 2- and 3-substituted isomers of **1a** in all cases (ca 3.2:1 ratio).

(16) ^{1}H NMR analysis of reaction crude shows generation of ca. 4:1 ratio of 2- and 3-substituted N-methylpyrrole. Only the major isomer is isolated and characterized.

(17) (a) Nadres, E. T.; Lazareva, A.; Daugulis, O. *J. Org. Chem.* **2011**, *76*, 471-483; (b) Liégault, B.; Petrov, I.; Gorelsky, S. I.; Fagnou, K. *J. Org. Chem.* **2010**, *75*, 1047-1060; (c) Liégault, B.; Lapointe, D.; Caron, L.; Vlassova, A.; Fagnou, K. *J. Org. Chem.* **2009**, *74*, 1826-1834; (d) Roger, J.; Doucet, H. *Adv. Synth. Catal.* **2009**, *351*, 1977-1990; (e) Wagner, A. M.; Sanford, M. S. *Org. Lett.* **2011**, *13*, 288-291; (f) Zhao, L.; Bruneau, C.; Doucet, H. *ChemCatChem* **2013**, *5*, 255-262.

(18) Bontemps, S.; Quesnel, J. S.; Worrall, K.; Arndtsen, B. A. *Angew. Chem. Int. Ed.* **2011**, *50*, 8948-8951.

(19) The reaction between pyrrole and **2a** in the absence of CO doesn't proceed cleanly due to side reactions, thus the initial rate of this reaction was observed to be 0.0015 min^{-1}; however, the observed rate constant for the reaction in the presence of 4 atm CO is 0.0100 min^{-1}.

(20) Anisoyl iodide reacts with NEt^iPr_2 at 125 ºC to form N-ethyl-N-isopropyl-4-methoxybenzamide via a Hofmann-type elimination.

(21) (a) Carson, J. R.; McKinstry, D. N.; Wong, S. *J. Med. Chem.* **1971**, *14*, 646-647; (b) Reddy, L. A.; Chakraborty, S.; Swapna, R.; Bhalerao, D.; Malakondaiah, G. C.; Ravikumar, M.; Kumar, A.; Reddy, G. S.; Naram, J.; Dwivedi, N.; Roy, A.; Himabindu, V.; Babu, B.; Bhattacharya, A.; Bandichhor, R. *Org. Process Res. Dev.* **2010**, *14*, 362-368.

(22) Zalesskiy, S. S.; Ananikov, V. P. *Organometallics* **2012**, *31*, 2302-2309.

(23) Miles, K. C.; Mays, S. M.; Southerland, B. K.; Auvil, T. J.; Ketcha, D. M. *ARKIVOC* **2009***, 2009,* 181-190.

(24) Islam, S.; Larrosa, I. *Chem. Eur. J.* **2013**, *19*, 15093-15096.

(25) Xu, S.; Huang, X.; Hong, X.; Xu, B. *Org. Lett.* **2012**, *14*, 4614-4617.

(26) Smith, N. D.; Huang, D.; Cosford, N. D. P. *Org. Lett.* **2002**, *4*, 3537-3539.

(27) Reddy, L. A.; Chakraborty, S.; Swapna, R.; Bhalerao, D.; Malakondaiah, G. C.; Ravikumar, M.; Kumar, A.; Reddy, G. S.; Naram, J.; Dwivedi, N.; Roy, A.; Himabindu, V.; Babu, B.; Bhattacharya, A.; Bandichhor, R. *Org. Process Res. Dev.* **2010**, *14*, 362-368.

(28) Wakeham, R. J.; Taylor, J. E.; Bull, S. D.; Morris, J. A.; Williams, J. M. J. *Org. Lett.* **2013**, *15*, 702-705.

(29) Taylor, J. E.; Jones, M. D.; Williams, J. M. J.; Bull, S. D. *Org Lett.* **2010**, *12*, 5740-5743.

(30) Carson, J. R.; Davis, N. M. *J. Org. Chem.* **1981**, *46*, 839-843.

(31) Jafarpour, F.; Hazrati, H.; Darvishmolla, M. *Adv. Synth. Catal.* **2014**, *356*, 3784-3788.

(32) Bernardi, D.; Dicko, A.; Kirsch, G. *Synthesis* **2006**, *2006*, 509-513.

(33) Miki, Y.; Tsuzaki, Y.; Kai, C.; Hachiken, H. *Heterocycles* **2002**, *57*, 1635-1643.

(34) Guchhait, S. K.; Kashyap, M. *Synthesis* **2012**, *44*, 619-627.

(35) Wu, X.-F.; Anbarasan, P.; Neumann, H.; Beller, M. *Angew. Chem. Int. Ed*. **2010**, *49*, 7316-7319.

(36) Lerebours, R.; Camacho-Soto, A.; Wolf, C. *J. Org. Chem.* **2005**, *70*, 8601-8604.

Chapter 5. Mechanism of the Palladium Catalyzed Synthesis of Münchnones: The Role of Ligands in N-Acyl Iminium Salt Carbonylation

5.1. Preface

As described in the introduction (Section 1.3.3.), our lab has previously reported the palladium catalyzed carbonylative coupling of imines and acid chlorides can provide a route to prepare Münchnones. Coupling the formation of these 1,3-dipoles with cycloaddition reactions provides efficient routes to prepare nitrogen-containing heterocycles. One challenge in developing this reaction, and the creation of more active catalyst systems, is the lack of data on how this complex transformation proceeds. To address this, we describe in this chapter the results of our mechanistic studies on this system, and in particular the formation of mesoionic Münchnones. This includes the synthesis of key catalytic intermediates, model reactions, and kinetic studies that support the role of these compounds in catalysis. Together, these studies provide a clear picture of the impact of catalyst structure, ligands and palladium nanoparticles on facilitating the carbonylation of *in situ* generated iminium salts, and suggest an avenue for the creation of more active catalyst systems. This work was done in collaboration with Dr. Yingdong Lu and Dr. Rajiv Dhawan. Dr. Dhawan performed the mercury poisoning experiments, obtained X-Ray crystal structures of compounds **5.2b** and **5.7b** and conducted some model reactions. Dr. Lu performed initial kinetic studies. This work was published in the *Chemistry - A European Journal* (**2016**, *22*, 15945-15954).

5.2. Introduction

Metal catalyzed multicomponent coupling reactions (MCRs) are of growing relevance in the design of efficient new synthetic methods.[1] By mediating the coupling of three or more reagents in a single synthetic step, multicomponent reactions offer the potential to simplify the synthesis of complex products, and are also of direct relevance to library generation. Transition metal catalysis can be an important tool in the design of new variants of these transformations, where the reactivity of the catalyst, rather than that designed into the reagents, can be used to

mediate the coupling of traditionally unreactive precursors. These features are demonstrated by many well established metal catalyzed MCRs, including the Pauson-Khand reaction,[2] metal catalyzed trimerization reactions (e.g. alkyne trimerization),[3] aldehyde amidocarbonylation,[4] and a range of more recently developed metal mediated or catalyzed processes.[5]

One challenge in the development of metal catalyzed multicomponent reactions can be the lack of a mechanistic information on how the multiple building blocks, along with the reactive catalyst, ligands, and other additives, all come together to selectively generate a single reaction product. These are often complex reactions, where a series of steps must occur in a selective fashion to form products. A wide range of side reactions are possible under these conditions, which can serve to either diminish yields or completely inhibit product formation. This complexity has also made mechanistic studies a challenge, and many times little is known about what is the rate determining step or steps in these systems.

We have recently reported the palladium catalyzed multicomponent synthesis of nitrogen-containing heterocycles and related products as shown in Scheme 5.1a.[6-8] A common feature of each of these reactions is the initial catalytic formation of 1,3-oxazolium-5-oxide (Münchnone, **5.1**) intermediates, generated via the palladium catalyzed coupling of imines, acid chlorides and carbon monoxide. Based upon several pieces of indirect data, we have postulated a mechanism for the palladium catalyzed formation of Münchnones as shown below. This involves the carbonylation of an *in situ* generated palladacycle **5.2**, followed by β-hydride elimination and cyclization to generate **5.1**. Evidence for this mechanism comes from stoichiometric studies that show that the 2,2-bipyridine (bipy) coordinated **5.2** can serve as a stoichiometric precursor for imidazolines, via both undergoing carbonylation to generate **5.1**, and equilibrium fragmentation to iminium salts, which are themselves the product of imine and acid chloride coupling.[6a] As such, it was postulated that complex **5.2** is an intermediate in catalysis, and generated upon addition of *N*-acyl iminium salt to palladium(0). These steps are mechanistically related to aldehyde amidocarbonylation reactions (Scheme 5.1b), where aldehyde/ amide condensation is postulated to lead to *N*-acyl iminium salt precursors under strongly acidic conditions, and ultimately allows carbonylation to α-amido acid derivatives via hydrolysis of **5.5**.[4] Nevertheless, the precise mechanism by which Münchnone is generated in

this reaction is not known, which has made the design of active catalysts for this transformation a challenge.

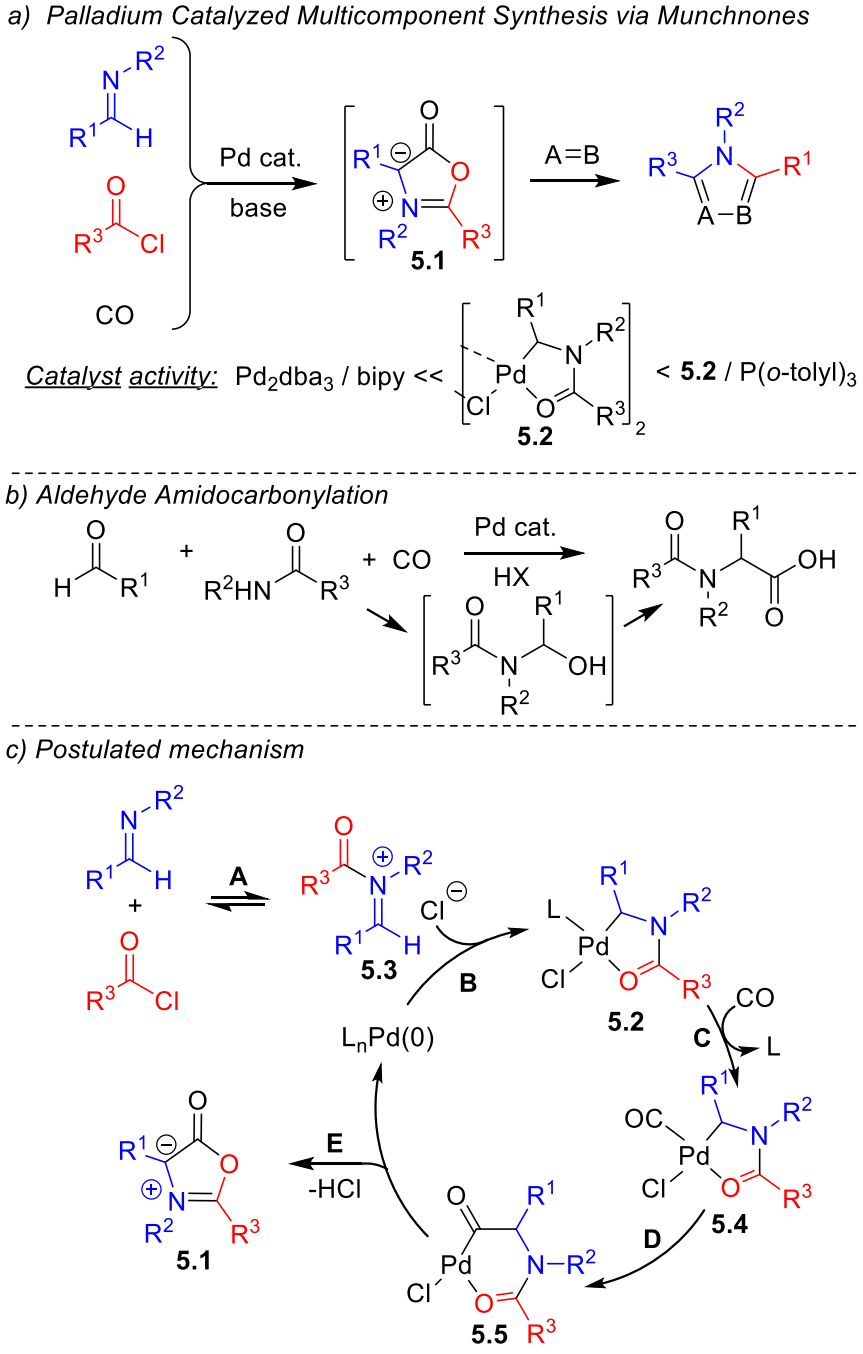

Scheme 5.1. Palladium Catalyzed Multicomponent Reactions via Münchnones.

For example, the initially developed catalyst for this reaction involved simple bipy/Pd_2dba_3.[6a] However, subsequent studies demonstrated that the formation of Münchnone is slowed by ligands such as bipy or dba (dibenzylideneacetone), and instead proceeds in highest yields with the palladacycle **5.4** with Bu_4NBr under pseudo ligandless conditions.[6b] More recently, we have reported that the addition bulky phosphine ligands such as P(*o*-Tol)$_3$ can accelerate Münchnone formation.[6c]

In order to understand the factors that control and influence catalytic Münchnone formation, we have undertaken a study of the mechanism of this reaction. The results of these studies are detailed below. These suggest not only the route by which Münchnones are formed in this system, but also the importance of balancing the factors that favor the various steps in this catalytic process (e.g. oxidative addition, carbonylation, and Pd(0) stabilization). In addition to providing an example of a mechanistically characterized metal catalyzed multicomponent coupling reaction, a comparison of the mechanism of both ligand free and phosphine containing catalytic systems shows what the precise role of the phosphine structure can have on this carbonylative coupling reaction, and the factors that can be used to accelerate catalysis.

5.3. Results and Discussion

5.3.1. Non-Ligated Palladium Catalysts

5.3.1.1. Synthesis of Reaction Intermediates.

In order to probe the mechanism of palladium catalyzed Münchnone formation in greater detail, we first examined the viability of these individual steps in the postulated catalytic cycle.

Formation of N-Acyl Iminium Salt (Step A). Monitoring the initial stages of the reaction by ^{1}H NMR spectroscopy provides insight into the first step of the catalytic process. The mixing of the imine, (*p*-Tol)HC=NBn (*p*-Tol = *p*-$C_6H_4CH_3$, Bn = CH_2Ph), and benzoyl chloride in CD_3CN leads to the rapid formation of *N*-acyl iminium salt **5.3a** (Scheme 5.2). The generation of **5.3a** is not complete, and approaches an equilibrium in which 91% of imine is converted to **5.3a** (K_{eq} = 1.4 (0.2) x 10^3 M^{-1}).[9] Compound **5.3a** can be isolated as a pale yellow solid by precipitation with pentane. ^{1}H and ^{13}C NMR spectra of **5.3a** in CD_3CN reveals the upfield shift of the former imine hydrogen (from δ 8.44 to δ 7.33) and carbon (from δ 161.6 to δ 78.0), both of which are similar to previously reported variants of **5.3a**, and suggest this product is best

described as a neutral α-chloroamide.[10] Interestingly, the benzylic hydrogens of **5.3a** appear as a singlet in the ^{1}H NMR spectra, despite the chirality in **5.3a**. This is consistent with a rapid equilibrium of **5.3a** with the ionic *N*-acyl iminium salt **5.3a'** on the NMR timescale. In the less polar benzene-d_6 solvent, this equilibrium is slowed, and the ^{1}H NMR spectra displays the anticipated diastereotopic benzylic hydrogens.

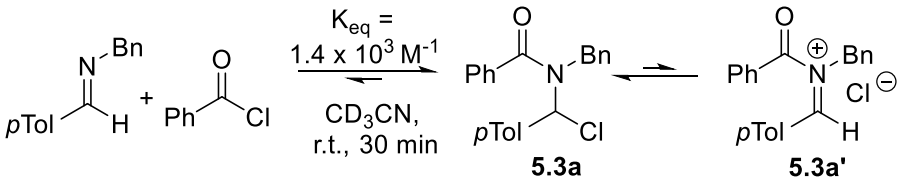

Scheme 5.2. Formation of α-chloroamide 5.3a.

*Synthesis of Palladacycle **5.2a** (Step B).* The addition of $Pd_2(dba)_3{\cdot}CHCl_3$ to the *in situ* generated *N*-acyl iminium salt **5.3a** leads to the rapid formation of the palladacycle $\{Pd(Cl)[\kappa^2$-CH(*p*-Tol)NBnCOPh]$\}_2$ **5.2a** (Scheme 5.3). Considering the rate of **5.2a** formation (1 h at ambient temperature) relative to catalysis (65 ºC, 24 h), this is also a viable step in catalysis. Complex **5.2a** can be isolated in 82% yield by a precipitation with diethyl ether. Spectroscopic data are consistent with a chelated amide structure. This includes the significant upfield shift of the former imine carbon and hydrogen in the ^{1}H and ^{13}C NMR spectra (to δ 5.21 and 59.5 ppm respectively), indicating the reduction of the imine C=N bond. In addition, the carbonyl resonance is observed at δ 180.3 in the ^{13}C NMR spectrum, which is shifted downfield of typical amides and suggestive of its chelation to palladium.[11] Electrospray mass spectroscopy shows this complex exists as in a dimeric structure (**5.2a**, M+Na$^+$ = 933.0429).

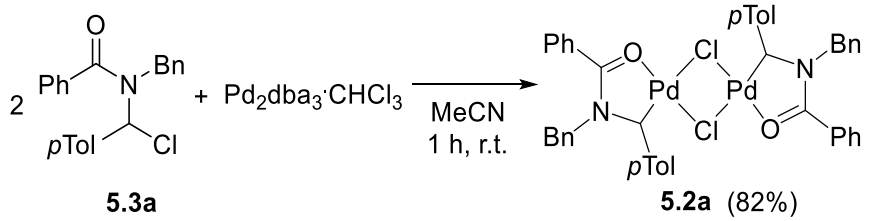

Scheme 5.3. Oxidative addition of *N*-acyl iminium salt 5.3a to Pd_2dba_3.

While **5.2a** could not be crystallized, the analogous *p*-methoxylbenzyl substituted {Pd(Cl)[κ^2-CH(*p*-Tol)N(PMB)COPh]}$_2$ **5.2b** can be generated via a similar reaction and isolated as an orange crystalline material upon recrystallization from toluene at –40ºC. The crystal structure of this complex is shown in Figure 5.1. Complex **5.2b** has a pseudo-square planar geometry about the palladium center (sum of angles = 360.0º). The Pd-Cl bond length cis to the amide oxygen O(4) is longer than the Pd-Cl^i bond, consistent with a stronger trans influence of the Pd-C bond. The C-O bond length is 1.264(7) Å is slightly longer than that observed in simple amides (PhCONMe$_2$, C=O = 1.231 Å).[12] In addition, the amide C-N bond length (1.312(8) Å) in **5.2b** is contracted (C-N = 1.368 Å in PhCONMe$_2$). Together, this data suggests a significant contribution of resonance form **5.2b'** to the structure of **5.2b**.

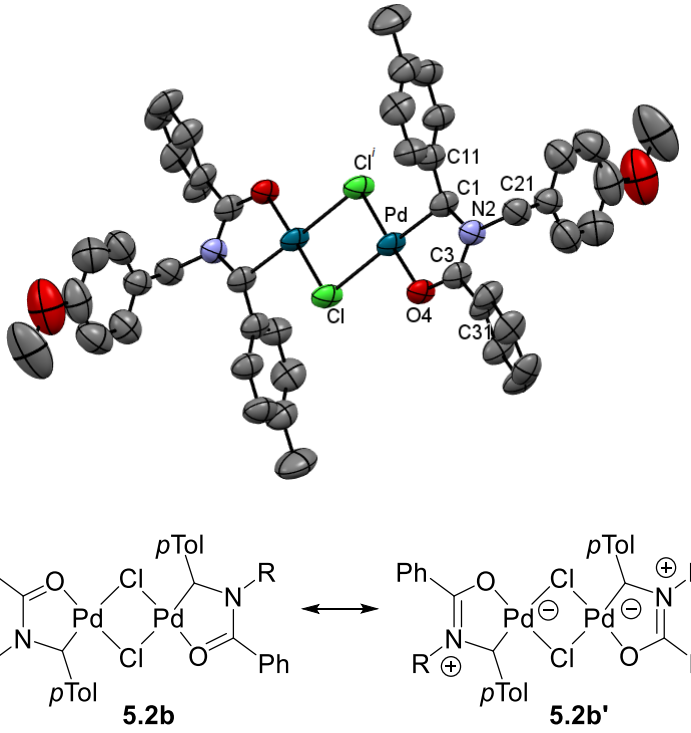

Figure 5.1. Crystal Structure of {Pd(Cl)[κ^2-CH(*p*-Tol)N(PMB)COPh]}$_2$ 5.2b.

Selected bond lengths (Å) and angles (deg): Pd-O(4), 2.2028 (4); O(4)-C(3), 1.264 (7); C(3)-N(2), 1.312 (8); N(2)-C(1), 1.519 (7); C(1)-Pd, 1.976 (6); Pd- Cli, 2.3198(16); Pd-Cl, 2.4655 (18); Cl-Pdi, 2.3198 (16); C(3)-C(31), 1.498 (8). Pdi-Cl-Pd, 93.08 (6); Pd-O(4)-C(3), 111.8 (4); O(4)-C(3)-N(2), 121.6 (5); C(3)-N(2)-C(1), 166.6 (5); N(2)-C(1)-Pd, 106.4 (4); C(1)-Pd-O(4), 83.6 (4); C(1)-Pd-Cli, 94.29 (17). The solvent (toluene) and hydrogen atoms in the lattice have been excluded for clarity.

*Reaction of **5.2** with CO (Step C).* The addition of the final reagent in the catalytic reaction, CO, to palladium complex **5.2a** leads to the rapid (<10 min) *in situ* formation of the carbonyl coordinated complex **5.4a** (Scheme 5.4). This complex displays shifted ^{1}H NMR signals for the chelated amide ligand, and IR analysis clearly shows the presence of a palladium bound carbonyl (ν_{CO} = 2114 cm^{-1} in CH_3CN).[13] Notably, no new IR stretch is observable between 1650 and 1800 cm^{-1}, indicating that CO insertion into the palladium-carbon bond has not occurred. Removal of CO reverts the CO-coordinated **5.4a** back to the palladium complex **5.2a**.

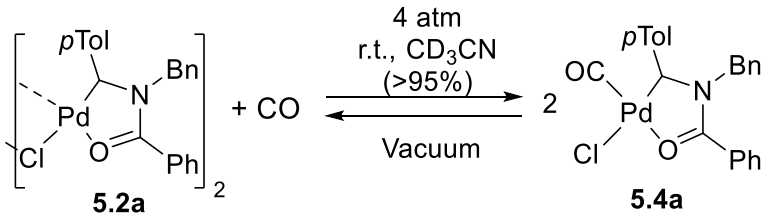

Scheme 5.4. Reaction of palladium complex 5.2a with CO.

Subsequent Steps in Catalysis. We see no evidence through stoichiometric experiments of any intermediate after complex **5.4a**. The warming of the CO coordinated **5.4a** to 65°C leads to a complex mixture of decomposition products, including significant amounts of palladium sediments and reversion back to imine and *N*-acyl iminium salt (Scheme 5.5). The addition of **5.3a** to palladium therefore appears to be an equilibrium process, and in the absence of excess iminium salt **5.3a** or stabilizing ligands, palladium precipitation occurs. In order to inhibit palladium black formation, Bu_4NBr was added to **5.4a**. Heating of **5.4a** under these conditions leads to the generation of Münchnone **5.1a** in 87% yield (Scheme 5.5). In light of these results, at least one role of the bromide source Bu_4NBr appears to be to stabilize palladium from irreversible precipitation. Under these conditions complex **5.4a** is a viable intermediate in Münchnone formation.

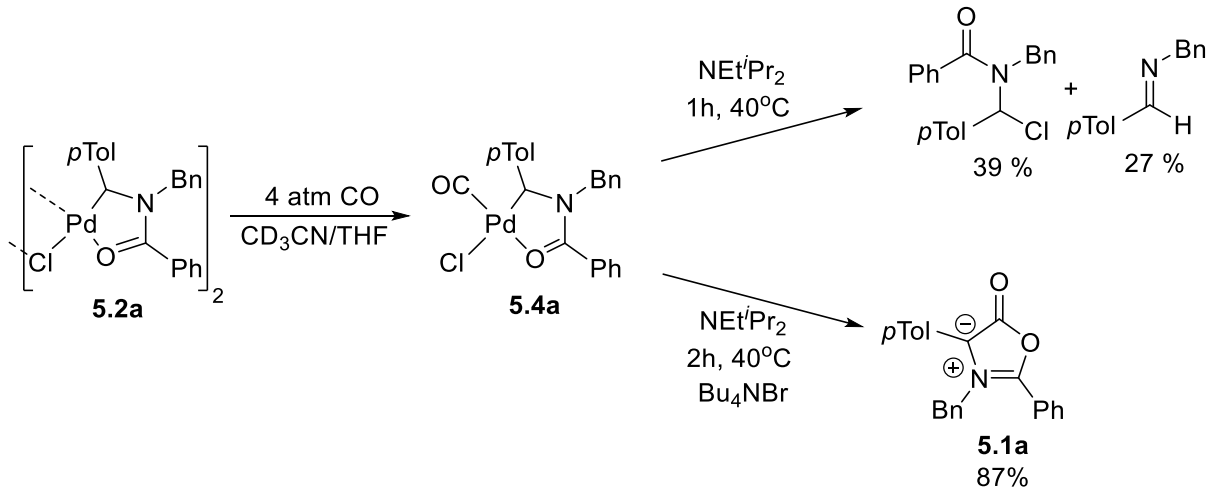

Scheme 5.5. Reactivity of palladacycle 5.4a and Münchnone formation.

5.3.1.2. Observation of 5.2-5.4 in Catalysis.

The relevance of the stoichiometric experiments above to catalysis can be probed by monitoring the formation of Münchnone by ^{1}H NMR spectroscopy. As illustrated in Figure 5.2, the initial spectrum of the catalytic reaction shows the rapid generation of *N*-acyl iminium salt **5.3a**. In addition, the palladacycle catalyst **5.2a** reacts with CO to form the carbonylated intermediate **5.4a**. Warming of this mixture to the reaction temperature of 65°C shows the slow disappearance of *N*-acyl iminium salt **5.3a** and the concomitant formation of Münchnone **5.1a** over the course of 12 hours. Interestingly, after 3 hours of reaction time, there is no evidence for any organometallic species in solution (i.e. **5.2a** or **5.4a**). This appears to be due to the rapid equilibration of these complexes with the excess *N*-acyl iminium salt, as the low temperature ^{1}H NMR (-10°C) of this mixture reveals the presence of **5.4a**, and the analogous bromide coordinated complex.[14] Integration of these signals show that palladacycle only accounts for 55% of the palladium added to the reaction. After 8 h reaction, or ca. 75% completion, almost no **5.4a** can be observed. The lack of any detectable organometallic intermediates during catalysis suggests that a significant amount of palladium may exist as Pd(0) during catalysis (*vide infra*).

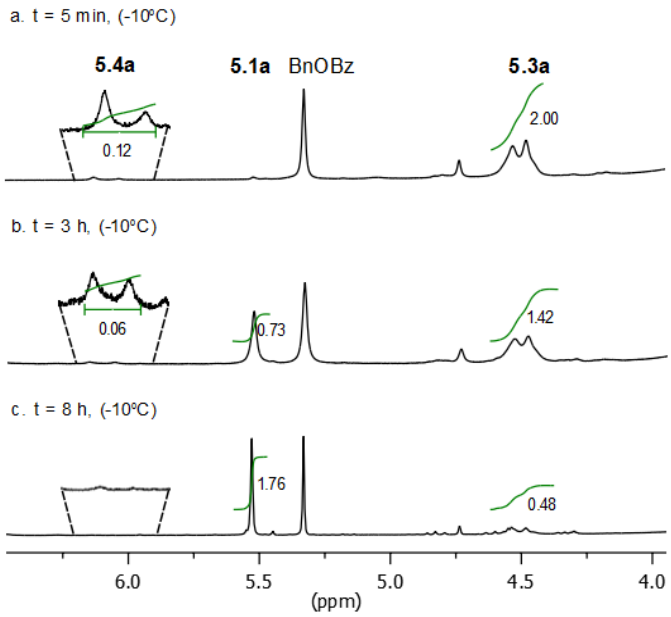

Figure 5.2. Monitoring the Catalytic Formation of Münchnone by ^{1}H NMR Analysis.

Catalytic reaction of benzoyl chloride (21 mg, 0.15 mmol), (*p*-Tol)HC=NBn (21 mg, 0.10 mmol), **5.2a** (4.5 mg, 0.005 mmol), Bu_4NBr (32 mg, 0.1mmol), EtN^iPr_2 (64 mg, 0.5 mmol), BnOBz standard, 4 atm CO in CD_3CN (0.7 mL) at 65°C Spectra shown were taken at -10°C.

5.3.1.3. Kinetics of Münchnone Formation.

We next turned towards determining which step or steps in this catalytic process influence the rate of product formation. The ambient temperature formation of palladacycle **5.2**, and its CO coordinated analogue **5.4**, suggest that the rate of Münchnone formation should be only dependent upon the intramolecular rearrangement of **5.4** (steps D and E, Scheme 5.1); i.e. a zero-order conversion of *N*-acyl iminium salt **5.3**. Our kinetic data is partially consistent with this interpretation. Monitoring the catalytic reaction by ^{1}H NMR analysis does show an initial linear disappearance of **5.3a**, but this quickly slows to a more first-order reaction as catalysis proceeds (Figure 5.3a). The zero-order behavior at the beginning of the reaction can be confirmed by probing the initial rates of catalysis at various concentration of **5.3a** (Figure 5.3b), which shows no rate dependence on N-acyl iminium salt **5.3a** concentration. We also see no significant rate dependence upon base (EtN^iPr_2) or the halide additive (Bu_4NBr) (Table 5.12), and first order dependence upon palladium concentration (Figure 5.3c). Interestingly, however, there is a clear linear dependence of rate on CO pressure (Figure 5.3d). In considering the

mechanism in Scheme 5.1, this would imply that either step C, the formation of CO coordinated **5.4**, is relatively slow or an equilibrium process under the catalytic conditions, or that carbon monoxide favors the subsequent steps in the catalytic cycle (e.g. stabilization of CO-insertion product **5.5**).

Evidence for the influence CO has on catalysis can be obtained by examining the stoichiometric reaction of palladacycle **5.2** at varying CO pressures. There is a clear first order rate dependence of Münchnone formation on CO pressure (Figure 5.15). As the conversion of palladacycle **5.2a** to the CO coordinated **5.4a** is quantitative in each of these reactions, this data suggests that CO favors the transformation of **5.4a** to Münchnone. The latter may arise from CO coordination to stabilize the product of insertion (e.g. complex **5.5**, Scheme 5.1), and allow the subsequent steps for the generation of Münchnone **5.1a** to proceed.

As noted above, the rate of **5.3a** disappearance deviates from zero-order behavior as catalysis proceeds, and shows a kinetic profile closer to first order behavior near the end of the reaction (Figure 5.3a). One rationale for this observation is a degradation or change in the palladium catalyst. In order to determine if the catalyst is degrading, a "same excess" kinetic experiment was performed (Figure 5.3a, inset),[15] wherein all reagent concentrations are identical to that at a midpoint in the reaction, but the catalyst is new. This shows that at identical **5.3a** concentration, the reaction with fresh catalyst proceeds at a higher rate, and the again zero-order disappearance of *N*-acyl iminium salt. Also consistent with the loss of catalyst activity as *N*-acyl iminium salt disappears, kinetic experiments at ten times lower **5.3a** concentration, which are also the conditions typically employed in synthesis,[6,16] show that the disappearance of *N*-acyl iminium salt does not follow zero-order kinetics at any stage of the reaction, and is instead first-order in **5.3a** (Figures 5.3e); i.e. the reaction of **5.3a** with Pd(0) is at least partially rate determining at these conditions. Together, this data implies that the palladium catalyst is undergoing degradation during catalysis, and that oxidative addition is becoming rate determining. The nature of the Pd(0) catalyst under these conditions is examined below.

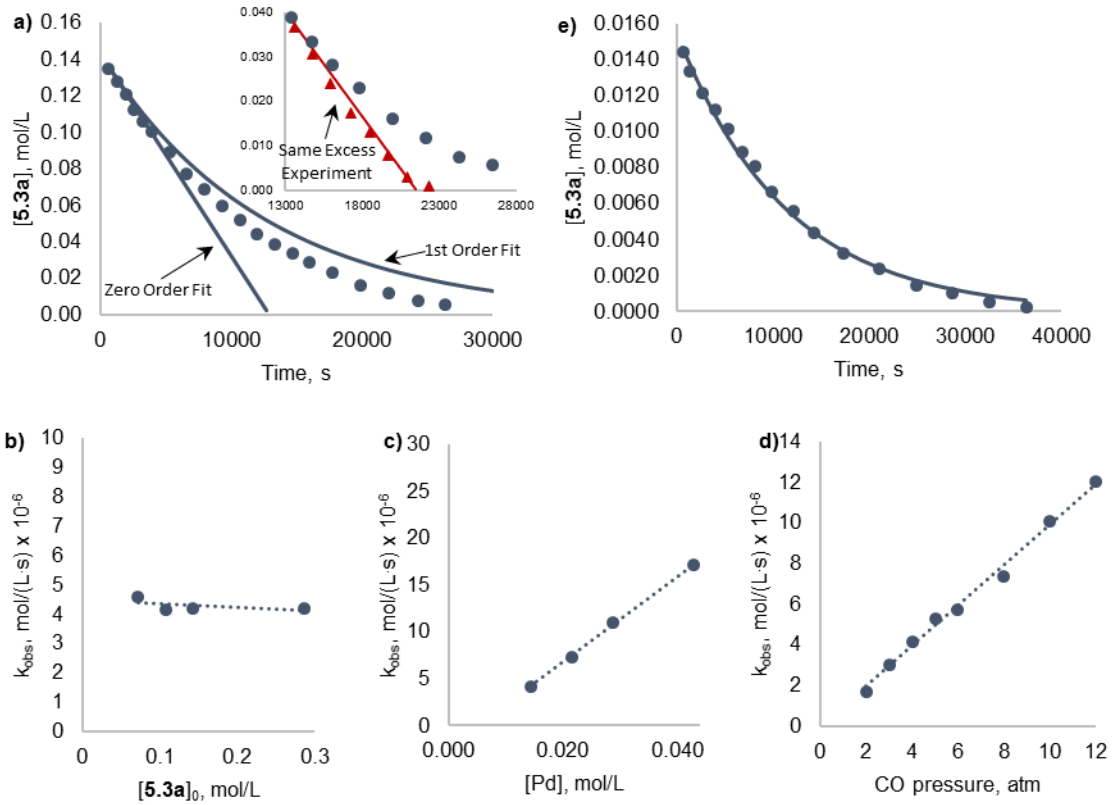

Figure 5.3. Kinetic Analysis of the 5.2a/Bu_4NBr Catalyzed Formation of Münchnone.

(a) Typical plot of the consumption of **5.3a** vs. time for the reaction of benzoyl chloride (21 mg, 0.15 mmol), (*p*-Tol)HC=NBn (21 mg, 0.10 mmol), [Pd(Cl)[κ^2-CH(*p*-Tol)NBn(COPh)]$_2$ **5.2a** (4.5 mg, 0.005 mmol), Bu_4NBr (32 mg, 0.1mmol), EtN^iPr_2 (64 mg, 0.5 mmol), 4 atm CO in 0.7 mL CD_3CN at 65°C. (b) Initial rate dependence on **5.3a** concentration. (c) Rate dependence on catalyst loading. (d) Rate dependence on CO pressure. (e) Typical plot of consumption of **5.3a** vs. time for a 10-fold diluted reaction.

5.3.1.4. Catalyst Resting State.

The observation that *N*-acyl iminium salt oxidative addition to palladium is rate determining, or becomes rate determining, contrasts with our control experiments, which show the rapid, ambient temperature formation of palladacycle **5.2**. However, this comparison is not entirely accurate, as these control experiments were performed with a well-defined Pd_2dba_3, while the Pd(0) generated during catalysis could take a number of forms. In considering potential pathways by which the palladium catalyst may lose reactivity, it is well-established that in the absence of strongly coordinating ligands, palladium(0) can deactivate via the formation of

colloids and subsequently palladium sediments.[17] In addition, bromide salts such as Bu_4NBr employed in catalysis have been demonstrated to facilitate the formation of palladium nanoparticles.[18] Consistent with the slow build-up of a colloidal palladium resting state during catalysis, the loss in catalyst activity as the reaction proceeds correlates with observed decrease of palladacycle complex **5.4a** concentration throughout the course of the reaction (Figure 5.2).

One test for the presence of heterogeneous catalysts involves mercury poisoning,[19] where heterogeneous reactions are more readily deactivated than their homogeneous variants (Scheme 5.6). As anticipated, the addition of metallic mercury to the partially completed catalytic reaction, followed by filtration, completely blocks further Münchnone formation.[20] The palladium catalyst under synthetic reaction conditions therefore appears to be colloidal palladium. These colloids presumably inhibit catalysis relative to well defined Pd(0) complexes (e.g. Pd_2dba_3) by slowing the oxidative addition of iminium salt to generate complex **5.2a** (*vide infra*).

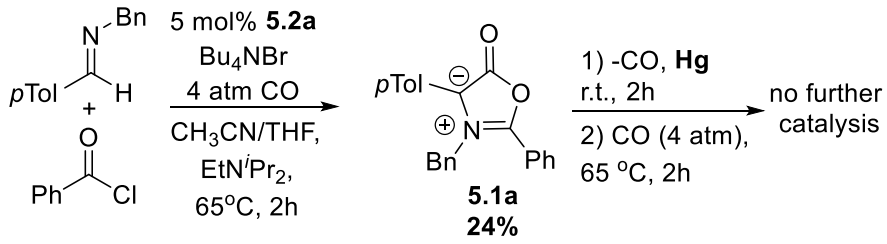

Scheme 5.6. Probe for nanoparticulate palladium with mercury poisoning.

5.3.2. Phosphine Ligands in Münchnone Formation.

We have previously reported that the addition of phosphines to the catalytic formation of Münchnones can influence the rate and scope of catalysis (Table 5.1).[6] In general, it was found that smaller or bidentate phosphines completely block Münchnone formation. Conversely, bulky phosphines such as P(*o*-Tol)$_3$ not only allowed catalysis, but lead to a rate enhancement over that with added Bu_4NBr. The role of phosphines in catalysis has been similarly first examined through stoichiometric experiments.

Table 5.1. Ligand Influence on Münchnone Formation.[a]

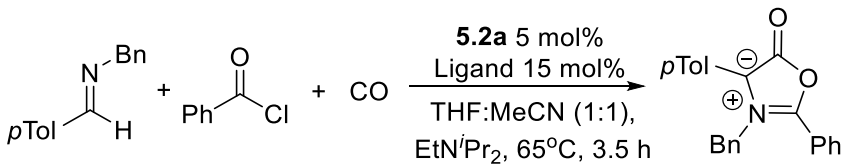

Entry	Ligand	Yield	Entry	Ligand	Yield
1	Bu_4NBr	33 %	5	dppb	0 %
2	PCy_3	0 %	6	P^tBu_3	29 %
3	PPh_3	0 %	7	P(1-naphyl)$_3$	51 %
4	dppe	0 %	8	P(*o*-Tol)$_3$	78 %

[a] Results from reference 6c.

5.3.2.1. Formation of PR_3-Coordinated Intermediates.

Synthesis of (PR$_3$)Pd(Cl)[κ^2-CH(p-Tol)N(Bn)COPh] The potential role of triphenylphosphine in catalysis inhibition was probed by examining its stoichiometric reaction with imine, acid chloride and Pd_2dba_3. As shown in Scheme 5.7, this leads to the rapid formation of the triphenylphosphine complex $(PPh_3)Pd(Cl)[\kappa^2$-CH(*p*-Tol)N(Bn)COPh] **5.6a** as a pale yellow solid in 90% yield. The ^{31}P NMR spectra of **5.6a** shows the presence of a single phosphorus ligand coordinated to palladium (δ 31.1 ppm), while the ^1H-NMR spectrum of **5.6a** reveals a new phosphine-coupled methine resonance at 4.17 ppm (d, $^3J_{P\text{-}H}$ = 4.3 Hz). NOE ^1H NMR studies confirm the *cis* relationship between the phosphine and this methine unit.

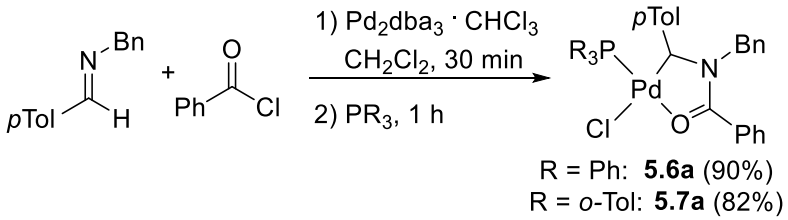

Scheme 5.7. Synthesis of [PR$_3$]Pd(Cl)[κ^2-CH(*p*-Tol)N(Bn)COPh.

The sterically bulky P(*o*-Tol)$_3$ displays similar behavior to PPh_3, with the reaction of imine, acid chloride and Pd_2dba_3, followed by the addition of P(*o*-Tol)$_3$ leading to the analogous formation

of [P(*o*-Tol)$_3$]Pd(Cl)[κ^2-CH(*p*-Tol)N(Bn)COPh] **5.7a**. Crystals of the *N*-4-methoxybenzyl analogue **5.7b** suitable for X-ray diffraction can be grown from CH_2Cl_2 and toluene at –40°C, and the formulation of this complex was confirmed by X-ray crystallography. As shown in Figure 5.4, the palladium center in **5.7b** is approximately square planar (sum of bond angles = 360.6°). The carbonyl bond length in **5.7b** (1.262 (4) Å) is similar to that in **5.2b** (1.264 (7) Å), while the amide C-N bond is slightly longer at 1.324 (4) Å than that in complex **5.2b** (1.312 (8) Å), though still shorter than those found in simple amides.[12] This again suggests significant Pd-O bonding in **5.7b**. In addition, the ∠C-Pd-O bond angle is slightly compressed in **5.7** (81.01°), relative to **5.2b** (83.6°), presumably due to the steric bulk of the phosphine ligand forcing the carbon bound to the palladium closer to the amide oxygen.

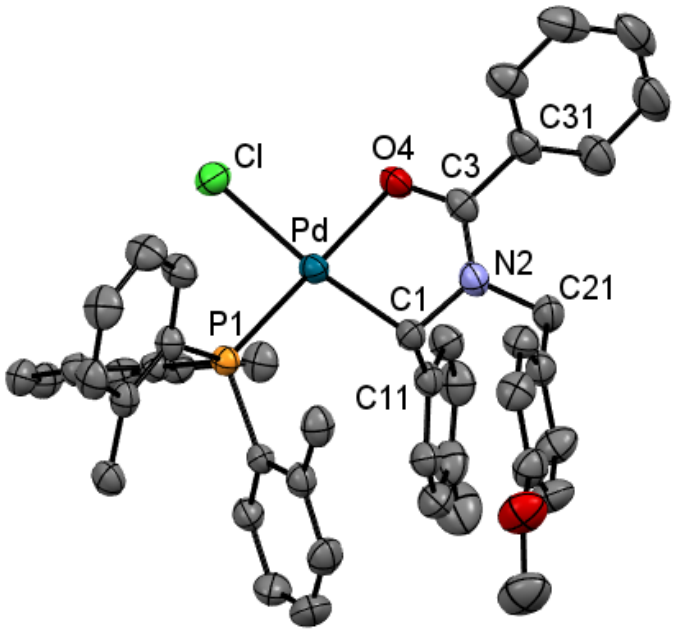

Figure 5.4. X-ray Structure of {[P(*o*-Tol)$_3$]Pd(Cl)[κ^2-CH(*p*-Tol)N(PMB)COPh} 5.7b.

Selected bond lengths (Å) and angles (deg.): Pd-C(1), 2.050(3); Pd-O(4), 2.078(2); Pd-P(1), 2.2563(7); Pd-Cl, 2.4030(8); C(1)-N(2), 1.495(4); N(2)-C(3), 1.324(4); C(3)-O(4), 1.262(4); C(1)-Pd-O(4), 81.01(10); C(1)-Pd-P(1), 98.50(8); O(4)-Pd-P(1), 173.29(6); C(1)-Pd-Cl, 170.36(8); O(4)-Pd-Cl, 91.37(6); P(1)-Pd-Cl, 89.76(3); N(2)-C(1)-C(11), 109.9(2); N(2)-C(1)-Pd, 105.17(19); C(11)-C(1)-Pd, 112.5(2); C(3)-N(2)-C(1), 118.2(3); C(21)-N(2)-C(1), 115.7(2); O(4)-C(3)-N(2), 120.3(3); 117.4(3); C(3)-O(4)-Pd, 112.45(18). Disordered solvent (CH_2Cl_2) and hydrogen atoms are removed for clarity.

*Solution Behavior of **5.6** and **5.7**.* While both PPh_3 and P(*o*-Tol)$_3$ form similar mono-ligated palladium complexes, they display distinct behavior in solution. In contrast to the static PPh_3 complex **5.6a**, the ^{1}H NMR spectrum of the P(*o*-Tol)$_3$ complex **5.7b** in CD_2Cl_2 at 25ºC shows it exists as two isomeric compounds, with two methoxy resonances at (δ 3.83 and 3.75) in a ~7:1 ratio, as well as a broadened methine (δ 3.93) and benzylic (δ 4.47 and 3.62) signals. The ^{31}P NMR spectrum of **5.7b** also has two resonances at δ 25.4 and 32.0 ppm in a ca. 7:1 ratio. In addition, three different *o*-tolyl signals for the phosphine ligand are seen, consistent with restricted rotation about the Pd-P bond. Mild warming of this mixture to 65ºC results in the coalescence of all of these signals (ca. $\Delta G^{\ddagger}$ = 15.5 kcal/mol barrier to exchange).

The existence of rotational isomers of **5.7** presumably results from close contacts between the large P(*o*-Tol)$_3$ ligand (cone angle = 194°) and the chelated amide.[21] We questioned if this steric bulk might lead to a labilization of this phosphine. To test this, the methoxy-labeled phosphine P(*o*-$MeOC_6H_4$)$_3$ was added to **5.7a**. This leads to rapid displacement of P(*o*-Tol)$_3$ at ambient temperature (Scheme 5.8). Notably, no reaction was observed under similar conditions with the PPh_3 coordinated **5.6a**.

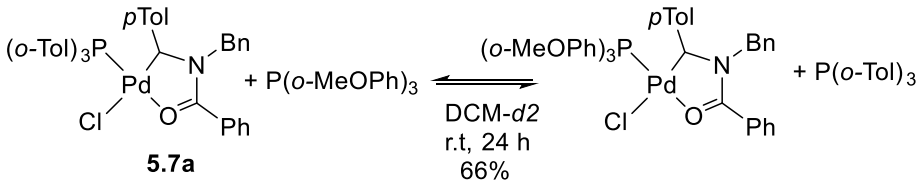

Scheme 5.8. Reaction of 5.7a with P(*o*-$MeOC_6H_4$)$_3$.

Carbonylation of [PR_3]Pd(Cl)[κ^2-CH(p-Tol)N(Bn)COPh] Complexes **5.6a** and **5.7a** also show different reactivity with carbon monoxide. The addition of CO to [PPh_3]Pd(Cl)[κ^2-CH(*p*-Tol)N(Bn)COPh] **5.6a** in CD_2Cl_2 results in no change, even upon prolonged heating at 65ºC. Instead, **5.6a** slowly decomposed with the formation of palladium sediments. The deactivation of catalysis with PPh_3 therefore appears to be due to the inability of palladacycle **5.6a** to undergo carbonylation.

In contrast, the addition of CO to **5.7a** results in its rapid, partial conversion to the CO coordinated complex **5.4a** in (8:1 ratio of **5.7a**: **5.4a**). Excess P(*o*-Tol)$_3$ suppresses this equilibrium, while increased CO pressure favors **5.4a** (Figure 5.5). Varying the CO pressure can allow the determination of the equilibrium constant for this reaction $K_{eq} = 7.3 \pm 0.1 \times 10^{-3}$ (or $\Delta G = 2.9 \pm 0.1$ kcal/mol at 25°C). The equilibrium mixture of **5.7a** and **5.4a** is stable for an hour at ambient temperature. However, mild warming in the presence of amine base leads to the generation of Münchnone in high yield. The rate of this transformation is comparable to that observed in the absence of phosphines (Scheme 5.5). The latter is intriguing, as P(*o*-Tol)$_3$ inhibits the formation of the CO bound complex **5.4a**, and suggests that the phosphine may assist in CO insertion (Step D in Scheme 5.1), much as CO pressure does in the absence of ligands.

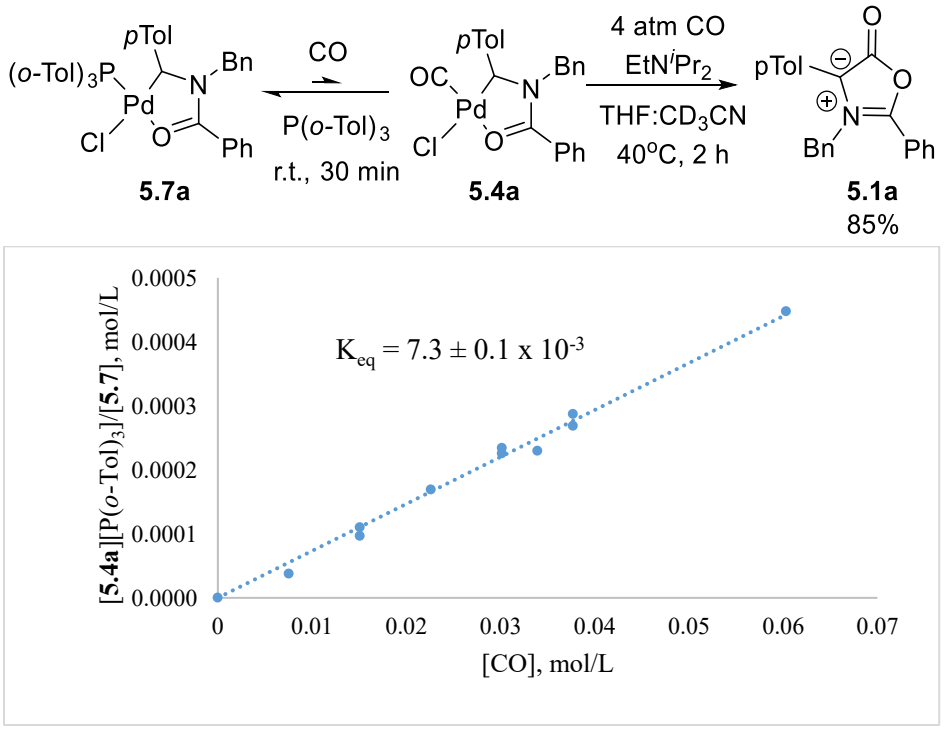

Figure 5.5. Reaction of 5.7a with CO and Münchnone formation.

5.3.2.2. Kinetics of Münchnone Formation with P(*o*-Tol)$_3$.

The facile generation of the P(*o*-Tol)$_3$ coordinated palladacycle **5.7** suggests that the oxidative addition to *N*-acyl iminium salt is not the rate determining step in catalysis. Consistent

with this analysis, kinetic studies on the catalytic reaction shows the clean, zero-order disappearance of *N*-acyl iminium salt **5.3a** (Figure 5.6a). As expected from the equilibrium displacement of P(*o*-Tol)$_3$ (Figure 5.5), the reaction shows first order rate dependence on CO pressure (Figure 5.6d), and is inhibited by added P(*o*-Tol)$_3$ (Figure 5.6c). Together, these suggest that the conversion of palladacycle **5.7** to Münchnone, via the intermediate formation of the CO-coordinated **5.4**, is the rate determining step in catalysis.

An interesting outcome of these kinetics is that the observed rate constant for the reaction with P(*o*-Tol)$_3$ (k_{obs} = 5.1 ± 0.3 x 10^{-6} M·s^{-1}) is similar to the initial rate noted with Bu$_4$NBr (k_{obs} = 4.1 ± 0.4 x 10^{-6} M·s^{-1}, Figure 5.3a). A difference is in the kinetic profile of these reactions, where we see no deviation from zero-order kinetic behavior with P(*o*-Tol)$_3$ (Figure 5.6a). Similarly, *in situ* ^{1}H and ^{31}P NMR analysis clearly shows the presence of the P(*o*-Tol)$_3$-coordinated **5.7** throughout the course of the catalytic reaction (Figure 5.16). This data contrasts with the rapid loss of palladacycle **5.4** as the catalyst resting state with Bu$_4$NBr, and the slowing of catalysis as the reaction proceeds. The ability of P(*o*-Tol)$_3$ to retain catalyst activity throughout the reaction becomes important at the more dilute concentrations typically employed in synthesis. As shown in Figure 5.6e, kinetic analysis at synthetically relevant concentrations (10-fold dilution) shows the rapid, zero order disappearance of **5.3a** is retained in the presence of P(*o*-Tol)$_3$. Thus, even at low concentrations, the oxidative addition of *N*-acyl iminium salt **5.3a** is rapid. The overall effect is a transformation that under synthetic conditions proceeds to completion nearly 3.5 times faster with P(*o*-Tol)$_3$ than with Bu$_4$NBr.

In the case of Bu$_4$NBr stabilized catalysis, the loss of catalyst activity as the reaction proceeds was attributed to the build-up of nanoparticulate palladium (Scheme 5.6). This does not appear to be the case with P(*o*-Tol)$_3$. The addition of metallic mercury to the partially completed catalytic reaction, followed by celite filtration, does not inhibit Münchnone formation, and catalysis proceeds at a similar rate to that observed prior to Hg (Scheme 5.9). Together, these data indicate that the main rate influence of P(*o*-Tol)$_3$ is to retain the palladium in its palladacyclic form **5.7** for rate determining conversion of product.

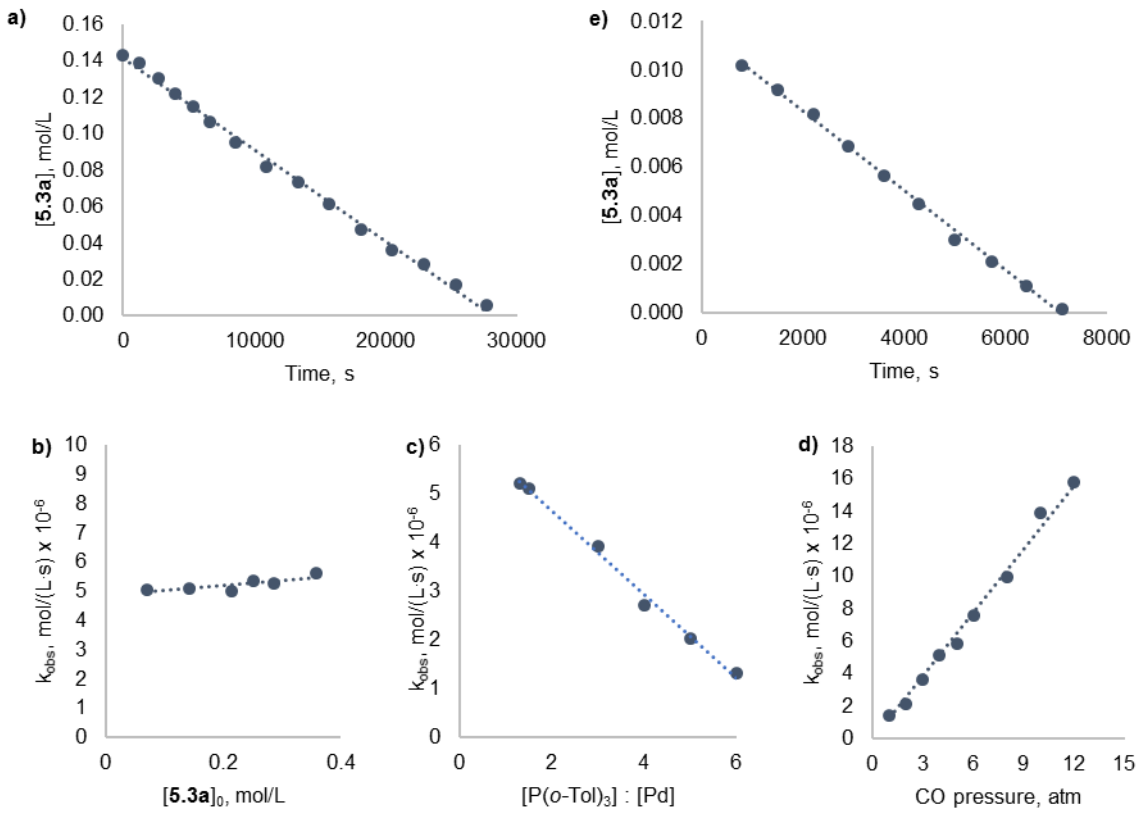

Figure 5.6. Kinetic Analysis of the 5.2a/P(*o*-Tol)$_3$ Catalyzed Formation of Münchnone.

(a) Typical plot of **5.3a** vs. time for the reaction of benzoyl chloride (21 mg, 0.15 mmol), (*p*-Tol)HC=NBn (21 mg, 0.10 mmol), [Pd(Cl)[κ^2-CH(*p*-Tol)NBn(COPh)]$_2$ **5.2a** (4.5 mg, 0.005 mmol), P(*o*-Tol)$_3$ (4.5 mg, 0.015mmol), EtN^{i}Pr$_2$ (64 mg, 0.5 mmol), 4 atm CO in CD_3CN:THF (1:1, 0.7 mL) at 65ºC. (b) Initial rate dependence on **5.3a** concentration. (c) Initial rate dependence on palladium catalyst : ligand ratio. (d) Rate dependence on CO pressure. (e) typical plot of **5.3a** vs. time for the reaction catalytic reaction of Münchnone formation at 10 fold dilution (note: 0.004 mM imine is not converted to iminium salt **5.3a** at these dilute conditions, and not considered in the plot).

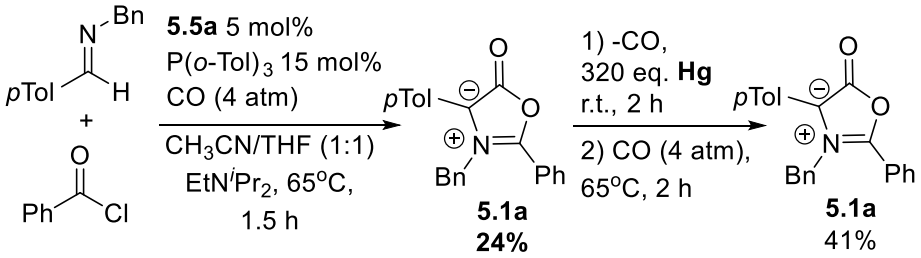

Scheme 5.9. Probe for heterogeneous processes with mercury poisoning.

5.3.2.3. Mechanistic Analysis

The above data demonstrate that the mechanism by which imine, acid chloride and carbon monoxide are coupled involves multiple reaction steps, several of which appear to be in equilibrium under catalysis conditions. The relative rates of each of these steps are well-suited to lead to selective Münchnone formation. Firstly, imine and acid chloride undergo a reaction to generate *N*-acyl iminium salt precursor **5.3** within minutes under the reaction conditions. This results in the constant presence of **5.3** during catalysis to undergo oxidative addition to palladium. The rapid formation of *N*-acyl iminium salt is important, since the acid chloride itself could undergo oxidative addition to palladium, as could functionalized substituents (e.g. aryl-halides) on the imine or acid chloride. This data provides a rationale for certain scope limitations in this reaction, where non-nucleophilic or enolizable imines are not viable substrates, as these cannot generate high concentrations of **5.3** that are sufficiently stable to exist throughout the course of catalysis.[6] Once complex **5.2** is generated, the only other reagents in solution are labile ligands (e.g. Br^-, EtN^iPr_2, P(*o*-Tol)$_3$), which can be readily displaced by CO to allow for both carbon monoxide coordination, and the subsequent carbonylation steps to occur.

Our initial catalyst for Münchnone formation, $[Pd(Cl)[\kappa^2\text{-}CH(R^2)NR^1(COR^3)]_2$, was designed based upon the postulate that the oxidative addition of the *N*-acyl iminium salt to Pd(0) was rapid and the subsequent carbonylation steps were rate limiting.[6b] It instead appears that **5.3** oxidative addition to palladium becomes significantly slowed in the absence of coordinating ligands. This can be attributed to the generation of colloidal palladium. The influence of palladium colloids on catalysis is most pronounced under the dilute conditions of synthesis, where the bimolecular oxidative addition of **5.3** to palladium is presumably slowed. The

formation of palladium colloids also provides a rationale for the required use of additives such as Bu_4NBr in catalysis, since unligated palladium in the absence of stabilizing halide sources can readily form inactive palladium precipitates.

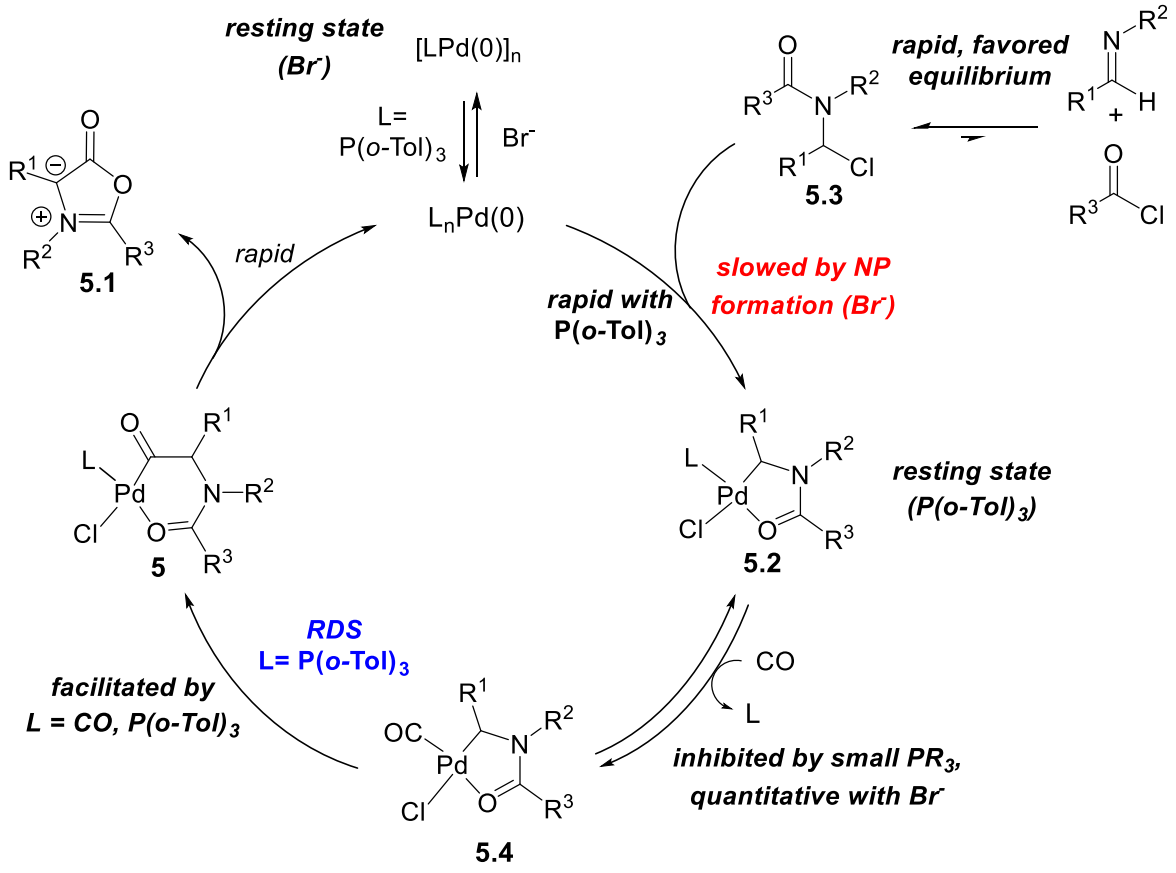

Scheme 5.10. Combined mechanism for the palladium catalyzed formation of Münchnones.

Based upon these results, we can formulate a reasonable rationale for the accelerating influence of P(*o*-Tol)$_3$ on catalysis. Firstly, the lability of this phosphine ligand is critical for the catalytic formation of Münchnones by providing access to CO coordinated intermediates such as **5.4**. This can be clearly seen by comparison to smaller phosphines such as PPh_3 (e.g. complex **5.6**), which show no evidence for either displacement by CO or subsequent insertion. The

lability of P(*o*-Tol)$_3$ is presumably a product of its steric bulk, and supported by reactivity data on [P(*o*-Tol)$_3$]Pd(Cl)[κ^2-CH(*p*-Tol)N(PMB)COPh], which shows rapid phosphine displacement at moderate temperatures. While access to the CO coordinated adduct **5.4** is less facile than without phosphines, this inhibition is partially offset by the ability of this ligand to facilitate subsequent steps in the catalysis.

Instead, the major influence of P(*o*-Tol)$_3$ is to retain the monometallic, phosphine-coordinated complex **5.2** as the catalyst resting state throughout the course of the reaction, rather than allowing the build-up of less active palladium colloids. This, combined with the lability of the phosphine in the presence of CO, translates into much higher rates of catalysis at synthetically relevant conditions where *N*-acyl iminium salt concentrations are typically low. The combined mechanistic data is summarized in Scheme 5.10.

5.3.3. New Catalyst

As a final test for this mechanistic postulate, and the importance of phosphine lability for catalytic activity, we have preliminarily examined the ability of other phosphines to allow catalytic Münchnone formation. For example, while steric encumbrance is one method to promote ligand loss, we postulated that similar influences might also be seen with phosphines of diminished donor ability. Indeed, after probing several different triarylphosphines, we have found that the electron deficient P(C$_6$F$_5$)$_3$ can also allow catalytic Münchnone formation (Scheme 5.11). Kinetic analysis shows that this catalyst once again proceeds with a zero-order loss of *N*-acyl iminium salt, suggesting that iminium salt oxidative addition is also rapid. Interestingly, the catalyst generated with P(C$_6$F$_5$)$_3$ is more active (k_{obs} = 7.4±0.3 x 10^{-6} M·s^{-1}) than that we have previously noted with P(*o*-Tol)$_3$ (k_{obs} = 5.1±0.3 x 10^{-6} M·s^{-1}). As the cone angle of P(C$_6$F$_5$)$_3$ is smaller than that of P(*o*-Tol)$_3$,[21] the activity of the perfluorinated phosphine is presumably related to its reduced donor ability, which can similarly favor CO substitution in palladacycle **5.2** and subsequent carbonylation.

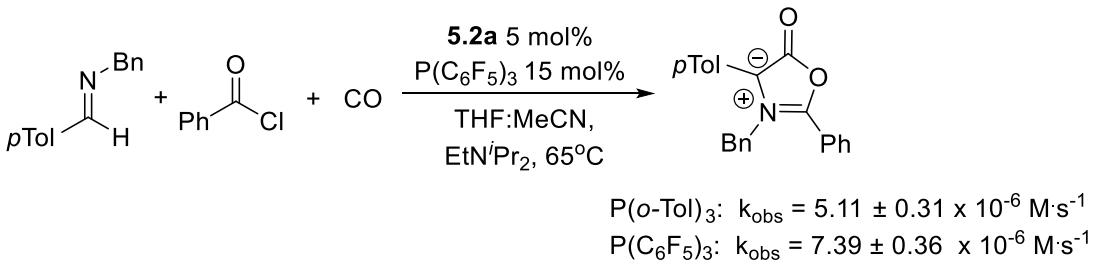

Scheme 5.11. Palladium catalyzed Münchnone formation with $P(C_6F_5)_3$ as ligand.

5.4. Conclusions

In summary, these studies have demonstrated the importance of finely balancing multiple steps in the palladium catalyzed multicomponent synthesis of Münchnones, including *N*-acyl iminium salt formation, Pd(0) stabilization, oxidative addition, ligand labilization and carbonylation. Each of these are critical for achieving efficient catalysis, and under optimal conditions can allow the selective cascade of catalytic steps to proceed with high selectivity. From a catalysis perspective, ligands designed to not only stabilize the palladium center from colloid formation, but also undergo ready labilization for carbon monoxide coordination, are important for catalysis. These features are presumably similar to those noted in aldehyde amidocarbonylation, and suggest at least some of these factors and intermediates are relevant for catalyst development and scope limitations in these transformations. Further studies aimed at exploiting these observations to generate more active carbonylation catalysts are in progress.

5.5. Supplementary Information

5.5.1. General Considerations

All reactions were carried out under an inert atmosphere in a glovebox or using standard Schlenk techniques, unless otherwise indicated. Research grade carbon monoxide (99.99%) was used as received. All solvents were dried with using a solvent purification system and stored in glovebox over activated 4 Å molecular sieves. Deuterated solvents were dried over CaH_2, vacuum transferred and stored over 4 Å molecular sieves. Tetrabutylammonium bromide

(Bu_4NBr) was dried in the glovebox by dissolving in dichloromethane, allowing it to stand overnight over activated 4 Å molecule sieves, then filtering and removing the solvent *in vacuo*. $Pd_2dba_3{\cdot}CHCl_3$ was prepared according to literature procedures and stored at -35 °C in the glovebox to avoid decomposition.[22] Imines were prepared according to literature procedures.[23] All other reagents were purchased from commercial suppliers and used as received. CO solution concentrations were determined by ^{13}C NMR analysis relative to a benzyl benzoate internal standard, with relaxation delays to compensate for differing T_1 values, based on literature precedent.[24] All ^{1}H, ^{31}P and ^{13}C NMR spectra were acquired on 400 and 500 MHz spectrometers. High resolution mass spectra were obtained using a quadrupole-time of flight and an orbitrap detector by direct infusion in positive ESI mode.

5.5.2. Generation and Characterization of Intermediates

Generation of N-acyl iminium salt 5.3a (Scheme 5.2)

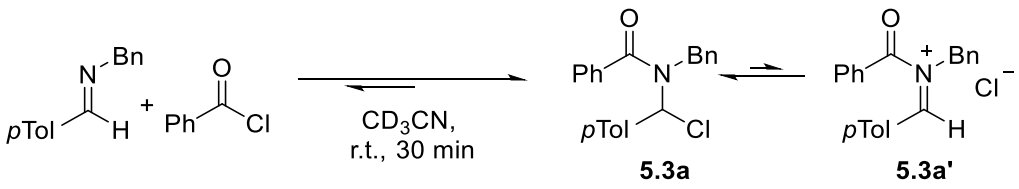

In a glovebox, (*p*-Tol)HC=NBn (11 mg, 0.05 mmol), benzoyl chloride (8 mg, 0.055 mmol), and benzyl benzoate internal standard were mixed in CD_3CN (1.4 mL). After 30 minutes, *in situ* ^{1}H NMR analysis shows the generation of **5.3a** in 91% yield together with unreacted imine and acid chloride. Monitoring the reaction over time shows no change in this ratio.

Isolation and characterization of 5.3a

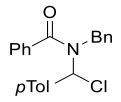

5.3a

In a glovebox, *p*-Tol(H)C=NBn (209 mg, 1.00 mmol), benzoyl chloride (140 mg, 1.00 mmol) were stirred in MeCN (5 mL) for 1 h. The solvent was evaporated and the obtained residue was washed with pentane (3 x 5 mL) to afford **5.3a** as a white solid in 95% yield.

^{1}H NMR (500 MHz, CD_3CN) δ 7.62 (d, *J* = 6.5 Hz, 2H), 7.56 – 7.49 (m, 3H), 7.44 (d, *J* = 8.2 Hz, 2H), 7.33 (s, 1H), 7.22 – 7.14 (m, 5H), 7.07 (d, *J* = 6.9 Hz, 2H), 4.57 (s, 2H), 2.32 (s, 3H). ^{13}C NMR (126 MHz, CD_3CN) δ 172.3, 139.2, 137.6, 135.3, 133.7, 130.4, 129.0, 128.9, 128.0, 127.5, 127.1, 126.7, 126.6, 78.0, 46.2, 20.1. HRMS. Calculated for $C_{22}H_{20}NO$ ($M\text{-}Cl^+$): 314.1539, found: 314.1539.

K_{eq} determination for 5.3a formation

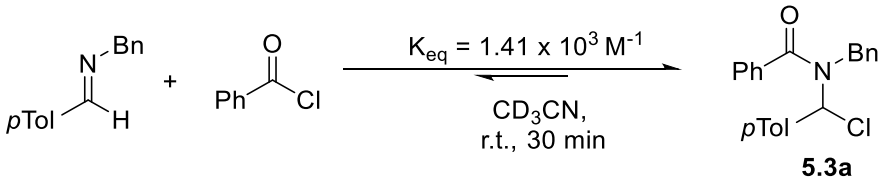

5.3a

In a glovebox, **5.3a** (12 mg, 0.035 mmol) and benzyl benzoate internal standard were combined in varying amounts of CD_3CN (0.7 mL, 1.0 mL 1.2 mL, 1.5 mL, 1.8 mL) and allowed to equilibrate for 30 min. *In situ* ^{1}H NMR analysis was used to determine the ratio of **5.3a** to imine/acid chloride at each concentration (see plot below). From this, K_{eq} was determined to be $1.41 \pm 0.02 \times 10^3\ M^{-1}$.

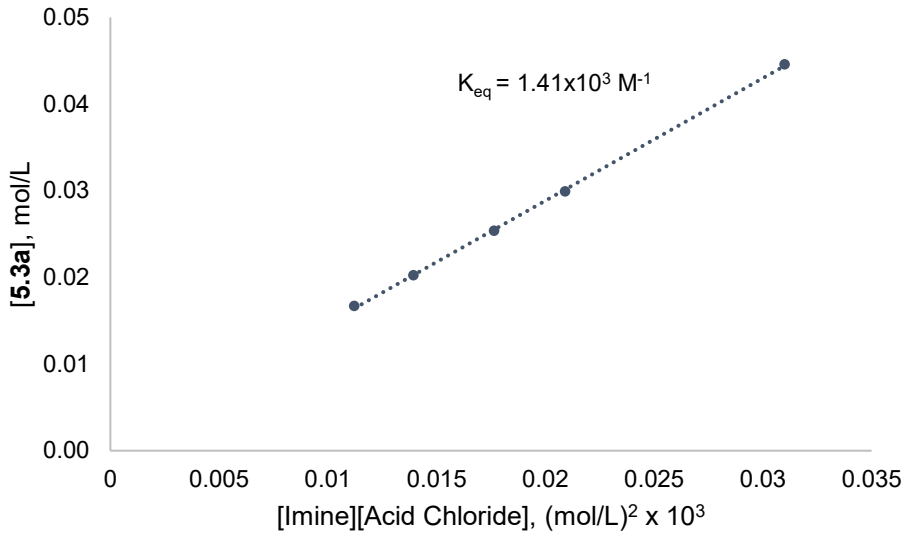

Figure 5.7. Plot of [Imine][Acid Chloride] vs [5.3a], the slope of the graph represents K_{eq}.

Synthesis of {Pd[κ²-C(p-Tol)HN(Bn)COPh]}₂ 5.2a (Scheme 5.3)

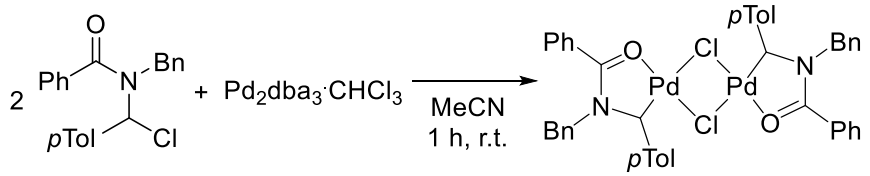

5.3a **5.2a**

In a glovebox, *p*-Tol(H)C=N(Bn) (209 mg, 1.00 mmol) and PhCOCl (154 mg, 1.10 mmol) were combined in MeCN (10 mL) and stirred for 15 min. This solution was added to $Pd_2(dba)_3{\cdot}CHCl_3$ (518 mg, 0.5 mmol) in CH_3CN (10 mL) and stirred for 1 hour at room temperature. The solution was subsequently filtered through celite and the solvent was removed *in vacuo* to provide a yellow residue. This residue was washed with diethyl ether (4 x 10 mL) to afford the product **5.2a** as a yellow solid in 82% yield.

^{1}H NMR (500 MHz, 60ºC, CD_3CN) δ 7.80 – 7.73 (m, 1H), 7.63 (dd, *J* = 9.1, 7.5 Hz, 2H), 7.56 (t, *J* = 7.4 Hz, 2H), 7.48 (dd, *J* = 5.1, 1.9 Hz, 1H), 7.41 – 7.35 (m, 2H), 7.21 (d, *J* = 8.0 Hz, 2H), 7.14 (d, *J* = 7.9 Hz, 2H), 7.09 (d, *J* = 6.6 Hz, 2H), 5.21 (s, 1H), 4.55 (d, *J* = 15.7 Hz, 1H), 3.98 (d, *J* = 15.5 Hz, 1H), 2.27 (s, 3H). ^{13}C NMR (126 MHz, CD_3CN) δ 180.3, 142.6, 139.3, 135.8, 134.7, 131.4, 130.5, 129.4, 129.0, 128.9, 127.6, 127.5, 126.1, 59.6, 52.2, 20.4. FT-IR-ATR (cm^{-1}): 1584.6 (C=O). HRMS. Calculated for $C_{44}H_{40}Cl_2N_2O_2Pd_2Na$ ($M+Na^+$): 933.0458, found: 933.0429.

Synthesis of {Pd[κ²-C(p-Tol)HN(p-CH₃OC₆H₄CH₂)COPh]}₂ 5.2b

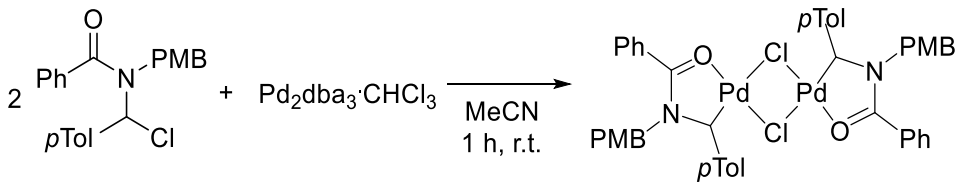

5.3b **5.2b**

In a glovebox, *p*-Tol(H)C=N(*p*-$CH_3OC_6H_4CH_2$) (239 mg, 1.00 mmol) and PhCOCl (154 mg, 1.10 mmol) were combined in MeCN (10 mL) and stirred for 15 min. This solution was added to $Pd_2(dba)_3{\cdot}CHCl_3$ (518 mg, 0.5 mmol) in CH_3CN (10 mL) and stirred for 1 hour at room

temperature. The resulting solution was filtered through celite and the solvent was removed *in vacuo* to provide a yellow residue. This residue was washed with diethyl ether (4 x 10 mL) to afford the product **5.2b** as a pale orange solid in 80% yield. Recrystallization from toluene at –40ºC provided complex **5.2b** as orange crystals for crystallographic analysis.

^{1}H NMR (400 MHz, CD_2Cl_2) δ 7.61 (m, 3H), 7.56 (d, *J* = 6.9 Hz, 2H), 7.20 (bs, 4H), 6.91 (bs, 4H), 5.39 (s, 1H), 4.51 (d, *J* = 15.0 Hz, 1H), 3.96 (d, *J* = 15.0 Hz, 1H), 3.84 (s, 3H), 2.30 (s, 3H). ^{13}C NMR (126 MHz, CD_2Cl_2) δ 179.8, 159.6, 138.9, 138.4, 136.3, 131.9, 131.4, 129.9, 129.1, 128.9, 127.6, 125.7, 114.2, 60.3, 55.2, 51.6, 21.2. FT-IR-ATR (cm^{-1}): 1543.5 (C=O). HRMS. Calculated for $C_{46}H_{44}N_2O_2Pd_2Cl_2Na$ ($M+Na^+$): 995.0644, found: 995.0637.

In Situ Generation of [Pd(Cl)(CO)[κ^2-CH(Tol)NBn(COPh)] 5.4a (Scheme 5.4)

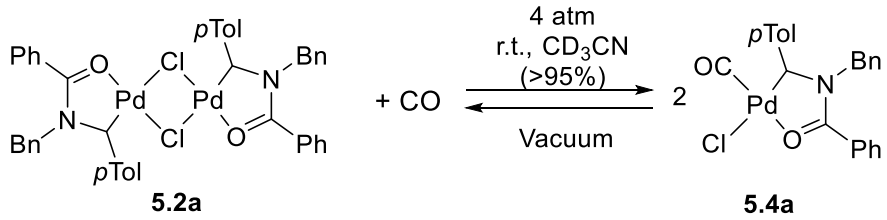

In a glovebox, {Pd(Cl)[κ^2-CH(*p*-Tol)N(Bn)COPh]}$_2$ **5.2a** (4.5 mg, 0.005 mmol) was dissolved in CD_3CN (0.7 mL) and transferred into a J-Young NMR tube. The NMR tube was brought outside of glovebox and pressurized with 4 atm CO. ^{1}H and ^{13}C NMR analysis of reaction mixture showed quantitative conversion to complex **5.4a**. The removal of CO shows reverse generation of **5.2a**.

In situ ^{1}H NMR (500 MHz, CD_3CN) δ 7.73 – 7.69 (m, 2H), 7.66 (d, *J* = 7.4 Hz, 1H), 7.59 (t, *J* = 7.5 Hz, 2H), 7.38 (m, 3H), 7.30 – 7.21 (m, 4H), 7.12 – 7.08 (m, 2H), 6.03 (s, 1H), 4.76 (d, *J* = 15.7 Hz, 1H), 4.12 (d, *J* = 15.7 Hz, 1H), 2.35 (s, 3H). *In situ* ^{13}C NMR (126 MHz, CD_3CN) δ 184.2, 181.9, 142.6, 137.6, 137.2, 133.7, 132.1, 130.4, 129.1, 128.9, 128.4, 128.3, 127.8, 125.6, 69.1, 53.1, 20.3. IR (MeCN): 2114 cm^{-1}.

***Münchnone generation from* [*Pd(Cl)(CO)[κ²-CH(p-Tol)NBn(COPh)]* 5.2a (Scheme 5.5)**

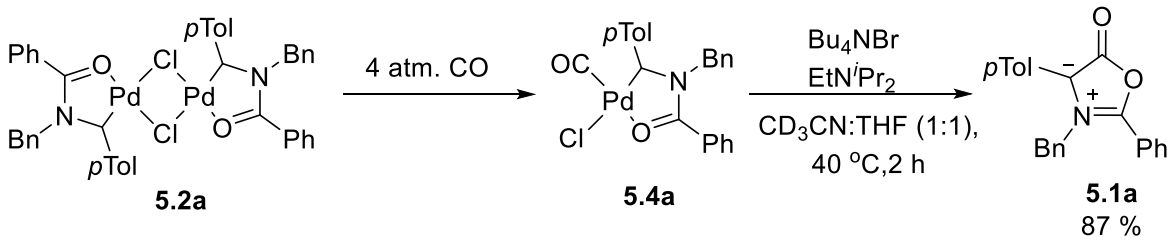

In a glovebox, {Pd(Cl)[κ²-CH(*p*-Tol)N(Bn)COPh]}$_2$ **5.2a** (4.5 mg, 0.005 mmol), EtN^iPr_2 (2.6 mg, 0.02 mmol) and benzyl benzoate internal standard were mixed in CD_3CN : THF (1:1, 0.7 mL) and transferred into a J-Young NMR tube. The NMR tube was brought outside of glovebox, pressurized with 4 atm CO, and heated at 40°C for 1 h. ^{1}H NMR analysis shows the degradation of **5.2a** to form imine (27% yield) and **5.3a** (39% yield).

The analogous experiment was performed in the presence of Bu_4NBr. In a glovebox, {Pd(Cl)[κ²-CH(*p*-Tol)N(Bn)COPh]}$_2$ **5.2a** (4.5 mg, 0.005 mmol), Bu_4NBr (3.2 mg, 0.01 mmol), EtN^iPr_2 (2.6 mg, 0.02 mmol) and benzyl benzoate internal standard were mixed in CD_3CN : THF (1:1, 0.7 mL) and transferred into a J-Young NMR tube. The NMR tube was brought outside of glovebox, pressurized with 4 atm CO, and heated at 40°C for 2 h. The reaction progress was followed by ^{1}H NMR analysis and showed generation of **5.1a** in 87% yield.[5c]

Monitoring the catalytic formation of Münchnone by ^{1}H NMR analysis (Figure 5.2)

In a glovebox, *p*-Tol(H)C=NBn (21 mg, 0.10 mmol), PhCOCl (21 mg, 0.15 mmol), EtN^iPr_2 (64 mg, 0.50 mmol), Bu_4NBr (32 mg, 0.10 mmol), [Pd(Cl)[κ²-CH(*p*-Tol)NBn(COPh)]$_2$ (4.5 mg, 0.005 mmol), and benzyl benzoate internal standard were combined in CD_3CN : THF (0.7 mL, 1:1) and transferred into a J-Young NMR tube. The tube was brought outside of the glovebox, the solution frozen, and 4 atm CO was condensed into the NMR tube. The NMR tube was heated at 65°C in an oil bath. Low temperature ^{1}H NMR (-10°C) was taken at 5 min, 3 h, 8h reaction times.

Mercury poisoning of catalysis with {Pd(Cl)[κ²-CH(p-Tol)N(Bn)COPh]}₂ 5.2a /Bu₄NBr (Scheme 5.6)

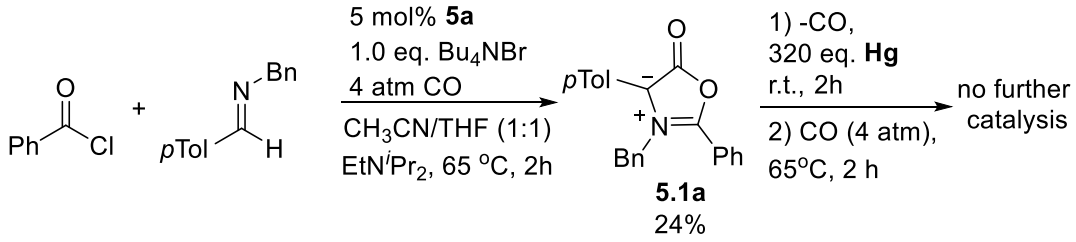

p-Tol(H)C=NBn (210 mg, 1.0 mmol), PhCOCl (210 mg, 1.5 mmol) and benzyl benzoate internal standard were dissolved in CH_3CN (2.5 mL) and stirred for 15 min. To this solution was added a solution of {Pd(Cl)[κ²-CH(*p*-Tol)NBnCOPh]}₂ **5.2a** (45 mg, 0.05 mmol), and Bu_4NBr (320 mg, 1.0 mmol) in CH_3CN (2.5 mL). The reaction mixture and NEt^iPr_2 (160 mg, 0.12 mmol) in THF (5 mL) was transferred to a 50 mL pressure vessel. The solution was degassed and 4 atm CO was added to the reaction mixture. The reaction mixture was stirred at 65°C for 2 hours. ^{1}H-NMR analysis showed generation of Münchnone **5.1a** in 24% yield. After degassing, the solution was vigorously stirred in the presence of mercury (8.7 g, 42.6 mmol) over a 2-hour period. After celite filtration, the solution was transferred back into the pressure vessel, pressurized with 4 atm CO, heated at 65°C for another 2 hours. ^{1}H-NMR analysis showed generation of Münchnone **5.1a** remained at 24% yield.

Synthesis of {[PPh₃]Pd(Cl)[κ²-CH(p-Tol)N(Bn)COPh} 5.6a (Scheme 5.7)

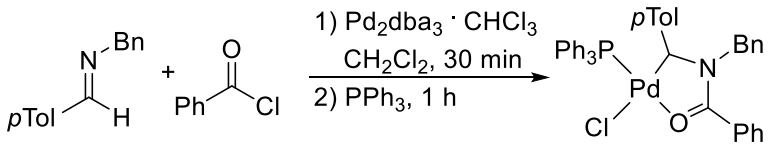

In a glovebox, *p*-Tol(H)C=N(Bn) (109 mg, 0.50 mmol) and PhCOCl (77 mg, 0.55 mmol) in dichloromethane (5 mL) were stirred for 15 min. To this solution $Pd_2(dba)_3{\cdot}CHCl_3$ (258 mg, 0.25 mmol) in dichloromethane (10 mL) was added and allowed to stir for 15 min. PPh_3 (131 mg, 0.5

mmol) was then added and the resulting mixture was stirred for 1 hour. The solution was then filtered through celite and solvent was removed *in vacuo.* The solid residue was washed with ether (4 x 5 mL), which resulted in the isolation of **5.6a** in 90% yield as a white grey solid.

^{1}H NMR (500 MHz, CD_3CN) δ 7.67 – 7.60 (m, 3H), 7.57 (dd, *J* = 7.9, 6.5 Hz, 2H), 7.48 – 7.40 (m, 6H), 7.30 – 7.23 (m, 12H), 7.14 (dd, *J* = 6.6, 2.6 Hz, 2H), 6.97 (d, *J* = 7.8 Hz, 2H), 6.24 (d, *J* = 7.8 Hz, 2H), 4.58 (d, *J* = 15.5 Hz, 1H), 4.16 (d, *J* = 4.3 Hz, 1H), 3.77 (d, *J* = 15.5 Hz, 1H), 2.31 (s, 3H). ^{13}C NMR (126 MHz, CD_3CN) δ 179.7, 138.8, 136.0, 135.2, 134.5 (d, *J* = 11.2 Hz), 133.6 (d, *J* = 184.7 Hz), 131.2, 130.6, 130.5, 129.1, 128.94, 128.90, 128.1, 128.0, 127.3, 126.9 (d, *J* = 148.7 Hz), 69.2, 52.8 (d, *J* = 3.6 Hz), 20.1. ^{31}P NMR (162 MHz, CD_3CN) δ 31.1. FT-IR-ATR (cm^{-1}): 1543.0 (C=O). HRMS. Calculated for $C_{40}H_{35}NOPPd$ ($M\text{-}Cl^{+}$): 682.1486, found: 682.1493.

Synthesis of {[P(o-Tol)$_3$]Pd(Cl)[κ^2-CH(p-Tol)N(Bn)COPh} 5.7a (Scheme 5.7)

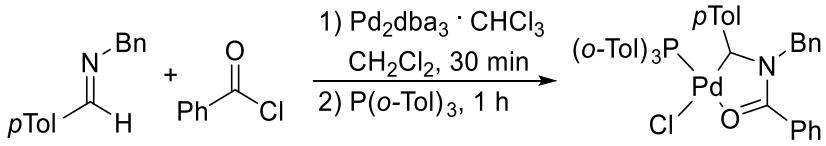

In a glovebox, *p*-Tol(H)C=N(Bn) (109 mg, 0.50 mmol) and PhCOCl (77 mg, 0.55 mmol) in dichloromethane (5 mL) were stirred for 15 min. To this solution $Pd_2(dba)_3{\cdot}CHCl_3$ (258 mg, 0.25 mmol) in dichloromethane (10 mL) was added and allowed to stir for 15 min. P(*o*-Tol)$_3$ (152 mg, 0.5 mmol) was then added and the resulting mixture was stirred for 1 hour. The solution was then filtered through celite and solvent was removed *in vacuo.* The solid residue was washed with ether (4 x 5 mL), which resulted in the isolation of **5.7a** in 82% yield as a pale yellow solid.

^{1}H NMR (500 MHz, CD_2Cl_2, -10°C) δ 9.44 (dd, *J* = 17.2, 7.3 Hz, 1H), 7.68 (d, *J* = 6.7 Hz, 2H), 7.48 (m, 7H), 7.33 (d, *J* = 18.6 Hz, 4H), 7.20 (s, 3H), 7.17 – 7.09 (m, 2H), 7.05 (d, *J* = 18.0 Hz, 3H), 6.98 (d, *J* = 11.6 Hz, 1H), 6.91 (s, 1H), 6.83 – 6.69 (m, 1H), 6.51 (s, 1H), 4.53 (d, *J* = 14.9 Hz, 1H), 4.36 (s, 1H), 3.65 (dd, *J* = 8.8, 5.7 Hz, 1H), 2.25 (s, 3H), 1.95 (s, 3H), 1.47 (s, 3H), 1.11 (s, 3H). ^{13}C NMR (126 MHz, CD_2Cl_2, 65°C) δ 179.2, 142.7, 140.0, 135.8, 135.3, 133.0, 131.5, 130.8, 130.2, 129.0, 128.8, 128.7, 128.2, 128.0, 127.5, 126.8, 126.4, 125.6, 125.1, 68.9, 52.8,

22.6, 20.7. ^{31}P NMR (162 MHz, CD_2Cl_2) δ 25.19. FT-IR-ATR (cm^{-1}): 1546.3 (C=O). HRMS. Calculated for $C_{43}H_{41}NOPPd$ ($M\text{-}Cl^+$): 724.1955, found: 724.1981.

Synthesis of {[P(o-Tol)$_3$]Pd(Cl)[κ^2-CH(p-Tol)N(p-CH$_3$OC$_6$H$_4$CH$_2$)COPh} 5.7b

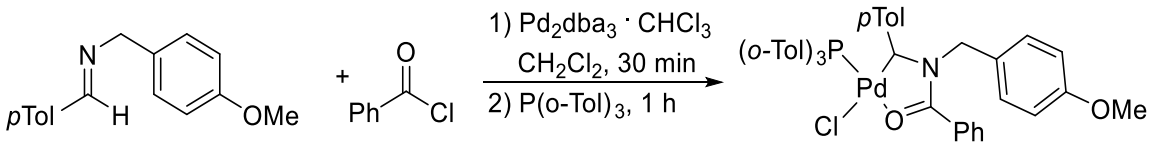

In a glovebox, *p*-Tol(H)C=N(*p*-$CH_3OC_6H_4CH_2$) (120 mg, 0.50 mmol) and PhCOCl (77 mg, 0.55 mmol) in dichloromethane (5 mL) were stirred for 15 min. To this solution $Pd_2(dba)_3{\cdot}CHCl_3$ (258 mg, 0.25 mmol) in dichloromethane (10 mL) was added and allowed to stir for 15 min. P(*o*-Tol)$_3$ (152 mg, 0.5mmol) was then added, and the resulting mixture was allowed to stir for 1 hour. The solution was then filtered through celite and solvent was removed *in vacuo.* The solid residue was washed with ether (4 x 5 mL), which resulted in the isolation of **5.7b** in 80% yield as a pale yellow solid. Recrystallization from dichloromethane at –40ºC provided complex **5.7b** as yellow crystals for crystallographic analysis.

^{1}H NMR (500 MHz, CD_2Cl_2, -10°C) δ 9.50 – 9.31 (m, 1H), 7.67 (d, *J* = 6.6 Hz, 2H), 7.58 – 7.41 (m, 7H), 7.31 (t, *J* = 7.5 Hz, 1H), 7.23 – 7.07 (m, 5H), 7.02 (d, *J* = 7.0 Hz, 1H), 6.95 (d, *J* = 8.3 Hz, 4H), 6.87 (d, *J* = 8.6 Hz, 2H), 6.80 – 6.71 (m, 1H), 6.51 (d, *J* = 6.6 Hz, 1H), 4.45 (d, *J* = 14.5 Hz, 1H), 4.35 (d, *J* = 6.6 Hz, 1H), 3.80 (s, 3H), 3.58 (d, *J* = 14.5 Hz, 1H), 2.25 (s, 3H), 1.94 (s, 3H), 1.47 (s, 3H), 1.16 (s, 3H). ^{13}C NMR (126 MHz, CD_2Cl_2, 65°C) δ 178.9, 159.8, 142.9, 140.1, 135.8, 133.13, 133.11, 131.6, 130.8, 130.4, 129.4, 129.0, 128.7, 128.3, 127.5, 127.1, 126.4, 125.4, 114.4, 68.5, 55.3, 52.3, 22.6, 20.7. ^{31}P NMR (162 MHz, $CDCl_3$) δ 25.01. FT-IR-ATR (cm^{-1}): 1547.7 (C=O). HRMS. Calculated for $C_{44}H_{43}NO_2PPd$ ($M\text{-}Cl^+$): 754.2061, found: 754.2080.

Reaction of {[P(o-Tol)$_3$]Pd(Cl)[κ^2-CH(p-Tol)N(Bn)COPh} 5.7a with P(*o*-MeOC$_6$H$_4$)$_3$ (Scheme 5.8)

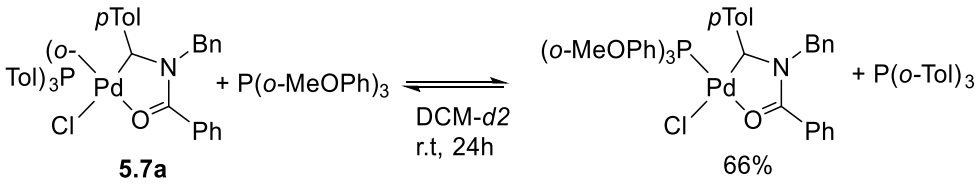

5.7a 66%

In a glovebox, {[P(*o*-Tol)$_3$]Pd(Cl)[□^{2}-CH(*p*-Tol)N(Bn)COPh} **5.7a** (7.6 mg, 0.01 mmol), P(*o*-MeOC$_6$H$_4$)$_3$ (3.5 mg, 0.01 mmol) and benzyl benzoate internal standard were mixed in dichloromethane-*d2* (0.7 mL). The reaction progress was followed by ^{1}H and ^{31}P NMR analysis, which showed equilibrium displacement of P(*o*-Tol)$_3$ in 66% yield after 24h.

Reaction of {[PPh$_3$]Pd(Cl)[κ^2-CH(p-Tol)N(Bn)COPh} 5.6a with P(*o*-MeOC$_6$H$_4$)$_3$

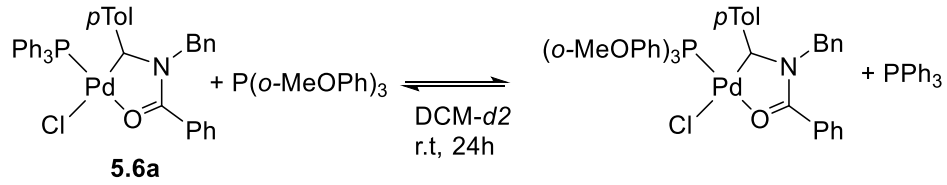

5.6a

In a glovebox, {[PPh$_3$]Pd(Cl)[κ^2-CH(p-Tol)N(Bn)COPh} **5.6a** (7.2 mg, 0.01 mmol), P(*o*-MeOC$_6$H$_4$)$_3$ (3.5 mg, 0.01 mmol) and benzyl benzoate internal standard were mixed in dichloromethane-*d2* (0.7 mL). ^{1}H and ^{31}P NMR analysis showed no reaction after 24 h at ambient temperature.

Reaction of {[P(o-Tol)$_3$]Pd(Cl)[κ^2-CH(p-Tol)N(Bn)COPh} 5.7a with CO (Figure 5.5)

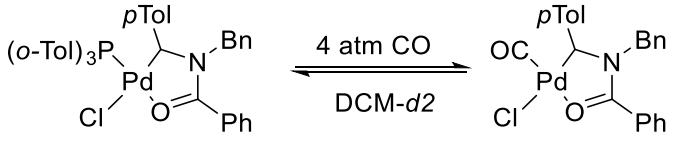

5.7a **5.7a:5.4a** (8:1) **5.4a**

In a glovebox, {[P(*o*-Tol)$_3$]Pd(Cl)[κ^2-CH(*p*-Tol)N(Bn)COPh} **5.7a** (7.6 mg, 0.01 mmol) and benzyl benzoate internal standard were combined in 0.7 mL of dichloromethane-*d2* and transferred to a J-Young NMR tube. The tube was brought outside of the glovebox. The solution was frozen and 4 atm carbon monoxide was condensed into the NMR tube. The *in situ* ^{1}H-NMR analysis showed equilibrium between **5.7a** and **5.4a** in an ~8:1 ratio. The procedure was repeated at various CO pressures.

Münchnone generation from{[P(o-Tol)$_3$]Pd(Cl)[κ^2-CH(p-Tol)N(Bn)COPh} 5.7a (Figure 5.5)

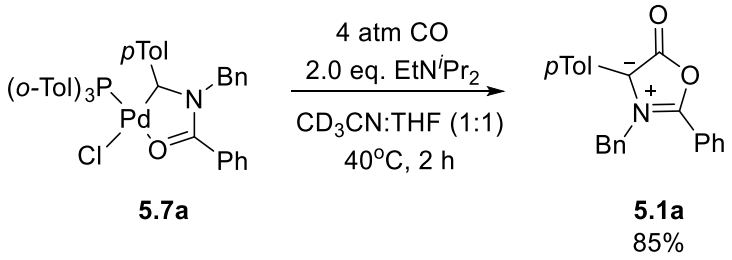

5.7a **5.1a** 85%

In a glovebox, {[P(*o*-Tol)$_3$]Pd(Cl)[κ^2-CH(*p*-Tol)N(Bn)COPh} **5.7a** (7.6 mg, 0.01 mmol), Et*N*^{i}Pr$_2$ (2.6 mg, 0.02 mmol) and benzyl benzoate internal standard were mixed in CD_3CN : THF (1:1, 0.7 mL) and transferred into a J-Young NMR tube. The NMR tube was brought outside of glovebox, pressurized with 4 atm CO, and heated at 40°C for 2 h. The reaction progress was followed by ^{1}H NMR analysis and showed generation of **5.1a** in 85% yield.

Mercury poisoning test with {Pd(Cl)[κ^2-CH(p-Tol)N(Bn)COPh]}$_2$ 5.2a and P(o-Tol)$_3$ (Scheme 5.9)

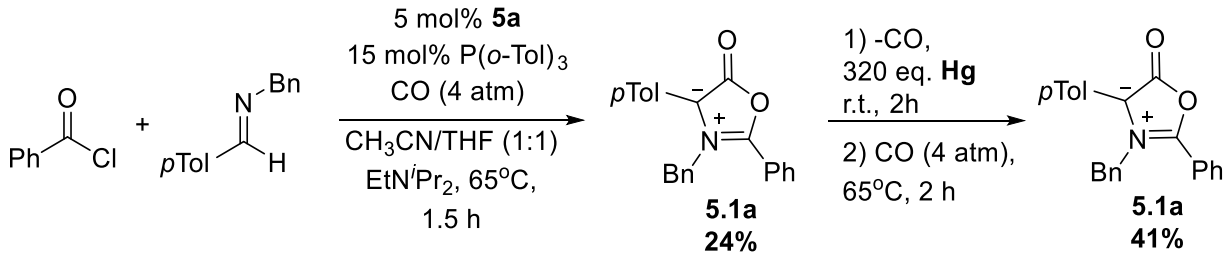

5.1a **24%** **5.1a** **41%**

In a glovebox, *p*-Tol(H)C=NBn (210 mg, 1.0 mmol), benzoyl chloride (210 mg, 1.5 mmol) and benzyl benzoate internal standard were dissolved in CH_3CN (2.5 mL) and stirred for 15 min. This solution was added to a solution of {Pd(Cl)[κ^2-CH(*p*-Tol)NBnCOPh]}$_2$ **5.2a** (45 mg, 0.05 mmol), and P(*o*-Tol)$_3$ (45 mg, 0.15 mmol) in CH_3CN (2.5 mL). The reaction mixture and NEt^{i}Pr$_2$ (160 mg, 0.12 mmol) in THF (5 mL) were transferred to a 50 mL pressure vessel. The solution was then degassed and 4 atm CO was added. The reaction mixture was stirred at 65°C for 2 hours. ^{1}H-NMR analysis of an aliquot showed generation of Münchnone **5.1a** in 21% yield. After degassing, the solution was vigorously stirred in the presence of mercury (8.7 g, 42.6 mmol) over a 2-hour period. After celite filtration, the solution was transferred back into the pressure vessel, pressurized with 4 atm CO and heated at 65°C another 2 hours. ^{1}H-NMR analysis showed generation of Münchnone **5.1a** in 41% yield.

Catalytic Münchnone formation with P(C$_6$F$_5$)$_3$ ligand (Scheme 5.11)

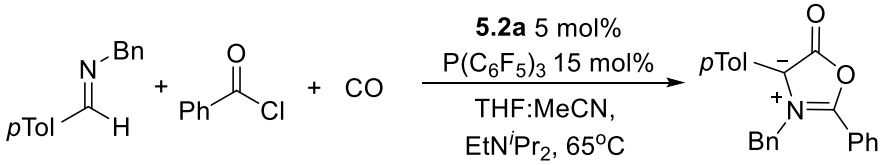

In a glovebox, *p*-Tol(H)C=NBn (21 mg, 0.10 mmol), PhCOCl (21 mg, 0.15 mmol), EtN^{i}Pr$_2$ (64 mg, 0.50 mmol), P(C$_6$F$_5$)$_3$ (8 mg, 0.015 mmol), [Pd(Cl)[κ^2-CH(*p*-Tol)NBn(COPh)]$_2$ (4.5 mg, 0.005 mol), and benzyl benzoate internal standard were combined in CD_3CN : THF (0.7 mL, 1:1) and transferred into a J-Young NMR tube. The tube was brought outside of the glovebox, the solution was frozen and 4 atm CO was condensed into the NMR tube. The NMR tube was heated at 65°C in an NMR spectrometer for 12 h and the reaction was monitored by ^{1}H NMR analysis. Generation of **5.1a** and disappearance of **5.3a** were determined in respect to benzyl benzoate internal standard.

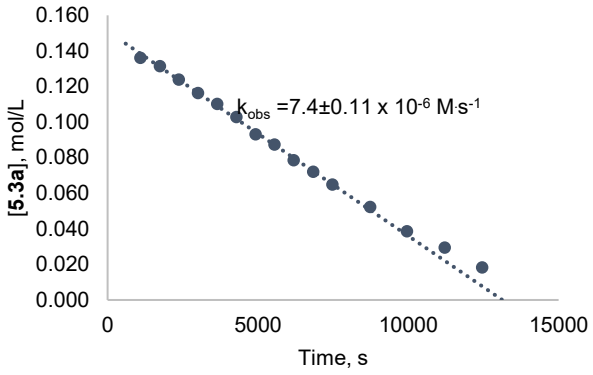

Figure 5.8. Kinetic Analysis of the 5.2a/P(C_6F_5)$_3$ Catalyzed Formation of Münchnone.

Plot of **5.3a** vs. time for the reaction of benzoyl chloride (21 mg, 0.15 mmol), (*p*-tolyl)HC=NBn (21 mg, 0.10 mmol), [Pd(Cl)[κ^2-CH(*p*-Tol)NBn(COPh)]$_2$ **5.2a** (4.5 mg, 0.005 mmol), P(C_6F_5)$_3$ (8.0 mg, 0.015mmol), EtN^iPr$_2$ (64 mg, 0.5 mmol), BnOBz standard, 4 atm CO in CD_3CN:THF (1:1, 0.7 mL) at 65°C.

Table 5.2. Rate data for **5.2a**/P(C_6F_5)$_3$ Catalyzed Formation of Münchnone.

Time	[**5.3a**], mol/L	Time	[**5.3a**], mol/L
600	0.139	7486	0.065
1102	0.136	8738	0.052
1748	0.131	9967	0.038
2383	0.124	11223	0.029
3018	0.116	12471	0.018
3654	0.110	13702	0.012
4291	0.103	14950	0.007
4928	0.093	16197	0.004
5564	0.087	17453	0.003
6201	0.078	18703	0.001
6844	0.072	19952	0.001

5.3.3. Kinetic Studies

Typical Procedure for Kinetic Studies on Münchnone Formation with Bu_4NBr (Figure 5.3)

In glovebox, *p*-Tol(H)C=NBn (21 mg, 0.10 mmol), PhCOCl (21 mg, 0.15 mmol), EtN^iPr_2 (64 mg, 0.50 mmol), Bu_4NBr (32 mg, 0.082 mmol), $[Pd(Cl)[\kappa^2\text{-}CH(p\text{-}Tol)NBn(COPh)]]_2$ (4.5 mg, 0.005 mmol), and benzyl benzoate internal standard were combined in CD_3CN : THF (0.7 mL, 1:1) and transferred into a J-Young NMR tube. The tube was brought outside of the glovebox, the solution frozen, and 4 atm CO was condensed into the NMR tube. The NMR tube was heated at 65°C in an NMR spectrometer and the reaction was monitored by ^1H NMR analysis. Generation of **5.1a** and disappearance of **5.3a** were determined in respect to benzyl benzoate internal standard. For studies employing only initial rates, the k_{obs} was determined by initial rate of **5.1a** formation up to 8000 seconds. Note: The uncertainty in k_{obs} was calculated by using the minimum and maximum slope method.[25] For each data point an uncertainty of ±0.002 mmol was assigned. Afterwards the best fit slope for the $k_{obs\ (MAX)}$ was plotted by taking the lowest uncertainty value of the first data point and the highest uncertainty value of the last data point. Alternatively, best fit slope for the $k_{obs\ (MIN)}$ was plotted by taking the highest uncertainty value of the first data point and the lowest uncertainty value of the last data point. The uncertainty of $k_{obs} = (k_{obs\ (MAX)} - k_{obs\ (MIN)})/2$.

Table 5.3. Rate data in Figure 5.3a

Time, s	[**5.3a**], mol/L	Time, s	[**5.3a**], mol/L
600	0.135	10661	0.052
1261	0.128	12019	0.044
1923	0.121	13377	0.039
2602	0.112	14734	0.033
3264	0.106	16044	0.028
3930	0.100	17799	0.023
5260	0.089	19964	0.016
6587	0.077	22127	0.012
7945	0.069	24292	0.008
9303	0.060	26441	0.006

Table 5.4. Rate data in Figure 5.3b

[**5.3a**]$_0$ = 0.072 mol/L		[**5.3a**]$_0$ = 0.107 mol/L		[**5.3a**]$_0$ = 0.143 mol/L		[**5.3a**]$_0$ = 0.286 mol/L	
k_{obs} = 4.58±0.43 mol/(L·s) x 10^{-6}		k_{obs} = 4.16±0.61 mol/(L·s) x 10^{-6}		k_{obs} = 4.17±0.35 mol/(L·s) x 10^{-6}		k_{obs} = 4.19±0.86 mol/(L·s) x 10^{-6}	
Time, s	**5.1a**, mol/L	Time, s	**5.1a**, mol/L	Time, s	**5.1a**, mol/L	Time, s	**5.1a**, mol/L
0	0	0	0	0	0	0	0
1200	0.0084	1500	0.008	900	0.006	300	0.002
2400	0.0169	3000	0.013	1560	0.007	960	0.005
3000	0.0211	4200	0.016	2220	0.009	1620	0.008
4200	0.0246	5400	0.022	3540	0.014	2940	0.011
6000	0.0331	6600	0.030	4860	0.020	3600	0.016
8000	0.0394	7800	0.033	5520	0.022	4920	0.021
				6180	0.025	6900	0.029
				7500	0.032	7560	0.0327

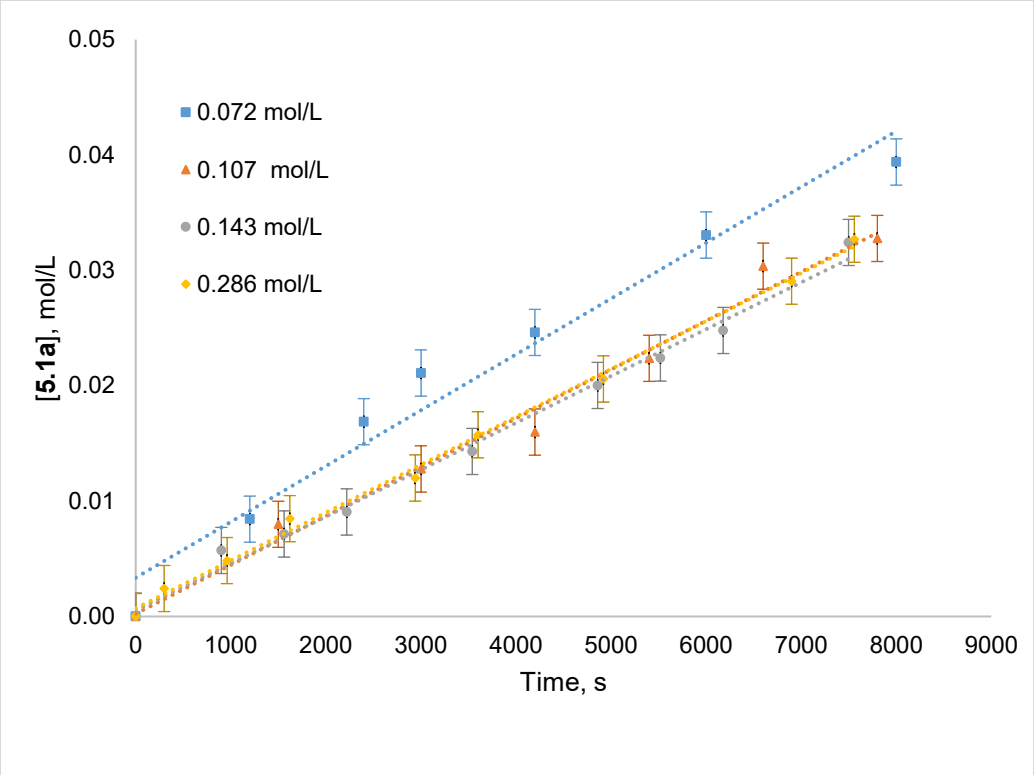

Figure 5.9. Kinetic plot of 5.1a formation vs time at various initial 5.3a concentrations.

Table 5.5. Rate data in Figure 5.3c

[Pd] = 0.014 mol/L		[Pd] = 0.021 mol/L		[Pd] = 0.029 mol/L		[Pd] = 0.043 mol/L	
k_{obs} = 4.17±0.35 mol/(L·s) x 10^{-6}		k_{obs} = 7.28±0.53 mol/(L·s) x 10^{-6}		k_{obs} = 10.7±0.7 mol/(L·s) x 10^{-6}		k_{obs} = 17.1±0.7 mol/(L·s) x 10^{-6}	
Time, s	**5.1a**, mol/L	Time, s	**5.1a**, mol/L	Time, s	**5.1a**, mol/L	Time, s	**5.1a**, mol/L
0	0	0	0	0	0	0	0
900	0.006	1200	0.009	1200	0.021	60	0.004
1560	0.007	2400	0.019	2400	0.032	1800	0.028
2220	0.009	5400	0.039	3600	0.043	3600	0.065
3540	0.014	6200	0.046	4600	0.058	5400	0.093
5520	0.022	8400	0.061	7200	0.079	7200	0.102
6180	0.025						
7500	0.032						

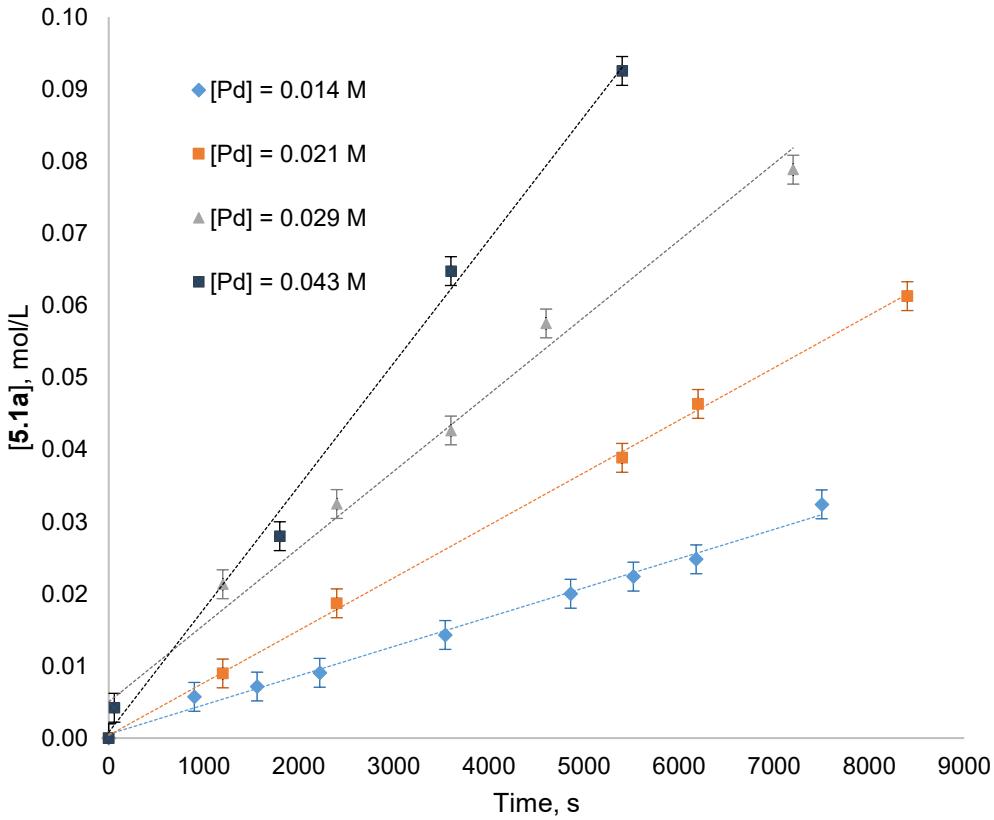

Figure 5.10. Kinetic plot of 5.1a formation vs time at various catalyst 5.2a concentrations

Table 5.6. Rate data in Figure 5.3d

2 atm CO		3 atm CO		4 atm CO		5 atm CO	
k_{obs} = 1.69±0.35 mol/(L·s) x 10^{-6}		k_{obs} = 2.98±0.44 mol/(L·s) x 10^{-6}		k_{obs} = 4.17±0.35 mol/(L·s) x 10^{-6}		k_{obs} = 5.26±0.59 mol/(L·s) x 10^{-6}	
Time, s	**5.1a**, mol/L	Time, s	**5.1a**, mol/L	Time, s	**5.1a**, mol/L	Time, s	**5.1a**, mol/L
0	0	0	0	0	0	0	0
660	0.001	600	0.003	900	0.006	480	0.008
1320	0.001	1620	0.006	1560	0.007	1380	0.011
1980	0.002	2640	0.010	2220	0.009	2280	0.016
2640	0.004	3600	0.014	3540	0.014	3180	0.020
3300	0.006	5460	0.016	4860	0.020	4080	0.028
5220	0.009	5940	0.021	5520	0.022	5880	0.035
7140	0.011	7800	0.023	6180	0.025	7680	0.042
				7500	0.032		
6 atm CO		8 atm CO		10 atm CO		12 atm CO	
k_{obs} = 5.69±0.53 mol/(L·s) x 10^{-6}		k_{obs} = 7.38±0.96 mol/(L·s) x 10^{-6}		k_{obs} = 10.1±1.0 mol/(L·s) x 10^{-6}		k_{obs} = 12.0±1.0 mol/(L·s) x 10^{-6}	
Time, s	**5.1a**, mol/L	Time, s	**5.1a**, mol/L	Time, s	**5.1a**, mol/L	Time, s	**5.1a**, mol/L
0	0	0	0	0	0	0	0
900	0.009	600	0.006	900	0.008	600	0.010
1800	0.012	1260	0.009	1560	0.012	1260	0.016
2700	0.017	1920	0.013	2220	0.019	1920	0.026
3600	0.021	2580	0.018	2880	0.029	2580	0.037
4500	0.027	3240	0.025	3540	0.035	3240	0.047
5400	0.030	3900	0.029	4200	0.042	3900	0.056
6300	0.040	4560	0.034	4860	0.048	5220	0.067
7200	0.046	5220	0.037	5520	0.053	5880	0.072
		5880	0.040	6180	0.055	6540	0.076
		6540	0.044	6840	0.059	7200	0.079
		7860	0.049	7500	0.063	7860	0.083

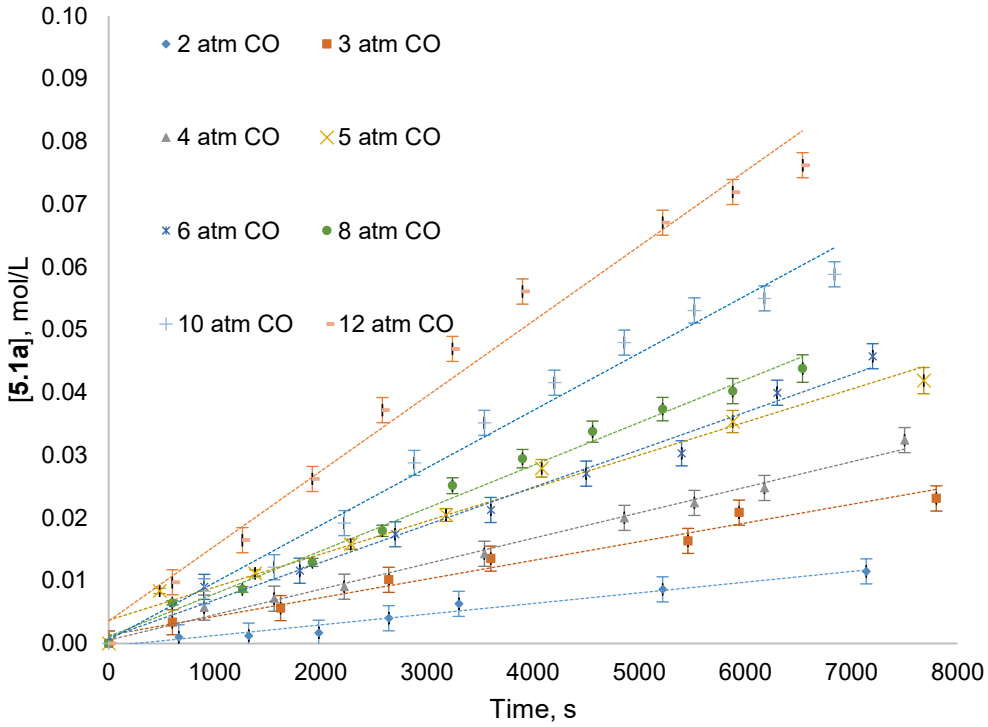

Figure 5.11. Kinetic plot of 6.1a formation vs time at various CO pressures

Table 5.7. Rate data in Figure 5.3e

Time, s	[**5.3a**], mol/L	Time, s	[**5.3a**], mol/L
600	0.0144	12062	0.0056
1282	0.0134	14230	0.0044
2636	0.0121	17245	0.0032
4003	0.0112	21054	0.0024
5369	0.0102	24863	0.0014
6725	0.0089	28678	0.0010
8104	0.0081	32501	0.0006
9879	0.0067	36319	0.0002

Typical Procedure for Kinetic Studies on Münchnone Formation with P(o-Tol)$_3$ (Figure 5.6)

In glovebox, *p*-Tol(H)C=NBn (21 mg, 0.10 mmol), PhCOCl (21 mg, 0.15 mmol), EtN^iPr_2 (64 mg, 0.50 mmol), P(*o*-Tol)$_3$ (4.5 mg, 0.015 mmol), [Pd(Cl)[κ^2-CH(*p*-Tol)NBn(COPh)]$_2$ (4.5 mg, 0.005 mmol), and benzyl benzoate internal standard were combined in CD_3CN : THF (0.7 mL, 1:1) and transferred into a J-Young NMR tube. The tube was brought outside of the glovebox, the solution was frozen, and 4 atm carbon monoxide was condensed into the NMR tube. The NMR tube was heated at 65°C in an NMR spectrometer for 12 h and the reaction was monitored by ^{1}H NMR analysis. Generation of **5.1a** and disappearance of **5.3a** were determined in respect to benzyl benzoate internal standard. For studies employing only initial rates, the k_{obs} was determined by initial rate of **5.1a** formation up to 8000 seconds.

Table 5.8. Rate data in Figure 5.6a

Time, s	[**5.3a**], mol/L	Time, s	[**5.3a**], mol/L
0	0.143	13320	0.073
1260	0.139	15720	0.061
2700	0.130	18120	0.047
4020	0.122	20520	0.036
5340	0.115	22920	0.028
6660	0.107	25320	0.017
8520	0.095	27720	0.006
10920	0.082		

Table 5.9. Rate data in Figure 5.6b

[**5.3a**]$_0$ = 0.072 mol/L		[**5.3a**]$_0$ = 0.143 mol/L		[**5.3a**]$_0$ = 0.215 mol/L	
k_{obs} = 5.06±0.29 mol/(L·s) x 10^{-6}		k_{obs} = 5.11±0.31 mol/(L·s) x 10^{-6}		k_{obs} = 4.98±0.22 mol/(L·s) x 10^{-6}	
Time, s	**5.1a**, mol/L	Time, s	**5.1a**, mol/L	Time, s	**5.1a**, mol/L
0	0	0	0	0	0
600	0.003	600	0.002	600	0.001
1200	0.004	1260	0.004	1260	0.003
1800	0.007	1980	0.007	1920	0.004
2400	0.008	2700	0.010	2580	0.007
3000	0.013	3360	0.013	3240	0.011
3600	0.016	4020	0.016	3900	0.013
4200	0.019	4680	0.020	4560	0.017
5100	0.024	5340	0.024	5640	0.023
6000	0.029	6000	0.027	6720	0.030
6900	0.034	6660	0.032	7800	0.035
7800	0.038	7320	0.036		
[**5.3a**]$_0$ = 0.250 mol/L		[**5.3a**]$_0$ = 0.286 mol/L		[**5.3a**]$_0$ = 0.358 mol/L	
k_{obs} = 5.36±0.30 mol/(L·s) x 10^{-6}		k_{obs} = 5.27±0.33 mol/(L·s) x 10^{-6}		k_{obs} = 5.60±0.35 mol/(L·s) x 10^{-6}	
Time, s	**5.1a**, mol/L	Time, s	**5.1a**, mol/L	Time, s	**5.1a**, mol/L
0	0	0	0	0	0
1000	0.001	600	0.003	600	0.002
1660	0.003	1500	0.010	1260	0.005
2320	0.005	2400	0.014	1920	0.009
2980	0.008	3300	0.017	2580	0.012
3640	0.010	4200	0.023	3240	0.015
4300	0.016	5100	0.028	3900	0.018
4960	0.020	6000	0.034	4560	0.023
6040	0.027	7800	0.040	5640	0.030
7120	0.033			6720	0.036
8200	0.036			7800	0.043

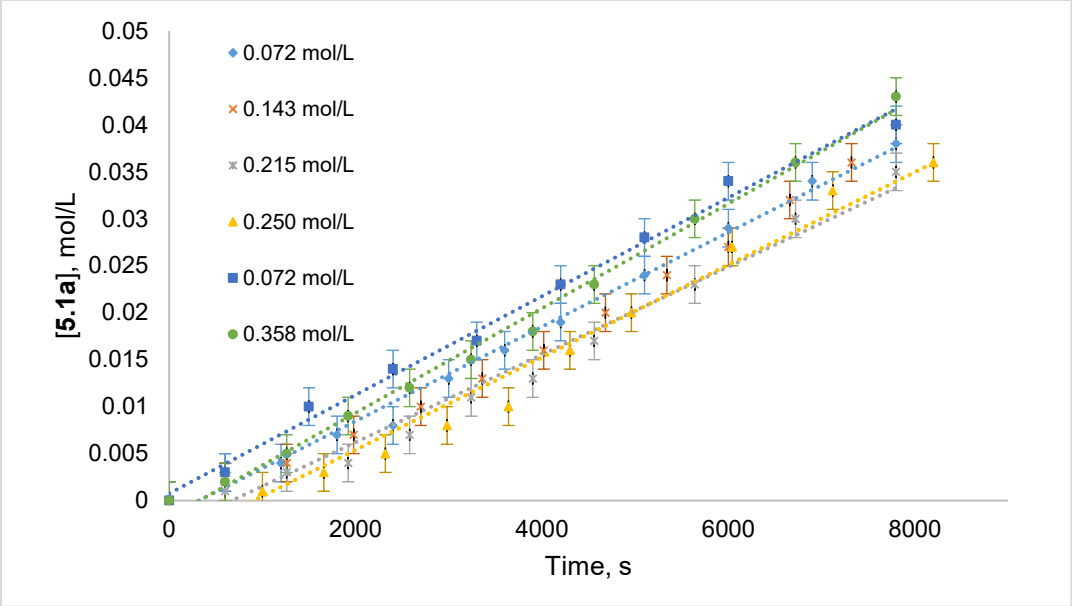

Figure 5.12. Kinetic plot of 5.1a formation vs time at various initial 5.3a concentrations

Table 5.10. Rate data in Figure 5.6c

[P(*o*-Tol)$_3$]: [Pd] = 1.3		[P(*o*-Tol)$_3$]: [Pd] = 1.5		[P(*o*-Tol)$_3$]: [Pd] = 3	
k_{obs} = 5.22±0.40 mol/(L·s) x 10^{-6}		k_{obs} = 5.11±0.31 mol/(L·s) x 10^{-6}		k_{obs} = 3.91±0.27 mol/(L·s) x 10^{-6}	
Time, s	**5.1a**, mol/L	Time, s	**5.1a**, mol/L	Time, s	**5.1a**, mol/L
0	0	0	0	0	0
600	0.003	600	0.002	600	0.003
1380	0.008	1260	0.004	1680	0.006
2160	0.012	1980	0.007	2700	0.008
2940	0.015	2700	0.010	3780	0.014
3720	0.019	3360	0.013	4800	0.018
4500	0.025	4020	0.016	5820	0.022
5280	0.030	4680	0.020	6840	0.026
6060	0.032	5340	0.024	7860	0.029
6840	0.036	6000	0.027		
7620	0.040	6660	0.032		
		7320	0.036		

[P(*o*-Tol)$_3$]: [Pd] = 4		[P(*o*-Tol)$_3$]: [Pd] = 5		[P(*o*-Tol)$_3$]: [Pd] = 6	
k_{obs} = 2.71±0.55 mol/(L·s) x 10^{-6}		k_{obs} = 2.02±0.26 mol/(L·s) x 10^{-6}		k_{obs} = 1.31±0.26 mol/(L·s) x 10^{-6}	
Time, s	**5.1a**, mol/L	Time, s	**5.1a**, mol/L	Time, s	**5.1a**, mol/L
0	0	0	0.000	0	0
600	0.002	600	0.001	480	0.001
1380	0.003	1380	0.002	1560	0.003
2160	0.005	2160	0.002	2640	0.003
2940	0.007	2940	0.003	3720	0.005
3720	0.008	3720	0.005	4800	0.006
4500	0.010	4500	0.006	5880	0.008
5280	0.014	5280	0.008	6960	0.009
6060	0.016	6060	0.010	8040	0.011
6840	0.017	6840	0.011		
7620	0.021	7620	0.013		

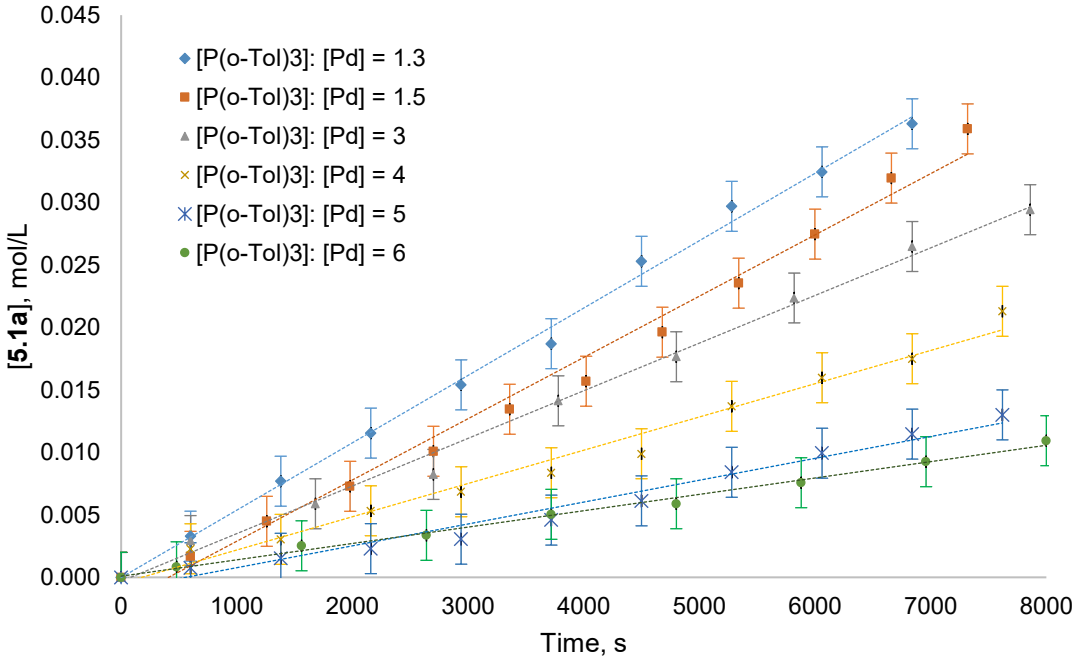

Figure 5.13. Kinetic plot of 5.1a formation vs time at various P(o-Tol)$_3$:5.2a ratios

Table 5.11. Rate data in Figure 5.6d

1 atm CO		2 atm CO		3 atm CO		4 atm CO		5 atm CO	
k_{obs} = 1.42±0.23 mol/(L·s) x 10^{-6}		k_{obs} = 2.09±0.65 mol/(L·s) x 10^{-6}		k_{obs} = 3.61±0.39 mol/(L·s) x 10^{-6}		k_{obs} = 5.11±0.31 mol/(L·s) x 10^{-6}		k_{obs} = 5.80±0.30 mol/(L·s) x 10^{-6}	
Time, s	**5.1a**, mol/L	Time, s	**5.1a**, mol/L	Time, s	**5.1a**, mol/L	Time, s	**5.1a**, mol/L	Time, s	**5.1a**, mol/L
0	0.000	0	0	0	0	0	0	0	0.000
600	0.001	600	0.001	600	0.000	600	0.002	600	0.002
1500	0.001	1500	0.002	1260	0.002	1260	0.004	1140	0.003
2400	0.001	2400	0.003	1920	0.003	1980	0.007	2220	0.010
3300	0.002	3300	0.004	2580	0.005	2700	0.010	3300	0.017
4200	0.003	4200	0.006	3240	0.009	3360	0.013	3840	0.020
5100	0.004	5100	0.008	3900	0.010	4020	0.016	4380	0.023
6000	0.006	6000	0.011	4560	0.012	4680	0.020	4920	0.026
7200	0.008	6900	0.013	5220	0.017	5340	0.024	5460	0.028
8400	0.011	7800	0.018	5880	0.020	6000	0.027	6000	0.033
				6960	0.024	6660	0.032	6540	0.036
						7320	0.036	7620	0.043

6 atm CO		8 atm CO		10 atm CO		12 atm CO	
k_{obs} = 7.53±0.51 mol/(L·s) x 10^{-6}		k_{obs} = 9.94±0.31 mol/(L·s) x 10^{-6}		k_{obs} = 13.9±0.7 mol/(L·s) x 10^{-6}		k_{obs} = 15.8±0.6 mol/(L·s) x 10^{-6}	
Time, s	**5.1a**, mol/L	Time, s	**5.1a**, mol/L	Time, s	**5.1a**, mol/L	Time, s	**5.1a**, mol/L
0	0	0	0	0	0	0	0
780	0.004	780	0.005	840	0.010	1000	0.015
1560	0.011	1560	0.014	1680	0.027	2080	0.035
2340	0.018	2340	0.025	2520	0.042	3220	0.064
3120	0.024	3120	0.030	3360	0.054	4300	0.081
3900	0.030	3900	0.038	5040	0.076	5380	0.090
4680	0.035	4680	0.048	5880	0.083	6460	0.094
5460	0.041	5460	0.054	6720	0.091	7540	0.104
6240	0.046	6240	0.060	7560	0.096		
7020	0.055	7020	0.066				
7800	0.063	7800	0.072				

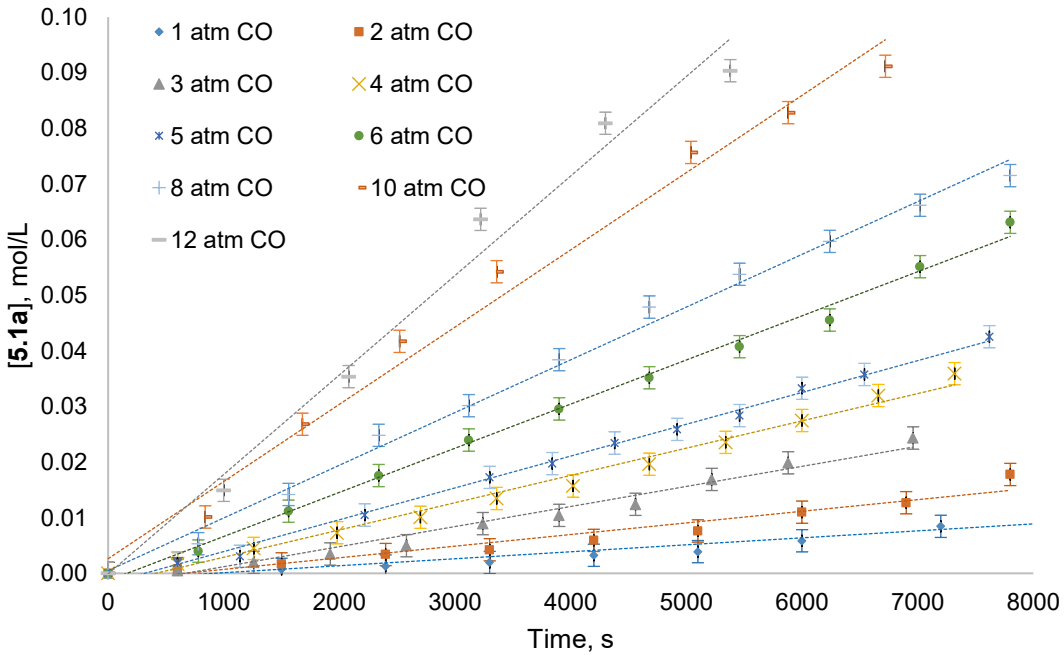

Figure 5.14. Kinetic plot of 5.1a formation vs time at various CO pressures

Table 5.12. Rate data in Figure 5.6e

Time, s	[**5.3a**], mol/L
800	0.0102
1501	0.0092
2196	0.0082
2893	0.0068
3589	0.0056
4286	0.0045
4999	0.0030
5715	0.0021
6418	0.0011
7124	0.0001

5.5.4. Supplementary Tables and Figures

EtN^iPr_2 and Bu_4NBr concentration influence on catalytic Münchnone formation

In glovebox, *p*-Tol(H)C=NBn (21 mg, 0.10 mmol), PhCOCl (21 mg, 0.15 mmol), EtN^iPr_2, Bu_4NBr, [Pd(Cl)[κ^2-CH(*p*-Tol)NBn(COPh)]$_2$ (4.5 mg, 0.005 mmol), and benzyl benzoate internal standard were combined in CD_3CN : THF (0.7 mL, 1:1) and transferred into a J-Young NMR tube. The tube was brought outside of the glovebox, the solution frozen, and 4 atm carbon monoxide was condensed into the NMR tube. The NMR tube was heated at 65°C in an NMR spectrometer and the reaction was monitored by ^{1}H NMR analysis. Generation of **5.1a** and disappearance of **5.3a** were determined in respect to benzyl benzoate internal standard. For studies employing only initial rates, the k_{obs} was determined by initial rate of **5.1a** formation up to 8000 seconds.

Table 5.13. EtN^iPr_2 and Bu_4NBr concentration influence formation on catalytic Münchnone

[EtN^iPr_2] 0.12 mmol [Bu_4NBr] = 0.1 mmol		[EtN^iPr_2] 0.12 mmol [Bu_4NBr] = 0.01 mmol		[EtN^iPr_2] 0.12 mmol [Bu_4NBr] = 0.01 mmol	
k_{obs} = 4.11 ± 0.35 mol/(L·s) x 10^{-6}		k_{obs} = 4.38 ± 0.64 mol/(L·s) x 10^{-6}		k_{obs} = 4.74 ± 0. 54 mol/(L·s) x 10^{-6}	
Time, s	[**5.1a**], mol/L	Time, s	[**5.1a**], mol/L	Time, s	[**5.1a**], mol/L
0	0	0	0	0	0
600	0.002	600	0.0049	900	0.006
1740	0.004	1800	0.0107	1560	0.007
2880	0.008	2880	0.0174	2220	0.009
4020	0.013	3960	0.0223	3540	0.014
5160	0.019	5040	0.0273	4860	0.020
6300	0.024	6120	0.0304	5520	0.022
7440	0.035	7200	0.0358	6180	0.025
				7500	0.032

***Influence of CO pressure on Münchnone generation from* 5.2a**

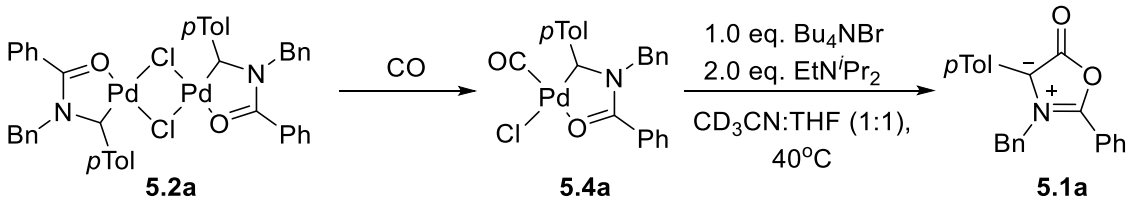

In a glovebox, {Pd(Cl)[κ^2-CH(*p*-Tol)N(Bn)COPh]}$_2$ **5.2a** (4.5 mg, 0.005 mmol), Bu_4NBr (3.2 mg, 0.01 mmol), EtN^iPr_2 (2.6 mg, 0.02 mmol) and benzyl benzoate internal standard were mixed in CD_3CN : THF (1:1, 0.7 mL) and transferred into a J-Young NMR tube. The NMR tube was brought outside of glovebox, pressurized with CO (3, 4, 5, 6, 8, 10 atm), and heated at 40°C. The rate of Münchnone **5.1a** formation was monitored by ^{1}H NMR analysis.

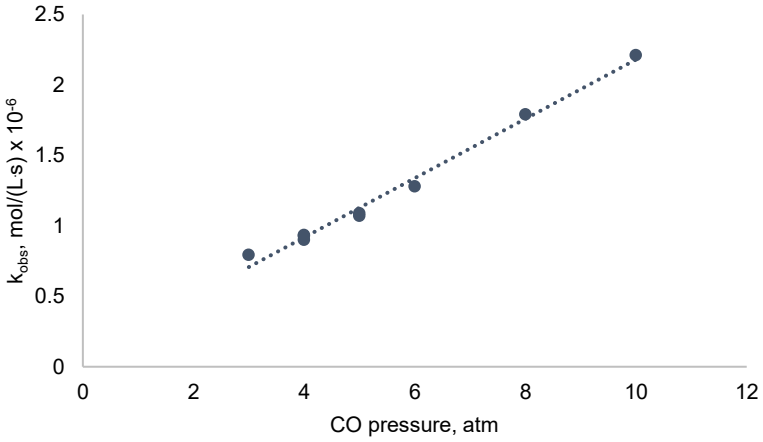

Figure 5.15. Influence of CO pressure on Münchnone generation from 5.2a.

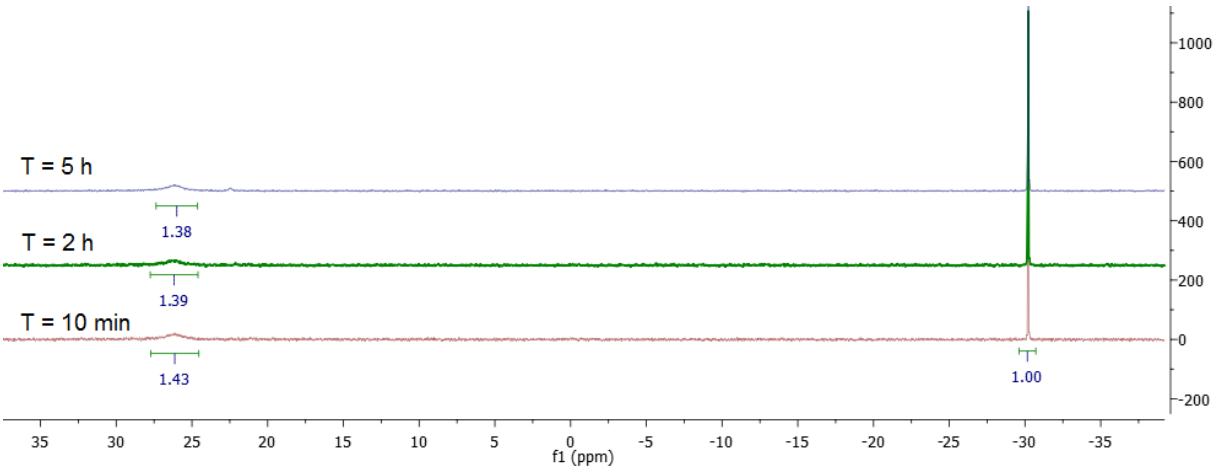

Figure 5.16. *In situ* ^{31}P NMR spectrum of the catalytic formation of 5.1.

Reaction of benzoyl chloride (21 mg, 0.15 mmol), (*p*-Tol)HC=NBn (21 mg, 0.10 mmol), [Pd(Cl)[κ^2-CH(*p*-Tol)NBn(COPh)]$_2$ **5.2a** (4.5 mg, 0.005 mmol), P(*o*-Tol)$_3$ (4.5 mg, 0.015mmol), EtN^iPr$_2$ (64 mg, 0.5 mmol), 4 atm CO in CD_3CN:THF (1:1, 0.7 mL) at 65°C. ^{31}P NMR taken at 10 min, 2 h, 5 h time points show the presence of free P(*o*-Tol)$_3$ (δ -30.2 ppm) and palladacycle **5.7a** (δ 26.1 ppm) in the ~ 1:1.4 ratio.

5.6. References

(1) For reviews on metal catalyzed multicomponent reactions: (a) D'Souza, D. M.; Müller, T. J. J. *Chem. Soc. Rev.* **2007**, *36*, 1095-1108; (b) Balme, G.; Bossharth, E.; Monteiro, N. *Eur. J. Org. Chem.* **2003**, 4101-4111; (c) Estevez, V.; Villacampa, M.; Menendez, J. C. *Chem. Soc. Rev.* **2010**, *39*, 4402-4421; (d) Arndtsen, B. A.; Tjutrins, J. In *Science of Synthesis, Multicomponent Reactions*; Georg Thieme Verlag: **2014**; Vol. 2, pp. 475-533; (e) Balme, G.; Bouyssi, D.; Mont, N. In *Multicomponent Reactions* (Eds.: J. Zhu, H. Bienaymé), Wiley-VCH, Weinheim, **2005**, pp. 224-276; (f) Lorenzini, F.; Tjutrins, J.; Quesnel, J. S.; Arndtsen, B. A. In *Multicomponent Reactions in Organic Synthesis*, Wiley-VCH Verlag GmbH & Co. KGaA, **2014**, pp. 207-230; (g) Montgomery, J. *Acc. Chem. Res.* **2000**, *33*, 467-473; (h) Orru, R. V. A.; de Greef, M. *Synthesis* **2003**, *2003*, 1471,1499.

(2) For reviews on the Pauson Khand reaction, see: (a) Kitagaki, S.; Inagaki, F.; Mukai, C. *Chem. Soc. Rev.* **2014**, *43*, 2956-2978; (b) Moulton, B. E. In *Organometallic Chemistry*: Volume

36; The Royal Society of Chemistry: **2010**; Vol. 36, pp. 93-120; (c) Lee, H.-W.; Kwong, F.-Y. *Eur. J. Org. Chem.* **2010**, 789-811; (d) Lam, F. L.; Lee, H. W.; Wang, J.; Kwong, F. Y. In *The Pauson-Khand Reaction*; John Wiley & Sons, Ltd: **2012**, pp. 181-210; (e) Brummond, K. M.; Kent, J. L. *Tetrahedron* **2000**, *56*, 3263-3283; (f) Shi, L.; Yang, Z. *Eur. J. Org. Chem.* **2016**, *2016*, 2356-2368; (g) Gibson, S. E.; Stevenazzi, A. *Angew. Chem. Int. Ed.* **2003**, *42*, 1800-1810; (h) Laschat, S.; Becheanu, A.; Bell, T.; Baro, *Synlett* **2005**, 2547-2570.

(3) For reviews on alkyne trimerization, see: (a) Galan, B. R.; Rovis, T. *Angew. Chem. Int. Ed.* **2009**, *48*, 2830-2834; (b) Broere, D. L. J.; Ruijter, E. *Synthesis* **2012**, *44*, 2639-2672; (c) Shibata, T.; Tsuchikama, K. *Org. Biomol. Chem.* **2008**, *6*, 1317-1323; (d) Dominguez, G.; Perez-Castells, J. *Chem. Soc. Rev.* **2011**, *40*, 3430-3444; (e) Domínguez, G.; Pérez-Castells, J. In *Comprehensive Organic Synthesis II* (Second Edition) (Ed.: P. Knochel), Elsevier, Amsterdam, **2014**, pp. 1537-1581; (f) Kotha, S.; Brahmachary, E.; Lahiri, K. *Eur. J. Org. Chem.* **2005**, *2005*, 4741-4767.

(4) For reviews on amidocarbonylation, see: (a) von Wangelin, A. J.; Neumann, H.; Gördes, D.; Beller, M. In *Transition Metals for Organic Synthesis*, Wiley-VCH Verlag GmbH, **2008**, pp. 133-148; (b) Ojima, I.; Commandeur, C.; Chiou, W. H. In C*omprehensive Organometallic Chemistry III* (Ed.: D. M. P. M. H. Crabtree), Elsevier, Oxford, **2007**, pp. 511-555; (c) von Wangelin, A. J.; Neumann, H.; Gördes, D.; Klaus, S.; Strübing, D.; Beller, *Chem. Eur. J.* **2003**, *9*, 4286-4294; (d) Beller, M.; Eckert, M. *Angew. Chem. Int. Ed.* **2000**, *39*, 1010-1027.

(5) For representative catalytic examples: (a) Yamamoto, K.; Bruun, T.; Kim, J. Y.; Zhang, L.; Lautens, M. *Org. Lett.* **2016**, *18*, 2644-2647; (b) Jackson, E. P.; Montgomery, J. *J. Am. Chem. Soc.* **2015**, *137*, 958-963; (c) Standley, E. A.; Tasker, S. Z.; Jensen, K. L.; Jamison, T. F. *Acc. Chem. Res.* **2015**, *48*, 1503-1514; (d) Deibl, N.; Ament, K.; Kempe, R. *J. Am. Chem. Soc.* **2015**, *137*, 12804-12807; (e) Moni, L.; Denißen, M.; Valentini, G.; Müller, T. J. J.; Riva, R. *Chem. Eur. J.* **2015**, *21*, 753-762; (f) Odom, A. L.; McDaniel, T. J. *Acc. Chem. Res.* **2015**, *48*, 2822-2833; (g) Ahlin, J. S. E.; Cramer, N. *Org. Lett.* **2016**, *18*, 3242-3245; (h) Xue, F.; Zhao, J.; Hor, T. S. A.; Hayashi, T. *J. Am. Chem. Soc.* **2015**, *137*, 3189-3192; (i) Nogi, K.; Fujihara, T.; Terao, J.; Tsuji, Y. *J. Am. Chem. Soc.* **2016**, *138*, 5547-5550; (j) Lei, C.; Jin, X.; Zhou, J. *Angew. Chem. Int. Ed.* **2015**, *54*, 13397-13400; (k) Zhang, M.; Fang, X.; Neumann, H.; Beller, M. *J. Am. Chem. Soc.* **2013**, *135*, 11384-1138; (l) Uhlig, N.; Yoo, W.-J.; Zhao, L.; Li, C.-J. In *Modern Alkyne*

Chemistry; Wiley-VCH Verlag: **2014**, pp. 239-268; (m) Lee, D. J.; Han, H. S.; Shin, J.; Yoo, E. J. *J. Am. Chem. Soc.* **2014**, *136*, 11606-11609; (n) Alford, J. S.; Davies, H. M. L. *J. Am. Chem. Soc.* **2014,** *136*, 10266-10269; (o) He, R.; Jin, X.; Chen, H.; Huang, Z.-T.; Zheng, Q.-Y.; Wang, C. *J. Am. Chem. Soc.* **2014**, 136, 6558-6561; (p) Xiao, Q.; Wang, B.; Tian, L.; Yang, Y.; Ma, J.; Zhang, Y.; Chen, S.; Wang, J. *Angew. Chem. Int. Ed.* **2013**, *52*, 9305-9308; (q) Gianino, J. B.; Ashfeld, B. L. *J. Am. Chem. Soc.* **2012**, *134*, 18217-18220; (r) Staben, S. T.; Blaquiere, N. *Angew. Chem. Int. Ed.* **2010**, *49*, 325-328. (s) Cao, H.; McNamee, L.; Alper, H. *Org. Lett.* **2008**, *10*, 5281-5284; t) Pinto, A.; Neuville, L.; Zhu, J. *Angew. Chem. Int. Ed.* **2007**, *46*, 3291.

(6) (a) Dghaym, R. D.; Dhawan, R.; Arndtsen, B. A. *Angew. Chem. Int. Ed.* **2001**, *40*, 3228-3230; (b) Dhawan, R.; Dghaym, R. D.; Arndtsen, B. A. *J. Am. Chem. Soc.* **2003**, *125*, 1474-1475; (c) Dhawan, R.; Arndtsen, B. A. *J. Am. Chem. Soc.* **2004**, *126*, 468-469; (d) Dhawan, R.; Dghaym, R. D.; St. Cyr, D. J.; Arndtsen, B. A. *Org. Lett.* **2006**, *8*, 3927-3930; (e) Siamaki, A. R.; Arndtsen, B. A. *J. Am. Chem. Soc.* **2006**, *128*, 6050-6051; (f) Worrall, K.; Xu, B.; Bontemps, S.; Arndtsen, B. A. *J. Org. Chem.* **2011**, *76*, 170-180; (g) Arndtsen, B. A. *Chem. Eur. J*. **2009**, *15*, 302-313.

(7) For examples in polymer synthesis: (a) Siamaki, A. R.; Sakalauskas, M.; Arndtsen, B. A. *Angew. Chem. Int. Ed.* **2011**, *50*, 6552-6556; (b) Leitch, D. C.; Kayser, L. V.; Han, Z.-Y.; Siamaki, A. R.; Keyzer, E. N.; Gefen, A.; Arndtsen, B. A. *Nat Commun* **2015**, *6*, 7411.

(8) For review of carbonylative approaches to heterocycle synthesis: Wu, X.-F.; Neumann, H.; Beller, M. *Chem. Rev.* **2013**, *113*, 1-35.

(9) See Section 5.5. Supporting Information for full details of this calculation.

(10) (a) Bose, A. K.; Spiegelman, G.; Manhas, M. S. *Tetrahedron Lett.* **1971**, *12*, 3167-3170; (b) Maryanoff, B. E.; Zhang, H.-C.; Cohen, J. H.; Turchi, I. J.; Maryanoff, C. A. *Chem. Rev.* **2004**, *104*, 1431-1628; (c) Nortey, S.; McComsey, D.; Maryanoff, B. *Heterocycles* **1993**, *35*, 1075-1088.

(11) Dghaym, R. D.; Yaccato, K. J.; Arndtsen, B. A. *Organometallics* **1998**, *17*, 4-6.

(12) Allen, F. H.; Kennard, O.; Watson, D. G.; Brammer, L.; Orpen, A. G.; Taylor, R. In *International Tables for Crystallography*, Vol. C (Ed.: A. J. C. Wilson), Kluwer, Boston, **1992**, pp. 685 - 706.

(13) For related Pd(II) carbonyl complexes see: Ledford, J.; Shultz, C. S.; Gates, D. P.; White, P. S.; DeSimone, J. M.; Brookhart, M. *Organometallics* **2001**, *20*, 5266-5276.

(14) The bromide versions of **5.2a** can be generated *in situ* by the reaction of: benzoyl bromide (94 mg, 0.5 mmol), *p*-TolC(H)=NBn (105 mg, 0.5 mmol) and $Pd_2dba_3.CHCl_3$ (259 mg, 0.25 mmol) in MeCN (5 mL) for 1 h. Filtration of this solution through celite, removal of the solvent in vacuo, washing with Et_2O (4 x 5 mL), followed by ^1H NMR analysis reveals the formation of the Br-**5.2a**. The bromide versions of **5.4a** was generated *in situ* by transferring a solution of **Br-5.2a** (4.5 mg, 0.005 mmol) in CD_3CN (0.7 mL) to a J-Young tube and adding 4 atm CO.

(15) (a) Blackmond, D. G. *Angew. Chem. Int. Ed.* **2005**, *44*, 4302-4320; (b) Mathew, J. S.; Klussmann, M.; Iwamura, H.; Valera, F.; Futran, A.; Emanuelsson, E. A. C.; Blackmond, D. G. *J. Org. Chem.* **2006**, *71*, 4711-4722.

(16) Synthetic conditions for the catalytic formation of Münchnones employ dilute conditions in order to minimize the generation of side products.

(17) Beletskaya, I. P.; Cheprakov, A. V. *Chem. Rev.* **2000**, *100*, 3009-3066.

(18) Reetz, M. T.; Westermann, E. *Angew. Chem. Int. Ed.* **2000**, *39*, 165-168.

(19) (a) Widegren, J. A.; Finke, R. G. *J. Mol. Cat. A.* **2003**, *198*, 317-341. (b) Davies, I. W.; Matty, L.; Hughes, D. L.; Reider, P. J. *J. Am. Chem. Soc.* **2001**, *123*, 10139-10140.

(20) Performing the same sequence of steps, without the addition of mercury results in further catalysis.

(21) Tolman, C. A. *Chem. Rev.* **1977**, *77*, 313-348.

(22) Zalesskiy, S. S.; Ananikov, V. P. *Organometallics* **2012**, *31*, 2302-2309.

(23) Layer W. R. *Chem. Rev*. **1963**, *63*, 489-510.

(24) Ohlin, C. A.; Dyson, P. J.; Laurenczy, G. *Chem. Commun*. **2004**, 1070-1071.

(25) Hughes, I.; Hase, T. *Measurements and Their Uncertainties: A Practical Guide to Modern Error Analysis*; OUP Oxford, 2010.

Chapter 6. Palladium Catalyst Design for the Carbonylative Synthesis of Pyrroles and the One Pot, Multicomponent Assembly to Atorvastatin

6.1. Preface

In this chapter, we show how the mechanistic insights presented in chapter 5 can be used to develop a highly active catalyst for carbonylative synthesis of Münchnones. This catalyst exploits the sterically encumbered phosphine $^{t}Bu_2P$(N-phenylpyrrole) to create a palladium intermediate that undergoes rapid CO coordination and insertion. The use of this catalyst allows the formation of Münchnones at milder reaction conditions, significantly higher rates and 10-fold lower catalyst loadings. Coupling the formation of Münchnones with cycloaddition can be used to synthesize a broad range of polysubstituted pyrroles, including the pharmaceutical Atorvastatin, from available imines, acid chlorides, alkenes and alkynes.

6.2. Introduction

The development of efficient and atom economical methods to assemble pharmaceutical cores represents a central thrust in synthetic chemistry. These efforts have taken even greater importance as we move to minimize the environmental impact and waste often associated with classical multistep synthesis. In this regard, one of the most heavily prescribed pharmaceutical in the world over the past decade has been the pyrrole Atorvastatin Calcium, commonly known as Lipitor (Figure 6.1a).[1] Lipitor is a member of pharmaceutical agents known as statins, used primarily as a cholesterol-lowering agent, and has been the largest market share pharmaceutical in the world over the past decade.[2] The utility of Lipitor as a pharmaceutical has attracted a number of studies directed towards its efficient formation.[3] For example, biosynthetic platforms are available to access the ethyl (R)-4-amino-3-hydroxybutyrate unit in Atorvastatin from available substrates, and were the subject of the 2006 Presidential Green Chemistry Challenge Award.[4] Related metal catalyzed methods can be similarly efficient. Nevertheless, the assembly of the pyrrole core of Atorvastatin has to date involved more classical synthetic methods, such as the Paal-Knorr reaction with functionalized diketones, reductive cyclizations, or 1,3-dipolar cycloaddition with alkynes (Figure 6.1b).[5] While effective, these methods also require multistep

assembly of precursor prior to cyclization, which can detract from the step and atom economy of these approaches, and also generate significant waste.

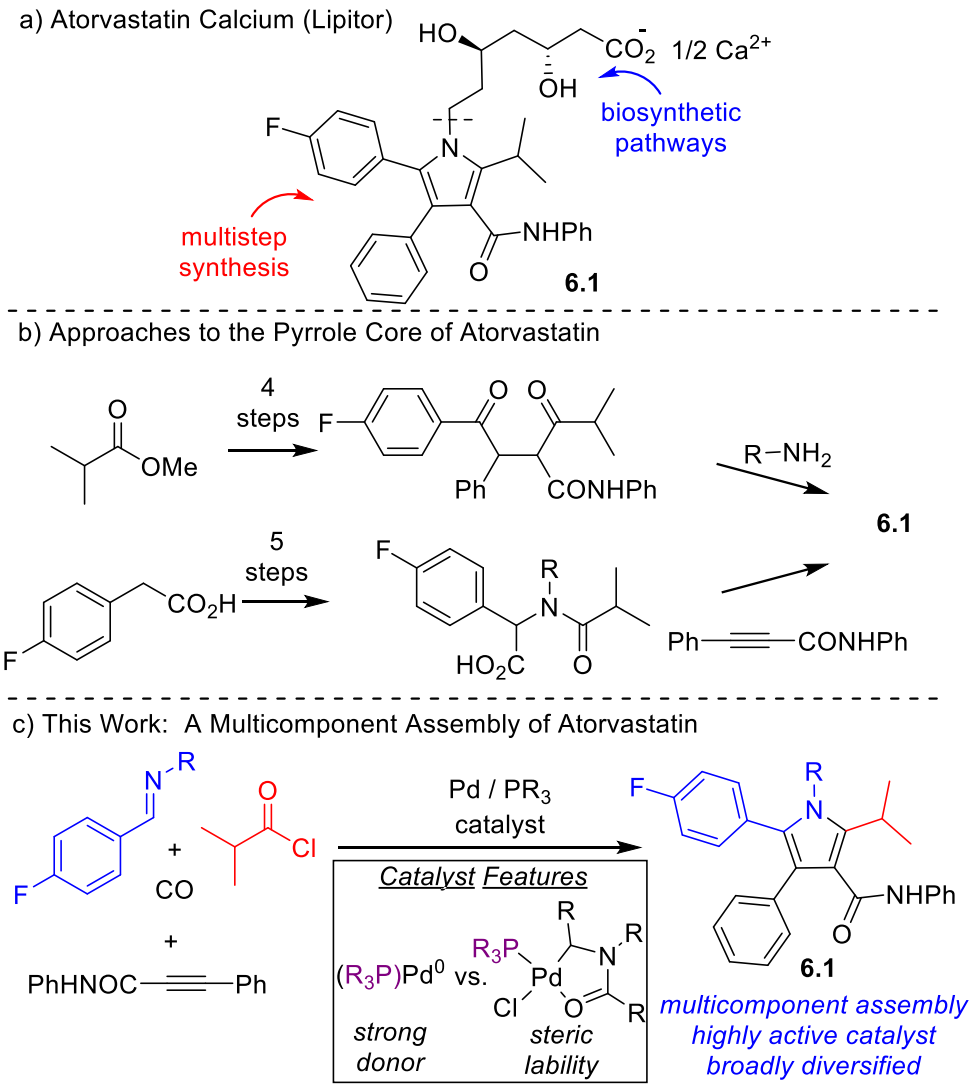

Scheme 6.1. Synthetic Approaches to Atorvastatin.

In principle, a more attractive approach to pyrroles such that in Atorvastatin would be to assemble these as well from available reagents. A number of efficient, often metal catalyzed, routes to access pyrroles have recently been reported, including those that exploit multicomponent reactions and tandem catalysis.[6] For example, our lab has demonstrated that pyrroles can be generated via a palladium catalyzed carbonylative coupling of acid chlorides,

imines and alkynes.[7] A feature of this latter reaction is the ability to access diversely substituted pyrroles with high chemoselectivity from three distinct and simple building blocks.

The efficiency of this transformation led us to question if we might develop a unique synthesis of a complex pharmaceutical core such as Atorvastatin in one step via a metal catalyzed multicomponent coupling reaction.[8] The development of this transformation presents several significant challenges. Firstly, the catalyst and complex catalytic cycle for this multicomponent reaction must be compatible with the dense functionality in **6.1**, which has not to date been viable. This includes moving beyond common aromatic substrates (e.g. aromatic acid chlorides) to employ more reactive alkyl acid chlorides. In addition, the reaction would ideally operate at low catalyst loadings, rather than the 10-20 mol% Pd currently required for efficient catalysis. We describe below our efforts towards the design of this synthesis. These have led to the unexpected discovery of a highly efficient palladium catalyst for the carbonylative formation of pyrroles. This catalyst system offers a broadly general approach to assemble pyrroles, including the multicomponent assembly of Atorvastatin, in a single palladium catalyzed operation from combinations of commercial, inexpensive, and easily modulated substrates.

6.3. Results and Discussion

At the outset, we probed the application of our previously developed palladium catalyst to the assembly of the model substrates for Atorvastatin. As shown in Scheme **6.2a**, this leads predominately to the recovery of starting materials together with some decomposition at the elevated temperatures required for reaction.[9] Mechanistic studies on the formation of pyrroles have previously shown that the reaction proceeds via the catalytic formation of a 1,3-dipolar Münchnone followed by alkyne cycloaddition (Scheme 6.2b). In this, iminium salt generation and its oxidative addition to palladium are rapid, and the rate determining step is $P(o\text{-}Tol)_3$ labilization for CO insertion.[10] We therefore postulated that the inefficiency of this synthesis may be tied to the slow carbonylative formation of Münchnone **6.2**, and could be addressed by employing ligands that can be more labile for this CO association step to palladium.

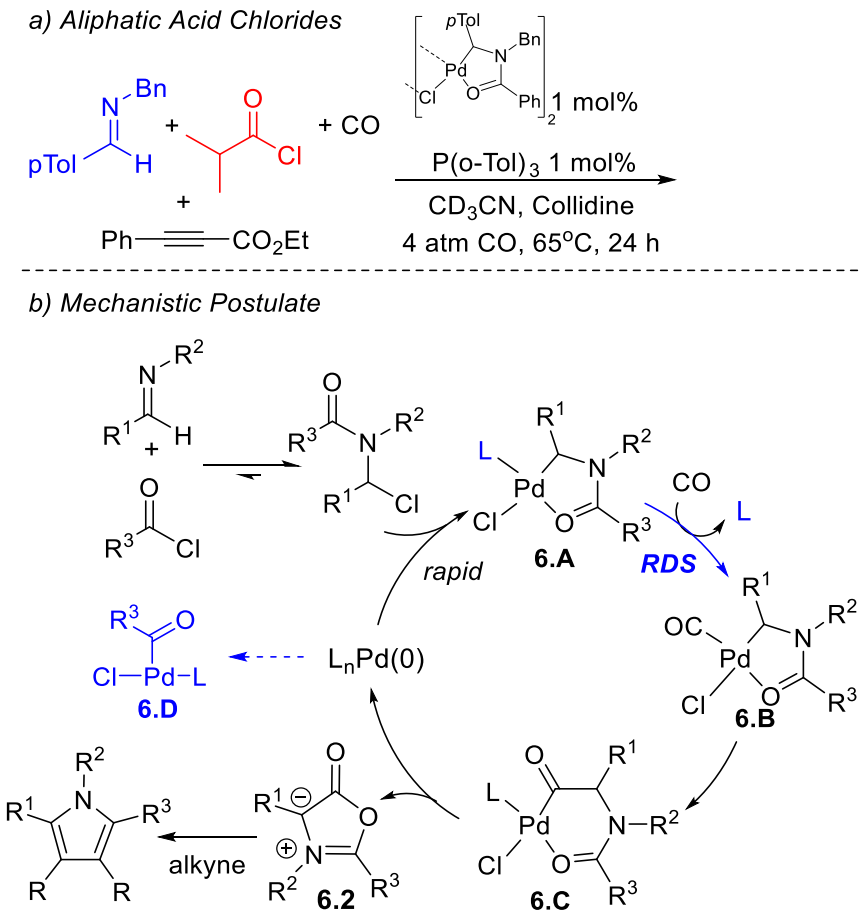

Scheme 6.2. Previous studies and Mechanistic Postulate.

In order to create a more active catalyst, we examined various ligands in the initial formation of Münchnone **6.2** at short reaction times (3 h, Table 6.1). As expected, smaller, strongly coordinating phosphines inhibit catalysis under these conditions (entries 1-4). In contrast, more sterically encumbered phosphines such as P^tBu_3 and P(1-adamantyl)$_2$Bu (entries 5, 6) lead to an increase in catalytic activity, potentially due to their size leading to more facile displacement by CO in **6.B**. Based upon this trend, we next examined the large 2-biaryl-phosphine ligands developed by Buchwald,[11] which significantly increase the reaction rate, and provide Münchnone product in now 57% yield together with unreacted imine (entry 7). Both the slightly smaller cyclohexyl variant of this ligand (entry 8), and more sterically encumbered systems (entries 9-11), lead to decreased activity, suggesting that catalysis requires balancing the

lability of the phosphine (e.g. in **6.A**) with its ability to coordinate and stabilize palladium in the catalytic cycle.

Table 6.1. Catalyst Optimization for Münchnone Formation

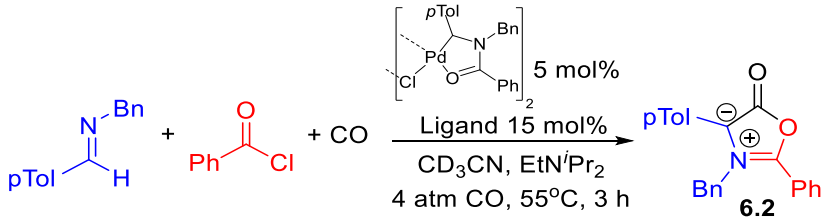

entry	L	% **6.2**[b]	entry	L	% **6.2**[b]	entry	L	% **6.2**[b]
1	P(*o*-Tol)$_3$	6	7		57	13	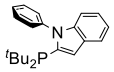	66
2	P(C$_6$F$_5$)$_3$	14	8		2	14		38
3	PCy$_3$	0	9		49	15	 **6.3**	70
4	P(OEt)$_3$	0	10		29	16[c]	**6.3**	52
5	P(^{t}Bu)$_3$	24	11		13	17[c,d]	**6.3**	87
6		24	12		31	18[d,e]	**6.3**	82

[a] Imine (21 mg, 0.1 mmol), benzoyl chloride (21 mg, 0.15 mmol), EtN^{i}Pr$_2$ (16 mg, 0.12 mmmol), Pd cat. (4.5 mg, 0.005 mmol), Ligand (0.015 mmol), CO 4 atm, 55°C, 3 h. [b] Yield determined in respect to BnOBz internal standard. [c] 0.5 mol% Pd cat., 24 h, 4 atm CO. [d] benzoyl chloride (14 mg, 0.1 mmol), [e] Pd cat. 5 mol%, r.t.

The more electron rich di-t-butyl-N-arylpyrrole phosphine motif developed by Beller was examined.[12] While sterically more encumbered variants of this ligand do not improve the reaction (entry 12), we were please to find that the use of 2-phenylpyrrole-based ligand **6.3** results in a significant increase in catalytic activity over the other ligands examined, and the formation of **6.2** in 70% yield (entry 15).

In order to further improve catalysis, we next performed mechanistic studies on the catalyst with ligand **6.3**. Interestingly, kinetic analysis shows a first order rate dependence on iminium salt concentration, implying that oxidative addition is now rate determining (see figure 6.1 in the supporting information). This was unexpected, since the stoichiometric oxidative addition of iminium salts to Pd(0) is typically rapid at ambient temperature. The origin of this change in the rate determining step can be seen by monitoring the reaction by ^{31}P NMR analysis, which shows the build-up of a single palladium intermediate that represents over 65 % of the catalyst (Figure 6.2 in the supporting information). This complex is not the expected phosphine coordinated palladacycle **6.B**, but instead the acid chloride oxidative addition product **6.D** (Scheme 6.2b).[13] **6.D** is presumably formed from the excess of acid chloride used in the reaction to drive the formation of N-acyl iminium salt. Complex **6.D** is an off-cycle resting state that must dissociate to enter the productive cycle. As such, by removing the excess acid chloride, and therefore keeping palladium in the catalytic cycle, catalyst activity with this ligand can be significantly increased (entry 15). This catalyst system can now allow the formation of Münchnone at catalyst loadings as low as 0.5 mol% and with commercial $[Pd(allyl)Cl]_2$ (entry 17), or at ambient temperature (entry 18). As illustrated in Figure 6.1, this represents a nearly two orders of magnitude increase activity relative to the original catalyst system.

The increased catalytic activity with **6.3** offers a broadly applicable system for the multicomponent synthesis of pyrroles with alkynes. As shown in Table 6.2-3, performing the reaction in the presence of ethyl phenylpropiolate leads to the high yield formation of pyrrole **6.4a** at low reaction temperatures (45°C) and with 0.5 mol% catalyst. In addition, this reaction can be straight-forward to diversify. For example, N-alkyl and N-benzyl substituted imines are viable substrates in this chemistry, as are electron rich N-aryl imines (**6.4a-d,p**). On the imine carbon, an array of electron rich or electron poor aryl-substituents can be employed (**6.4a-n**), as can heterocyclic units (**6.4o,q**). The reaction also tolerates electron rich and electron poor acid

chlorides (**6.4r-u**). The high catalyst activity even allows the use of alkyl substituted acid chlorides without competing ketene formation by employing a slightly weaker collidine base (**6.4v-z**). Finally, various electron deficient alkyne dipolarophiles can be incorporated into this platform to modulate the 3,4-pyrrole substituents. These more reactive alkynes must be added subsequent to Münchnone generation to avoid side reactions with the amine base. Examples include alkynes with esters (**6.4aa-bb**) and terminal alkynes (**6.4cc**). In analogy to previous reports, electron deficient alkenes are also viable substrates for cycloaddition and pyrrole formation, and offer access to cyano (**6.4ff**) and phenyl (**6.4ee**) substituted pyrrole, and even simple 3,4-unsubstituted pyrroles (**6.4dd**).

Table 6.2. Multicomponent Synthesis of Pyrroles: Imine Diversity

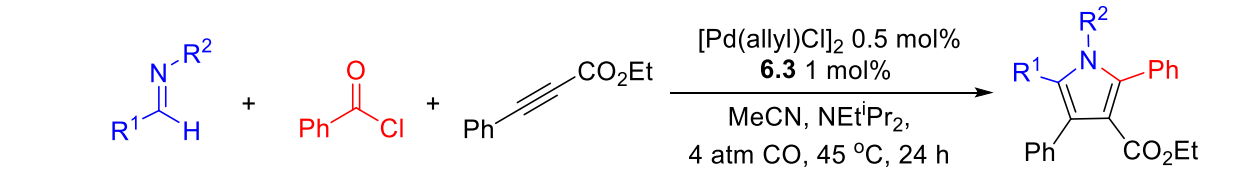

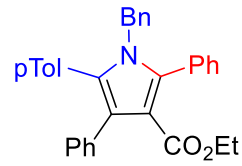

6.4a, 87%

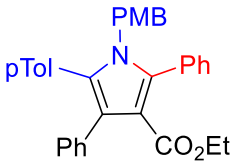

6.4b, 91%

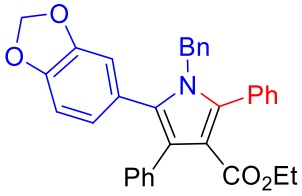

6.4c, 83%

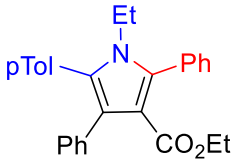

6.4d, 88%

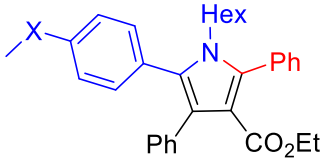

6.4e, X = S 83%
6.4f, X = O 87%

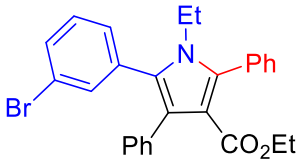

6.4g, 79%

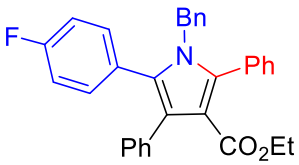

6.4h, 80%

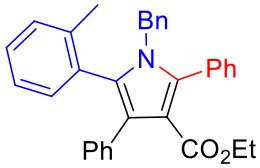

6.4i, 81%

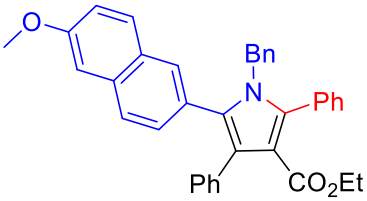

6.4j, 86%

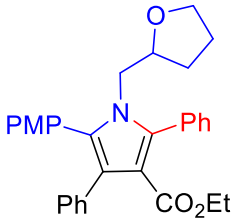

6.4k, 84%

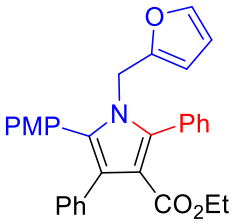

6.4l, 79%

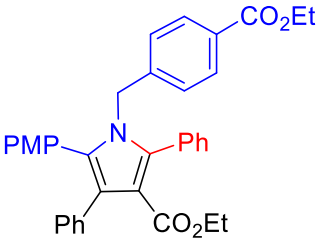

6.4m, 85%

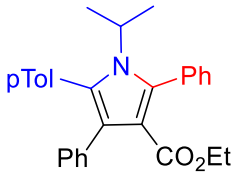

6.4n, 75%

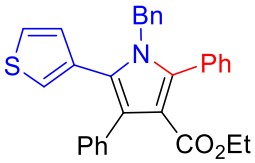

6.4o, 75%

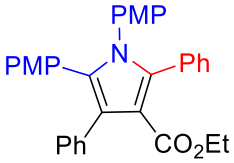

6.4p, 82%

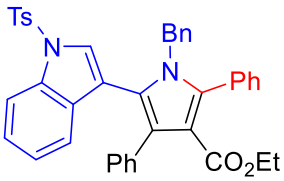

6.4q, 65%

[a] Imine (0.5 mmol), acid chloride (0.5 mmol), EtN^iPr_2 (0.6 mmol), alkyne (0.6 mmol), Pd cat. (0.0025 mmol), ligand **6.3** (0.0025 mmol), CO 4 atm, 45°C, 24 h. [b] Collidine (0.6 mmol) used instead of EtN^iPr_2.

.

Table 6.3. Multicomponent Synthesis of Pyrroles: Alkyne, Alkene and Acid Chloride Diversity

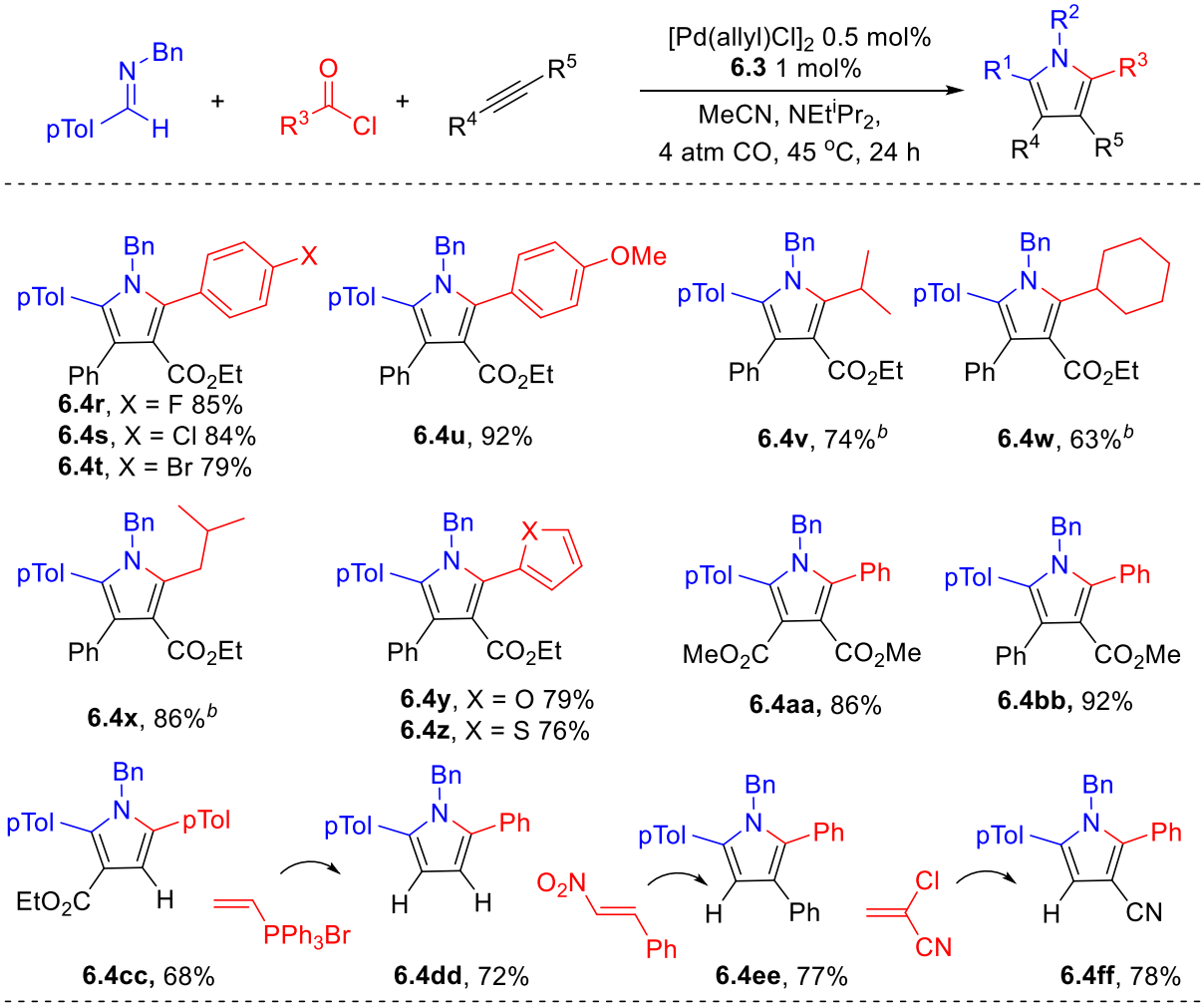

[a] Imine (0.5 mmol), acid chloride (0.5 mmol), EtN^iPr_2 (0.6 mmol), alkyne (0.6 mmol), Pd cat. (0.0025 mmol), ligand **6.3** (0.0025 mmol), CO 4 atm, 45°C, 24 h. [b] Collidine (0.6 mmol) used instead of EtN^iPr_2.

Overall, this palladium catalyst offers a straightforward method to generate pyrroles with a diverse array of substituted reagents and under mild conditions. This chemistry can also be applied to the assembly Atorvastatin. The palladium catalyzed coupling of imine **6.5** with acid chloride and CO followed by alkyne addition leads to the formation of **6.1** in 71% yield following hydrolysis. Of note, this transformation exploits substrates that are each inexpensive and commercially available, including imine **6.5**, generated in a single step from a commercially available amine and 4-fluorobenzaldehyde, isobutyroyl chloride and diphenylpropiolamide, and

offers what is to our knowledge a unique platform to directly assemble a high-volume drug core in a metal catalyzed multicomponent reaction. The reaction proceeds at low catalyst loading, in high overall yield and with minimal byproducts.

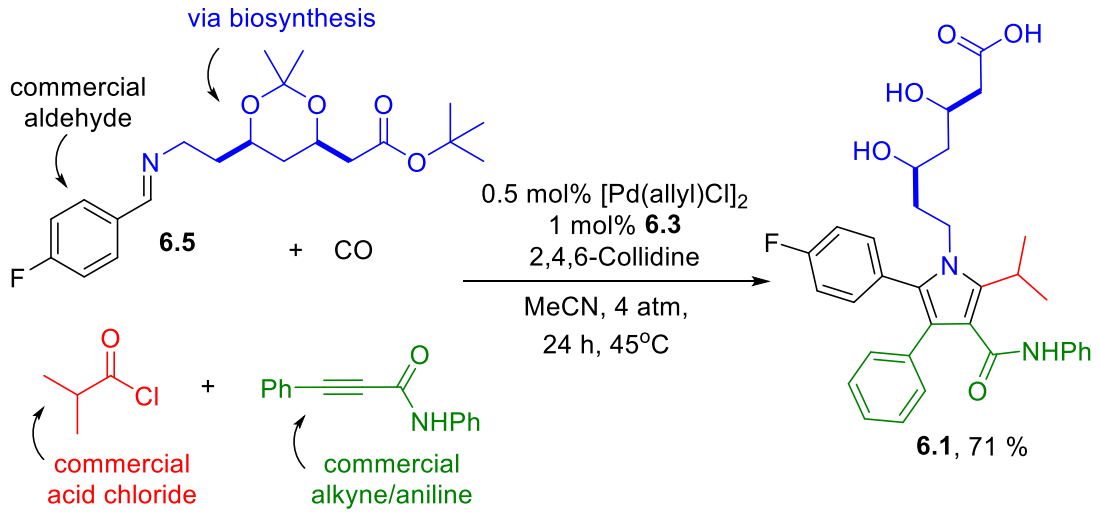

Scheme 6.3. Palladium Catalyzed Carbonylative Multicomponent Synthesis of Atorvastatin.

6.4. Conclusions

In conclusion, we have developed an efficient and broadly applicable palladium catalyst for the multicomponent assembly of pyrroles from imines, alkynes and acid chlorides. This transformation proceeds at low catalyst loadings, and illustrates how phosphine steric labilization can lead to an exceptionally active palladium catalyst for the carbonylation for iminium salts. Relative to other approaches to pyrroles, this offers a method to generate pyrroles from three different units, and therefore can be exploited to generate these heterocycles with independent control over all five substituents, and each can be broadly diversified. Overall, this has allowed the development of a multicomponent assembly of Atorvastatin in one pot, and from combinations of available reagents.

6.5. Supporting Information

6.5.1. General Considerations

All reactions were carried out under an inert atmosphere in a glovebox or using standard Schlenk techniques, unless otherwise indicated. Research grade carbon monoxide (99.99%) was used as received. All solvents were dried using a solvent purification system and stored in glovebox over activated 4 Å molecular sieves. Deuterated solvents were dried over CaH_2, vacuum transferred and stored over 4 Å molecular sieves. N-alkyl, N-aryl imines were prepared according to literature procedures.[14] Palladium precatalyst was synthesized according to literature procedure.[14] All other reagents were purchased from commercial suppliers and used as received. All ^1H and ^{13}C NMR spectra were acquired on 400 and 500 MHz spectrometers. High resolution mass spectra were obtained using a quadrupole-time of flight and an Orbitrap detector by direct infusion in positive ESI mode.

6.5.2. Synthetic Procedures

Typical Procedure for Catalyst Screening (Table 6.1)

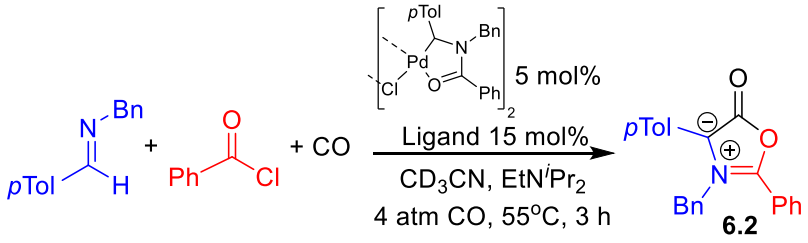

In a glovebox, benzoyl chloride (21 mg, 0.15 mmol), *p*-TolC=NBn (21 mg, 0.10 mmol), EtN^iPr_2 (16 mg, 0.12 mmol), palladium precursor (4.5 mg, 0.005 mmol), ligand (0.015 mmol), and benzyl benzoate internal standard were dissolved in CD_3CN (0.7 mL) and added to a J-Young NMR tube. The tube was removed from the glovebox, frozen in liquid nitrogen, the headspace evacuated, and 4 atm carbon monoxide was condensed into the NMR tube. The reaction was heated at 55 °C and monitored by ^1H NMR spectroscopy. The yield of **6.2** was determined by ^1H NMR analysis relative to the internal standard.

General Procedure for Pyrrole **6.4** formation (Table 2)

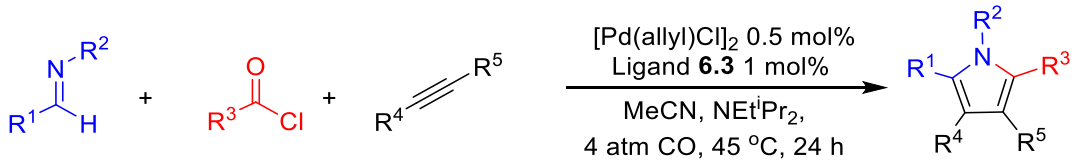

In a glovebox, acid chloride (0.5 mmol), imine (0.50 mmol), alkyne (0.6 mmol), EtN^iPr_2 (77.8 mg, 0.6 mmol) were combined in MeCN (4 mL). To this solution 1 mL of palladium catalyst stock solution was added ($[Pd(allyl)Cl]_2$ (9.1 mg, 0.025 mmol) and CataCXiumPtB (14.4 mg, 0.05 mmol) dissolved in MeCN (10 mL)). The obtained solution was transferred into a 50 mL pressure vessel. The pressure vessel was pressurized with CO (4 atm) and heated at 45 °C for 24 hours. Products were purified by silica gel chromatography using hexanes/ethyl acetate as eluent.

Procedure for the synthesis of Complex **6.D**

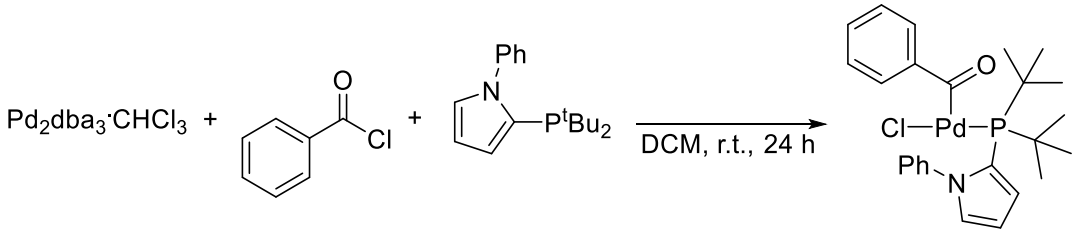

6.D, 82%

In a glovebox, $Pd_2dba_3{\cdot}CHCl_3$ (207 mg, 0.2 mmol) and benzoyl chloride (56 mg, 0.4 mmol) were combined in dichloromethane (10 mL). Obtained solution was allowed to stir for 5 min, after which 2-(di-tert-butylphosphanyl)-1-phenyl-1H-pyrrole (115 mg, 0.4 mmol) solution in dichloromethane (10 mL) was added. The obtained solution was allowed to stir overnight. Afterwards the reaction mixture was filtered through celite and evaporated. Obtained crude product was washed with diethyl ether (4 x 5 mL) affording complex **6.D** as a yellow solid in 82% yield (175 mg). ^{1}H NMR (500 MHz, Acetonitrile-d_3) δ 7.94 (d, J = 7.0 Hz, 2H), 7.78 – 7.72 (m, 1H), 7.71 – 7.65 (m, 2H), 7.57 – 7.53 (m, 1H), 7.43 (t, J = 7.8 Hz, 2H), 7.35 (d, J = 7.5 Hz, 2H), 6.95 – 6.92 (m, 1H), 6.89 – 6.84 (m, 1H), 6.47 (ddd, J = 3.8, 2.7, 0.9 Hz, 1H), 1.30 (d, J = 15.1 Hz, 18H). ^{13}C NMR (126 MHz, Acetonitrile-d_3) δ 203.4 (d, J = 6.7 Hz), 139.1, 132.5, 132.4, 131.2, 131.1, 129.9 (d, J = 4.3 Hz), 128.1, 125.5, 123.8 (d, J = 46.7 Hz), 121.4 (d, J = 1.4

Hz), 117.0, 110.9 (d, J = 5.7 Hz), 37.5 (d, J = 20.0 Hz), 29.2 (d, J = 6.2 Hz). ^{31}P NMR (203 MHz, Acetonitrile-d_3) δ 35.08.

Procedure for the synthesis of 2-(di-tert-butylphosphanyl)-1-methyl-1H-pyrrole

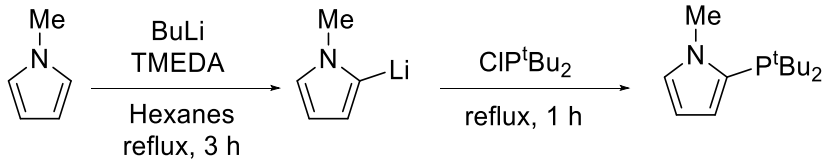

In glovebox, N-methylpyrrole (0.811 g, 10 mmol) was dissolved in n-hexanes (20 mL) and added to a sealable flask. To this solution TMEDA (1.74 g, 15 mmol) and n-BuLi (10 mmol, 1.6 M in hexanes) were added at room temperature. Afterwards the flask was sealed and heated to reflux temperature for 3 h. Afterwards the reaction mixture was cooled down and solution of di-tert-butylchlorophosphine (1.81 g, 10 mmol) in hexanes (5 mL) was added. The reaction mixture was heated again to reflux for an additional hour. After cooling down to room temperature, degassed water (15 mL) was added and the mixture was stirred to get a clear solution. The organic layer was collected and washed once more with degassed distilled water (15 mL). The obtained organic layer was dried over Na_2SO_4 and concentrated in vacuo giving the desired product as a pale yellow liquid in 86% yield (1.94 g). ^{1}H NMR (400 MHz, $CDCl_3$) δ 6.83 (ddd, J = 4.2, 2.4, 1.7 Hz, 1H), 6.56 (dd, J = 3.7, 1.6 Hz, 1H), 6.22 (dd, J = 3.7, 2.6 Hz, 1H), 3.81 (s, 3H), 1.19 (d, J = 12.3 Hz, 18H). ^{13}C NMR (101 MHz, $CDCl_3$) δ 126.9 (d, J = 7.0 Hz), 125.0 (d, J = 2.6 Hz), 117.1 (d, J = 4.8 Hz), 107.4, 36.0 (d, J = 19.4 Hz), 32.6 (d, J = 14.7 Hz), 30.2 (d, J = 14.7 Hz). ^{31}P NMR (162 MHz, $CDCl_3$) δ 2.12.

Procedure for the synthesis of Atorvastatin **6.1**

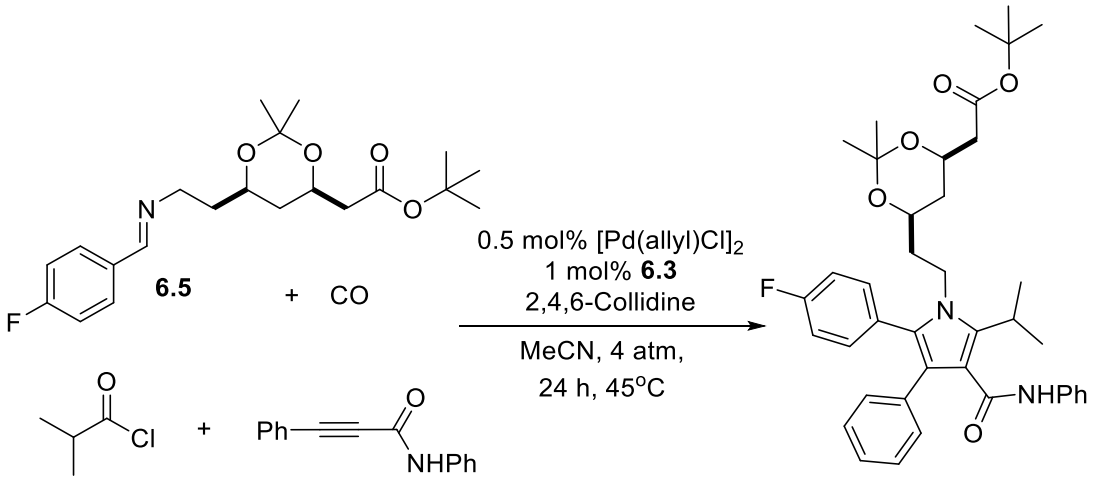

In a glovebox, isobutyryl chloride (64 mg, 0.6 mmol), imine **6.5** (188 mg, 0.50 mmol), collidine (73 mg, 0.6 mmol) were combined in MeCN (4 mL). To this solution 1 mL of palladium catalyst stock solution was added ($[Pd(allyl)Cl]_2$ (9.1 mg, 0.025 mmol) and CataCXiumPtB (14.4 mg, 0.05 mmol) dissolved in MeCN (10 mL)). The obtained solution was transferred into a 50 mL pressure vessel. The pressure vessel was pressurized with CO (4 atm) and heated at 45 ºC for 24 hours. Afterwards the carbon monoxide was removed and the pressure vessel was brought back to the glove box. N,3-diphenylpropiolamide (133 mg, 0.6 mmol) and N,N′-Diisopropylcarbodiimide (126 mg, 0.1 mmol) were added to the pressure vessel. The reaction flask was sealed and heated overnight at 65 ºC. Products was purified by silica gel chromatography using hexanes/ethyl acetate as eluent affording the product as pale white solid.

Tert-butyl 2-((4R,6R)-6-(2-(2-(4-fluorophenyl)-5-isopropyl-3-phenyl-4-(phenylcarbamoyl)-1H-pyrrol-1-yl)ethyl)-2,2-dimethyl-1,3-dioxan-4-yl)acetate ^{1}H NMR (500 MHz, $CDCl_3$) δ 7.18–7.14 (m, 9H), 7.07 (d, 2H, *J* = 8.0 Hz), 6.99–6.94 (m, 3H), 6.88 (s, 1H), 4.18–4.04 (m, 2H), 3.86–3.80 (m, 1H), 3.70–3.68 (m, 1H), 3.60–3.54 (m, 1H), 2.37 (dd, 1H, *J* = 15.3, 7.1 Hz), 2.23 (dd, 1H, *J* = 15.3, 6.1 Hz), 1.69–1.66 (m, 2H), 1.53 (d, 6H, J = 7.1 Hz), 1.43 (s, 9H), 1.36 (s, 3H), 1.29 (s, 3H), 1.09–1.01 (m, 1H). ^{13}C NMR (126 MHz, $CDCl_3$) δ 170.2, 164.8, 163.2, 161.2, 141.5, 138.4, 134.6, 133.2, 133.1, 130.5, 129.0, 128.9, 128.8, 128.6, 128.3, 126.5, 123.5, 121.8, 119.5, 115.4, 115.2, 98.7, 80.7, 66.4, 65.9, 42.5, 40.8, 38.1, 36.0, 28.1, 26.1, 21.7, 21.5, 19.7. ^{19}F NMR (471 MHz, $CDCl_3$) δ -113.7. HRMS. Calculated for $C_{40}H_{47}N_2O_5FNa$ ($M+H^+$): 677.3361, found: 677.33431.

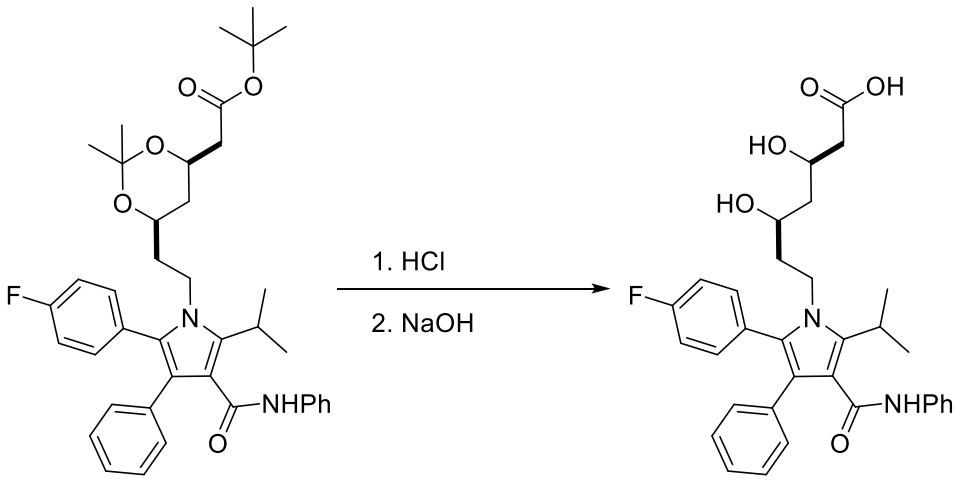

6.1

In a 25 mL round bottom flask, tert-butyl 2-((4R,6R)-6-(2-(2-(4-fluorophenyl)-5-isopropyl-3-phenyl-4-(phenylcarbamoyl)-1H-pyrrol-1-yl)ethyl)-2,2-dimethyl-1,3-dioxan-4-yl)acetate (165 mg, 0.25 mmol) was dissolved in THF (10 mL), then aqueous HCl (1 mL, 10%) was added and the solution was stirred at room temperature for 15 hours. Afterwards NaOH (0.24 g, 6 mmol) were added and the solution was further stirred for 3 hours. The pH of the solution was adjusted to ~ 2 using 1M HCl solution. Solvents were evaporated in vacuo and the product was extracted with EtOAc/H_2O (2 x). The product was purified using flash chromatography using hexanes/ethyl acetate as eluent affording atorvastatin **6.1** as a pale white solid 112 mg, 69% yield. ^{1}H NMR (500 MHz, $CDCl_3$) δ 7.30–7.29 (m, 2H), 7.25–7.20 (m, 4H), 7.15–7.13 (m, 2H), 7.11–7.02 (m, 6H), 4.08 (ddd, *J* = 16.0, 7.8, 5.3 Hz 1H), 4.02–3.98 (m, 1H), 3.91 (ddd, *J* = 16.0, 7.6, 5.3 Hz, 1H), 3.69–3.63 (m, 1H), 3.40–3.34 (m, 1H), 2.41 (dd, J=5.2, 15.5 Hz, 1H), 2.35 (dd, *J* = 7.6, 15.5 Hz, 1H), 1.75–1.6 (m, 2H), 1.56–1.51 (m, 1H), 1.49 (d, J=7.1 Hz, 3H), 1.48 (d, *J* = 7.1 Hz, 3H), 1.47–1.43 (m, 1H); ^{13}C NMR (126 MHz, $CDCl_3$) δ 175.9, 169.5, 163.8 (1JCF=245.5 Hz), 139.9, 139.1, 139.1, 136.4, 134.7 (3JCF=7.2 Hz), 131.0, 130.3 (4JCF=2.9 Hz), 129.6, 128.9, 126.9, 125.2, 123.3, 121.5, 118.1, 116.3 (2JCF=21.6 Hz), 68.6, 67.9, 44.2, 43.3, 42.2, 40.1, 27.7, 22.9, 22.8; ^{19}F NMR (471 MHz, $CDCl_3$) δ −113.1;

6.5.3 Kinetic Studies

In glovebox, *p*-Tol(H)C=NBn (21 mg, 0.10 mmol), PhCOCl (21 mg, 0.15 mmol), EtN^iPr_2 (64 mg, 0.50 mmol), and benzyl benzoate internal standard were combined in CD_3CN stock solution (0.7 mL) containing **6.3** (0.43 mg, 0.0015 mmol), [Pd(Cl)[κ^2-CH(*p*-Tol)NBn(COPh)]$_2$ (0.45 mg,

0.0005 mmol), and transferred into a J-Young NMR tube. The tube was brought outside of the glovebox, the solution was frozen, and 4 atm carbon monoxide was condensed into the NMR tube. The NMR tube was heated at 45°C in an NMR spectrometer for 12 h and the reaction was monitored by ^{1}H NMR analysis. Generation of **6.2** and disappearance of imine were determined in respect to benzyl benzoate internal standard.

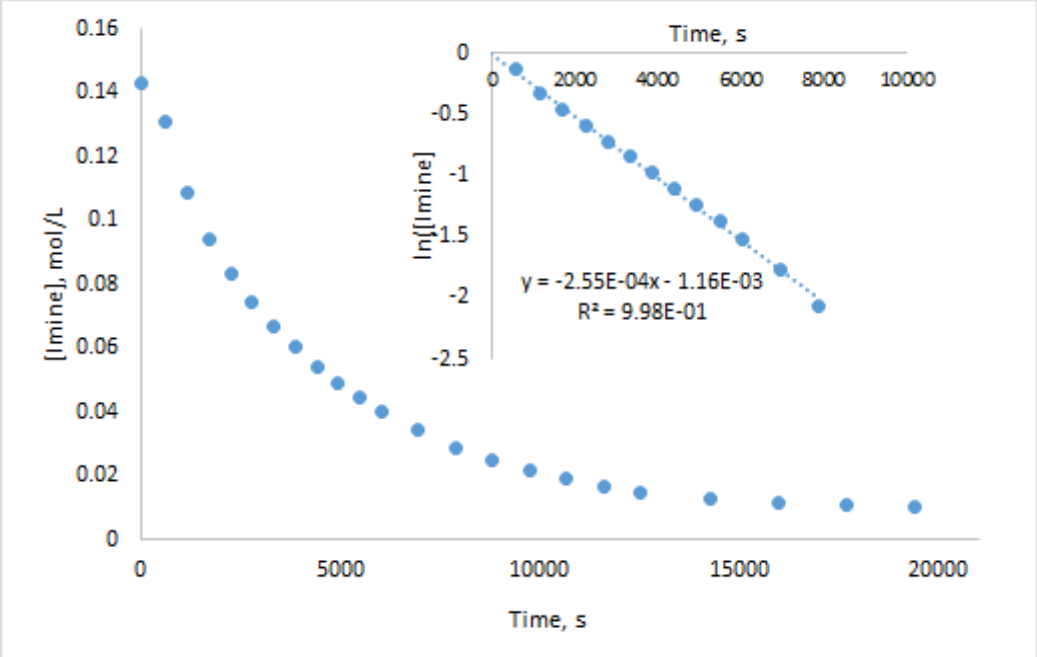

Figure 6.1. Kinetic Plot for imine consumption vs time.

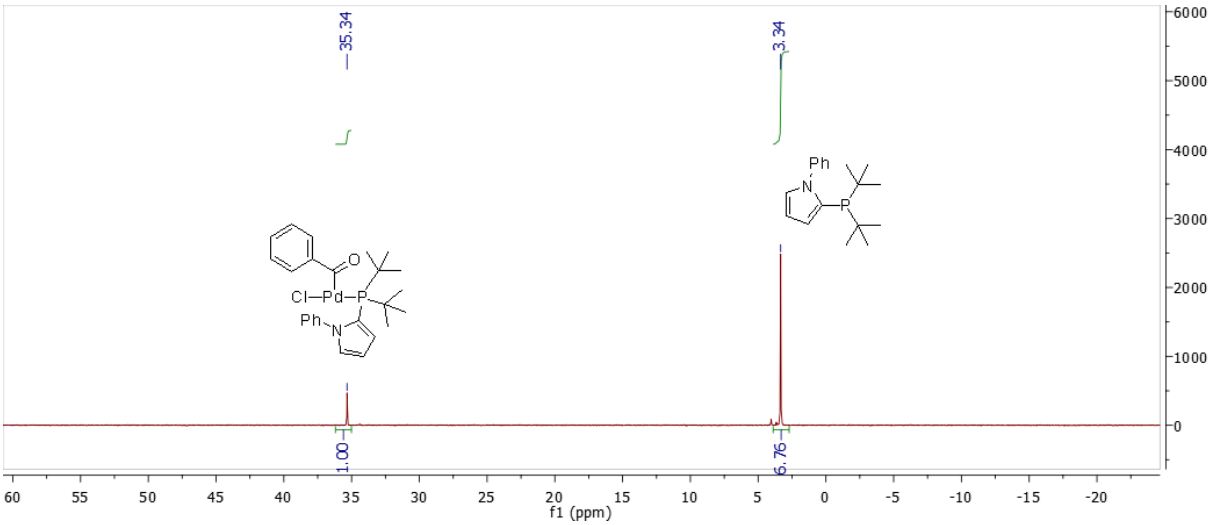

Figure 6.2. *In situ* ^{31}P NMR spectrum of the catalytic formation of 6.2.

6.5.4. Spectroscopic Data on 6.4

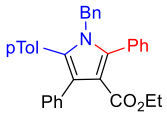

Ethyl 1-benzyl-2,4-diphenyl-5-(p-tolyl)-1H-pyrrole-3-carboxylate 6.4a. White solid, 203 mg, 86% yield. ^{1}H NMR (500 MHz, $CDCl_3$) δ 7.41 – 7.33 (m, 5H), 7.33 – 7.26 (m, 2H), 7.24 (t, J = 7.3 Hz, 2H), 7.21 – 7.15 (m, 4H), 7.04 (q, J = 8.1 Hz, 4H), 6.69 (dd, J = 6.5, 2.8 Hz, 2H), 5.01 (s, 2H), 3.97 (q, J = 7.1 Hz, 2H), 2.30 (s, 3H), 0.85 (t, J = 7.2 Hz, 3H). ^{13}C NMR (126 MHz, $CDCl_3$) 165.2, 138.6, 138.2, 137.4, 135.4, 132.9, 132.5, 131.2, 130.85, 130.79, 128.8, 128.7, 128.22, 128.18, 127.8, 127.2, 127.0, 126.1, 125.9, 124.4, 113.5, 59.4, 48.5, 21.3, 13.6. HRMS. Calculated for $C_{33}H_{30}NO_2$ ($M+H^+$): 472.2271, found: 472.2259.

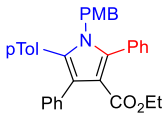

Ethyl 1-(4-methoxybenzyl)-2,4-diphenyl-5-(p-tolyl)-1H-pyrrole-3-carboxylate 6.4b. White solid, 228 mg, 91% yield. ^{1}H NMR (500 MHz, $CDCl_3$) δ 7.37 (s, 5H), 7.29 – 7.26 (m, 2H), 7.22 (t, J = 7.3 Hz, 2H), 7.17 (t, J = 7.2 Hz, 1H), 7.04 (d, J = 2.1 Hz, 4H), 6.68 (d, J = 8.7 Hz, 2H), 6.55 (d, J = 8.7 Hz, 2H), 4.93 (s, 2H), 3.95 (q, J = 7.1 Hz, 2H), 3.76 (s, 3H), 2.31 (s, 3H), 0.83 (t, J = 7.1 Hz, 3H). ^{13}C NMR (126 MHz, $CDCl_3$) δ 165.2, 158.5, 138.5, 137.4, 135.4, 132.7, 132.5, 131.2, 130.9, 130.8, 130.8, 130.3, 128.8, 128.7,

128.1, 127.8, 127.4, 127.2, 125.8, 124.4, 113.6, 113.5, 59.3, 55.2, 47.9, 21.3, 13.6. HRMS. Calculated for $C_{34}H_{31}NKO_3$ ($M+K^+$): 540.1936, found: 540.1950.

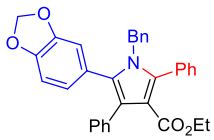

Ethyl 5-(benzo[d][1,3]dioxol-5-yl)-1-benzyl-2,4-diphenyl-1H-pyrrole-3-carboxylate 6.4c. White solid, 208 mg, 83% yield. ^{1}H NMR (500 MHz, $CDCl_3$) δ 7.35 (s, 5H), 7.29 – 7.21 (m, 4H), 7.20 – 7.14 (m, 4H), 6.69 – 6.56 (m, 5H), 5.91 (s, 2H), 4.97 (s, 2H), 3.94 (q, J = 7.1 Hz, 2H), 0.82 (t, J = 7.2 Hz, 3H). ^{13}C NMR (126 MHz, $CDCl_3$) δ 165.2, 147.2, 147.2, 138.5, 138.1, 135.2, 132.3, 132.2, 130.8, 130.7, 128.24, 128.19, 127.8, 127.2, 127.0, 126.1, 125.9, 125.4, 125.2, 124.6, 113.4, 111.6, 108.0, 101.0, 59.4, 48.4, 13.5. HRMS. Calculated for $C_{33}H_{28}NO_4$ ($M+H^+$): 502.2013, found: 502.1996.

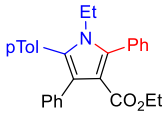

Ethyl 1-ethyl-2,4-diphenyl-5-(p-tolyl)-1H-pyrrole-3-carboxylate 6.4d. White solid, 180 mg, 88% yield. ^{1}H NMR (500 MHz, $CDCl_3$) δ 7.55 – 7.44 (m, 5H), 7.26 – 7.12 (m, 9H), 3.93 (q, J = 7.2 Hz, 2H), 3.81 (q, J = 7.1 Hz, 2H), 2.36 (s, 3H), 0.91 (t, J = 7.2 Hz, 3H), 0.82 (t, J = 7.1 Hz, 3H). ^{13}C NMR (126 MHz, $CDCl_3$) δ 165.2, 137.7, 137.4, 135.5, 132.9, 131.8, 131.2, 130.8, 130.7, 130.6, 129.1, 129.0, 128.9, 128.8, 128.21, 128.16, 128.0, 127.1, 125.7, 124.1, 113.0, 59.2, 39.8, 21.3, 16.3, 13.6. HRMS. Calculated for $C_{28}H_{28}NO_2$ ($M+H^+$): 410.2115, found: 410.2112.

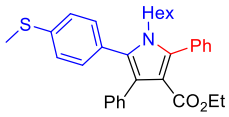

Ethyl 1-hexyl-5-(4-(methylthio)phenyl)-2,4-diphenyl-1H-pyrrole-3-carboxylate 6.4e. pale yellow oil, 207 mg, 83% yield. ^{1}H NMR (500 MHz, $CDCl_3$) δ 7.52 – 7.43 (m, 5H), 7.24 – 7.15 (m, 9H), 3.92 (q, J = 7.2 Hz, 2H), 3.78 – 3.72 (m, 2H), 2.49 (s, 3H), 1.26 (p, J = 7.6, 7.0 Hz, 2H), 1.06 (q, J = 7.3 Hz, 2H), 0.95 – 0.85 (m, 4H), 0.82 (t, J = 7.1 Hz, 3H), 0.76 (t, J = 7.3 Hz, 3H). ^{13}C NMR (126 MHz, $CDCl_3$) δ 165.2, 138.3, 138.0, 135.4, 132.8, 131.5, 130.8, 130.8, 128.7, 128.2, 127.9, 127.2, 125.8, 124.3, 113.0, 59.3, 44.9, 30.8, 30.4, 25.9, 22.2, 15.3, 13.9, 13.6. HRMS. Calculated for $C_{32}H_{36}NSO_2$ ($M+H^+$): 498.2461, found: 498.2477.

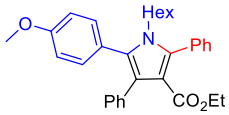

Ethyl 1-hexanoyl-5-(4-methoxyphenyl)-2,4-diphenyl-1H-pyrrole-3-carboxylate 6.4f. colorless oil, 209 mg, 87% yield. ^{1}H NMR (500 MHz, $CDCl_3$) δ 7.52 – 7.44 (m, 5H), 7.25 – 7.13 (m, 7H), 6.86 (d, *J* = 8.7 Hz, 2H), 3.93 (q, *J* = 7.1 Hz, 2H), 3.82 (s, 3H), 3.75 – 3.70 (m, 2H), 1.32 – 1.22 (m, 2H), 1.05 (p, *J* = 7.2 Hz, 2H), 0.93 – 0.86 (m, 4H), 0.82 (t, *J* = 7.2 Hz, 3H), 0.75 (t, *J* = 7.3 Hz,3). ^{13}C NMR (126 MHz, $CDCl_3$) δ 165.3, 159.0, 137.9, 135.5, 132.9, 132.5, 131.9, 130.8, 130.8, 128.1, 127.9, 127.1, 125.7, 124.4, 124.0, 113.7, 112.8, 59.2, 55.2, 44.8, 30.8, 30.4, 25.9, 22.2, 13.8, 13.6. HRMS. Calculated for $C_{32}H_{36}NO_3$ ($M+H^+$): 482.2690, found: 482.2695.

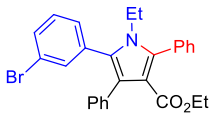

Ethyl 5-(3-bromophenyl)-1-ethyl-2,4-diphenyl-1H-pyrrole-3-carboxylate 6.4g. White solid, 187 mg, 79% yield. ^{1}H NMR (500 MHz, $CDCl_3$) δ 7.50 – 7.42 (m, 7H), 7.23 – 7.15 (m, 7H), 3.91 (q, *J* = 7.1 Hz, 2H), 3.81 (q, *J* = 7.1 Hz, 2H), 0.91 (t, *J* = 7.1 Hz, 3H), 0.80 (t, *J* = 7.1 Hz, 3H). ^{13}C NMR (126 MHz, $CDCl_3$) δ 164.9, 138.3, 134.9, 134.2, 133.9, 132.6, 130.8, 130.7, 130.7, 130.1, 130.0, 129.7, 128.3, 128.0, 127.3, 126.1, 125.0, 122.1, 113.3, 59.3, 39.9, 16.3, 13.5. HRMS. Calculated for $C_{27}H_{25}BrNO_2$ ($M+H^+$): 474.1063, found: 474.1064.

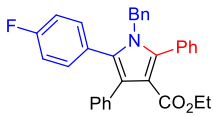

Ethyl 1-benzyl-5-(4-fluorophenyl)-2,4-diphenyl-1H-pyrrole-3-carboxylate 6.4h. White solid, 190 mg, 80% yield. ^{1}H NMR (500 MHz, $CDCl_3$) δ 7.39 (m, 5H), 7.27 – 7.15 (m, 8H), 7.09 – 7.05 (m, 2H), 6.88 (t, *J* = 8.7 Hz, 2H), 6.67 (dd, *J* = 6.6, 2.9 Hz, 2H), 4.97 (s, 2H), 3.96 (q, *J* = 7.1 Hz, 2H), 0.84 (t, *J* = 7.1 Hz, 3H) . ^{13}C NMR (126 MHz, $CDCl_3$) δ 165.1, 162.2 (d, *J* = 247.7 Hz), 138.9, 137.9, 135.0, 133.1 (d, *J* = 8.2 Hz), 131.9 (d, *J* = 83.3 Hz), 130.81, 130.75, 130.7, 128.3, 128.8 127.9, 127.7 (d, *J* = 3.2 Hz), 127.3, 127.1, 126.06, 126.04, 125.0, 115.1 (d, *J* = 21.5 Hz), 113.5, 59.4, 48.5, 13.6. HRMS. Calculated for $C_{32}H_{27}NO_2F$ ($M+H^+$): 467.2020, found: 476.2027.

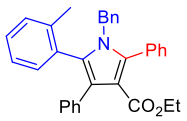

Ethyl 1-benzyl-2,4-diphenyl-5-(o-tolyl)-1H-pyrrole-3-carboxylate 6.4i. colorless oil, 191 mg, 81% yield. ^{1}H NMR (500 MHz, $CDCl_3$) δ 7.49 – 7.38 (m,

5H), 7.25 – 7.08 (m, 11H), 7.03 (d, J = 7.5 Hz, 1H), 6.60 (dd, J = 7.6, 1.5 Hz, 2H), 4.91 (d, J = 15.6 Hz, 1H), 4.80 (d, J = 15.7 Hz, 1H), 4.09 – 3.83 (m, 2H), 1.78 (s, 3H), 0.87 (t, J = 7.1 Hz, 3H). ^{13}C NMR (126 MHz, $CDCl_3$) δ 165.3, 138.9, 138.7, 137.6, 135.3, 132.5, 132.4, 131.7, 131.1, 131.0, 130.2, 129.9, 128.5, 128.2, 128.1, 127.9, 127.2, 127.1, 126.6, 125.8, 125.3, 124.6, 113.0, 59.4, 48.4, 19.6, 13.6. HRMS. Calculated for $C_{33}H_{30}NO_2$ ($M+H^+$): 472.2271, found: 472.2271.

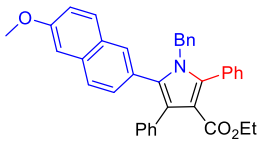

Ethyl 1-benzyl-5-(6-methoxynaphthalen-2-yl)-2,4-diphenyl-1H-pyrrole-3-carboxylate 6.4j. White solid, 231 mg, 86% yield. ^{1}H NMR (500 MHz, $CDCl_3$) δ 7.53 (dd, J = 9.0, 3.7 Hz, 3H), 7.41 (dd, J = 6.7, 2.7 Hz, 2H), 7.37 (dd, J = 4.2, 2.1 Hz, 3H), 7.30 – 7.28 (m, 2H), 7.17 (t, J = 7.2 Hz, 2H), 7.14 – 7.09 (m, 6H), 7.06 (d, J = 2.3 Hz, 1H), 6.67 – 6.64 (m, 2H), 5.02 (s, 2H), 3.96 (q, J = 7.0 Hz, 2H), 3.91 (s, 3H), 0.84 (t, J = 7.1 Hz, 3H). ^{13}C NMR (126 MHz, $CDCl_3$) 165.2, 158.0, 138.8, 138.2, 135.2, 133.7, 132.8, 132.4, 130.8, 130.8, 130.4, 129.6, 129.6, 128.4, 128.2, 127.8, 127.2, 127.0, 126.9, 126.4, 126.1, 125.9, 124.8, 118.9, 113.6, 105.5, 59.4, 55.3, 48.6, 13.6. HRMS. Calculated for $C_{37}H_{32}NO_3$ ($M+H^+$): 538.2377, found: 538.2357.

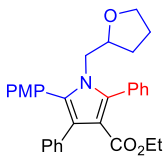

Ethyl 5-(4-methoxyphenyl)-2,4-diphenyl-1-((tetrahydrofuran-2-yl)methyl)-1H-pyrrole-3-carboxylate 6.4k. White solid, 202 mg, 84% yield. ^{1}H NMR (500 MHz, $CDCl_3$) δ 7.53 (d, J = 1.5 Hz, 2H), 7.50 – 7.40 (m, 3H), 7.25 – 7.13 (m, 7H), 6.84 (d, J = 8.9 Hz, 2H), 3.95 – 3.86 (m, 3H), 3.84 – 3.78 (m, 4H), 3.65 (p, J = 6.2, 5.6 Hz, 1H), 3.53 – 3.48 (m, 1H), 3.35 (ddd, J = 8.4, 7.2, 5.9 Hz, 1H), 1.58 (tdd, J = 12.4, 7.6, 3.7 Hz, 2H), 1.48 – 1.38 (m, 1H), 1.16 – 1.09 (m, 1H), 0.80 (t, J = 7.1 Hz, 3H). ^{13}C NMR (126 MHz, $CDCl_3$) δ 165.2, 158.9, 138.3, 135.5, 132.8, 132.6, 132.2, 131.2, 130.8, 128.1, 127.9, 127.1, 125.7, 124.3, 124.2, 113.7, 113.3, 67.5, 59.2, 55.1, 48.5, 28.8, 25.1, 13.5. HRMS. Calculated for $C_{31}H_{32}NO_4$ ($M+H^+$): 482.2326, found: 482.2311.

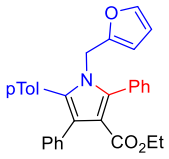

Ethyl 1-(furan-2-ylmethyl)-2,4-diphenyl-5-(p-tolyl)-1H-pyrrole-3-carboxylate 6.4l. White solid, 188 mg, 79% yield. ^{1}H NMR (500 MHz, $CDCl_3$) δ 7.44 (h, *J* = 4.2 Hz, 5H), 7.26 – 7.19 (m, 5H), 7.17 (d, *J* = 7.0 Hz, 1H), 7.10 (q, *J* = 8.2 Hz, 4H), 6.15 (dd, *J* = 3.2, 1.8 Hz, 1H), 5.53 (d, *J* = 2.6 Hz, 1H), 4.89 (s, 2H), 3.94 (q, *J* = 7.1 Hz, 2H), 2.34 (s, 3H), 0.83 (t, *J* = 7.1 Hz, 3H). ^{13}C NMR (126 MHz, $CDCl_3$) δ 165.1, 150.4, 141.7, 138.4, 137.5, 135.3, 132.6, 132.4, 131.3, 130.9, 130.7, 128.9, 128.6, 128.3, 127.8, 127.2, 125.8, 124.2, 113.5, 110.2, 107.6, 59.3, 42.1, 21.3, 13.5. HRMS. Calculated for $C_{31}H_{28}NO_3$ ($M+H^+$): 462.2064, found: 462.2068.

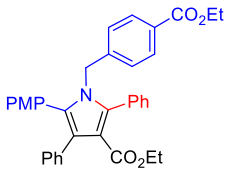

Ethyl 1-(4-(ethoxycarbonyl)benzyl)-5-(4-methoxyphenyl)-2,4-diphenyl-1H-pyrrole-3-carboxylate 6.4m. White solid, 238 mg, 85% yield. ^{1}H NMR (500 MHz, $CDCl_3$) δ 7.85 (d, *J* = 8.2 Hz, 2H), 7.35 (s, 5H), 7.27 – 7.14 (m, 5H), 7.01 (d, *J* = 8.9 Hz, 2H), 6.73 (dd, *J* = 12.7, 8.5 Hz, 4H), 4.99 (s, 2H), 4.36 (q, *J* = 7.2 Hz, 2H), 3.94 (q, *J* = 7.2 Hz, 2H), 3.75 (s, 3H), 1.40 (t, *J* = 7.2 Hz, 3H), 0.82 (t, *J* = 7.2 Hz, 3H). ^{13}C NMR (126 MHz, $CDCl_3$) δ 166.3, 165.1, 159.1, 143.3, 138.4, 135.2, 132.5, 132.2, 130.7, 130.7, 129.6, 129.3, 128.3, 127.9, 127.2, 125.9, 125.9, 124.6, 123.6, 113.6, 61.0, 59.4, 55.1, 48.2, 14.3, 13.5. HRMS. Calculated for $C_{36}H_{34}NNaO_5$ ($M+H^+$): 560.2432, found: 560.2423.

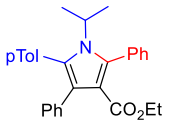

Ethyl 1-isopropyl-2,4-diphenyl-5-(p-tolyl)-1H-pyrrole-3-carboxylate 6.4n. White solid, 155 mg, 73% yield. ^{1}H NMR (500 MHz, $CDCl_3$) δ 7.55 – 7.49 (m, 2H), 7.46 (dd, *J* = 5.0, 2.1 Hz, 3H), 7.23 – 7.13 (m, 6H), 7.14 – 7.08 (m, 3H), 4.34 (p, *J* = 7.0 Hz, 1H), 3.88 (q, *J* = 7.2 Hz, 2H), 2.36 (s, 3H), 1.19 (d, *J* = 7.0 Hz, 6H), 0.77 (t, *J* = 7.1 Hz, 3H). ^{13}C NMR (126 MHz, $CDCl_3$) δ 165.2, 137.6, 137.5, 135.6, 133.8, 132.2, 132.0, 131.5, 131.3, 130.6, 130.0, 128.6, 128.4, 128.2, 127.8, 127.6, 127.0, 125.5, 124.4, 113.4, 59.1, 49.7, 23.5, 21.3, 13.5. HRMS. Calculated for $C_{29}H_{30}NO_2$ ($M+H^+$): 424.2271, found: 424.2264.

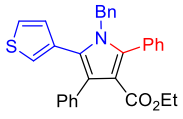

Ethyl 1-benzyl-2,4-diphenyl-5-(thiophen-3-yl)-1H-pyrrole-3-carboxylate 6.4o. White solid, 174 mg, 75% yield. ^{1}H NMR (500 MHz, $CDCl_3$) δ 7.35 (m, 5H), 7.30 – 7.19 (m, 9H), 7.14 (dd, *J* = 5.0, 3.0 Hz, 1H), 6.95 (dd, *J* = 3.0, 1.1 Hz, 1H), 6.79 – 6.76 (m, 2H), 6.74 (dd, *J* = 5.0, 1.2 Hz, 1H), 5.01 (s, 2H), 3.94 (q, *J* = 7.2 Hz, 2H), 0.82 (t, *J* = 7.1 Hz, 3H). ^{13}C NMR (126 MHz, $CDCl_3$) δ 165.0, 138.9, 138.4, 135.3, 132.2, 131.5, 130.7, 130.6, 129.7, 128.4, 128.3, 127.8, 127.4, 127.3, 127.1, 126.1, 125.9, 125.8, 125.2, 124.9, 113.5, 59.4, 48.6, 13.5. HRMS. Calculated for $C_{30}H_{26}NSO_2$ ($M+H^+$): 464.1652, found: 464.1673.

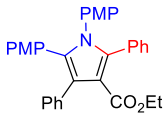

Ethyl 1,5-bis(4-methoxyphenyl)-2,4-diphenyl-1H-pyrrole-3-carboxylate 6.4p. Pale pink solid, 206 mg, 82% yield. ^{1}H NMR (500 MHz, $CDCl_3$) δ 7.25 (m, 10H), 6.87 – 6.82 (m, 4H), 6.62 (dd, *J* = 15.1, 8.9 Hz, 4H), 4.01 (q, *J* = 7.0 Hz, 2H), 3.72 (s, 3H), 3.71 (s, 3H), 0.89 (t, *J* = 7.1 Hz, 3H). ^{13}C NMR (126 MHz, $CDCl_3$) δ 165.6, 158.3, 158.3, 137.8, 135.4, 132.6, 132.4, 132.1, 131.0, 130.8, 130.7, 130.0, 127.4, 127.4, 127.4, 125.9, 123.9, 123.6, 113.8, 113.5, 113.1, 59.7, 55.2, 55.0, 13.6. HRMS. Calculated for $C_{33}H_{30}NO_4$ ($M+H^+$): 504.2169, found: 504.2155.

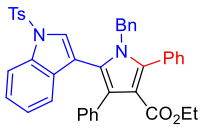

Ethyl 1-benzyl-2,4-diphenyl-5-(1-tosyl-1H-indol-3-yl)-1H-pyrrole-3-carboxylate 6.4q. White solid, 212 mg, 65% yield. ^{1}H NMR (500 MHz, $CDCl_3$) δ 7.88 (d, *J* = 8.7 Hz, 1H), 7.42 (d, *J* = 8.4 Hz, 2H), 7.38 (m, 5H), 7.28 (d, *J* = 4.1 Hz, 2H), 7.27 – 7.21 (m, 3H), 7.18 – 7.10 (m, 9H), 6.62 – 6.47 (m, 2H), 4.89 (s, 2H), 3.96 (q, *J* = 7.1 Hz, 2H), 2.35 (s, 3H), 0.84 (t, *J* = 7.1 Hz, 3H). ^{13}C NMR (126 MHz, $CDCl_3$) 164.9, 144.8, 139.8, 137.8, 135.1, 134.9, 134.5, 132.1, 131.0, 130.7, 130.2, 129.8, 128.4, 128.3, 127.9, 127.6, 127.21, 127.20, 127.0, 126.6, 126.1, 125.9, 124.8, 123.6, 123.3, 120.3, 113.8, 113.6, 113.5, 59.5, 48.9, 21.6, 13.5. HRMS. Calculated for $C_{41}H_{35}N_2SO_4$ ($M+H^+$): 651.2312, found: 651.22913.

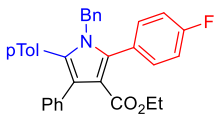

Ethyl 1-benzyl-2-(4-fluorophenyl)-4-phenyl-5-(p-tolyl)-1H-pyrrole-3-carboxylate 6.4r. White solid, 208 mg, 85% yield. ^{1}H NMR (500 MHz, $CDCl_3$) δ 7.31 – 7.23 (m, 4H), 7.21 (t, *J* = 7.2 Hz, 2H), 7.17 (td, *J* = 4.6, 2.2 Hz, 4H), 7.06 – 6.99 (m, 6H), 6.68 – 6.64 (m, 2H), 4.95 (s, 2H), 3.94 (q, *J* = 7.0 Hz, 2H), 2.29 (s, 3H), 0.84 (t, *J* = 7.1 Hz, 3H). ^{13}C NMR (126 MHz, $CDCl_3$) δ 165.08, 162.67 (d, *J* = 247.7 Hz), 138.09, 137.52, 137.33, 135.30, 133.03, 132.61 (d, *J* = 8.2 Hz), 131.14, 130.73, 130.66, 128.87, 128.67, 128.45, 128.38 (d, *J* = 3.2 Hz), 128.29, 127.19, 127.05, 126.00, 125.88, 124.37, 114.82 (d, *J* = 22.0 Hz), 113.74, 59.41, 48.45, 21.23, 13.59. HRMS. Calculated for $C_{33}H_{29}FNO_2$ ($M+H^+$): 490.2177, found: 490.2182.

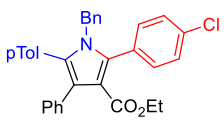

Ethyl 1-benzyl-2-(4-chlorophenyl)-4-phenyl-5-(p-tolyl)-1H-pyrrole-3-carboxylate 6.4s. Off white solid, 232 mg, 84% yield. ^{1}H NMR (500 MHz, $CDCl_3$) δ 7.33 – 7.30 (m, 2H), 7.28 – 7.21 (m, 6H), 7.18 – 7.15 (m, 4H), 7.05 – 6.98 (m, 4H), 6.66 (dd, *J* = 6.4, 2.7 Hz, 2H), 4.95 (s, 2H), 3.95 (q, *J* = 7.1 Hz, 2H), 2.29 (s, 3H), 0.85 (t, *J* = 7.1 Hz, 3H).^{13}C NMR (126 MHz, $CDCl_3$) δ 165.0, 138.0, 137.6, 137.1, 135.2, 134.3, 133.2, 132.2, 131.1, 130.9, 130.7, 128.9, 128.4, 128.3, 128.0, 127.2, 127.1, 126.0, 125.9, 124.5, 113.8, 59.5, 48.5, 21.2, 13.6. HRMS. Calculated for $C_{33}H_{29}ClNO_2$ ($M+H^+$): 506.1881, found: 506.1877.

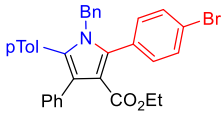

Ethyl 1-benzyl-2-(4-bromophenyl)-4-phenyl-5-(p-tolyl)-1H-pyrrole-3-carboxylate 6.4t. White solid, 217 mg, 79% yield. ^{1}H NMR (500 MHz, $CDCl_3$) δ 7.47 (s, 2H), 7.25 – 7.15 (m, 10H), 7.01 (m, 4H), 6.66 (dd, *J* = 6.6, 2.8 Hz, 2H), 4.95 (s, 2H), 3.95 (q, *J* = 7.1 Hz, 2H), 2.28 (s, 3H), 0.85 (t, *J* = 7.1 Hz, 3H). ^{13}C NMR (126 MHz, $CDCl_3$) 165.0, 138.0, 137.6, 137.1, 135.2, 133.3, 132.5, 131.4, 131.1, 131.0, 130.7, 128.9, 128.4, 128.3, 127.2, 127.1, 126.0, 125.9, 124.5, 122.6, 113.8, 59.5, 48.5, 21.2, 13.6. HRMS. Calculated for $C_{33}H_{29}BrNO_2$ ($M+H^+$): 550.1376, found: 550.1382.

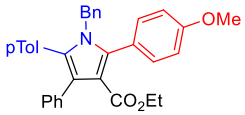

Ethyl 1-benzyl-2-(4-methoxyphenyl)-4-phenyl-5-(p-tolyl)-1H-pyrrole-3-carboxylate 6.4u. White solid, 231 mg, 92% yield. ^{1}H NMR (500 MHz, $CDCl_3$) δ 7.29 – 7.23 (m, 4H), 7.20 (t, *J* = 7.3 Hz, 2H), 7.15 (dd, *J* = 5.0, 1.9 Hz, 4H), 7.00 (d, *J* = 2.1 Hz, 4H), 6.87 (s, 2H), 6.67 (dd, *J* = 6.3, 2.7 Hz, 2H), 4.97 (s, 2H), 3.95 (q, *J* = 7.2 Hz, 2H), 3.83 (s, 3H), 2.28 (s, 3H), 0.85 (t, *J* = 7.1 Hz, 3H). ^{13}C NMR (126 MHz, $CDCl_3$) δ 165.4, 159.5, 138.5, 138.4, 137.3, 135.6, 132.6, 132.1, 131.2, 130.7, 128.8, 128.7, 128.2, 127.2, 126.9, 126.1, 125.8, 124.5, 124.3, 113.5, 113.3, 59.4, 55.2, 48.4, 21.2, 13.7. HRMS. Calculated for $C_{34}H_{32}NO_3$ ($M+H^+$): 502.2377, found: 502.2365.

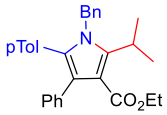

Ethyl 1-benzyl-2-isopropyl-4-phenyl-5-(p-tolyl)-1H-pyrrole-3-carboxylate 6.4v. White solid, 162 mg, 74% yield. ^{1}H NMR (500 MHz, $CDCl_3$) δ 7.34 (t, *J* = 7.4 Hz, 2H), 7.28 (d, *J* = 7.0 Hz, 1H), 7.20 – 7.10 (m, 5H), 6.96 (dd, *J* = 8.1, 5.8 Hz, 6H), 5.08 (s, 2H), 4.10 (q, *J* = 7.1 Hz, 2H), 3.18 (p, *J* = 7.1 Hz, 1H), 2.27 (s, 3H), 1.34 (d, *J* = 7.0 Hz, 6H), 1.00 (t, *J* = 7.1 Hz, 3H).^{13}C NMR (126 MHz, $CDCl_3$) δ 166.9, 142.5, 138.6, 137.3, 136.1, 131.1, 130.9, 130.3, 128.9, 128.8, 128.7, 127.2, 127.2, 125.6, 125.4, 123.7, 112.0, 59.8, 48.0, 26.7, 21.2, 21.1, 13.7. HRMS. Calculated for $C_{29}H_{30}NO_2$ ($M+H^+$): 424.2271, found: 424.2264.

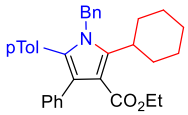

Ethyl 1-benzyl-2-cyclohexyl-4-phenyl-5-(p-tolyl)-1H-pyrrole-3-carboxylate 6.4w. White solid, 150 mg, 63% yield. ^{1}H NMR (500 MHz, $CDCl_3$) δ 7.33 (t, *J* = 7.4 Hz, 2H), 7.28 (d, *J* = 6.6 Hz, 1H), 7.20 – 7.10 (m, 5H), 7.01 – 6.95 (m, 6H), 5.09 (s, 2H), 4.11 (q, *J* = 7.2 Hz, 2H), 2.78 (t, *J* = 12.2 Hz, 1H), 2.28 (s, 3H), 2.06 (qd, *J* = 12.7, 3.2 Hz, 2H), 1.75 (d, *J* = 13.1 Hz, 2H), 1.63 (d, *J* = 12.1 Hz, 2H), 1.29 (q, *J* = 13.0 Hz, 2H), 1.13 (q, *J* = 13.0 Hz, 2H), 1.01 (t, *J* = 7.2 Hz, 3H). ^{13}C NMR (126 MHz, $CDCl_3$) δ 167.0, 141.5, 138.7, 137.3, 136.2, 131.2, 131.0, 130.2, 129.0, 128.8, 128.6, 127.2, 127.2, 125.7, 125.4, 123.6, 112.4, 59.8, 48.2, 37.6, 30.7, 27.2, 25.7, 21.2, 13.7. HRMS. Calculated for $C_{33}H_{36}NO_2$ ($M+H^+$): 478.2741, found: 478.2734.

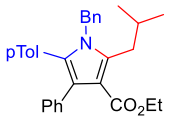

Ethyl 1-benzyl-2-isobutyl-4-phenyl-5-(p-tolyl)-1H-pyrrole-3-carboxylate 6.4x. White solid, 194 mg, 86% yield. ^{1}H NMR (500 MHz, $CDCl_3$) δ 7.31 (dd, *J* = 7.9, 6.6 Hz, 2H), 7.25 (t, *J* = 7.2 Hz, 1H), 7.21 – 7.14 (m, 5H), 6.99 – 6.92 (m, 4H), 6.89 (d, *J* = 7.3 Hz, 2H), 5.11 (s, 2H), 4.13 (q, *J* = 7.2 Hz, 2H), 2.85 (d, *J* = 7.3 Hz, 2H), 2.27 (s, 3H), 2.05 (m, 1H), 1.07 (t, *J* = 7.1 Hz, 3H), 1.02 (d, *J* = 6.7 Hz, 6H). ^{13}C NMR (126 MHz, $CDCl_3$) δ 166.0, 139.3, 138.2, 137.2, 136.3, 132.0, 131.2, 130.8, 128.8, 128.7, 128.7, 127.2, 127.0, 125.6, 125.5, 124.2, 112.1, 59.2, 47.9, 34.3, 29.8, 22.6, 21.2, 13.9. HRMS. Calculated for $C_{31}H_{34}NO_2$ ($M+H^+$): 452.2584, found: 452.2574.

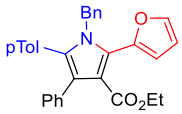

Ethyl 1-benzyl-2-(furan-2-yl)-4-phenyl-5-(p-tolyl)-1H-pyrrole-3-carboxylate 6.4y. colorless oil, 175 mg, 76% yield. ^{1}H NMR (500 MHz, $CDCl_3$) δ 7.52 (dd, *J* = 1.8, 0.8 Hz, 1H), 7.25 – 7.17 (m, 8H), 7.03 – 6.98 (m, 4H), 6.81 (dd, *J* = 7.6, 1.8 Hz, 2H), 6.50 (dd, *J* = 3.4, 0.6 Hz, 1H), 6.44 (dd, *J* = 3.4, 1.8 Hz, 1H), 5.10 (s, 2H), 4.06 (q, *J* = 7.1 Hz, 2H), 2.30 (s, 3H), 0.98 (t, *J* = 7.2 Hz, 3H). ^{13}C NMR (126 MHz, $CDCl_3$) δ 164.9, 144.5, 142.7, 138.1, 137.7, 135.0, 134.2, 131.1, 130.6, 128.9, 128.3, 128.3, 128.2, 127.4, 127.3, 127.1, 126.8, 126.2, 126.0, 124.7, 115.9, 112.3, 110.9, 59.8, 49.1, 21.3, 13.8. HRMS. Calculated for $C_{31}H_{28}NO_3$ ($M+H^+$): 462.2064, found: 462.2060.

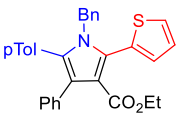

Ethyl 1-benzyl-4-phenyl-2-(thiophen-2-yl)-5-(p-tolyl)-1H-pyrrole-3-carboxylate 6.4z. pale yellow solid, 188 mg, 79% yield. ^{1}H NMR (500 MHz, $CDCl_3$) δ 7.40 (dd, *J* = 4.4, 2.0 Hz, 1H), 7.30 – 7.15 (m, 8H), 7.01 (d, *J* = 5.6 Hz, 6H), 6.81 – 6.77 (m, 2H), 5.05 (s, 2H), 4.01 (q, *J* = 7.2 Hz, 2H), 2.29 (s, 3H), 0.91 (t, *J* = 7.1 Hz, 3H). ^{13}C NMR (126 MHz, $CDCl_3$) δ 165.0, 138.4, 137.6, 135.1, 133.8, 132.1, 131.1, 130.7, 130.0, 129.5, 128.9, 128.4, 128.3, 127.5, 127.2, 127.0, 126.5, 126.0, 126.0, 124.7, 115.9, 59.6, 48.6, 21.3, 13.6. HRMS. Calculated for $C_{31}H_{28}NO_2S$ ($M+H^+$): 478.1835, found: 478.1834.

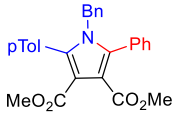

Dimethyl 1-benzyl-2-phenyl-5-(p-tolyl)-1H-pyrrole-3,4-dicarboxylate 6.4aa. White solid, 189 mg, 86% yield. ^{1}H NMR (500 MHz, $CDCl_3$) δ 7.39 – 7.28 (m,

5H), 7.23 (d, J = 8.1 Hz, 2H), 7.17 (d, J = 7.9 Hz, 2H), 7.14 – 7.10 (m, 3H), 6.60 – 6.57 (m, 2H), 4.94 (s, 2H), 3.71 (s, 3H), 3.68 (s, 3H), 2.37 (s, 3H) . ^{13}C NMR (126 MHz, $CDCl_3$) δ 165.5, 165.4, 138.6, 137.4, 137.2, 137.0, 130.7, 130.6, 130.4, 128.9, 128.7, 128.3, 128.1, 127.5, 127.2, 126.1, 114.8, 114.7, 51.6, 51.6, 48.5, 21.4. HRMS. Calculated for $C_{28}H_{26}NO_4$ ($M+H^+$): 440.1856, found: 440.1847.

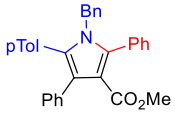

methyl 1-benzyl-2,4-diphenyl-5-(p-tolyl)-1H-pyrrole-3-carboxylate 6.4bb. White solid, 210 mg, 92% yield. ^{1}H NMR (500 MHz, $CDCl_3$) 1H NMR (500 MHz, Chloroform-d) δ 7.35 (s, 5H), 7.27 – 7.19 (m, 4H), 7.18 – 7.13 (m, 4H), 7.00 (m, 4H), 6.71 – 6.61 (m, 2H), 4.97 (s, 2H), 3.45 (s, 3H), 2.29 (s, 3H). ^{13}C NMR (126 MHz, $CDCl_3$) δ 165.7, 138.6, 138.2, 137.4, 135.3, 133.0, 132.3, 131.2, 130.7, 130.6, 128.8, 128.6, 128.2, 127.8, 127.2, 126.9, 126.1, 125.8, 124.3, 113.2, 50.6, 48.5, 21.2. HRMS. Calculated for $C_{32}H_{28}NO_2$ ($M+H^+$): 458.2115, found: 458.2111.

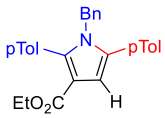

Ethyl 1-benzyl-2,5-di-p-tolyl-1H-pyrrole-3-carboxylate 6.4cc. colorless oil, 140 mg, 68% yield. ^{1}H NMR (500 MHz, $CDCl_3$) δ 7.25 (d, J = 8.1 Hz, 2H), 7.20 – 7.13 (m, 9H), 6.80 (s, 1H), 6.67 (dd, J = 6.5, 3.0 Hz, 2H), 5.06 (s, 2H), 4.17 (q, J = 7.2 Hz, 2H), 2.38 (s, 3H), 2.37 (s, 3H), 1.19 (t, J = 7.2 Hz, 3H). ^{13}C NMR (126 MHz, $CDCl_3$) δ 164.8, 140.0, 138.4, 138.0, 137.4, 135.0, 130.6, 129.8, 129.2, 129.1, 129.0, 128.5, 128.3, 126.9, 125.9, 114.0, 110.5, 59.4, 48.4, 21.4, 21.2, 14.2. HRMS. Calculated for $C_{28}H_{28}NO_2$ ($M+H^+$): 410.2115, found: 410.2115.

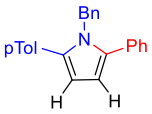

1-Benzyl-2-phenyl-5-(p-tolyl)-1H-pyrrole 6.4dd. White solid, 116 mg, 72% yield. ^{1}H NMR (500 MHz, $CDCl_3$) δ 7.42 – 7.38 (m, 2H), 7.35 (t, J = 7.4 Hz, 2H), 7.32 – 7.28 (m, 3H), 7.21 – 7.14 (m, 5H), 6.74 (d, J = 6.6 Hz, 2H), 6.45 – 6.30 (m, 2H), 5.28 (s, 2H), 2.39 (s, 3H). ^{13}C NMR (126 MHz, $CDCl_3$) δ 139.4, 136.8, 136.4, 133.8, 130.8, 128.99, 128.98, 129.0, 128.28, 128.27, 128.3, 126.9, 126.7, 125.9, 109.6, 109.4, 48.6, 21.2. HRMS. Calculated for $C_{24}H_{22}N$ ($M+H^+$): 324.1747, found: 324.1744.

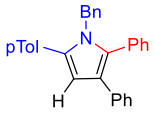

1-Benzyl-2,3-diphenyl-5-(p-tolyl)-1H-pyrrole 6.4ee. White solid, 154 mg, 77% yield. ^{1}H NMR (500 MHz, $CDCl_3$) δ 7.35 (d, *J* = 8.1 Hz, 2H), 7.30 – 7.12 (m, 14H), 7.11 (t, *J* = 7.3 Hz, 1H), 6.73 – 6.69 (m, 2H), 6.59 (s, 1H), 5.12 (s, 2H), 2.38 (s, 3H). ^{13}C NMR (126 MHz, $CDCl_3$) δ 139.2, 136.9, 136.3, 135.6, 133.2, 132.0, 131.3, 130.5, 129.1, 129.0, 128.3, 128.2, 128.0, 127.6, 127.6, 126.7, 126.0, 125.1, 123.2, 109.2, 48.4, 21.2. HRMS. Calculated for $C_{30}H_{26}N$ ($M+H^+$): 400.2060, found: 400.2050.

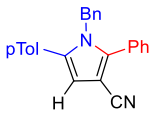

1-Benzyl-2-phenyl-5-(p-tolyl)-1H-pyrrole-3-carbonitrile 6.4ff. Colorless oil, 136 mg, 78% yield. ^{1}H NMR (500 MHz, $CDCl_3$) δ 7.38 – 7.30 (m, 7H), 7.24 (d, *J* = 7.9 Hz, 2H), 7.21 – 7.16 (m, 3H), 6.69 – 6.64 (m, 2H), 6.60 (s, 1H), 5.19 (s, 2H), 2.40 (s, 3H). ^{13}C NMR (126 MHz, $CDCl_3$) δ 143.0, 139.2, 137.6, 136.4, 131.7, 129.6, 129.6, 129.4, 129.4, 129.3, 128.6, 128.5, 128.3, 127.4, 126.7, 125.9, 117.4, 112.0, 93.1, 49.1, 21.4. HRMS. Calculated for $C_{25}H_{20}N_2Na$ ($M+Na^+$): 371.1519, found: 371.1522.

6.6. References

(1) Kantor, E. D.; Rehm, C. D.; Haas, J. S.; Chan, A. T.; Giovannucci, E. L. *JAMA* **2015**, *314*, 1818-1830.

(2) (a) Harrison, C. *Nat. Rev. Drug Discov.* **2013**, *12*, 14-15; (b) Kidd, J. *Nat. Rev. Drug Discov.* **2006**, *5*, 813-814.

(3) (a) Andrushko, N.; Andrushko, V.; Tararov, V.; Korostylev, A.; König, G.; Börner, A. *Chirality* **2010**, *22*, 534-541; (b) Pandey, P. S.; Srinivasa Rao, T. *Bioorg. Med. Chem. Lett.* **2004**, *14*, 129-131; (c) George, S.; Sudalai, A. *Tetrahedron Lett.* **2007**, *48*, 8544-8546; (d) Liu, J.; Hsu, C.-C.; Wong, C.-H. *Tetrahedron Lett.* **2004**, *45*, 2439-2441; (e) Rádl, S.; Stach, J.; Hajicek, J. *Tetrahedron Lett.* **2002**, *43*, 2087-2090; (f) Baumann, K. L.; Butler, D. E.; Deering, C. F.;

Mennen, K. E.; Millar, A.; Nanninga, T. N.; Palmer, C. W.; Roth, B. D. *Tetrahedron Lett.* **1992**, *33*, 2283-2284.

(4) *Green Chem.* **2006**, *8*, 675-676.

(5) (a) Roth, B. D. *Prog. Med. Chem.* **2002**, *40*, 1-22; (b) Kawato , Y.; Chaudhary, S.; Kumagai, N.; Shibasaki , M. *Chem. Eur. J.* **2013**, *19*, 3802-3806; (c) Lopchuk, J. M.; Gribble, G. W. *Tetrahedron Lett.* **2015**, *56*, 3208-3211; (d) Dias, L. C.; Vieira, A. S.; Barreiro, E. J. *Org. Biomol. Chem.* **2016**, *14*, 2291-2296; (e) Kawato, Y.; Iwata, M.; Yazaki, R.; Kumagai, N.; Shibasaki, M. *Tetrahedron* **2011**, *67*, 6539-6546.

(6) For reviews on multicomponent approaches to pyrroles, see: (a) Balme, G. *Angew. Chem. Int. Ed.* **2004**, *43*, 6238-6241; (b) Estevez, V.; Villacampa, M.; Menendez, J. C. *Chem. Soc. Rev.* **2014**, *43*, 4633-4657; (c) Estevez, V.; Villacampa, M.; Menendez, J. C. *Chem. Soc. Rev.* **2010**, *39*, 4402-4421; (d) Reddy, G. R.; Reddy, T. R.; Joseph, S. C.; Reddy, K. S.; Reddy, L. S.; Kumar, P. M.; Krishna, G. R.; Reddy, C. M.; Rambabu, D.; Kapavarapu, R.; Lakshmi, C.; Meda, T.; Priya, K. K.; Parsa, K. V. L.; Pal, M. *Chem. Commun.* **2011**, *47*, 7779-7781; (e) Odom, A. L.; McDaniel, T. J. *Acc. Chem. Res.* **2015**, *48*, 2822-2833.

(7) Dhawan, R.; Arndtsen, B. A. *J. Am. Chem. Soc.* **2004**, *126*, 468-469.

(8) (a) Zarganes-Tzitzikas, T.; Domling, A. *Or. Chem. Front.* **2014**, *1*, 834-837; (b) Taylor, A. P.; Robinson, R. P.; Fobian, Y. M.; Blakemore, D. C.; Jones, L. H.; Fadeyi, O. *Org. Biomol. Chem.* **2016**, *14*, 6611-6637; (c) Cioc, R. C.; Ruijter, E.; Orru, R. V. A. *Green Chem.* **2014**, *16*, 2958-2975; (d) Slobbe, P.; Ruijter, E.; Orru, R. V. A. *MedChemComm* **2012**, *3*, 1189-1218; (e) Hulme, C. In *Multicomponent Reactions*; Wiley-VCH Verlag GmbH & Co. KGaA: 2005, p 311-341; (f) Akritopoulou-Zanze, I.; Djuric, S. W. In *Synthesis of heterocycles via multicomponent reactions II*; Orru, R. V. A., Ruijter, E., Eds.; Springer-Verlag: Berlin; Heidelberg, 2010, p 231-287.

(9) Staudinger, H. *Justus Liebigs Ann. Chem.* **1907**, *356*, 51-123.

(10) Tjutrins, J.; Dhawan, R.; Lu, Y.; Arndtsen, B. A. *Chem. Eur. J.* **2016**, *22*, 15945-15954.

(11) (a) Martin, R.; Buchwald, S. L. *Acc. Chem. Res.* **2008**, *41*, 1461-1473; (b) Surry, D. S.; Buchwald, S. L. *Angew. Chem. Int. Ed.* **2008**, *47*, 6338-6361.

(12) Zapf, A.; Jackstell, R.; Rataboul, F.; Riermeier, T.; Monsees, A.; Fuhrmann, C.; Shaikh, N.; Dingerdissen, U.; Beller, M. *Chem. Commun.* **2004**, 38-39.

(13) See supporting information for the synthetic procedure and product characterization.

(14) Layer, W. R. *Chem. Rev.* **1963**, 63, 489.

Chapter 7. Conclusions, Contributions to Original Knowledge, and Suggestion for Future Work

This chapter briefly summarizes the research presented throughout this thesis and its contribution to our understanding of palladium and nickel catalyzed carbonylation chemistry. Areas of future research exploiting the results from this body of work will also be suggested.

7.1. Conclusions and Contributions to Knowledge

As laid out in the introductory chapter of this thesis, transition metal catalyzed carbonylation reactions, and their use in multicomponent coupling reactions, have proven to be a very powerful tool in molecular synthesis. As such, large interest in the Arndtsen research group has been the development of both – transition metal catalyzed carbonylations and multicomponent reactions. The results presented in this thesis show further developments in the design and mechanistic understanding of such palladium and nickel catalyzed reactions.

In chapter 2, we described a palladium catalyzed tandem approach to synthesize tetra-substituted imidazoles by coupling two electronically different imines, aryl-iodides and CO. It was found that a single palladium catalyst can mediate two catalytic processes at once – aryl halide carbonylation to generate *in situ* acid chlorides, as well as cyclocarbonylation of α-chloroamides into 1,3-dipoles (Münchnones). The electronic differences between the imines employed in this transformation allows the selective incorporation of two different imines into the imidazole product, where more electron deficient N-tosyl imine undergoes selective 1,3-dipolar cycloaddition to Münchnones, while a more electron rich imine reacts with acid chloride to form the Münchnone. Overall, this provides a modular route to synthesize imidazoles with control of all four substituents.

In chapter 3, we continued our interest in the carbonylation of aryl halides in the presence of imines. In contrast to the palladium catalyzed reaction describe above, it was found that by using nickel (i.e., $Ni(COD)_2$) as the catalyst in this transformation, a range of isoindolinones

could be prepared. This transformation is believed to proceed via a tandem nickel catalyzed carbonylation to form *N*-acyl iminium chloride salts, followed by a spontaneous nickel catalyzed cyclization. This provides an efficient platform to synthesize isoindolinones, as well as a demonstration of how this slower carbonylation with nickel catalysts relative to palladium can be exploited to create new products from imines and aryl iodides.

In chapter 4, we described how palladium catalyzed aryl halide carbonylation can be used as a tool to generate electrophilic aroylating agents for the C-H functionalization of activated heterocycles. Previous work in our lab has shown that acid chlorides can be generated from the palladium catalyzed carbonylation of aryl halides in the presence of chloride salts. In this, the use of P^tBu_3 ligand is critical to facilitate the reductive elimination of acid chlorides from palladium-aroyl intermediates. The generation of electrophilic species such as acid chlorides from carbonylation inspired us to explore the combination of this chemistry with trapping by heterocycles as a new approach to C-H bond functionalization. These led to the discovery of a general, acid chloride free, method to carbonylatively couple aryl halides with heterocycles to form ketones. Mechanistic studies showed that in the absence of chloride source a more electrophilic intermediate, presumably aroyl iodide, is generated during the transformation. Overall this provides with a general synthetic route to generate aryl-(hetero)aryl ketones using readily available aryl iodides, heterocycles and CO, and without the typical need of using pre-metallated heterocycles in carbonylative coupling chemistry.

Chapter 5 provides probes the mechanism of the synthesis of Münchnones via a palladium catalyzed carbonylative coupling of imines and acid chlorides. Two catalytic systems were examined using Bu_4NBr or P(*o*-Tol)$_3$ as additives or ligands, respectively. In both cases, the key catalytic intermediates were synthesized and characterized using NMR spectroscopy and X-ray structural analysis. Evidence gathered through kinetic and stoichiometric experiments suggests that utilization of Bu_4NBr in the reaction results in generation of a nanoparticulate palladium catalyst which undergoes slow, rate determining oxidative addition. Conversely the use of bulky phosphine ligands such as P(o-Tol)$_3$ result in a much more active, monomeric Pd(0) catalyst. The steric bulk of this ligand is critical in catalysis to allow rate limiting CO coordination and insertion. Overall this study provides insights that can be further used to create more active catalysts for this reaction.

In chapter 6, we described how the mechanistic results laid out in chapter 5 can be applied to create a highly active catalyst for synthesis of Münchnones. This catalyst exploits the sterically encumbered and electron donating pyrrole-based phosphine, $^{t}Bu_2P$(N-phenylpyrrole), to create a palladium intermediate that undergoes rapid CO coordination and insertion to form Münchnones under more mild reaction conditions, significantly higher rates. The generation of Münchnones can be coupled with alkyne and alkene 1,3-dipolar cycloaddition reactions, thus offering a broadly generalizable route to form polysubstituted pyrroles from simple imines, acid chlorides and alkynes/alkenes. This approach has been applied to the multicomponent synthesis of Atorvastatin (i.e., Lipitor) in a highly convergent manner from a commercially available amine, 4-fluorobenzaldehyde, isobutyroyl chloride and diphenylpropiolamide.

7.1. Suggestions for Future Work

Previous studies in our research group have shown that the bulky $P^{t}Bu_3$ ligand in the presence of CO can facilitate the reductive elimination of acid chlorides from palladium aroyl complexes. In chapter 4, this transformation inspired us to develop an electrophilic approach to the C-H bond functionalization of heterocycles via palladium catalyzed carbonylation of aryl halides. Mechanistic analysis showed that this transformation relies on rapid reversible reductive elimination of aroyl iodides, which are stronger acylating reagents than acid chlorides and allow functionalization of a range of activated heterocycles. However, our preliminary studies have shown that aroyl iodides are not sufficiently reactive to directly functionalize less activated substrates such as thiophene or benzene.

The C-H functionalization of simple arenes in principle would require the development of a catalytic system that would be able to reductively eliminate even more reactive aroyl electrophiles. An approach to enhance electrophilicity would be to employ even more ionizable carboxylic acid derivatives, such as triflates, by intercepting the palladium-aroyl intermediate with anion exchange. In preliminary studies, I have found that this is possible by adding AgOTf to the catalytic reaction and offers an approach to perform the C-H bond functionalization of benzene into ketones (Scheme 7.1). Preliminary data from this study shows that reaction does

proceed via the formation of aroyl triflate intermediates that react with benzene. This project is currently being persued by Garrison Kinney in our laboratory.

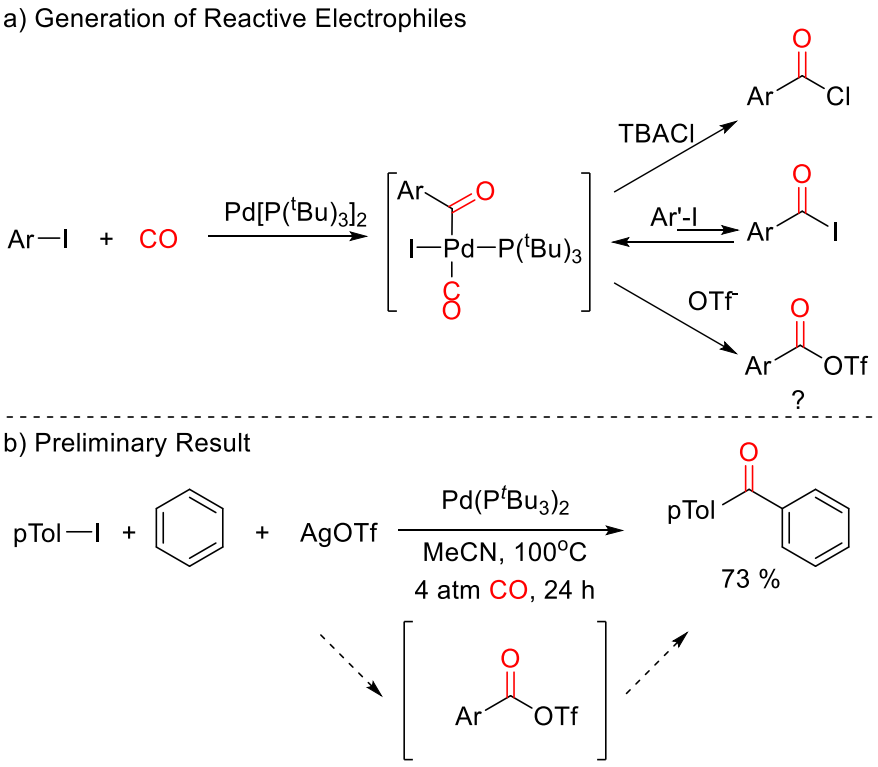

Scheme 7.1. Palladium Catalyzed Carbonylative Generation of Electrophiles.

An alternative approach to generate reactive electrophiles such as aroyl triflates would be to utilize aryl triflates as substrates for carbonylation chemistry. This would provide with an atom economical approach to generate these reactive electrophiles without the use of silver salts. As highlighted in the introductory chapter of this thesis, aryl triflates are attractive substrates since they can be readily derived from phenols. A plausible mechanism for this transformation is highlighted below. A key challenge to this reaction would be to overcome the relative rate differences of oxidative addition of the strong aryl triflate bond in the presence of reactive aroyl triflate generated during catalysis. A plausible solution could be to employ excess amounts of

electron rich heterocycles, that could undergo C-H bond functionalization at rates high enough to offset the competitive re-oxidative addition of aroyl triflates.

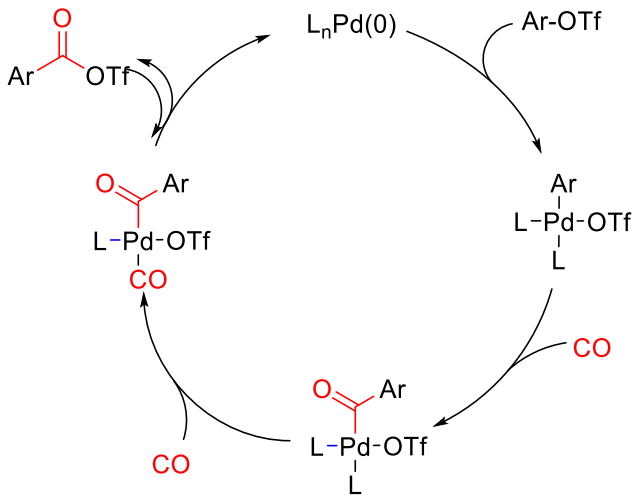

Scheme 7.2. Palladium Catalyzed Carbonylation of Aryl Triflates.

Appendix 1. Preliminary Studies: New Nickel Catalysts for Carbonylative Coupling Reactions and Carbonylative Decarboxylations

A1.1. Preface

Throughout the course of these studies, several side projects were initiated to explore wider chemical space on carbonylation reactions. While these studies cannot be summarized as whole chapters themselves, they could provide with interesting insights and observations for future projects in the Arndtsen research group. Efforts towards development of new nickel catalysts for the aminocarbonylation or aryl iodides, the synthesis of $Ni(CO)_3(PR_3)$ complexes, as well as efforts towards development of palladium catalyzed carbonylative decarboxylation reactions are described below.

A1.2. Nickel Catalyzed Aminocarbonylation

In contrast to palladium catalyzed carbonylation reactions of aryl halides, which have seen significant use in the last several decades, nickel catalyzed carbonylation reactions has gathered much less interest, presumably due to their lower catalytic activity than palladium and the formation of toxic $Ni(CO)_4$ by-products. This is despite significant developmental work on nickel catalyst systems up until the 1980s. Considering the vast advances in phosphine ligand design in the past decade, we sought out to investigate whether new ligand scaffolds could be beneficial in improving catalytic activity using nickel complexes (See section 1.2.2). In addition, we were interested if chloride salt additives would be beneficial in nickel catalyzed aminocarbonylations, through allowing the *in situ* generation of acid chlorides.

To probe for potential influence of chloride salts on catalysis, we first carried out a control experiment using a $Ni(CO)_3(P^tBu_3)$ catalyst to carbonylate 4-iodotoluene in the presence of a bulky 2,6-diisopropylaniline. It was found that adding a soluble chloride source (Bu_4NCl)

led to the formation of amide in 82% yield, compared to 23% in a control experiment where no additive was added.

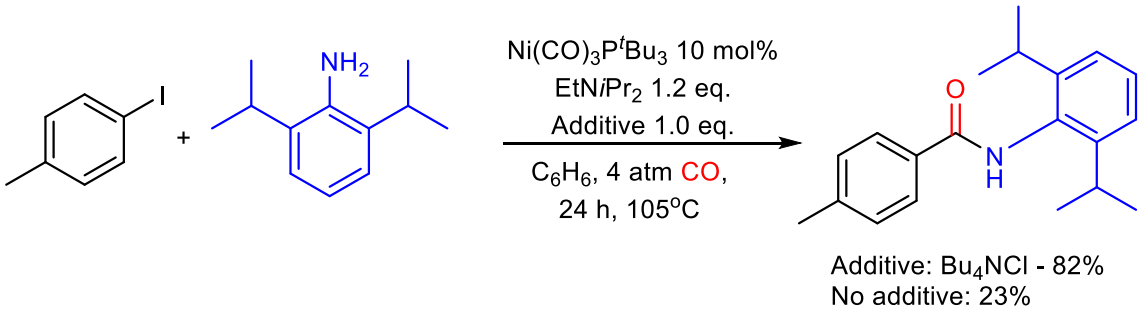

Scheme A1.1. Chloride Effect on Nickel Catalyzed Aminocarbonylation.

There are several potential roles of chloride could play in catalysis. For example, Cassar and Foa have previously reported that the build-up of halide ions during catalysis facilitates the rate of carbonylation via generation of a more active anionic nickel catalyst – $[Ni(CO)_3X]^-$ for oxidative addition of the aryl halide.[1] Alternatively, the increased yield of amide might be attributed to the *in situ* generation of acid chlorides, similarly to our palladium system previously described.[2] In order to probe the latter postulate, we set out to catalytically build up acid chlorides from aryl iodides in the presence of various chloride salt additives, and trap them out with a nucleophile (benzylamine) (Table A1.1). It was found that after 4 days of heating 4-iodotoluene in the presence of Ph_3BnPCl and $Ni(CO)_3(P^tBu_3)$ catalyst followed by quenching with benzylamine, we were able to isolate the corresponding amide in 49% yield. These results suggest the catalytic formation of 4-methylbenzoyl chloride. This was further confirmed via *in situ* monitoring of this reaction by ^1H NMR in C_6D_6. ^1H NMR analysis shows the generation signals corresponding to acid chloride (δ 7.75 (d, J = 8.4 Hz, 2H), 6.61 (d, J = 8.1 Hz, 2H), 1.77 (s, 3H)) corresponding to 4-methylbenzoyl chloride (34% *in situ* yield). Upon addition of benzylamine to the reaction mixture, these aforementioned signals disappear and the N-benzyl-4-methylbenzamide can be observed.

Table A1.1. Catalytic Generation of Acid Chlorides using Nickel Catalysis.

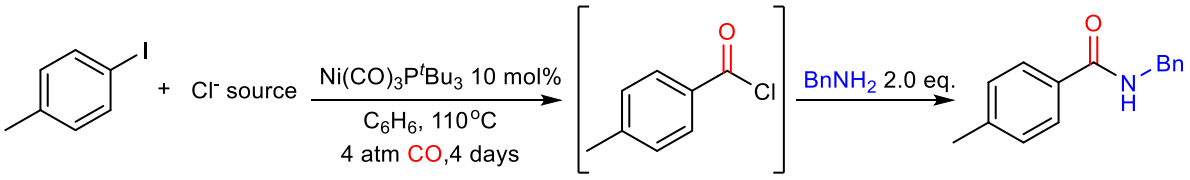

Entry	Chloride source	Isolated yield, %
1	TBACl	23 %
2	Ph_3BnPCl	49 %
3	PPNCl	0 %
4	LiCl	25 %
5	CsCl	22 %

Further we investigated the temperature influence on this transformation. High temperature carbonylation of 4-iodotoluene, in the presence of benzylamine and Bu_4NCl led to high conversion of the starting material to the desired amide (Table A1.2.). Interestingly, lowering the reaction temperature to 75°C not only lowered the yield of amide, but also led to the formation of a doubly carbonylated keto amide product. Further decreasing the reaction temperature to 55 °C yielded only the double carbonylated product, along with unreacted 4-iodotoluene.

Table A1.2. Temperature Influence on Nickel Catalyzed Aminocarbonylation.

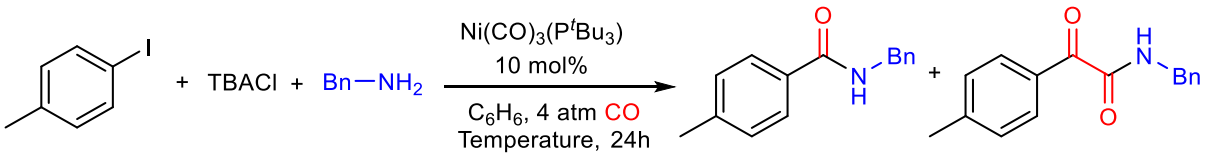

Entry	Temperature	Amide yield, %	Keto amide yield, %
1	110°C	88 %	0 %
2	75°C	25 %	40 %
3	55°C	0 %	42 %

We also explored the effect of various phosphine ligands on the carbonylation of 4-iodotoluene in the presence of benzylamine without chloride additives (Table A1.3.). It was found that in the absence of any phosphine ligand, 59% of amide was generated alongside with 4% of the keto amide side product. Addition of small, electron donating phosphine ligands significantly diminished the yield of amide, while bulky ligands such as P(*o*-Tol)$_3$ or P(TMS)$_3$ approached the activity of phosphine free reaction. These observations can be attributed to the slower dissociation of CO from a phosphine coordinated nickel catalyst for rate determining oxidative addition.

Table A1.3. Ligand Influence on Nickel Catalyzed Aminocarbonylation.

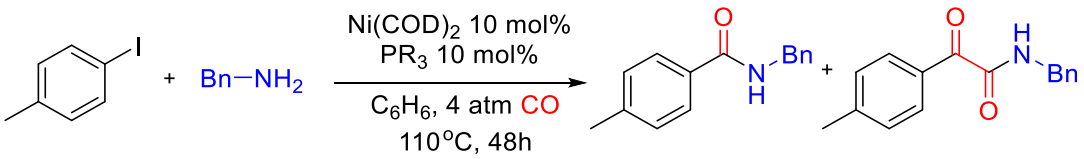

Entry	PR_3	Amide yield, %	Keto amide yield, %	Entry	PR_3	Amide yield, %	Keto amide yield, %
1	-	59 %	4 %	8	PCy_3	30 %	3 %
2	PPh_3	12 %	13 %	9	$P(o\text{-}MeOPh)_3$	13 %	0 %
3	$P(OPh)_3$	33 %	7 %	10	$P(o\text{-}Tol)_3$	58 %	0 %
4	$P(OEt)_3$	18 %	7 %	11	$P(TMS)_3$	66 %	0 %
5	$P(OCH_2CF_3)_3$	34 %	8 %	12	P^tBu_3	39 %	7 %
6	P(OPh)Cathecol	41 %	4 %	13	PPh_3 (20 mol%)	17 %	10 %
7	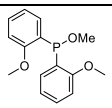	22 %	18 %	14		53 %	0 %

p-Tol-I (48 mg, 0.22 mmol), $BnNH_2$ (19 mg, 0.18 mmol), $Ni(COD)_2$ (5 mg, 0.018 eq.), EtN^iPr_2 (28 mg, 0.22 mmol), phosphine (0.18 mmol), 0.7 mL of C_6D_6, 4 atm CO, 48h. Yield determined by ^1H NMR in respect to BnOBz internal standard.

A1.3. Synthesis of Nickel Tricarbonyl Phosphine Complexes

During the course of our studies on nickel catalyzed carbonylative coupling reactions, we initiated a collaboration with researchers at Texas A&M Qatar on the mechanism of these transformations, and in particular the role of phosphines in inhibiting aryl halide oxidative addition. These required us to synthesis several $Ni(CO)_3PR_3$ complexes for their studies. Traditionally, these nickel carbonyl complexes are prepared from $Ni(CO)_4$ via substitution reaction. However, $Ni(CO)_4$ is extremely toxic and, due to its high volatility, difficult to handle. As an alternative, we show here how various $Ni(CO)_3PR_3$ complexes can be generated instead from $Ni(COD)_2$ via simple displacement of the labile 1,5-cyclooactadiene ligand.

As shown in Scheme A1.2, the combination of $Ni(COD)_2$ and phosphine in benzene (5 min), followed by addition of 4 atm CO led to the straightforward generation of various $Ni(CO)_3PR_3$ complexes. Evaporation of solvent and 1,5-cyclooactadiene on a Schlenk line leads to the generation of pure $Ni(CO)_3PR_3$ which needed no additional purification (NOTE: any $Ni(CO)_4$ collected in the vacuum trap was immediately quenched by precharging the trap charged with excess PPh_3. Upon thawing of the trap, water was then added, as previously reported by Nolan).[3] The $Ni(CO)_3PR_3$ complexes were all isolated in high yields.

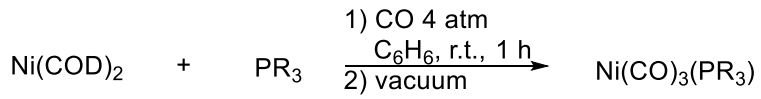

$Ni(CO)_3(P^tBu_3)$	$Ni(CO)_3(PPh_3)$	$Ni(CO)_3(P(o\text{-}Tol)_3)$	$Ni(CO)_2(DPPE)$
93%	95%	94%	97%

Scheme A1.2. Synthesis of $Ni(CO)_3(PR_3)$ Complexes.

A1.4. Palladium Catalyzed Decarboxylative Carbonylation Reactions

A potential alternative to palladium catalyzed carbonylation reactions of aryl halides would be the decarboxylative carbonylation of carboxylic acids or their salts. Unlike aryl halides, which are the product of petrochemical industry, carboxylic acids are widely available at low cost, and often are readily obtained from natural sources. In the last decade, several powerful decarboxylative cross-coupling methodologies have been developed as an alternative to classical cross-coupling reactions of aryl halides.[4] Thus we envisioned to develop a palladium catalyzed decarboxylative carbonylation reaction. This section highlights the preliminary results obtained.

The decarboxylative aminocarbonylation of carboxylic acids would to be of great interest, considering that it would allow the construction of amides without the need of stoichiometric activating agents (DCC, EDC, HOBt etc). As a test for this reaction, benzoic acid was reacted with benzylamine and 4 atm of CO using a catalyst system similar to that reported

by Goossen for benzoic acid decarbonylation.[5] This results in the formation of 1,3-dibenzylurea due to the carbonylative dimerization of the amine, with small amounts of N-benzylacetamide (Scheme A1.3.a). In order to prevent the generation of the urea product, an *ortho*-amide substituted benzoic acid (2-(benzylcarbamoyl)benzoic acid) was employed as both the decarboxylative unit and as the nucleophile trap. Upon subjecting the starting material to the reaction conditions we observed the generation of phtalimide in high yield (Scheme A1.3.b). However, upon on examining the background reaction of the non-carbonylative cyclization of the starting material we found that the product could be generated also in the absence of CO in similar yield, suggesting that decarboxylation and carbonylation had not occurred.

As the presence of an amine or amide in the reaction appeared to lead to side reaction, we next examined the potential decarboxylative carbonylation of benzoic acid derived by themselves, which could potentially lead to the formation of anhydrides. However, subjecting 2-methylbenzoic acid to reaction conditions described by Myers[6] led to no anhydride products. In retrospect, the anhydride product might have been lost during the aqueous workup of DMSO prior taking a crude ^{1}H NMR, and only starting material was observed (Scheme A1.3.c). Employing other highly polar solvents such as NMP, DMF also only led to the recovery of starting material.

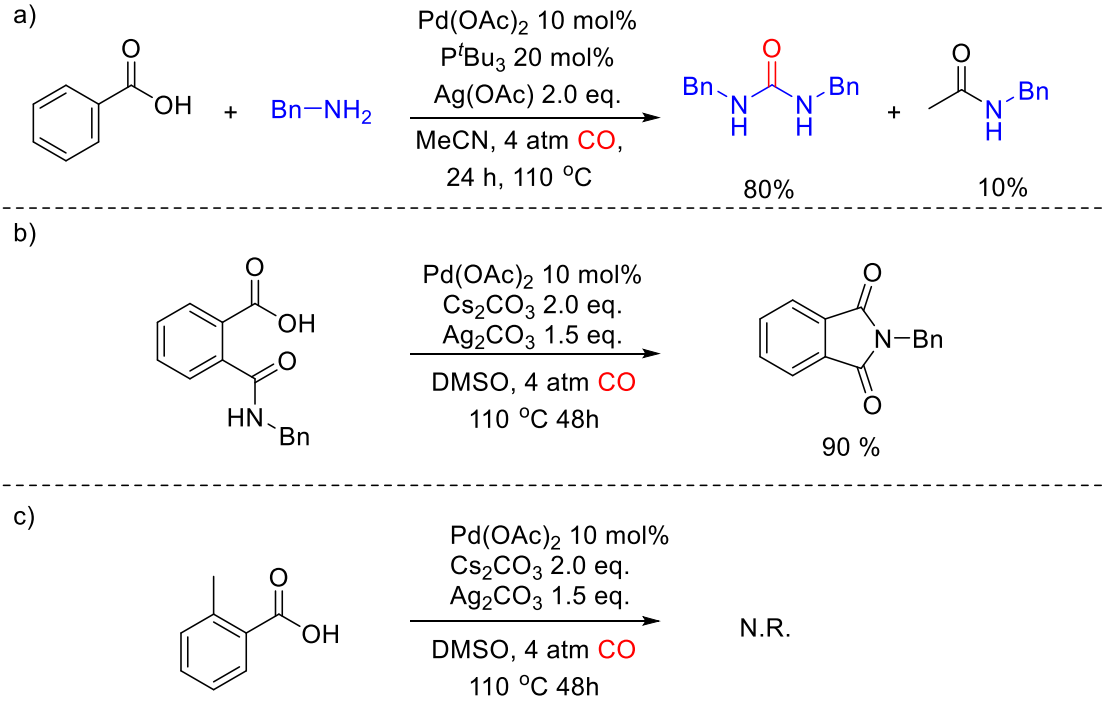

Scheme A1.3. Decarboxylative carbonylation of Benzoic Acids.

We also examined the feasibility of a decarboxylative carbonylative Heck-type reaction. When be subjected 2,6-dimethoxybenzoic acid and styrene in the presence of 4 atm of CO to catalytic reaction conditions, no carbonylative product was obtained and most of the carboxylic acid starting material was recovered. This could be the result of CO binding to palladium center and preventing the decarboxylation step all together.

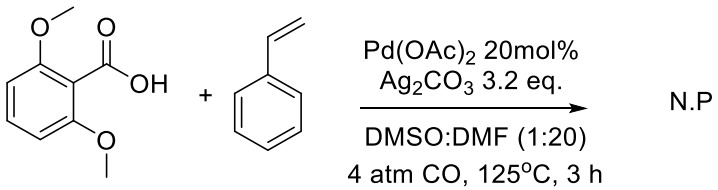

Scheme A1.4. Decarboxylative Carbonylative Heck Type Reaction.

A1.5. Synthetic Procedures and Characterization Data

Safety note: ***Ni(CO)$_4$ is a potential product generated in nickel-based carbonylations, and is extremely toxic and volatile.*** Precautions must be taken to avoid all contact with the reaction prior to quenching. All manipulations of the catalysis solutions after CO introduction were therefore rigorously performed in sealed vessels with no contact to air or person. In order to quench any possible traces of $Ni(CO)_4$, all volatiles from reaction mixtures were removed *in vacuo* on a Schlenk line and collected into a solvent trap charged with excess PPh_3, followed by the addition of water, as noted by Nolan.[3]

Typical Procedure for the Catalytic Generation of Acid Chlorides using Nickel Catalysis (Table A1.1.)

In a glovebox, 4-iodotoluene (126 mg, 0.58 mmol), tetrabutylammonium chloride (161 mg, 0.58 mmol), $Ni(CO)_3(P^tBu_3)$ (20 mg, 0.0058 mmol) were combined in C_6H_6 (5 mL) and added to a 50 mL sealable pressure vessel. The vessel was closed, removed from the glovebox. The pressure vessel was connected to a CO gas cylinder via a rubber hose (Figure 2.2). The hose was evacuated and backfilled with CO 3 times. Afterwards the pressure vessel was opened to the line, and pressurized to 4 atm of carbon monoxide per the reading on the pressure gauge on the gas cylinder. The reaction was heated at 110 °C for 4 days. After the reaction was cooled to room temperature, and all volatiles were removed in vacuo according to the procedure noted above. The pressure vessel was brought into to the glove box and a solution of benzylamine (124 mg, 1.16 mmol) in C_6H_6 (2 mL) was a added to the crude solid. The reaction was allowed to stir at room temperature for 1 h. Afterwards the solvent was removed, and the crude solid was redissolved in dichloromethane (50 mL) and extracted with 1M aqueous HCl solution (3x 50 mL). The organic layer was collected, concentrated onto silica and purified by flash column chromatography (EtOAc : Hexanes, 0 – 25% gradient) affording pure N-benzyl-4-methylbenzamide in 23 % yield (30 mg).

Procedure for the Determination of Chloride Effect on Nickel Catalyzed Aminocarbonylation (Scheme A1.1.)

In a glovebox, 4-iodotoluene (126 mg, 0.58 mmol), tetrabutylammonium chloride (161 mg, 0.58 mmol), 2,6-diisopropylaniline (105 mg, 0.58 mmol), $Ni(CO)_3(P^tBu_3)$ (20 mg, 0.058 mmol) were combined in C_6H_6 (5 mL) and added to a 50 mL sealable pressure vessel. The vessel was closed, removed from the glovebox. The pressure vessel was connected to a CO gas cylinder via a rubber hose (Figure 2.2). The hose was evacuated and backfilled with CO 3 times. Afterwards the pressure vessel was opened to the line, and pressurized to 4 atm of carbon monoxide per the reading on the pressure gauge on the gas cylinder. The reaction was heated at 110 °C for 24 h. After the reaction was cooled to room temperature, and all volatiles were removed in vacuo according to the procedure noted above. Afterwards the solvent was removed, and the crude solid was redissolved in dichloromethane (50 mL) and extracted with 1M aqueous HCl solution

(3x 50 mL). The organic layer was collected, concentrated onto silica and purified by flash column chromatography (EtOAc : Hexanes, 0 – 25 % gradient) affording pure N-(2,6-diisopropylphenyl)-4-methylbenzamide as a pale white solid in 82 % yield (140 mg). ^{1}H NMR (400 MHz, $CDCl_3$) δ 7.81 (d, *J* = 8.0 Hz, 2H), 7.40 (s, 1H), 7.33 (d, *J* = 7.7 Hz, 1H), 7.28 (d, *J* = 7.9 Hz, 2H), 7.22 (d, *J* = 7.7 Hz, 2H), 3.14 (hept, *J* = 6.7 Hz, 2H), 2.44 (s, 3H), 1.21 (d, *J* = 6.9 Hz, 12H). ^{13}C NMR (75 MHz, $CDCl_3$) δ 166.8, 146.4, 142.2, 131.7, 131.3, 129.4, 128.4, 127.2, 123.5, 28.9, 23.6, 21.5.

General Procedure for Determining Temperature Influence on Nickel Catalyzed Aminocarbonylation (Table A1.2.)

In a glovebox, 4-iodotoluene (126 mg, 0.58 mmol), tetrabutylammonium chloride (161 mg, 0.58 mmol), benzylamine (62 mg, 0.58 mmol), $Ni(CO)_3(P^tBu_3)$ (20 mg, 0.058 mmol) were combined in C_6H_6 (5 mL) and added to a 50 mL sealable pressure vessel. The vessel was closed, removed from the glovebox. The pressure vessel was connected to a CO gas cylinder via a rubber hose (Figure 2.2). The hose was evacuated and backfilled with CO 3 times. Afterwards the pressure vessel was opened to the line, and pressurized to 4 atm of carbon monoxide per the reading on the pressure gauge on the gas cylinder. The reaction was heated at temperature indicated in table A2.2. for 24 h. After the reaction was cooled to room temperature, and all volatiles were removed in vacuo according to the procedure noted above. Afterwards the solvent was removed, and the crude solid was redissolved in dichloromethane (50 mL) and extracted with 1M aqueous HCl solution (3x 50 mL). The organic layer was collected, concentrated onto silica and purified by flash column chromatography (EtOAc : Hexanes, 0 – 25 % gradient) affording pure N-benzyl-4-methylbenzamide and N-benzyl-2-oxo-2-(*p*-tolyl)acetamide in yields as indicated in table A1.2.

Typical Procedure for Determining Ligand Influence on Nickel Catalyzed Aminocarbonylation (Table A1.3.)

In a glovebox, 4-iodotoluene (48 mg, 0.22 mmol), benzylamine (1+ mg, 0.18 mmol), $Ni(COD)_2$ (5 mg, 0.018 mmol), EtN^iPr_2 (28 mg, 0.22 mmol), phosphine (0.18 mmol), and benzyl benzoate

internal standard were combined in C_6D_6 (0.7 mL) and added to a J-Young tube. The tube was removed from the glovebox, connected to the Schlenk line (Figure 2.1.), the solvent was frozen in liquid nitrogen, the headspace of the NMR evacuated, and 4 atm carbon monoxide was condensed into the NMR tube. The reaction was heated at 110 ºC and monitored by ^{1}H NMR spectroscopy. The yield of amide product was determined by ^{1}H NMR analysis relative to the internal standard.

General procedure for the synthesis of $Ni(CO)_3(PR_3)$ Complexes (Scheme A1.2)

In a glovebox, $Ni(COD)_2$ (100 mg, 0.36 mmol), phosphine (0.36 mmol) were combined in C_6H_6 (3 mL) and added to a 50 mL sealable pressure vessel. The vessel was closed, removed from the glovebox. The pressure vessel was connected to a CO gas cylinder via a rubber hose (Figure 2.2). The hose was evacuated and backfilled with CO 3 times. Afterwards the pressure vessel was opened to the line, and pressurized to 4 atm of carbon monoxide per the reading on the pressure gauge on the gas cylinder. The reaction was allowed to stir at room temperature for 1 h. Afterwards all the volatiles were removed in vacuo according to the safety procedure noted above affording pure product.

$Ni(CO)_3(PPh_3)$. Grey solid, 147 mg, 95% yield. ^{1}H NMR (200 MHz, C_6D_6) δ 7.40 (s, 2H), 6.94 (s, 3H). ^{31}P NMR (81 MHz, C_6D_6) δ 31.35. FT-IR-ATR (cm^{-1}): 2068, 1978 (CO).

$Ni(CO)_3(P^tBu_3)$. White solid, 93% yield. ^{1}H NMR (500 MHz, C_6D_6) δ 1.12 (d, J = 11.7 Hz, 27H). ^{31}P NMR (202 MHz, C_6D_6) δ 90.65.FT-IR-ATR (cm^{-1}): 2056, 1961 (CO).

$Ni(CO)_3(P(o\text{-}Tol)_3)$. White solid, 163 mg, 94% yield. ^{1}H NMR (200 MHz, C_6D_6) δ 7.37 – 6.68 (m, 12H), 2.37 (s, 9H). ^{31}P NMR (81 MHz, C_6D_6) δ 18.32. FT-IR-ATR (cm^{-1}): 2068, 1979 (CO).

$Ni(CO)_2$(DPPE). Grey solid, 186 mg, 97% yield. ^{1}H NMR (200 MHz, C_6D_6) δ 7.56 (s, 8H), 6.97 (bs, Hz, 12H), 1.96 (d, J = 15.5 Hz, 4H). ^{31}P NMR (81 MHz, C_6D_6) δ 45.92. FT-IR-ATR (cm^{-1}): 1996, 1934 (CO).

A1.6. References

(1) Cassar, L.; Foà, M. *J. Organomet. Chem.* **1973**, *51*, 381-393.

(2) Quesnel, J. S.; Arndtsen, B. A. *J. Am. Chem. Soc.* **2013**, *135*, 16841-16844.

(3) Dorta, R.; Stevens, E. D.; Scott, N. M.; Costabile, C.; Cavallo, L.; Hoff, C. D.; Nolan, S. P. *J. Am. Chem. Soc.* **2005**, *127*, 2485-2495.

(4) Rodriguez, N.; Goossen, L. J. *Chem. Soc. Rev.* **2011**, *40*, 5030-5048.

(5) (a) Gooßen, L. J.; Deng, G.; Levy, L. M. *Science* **2006**, *313*, 662-664; (b) Goossen, L. J.; Rodríguez, N.; Melzer, B.; Linder, C.; Deng, G.; Levy, L. M. *J. Am. Chem. Soc.* **2007**, *129*, 4824-4833.

(6) Myers, A. G.; Tanaka, D.; Mannion, M. R. *J. Am. Chem. Soc.* **2002**, *124*, 11250-11251.

Appendix 2. Spectroscopic Data for Chapter 6

^{1}H and ^{13}C NMR spectra of **6.4a**

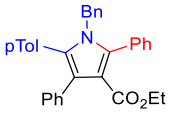

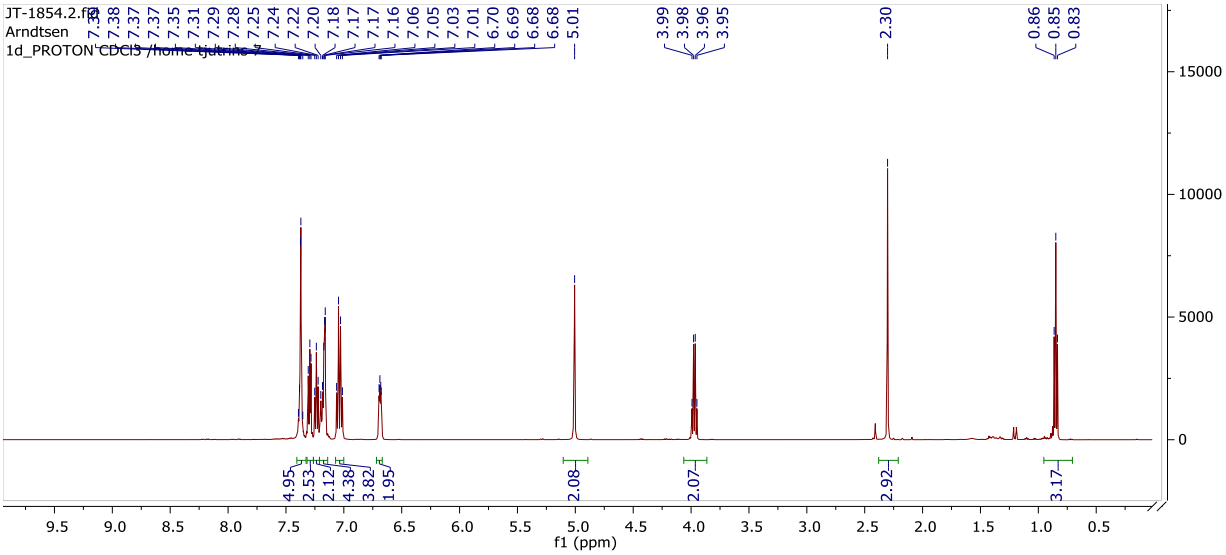

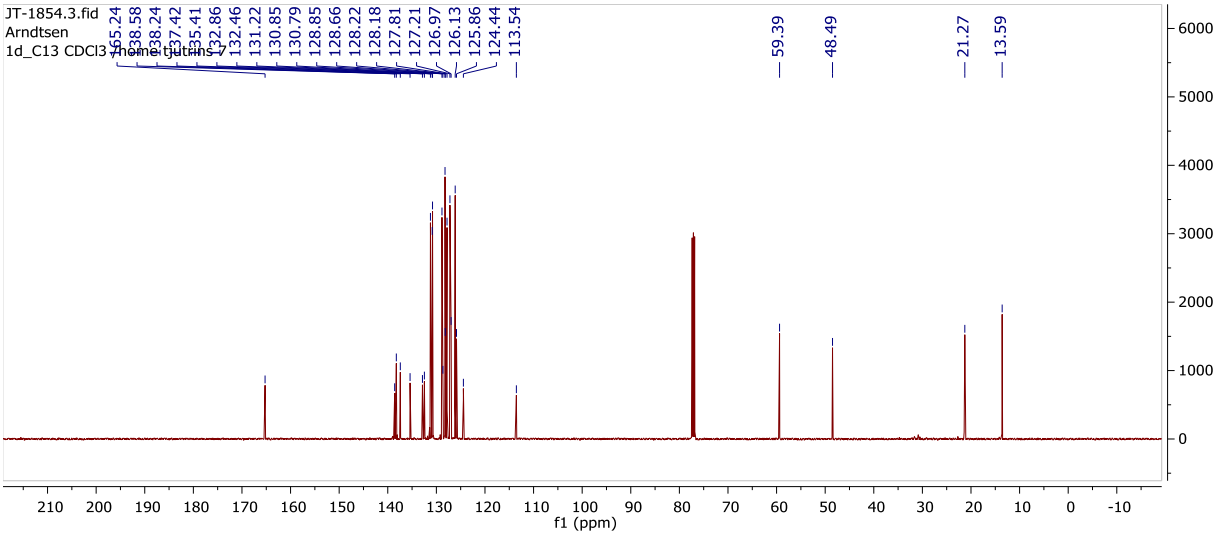

^{1}H and ^{13}C NMR spectra of **6.4b**

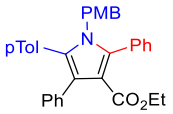

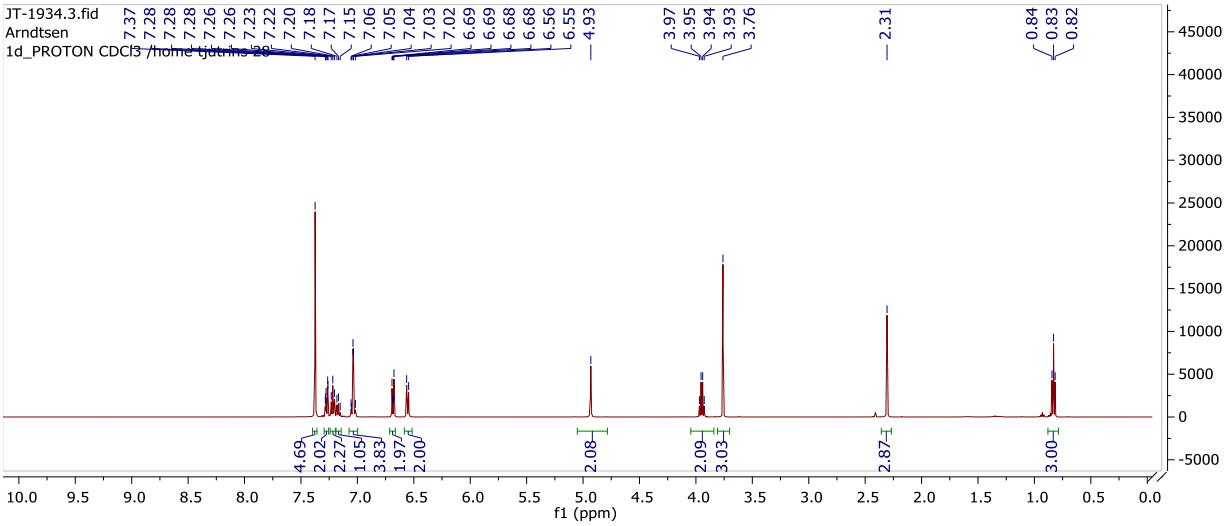

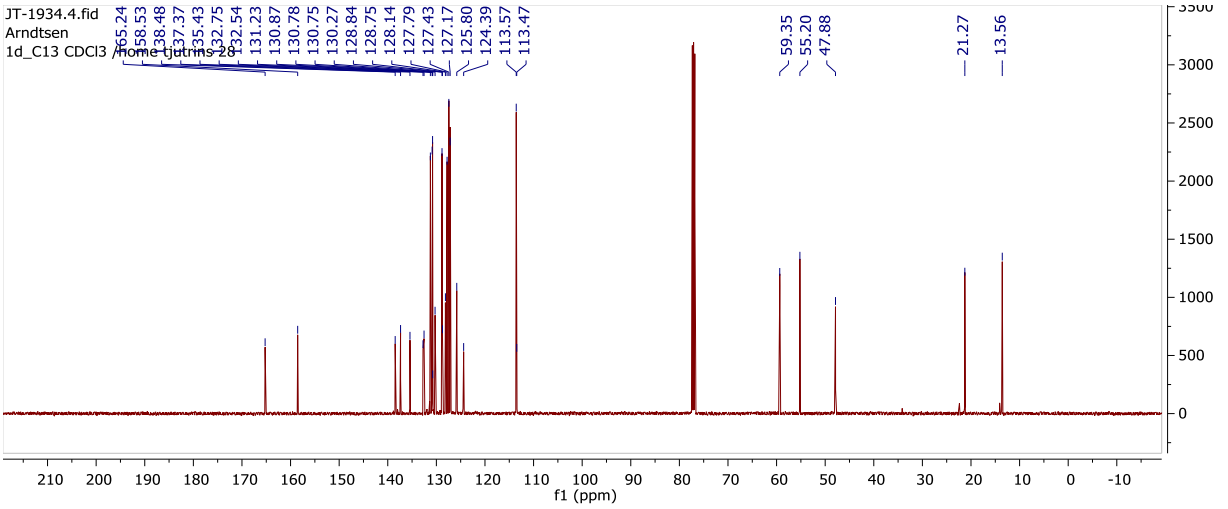

^{1}H and ^{13}C NMR spectra of **6.6.4c**

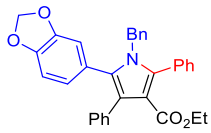

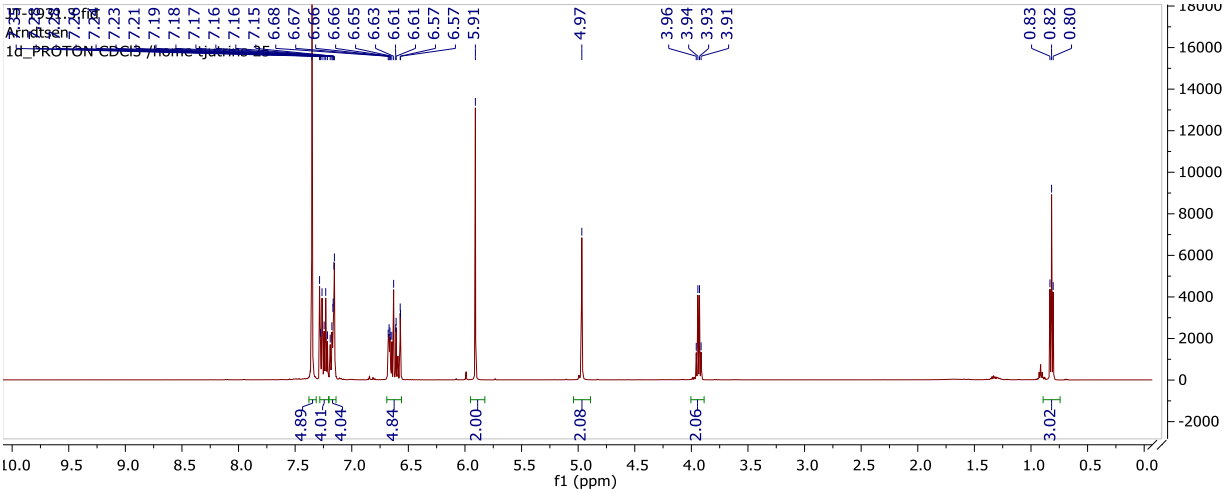

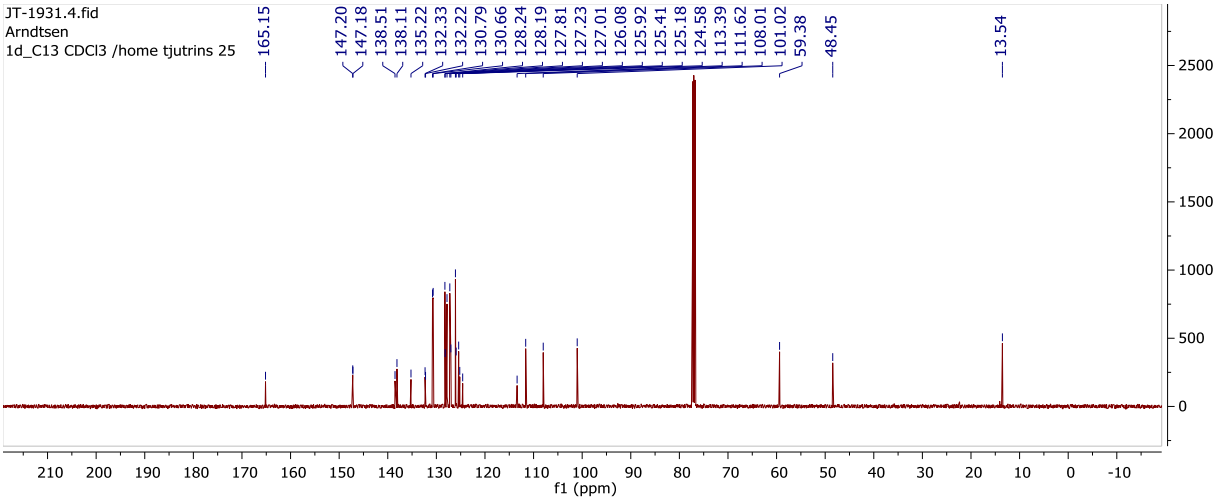

^{1}H and ^{13}C NMR spectra of **6.6.4d**

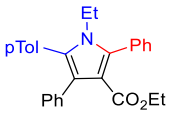

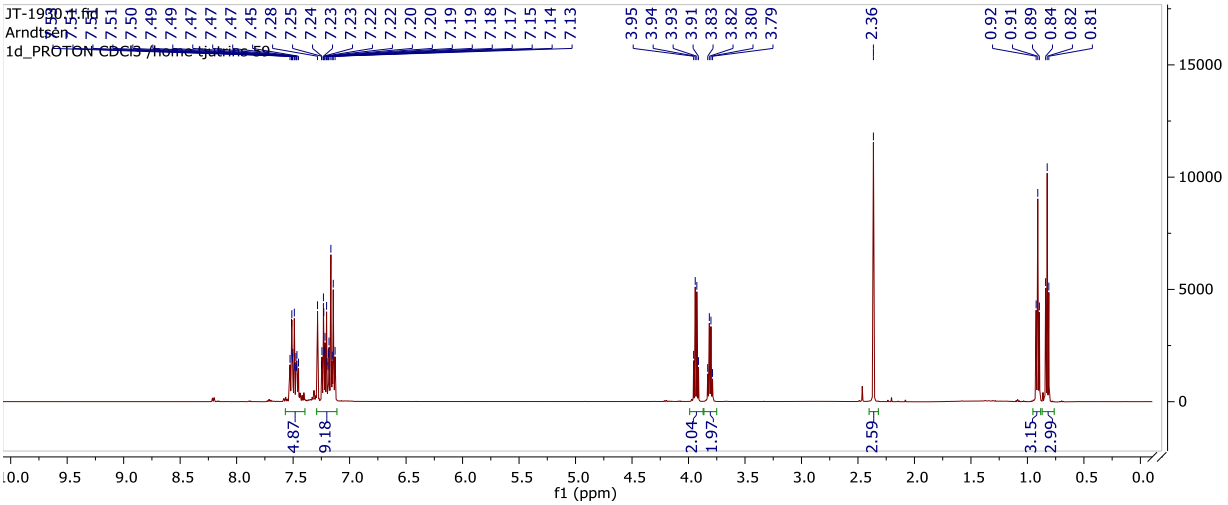

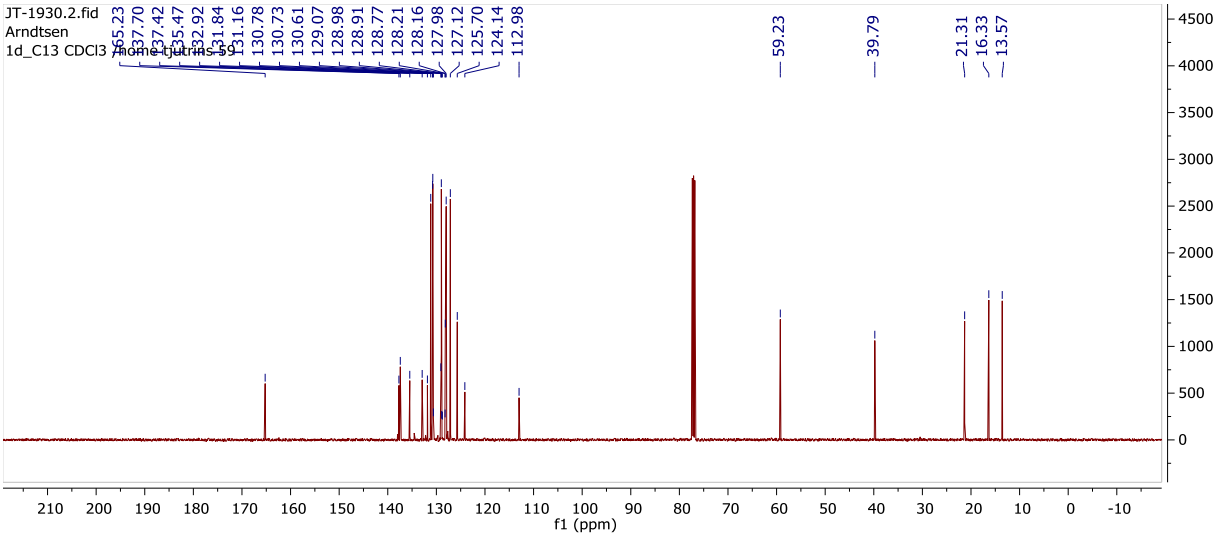

^{1}H and ^{13}C NMR spectra of **6.4e**

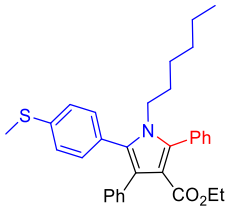

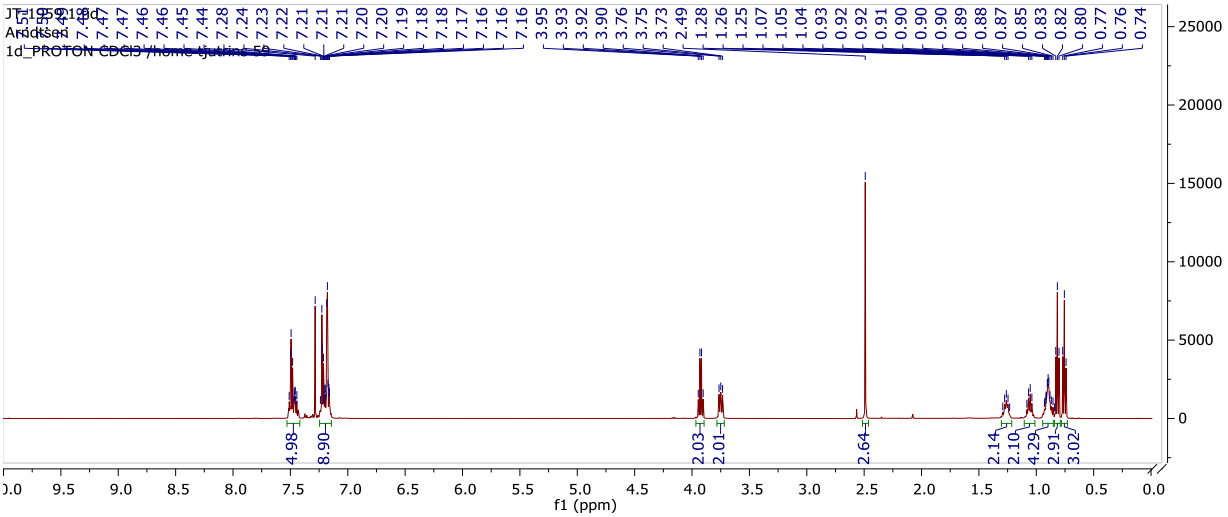

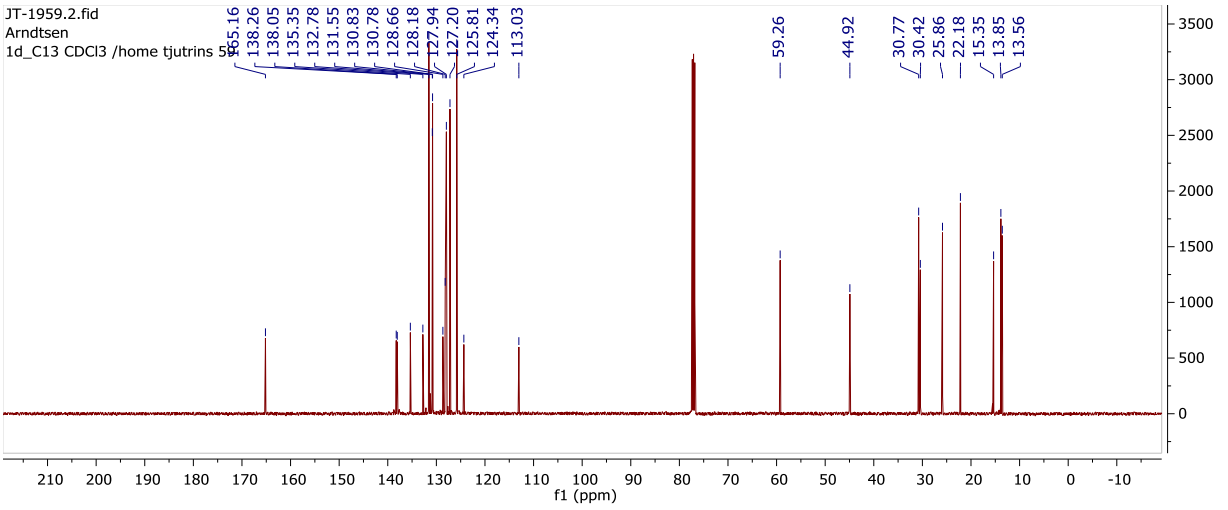

^{1}H and ^{13}C NMR spectra of **6.4f**

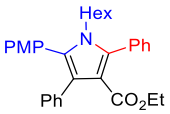

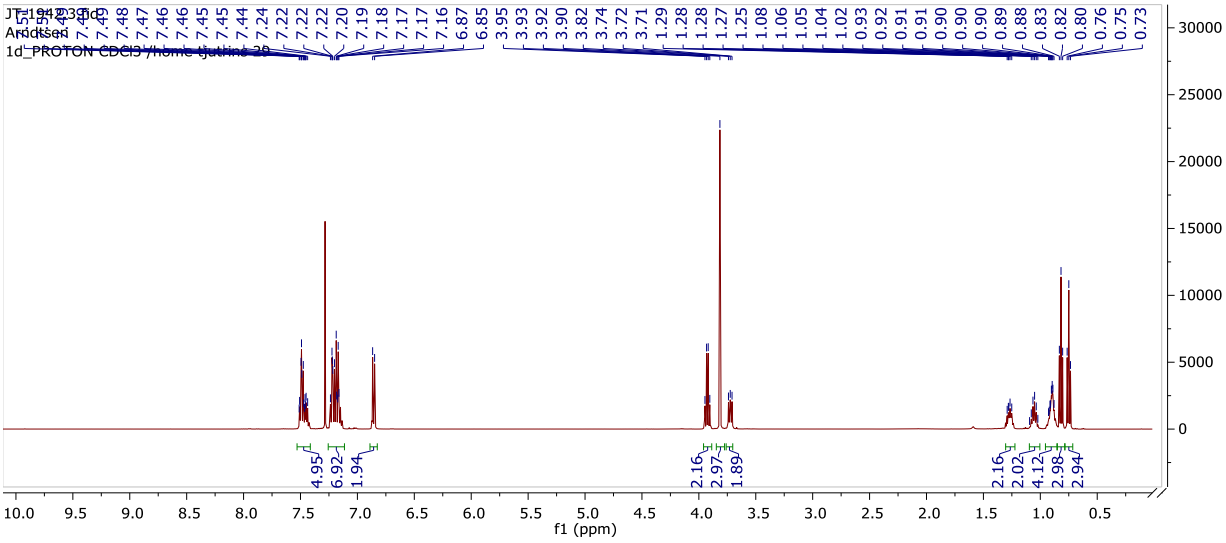

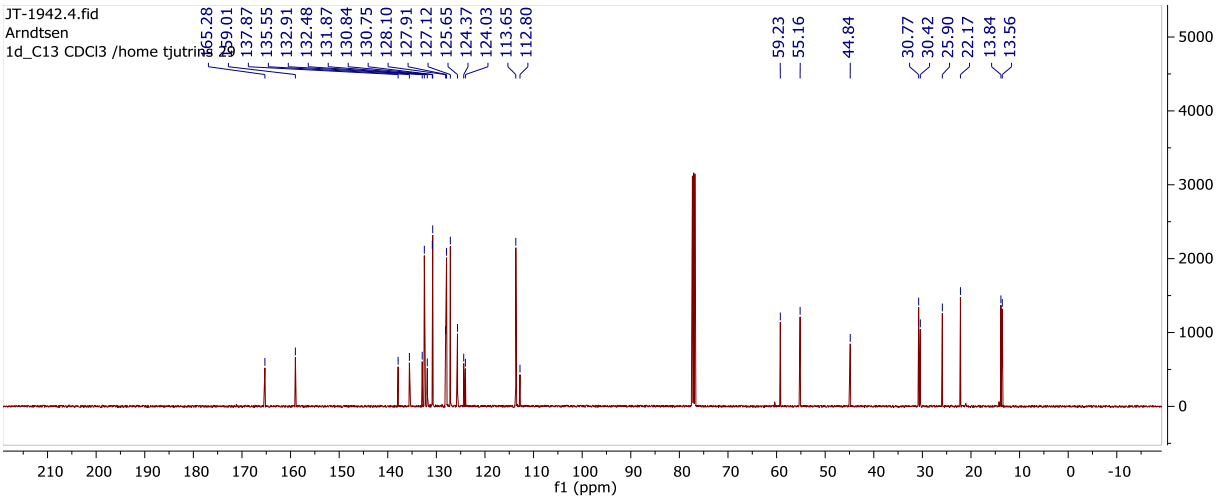

^{1}H and ^{13}C NMR spectra of **6.4g**

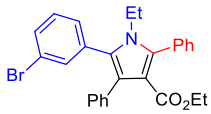

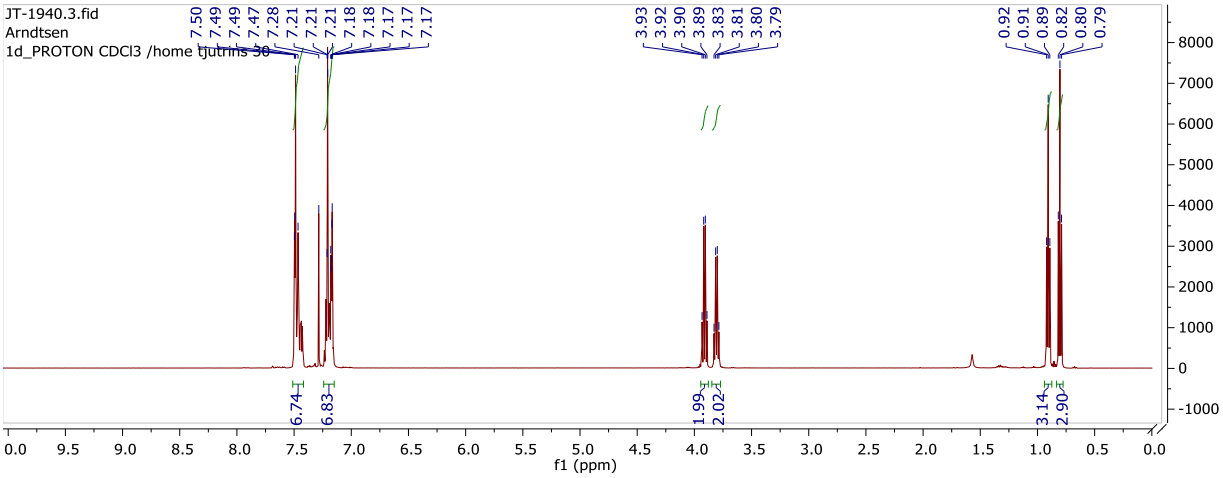

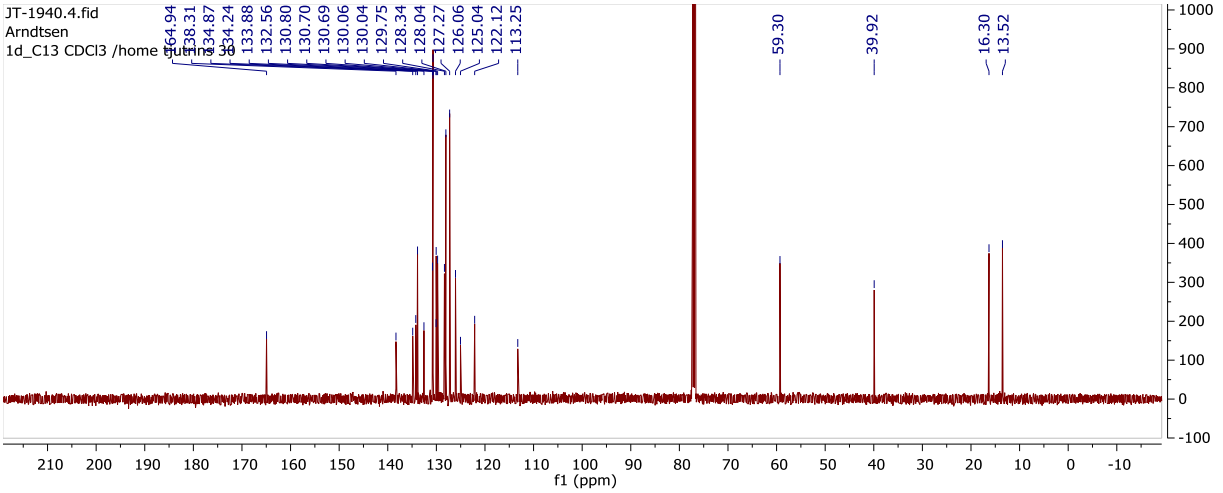

^{1}H and ^{13}C NMR spectra of **6.4h**

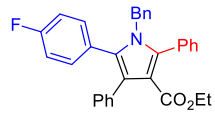

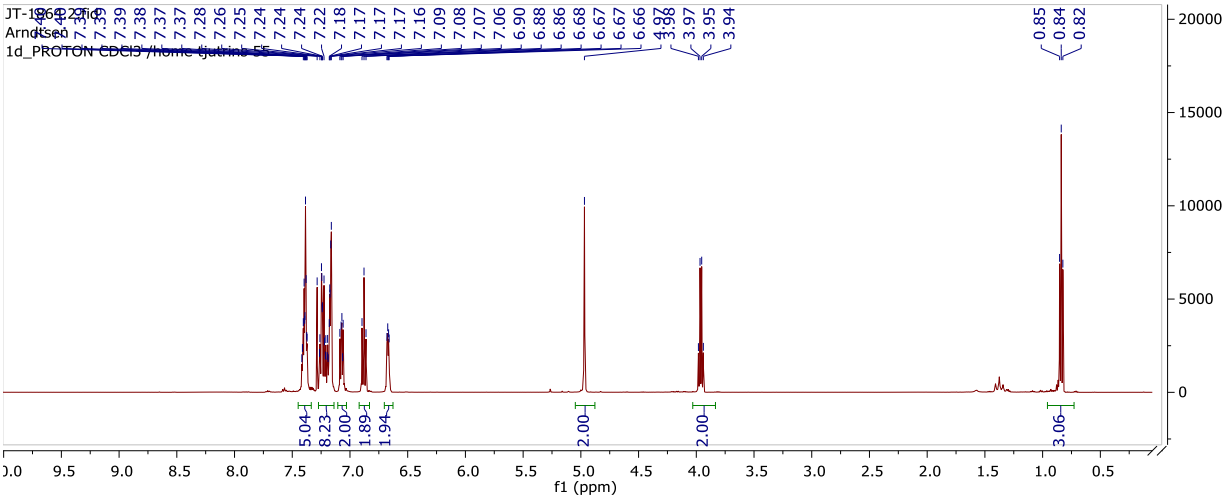

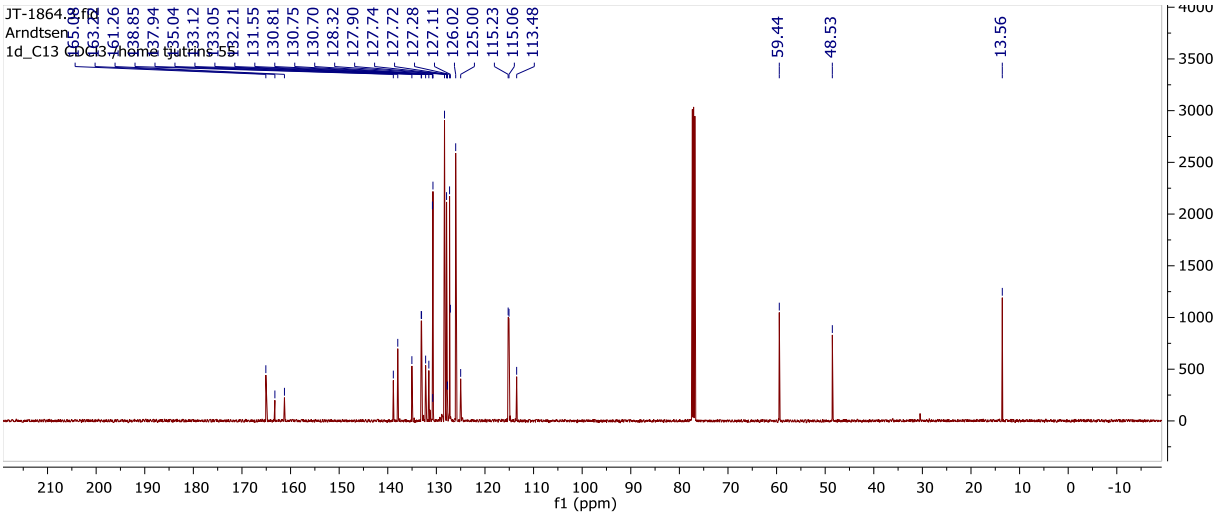

^{1}H and ^{13}C NMR spectra of **6.4i**

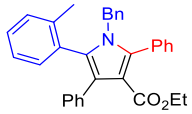

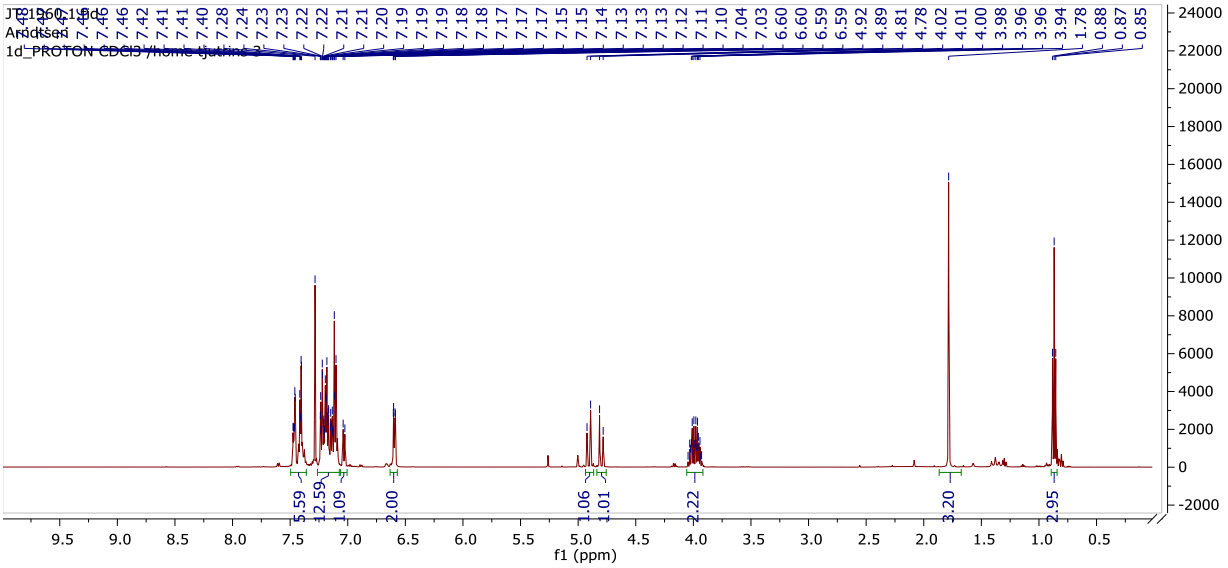

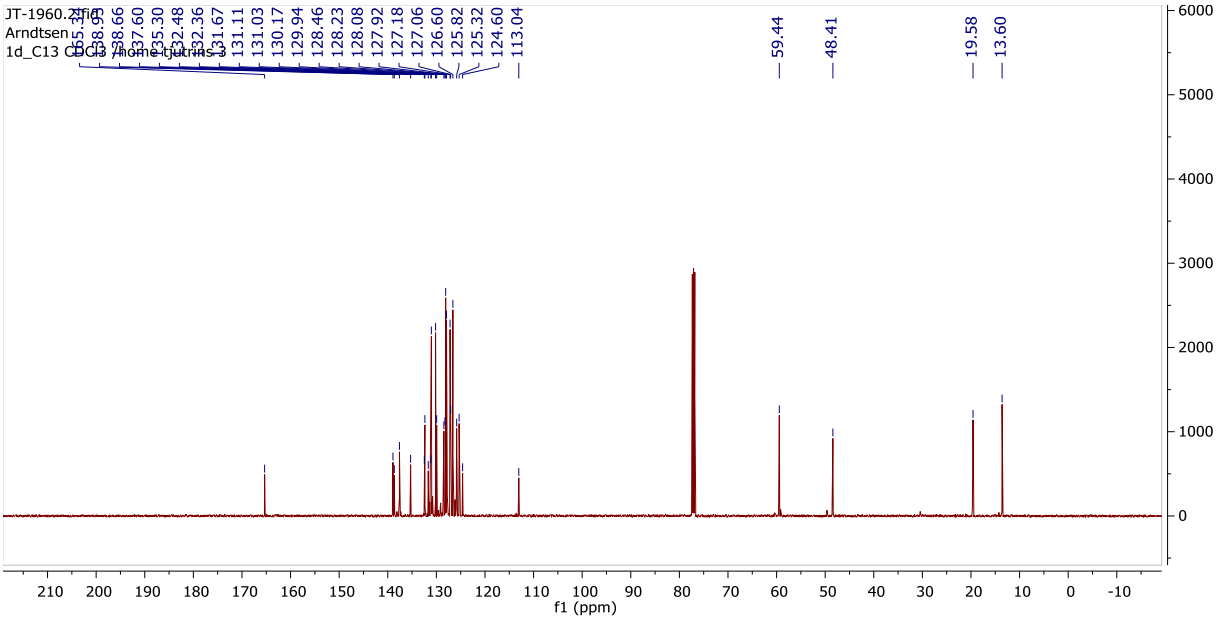

^{1}H and ^{13}C NMR spectra of **6.4j**

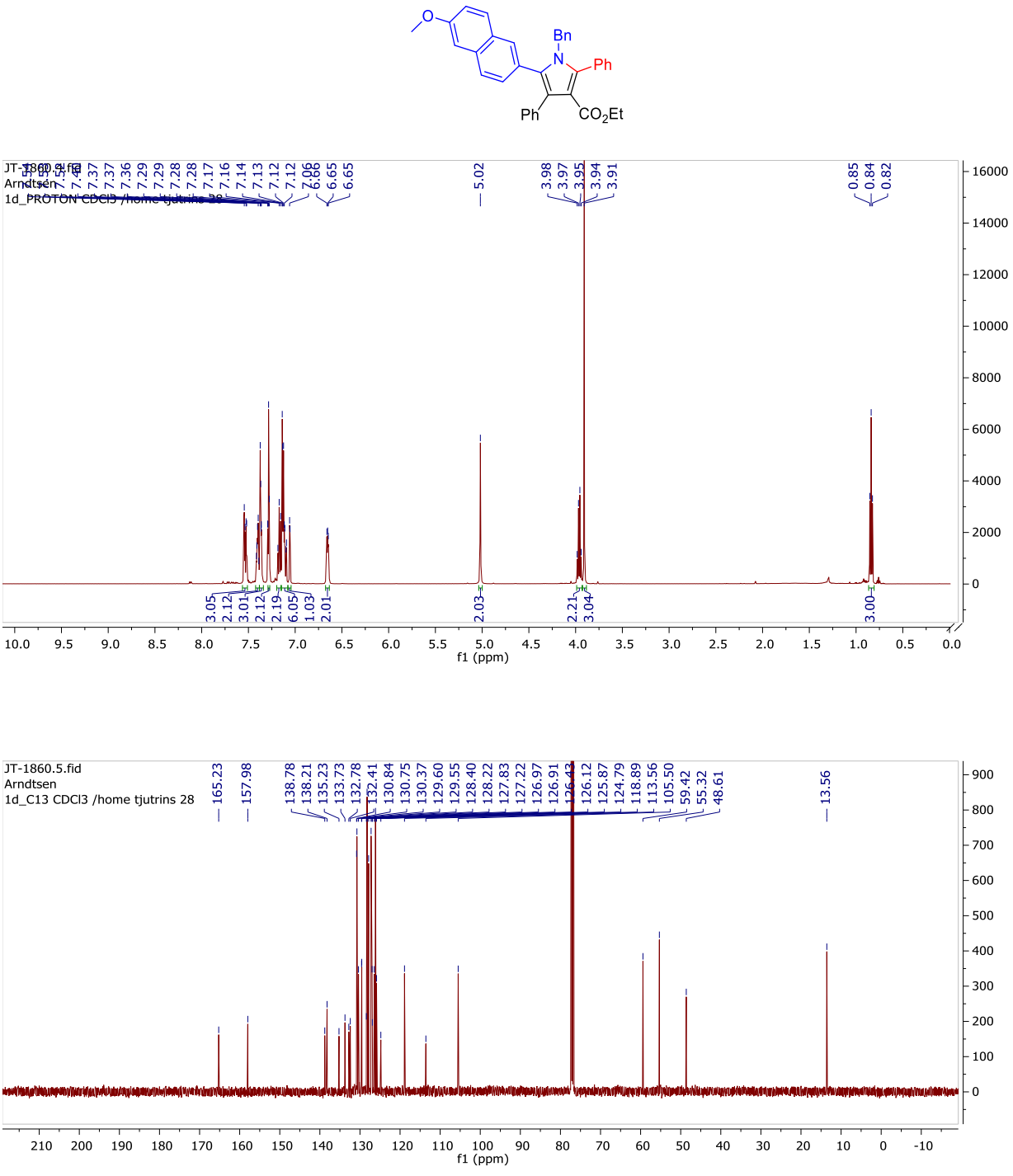

^{1}H and ^{13}C NMR spectra of **6.4k**

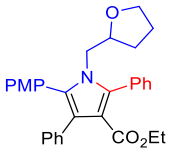

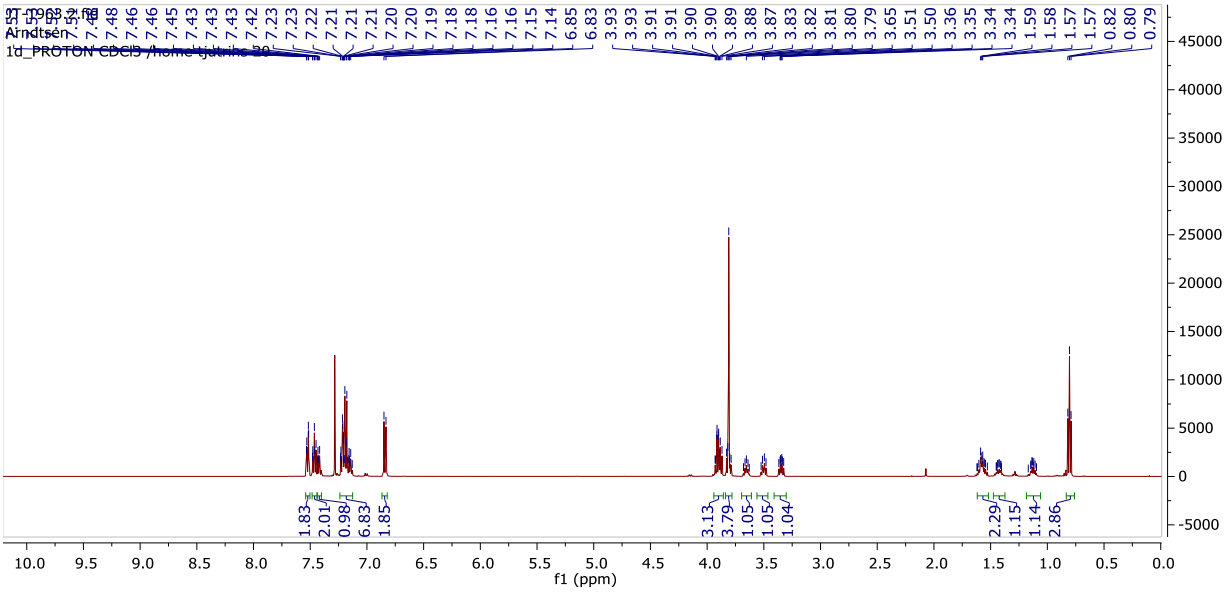

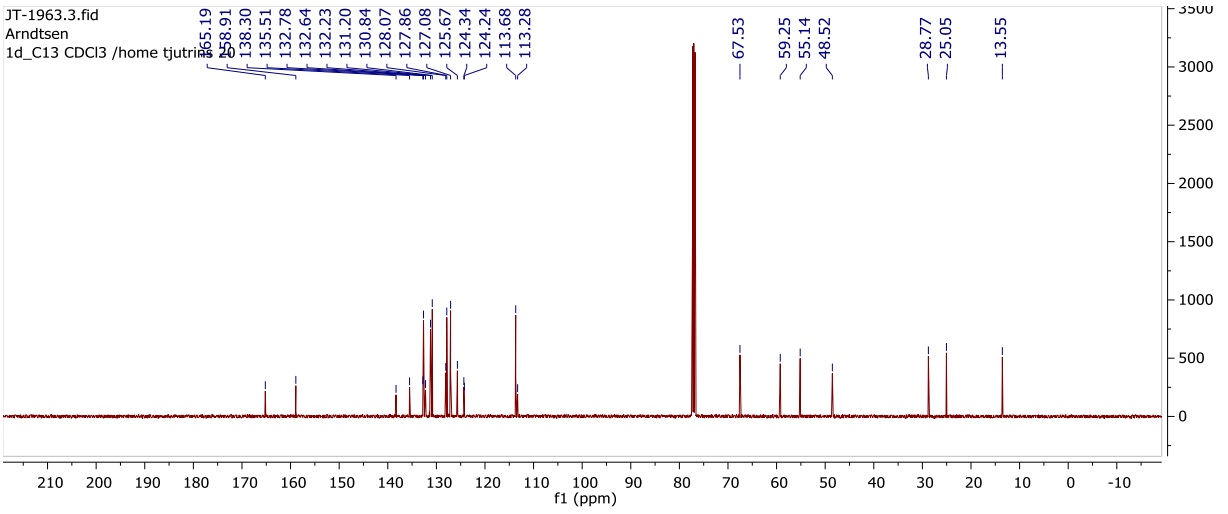

^{1}H and ^{13}C NMR spectra of **6.4l**

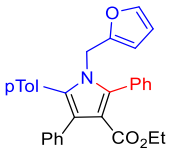

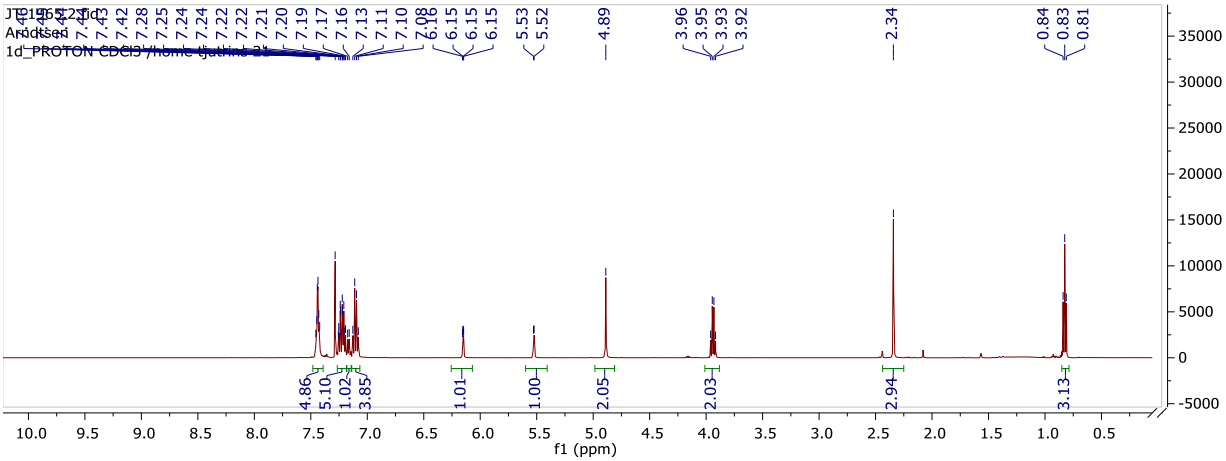

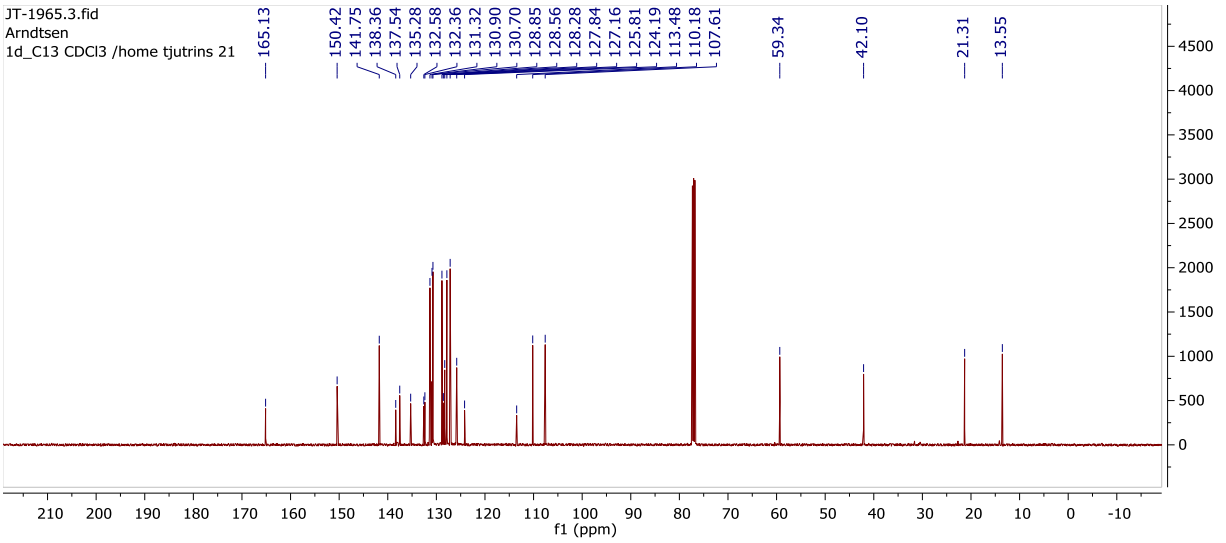

^{1}H and ^{13}C NMR spectra of **6.4m**

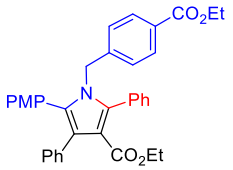

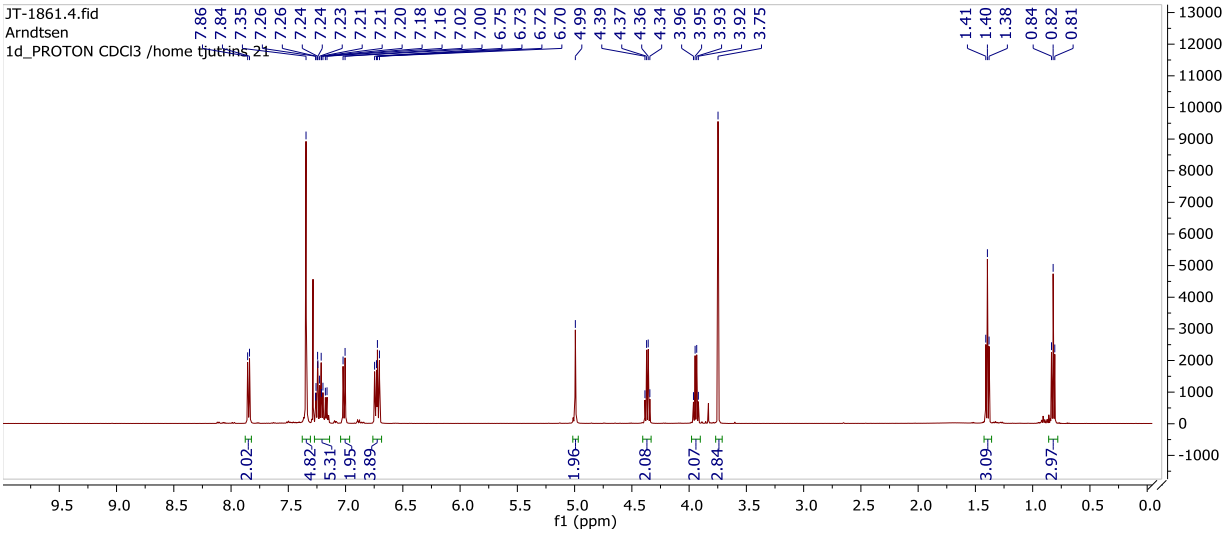

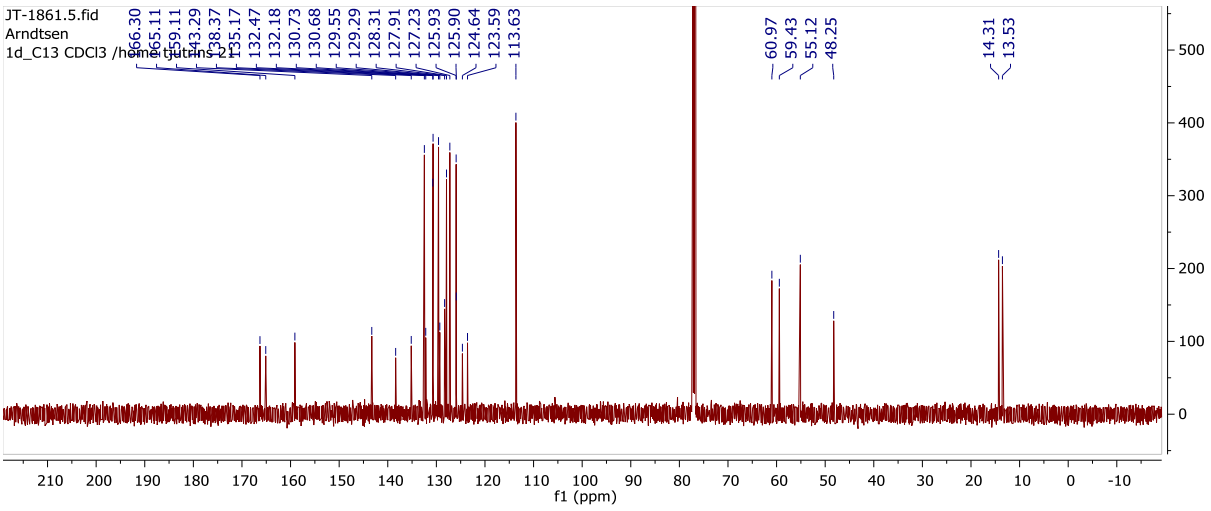

^{1}H and ^{13}C NMR spectra of **6.4n**

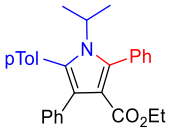

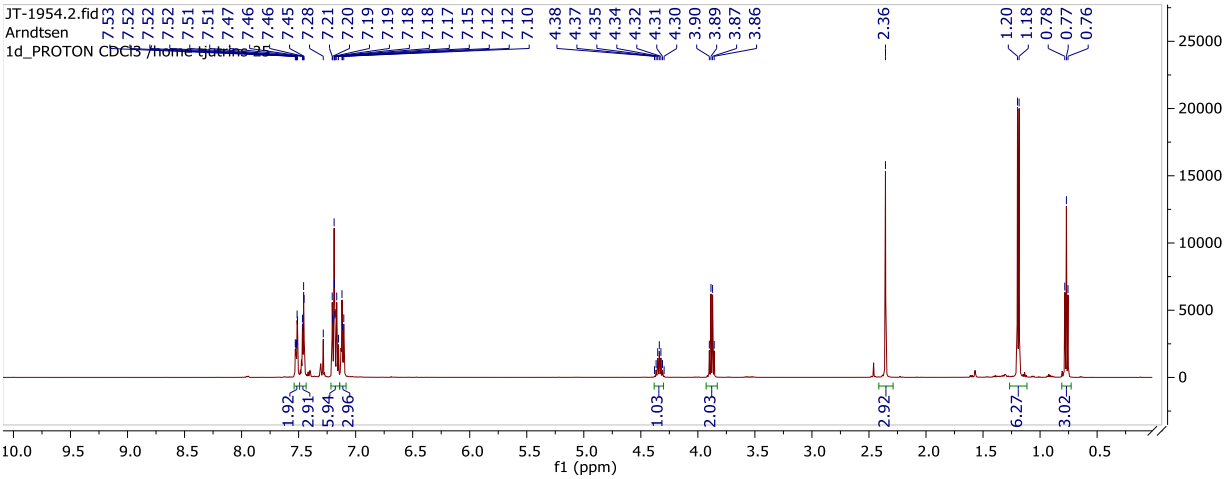

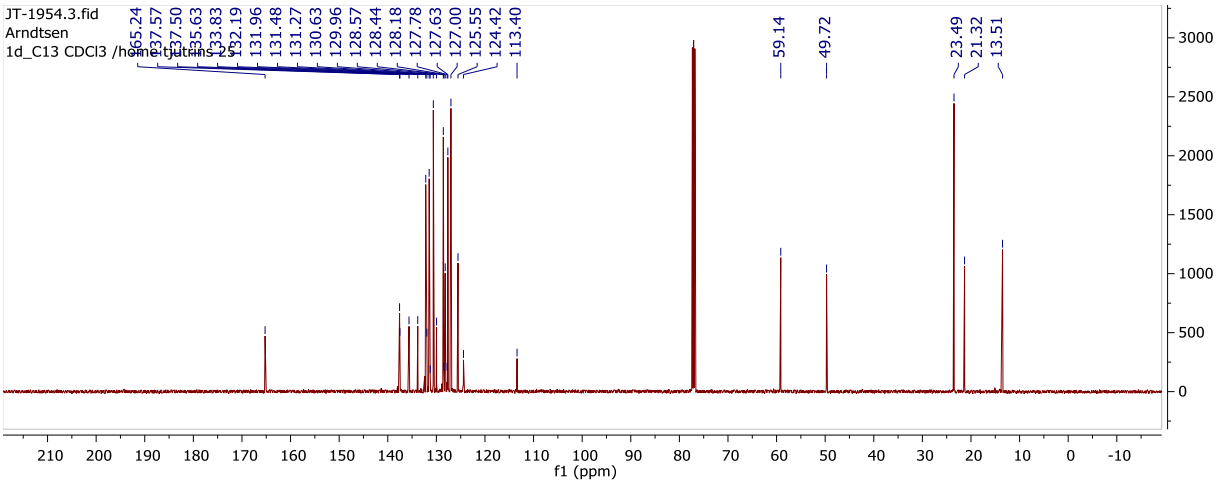

^{1}H and ^{13}C NMR spectra of **6.4o**

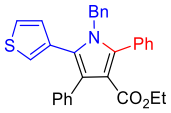

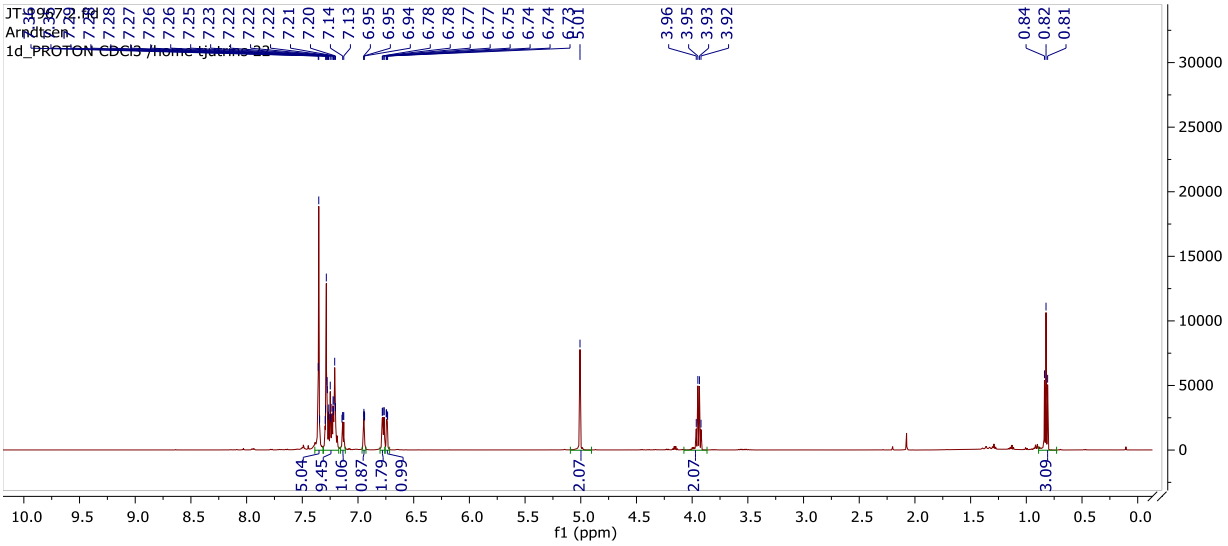

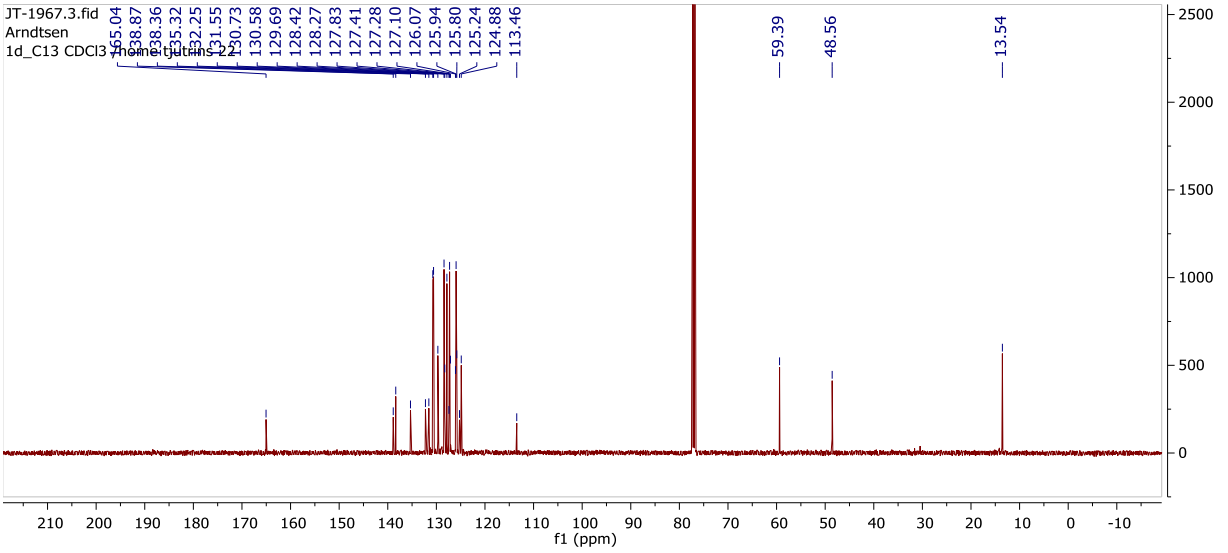

^{1}H and ^{13}C NMR spectra of **6.4p**

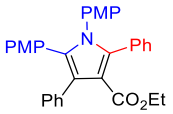

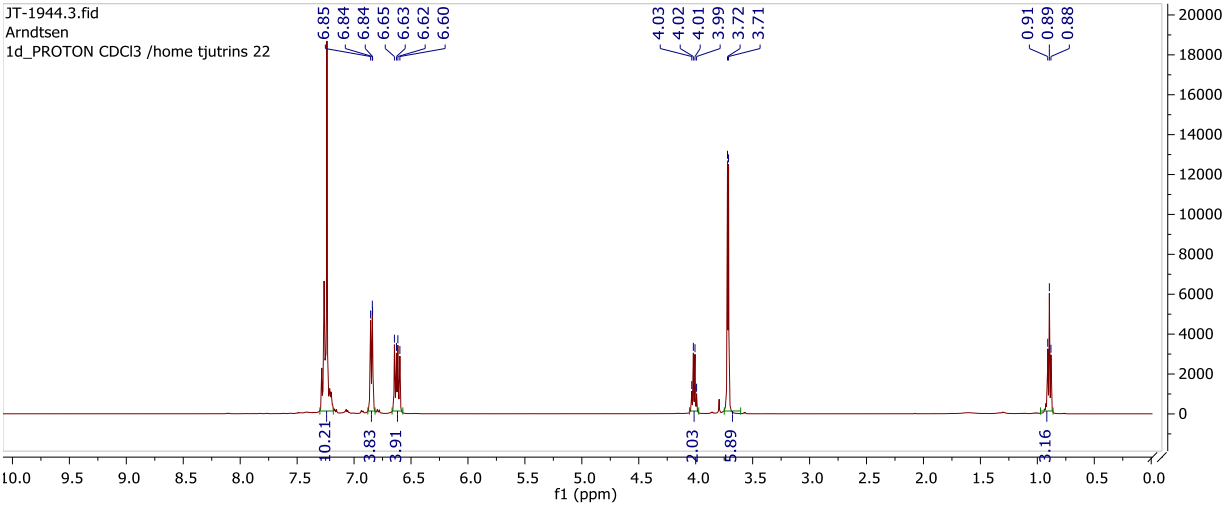

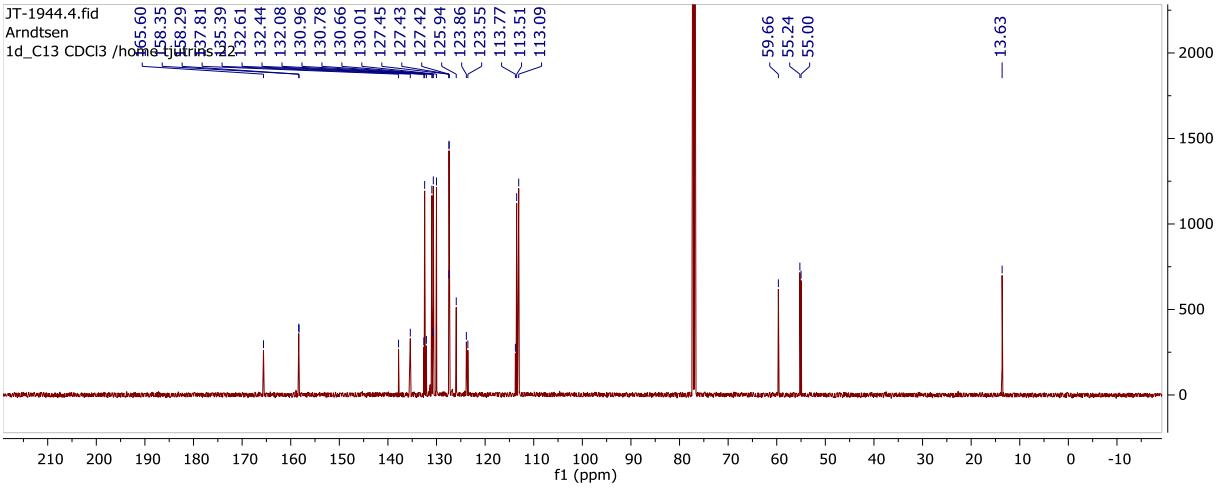

^{1}H and ^{13}C NMR spectra of **6.4q**

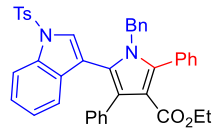

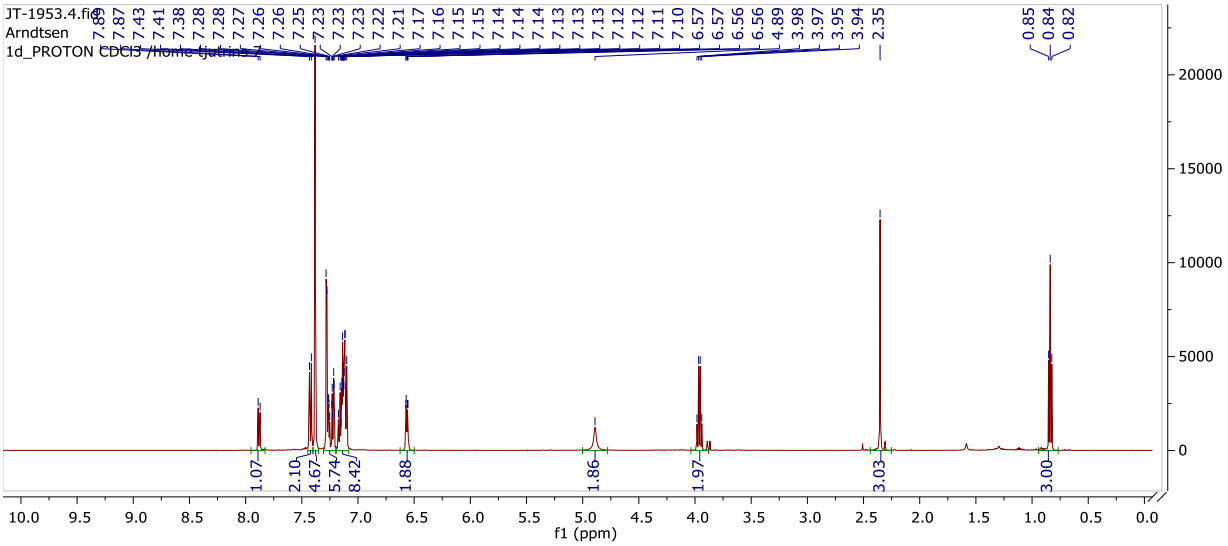

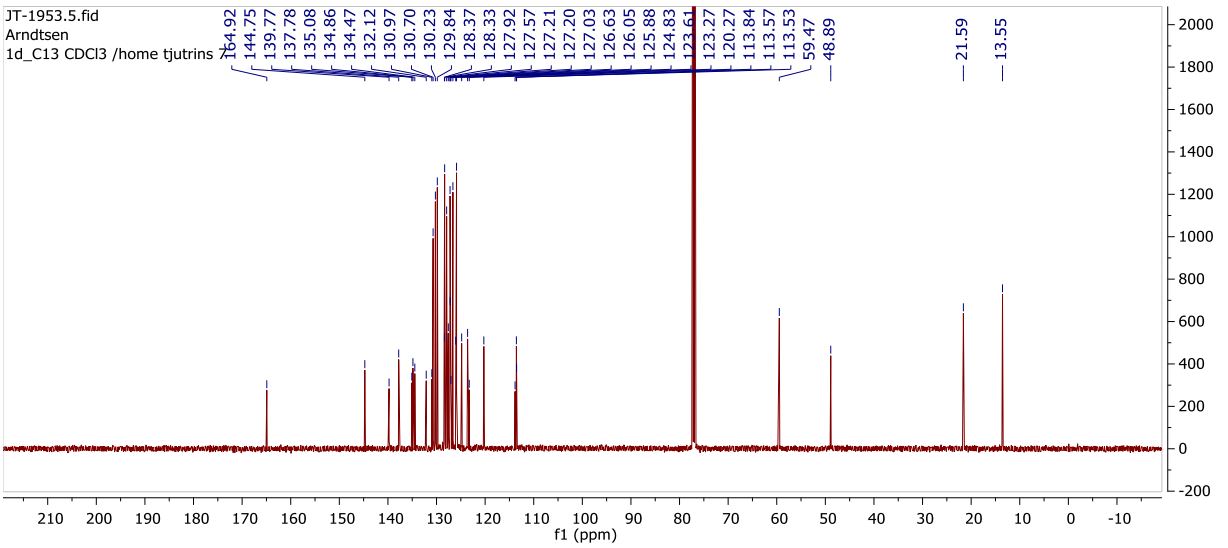

^{1}H and ^{13}C NMR spectra of **6.4r**

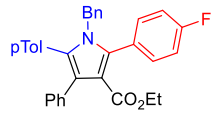

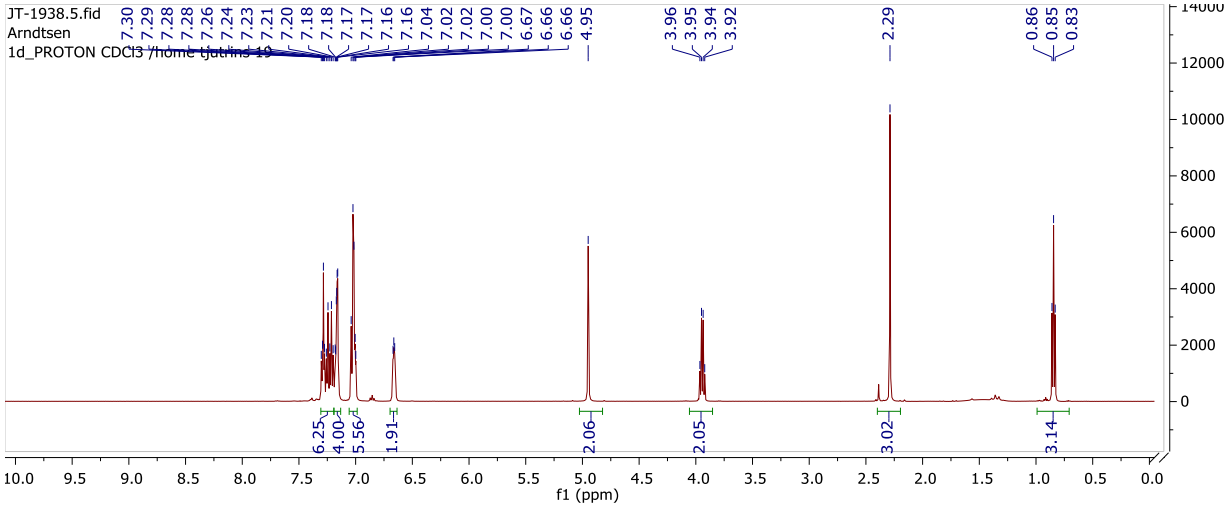

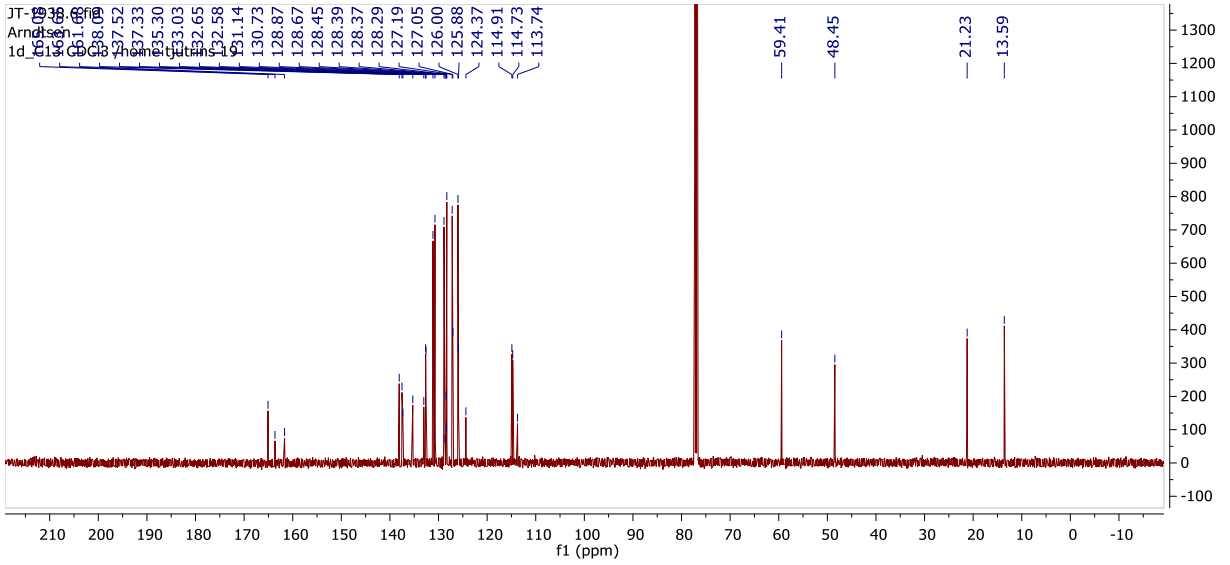

^{1}H and ^{13}C NMR spectra of **6.4s**

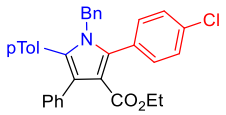

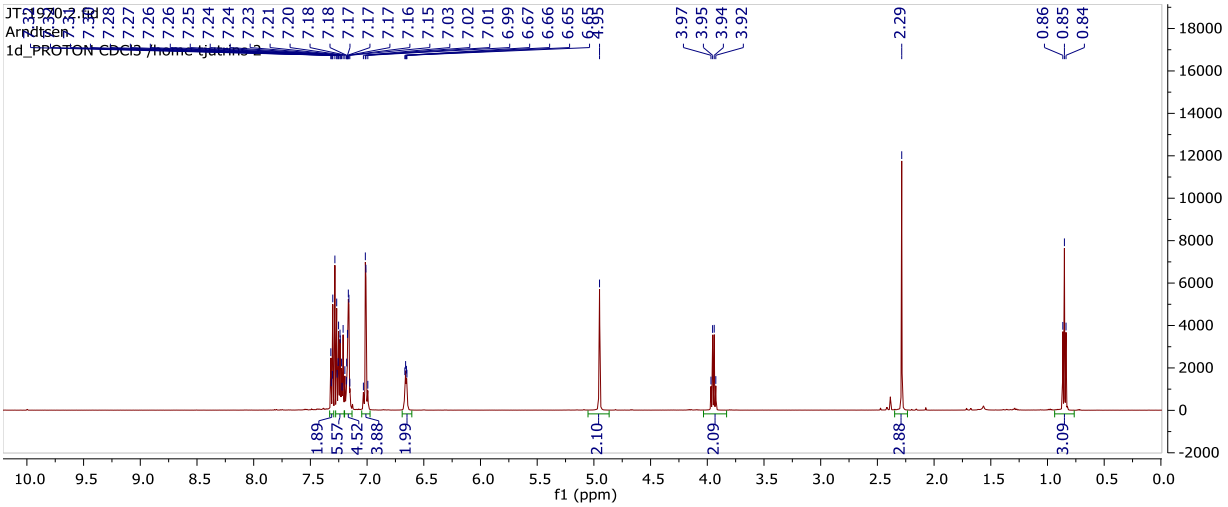

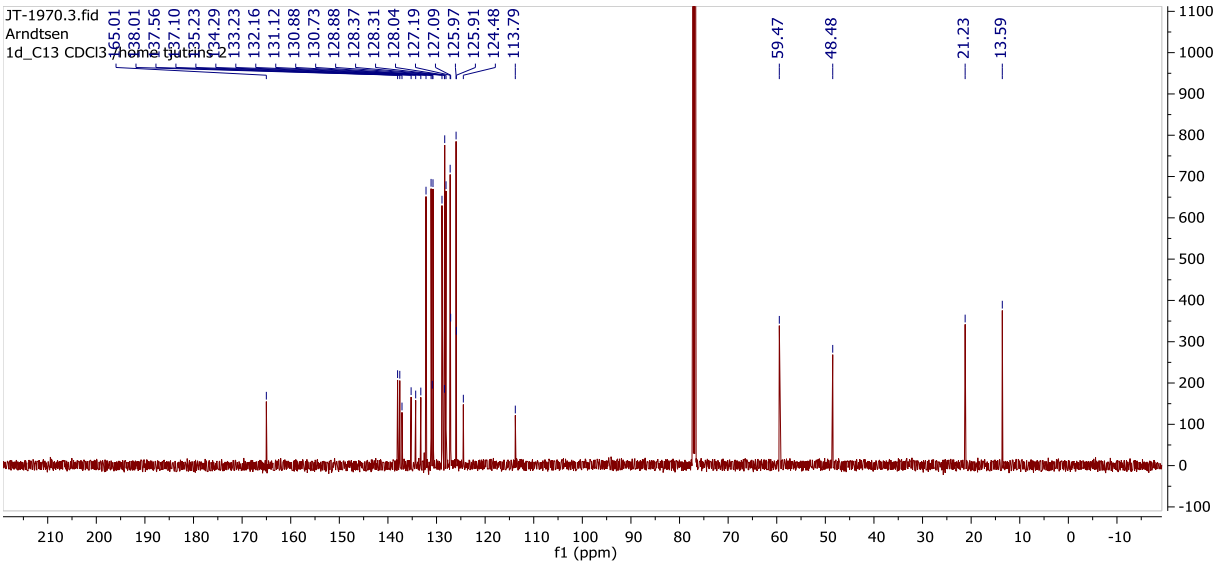

^{1}H and ^{13}C NMR spectra of **6.4t**

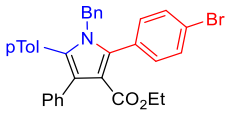

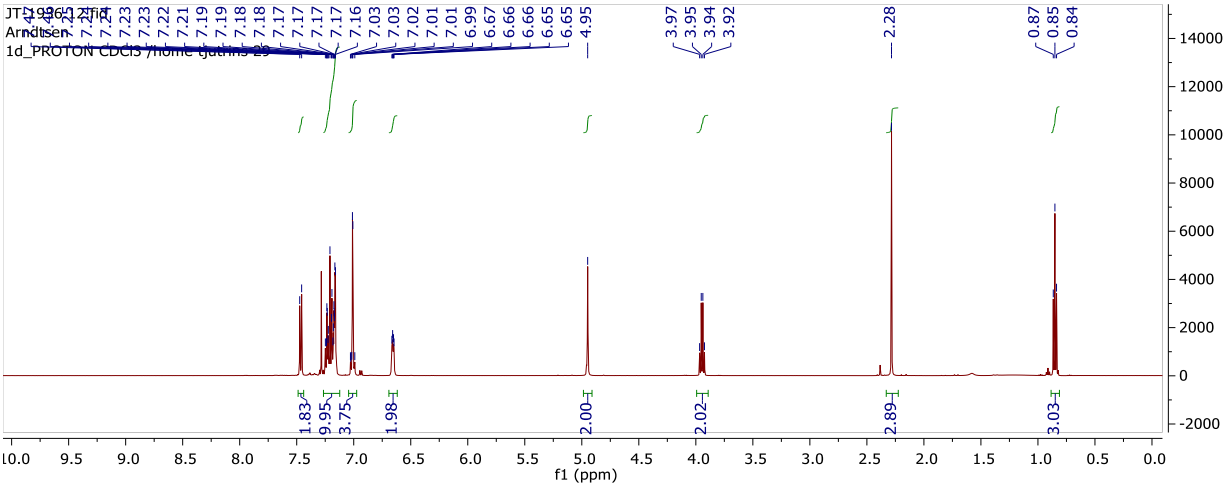

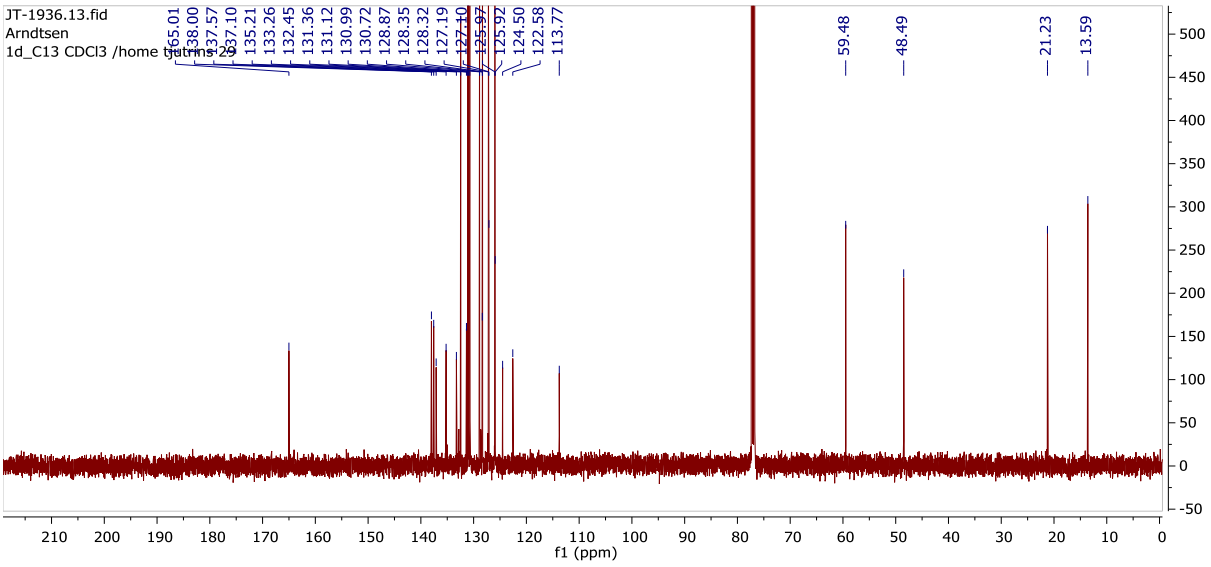

^{1}H and ^{13}C NMR spectra of **6.4u**

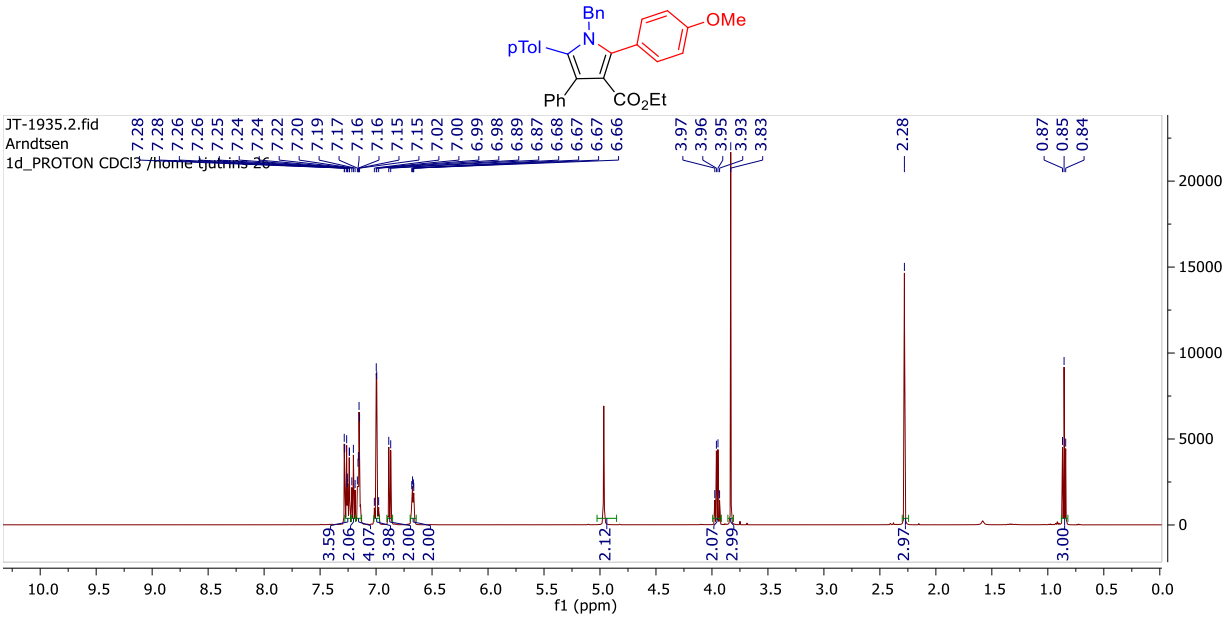

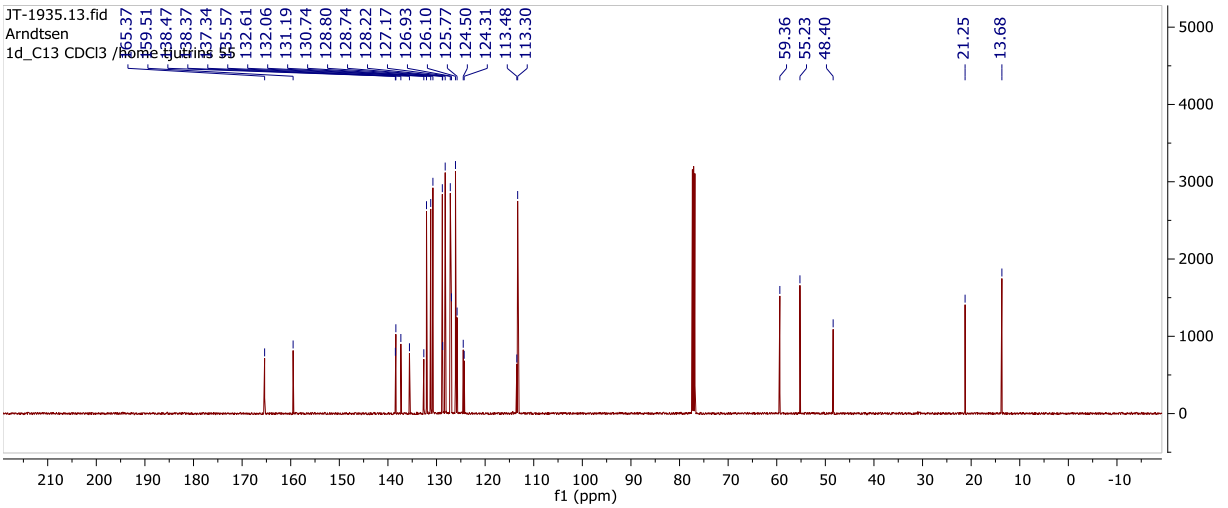

^{1}H and ^{13}C NMR spectra of **6.4v**

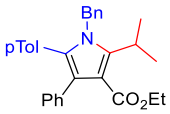

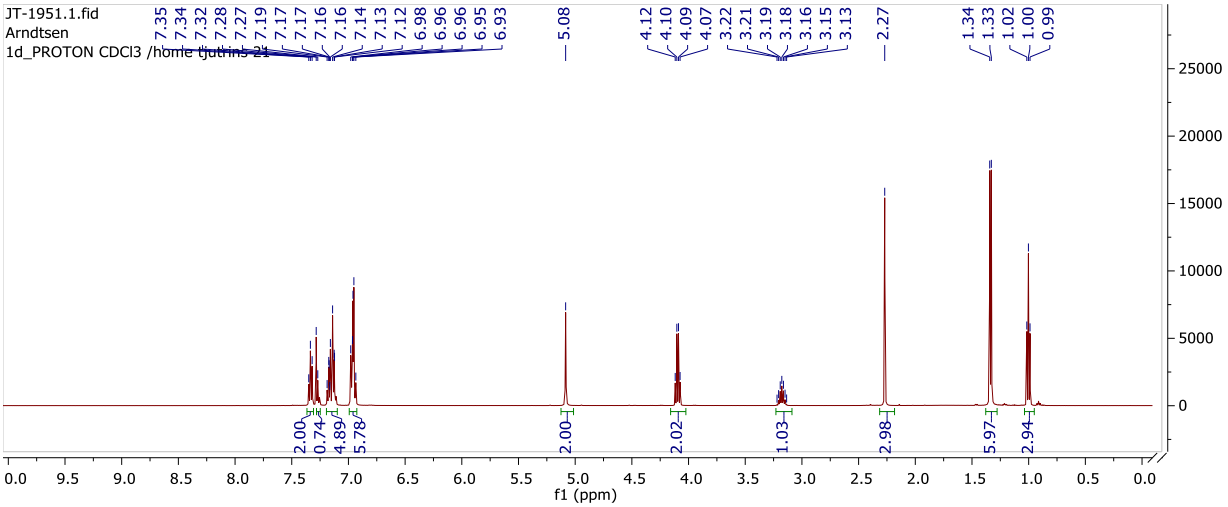

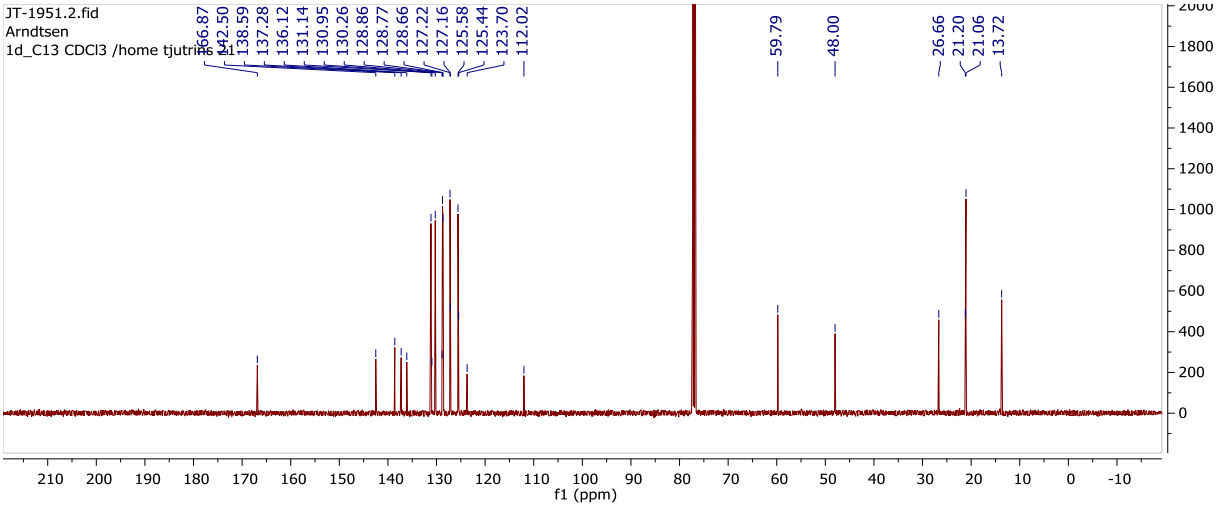

^{1}H and ^{13}C NMR spectra of **6.4w**

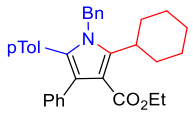

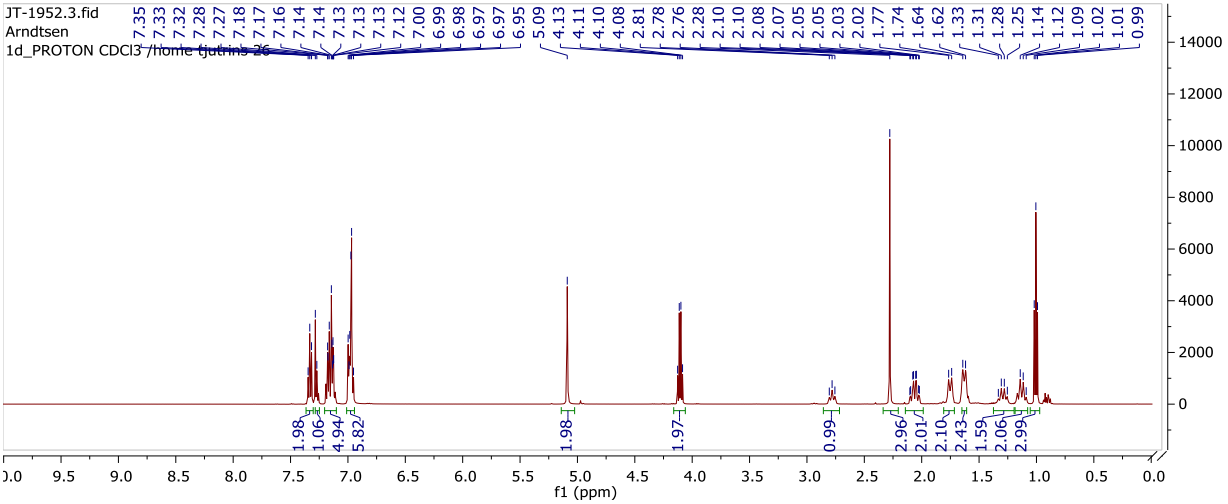

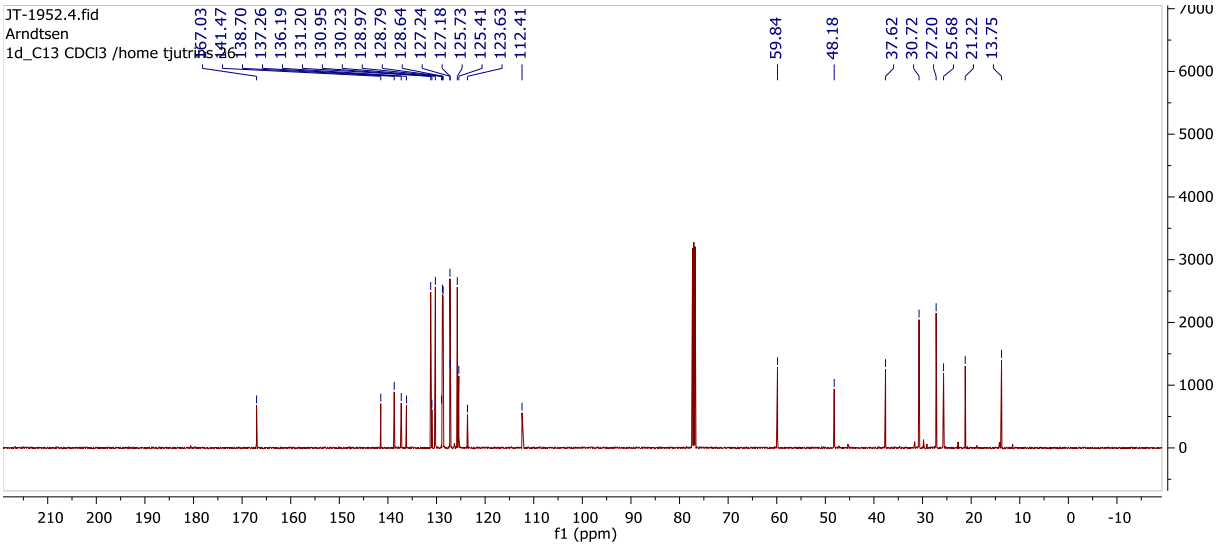

^{1}H and ^{13}C NMR spectra of **6.4x**

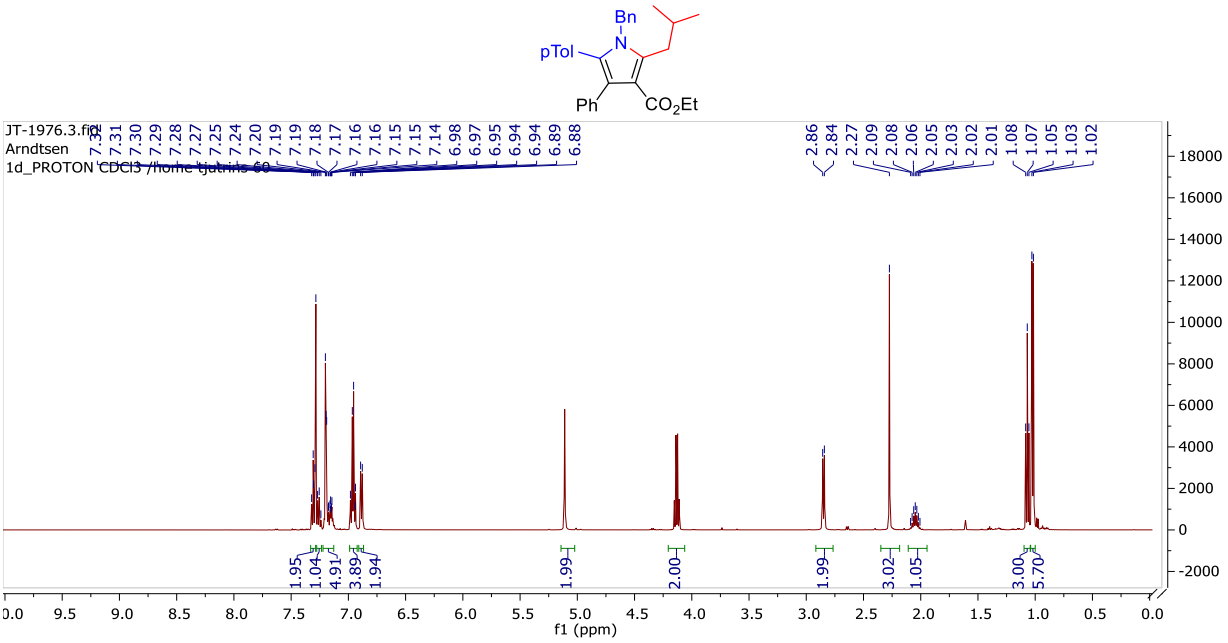

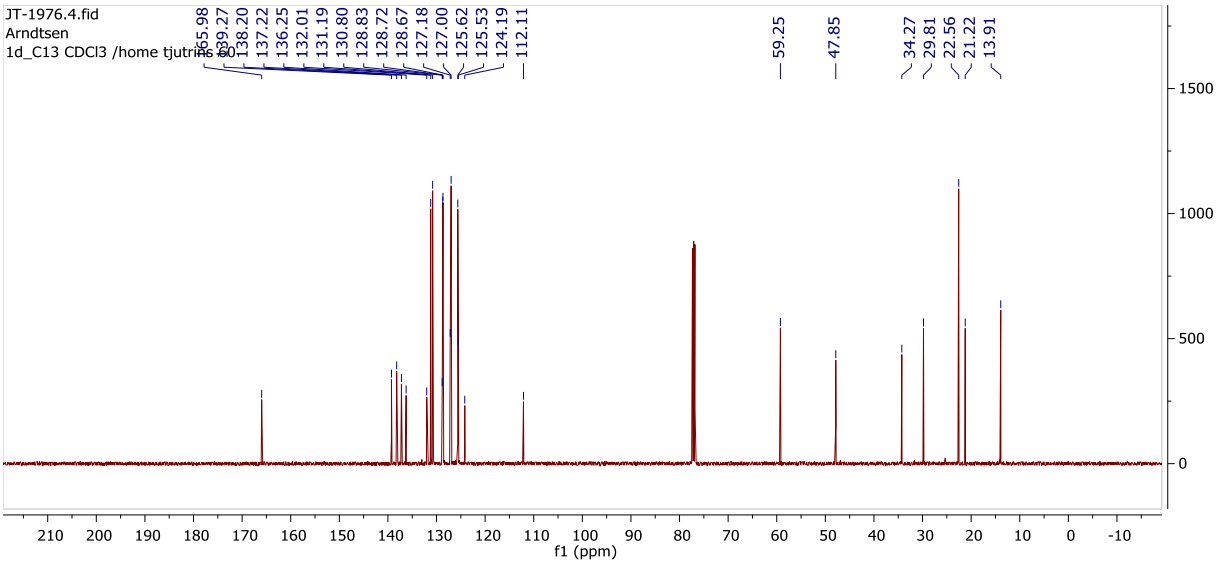

^{1}H and ^{13}C NMR spectra of **6.4y**

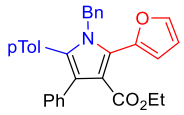

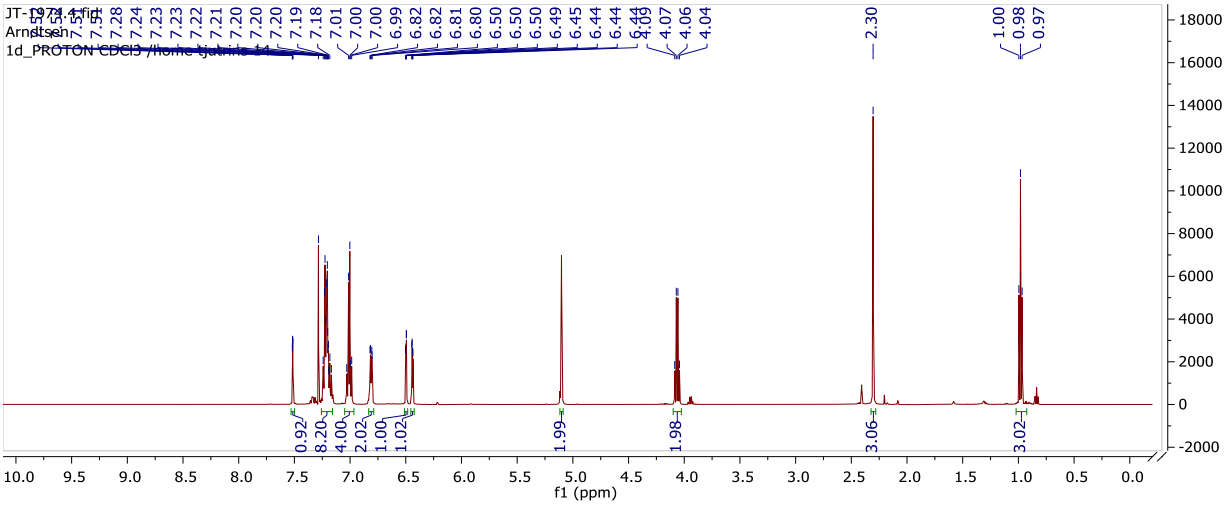

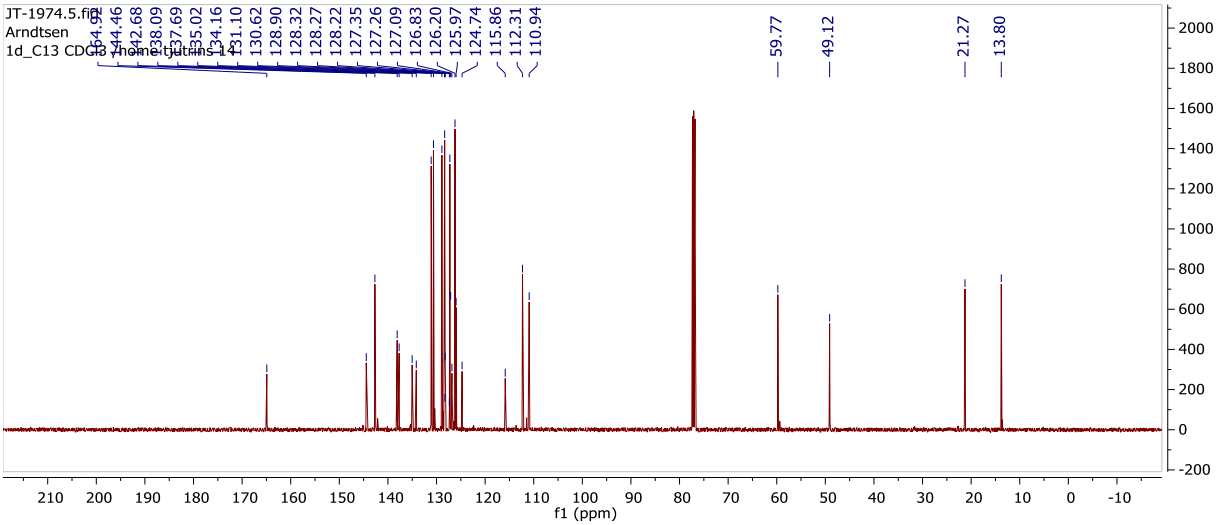

^{1}H and ^{13}C NMR spectra of **6.4z**

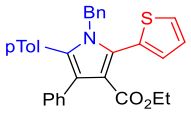

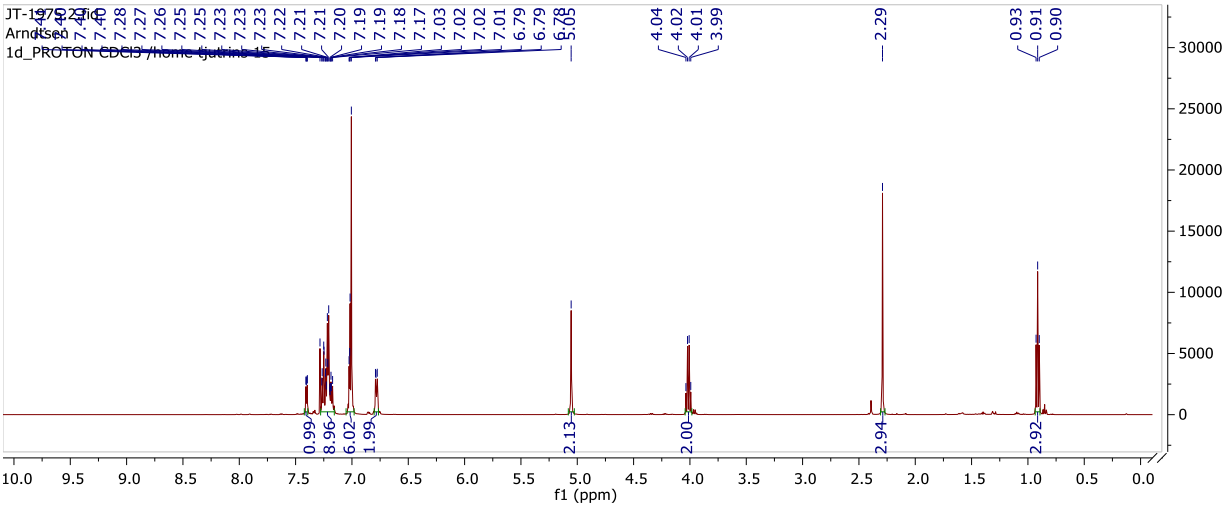

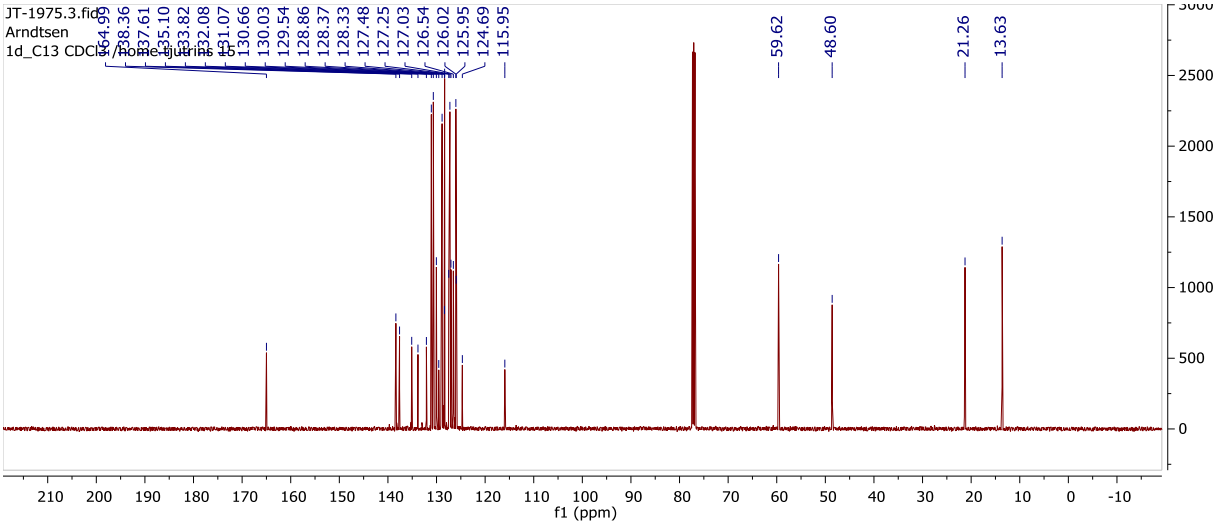

^{1}H and ^{13}C NMR spectra of **6.4aa**

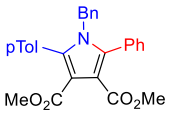

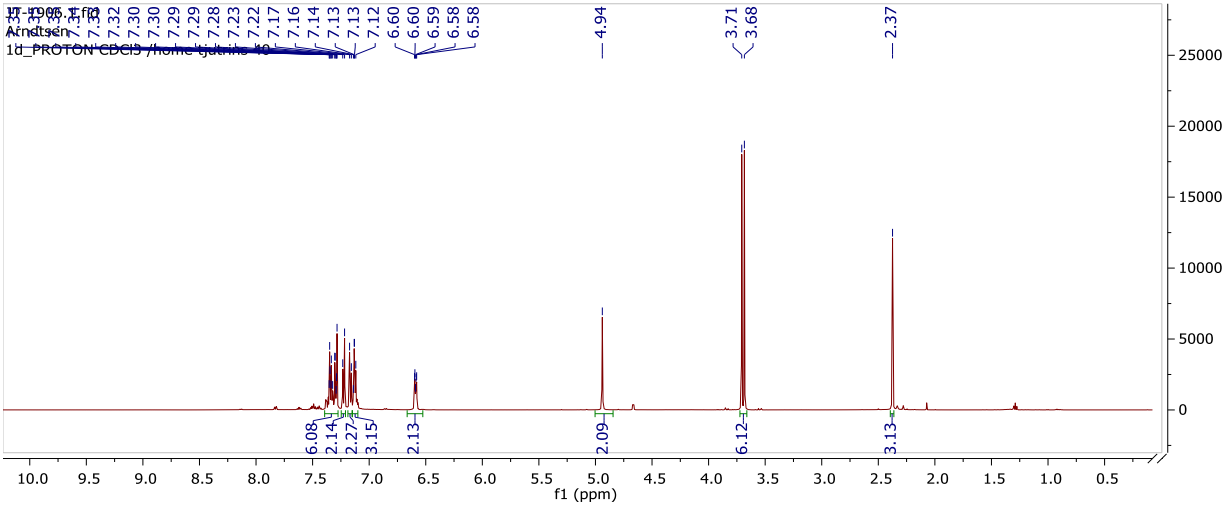

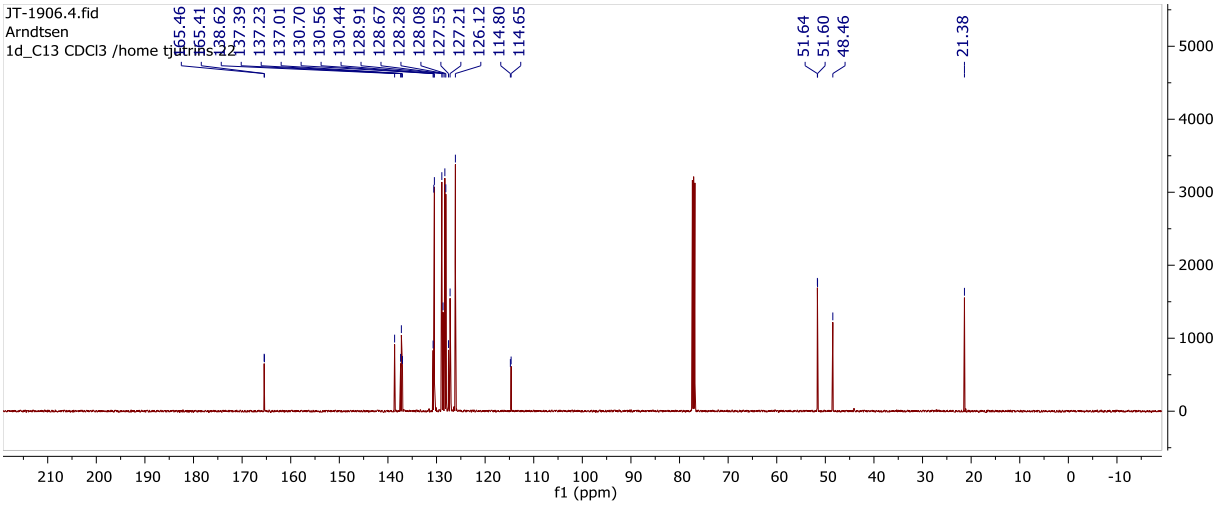

^{1}H and ^{13}C NMR spectra of **6.4bb**

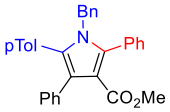

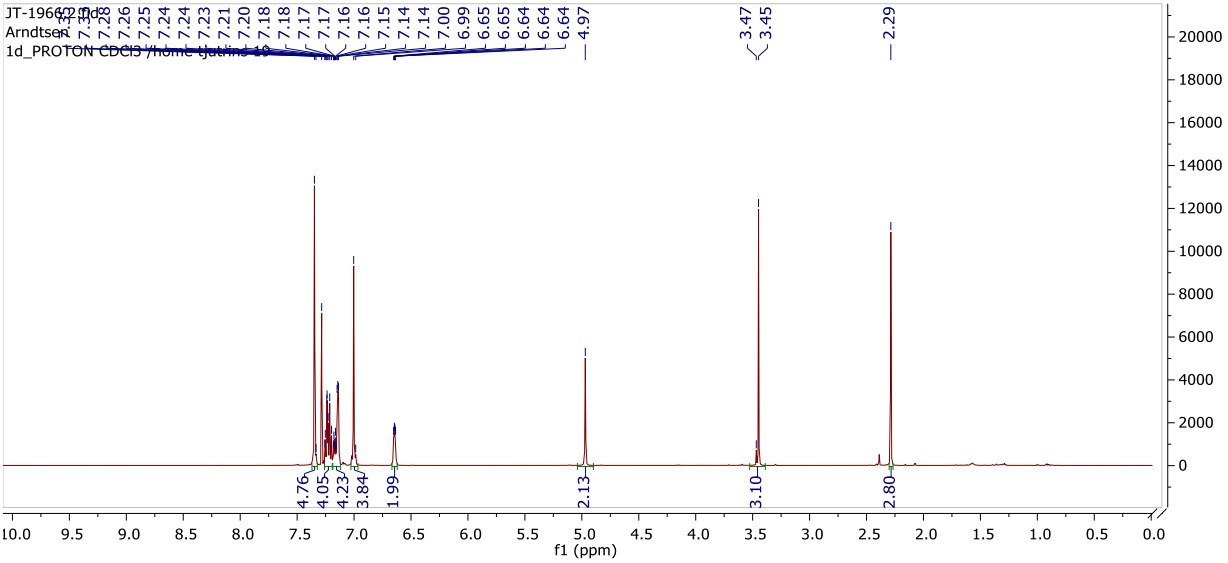

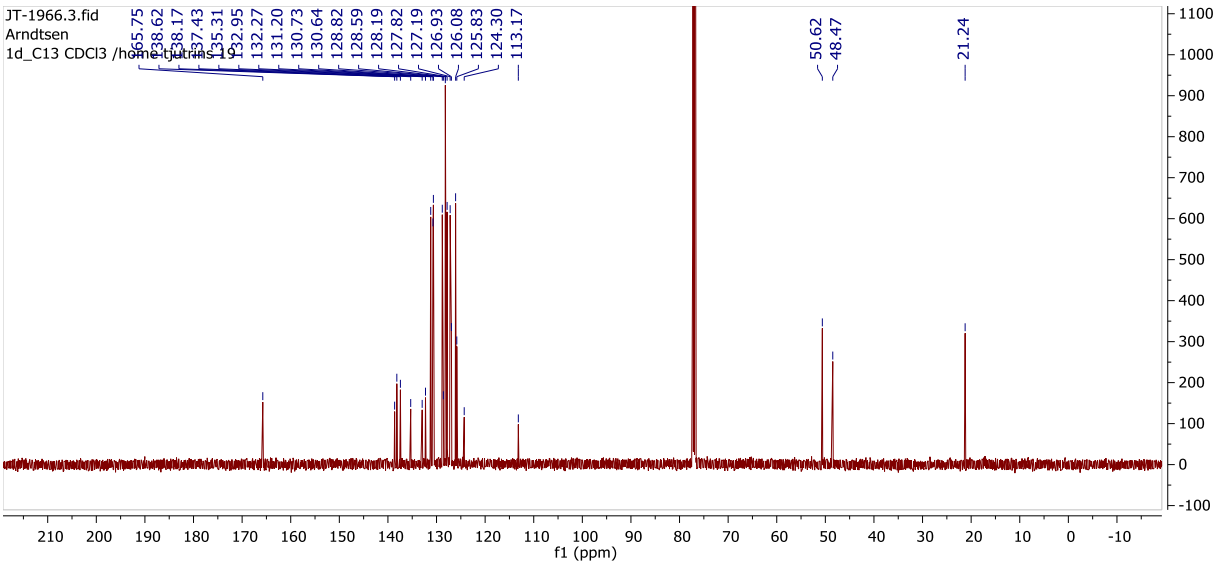

^{1}H and ^{13}C NMR spectra of **6.4cc**

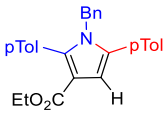

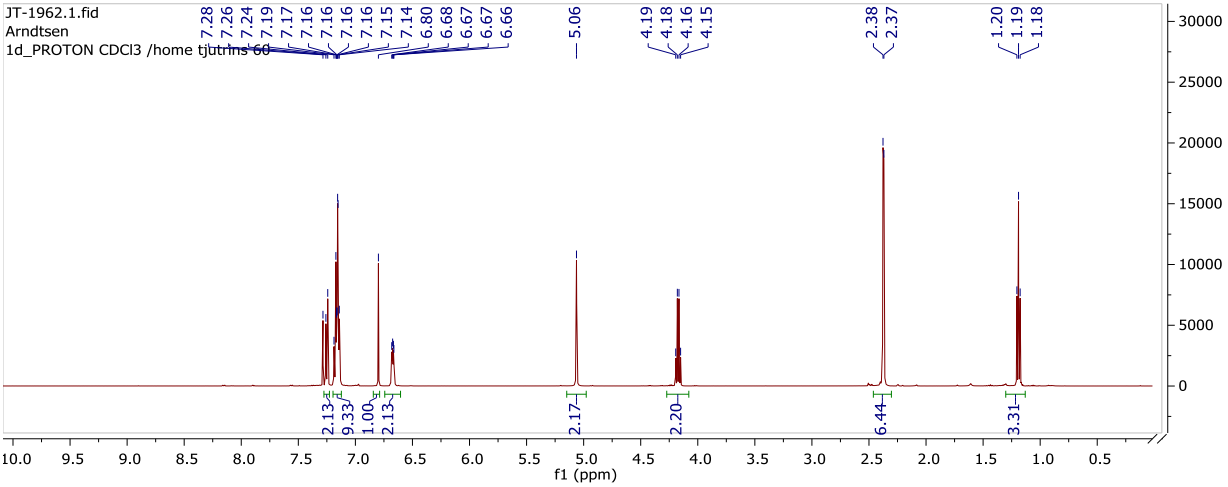

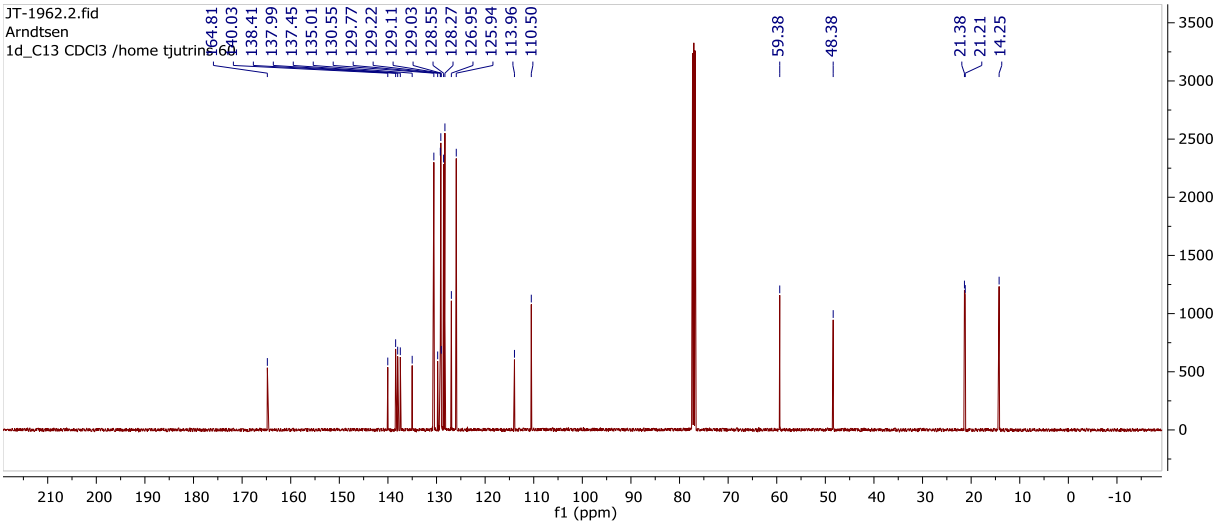

^{1}H and ^{13}C NMR spectra of **6.4dd**

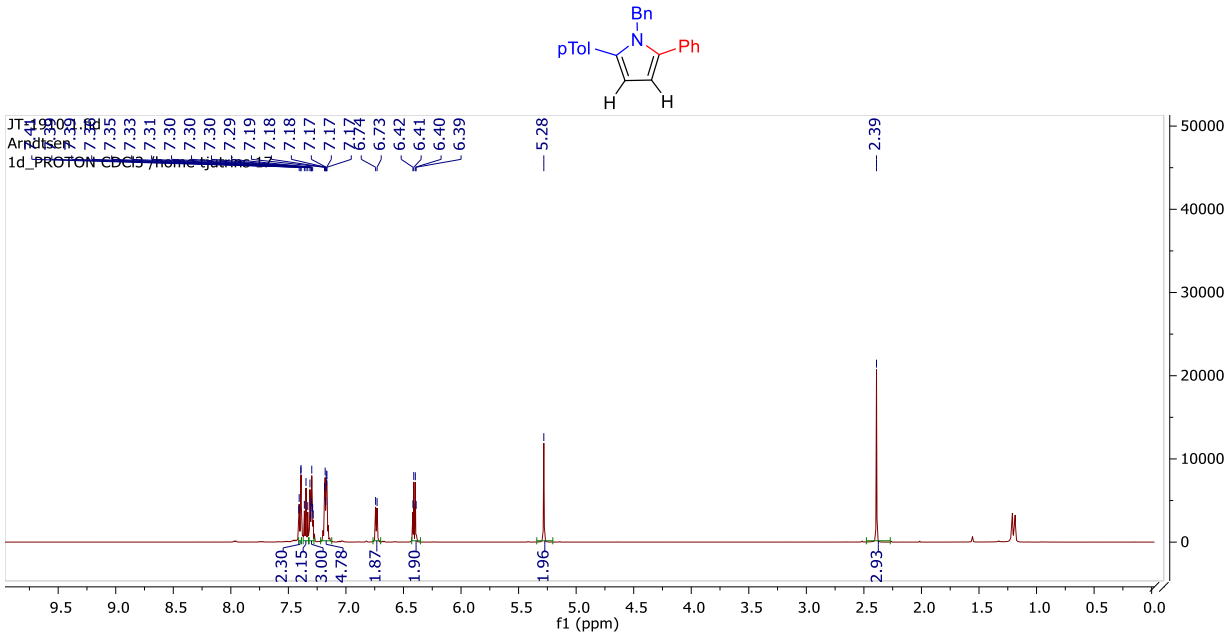

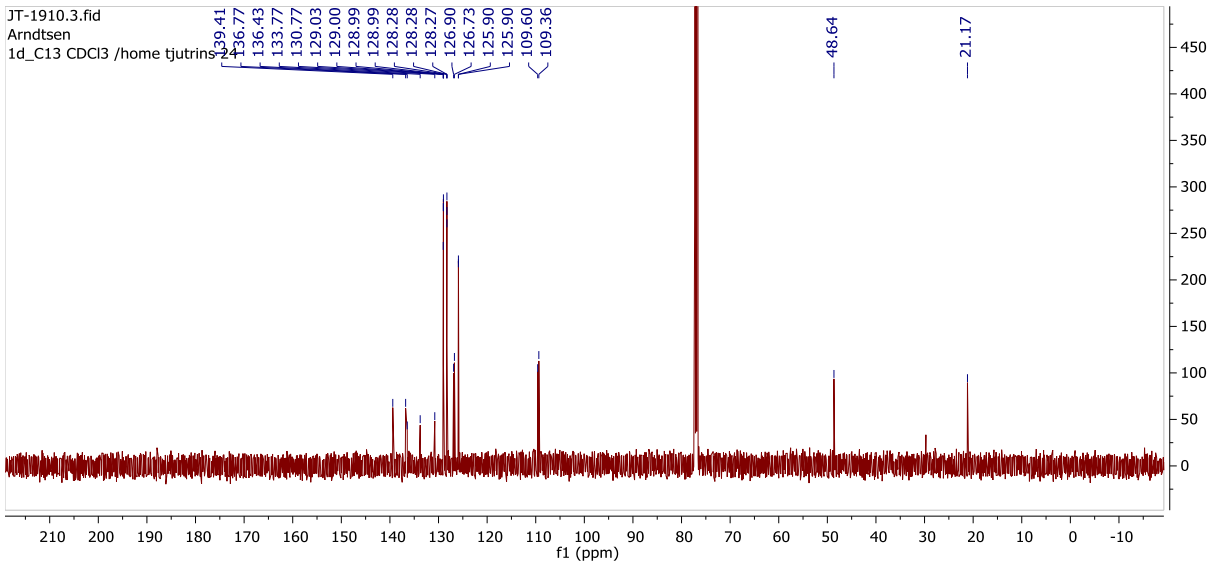

^{1}H and ^{13}C NMR spectra of **6.4ee**

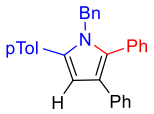

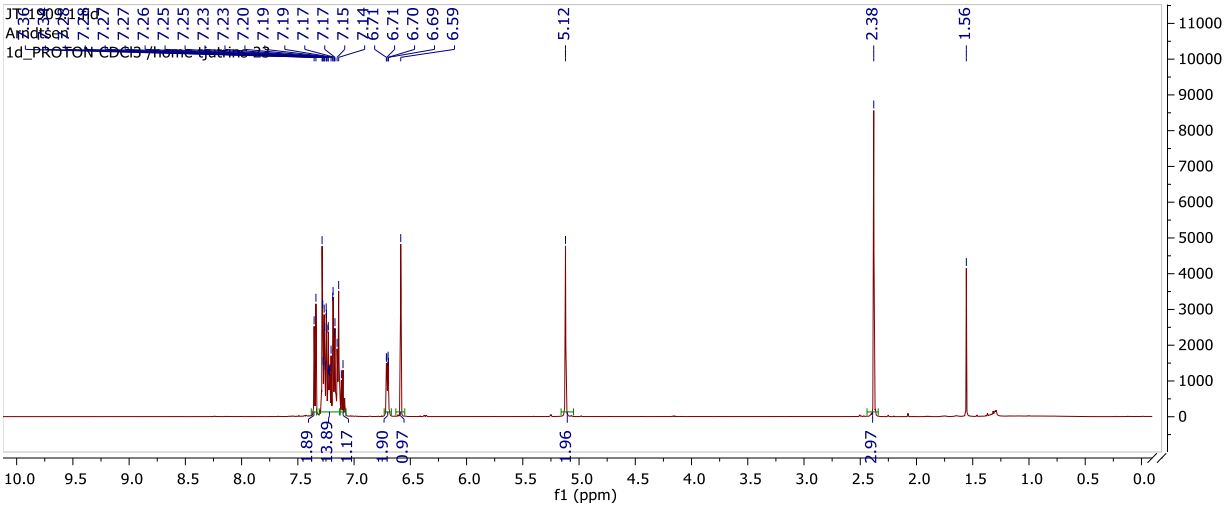

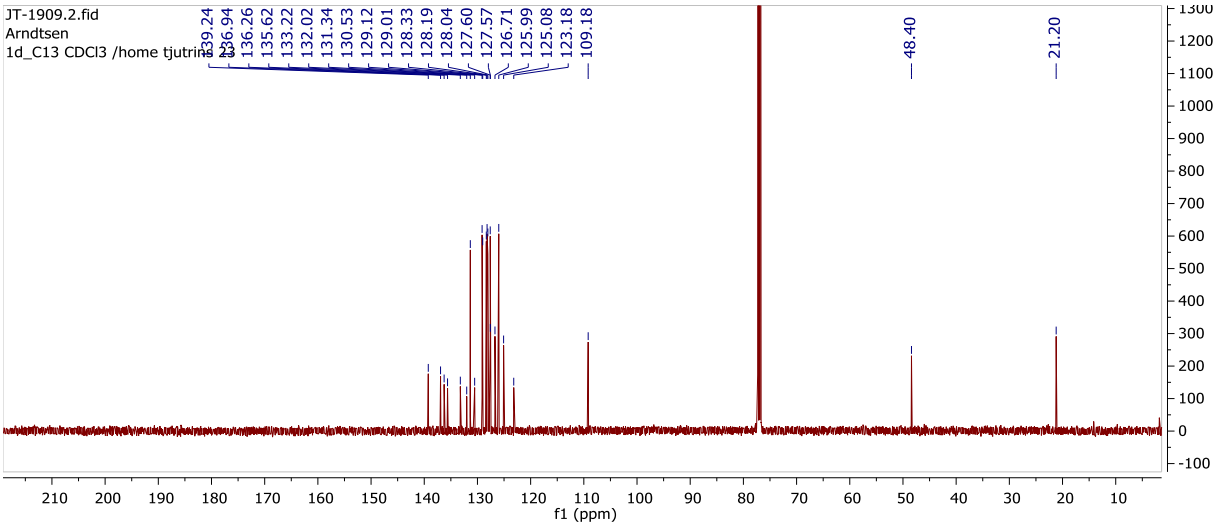

^{1}H and ^{13}C NMR spectra of **6.4ff**

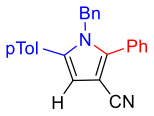

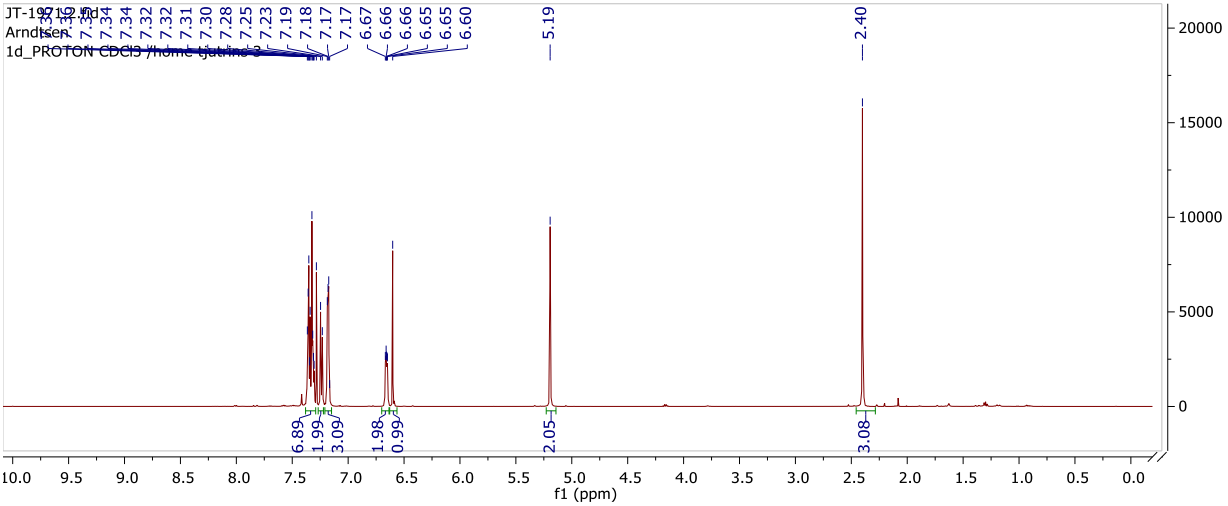

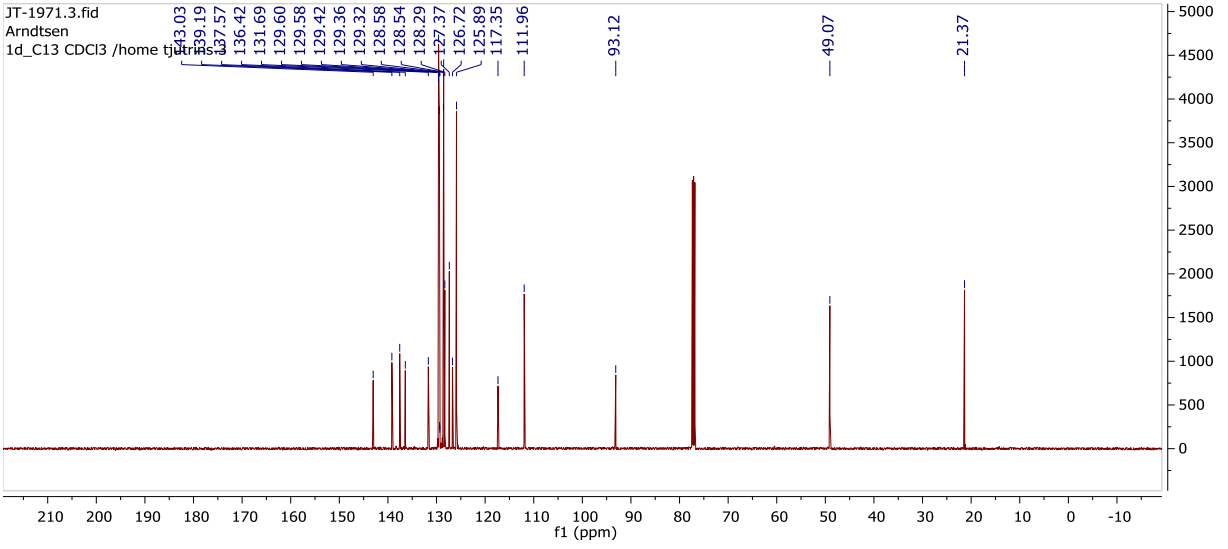

^{1}H,^{13}C and ^{19}F NMR spectra of **6.1**

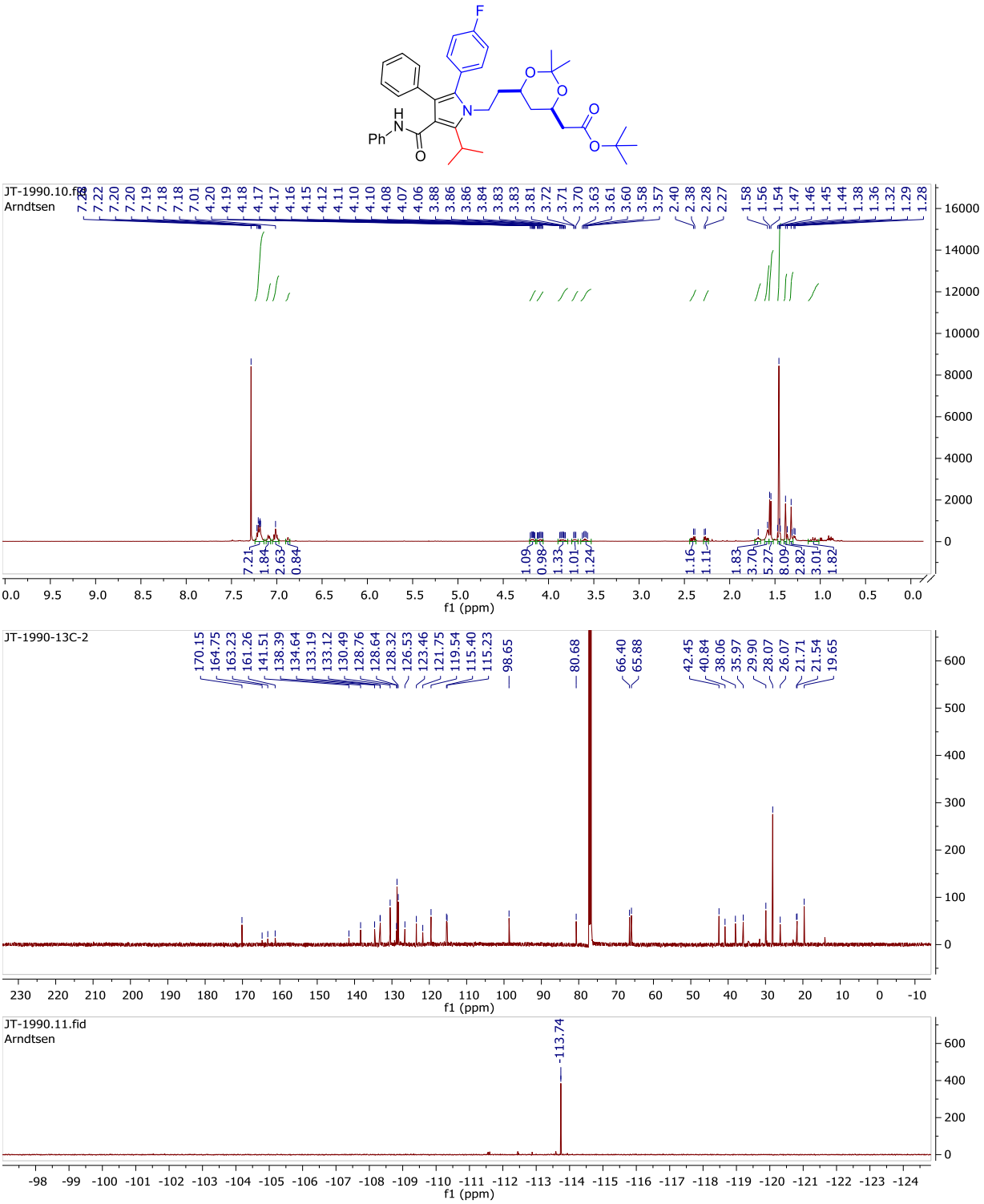

^{1}H, ^{13}C and ^{31}P NMR spectra of complex **6.D**

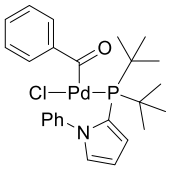

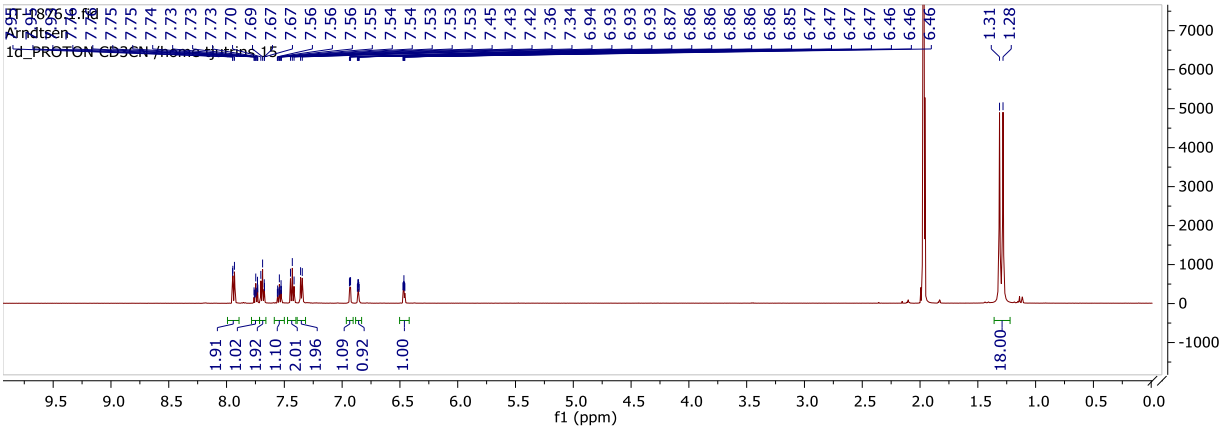

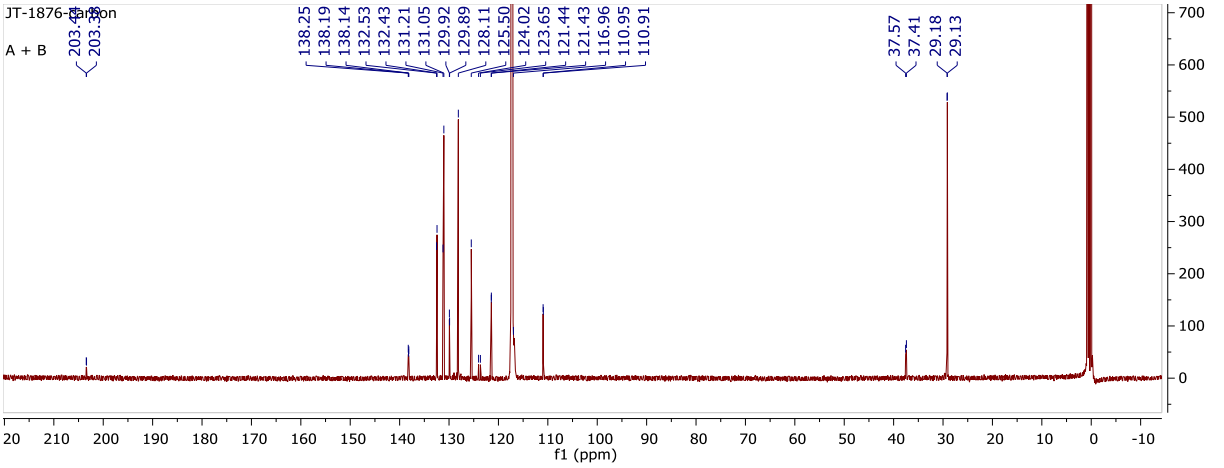

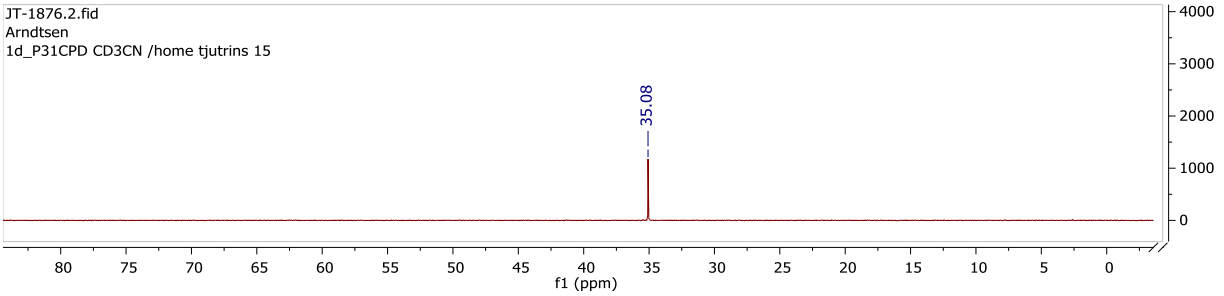

^{1}H, ^{13}C and ^{31}P NMR spectra of complex 2-(di-tert-butylphosphanyl)-1-methyl-1H-pyrrole